Urychlené černé díry a struktura záření v prostoročasech s nenulovou kosmologickou konstantou

Pavel Krtouš

Ústav teoretické fyziky
Matematicko-fyzikální fakulta
Univerzita Karlova v Praze

HABILITAČNÍ PRÁCE
OBOR: FYZIKA SMĚR: TEORETICKÁ FYZIKA

Praha, 2005

Obsah

Část I

Přehledová část

Úvod

V této habilitační práci předkládám své výsledky publikované během posledních let v recenzovaných mezinárodních časopisech. Práce se skládá z přehledové části a souboru publikací. Přehledová část shrnuje hlavní výsledky přiložených prací a navozuje kontext, do kterého jsou tyto práce zasazeny.

Habilitační práce se zabývá zejména tematikou urychlených černých děr a asymptotickými vlastnostmi polí v případě nenulové kosmologické konstanty. Tomu odpovídá i členění přehledové části. Ta se skládá ze tří kapitol.

První kapitola uvádí čtenáře do problematiky černých děr – objektů jejichž podstata spočívá v degeneraci kauzálních vlastností prostoročasu. Tato kapitola má více pedagogický charakter, jsou zde krátce vyloženy i některé standardní pojmy a metody užívané při zkoumání globálních a kauzálních vlastností prostoročasů. Vedle toho zde jsou shrnuty původní výsledky týkající se urychlených černých děr v asymptoticky de sitterovských a anti-de sitteriovských prostoročasech.

Tuto kapitolu doplňuje též 'digitální příloha' – prezentace na přiloženém CD obsahující obrázky, interaktivní třídimenzionální diagramy a animace ilustrující strukturu prostoročasů vně černých děr různých typů.

Druhá kapitola se zabývá strukturou zářivých polí v asymptotických oblastech různého typu (v závislosti na hodnotě kosmologické konstanty). Je zde krátce shrnuta problematika záření v obecné teorii relativity a jako hlavní původní výsledek je zde diskutována směrová charakteristika zářivé komponenty gravitačního pole.

Třetí kapitola se krátce zabývá pracemi souvisejícími s formulací teorie gravitace v prostoročasech vyšší dimenze. Jedná se o zobecnění výsledků diskutovaných v druhé kapitole a dále o výsledky týkající se ultrarelativisticky se pohybujících černých prstenců – vícedimenzionálních alternativ k černým dírám.

Přehledová část má poměrně obecný charakter. Jejím cílem je nastínit význam přiložených odborných prací a přiblížit jejich hlavní výsledky. Vedle toho jsem se snažil též shrnout širší souvislosti formou přístupnou i pro čtenáře, který nepracuje aktivně v obecné teorii relativity. Zejména první kapitola obsahuje i přehledový materiál, druhá a třetí kapitola se již více zaměřují na původní odborné výsledky. Pro podrobný technický výklad čtenáře odkazuji na samotné přiložené články, zvláště pak na zastřešující rozsáhlé práce [3, 7, 10, 12].

Na přiloženém CD lze nalézt vedle zmíněné digitální přílohy a souboru většiny mých odborných publikací též několik studijních textů a dva popularizační projekty přibližující některé aspekty speciální teorie relativity. Obsah přiloženého CD lze nalézt v závěru přehledové části.

* * *

Většina předkládaných výsledků byla dosažena ve spolupráci s kolegy z Ústavu teoretické fyziky MFF UK. V první řadě bych chtěl jmenovat svého učitele prof. Jiřího Bičáka, který zásadním způsobem formoval mojí odbornou orientaci. Již během mého studia na MFF UK mě uvedl do světa zachyceného Einsteinovu teorií relativity a upoutal mojí pozornost na problematiku boost-rotačně symetrických prostoročasů, která stojí v centru či alespoň pozadí většiny zde uváděných prací. Za jeho inspirující a nedocenitelný vliv a možnost plodné spolupráce mu patří můj upřímný dík. Poděkovat bych chtěl i svému kolegovi a příteli doc. Jiřímu Podolskému za potěšení z mnoha diskuzí a společně dosažených výsledků. Naše vzájemná spolupráce těží z podobné 'naladěnosti' na vnímání problémů v obecné teorii relativity a věřím, že i nadále povede k dalším zajímavým výsledkům. Rád bych též zmínil dr. Marcella Ortaggia a poděkoval mu zejména za to, že obrátil mojí pozornost i na problematiku teorií ve více dimenzích. Nakonec musím vyzdvihnout prostředí Ústavu teoretické fyziky a kolektivu kolem Relativistického semináře ÚTF, které mi poskytovalo velmi vstřícné a stimulující zázemí jak po odborné a technické, tak i po lidské stránce.

Výsledky předkládané v této práci vznikly za podpory grantů GAČR "Relativistická fyzika a astrofyzika" (roky 1997–98, 1999–2001 a 2002–2004), grantů GAUK "Relativistické teorie gravitace, astrofyzika a kosmologie" (roky 1997–1998, 2000–2002 a 2003), výzkumného záměru "Výzkum Země a vesmíru metodami teoretické, experimentální a počítačové fyziky" a rozvojového projektu MŠMT č. 360/2005.

V neposlední řadě bych chtěl poděkovat svým nejbližším – Simoně a Míšovi – za to, že se mnou a mým zájmem o fyziku měli a mají dostatek trpělivosti.

Kapitola 1

Urychlené černé díry

Shrnutí

Je známo pouze málo přesných řešení Einsteinových rovnic popisujících netriviálně se pohybující zdroje. Jednou třídou takových řešení jsou rovnoměrně urychlené černé díry popsané tzv. C-metrikou. Tato metrika je známá v podstatě od počátků obecné teorie relativity [21, 22], geometrická struktura samotného prostoročasu byla však pochopena mnohem později. Pro nulovou kosmologickou konstantu Λ byla C-metrika interpretována jako prostoročas urychlených černých děr až v 70-tých a 80-tých letech minulého století [23–25].

Zobecnění C-metriky pro nenulovou kosmologickou konstantu [26–28] bylo plně vysvětleno ještě později. K podrobné geometrické analýze prostoročasů popsaných touto metrikou přispěla i série prací [3, 5, 12] zařazených do této habilitace. Prostoročasy s $\Lambda \neq 0$ se od případu nulového Λ zásadně odlišují v asymptotické oblasti. Tato oblast byla v přiložených pracích vizualizována pomocí kompaktifikovaných třídimenzionálních diagramů zachycujících zejména kauzální strukturu. Byly též zavedeny různé souřadnicové systémy vhodné pro diskuzi vlastností prostoročasů a umožňující provedení různých fyzikálně zajímavých limit.

Jednou ze zajímavých limit je případ slabých polí, tj. případ zanedbatelných hmotnosti černých děr. V tomto případě C-metrika popisuje vakuové maximálně symetrické prostoročasy, jejichž geometrické struktura je plně dána kosmologickou konstantou. Jako pozůstatek černých děr však tyto prostoročasy obsahují rovnoměrně urychlené (elektromagneticky nabité) testovací částice. V přiložených pracích [1, 10] byly podrobně analyzovány vlastnosti rovnoměrně urychlených částic v de Sitterově vesmíru (případ $\Lambda > 0$) a odvozeno a diskutováno jejich elektromagnetické a skalární pole. Rozsáhlá práce [10] navíc obsahuje vyčerpávající přehled souřadnic užívaných v de Sitterově prostoročase, včetně souřadnic přizpůsobených urychleným pozorovatelům.

Tato kapitola krátce představí pojem černých děr, nastíní techniky užívané ke globální analýze prostoročasů a popíše strukturu prostoročasů s pohybujícími se černými dírami. Některé rysy těchto prostoročasů jsou dokumentovány a vizualizovány též pomocí obrázků, interaktivních třídimenzionálních diagramů a animací obsažených na přiloženém CD. Podkapitoly 1.1 a 1.3 jsou přehledové, uvádějí kontext, do kterého zkoumaná problematika zapadá. Podkapitoly 1.2 a 1.4 se dotýkají konkrétněji přiložených původních prací.

Publikace

Původní výsledky týkající se tématu této kapitoly jsou obsaženy v následujících pracích:

[3] Pavel Krtouš, Jiří Podolský: *Radiation from accelerated black holes in a de Sitter universe*, Phys. Rev. D 68, 024005 (2003).

[5] Jiří Podolský, Marcello Ortaggio, Pavel Krtouš: *Radiation from accelerated black holes in an anti-de Sitter universe*, Phys. Rev. D **68**, 124004 (2004).

[12] Pavel Krtouš: *Accelerated black holes in an anti-de Sitter universe*, Phys. Rev. D **72**, 124019 (2005).

[10] Jiří Bičák, Pavel Krtouš: *Fields of accelerated sources: Born in de Sitter*, J. Math. Phys. **46**, 102504 (2005).

[2] Jiří Bičák, Pavel Krtouš: *The fields of uniformly accelerated charges in de Sitter spacetime*, Phys. Rev. Lett. **88**, 211101 (2002).

[1] Jiří Bičák, Pavel Krtouš: *Accelerated sources in de Sitter spacetime and the insufficiency of retarded fields*, Phys. Rev. D, **64**, 124020 (2001).

Plné znění těchto publikací lze nalézt v druhé části habilitační práce.

1.1 Kauzální struktura prostoročasu

Uvedení do problematiky

Základní myšlenkou obecné teorie relativity je popisovat gravitační působení pomocí geometrických vlastností prostoročasu. To co vnímáme jako gravitační sílu má tak svůj původ (i) v naší volbě lokálně neinerciální soustavy a (ii) v zakřivení prostoročasu samotného. Podle obecné teorie relativity by např. v blízkosti Země byla přirozená lokálně inerciální soustava spojená s volně padajícími pozorovateli. Při volbě soustavy spojené s povrchem Země proto musíme zavést nepravou sílu zohledňující neinercialitu této soustavy. Tu běžně interpretujeme jako sílu gravitační. Takto zavedenou sílu lze eliminovat přechodem do lokálně inerciální soustavy. Tento přechod však nelze provést globálně – pokud je prostoročas zakřivený, globální inerciální soustava neexistuje. Vlastní zakřivení prostoročasu se projevuje tzv. slapovým působením – díky němu se i ve volně padající soustavě v blízkosti Země začnou blízká volná tělíska, na počátku připravená v klidu, vůči sobě pohybovat.

Spolu s těmito základními rysy přinesla obecná teorie relativity mnoho zajímavých a překvapivých předpovědí. Mimo jiné otevřela možnost netriviální kauzální struktury celého prostoročasu. Pod kauzální strukturou se rozumí znalost, které události v prostoročase mohou být (alespoň v principu) kauzálně spojené. Fakt, že tato struktura může být gravitačním polem pozměněna, odráží univerzalitu působením gravitačního pole na všechny procesy. Gravitační pole nelze odstínit a způsobuje stejný pohyb nezávisle na struktuře objektu, na který působí. Díky tomu můžeme zachytit působení gravitačního pole přímo v popisu prostoročasových vztahů. Gravitace tak determinuje jeviště, ve kterém se odehrává zbytek fyziky.

Kauzální struktura prázdného nepokřiveného prostoročasu je známá již ze speciální teorie relativity. Dvě události mohou být vůči sobě položeny buď *časupodobně* (jedna následuje druhou, tj. lze poslat fyzikální signál z jedné do druhé) nebo *prostorupodobně* (nelze kanonicky určit, která z událostí nastala dříve; události jsou příliš daleko, aby je mohl spojit podsvětelně se pohybující signál). Na rozdíl od předrelativistické představy, prostorupodobné události nejsou události současné: všechny události prostorupodobně položené vzhledem k jedné zvolené události tvoří oblast *stejné dimenze* jako prostoročas samotný. Hranici mezi událostmi časupodobně a prostorupodobně vztaženými ke zvolené události O nazýváme *světelný kužel* s vrcholem v O, viz obr. 1.1. Jak název napovídá, světelný kužel je tvořen drahami světelných paprsků vyslaných či přijatých v O.

Minkowského prostoročas speciální teorie relativity je homogenní a isotropní, jeho kauzální struktura (struktura světelných kuželů) je tak všude stejná. Obecná teorie relativity přebírá tuto strukturu lokálně – v malé oblasti zakřiveného prostoročasu se lokální fyzika odehrává podle stejných zákonů jako ve speciální teorii relativity. Na větších vzdálenostech se však vzájemná poloha světelných kuželů v zakřiveném prostoročase mění a deformuje. A na globální škále se kauzální struktura může změnit i zcela zásadním způsobem. Obecná teorie relativity tak např. připouští, že prostoročas může mít jinou kauzální asymptotiku – tzn. jinou kauzální dosažitelnost velmi vzdálených událostí. Nebo naopak připouští existenci

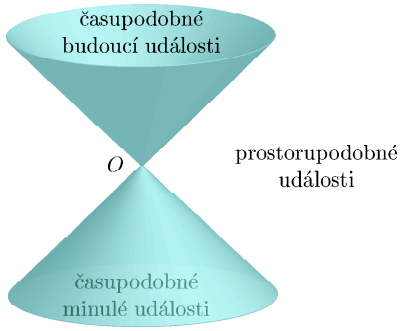

Obrázek 1.1: **Světelný kužel události O.** Světelný kužel rozděluje prostoročas na události, které jsou vzhledem k O položeny časupodobně a prostorupodobně. Časupodobné události se dále dělí na události budoucí k O (ty, ke kterým lze z O zaslat fyzikální signál) a události minulé k O (ze kterých lze do O poslat signál). Světelný kužel je generován světelnými (též nulovými) paprsky procházejícími událostí O.

oblastí, ze kterých se již nelze dostat do okolního prostoročasu. Lze v ní popsat prostoročasy s odlišnou topologií, případně i s patologickou kauzální strukturou připouštějící např. návraty do minulosti.

Kauzální struktura – zakódována v prostoročasové geometrii – determinuje tedy přípustné kauzální vztahy. Všechny známé fyzikální zákony respektují kauzální strukturu a proto jsou omezení daná touto strukturou fundamentální. Pokud zjistíme, že je nějaký proces omezen z kauzálních důvodů, neznamená to jen jakési technologické omezení, které může být v průběhu dalšího vývoje překonáno. Jedná se o omezení tak principiální, že je zabudováno (skrze prostoročasovou geometrii) přímo do jádra našeho popisu, a jeho porušení by s sebou nutně neslo velmi závažnou a rozsáhlou změnu celého tohoto popisu.

Níže se zaměříme zejména na dva netriviální projevy kauzální struktury: na *asymptotickou strukturu* prostoročasů a na objekty zvané *černé díry*. Nejdříve se však musíme seznámit s některými technikami používanými při zkoumání kauzální struktury.

Konformní geometrie a konformní nekonečno[1]

Při zkoumání asymptotických vlastností fyzikálních polí je důležité míti pod kontrolou velmi vzdálené části prostoročasu. Pro tento účel se zavádí pojem *konformního nekonečna*, označovaného $\mathcal{I}$, umožňující rigorózně a detailně popsat strukturu vzdálených oblastí. Podrobné zavedení je možné nalézt ve standardní literatuře [29, 30], ucelený přehled je též podán v [7] či v češtině v [31].

Technika konformního nekonečna umožňuje přidat ke zkoumanému prostoročasu 'body v nekonečnu' způsobem zachycujícím správně kauzální strukturu vzdálených oblastí. Zhruba řečeno, různé body v konformním nekonečnu mají k prostoročasu různý kauzální vztah. Můžeme si je představit jako limitní body *světelných* světočar, přičemž řekneme, že dvě světočáry vedou směrem do budoucnosti do stejného bodu nekonečna, pokud mají stejnou minulost (tedy souhrn

[1] Část tohoto oddílu je s úpravami převzata z úvodní partie práce [20].

všech událostí, ze kterých lze poslat k světočáře fyzikální signál). Dvě světelné světočáry tak končí v různých bodech konformního nekonečna, pokud jsou z těchto (do nekonečna protažených) světočar pozorovatelné různé oblasti prostoročasu.

Body dosažitelné nulovými světočárami směrem do budoucna tvoří *budoucí nekonečno* $\mathcal{I}^+$, obdobně definované body dosažitelné směrem do minula tvoří tzv. *minulé nekonečno* $\mathcal{I}^-$. Přitom jeden a týž bod v nekonečnu může nebo nemusí být dosažitelný jak z minula, tak z budoucna – to závisí na konkrétní struktuře konformního nekonečna.

Vedle toho lze analogicky zavést též *časové* a *prostorové* nekonečno – limitní body časových, resp. prostorových, asymptoticky geodetických křivek.

Z matematického hlediska je prostoročas $\mathcal{M}$ varietou s metrikou $\boldsymbol{g}$. Vlastnosti a strukturu konformního nekonečna této variety lze studovat Penroseovou metodou [29, 32]. Ta spočívá ve vnoření fyzikálního prostoročasu $\mathcal{M}$ s metrikou $\boldsymbol{g}$ do pomocného prostoročasu $\tilde{\mathcal{M}}$ s nefyzikální metrikou $\tilde{\boldsymbol{g}}$, která se od fyzikální metriky liší pouze lokální konformní transformací – přeškálováním konformním faktorem Ω^2:

$$\tilde{\boldsymbol{g}} = \Omega^2 \boldsymbol{g} \,. \tag{1.1}$$

Klíčové pozorování je, že konformní přeškálování nemění lokální kauzální strukturu. Časupodobné směry vycházející z dané události jsou totiž dány vektory se záporným kvadrátem velikosti spočteným pomocí metriky $\boldsymbol{g}$, prostorupodobné směry pomocí vektorů s kvadrátem velikosti kladným. Toto rozlišení se při přeškálování (1.1) nezmění. Pojmy *minulost* a *budoucnost* zůstávají tak pro konformní metriku stejné jako pro metriku fyzikální. Stejně tak nulové (světelné) křivky ve smyslu fyzikální geometrie jsou nulové i ve smyslu geometrie konformní.

Škálování metriky volíme takové, aby faktor Ω klesal k nule směrem do nekonečna fyzikálního prostoročasu. Fyzikální prostoročas $\mathcal{M}$ se pak stává částí nefyzikálního prostoročasu $\tilde{\mathcal{M}}$ ohraničenou hranicí $\partial\mathcal{M} = \mathcal{I}$, která je dána podmínkou

$$\Omega = 0 \,. \tag{1.2}$$

Řekneme, že nekonečno $\mathcal{I}$ je regulární, pokud z hlediska 'rozšířeného' prostoročasu $\tilde{\mathcal{M}}$ je metrika $\tilde{\boldsymbol{g}}$ na hranici $\mathcal{I}$ regulární.[2] Naproti tomu, fyzikální metrika je na $\mathcal{I}$ degenerovaná – vzdálenosti mezi body uvnitř fyzikálního prostoročasu a hranicí $\mathcal{I}$ měřené pomocí fyzikální metriky jsou nekonečné a proto hranice $\mathcal{I}$ reprezentuje body v nekonečnu fyzikálního prostoročasu. Z hlediska pomocné variety $\tilde{\mathcal{M}}$ je však regulární nekonečno obyčejnou nadplochou ohraničující fyzikální prostoročas a můžeme ji proto zkoumat běžnými prostředky diferenciální geometrie.

Zavedení konformního nekonečna $\mathcal{I}$ je analogické přidání nevlastních bodů známé z běžné geometrie. Konformní nekonečno ale může mít bohatou strukturu. Typicky se jedná o třídimenzionální varietu 'ohraničující' fyzikální prostoročas. Můžeme však mít konformní nekonečna lišící se jak svojí topologií, tak geometrii.

[2] Regularita není samozřejmá. Neregulární bývá např. prostorové nekonečno v netriviálních prostoročasech s $\Lambda = 0$ či např. části nekonečna $\mathcal{I}$ na ose symetrie prostoročasu C-metriky diskutovaného v podkapitole 1.4 níže.

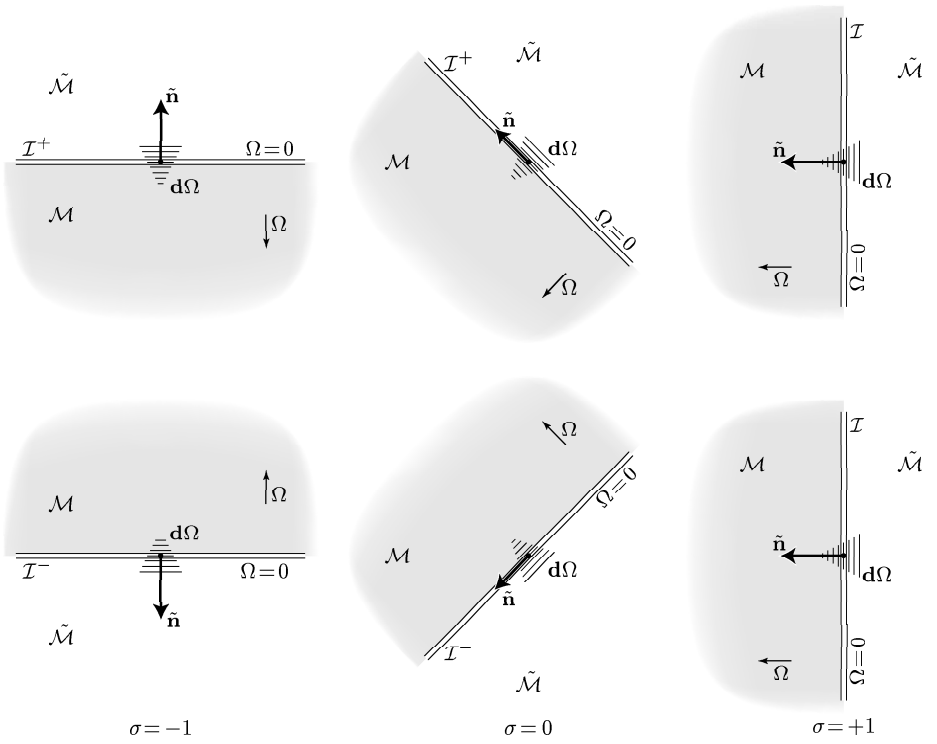

Obrázek 1.2: **Charakter konformního nekonečna.** Lokální charakter konformního nekonečna $\mathcal{I}$ (definovaného jako hranice $\Omega=0$ fyzikálního prostoročasu $\mathcal{M}$ v pomocné varietě $\tilde{\mathcal{M}}$) je určen normou σ vektoru $\tilde{\boldsymbol{n}}$ kolmého k nekonečnu $\mathcal{I}$. Pro $\sigma=-1,0$, nebo $+1$ je nekonečno $\mathcal{I}$ prostorupodobné, nulové, respektive časupodobné. Když $\sigma=-1$ nebo $\sigma=0$, lze rozlišit budoucí a minulé nekonečno $\mathcal{I}^+$ a $\mathcal{I}^-$; příslušné diagramy jsou nakresleny v horní a dolní části obrázku. Pro $\sigma=+1$ obě nekonečna splývají a příslušné diagramy jsou tudíž totožné.

Základní geometrickou charakteristikou konformního nekonečna $\mathcal{I}$ je jeho orientace. Zavedeme-li vektor $\tilde{\boldsymbol{n}}$ kolmý k nekonečnu $\mathcal{I}$ a normalizovaný pomocí metriky $\tilde{\boldsymbol{g}}$ vztahy

$$\tilde{\boldsymbol{n}} \propto \mathbf{d}\Omega\,, \qquad \tilde{\boldsymbol{g}}_{ab}\tilde{\boldsymbol{n}}^a\tilde{\boldsymbol{n}}^b=\sigma\,, \qquad \sigma=-1,0,+1\,, \tag{1.3}$$

pak říkáme, že konformní nekonečno je

$$\begin{array}{ll} \text{prostorupodobné} & \text{pokud } \sigma=-1\,,\\ \text{nulové} & \text{pokud } \sigma=0\,,\\ \text{časupodobné} & \text{pokud } \sigma=+1\,. \end{array} \tag{1.4}$$

Prostorupodobné a nulové nekonečno může být dosaženo pomocí nulových křivek pouze z minulosti nebo pouze z budoucnosti. Podle toho rozlišujeme *budoucí* a *minulé* konformní nekonečno (viz obr. 1.2). Bod časupodobného nekonečna může být zároveň dosažen jak z minulosti, tak z budoucnosti; budoucí a minulé nekonečno v tomto případě splývají.

Důležitým důsledkem Einsteinova gravitačního zákona je, že charakter konformního nekonečna souvisí se znaménkem kosmologické konstanty Λ. Za předpokladu, že stopa tenzoru energie-hybnosti je nulová (což je např. splněno ve vakuu či v přítomnosti elektromagnetického pole) platí (viz [29], případně (2.10) v [7]), že

$$\sigma = -\operatorname{sgn}\Lambda\,. \tag{1.5}$$

Prostoročasy bez kosmologické konstanty (např. plochý Minkowského vesmír) mají konformní nekonečno nulové, prostoročasy s kladnou kosmologickou konstantou (např. de Sitterův vesmír) 'začínají' prostorupodobným minulým nekonečnem a 'končí' prostorupodobným budoucím nekonečnem. Konečně prostoročasy se zápornou kosmologickou konstantou (např. anti-de Sitterův vesmír) jsou ohraničené časupodobným nekonečnem.

Poznamenejme, že existují situace, kdy nelze konformní nekonečno zavést. Prostoročas se nemusí na velkých vzdálenostech chovat regulárně, může být 'ohraničen' singularitami (jako je např. velký třesk) či může obsahovat černé díry (viz níže). Nekonečno nemusí být souvislé – může se rozpadat nejen na budoucí a minulou část, ale i na několik navzájem oddělených komponent. Na konformní nekonečno $\mathcal{I}$ lze klást další omezující podmínky, týkající se např. asymptotického chování metriky v okolí $\mathcal{I}$. Nejznámější je pojem tzv. *asymptotické plochosti* [29, 33] vymezující, že konformní nekonečno je nulové a asymptoticky velmi blízké nekonečnu prázdného Minkowského prostoročasu.

Konformní diagramy

Vnoření fyzikálního prostoročasu do pomocné variety $\tilde{\mathcal{M}}$ umožňuje přirozenou vizualizaci globálních aspektů kauzální struktury. Celý fyzikální prostoročas se zde totiž zobrazuje jako kompaktní objekt.

Typicky se tato technika používá pro dvoudimenzionální řezy. Pro symetrické prostoročasy bývá dvoudimenzionální řez dostatečně informativní. Např. pro sféricky symetrické prostoročasy řez v radiálním a časovém směru zachycuje většinu podstatných rysů kauzální struktury. Přeškálování fyzikální metriky lze vždy zvolit tak, aby restrikce konformní metriky $\tilde{\boldsymbol{g}}$ na vybraný dvoudimenzionální řez $\mathcal{K}$ byla Minkowského metrika[3]

$$\tilde{\boldsymbol{g}}\big|_{\mathcal{K}} = -\mathbf{d}\tilde{t}^2 + \mathbf{d}\tilde{r}^2\,. \tag{1.6}$$

Konformní diagram je pak zobrazení řezu $\mathcal{K}$ s vertikální a horizontální osou ve směru souřadnic $\tilde{t}$ a $\tilde{r}$. Diagonální směry odpovídají nulovým křivkám $\tilde{r} \pm \tilde{t} =$ konst., které jsou nulové i ve smyslu fyzikální metriky $\boldsymbol{g}$ a určují tak světelné kužele, tj. určují kauzální strukturu. V tomto diagramu bude celý fyzikální prostoročas zobrazen jako omezená oblast ohraničená konformním nekonečnem $\mathcal{I}$.

Konformní diagramy byly zavedeny Carterem a zpopularizovány Penrosem. Detailní popis jejich konstrukce a vlastností (zejména s aplikací na prostoročasy s černými dírami) je možné najít v [34].

[3] Každé dvě metriky na dvoudimenzionální ploše jsou spojené konformní transformací, proto lze konformní faktor vždy zvolit tak, aby $\tilde{\boldsymbol{g}}\big|_{\mathcal{K}}$ byla plochá.

Nejjednodušším příkladem je konformní diagram Minkowského prostoročasu. Minkowského metriku zapsanou ve sférických, případně nulových souřadnicích

$$\begin{aligned} \boldsymbol{g} &= -\mathbf{d}t^2 + \mathbf{d}r^2 + r^2\big(\mathbf{d}\vartheta^2 + \sin^2\vartheta\,\mathbf{d}\varphi^2\big) \\ &= -\tfrac{1}{2}\,\mathbf{d}u \vee \mathbf{d}v + \tfrac{1}{4}\,(v-u)^2\big(\mathbf{d}\vartheta^2 + \sin^2\vartheta\,\mathbf{d}\varphi^2\big) \end{aligned} \tag{1.7}$$

(kde $t \in \mathbb{R}$, $r \in \mathbb{R}^+$, $\vartheta \in (0,\pi)$, $\varphi \in (-\pi,\pi)$ a $u = t-r$, $v = t+r$) lze přeškálovat konformním faktorem

$$\Omega^2 = 4\,(1+u^2)^{-1}(1+v^2)^{-1}\,. \tag{1.8}$$

To vede ke konformní metrice $\tilde{\boldsymbol{g}}$, která má po zavedení souřadnic $\tilde{t}$, $\tilde{r}$

$$\begin{aligned} \tilde{t} &= \tfrac{1}{2}(\tilde{v}+\tilde{u})\,, \quad \tan\frac{\tilde{u}}{2} = u\,, \\ \tilde{r} &= \tfrac{1}{2}(\tilde{v}-\tilde{u})\,, \quad \tan\frac{\tilde{v}}{2} = v\,, \end{aligned} \tag{1.9}$$

tvar

$$\tilde{\boldsymbol{g}} = \Omega^2\boldsymbol{g} = -\mathbf{d}\tilde{t}^2 + \mathbf{d}\tilde{r}^2 + \sin^2\big(\mathbf{d}\vartheta^2 + \sin^2\vartheta\,\mathbf{d}\varphi^2\big)\,. \tag{1.10}$$

Zřejmě zúžení např. na řez $\vartheta = \pi/2$, $\varphi = 0$ vede na metriku (1.6). Konformní nekonečno $\mathcal{I}$ původního Minkowského prostoročasu je dáno podmínkou (1.2), tj. podmínkami[4] $u = -\infty$, resp. $v = \infty$. V souřadnicích $\tilde{u}$, $\tilde{v}$ tyto podmínky přejdou na $\tilde{u} = -\pi$ a $v = \pi$, konformní nekonečno $\mathcal{I}$ je tak vskutku lokalizované v konečné oblasti konformní variety $\tilde{\mathcal{M}}$. Konformní diagram radiálního řezu Minkowského prostoročasu je kosočtverec ohraničený konformním nekonečnem $\mathcal{I}$ nulového charakteru, viz obr. 1.3. Vrcholy kosočtverce jsou minulé a budoucí nekonečna i_- a i_+ a prostorové nekonečno i_0.

Pro prostoročasy s nižší symetrií nemusí být konformní diagram dvoudimenzionálních řezů již dostatečný – nemusí postihovat důležité rysy prostoročasu či dokonce může zkreslovat charakter konformního nekonečna. Záleží totiž na tom, jak je dvoudimenzionální řez do prostoročasu vnořen. Např. u C-metriky, o které se zmíníme podrobněji níže, typický řez, pro který se kreslí dvoudimenzionální konformní diagram, protíná konformní nekonečno v linii prostorového charakteru, ačkoli samotné nekonečno je charakteru nulového – viz diskuzi C-metriky v podkapitole 1.4 (např. obr. 1.11) či práci [12].

Proto je v těchto případech výhodné vizualizovat kauzální strukturu pomocí třídimenzionálních diagramů sestrojených opět pomocí konformní geometrie pomocné variety $\tilde{\mathcal{M}}$. V případě třídimenzionálního řezu však již není možné vždy dosáhnout, aby konformní metrika zúžená na řez byla plochá jako v (1.6). Při vykreslování třídimenzionálního diagramu je proto potřeba zvolit vhodné vnoření konformní geometrie do euklidovského prostoru, ve kterém diagram zobrazujeme. Pro takto zkonstruované diagramy nebude již platit, že všechny diagonální linie jsou nulové; světelné kužele mohou být zobrazeny deformovaně. Třídimenzionální diagram však lze chápat jako 'poslepování' diagramů dvoudimenzionálních – dvoudimenzionální řezy tvoří foliaci třídimenzionálního diagramu a v každém listu této foliace můžeme užít vlastností diagramů dvoudimenzionálních.

[4] Znaménka jsou dána požadavkem $r > 0$.

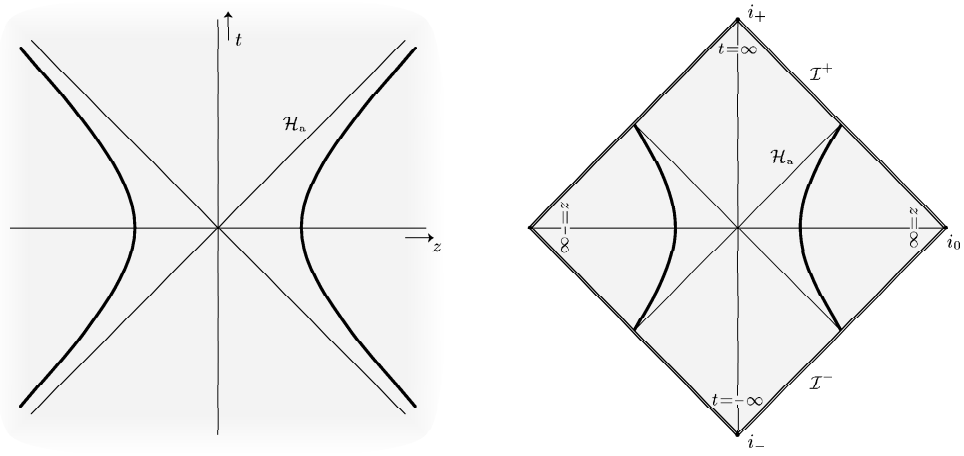

Obrázek 1.3: **Konformní diagram Minkowského prostoročasu.** Konformní diagram slouží k zachycení celého prostoročasu včetně jeho konformního nekonečna $\mathcal{I}$, prostorového nekonečna i_0 a časového nekonečna $i_\pm$. Diagram využívá ploché struktury pomocné variety, do které je fyzikální prostoročas vnořen. V obrázku nalevo je schematicky zachycen nepřeškálovaný Minkowského prostoročas, napravo jeho konformní diagram. V obou diagramech jsou znázorněny dva rovnoměrně urychlení pozorovatelé (tučně) a s nimi asociované akcelerační horizonty $\mathcal{H}_\mathrm{a}$(diagonální linie).

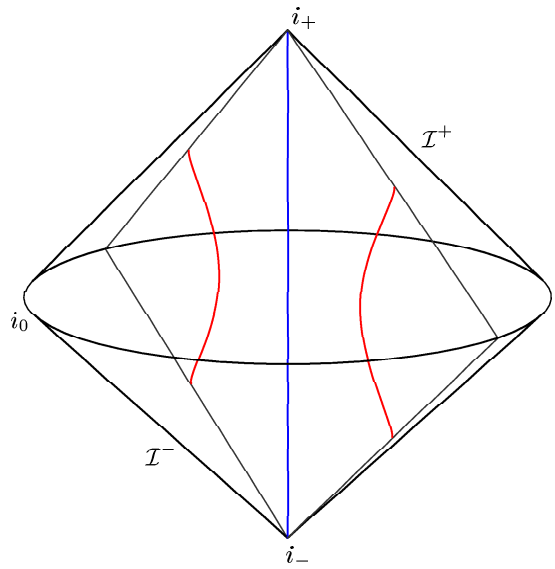

Obrázek 1.4: **Třídimenzionální diagram Minkowského prostoročasu.** Diagram třídimenzionálního řezu Minkowského prostoročasu z hlediska pomocné konformní geometrie, do které je fyzikální prostoročas vnořen. Hranice dvojitého kužele odpovídá konformnímu nekonečnu, vrcholy časovému nekonečnu a obvod společné podstavy kuželů prostorovému nekonečnu fyzikálního prostoročasu. V diagramu jsou znázorněny světočáry dvou rovnoměrně urychlených pozorovatelů a jednoho volného pozorovatele stojícího mezi nimi.

Pro Minkowského prostoročas můžeme zkonstruovat třídimenzionální diagram např. řezu $\vartheta = \pi/2$. Tento diagram lze též získat rotací diagramu dvoudimenzionálního – viz obr. 1.4. Interaktivní verzi a animaci tohoto diagramu lze též nalézt v digitální příloze. Interaktivní třídimenzionální diagramy lze prohlížet z různých stran, přiložené animace umožňují pohled 'dovnitř' prostoročasu ('otevřít' a 'zavřít' konformní nekonečno) a zobrazují vnoření dvoudimenzionálních konformních diagramů. V případě Minkowského prostoročasu jsou tato zobrazení poměrně triviální, nicméně do digitální přílohy byly zařazeny pro srovnání s komplikovanějšími diagramy prostoročasů obsahujících černé díry.

1.2 Rovnoměrně urychlené částice v maximálně symetrických prostoročasech

Motivace pro kosmologickou konstantu

Při zavedení konformních diagramů jsme se letmo seznámili s asymptotickou strukturou Minkowského prostoročasu – vakuového prostoročasu bez jakéhokoli gravitačního pole. Připomeňme, že i vakuový prostoročas (tj. prostoročas bez hmotných zdrojů) by mohl obsahovat netriviální gravitační pole – tzv. gravitační vlny. My se však nyní zaměříme na 'zcela prázdné' prostoročasy neobsahující ani gravitační vlny. Vedle Minkowského prostoročasu však navíc připustíme prostoročasy s nenulovou kosmologickou konstantou Λ. Nepřítomnost gravitačních vln můžeme matematicky vyjádřit požadavkem homogenity a isotropie těchto prostoročasů. Budeme se tedy zabývat maximálně symetrickými prostoročasy konstantní křivosti – tj. Minkowského (pro $\Lambda = 0$), de Sitterovým (pro $\Lambda > 0$) a anti-de Sitterovým (pro $\Lambda < 0$) prostoročasem.

Původně Einstein zahrnul do svého gravitačního zákona člen s kosmologickou konstantou, aby zajistil existenci řešení odpovídající statickému vesmíru vyplněného homogenně rozloženou hmotou (tzv. Einsteinův vesmír). Po experimentální evidenci toho, že se náš vesmír rozpíná, význam kosmologické konstanty na určitou dobu poklesl – přestože právě znalost de Sitterova řešení sehrála při akceptování expandujících kosmologických modelů pozitivní roli [35, 36]. Zájem o de Sitterovo řešení opět vzrostl v kontextu tzv. 'steady-state' modelu vesmíru v 50-tých letech 20. století a zejména v 80-tých letech v souvislosti s inflačními modely počátku vesmíru [36]. Kosmologická konstanta se nakonec vrátila na scénu v plné slávě s nedávným zjištěním, že se rozpínání našeho vesmíru urychluje (viz např. přehled [37]). K vysvětlení tohoto jevu je potřeba přítomnost $\Lambda > 0$ či nějakého fyzikálního pole – skrývajícího se pod přezdívkou *temná energie* – které se jako kosmologická konstanta efektivně chová.[5] De Sitterův model vesmíru tak hraje v současné kosmologie klíčovou roli jak při vysvětlování počátečních stavů vesmíru (inflační fáze), tak při popisu konečných fází, kdy je limitou obecné třídy kosmologických modelů s $\Lambda > 0$.

Vedle toho jsou prostoročasy jak s kladnou tak zápornou kosmologickou kon-

[5] Hodnota kosmologické konstanty konzistentní se současným pozorováním je $\Lambda = 3H^2\Omega_\Lambda = 0,12\,\mathrm{Gpc}^{-2} = 1,2\cdot 10^{-35}\,\mathrm{s}^{-2}$. Hubbleova konstanta $H = 71\,\mathrm{km\,s^{-1}Mpc^{-1}}$ a relativní hustota 'temné energie' $\Omega_\Lambda = 0,73$ jsou dány analýzou dat [38, 39].

stantou široce využívány při zkoumání působení gravitace na kvantová pole (viz např. [40]) a hrají podstatnou roli při pokusech o spojení kvantové teorie pole a obecné teorie relativity – ať již v teorii supergravitace, bránových kosmologiích či teorii superstrun. Jedním z klíčových pozorování využívaných v těchto teoriích, zvýrazňující význam anti-de Sitterova vesmíru, je AdS/CFT korespondence – skutečnost, že lze nalézt určitý vztah mezi kvantovými poruchami gravitačního pole uvnitř anti-de Sitterova vesmíru a jistými kvantovými poli žijícími na konformním nekonečnu.

Maximálně symetrické prostory sehrály také důležitou roli v matematické relativitě, kde slouží jako základní prototypy prostoročasů. Obvykle se předpokládá, že hmota obsažená ve vesmíru prostoročas deformuje pouze lokálně. Daleko od zdrojů by se vlastnosti prostoročasu alespoň v některých oblastech měly blížit vlastnostem prázdného vesmíru – podle znaménka kosmologické konstanty vlastnostem Minkowského, de Sitterova či anti-de Sitterova vesmíru.

Rovnoměrně urychlené zdroje

Rovnoměrně urychlené částice jsou asi nejjednodušší netriviálně se pohybující zdroje. Přesto analýza vlastností elektromagnetického pole těchto zdrojů (tzv. Bornovo řešení [41]) není přímočará a v odborné literatuře je možné nalézt nepřebernou řadu článků věnovaných tomuto tématu (viz citace v [42] a [10]). Zájem a kontroverzi působí zejména absence brzdné síly u pole, které má zářivý charakter. Bornovo řešení popisuje pole netriviálních zdrojů, přitom je však analyticky relativně snadno vyjádřitelné a může tak sloužit jako modelový příklad pro analýzu různých fenoménů, např. k porozumění asymptotické struktury záření.

Rovnoměrně urychlená částice se v obecné teorii relativity popisuje světočárou, jejíž 4-zrychlení se mění pouze ve směru 4-rychlosti. V Minkowského prostoročasu jsou takové světočáry hyperboly ve smyslu inerciálních souřadnic a mluví se o hyperbolickém pohybu. Bornovo řešení popisuje pole dvou nábojů, které se k sobě přibližují z nekonečna s konstantním zpomalením[6] – až se zastaví a poté se začnou od sebe s konstantním zrychlením vzdalovat. Tyto částice se asymptoticky pohybují rychlostí světla a proto se v kompaktifikovaném obrazu vynořují z konformního nekonečna a opět se do něho vrací – viz obr. 1.3, případně interaktivní diagramy v digitální příloze. Díky tomu ani jedna z těchto částic nemůže pozorovat všechny události v celém prostoročase a ani nemůže být pozorována ze všech událostí v prostoročase. Hranice oblasti, ze které může být částice pozorována, a oblasti, kterou může pozorovat, se nazývá akcelerační horizont. Jedná se o historii dvou roviny kolmých na pohyb částice pohybujících se rychlostí světla proti sobě podél směru pohybu částic. Obě částice jsou akceleračními horizonty od sebe kauzálně odděleny. V třídimenzionálním konformním diagramu můžeme nahlédnout, že akcelerační horizont je vlastně tvořen světelnými kuželi s vrcholy v bodech, ve kterých částice 'vstupují' či 'vystupují' skrze konformní nekonečno do prostoročasu. Digitální příloha obsahuje diagramy zobrazující Minkowského prostoročas s vyznačeným i nevyznačeným akceleračním horizontem a animace, ve kterých je možno tento horizont 'otevírat' a 'zavírat'.[7]

[6] Konstantní je zpomalení/zrychlení v klidové soustavě částice.

[7] Podrobněji se 'ovládáním' diagramů a animací v digitální příloze budeme zabývat v podkapitole 1.4, v oddíle popisujícím zobrazení C-metriky s $\Lambda = 0$.

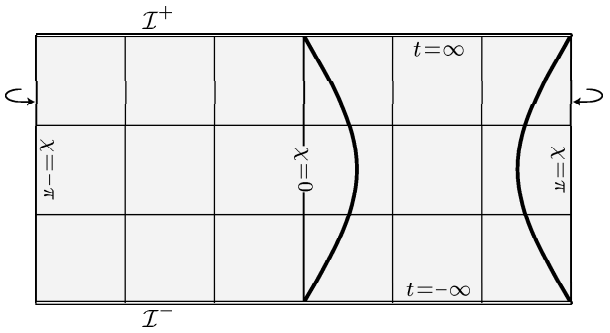

Obrázek 1.5: **Konformní diagram de Sitterova prostoročasu**. V diagramu je zobrazen radiální řez de Sitterovým vesmírem. Prostorová geometrie de Sitterova vesmíru je S^3, radiální řez tak odpovídá hlavní kružnici této třísféry. Horizontální linie v diagramu proto musejí být na krajích identifikovány. V diagramu jsou znázorněny linie standardních kosmologických souřadnic a světočáry dvou urychlených pozorovatelů (tučně). Dvojité čáry vyznačují konformní nekonečno prostoročasu, které se rozpadá na minulé nekonečno $\mathcal{I}^-$ a $\mathcal{I}^+$.

De Sitterův vesmír

V pracích [1, 2, 10] jsme se podrobně zabývali zobecněním Bornova řešení pro případ kladné kosmologické konstanty, tj. nalezením elektromagnetického a skalárního pole dvou rovnoměrně urychlených nábojů v de Sitterově vesmíru.

Kladná kosmologická konstanta efektivně působí jako rovnoměrně rozložená hmota se speciální stavovou rovnicí, která má *odpudivé* či *repulzní* gravitační účinky. Proto může kosmologická konstanta v Einsteinově vesmíru kompenzovat přitažlivé působení běžné hmoty, která by se jinak gravitačně zhroutila. De Sitterův vesmír neobsahuje žádnou hmotu a má proto tendenci se pod vlivem kosmologické konstanty rozpínat. Toto kosmologické rozpínání je ve vzdálené budoucnosti tak rychlé, že mu nemůže 'uniknout' ani světelný paprsek. Jednotlivé části prostoročasu se díky tomuto rozpínání vzdalují od sebe v daleké budoucnosti tak rychle, že je ani světelné paprsky nestihnou kauzálně spojit. Tyto oblasti jsou proto od sebe *prostorupodobně* oddělené. Budoucí konformní nekonečno $\mathcal{I}^+$ má tak prostorupodobný charakter – má podobu nadplochy (ve smyslu pomocné variety $\tilde{\mathcal{M}}$), jejíž jednotlivé body jsou navzájem prostorupodobně položené, viz obr. 1.5.

Díky rychlému rozpínání nemůže žádný pozorovatel v de Sitterově vesmíru (ani pozorovatel žijící nekonečně dlouho) uvidět celý vesmír – z některých oblasti k pozorovateli nestihne doletět žádná informace, protože žádný signál nepřekoná kosmologické vzdalování těchto oblastí. Hranice oblasti, kterou může pozorovatel (částice) vidět, se nazývá *částicový* či *kosmologický horizont*. Je tvořen světelnými paprsky asymptoticky přicházejícími do stejného bodu v budoucím konformním nekonečnu jako samotný pozorovatel (částice).

Tato situace je odlišná od Minkowského prostoročasu. V něm se paprsky pohybující se rychlostí světla vzdalují do konformního nekonečna $\mathcal{I}$, kdežto světočáry částic pohybujících se asymptoticky bez zrychlení vedou do časového nekonečna. V případě Minkowského prostoročasu lze časové nekonečno chápat jako vrchol

světelného kužele tvořícího konformní nekonečno (ve smyslu konformní geometrie pomocné variety $\tilde{\mathcal{M}}$). Světelné paprsky tak 'opouštějí' prostoročas 'jinde', než podsvětelní pozorovatelé. V de Sitterově prostoročasu je však konformní nekonečno zároveň i nekonečno časové.

Extrapolujeme-li de Sitterův vesmír do daleké minulosti zjistíme, že je časově symetrický. Fázi rozpínání předchází fáze smršťování.[8] Podobné argumenty uvedené pro budoucí konformní nekonečno lze tak uvést i pro nekonečno minulé. V prostorovém směru je de Sitterův vesmír uzavřený – lze si ho představit jako třídimenzionální sféru S^3 s poloměrem měnícím se s časem t jako $\ell\,\mathrm{ch}(t/\ell)$. Metrika tak lze zapsat ve tvaru

$$\boldsymbol{g} = -\mathbf{d}t^2 + \ell^2\,\mathrm{ch}^2\frac{t}{\ell}\left(\mathbf{d}\chi^2 + \sin^2\chi\left(\mathbf{d}\vartheta^2 + \sin^2\vartheta\,\mathbf{d}\varphi^2\right)\right). \tag{1.11}$$

Zde $\ell = \sqrt{3/\Lambda}$ je typická délková škála de Sitterova vesmíru určující jeho poloměr v okamžiku přechodu z fáze smršťování do fáze rozpínání.

Je přirozené nakreslit konformní diagram řezu odpovídajícího historii osy. V každý časový okamžik je osa dána hlavní kružnicí de sitterovské sféry S^3. Historie osy (tj. její časový vývoj) je proto topologicky povrch válce. Konformním přeškálováním lze potlačit rozpínání de Sitterova vesmíru a smrsknout trvání celého vesmíru na konečný úsek konformního času. Přitom se však zachová kauzální povahu konformního nekonečna. Dvoudimenzionální konformní diagram má tak podobu části povrchu (vertikálně orientovaného) válce. Tato část je ohraničena dvěma (horizontálními) kružnicemi okolo válce, které reprezentují minulé a budoucí konformní nekonečno. Typicky se tento cylindr 'rozřízne' ve vertikálním směru a zobrazí v rovině jako obdélník, viz obr. 1.5. Poměr časového (vertikálního) rozměru a prostorového (horizontálního) rozměru je takový, že světelné paprsky vyslané v minulém nekonečnu z jednoho bodu všemi směry se v budoucím nekonečnu sejdou přesně v bodě protilehlém k bodu vyslání.

Třídimenzionální konformní diagram by měl mít geometrii $S^2 \times \mathbb{R}$. Bohužel, sekvence dvousfér 'naskládaných ve vertikálním směru' se již v euklidovské rovině špatně zobrazuje. Jedna z možností je dvousféru 'propíchnout' a roztáhnout na kruh (jehož obvod tak odpovídá jednomu bodu). Tyto kruhy již ve vertikálním směru naskládat lze. Konformní diagram třídimenzionálního řezu de Sitterova prostoročasu má pak podobu vnitřku válce mezi dvěmi horizontálními podstavami reprezentujícími minulé a budoucí konformní nekonečno. Tento diagram s podrobnou diskuzí lze nalézt v práci [1].

Vzhledem k tomu, že se de Sitterův vesmír rozpíná, pozorovatel, který se snaží zachovat od jiného volně se pohybujícího pozorovatele konstantní vzdálenost, se musí pohybovat se zrychlením kompenzujícím kosmologickou expanzi. Díky homogenitě vesmíru se ukazuje, že toto zrychlení musí být konstantní – jedná se o rovnoměrně urychleného pozorovatele. Více takto navzájem nepohybujících se pozorovatelů tvoří tzv. statický systém. Všichni tito pozorovatelé 'vstupují' do prostoročasu v jenom bodě minulého konformního nekonečna, pohybují se

[8] Poznamenejme, že kosmologická repulze způsobená kosmologickou konstantou určuje 'zrychlení' rozpínání vesmíru, tj. druhou derivaci jeho 'velikosti'. Zda se se vesmír smršťuje či rozpíná závisí na 'počátečních podmínkách' pro velikost vesmíru. De Sitterův vesmír odpovídá časově symetrické situaci, kdy smršťování přejde v rozpínání.

s konstantním zrychlením a 'opouštějí' prostoročas opět v jednom bodě budoucího konformního nekonečna. Dosáhnout nekonečna jim samozřejmě trvá nekonečný vlastní čas.

V rozsáhlém článku [10] zařazeném do této práce je vyčerpávajícím způsobem rozebraná struktura de Sitterova vesmíru, jeho popis v různých souřadnicích, popis rovnoměrně urychlených pozorovatelů v těchto souřadnicích a konečně různé podoby elektromagnetického a skalárního pole urychlených zdrojů. Práce obsahuje podrobnou charakteristiku souřadnic přizpůsobených urychleným pozorovatelům včetně detailních diagramů. Apendix práce [10] tvoří jakýsi slovník všech souřadnic a vztahů mezi nimi s vyobrazením souřadnicových čar v konformních diagramech.

Pole dvou rovnoměrně urychlených nábojů v de Sitterově vesmíru bylo již nalezeno v pracích [1, 2]. Jedná se o pole nábojů, vstupujících do prostoročasu v antipodálních pólech, pohybujících se proti sobě se stejným zrychlením tak, že zachovávají během celé své existence od svých pólů konstantní vzdálenost. Nalezené pole je (obdobně klasickému Bornovu řešení) analytické v celém prostoročase (samozřejmě mimo zdroje) a lze ho interpretovat jako kombinaci retardovaného působení od jednoho náboje a advancovaného působení od druhého náboje, případně jako vhodnou kombinaci obou těchto působení od obou nábojů (viz např. rov. (6.6) v [1]).

Nabízí se přirozeně otázka, zda nelze nalézt čistě retardované pole obou nábojů, tj. pole, které je nenulové pouze v kauzální budoucnosti světočar nábojů. Na rozdíl od Minkowského prostoročasu je odpověď pro elektrické náboje v de Sitterově vesmíru záporná: nelze zkonstruovat čistě retardované elektromagnetické pole bodových nábojů! Příčina je přitom poměrně jednoduchá a má obecnější platnost než jen pro de Sitterův vesmír. Jedna z Maxwellových rovnic totiž říká, že v jednom časovém řezu mohou siločáry elektrického pole začínat pouze na náboji nebo musejí ubíhat do nekonečna. Časový řez de Sitterova vesmíru však může být zvolen uzavřený (sféra S^3) a tak všechny siločáry musejí začínat a končit na náboji. To nám okamžitě dává globální vazbu na celkový náboj ve vesmíru: celkový elektricky náboj v libovolném prostorově uzavřeném vesmíru musí být nulový. Toto však ještě není omezení, který by vylučovalo existenci čistě retardovaného pole – v našem případě jsou zdrojem pole dva náboj stejné velikosti, ale opačného znaménka a globální omezení na náboj je tedy splněno.

V případě, že minulé konformní nekonečno je prostorupodobné (jak je tomu i v de Sitterově vesmíru) můžeme navíc zformulovat i lokální omezení na rozložení náboje čistě retardovaného pole. Jak bylo řečeno, čistě retardované pole je pole nenulové pouze v kauzální budoucnosti zdrojů. Mělo by být tedy identicky nulové v minulém nekonečnu. Pokud je toto nekonečno prostorupodobné, lze na něm aplikovat vazbu plynoucí z Maxwellových rovnic a zjišťujeme, že v minulém nekonečnu nemohou být přítomny náboje ani lokálně (nemáme žádné siločáry, které by z nich vycházely).

Jediná možnost, jak by se v takovém prostoročasu mohl vyskytovat náboj s čistě retardovaným polem je, že by v jednom bodě minulého nekonečna vstoupilo do prostoročasu více nábojů, jejichž celková hodnota by byla nulová. Příklady takových nábojových rozložení jsou diskutovány v práci [1].

Poznamenejme ještě, že pro skalární pole obdobná omezení neexistují – pro skalární pole lze nalézt čistě retardované pole i jediného náboje – viz diskuzi v [1].

Anti-de Sitterův vesmír

Obdobou de Sitterova vesmíru pro zápornou kosmologickou konstantu je anti-de Sitterův vesmír. V něm kosmologická konstanta působí opačně – můžeme tak mluvit o neustálé kosmologické *atrakci*. Situace je však trochu složitější – anti-de Sitterův vesmír můžeme zároveň popsat jako statický (v čase neměnný) prostoročas.

Zvolíme-li jednoho volného pozorovatele jako centrum vesmíru (je jedno kterého, protože všichni si jsou ekvivalentní), tento pozorovatel popíše anti-de Sitterův vesmír jako časovou sekvenci prostorů H^3 s Lobačevského geometrií. Zavedeme-li sférické souřadnice t, r, ϑ, φ, kde t je vlastní čas centrálního pozorovatele a r prostorová vzdálenost od centra, metrika anti-de Sitterova prostoru má tvar

$$\boldsymbol{g} = -\operatorname{ch}^2\frac{r}{\ell}\,\mathbf{d}t^2 + \mathbf{d}r^2 + \ell^2 \operatorname{sh}^2\frac{r}{\ell}\left(\mathbf{d}\vartheta^2 + \sin^2\vartheta\,\mathbf{d}\varphi^2\right), \tag{1.12}$$

kde $\ell = \sqrt{-3/\Lambda}$ je opět typická délková škála související s poloměrem křivosti prostoročasu. Vidíme, že časová 'vzdálenost' mezi po sobě jdoucími časovými řezy závisí na vzdálenosti od centrálního pozorovatele. Pozorovateli setrvávajícímu ve vzdálenosti r od centra běží hodiny $\operatorname{ch}(r/\ell)$-krát rychleji než pozorovateli v centru.

Dvoudimenzionální diagram odpovídající historii polopřímky vedoucí z počátku do nekonečna je zobrazen v obr. 1.6. Jsou zde zobrazeny dvě alternativy užívající různou kompaktifikaci. Diagram 1.6a užívá časově nezávislého přeškálování a nekompaktifikuje tak časový směr – konformní geometrie i nadále zůstává statická (mimochodem, jedná se o geometrii hemisféry Einsteinova vesmíru) a časový směr tak nadále ubíhá po nekonečný úsek konformního času. Tento diagram zobrazuje konformní nekonečno, do kterého ubíhají světelné (a i prostorupodobné) křivky, a věrně odráží statickou povahu prostoročasu, nezobrazuje však časové nekonečno kam směřují volní pozorovatelé. K jeho zobrazení je potřeba provést časově závislé konformní přeškálování, což vede k diagramu 1.6b. Odpovídající třídimenzionální diagramy se získají rotováním dvoudimenzionálních diagramů kolem počátku a lze je nalézt např. v práci [12], v obr. 13.

Přestože je metrika (1.12) časově neměnná, můžeme mluvit o kosmologické atrakci. Pozorovatelé, kteří chtějí zůstat konstantní vzdálenost od centra, se musí totiž pohybovat se zrychlením kompenzujícím tuto kosmologickou atrakci, tj. např. musí mít zapnuté raketové motory odpuzující ji od centra. Čím dále jsou od centra, tím větší zrychlení musí pozorovatelé vyvinout. Hodnota zrychlení se pro velmi vzdálené pozorovatele limitně blíží hodnotě $1/\ell$. Statičtí pozorovatelé jsou tedy podobně jako v de Sitterově vesmíru rovnoměrně urychleni, tentokrát však s horním omezením na velikost jejich zrychleni.

Než se zmíníme o rovnoměrně urychlených pozorovatelích s větším zrychlením, vraťme se ještě k pozorovatelům volným. Jakýkoli volný pozorovatel, který je v určitý okamžik vůči centrálnímu pozorovateli v klidu, se k němu začne díky kosmologické kontrakci vesmíru přibližovat, až kolem něj proletí, poté se začne zpomalovat, až se opět zastaví na opačné straně od centra. Tento proces se bude opakovat znovu a znovu – dva volní pozorovatelé pohybující se po společné ose tedy kolem sebe vlivem kosmologické atrakce oscilují. Alternativně, dva volní pozorovatelé, jejichž rychlosti nejsou ve směru jejich spojnice, budou kolem sebe obíhat. Můžeme říci, že kosmologická atrakce je kompenzovaná odstředivou silou.

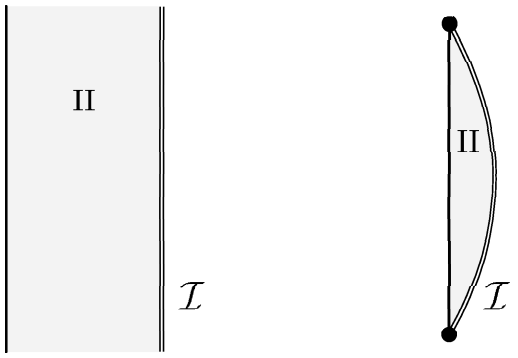

Obrázek 1.6: **Konformní diagramu anti-de Sitterova vesmíru.** Diagram znázorňuje radiální řez anti-de Sitterova vesmíru, konkrétně historii radiální polopřímky vedoucí z počátku do nekonečna. Levá hraniční linie je světočára pozorovatele v počátku. Dvojitá linie odpovídá konformnímu nekonečnu, které má časupodobný charakter. Nalevo je diagram získaný přeškálováním fyzikální metriky časově nezávislým faktorem, zůstává proto zachována 'nekonečnost' časového (vertikálního) směru. Diagram napravo využívá časově závislého škálování, které kompaktifikuje i časový směr.

Žádný volný pozorovatel se nemůže vymanit kosmologické atrakci, žádný podsvětelný pozorovatel bez zrychlení se od centrálního pozorovatele nevzdálí na nekonečnou vzdálenost. 'Únikovou rychlostí' do nekonečna je až rychlost světla: Jen signál pohybující se rychlostí světla či pozorovatel urychlující se k ní s dostatečně velkým zrychlením unikne až do konformního nekonečna. To má tentokrát *časupodobný* charakter (viz (1.5)). Na to, aby se podsvětelný pozorovatel do nekonečna vzdálil, musí se pohybovat alespoň nadkritickým zrychlením.

Příkladem jsou pozorovatelé pohybující se s rovnoměrným zrychlením větším než $1/\ell$. Ti překonají kosmologickou atrakci a jejich světočára vede až do konformního nekonečna. Jelikož je anti-de Sitterův vesmír symetrický vůči časové reverzi, pokud protáhneme jejich světočáru zpět v čase zjistíme, že z konformního nekonečna též přilétají. Jedná se tedy o pozorovatele, kteří vstupují do prostoročasu skrze časupodobné konformní nekonečno s nenulovou počáteční rychlostí směrem k centru, okamžitě však začnou brzdit svůj pohyb až se zastaví a začnou se vzdalovat až opět prostoročas opustí skrze konformní nekonečno. Pro každého z těchto pozorovatelů dosažení nekonečna samozřejmě trvá nekonečný vlastní čas. Avšak měřeno kosmologickým časem centrálního pozorovatele, celá existence takto urychlených pozorovatelů je omezena na konečný úsek $\Delta t = \pi\ell$. Zobrazení těchto pozorovatelů v třídimenzionálním konformním diagramu je možné nalézt na obr. 1.7.

Práce diskutující elektromagnetické a skalární pole rovnoměrně urychlených nábojů v anti-de Sitterově vesmíru, tj. zobecnění Bornova řešení pro $\Lambda < 0$, se připravuje. Diskuzi vlastností urychlených pozorovatelů a souřadnic s nimi spojených lze nalézt v části V práce [12]. V této práci se primárně diskutují pole urychlených černých děr. V limitě zanedbatelné hmotnosti a testovacího náboje však zkoumaný prostoročas přejde na anti-de Sitterův vesmír, černé díry se smrsknou na bodové náboje a elektromagnetické pole přejde na hledané zobecněné Bornovo

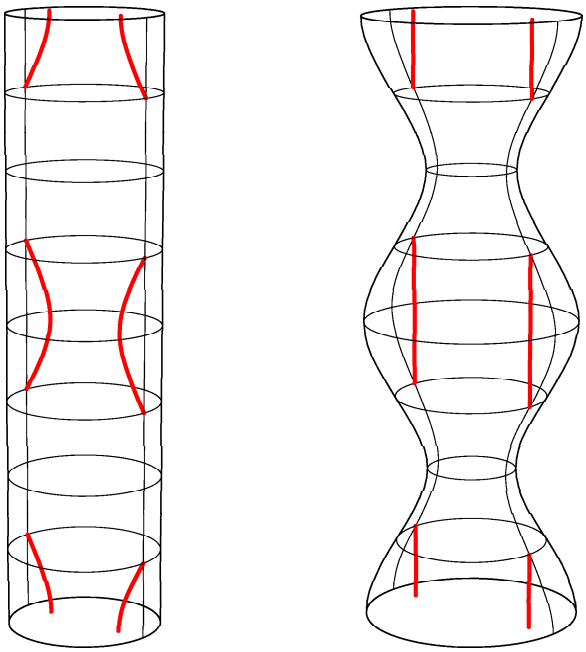

Obrázek 1.7: **Nadkriticky urychlení pozorovatelé v anti-de Sitteorvě vesmíru.** Pozorovatelé rovnoměrně urychlení se zrychlením větším než $1/\ell$ vstupují do prostoročasu skrze konformní nekonečno, zpomalují směrem k počátku až se zastaví a pak zrychlují zpět do nekonečna. Nalevo jsou světočáry těchto pozorovatelů znázorněny v třídimenzionálním diagramu získaném rotací diagramu z obr. 1.6. Napravo je tento diagram zdeformován tak, že světočáry urychlených pozorovatelů jsou znázorněný jako přímé linie. Toho lze dosáhnout vhodnou volnou konformního faktoru při kompaktifikaci. Tento diagram odpovídá analogickým diagramů pro nadkriticky urychlené černé díry v anti-de Sitterově vesmíru – viz podkapitolu 1.4.

řešení. Porovnání různých souřadnic a různých konformních diagramů diskutovaných v práci [12] (diagramů přizpůsobených jak statickým, tak urychleným pozorovatelům) lze též nalézt v digitální příloze.

1.3 Černé díry

Co jsou černé díry?

Jak jsme se již zmínili, černé díry souvisí se zásadní změnou kauzální struktury prostoročasu. Ukazuje se, že gravitační pole může být tak silné, že zamezí všem fyzikálním signálům (tj. veškeré hmotě, polím, pozorovatelům, ...) opustit jistou oblast prostoročasu.

Prostoročas s pouze slabým gravitačním polem (a nulovou kosmologickou konstantou) má globální kauzální strukturu podobnou Minkowského prostoročasu. Konformní nekonečno má stejnou topologii a v jistém smyslu i stejnou geometrii.[9] Každý pozorovatel může (v principu) existovat libovolně dlouhý vlastní čas

[9] Přesný význam těmto tvrzením dává pojem asymptotické plochosti, viz např. [29, 33].

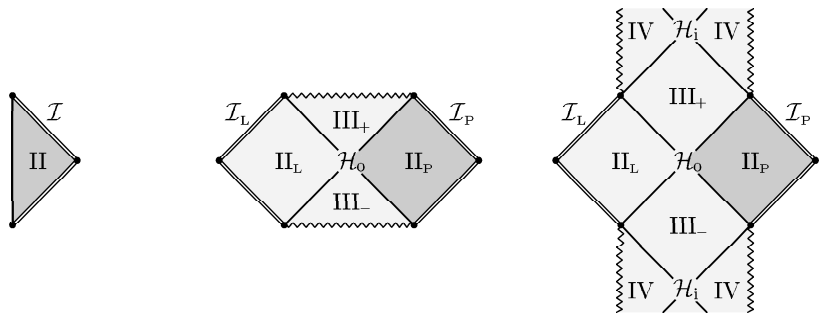

(a) (b) (c)

Obrázek 1.8: **Konformní diagramy statických černých děr.** Diagramy zobrazují radiální řez (a) prázdného Minkowského prostoročasu a maximálně rozšířeného (a) Schwarzschildova a (b) Reissnerova-Nordströmova prostoročasu. Ty reprezentují statickou nerotující nenabitou, respektive nabitou černou díru. Oblasti II odpovídají asymptoticky plochým oblastem, oblasti III a IV vnitřku černých/bílých děr. Dvojité čáry značí konformní nekonečno, zubatá čára singularity, diagonální čáry vnější (a případně vnitřní) horizonty černých děr. V případě nabité díry by měl diagram pokračovat skrze černou díru stejným způsobem jak do budoucnosti tak do minulosti.

a asymptoticky dosáhne buď časového nebo konformního nekonečna. V prostoročase se silným gravitačním polem se však může stát, že někteří pozorovatelé jsou zachyceni gravitačním polem a nekonečna dosáhnout nemohou.

Přesněji řečeno, vybereme-li maximální možnou souvislou komponentu budoucího konformního nekonečna a vezmeme-li její kauzální minulost $\mathcal{P}$ (všechny události, ze kterých se lze do tohoto nekonečna podsvětelnou či světelnou rychlostí dostat), nemusíme vždy dostat celý prostoročas. Pokud v prostoročasu existují i události nepatřící do $\mathcal{P}$, a přitom se do těchto událostí z $\mathcal{P}$ dá dostat, řekneme, že tyto události tvoří *černou díru* vzhledem k vybrané komponentě konformního nekonečna. Obdobným způsobem, ale opačně v čase – tj. pomocí doplňku k budoucnosti minulého nekonečna – definujeme *bílé díry*, oblasti, do kterých se fyzikální pozorovatel z vybraného nekonečna dostat nemůže. Pokud budeme mluvit společně o černých a bílých dírách, budeme je často pro jednoduchost označovat pouze jako černé díry.

Statická černá díra v asymptoticky plochém prostoročasu

Učebnicovými příklady [43,44] černé díry jsou prostoročasy popsané Schwarzschildovou a Reissnerovou-Nordströmovou metrikou. Jedná se o sféricky symetrické metriky řešící Einsteinovy gravitační rovnice ve vakuu respektive v přítomnosti sféricky symetrického elektromagnetického pole. Výše nastíněnou definici černé díry nejlépe dokumentují konformní diagramy radiálního směru těchto prostoročasů znázorněné na obr. 1.8. Poznamenejme, že je zde zobrazeno tzv. analytické rozšíření těchto metrik na maximální možný prostoročas, které nepopisuje astrofyzikálně realistickou situaci vzniku černé díry – o kolapsu vedoucímu k černé díře se zmíníme později.

Maximální rozšíření Schwarzschildovy metriky popisuje prostoročas, který má asymptoticky ploché nekonečno podobné nekonečnu Minkowského prostoročasu[10] (nekonečno $\mathcal{I}_{\mathrm{P}}$ ohraničující oblast II_{P} v obr. 1.8b; pro srovnání je na obr. 1.8a znázorněn diagram prázdného Minkowského prostoročasu). Uvnitř tohoto prostoročasu je však oblast III_{+} – černá díra, ze které se již do nekonečna $\mathcal{I}_{\mathrm{P}}$ nedá dostat. A to přesto, že z oblasti II_{P} se do této oblasti dostat dá. Analogicky je zde oblast III_{-} – bílá díra, do které se z nekonečna $\mathcal{I}_{\mathrm{P}}$ nedá dostat, přestože z bílé díry je možno do $\mathcal{I}_{\mathrm{P}}$ doletět. Pozoruhodné je, že metriku lze analyticky prodloužit i do jiné asymptoticky ploché oblasti II_{L}. Připomeňme, že diagramy na obr. 1.8 zobrazují radiální směr. Pravá polovina diagramu 1.8b (oblast II_{P}) zobrazuje historii polopřímky od díry do nekonečna v jedné asymptoticky ploché oblasti. Levá polovina (oblast II_{L}) reprezentuje historii radiální polopřímky v *zcela jiné* asymptotické oblasti. Obě asymptotické oblasti II_{L} a II_{P} jsou spojeny skrze černou a bílou díru tzv. Einsteinovým-Rosenovým mostem. Toto spojení je však *akauzální* v tom smyslu, že žádný pozorovatel či fyzikální signál nemůže proletět z jedné asymptotické oblasti do druhé.

Černá a bílá díra jsou od oblastí II_{L} a II_{P} oddělené *horizontem událostí* – nulovou nadplochou tvořenou paprsky, které jako poslední (chápáno z oblasti vně díry) mohou odletět do nekonečna (respektive – v případě bílé díry – jako první mohou z nekonečna přiletět).

Prostoročas nabité sféricky symetrické černé a bílé díry popsaný Reissnerovou-Nordströmovou metrikou se od Schwarzschildova prostoročasu z kauzálního hlediska vně děr příliš neliší. Zásadně se však odlišuje uvnitř děr. Co můžeme pod horizontem obou typů děr nalézt se zmíníme v následujícím oddíle. Nyní pouze konstatujme, že u nabité černé díry je možné touto dírou proletět do dalších asymptotických oblastí, které mají všechny obdobnou strukturu. Maximálně rozšířená Reissnerova-Nordströmova metrika tak popisuje prostoročas s nekonečně mnoha asymptoticky plochými oblastmi, které jsou vždy v páru spojeny Einsteinovým-Rosenovým mostem a tyto páry jsou propojeny mezi sebou skrze vnitřek černých/bílých děr. Pro více detailů viz např. [44]

Kauzální struktura libovolné asymptoticky ploché vnější oblasti (u Schwarzschildovy díry buď II_{L} nebo II_{P}, u nabité díry kterékoli z nekonečně mnoha vnějších oblastí II) je však stejná. Na jedné straně je oblast omezena horizontem oddělující ji od černé a bílé díry, na druhé straně konformním nekonečnem. Nás bude zajímat hlavně tato vnější oblast, jelikož právě její struktura se liší od struktury obdobných oblastí kolem *urychlených* černých děr, případně děr v prostoročasech s *nenulovou kosmologickou konstantou.*

Vybereme-li jednu takovou oblast, můžeme nakreslit její třídimenzionální konformní diagram. Jelikož se jedná o sféricky symetrické prostoročasy, takový diagram se dostane rotací části (např. oblasti II_{P}) dvoudimenzionálního diagramu. Výsledný diagram lze nalézt na obr. 1.9, jeho interaktivní verzi pak v digitální příloze. Zde se nachází také a animace 'otevírající' a 'zavírající' nekonečno a animace ukazující vnoření dvoudimenzionálních diagramů.[11]

[10] Poznamenejme, že asymptotická plochost se týká konformního nekonečna $\mathcal{I}$. Struktura prostorového nekonečna i_0 se u Schwarzschildova řešení (a stejně tak pro obecný asymptoticky plochý prostoročas) od struktury prostorového nekonečna Minkowského prostoru liší.

[11] Podrobněji 'ovládání' diagramů v digitální příloze popíšeme v příští podkapitole, v oddíle popisujícím zobrazení C-metriky s $\Lambda = 0$.

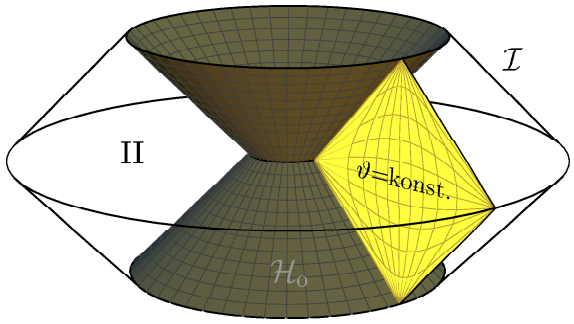

Obrázek 1.9: **Vnější oblast statické černé díry.** Diagram zobrazuje třídimenzionální radiální řez vnější oblasti prostoročasu okolo statické černé díry. Žlutá plocha odpovídá tmavě zvýrazněné oblasti II z obr. 1.8. Kónický povrch reprezentuje konformní nekonečno $\mathcal{I}$, tmavá plocha vnější horizont černé díry $\mathcal{H}_o$.

Co je uvnitř černých děr?

Než se dostaneme k hlavnímu tématu této kapitoly – zkoumání okolí urychlených černých děr – zmíníme se ještě o tom, jak vypadají černé díry uvnitř. Pro Schwarzschildovu a Reissnerovu-Nordströmovu metriku je charakter vnitřku černých děr dobře znám a popsán jak v odborné [43,44], tak populární literatuře (např. [45]). A ač je geometrie vnitřku urychlených děr odlišná, její kauzální aspekty zůstanou stejné. Proto nyní krátce připomeneme kauzální strukturu vnitřku statických černých děr a v případě urychlených děr se k ní již nebudeme vracet.

Pozorovatel, který se odhodlá vletět se svou kosmickou lodí dovnitř do (dostatečně velké) černé díry při průletu horizontem nebude cítit nic výjimečného – alespoň pokud se nedívá z okna lodě. Obraz jeho okolí by byl totiž již před průletem horizontem značně deformován gravitačním polem díry (zakřivením prostoročasu na škále velikosti horizontu díry). Ještě nad horizontem by mohl pozorovat větší část povrchu díry, než by očekával na základě zkušenosti z euklidovské geometrie; děje v blízkosti horizontu by mu připadaly zpomalené a barevně posunuté do červena; viděl by několikanásobné obrazy hvězd na druhé straně díry, atd. (ilustraci těchto jevů je možno nalézt např. v prezentaci [46]). Pokud by se však uzavřel do laboratoře uvnitř rakety, průlet horizontem by nedokázal lokálně detegovat – horizont jsme definovali jako hranici minulosti komponenty budoucího nekonečna, a jeho podoba tak závisí na celém dalším vývoji prostoročasu. Přesto by průlet horizontem měl pro další život pozorovatele zásadní vliv – zpoza horizontu se již nebude moci vrátit zpět do asymptotické oblasti, ze které vystartoval.

V případě nenabité černé díry pozorovateli za horizontem zbývá navíc již jen konečné množství času, než se přiblíží k singularitě, která se uvnitř černé díry skrývá. Jedná se o křivostní singularitu – oblast, kde křivost prostoročasu roste nade všechny meze (alespoň podle klasické obecné teorie relativity). To znamená, že při přibližování se k singularitě by pozorovatel začal pociťovat silnější a silnější slapové síly – nehomogenitu gravitačního působení, která by způsobovala, že by se v radiálním směru natahoval a v ostatních směrech smršťoval. Při dostatečném přiblížení k singularitě by toto působení bylo již tak silné, že by rozervalo

a rozmačkalo libovolně pevný materiál. Pádu do singularity uvnitř Schwarzschildovy černé díry se přitom nedá vyhnout. V diagramu 1.8b vidíme, že singularita (vyznačená zubatou čarou na horním okraji) leží 'v budoucnosti' pozorovatele, který vstoupil za horizont. Světočára libovolného pozorovatele či fyzikálního signálu musí směřovat do singularity. Singularita tak znamená pro vše uvnitř černé díry jakýsi 'konec času' – singularita má prostorupodobný charakter.

V případě nabité černé díry jsou vyhlídky pozorovatele, který se do ní vydá, mnohem zajímavější (alespoň v případě Reissnerovy-Nordströmovy černé díry, viz ale poznámku o realistických černých dírách v následujícím oddíle). Její konformní diagram je na obr. 1.8c. Vidíme, že singularita má zde časupodobný charakter a lze se jí vyhnout. Pozorovatel který se vydá na cestu skrze černou díru po průletu horizontem událostí $\mathcal{H}_{\mathrm{O}}$ (zde též nazývaným vnějším horizontem) již nemůže své rozhodnutí zvrátit a vrátit se zpět nad horizont. Může však zevnitř díry pozorovat celý další vývoj okolního světa. Za konečný časový úsek, kdy prolétá oblastí III_{+}, uvidí celou budoucí historii asymptotické oblasti, ze které se do díry dostal (a stejně tak i historii druhé asymptotické oblasti za Einsteinovým-Rosenovým mostem). Pozorovatel v černé díře 'přežije' celou existenci vnějšího vesmíru (která je ale pro vnějšího pozorovatele nekonečná) a poté, co obě vnější oblasti již přestanou existovat (tyto oblasti 'končí' konformním nekonečnem $\mathcal{I}_{\mathrm{L}}$ a $\mathcal{I}_{\mathrm{P}}$) 'odtrhne' se od nich v jakési časuprostorové bublině. V místě 'odtrhnutí' zbydou v bublině dvě křivostní singularity, v jejichž blízkosti opět působí velké slapové síly. Tentokrát se však lze těmto singularitám vyhnout. Naopak, tyto singularity může pozorovatel zkoumat. Uvidět je může po průletu tzv. *vnitřním horizontem* $\mathcal{H}_{\mathrm{i}}$. Při jeho průletu za krátký okamžik zahlédne i nekonečně dlouhé období prostoročasu vně černé díry. Za vnitřním horizontem, v oblasti IV je pozorovatel uzavřen v bublině o prostorové topologii $\mathbb{R} \times S^2$, kde na 'koncích' radiálního 'směru $\mathbb{R}$' leží právě zmíněné singularity. Ty však mají povahu objektu, ke kterému se sice není radno přibližovat, není však ani nevyhnutelné nutné se k němu přibližovat. Singularity tentokrát netvoří 'konec času', ale pouze uzavírají 'ze stran' bublinu, v které se pozorovatel nachází. Poté, co se pozorovatel 'nabažil' pohledu na singularity, dospěje k dalšímu vnitřnímu horizontu. Po jeho průchodu do oblasti III_{-} se již nemůže k singularitám přiblížit – ty se totiž dřív než k nim stačí doletět napojí na nové asymptoticky ploché oblasti typu II, do kterých se může dostat skrze vnější horizont $\mathcal{H}_{\mathrm{O}}$. Tentokrát se však v nové asymptotické oblasti vynoří z bílé díry, do které se žádný z vnějších pozorovatelů této oblasti nikdy nemůže dostat.

Tímto krátkým shrnutím známých faktů uzavřeme diskuzi statických černých děr. Zmíníme se však ještě krátce o tom, jak jsou tyto modely realistické z astrofyzikálního hlediska.

Existují černé díry?

Krátká odpověď je: „Ano, existují". Přesněji řečeno, máme průkazné evidence, že existují ve vesmíru objekty, které jinak než jako černé díry neumíme vysvětlit.

V první řadě poznamenejme, že realistické černé díry nebudou popsány maximálně rozšířeným prostoročasem, kterým jsme se zabývali výše. Tyto modely by spíše odpovídaly tzv. *primordiálním* černým dírám (černým dírám vzniklým

na počátku vesmíru), jejich množství a vůbec existence je však podle současných znalostí a pozorování jen těžko odhadnutelná. Realistické černé díry vznikají kolapsem hmotných těles a prostoročasy popisované výše žádnou hmotu neobsahují. Tyto prostoročasy však dobře popisují okolí vzniklé černé díry. Ukazuje se totiž, že závěrečné stádium gravitačního kolapsu libovolného dostatečně hmotného tělese vede k černé díře v podstatě vždy stejného typu – černé díry se od sebe mohou odlišovat pouze svojí velikostí (která je dána hmotností), nábojem a rotací. Přitom se neočekává, že by v astrofyzikálních situacích vznikaly podstatně nabité černé díry. Naopak většina děr bude mít určitou rotaci, kterou jsme v diskuzi výše pominuli.

Model realisticky kolabující hvězdy se tak v pozdních fázích bude vně hvězdy či vzniklé díry shodovat s prostoročasem popsaným výše, toto vnější řešení však musí být napojeno na vnitřní řešení v kterém hraje roli i kolabující hmota. Typicky toto vnitřní řešení odřízne Einsteinův-Rosenův most a prostoročas tak nebude obsahovat druhou asymptotickou oblast. Dále se očekává, že i kdyby kolabující objekt měl nenulový náboj, nevznikla by prostoročasová bublina vedoucí do dalších asymptotických oblastí. Jejímu vzniku by totiž zabránila hmota, která by se nakupila podél vnitřního černoděrového horizontu a prostoročas by zde 'odřízla' v jisté formě singularity. K nakupení hmoty podél vnitřního horizontu dojde z jednoduchého důvodu – jak jsme se zmínili, v jeho blízkosti by pozorovatel v konečném čase přehlédl nekonečnou historii vnějšího vesmíru. Čili i zanedbatelný tok záření z vnějšího vesmíru se podél horizontu zkoncentruje v divergující šokovou vlnu.

V současnosti se v našem vesmíru pozorují dva typy černých děr – černé díry vzniklé kolapsem jednotlivých hvězd a superhmotné černé díry v centrech galaxií. Stelární černé díry mají hmotnosti zhruba od 1,5 do 14 hmot našeho Slunce, přičemž černá díra vznikne z hvězdy, pokud je tato hvězda ve svém konečném stádiu cca třikrát hmotnější než Slunce. Nejdéle známou [47,48] stelární černou dírou je Cygnus X-1. Jedná se o binární systém jehož jedna složka je černá díra hmotnosti cca 10 Sluncí. Superhmotné černé díry mají hmotnosti miliónů až miliard hmot Slunce a nejbližší takovouto černou díru (a observačně nejlépe prokázanou) máme v centru naší galaxie [49].

A jak můžeme černou díru pozorovat, když ji nemůže nic uniknout? Velmi stručně řečeno, můžeme pozorovat její okolí a z jeho chování usoudit na přítomnost velmi hmotného a velmi kompaktního objektu, který neumíme vysvětlit jinak než jako černou díru.

Tímto uzavřeme stručný přehled obecných aspektů černých děr a ve zbytku kapitoly se budeme věnovat urychleným černým dírám popsaným tzv. C-metrikou.

1.4 C-metrika: urychlené černé díry

C-metrika

Vedle statických černých děr je známo také řešení Einsteinových gravitačních rovnic popisující rovnoměrně urychlené černé díry, tzv. *C-metrika*. Toto řešení bylo pro $\Lambda = 0$ nalezeno již v roce 1917 Levi-Civitou [21] a Weylem [22]. Pojmenováno bylo Ehlersem a Kundtem [50]. Fyzikální význam tohoto řešení jako pro-

storočasu s urychlenými černými dírami je ale podrobně analyzován až v pracích Kinnersleyho a Walkera [23], Ashtekara a Draye [24] a Bonnora [25]. V následujících letech byly zkoumány mnohé vlastnosti tohoto prostoročasu a metrika byla zobecněna pro případ rotujících černých děr a nenulové kosmologické konstanty. Přehled výsledků lze nalézt např. v pracích [51–54]; pro nedávné práce viz např. [55–57].

C-metrika patří do široké třídy tzv. *boost-rotačně symetrických řešení*, reprezentující asymptoticky ploché prostoročasy rovnoměrně urychlených zdrojů, která byla podrobně studována Bičákem a Schmidtem v [51]. Doposud však není známá analogie této třídy řešení pro případ nenulové kosmologické konstanty. Speciální případ C-metriky s $\Lambda \neq 0$ však znám je. Nabízí se tedy možnost, že by právě toto řešení mohlo být klíčem k nalezení obecné třídy asymptoticky (anti-)de sitteorovských prostoročasů rovnoměrně urychlených zdrojů. Toto byla jedna z motivací proč jsme v pracích [3, 5, 12] zkoumali vlastnosti právě C-metriky s $\Lambda \neq 0$.

Toto řešení bylo nalezeno v pracích [26–28] již v 70-tých letech. Až donedávna však nebyla provedena důkladná analýza jeho globálních vlastností. Pro případ $\Lambda > 0$ byla tato analýza provedena až v pracích [3, 58, 59] a pro případ $\Lambda < 0$ v [5, 12, 60, 61]. Různé degenerované a speciální případy byly diskutovány též v [62–65].

C-metrika s $\Lambda = 0$ a celá třída boost-rotačně symetrických řešení je zajímavá zejména proto, že se jedná o jediná explicitně známá řešení reprezentující zářivá gravitační pole netriviálně se pohybujících kompaktních zdrojů. Tyto prostoročasy hrály proto zásadní roli při zkoumání zářivých vlastností gravitačního pole. Je pro ně známa např. explicitní forma informační funkce gravitačního pole či Bondiho hmota [66–68]. Přehled výsledků týkajících se jejich zářivých vlastností je možné nalézt např. v [54, 69–71]. Povaha záření pro $\Lambda \neq 0$ není naproti tomu dobře uchopena dodnes a C-metrika s $\Lambda \neq 0$ je jeden z mála prostoročasů, kde můžeme zářivá pole v asymptoticky netriviálních prostoročasech explicitně zkoumat.

Třída boost-rotačně symetrických řešení je též populární v numerické relativitě, kde slouží jako testovací příklad pro funkčnost kódů numericky simulujících vývoj řešení Einsteinových rovnic; viz např. [72]. Velké využití nalezla C-metrika také v kvantové teorii kde se používá k analýze tvorby párů černých děr [73–76].

Motivováni důvody uvedenými výše jsme se v pracích [3, 5, 12] zabývali studiem globálních vlastností prostoročasů popsaných C-metrikou s $\Lambda \neq 0$ a diskuzí charakteru zde přítomného zářivého gravitačního a elektromagnetického pole. Výsledky týkající se globální struktury nyní krátce shrneme, diskusi vlastností záření ponecháme do příští kapitoly.

Ač se předkládané původní práce zabývají případem $\Lambda \neq 0$, pro úplnost a pro srovnání zmíníme i případ $\Lambda = 0$. Poznatky týkající této situace nejsou původní, nicméně níže prezentované třídimenzionální diagramy zobrazující urychlené černé díry v asymptoticky plochém prostoru jsou nové. Stejně tak všechny interaktivní diagramy a animace v digitální příloze jsou původní a prvně publikované v této práci.

Urychlené černé díry v Minkowského prostoročase

Řešení Einsteinových-Maxwellových rovnic nazývané C-metrika má tvar [23]:

$$\boldsymbol{g} = \omega^{-2}\left(-\mathcal{F}\,\mathbf{d}\tau^2 + \frac{1}{\mathcal{F}}\,\mathbf{d}\upsilon^2 + \frac{1}{\mathcal{G}}\,\mathbf{d}\xi^2 + \mathcal{G}\,\mathbf{d}\varphi^2\right), \tag{1.13}$$

$$\boldsymbol{F} = e\,\mathbf{d}\upsilon\wedge\mathbf{d}\tau\,, \tag{1.14}$$

kde metrické funkce $\mathcal{F}$ a $\mathcal{G}$ jsou polynomy čtvrtého stupně v υ a ξ

$$\begin{aligned} -\mathcal{F} &= 1-\upsilon^2+2mA\,\upsilon^3-e^2A^2\,\upsilon^4\,,\\ \mathcal{G} &= 1-\xi^2+2mA\,\xi^3-e^2A^2\,\xi^4\,,\\ \omega &= A\,(\upsilon-\xi)\,. \end{aligned} \tag{1.15}$$

(Odlišné, i když ekvivalentní tvary lze nalézt např. v [26, 55, 57].) Za jistých dodatečných předpokladů a při vhodném výběru definičního oboru souřadnic tato metrika reprezentuje dvě urychlené nabité černé díry pohybující se v asymptoticky plochém prostoročase. Parametry m, e, A charakterizují hmotnost, náboj a zrychlení černých děr. Vedle toho ještě máme parametr C charakterizující kónicitu osy symetrie, vstupující do definice prostoročasu skrze definiční interval souřadnice φ: $\varphi\in(-C\pi, C\pi)$. Aby metrika popisovala nabité černé díry, musí mít funkce $\mathcal{F}$ a $\mathcal{G}$ čtyři kořeny[12] (pro nenabitý případ $e=0$ kořeny tři) a musí být splněno $m, A, C>0$ a $m^2>e^2$. Souřadnice τ probíhá celé $\mathbb{R}$, souřadnice ξ musí ležet v intervalu kolem nuly, na kterém je $\mathcal{G}$ kladné, a souřadnice υ musí být z intervalu $\upsilon\in(-\xi,\infty)$.

Souřadnice $\tau, \upsilon, \xi, \varphi$ nepokrývají celý prostoročas hladce. Jak bude vidět níže, je potřeba použít několik kopií těchto souřadnic k pokrytí celého prostoročasu. Definiční interval souřadnice υ je potřeba rozdělit na čtyři části (tři v nenabitém případě) kořeny[13] $\upsilon_{\mathrm{i}}>\upsilon_{\mathrm{o}}>\upsilon_{\mathrm{a}}$ funkce $\mathcal{F}$. V prostoročasu těmto kořenům odpovídají tzv. *horizonty*. Mezi horizonty a mimo osu symetrie jsou souřadnice $\tau, \upsilon, \xi, \varphi$ hladké.

Význam souřadnic je následující: τ hraje roli časové souřadnice kolem černých děr, má však povahu rindlerovského času – vlastního času rovnoměrně urychlených pozorovatelů v Minkowského prostoročasu: na horizontech mění svojí povahu a stává se prostorovou souřadnicí. φ je úhlová souřadnice kolem osy symetrie. Obě tyto souřadnice odpovídají symetriím prostoročasu – geometrie se při posunu v jejich směru nemění. Prostoročas má tak dva Killingovy vektory $\boldsymbol{\partial}_\tau$ a $\boldsymbol{\partial}_\varphi$.

Souřadnice υ a ξ vně černých děr (oblast $\upsilon\in(\upsilon_{\mathrm{a}},\upsilon_{\mathrm{o}})$) mají povahu bipolárních souřadnic. υ je 'radiální' souřadnice běžící od jedné díry k druhé a ξ je úhlová souřadnice měřící zhruba 'kosinus úhlu' od osy symetrie měřeno z pohledu jedné či druhé černé díry, viz obr. 1.10. Hranice definičního intervalu $(\xi_{\mathrm{b}},\xi_{\mathrm{f}})$ souřadnice ξ odpovídají ose symetrie: $\xi=\xi_{\mathrm{b}}$ je osa spojující obě černé díry a $\xi=\xi_{\mathrm{f}}$ jsou části osy vedoucí z děr do nekonečna.

K tomu, abychom získali lepší představu o struktuře prostoročasu a jejích kauzálních aspektech, je potřeba zavést globální souřadnice. Standardním způsobem (viz [23, 34] nebo analogický postup v dodatku v [3]) lze nahradit souřadnice

[12] Poznamenejme, že $-\mathcal{F}$ a G jsou stejné polynomy pouze odlišné proměnné.

[13] Čtvrtý (záporný) kořen je na hranici definičního oboru υ.

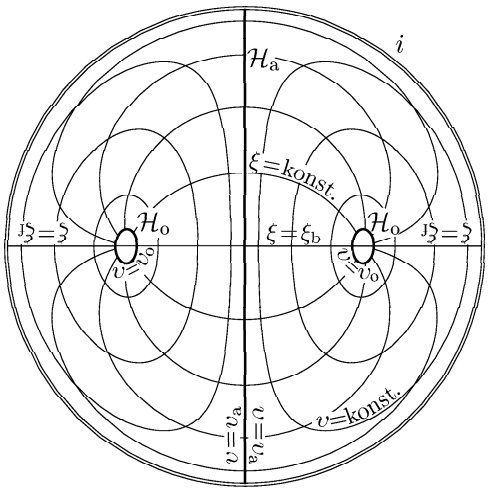

Obrázek 1.10: **Prostorový řez prostoročasem dvou urychlených černých děr.** Diagram znázorňuje souřadnice υ, ξ v prostorovém řezu $\tau, \varphi = \mathrm{konst.}$ skrze vnější oblasti černých děr prostoročasu C-metriky s $\Lambda = 0$. Souřadnice mají bipolární charakter – souřadnicové plochy $\upsilon = \mathrm{konst.}$ se nabalují kolem dvou 'center' tvořených vnějšími horizonty černých děr $\mathcal{H}_\mathrm{o}$ ($\upsilon = \upsilon_\mathrm{o}$), čáry měnícího se υ běží od jedné díry k druhé. Diagram zahrnuje dvě souřadnicové mapy, které jsou od sebe odděleny akceleračním horizontem $\mathcal{H}_\mathrm{a}$ ($\upsilon = \upsilon_\mathrm{a}$). Souřadnice ξ parametrizuje 'úhel' odklonu od osy z hlediska jedné či druhé černé díry. Dvojitá hraniční čára odpovídá prostorovému nekonečnu i.

τ, υ nulovými souřadnicemi u, v, které pokrývají prostoročas i přes horizonty. Typický konformní diagram 'radiálního' řezu $\xi, \varphi = \mathrm{konst.}$ je na obr. 1.11a. Souřadnice u, v v něm běží v diagonálních směrech a jejich souřadnicové čáry odpovídají trajektoriím světelných paprsků – určují tedy kauzální strukturu prostoročasu.

Diagram se rozpadá do bloků označených I, II, III, IV, které jsou odděleny horizonty $\mathcal{H}_\mathrm{i}$, $\mathcal{H}_\mathrm{o}$, $\mathcal{H}_\mathrm{a}$ ($\upsilon = \upsilon_\mathrm{i}, \upsilon_\mathrm{o}, \upsilon_\mathrm{a}$). Vnitřek černých/bílých děr má podobnou strukturu jakou jsme diskutovali v podkapitole 1.3, na obrázku odpovídá oblastem III (a v nabitém případě též IV). Singularita je opět vyznačena zubatou čarou a horizonty $\mathcal{H}_\mathrm{o}$ a $\mathcal{H}_\mathrm{i}$ odpovídají vnějšímu a vnitřnímu horizontu černých děr.

Vnější oblasti I a II jsou méně intuitivní – očekávali bychom, že vně děr bude mít prostoročas strukturu asymptoticky plochého prostoročasu s diagramem podobným obr. 1.3 či 1.8. Na obr. 1.11a však má konformní nekonečno (vyznačené dvojitou čárou) zdánlivě prosturopodobný charakter. Příčina neintuitivní podoby diagramu spočívá v tom, že řez $\xi, \varphi = \mathrm{konst.}$ neběží od černé díry do nekonečna (myšleno v prostorovém směru, tj. v nadploše $\tau = \mathrm{konst.}$), ale je napnut mezi dírami, viz obr. 1.10.

Jediná hodnota ξ, pro kterou tento řez běží z díry přímo do nekonečna, je vnější část osy symetrie $\xi = \xi_\mathrm{f}$. Vskutku, konformní diagram odpovídající tomuto řezu má jiný charakter, jak je vidět z obr. 1.11b. Vidíme, že se rozpadl na dvě části odpovídající vnějším osám jdoucím z jedné a z druhé díry. Každá z těchto částí již je analogická diagramům 1.8 pro statickou černou díru. Zobrazuje vnější oblast II, vnitřek díry III, resp. IV (pro nabité díry), a skrze každou z děr Einsteinův-Rosenův most do další asymptoticky ploché oblasti typu II.

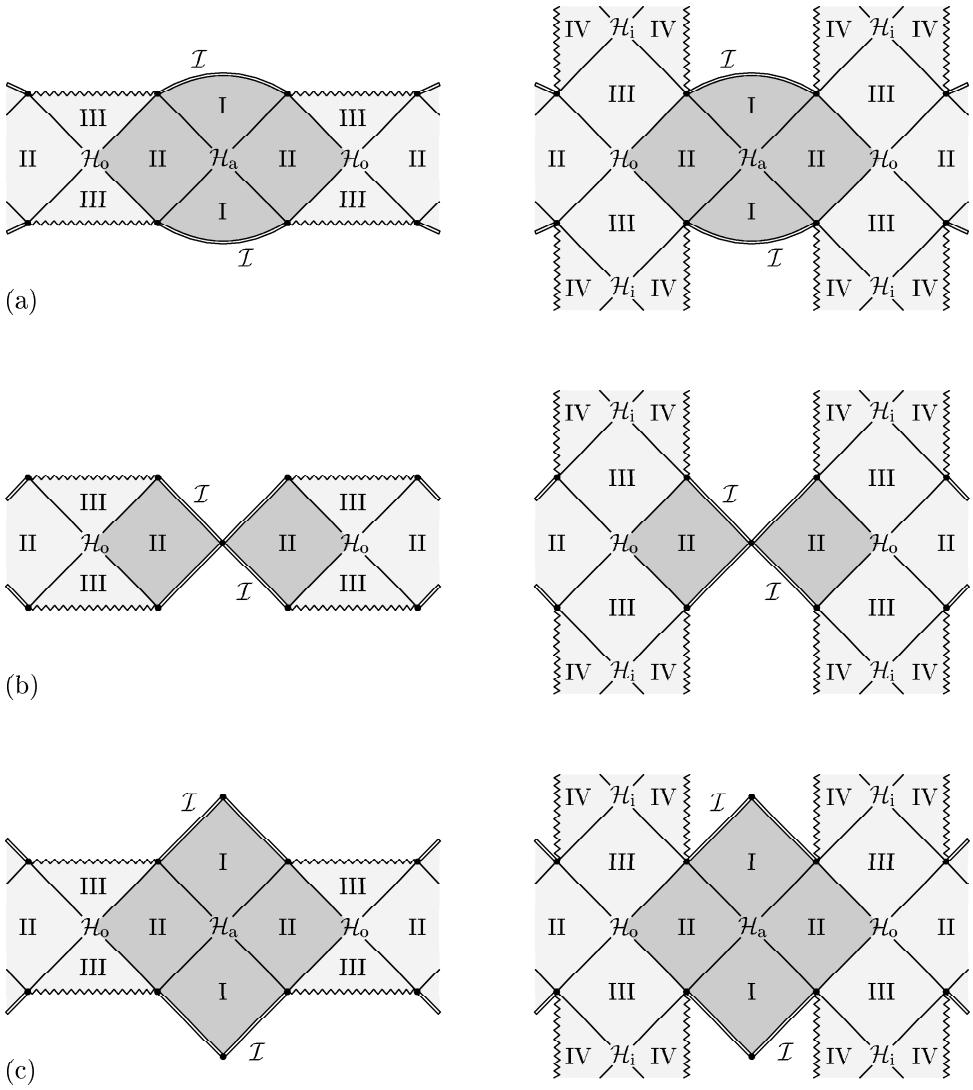

Obrázek 1.11: **Konformní diagramy prostoročasu C-metriky s $\Lambda = 0$.** Diagramy nalevo reprezentují prostoročas nenabité C-metriky, diagramy napravo prostoročas nabité C-metriky. Diagramy znázorňují řez $\xi, \varphi = \text{konst.}$ (a) pro obecnou hodnotu ξ, (b) pro $\xi = \xi_f$ odpovídající ose jdoucí od díry do nekonečna a (c) hodnotě $\xi = \xi_b$ odpovídající ose mezi dírami. Oblasti I, II leží vně děr, oblasti III a IV uvnitř a mají strukturu obdobnou struktuře statických děr, viz obr. 1.8. Konformní nekonečno je vyznačeno dvojitou čarou, singularity zubatou čarou a horizonty diagonálními liniemi mezi jednotlivými oblastmi. Různý charakter diagramů (a)–(c) souvisí se způsobem, jak jsou řezy $\xi = \text{konst.}$ vnořeny do prostoročasu – viz diskuzi v textu a obr. 1.12.

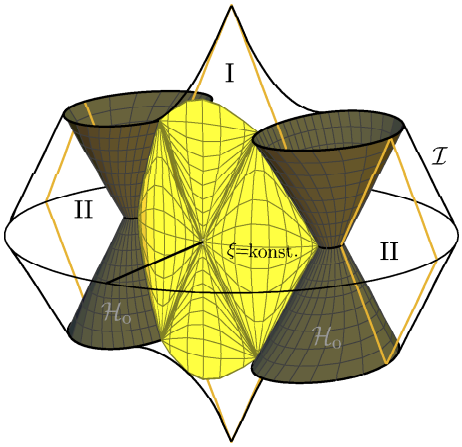

Obrázek 1.12: **Urychlené černé díry v asymptoticky plochém prostoročase.** Tento diagram 'slepuje' dvoudimenzionální diagramy z obr. 1.11. Zobrazena je pouze jedna vnější část černých děr (v obr. 1.11 vyznačena tmavě). Obalová plocha reprezentuje konformní nekonečno, tmavé kónické plochy vnější horizont černých děr. Žlutá plocha odpovídá typickému řezu $\xi = \text{konst.}$, tj. diagramu 1.11a. Speciální řezy 1.11b a 1.11c odpovídají vertikální rovině skrze díry.

Druhý speciální případ je osa mezi dírami $\xi = \xi_{\rm b}$. Konformní diagram je na obr. 1.11c. Zde vidíme, že obě díry jsou odděleny oblastmi II a I. Oblasti II odpovídají bezprostřednímu okolí černých děr. V těchto oblastech hraje souřadnice τ roli času pozorovatelů, kteří zůstavají v konstantní vzdálenosti od děr. Obě díry jsou však od sebe kauzálně odděleny *akceleračním horizontem* $\mathcal{H}_{\rm a}$ – nulovou plochou oddělující oblasti II od oblastí I. Žádný pozorovatel z jedné oblasti II nemůže kauzálním způsobem přeletět přes tento horizont do druhé oblasti II. Oblasti I pak zahrnují prostoročas od akceleračního horizontu do konformního nekonečna a vidíme, že na ose spojující obě díry má nekonečno $\mathcal{I}$ očividně nulový charakter – tyto části konformního diagramu se vskutku podobají diagramu Minkowského prostoročasu 1.3.

Zbývá vysvětlit konformní diagram 1.11a pro obecnou hodnotu ξ. Nejnázorněji to lze provést nakreslením třídimenzionálního diagramu potlačujícího pouze souřadnici φ. V obr. 1.12 je znázorněno, jakým způsobem je dvoudimenzionální diagram $\xi = \text{konst.}$ vnořen do diagramu třídimenzionálního. Tento diagram zobrazuje pouze vnějšek černých děr, konkrétně oblasti I a II zvýrazněné v diagramech 1.11. Dvě tmavé plochy v třídimenzionálním diagramu znázorňují vnější horizonty černých/bílých děr. Vnější hranice celého diagramu odpovídá konformnímu nekonečnu. Žlutá plocha pak odpovídá řezu $\xi = \text{konst.}$, tj. řezu dvoudimenzionálního diagramu z obr. 1.11a. Vidíme, že zdánlivě prostorupodobný charakter konformního nekonečna v diagramu 1.11a má původ v tom, že se jedná o průsečík konformního nekonečna nulové povahy s časupodobným řezem $\xi = \text{konst.}$.

Nakonec ještě proberme, proč mluvíme o *rovnoměrně urychlených* černých dírách. Pro bodovou testovací částici pohybující se v prostoročase je jednoduché definovat její čtyřzrychlení – v podstatě je dáno druhou derivací trajektorie z hlediska lokálně inerciálních pozorovatelů. Pro gravitující objekt jako je černá

díra to již tak jednoduché není. Gravitační působení totiž zakřivuje prostoročas a určuje, co to jsou lokálně inerciální pozorovatelé. Pohybující černé díry strhávají lokální inerciální systémy s sebou a nedá se tedy očekávat, že bychom vůči těmto systémů naměřili černým dírám zrychlení.

O zrychlení přesto mluvíme z několika důvodů. Boostová struktura Killingova vektoru $\boldsymbol{\partial}_\tau$ je typická pro analogický Killingův vektor spojený s rovnoměrně urychlenými pozorovateli v Minkowském prostoročase. Limita C-metriky pro zanedbatelné hmotnosti černých děr změní černé díry právě na takové rovnoměrně urychlené pozorovatele. Nadto geometrie horizontu děr není u C-metriky čistě sférická, horizont je zdeformován ve směru pohybu (podél osy φ symetrie). A v neposlední řadě, prostoročas C-metriky není čistě (elektro-)vakuový – obsahuje objekty, lokalizované na ose symetrie, které jsou příčinou pohybu černých děr. Geometrie C-metriky není totiž regulární na ose, obsahuje zde tzv. *kónickou singularitu* (podobnou singularitě povrchu kužele v jeho vrcholu). Taková singularita standardně popisuje lineární hmotný objekt zvaný *kosmická struna* [77]. Tato struna obecně vede podél celé osy, tj. z nekonečna do obou černých děr a je též stlačená mezi nimi. Volbou parametru kónicity C lze měnit napětí jednotlivých částí této struny, ale vždy tak, že úhrnný účinek struny na díry odpovídá síle tlačící díry od sebe do nekonečna. Vhodnou volbou C lze eliminovat strunu mezi dírami (díry jsou pak taženy strunami z nekonečna) nebo vně děr (díry jsou pak tlačeny stlačenou strunou mezi nimi). Nelze však zároveň eliminovat strunu na celé ose. (Existují ale zobecnění C-metriky, v nichž je struna nahrazena jiným 'urychlujícím faktorem' – např. dodatečným 'homogenním' elektrickým nebo gravitačním polem [78–80].)

Prezentace v digitální příloze

Kauzální struktura prostoročasu je zachycena také na obrázcích a animacích v digitální příloze. V tomto oddíle krátce popíšeme přístup k těmto materiálům. Obdobná 'navigace' platí i pro materiály týkající se prázdného Minkowského prostoročasu a černých děr v anti-de Sitterově vesmíru.

Z úvodní stránky týkající se C-metriky s $\Lambda = 0$ začněme volbou `[černé díry s horizontem kónického tvaru]`. Zobrazí se nám pohled na prostoročas 'zvenčí' (z pohledu pomocné konformní variety $\tilde{\mathcal{M}}$). Vidíme konformní nekonečno (tmavě modře), které je porušeno dvěma páry 'otvorů', které budou odpovídat černý dírám. Nekonečno má nulový charakter.

Volbou `[otevři nekonečno]` se lze podívat pod konformní nekonečno $\mathcal{I}$. Zobrazí se nám vnitřek prostoročasu s vyobrazeným akceleračním horizontem (světle modrý). Vidíme, že ten zcela 'zabaluje' oblast kolem černých děr a odděluje ji, s výjimkou čtyřech linií, od konformního nekonečna. Speciální linie, kde se akcelerační horizont dotýká konformního nekonečna, odpovídají směru os symetrie běžících od děr do nekonečna. Obrázek si lze prohlédnout z různých stran po kliknutí na `[interaktivní pohled]`. Tlačítko `[zavři nekonečno]` nás naopak vrátí k předchozímu zobrazení.

Nejdříve se však podíváme pod akcelerační horizont kliknutím na `[otevři horizont]`. Poté konečně uvidíme vnější horizonty dvou černých/bílých děr, každý tvořený párem kónických ploch. Vyznačeny jsou taky průsečíky osy symetrie s ho-

rizonty a s nekonečnem. Tlačítkem `[interaktivní pohled]` si opět můžeme díry prohlédnout z různých stran, tlačítkem `[zavři horizont]` se vrátíme k předchozímu zobrazení.

Kliknutím na tlačítko `[spusť` $\xi =$ `konst.]` spustíme animaci vnoření dvoudimenzionálních diagramů $\xi =$ konst. s měnícím se ξ. Napravo se nám zobrazí dvoudimenzionální diagram pro konkrétní ξ, nalevo jeho vnoření. Animaci zastavíme buď tlačítkem `[zastav]` nebo výběrem řezu `[0]` či `[`π`]`. V druhém případě si vnoření diagramů $\xi =$ konst. můžeme prohlédnout krok po kroku. Mezi jednotlivými hodnotami ξ se pohybujeme pomocí šipek. Zpět k zobrazení pouze horizontů děr se dostaneme pomocí tlačítka `[vnější horizonty]`.

Pokud se přepneme do módu interaktivního pohledu, můžeme obrázkem otáčet pomocí myši, případně ho přibližovat a vzdalovat. Zpět se dostaneme pomocí volby `[statický pohled]`.

Všechny diagramy si lze též prohlédnout v alternativní podobě po přepnutí pomocí `[zmáčkni horizonty]`. Tento alternativní pohled zdeformuje vnější horizont černých děr do 'kapkovitého' tvaru. Toto zobrazení je výhodnější při zkoumání limity zanedbatelných hmotností černých děr. V této limitě se prostoročas C-metriky redukuje na plochý Minkowského prostoročas a z černých děr zbydou pouze světočáry bodových částic. Evidentně, zobrazení pomocí kapkovitých horizontů přechází při smrsknutí horizontů v přímku na analogický diagram Minkowského prostoročasu (viz část prezentace týkající se prázdného Minkowského prostoročasu). Zpět k zobrazení pomocí kónických horizontů se dostaneme kliknutím na `[roztáhni horizonty]`.

Urychlené černé díry v de Sitterově prostoročase

C-metrika řešící Einsteinovy-Maxwellovy rovnice s kladnou kosmologickou konstantou má stejný tvar (1.13) (a tenzor elektromagnetického pole je opět dán rovnicí (1.14)), liší se však metrické funkce $\mathcal{F}$, $\mathcal{G}$ a ω:

$$\begin{aligned} -\mathcal{F} &= 1 - v^2 + \operatorname{ch}\alpha_{\mathrm{o}}\,\frac{2m}{\ell}\,v^3 - \operatorname{ch}^2\!\alpha_{\mathrm{o}}\,\frac{e^2}{\ell^2}\,v^4\,, \\ \mathcal{G} &= 1 - \xi^2 + \operatorname{sh}\alpha_{\mathrm{o}}\,\frac{2m}{\ell}\,\xi^3 - \operatorname{sh}^2\!\alpha_{\mathrm{o}}\,\frac{e^2}{\ell^2}\,\xi^4\,, \\ \omega &= \ell^{-1}\big(-v\cosh\alpha_{\mathrm{o}} + \xi\sinh\alpha_{\mathrm{o}}\big)\,, \end{aligned} \tag{1.16}$$

srovnej s (1.15). Podrobná diskuse tohoto řešení je obsažena v přiložené práci [3], zejména v kapitolách II, III a v dodatcích A–C. Níže shrneme pouze nejobecnější fakta.

Parametry m, e a C opět charakterizují hmotnost, náboj a kónicitu. Zrychlení A je tentokrát parametrizováno konstantou α_{o}:

$$A = \ell^{-1}\sinh\alpha_{\mathrm{o}}\,. \tag{1.17}$$

Kosmologická konstanta je skryta v délkové škále ℓ:

$$\ell = \sqrt{\frac{3}{\Lambda}}\,. \tag{1.18}$$

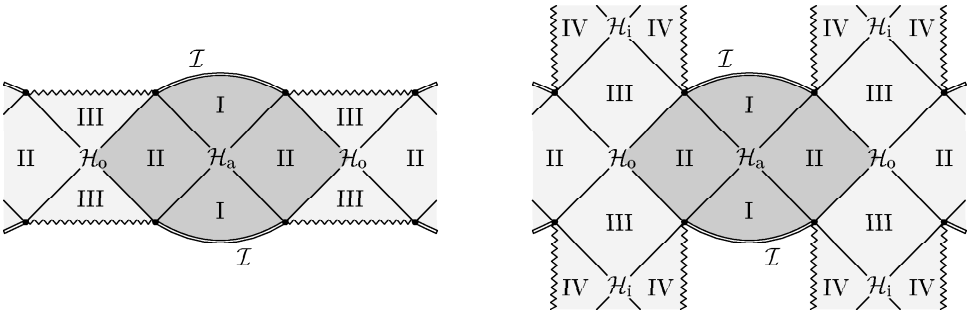

Obrázek 1.13: **Konformní diagramy prostoročasu urychlených černých děr s $\Lambda > 0$.** Konformní diagram řezu $\xi = \text{konst.}$ pro nenabitou (nalevo) a nabitou (napravo) C-metriku. Konformní nekonečno, singularity a horizonty jsou opět vyznačeny dvojitými, zubatými, respektive diagonálními čarami. Konformní nekonečno $\mathcal{I}$ má prostorupodobný de sitterovský charakter. Diagram je centrován na urychlené černé díry, což má za důsledek, že pro různé hodnoty ξ bude nekonečno různě 'prohnuté'.

Význam souřadnic $\tau, \upsilon, \xi, \varphi$ je obdobný případu $\Lambda = 0$ diskutovanému výše. Metrika opět popisuje dvě urychlené černé díry, tentokrát se však tyto díry pohybují v asymptoticky de Sitterově prostoročasu. Globální struktura je zachycena na dvoudimenzionálních diagramech na obr. 1.13. Jedná se o řezy $\xi, \varphi = \text{konst.}$ napnuté mezi černými dírami. Tentokrát mají diagramy pro všechny hodnoty ξ stejný charakter. Pro různá ξ se liší pouze různým 'prohnutím' konformního nekonečna (viz diskuse na str. 7 práce [3]). Prostorupodobný charakter nekonečna v dvoudimenzionálních diagramech odpovídá skutečnému charakteru konformního nekonečna.

Prostoročas vně děr (oblasti I a II) si můžeme představit jako de sitterovskou třísféru, která se nejdříve smršťuje a později roztahuje (viz diskuzi de Sitterova vesmíru v podkapitole 1.2). Na počátku, v minulém nekonečnu $\mathcal{I}^-$, do ní však v antipodálních pólech vstoupí dvě bílé díry, které během vývoje přejdou na černé díry a v budoucím nekonečnu opět opustí prostoročas v antipodálních pólech. Černé díry však nejsou během svého vývoje lokalizovány na pólech, naopak udržují se v nesymetrické pozici – vágně řečeno, v 'konstantní vzdálenosti' od pólů. Vybaveni intuicí o rovnoměrně urychlených pozorovatelích v de Sitterově prostoročase (podkapitola 1.2) řekneme, že se díry pohybují se zrychlením, které kompenzuje kosmologickou repulzi vesmíru a udržuje je v jejich nesymetrické pozici. Pouze v daleké minulosti a budoucnosti se odchylka děr od pólů stírá a proto jsme konstatovali, že díry vstupují a opouštějí prostoročas v antipodálních pólech. Použité souřadnice τ, υ, ξ, φ jsou však 'centrované' na obě díry. Při změně ξ (směru, ve kterém řez diagramu z děr vychází) se proto poloha děr nemění. Nesymetrická pozice děr se však projeví již zmíněnou změnou 'prohnutí' nekonečna.

Původcem zrychlení děr a jejich nesymetrické pozice je opět kosmická struna. Ta je napnutá na delší části osy symetrie, případně stlačená na její kratší části. (Tentokrát má osa pouze dvě části a obě dvě jsou napnuty mezi dírami. Struna

tedy nemůže ubíhat do prostorového nekonečna, jak tomu bylo v asymptoticky plochém prostoročase, protože žádné takové nekonečno v de Sitterově vesmíru není – prostoročas je vně děr prostorově uzavřený.)

Pokud položíme zrychlení rovno nule, působení struny z obou stran díry se vyrovná (případně struna zcela vymizí) a prostoročas popsaný C-metrikou se redukuje na prostoročas dvou statických černých děr v de Sitterově vesmíru umístěných v antipodálních pólech prostorového řezu.

Podkriticky urychlené díry v anti-de Sitterově prostoročase

Prostoročasy obsahující černé díry popsané C-metrikou s negativní kosmologickou konstantou se rozpadají do tří typů podle velikosti zrychlení děr. Pro podkritické zrychlení $A < 1/\ell$ prostoročas reprezentuje jednu urychlenou černou díru, pro kritické zrychlení $A = 1/\ell$ sekvenci urychlených černých děr vstupujících a opouštějících jednotlivě asymptoticky anti-de Sitterův vesmír, a konečně pro nadkritické zrychlení $A > 1/\ell$ popisuje sekvenci párů urychlených černých děr. Podkritický a nadkritický případ byl analyzován v pracích [5, 12], obdobná diskuse kritického případu se připravuje.

Pro $\Lambda < 0$ a $A < 1/\ell$, kde tentokrát

$$\ell = \sqrt{-\frac{3}{\Lambda}}\,, \tag{1.19}$$

lze C-metriku zapsat opět ve formě (1.13) s metrickými funkcemi $\mathcal{F}$, $\mathcal{G}$, ω danými [12]:

$$\begin{aligned} -\mathcal{F} &= -1 - v^2 + 2\,\frac{m}{\ell}\,\cos\chi_{\mathrm{o}}\,v^3 - \frac{e^2}{\ell^2}\,\cos^2\chi_{\mathrm{o}}\,v^4\,, \\ \mathcal{G} &= 1 - \xi^2 + 2\,\frac{m}{\ell}\,\sin\chi_{\mathrm{o}}\,\xi^3 - \frac{e^2}{\ell^2}\,\sin^2\chi_{\mathrm{o}}\,\xi^4\,, \\ \omega &= \ell^{-1}\big(v\,\cos\chi_{\mathrm{o}} - \xi\,\sin\chi_{\mathrm{o}}\big)\,. \end{aligned} \tag{1.20}$$

Zrychlení A je parametrizováno konstantou χ_{o}:

$$A = \frac{1}{\ell}\,\sin\chi_{\mathrm{o}}\,. \tag{1.21}$$

Význam ostatních parametrů zůstává stejný. Funkce $\mathcal{F}$ má však jen dva kořeny (dva kořeny v nabitém případě a pouze jeden kořen pro $e = 0$). Ty odpovídají vnějšímu a vnitřnímu horizontu díry. Akcelerační horizont v tomto případě neexistuje.

Struktura prostoročasu se nejvíce podobá struktuře jedné statické černé díry v asymptoticky plochém vesmíru s tím rozdílem, že konformní nekonečno má časupodobný charakter. Vskutku, pokud porovnáme konformní diagramy řezů $\xi = \mathrm{konst.}$ na obr. 1.14 s diagramy 1.8, vidíme odlišnost pouze v tvaru konformního nekonečna. Pro nulové zrychlení, $\chi_{\mathrm{o}} = 0$, je tato analogie přesná – jedná se o statickou sféricky symetrickou černou díru v anti-de Sitterově vesmíru. Pro nenulové zrychlení však není černá díra v prostoročase umístěna symetricky. Na ose je struna, která drží černou díru v nesymetrické pozici. Mluvíme proto opět

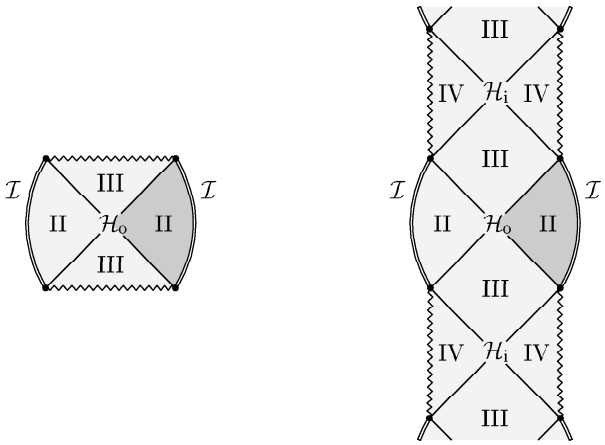

Obrázek 1.14: **Konformní diagram podkriticky urychlené černé díry v anti-de Sitterově vesmíru.** Nalevo je znázorněn nenabitý, napravo nabitý případ. Diagram zobrazuje řez $\xi, \varphi = \text{konst.}$. Značení je stejné jako v obrázcích obr. 1.11 a 1.13. Diagram je centrován na urychlenou černou díru, která je vůči anti-de sitterovskému nekonečnu situována nesymetricky. To se projeví různým 'prohnutím' konformního nekonečna pro různé hodnoty ξ – srovnej s třídimenzionálním diagramem 1.15.

o urychlené černé díře, přičemž její zrychlení kompenzuje kosmologickou atrakci a udržuje tak díru *statickou*.

Tato skutečnost je poměrně překvapivá. Speciálně je zvláštní, že prostoročas je statický *všude* vně děr. V případě $\Lambda \geq 0$ jsme vně urychlených děr měli také statický Killingův vektor, ten však na akceleračním horizontu měnil svoji povahu na prostorupodobný vektor. To je považováno za známku toho, že pole je dynamické, že se jedná o pole, u kterého lze očekávat zářivou složku. U podkriticky urychlené černé díry v anti-de Sitterově vesmíru však žádný akcelerační horizont nenajdeme a prostoročas vně díry je statický všude. Dynamická povaha urychleného zdroje je zde kompenzovaná kosmologickou atrakcí vesmíru. Je na místě se tedy ptát, zda je pole této díry zářivé. Odpověď je nejasná, protože prozatím neexistuje ucelená teorie gravitačního záření v prostoročasech s časupodobným konformním nekonečnem. K této otázce se ještě vrátíme v příští kapitole.

Lepší intuici pro globální kauzální strukturu nám dá třídimenzionální diagram zkoumaného prostoročasu vyobrazený na obr. 1.15a. Zde je zobrazena jedna oblast II vně černé díry (prostoročas má opět více vnějších oblastí propojených – i když ne vždy kauzálně – skrze černou díru). Upozorněme, že stejně jako v případě $\Lambda > 0$ používáme souřadnice centrované na díru. Proto horizont díry v obr. 1.15 má symetrický tvar, kdežto konformní nekonečno je deformováno. To je projev nesymetrické polohy díry způsobené jejím zrychlením. Kdybychom přizpůsobili obrázek asymptotickým pozorovatelům (nakreslili bychom konformní nekonečno symetricky), deformovaná by byla naopak černá díra.[14]

Alternativně můžeme prostoročas zobrazit s černoděrovým horizontem zdeformovaným do kapkovitého tvaru. Tato podoba je opět vhodná pro zkoumání

[14] Viz též analogickou diskuzi s diagramy týkající se podkriticky urychlených bodových zdrojů v kapitole V.A práce [12].

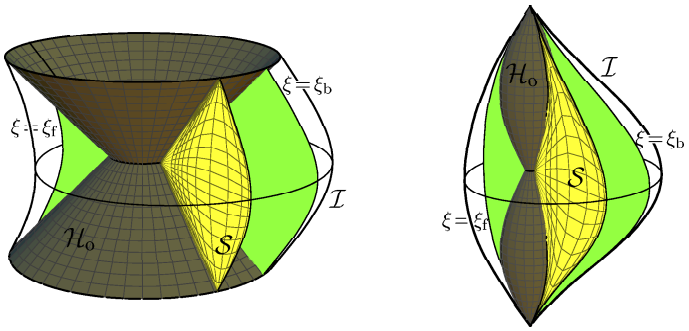

(a) (b)

Obrázek 1.15: **Podkriticky urychlená černá díra v anti-de Sitterově vesmíru.** Diagram zobrazuje oblast okolo černé díry odpovídající tmavě vyznačené oblast II v obr. 1.14. Obalová plocha reprezentuje konformní nekonečno, tmavá plocha vnější horizont díry. Konformní nekonečno je nesymetrické, jelikož diagram využívá souřadnic centrovaných na urychlenou černou díru. Horizont je znázorněn (a) jako kónická plocha, což odpovídá jeho kauzálnímu charakter – jedná se o nulovou plochu generovanou světelnými paprsky, nebo (b) zdeformován jako kapkovitá plocha – což je výhodnější při zkoumání limity malé hmotnosti, kdy černá díra přejde na bodovou částici.

limity slabých polí, kdy černá díra přechází na světočáru bodové částice. Vskutku, diagram 1.15b přejde na konformní diagram prázdného anti-de Sitterova vesmíru (srovnej s obr. 13b z práce [12]) získaný kompaktifikací pomocí časově proměnného konformního fakturu (viz diskuze z podkapitoly 1.2).

Třídimenzionální podobu prostoročasu si lze prohlédnout také v digitální příloze. Ovládáni je obdobné případu popsanému výše. Pouze se zde vzhledem k absenci akceleračního horizontu nevyskytují příslušné ovládací prvky.

Detailně je diskutovaný prostoročas popsán v kapitole III práce [12], případně v kapitole II.A práce [5].

Nadkriticky urychlené díry v anti-de Sitterově prostoročase

Pro nadkritické zrychlení $A > 1/\ell$ je metrika při $\Lambda < 0$ dána formou (1.13) s metrickými funkcemi

$$\begin{aligned} -\mathcal{F} &= 1 - v^2 + 2\,\frac{m}{\ell}\,\mathrm{sh}\,\alpha_\mathrm{o}\,v^3 - \frac{e^2}{\ell^2}\,\mathrm{sh}^2\,\alpha_\mathrm{o}\,v^4\,, \\ \mathcal{G} &= 1 - \xi^2 + 2\,\frac{m}{\ell}\,\mathrm{ch}\,\alpha_\mathrm{o}\,\xi^3 - \frac{e^2}{\ell^2}\,\mathrm{ch}^2\,\alpha_\mathrm{o}\,\xi^4\,, \\ \omega &= \ell^{-1}\big(v\,\mathrm{sh}\,\alpha_\mathrm{o} - \xi\,\mathrm{ch}\,\alpha_\mathrm{o}\big)\,, \end{aligned} \tag{1.22}$$

se zrychlením A daným

$$A = \frac{1}{\ell}\cosh\alpha_\mathrm{o}\,. \tag{1.23}$$

Význam ostatních parametrů zůstává stejný. Souřadnice mají význam obdobný případu páru urychlených černých děr v Minkowského prostoročasu. Definiční

intervaly souřadnic, podmínky kladené na parametry a podrobná diskuse vlastností prostoročasu jsou obsaženy v přiložených pracích [5] (kapitola II.B) a [12] (kapitola IV).

Globální struktura prostoročasu je v tomto případě složitější, jak napovídá rozmanitost a komplexita konformních diagramů na obr. 1.16. Lepší intuici je možné získat z třídimenzionálního diagramu 1.17a. Vidíme zde asymptoticky anti-de Sitterův prostoročas, do jehož časupodobného nekonečna vstupují a později z něho vystupují páry černých děr. V oblasti kolem jednoho páru černých děr se prostoročas podobá obdobné situaci v Minkowského prostoru – díry začínají a končí v konformním nekonečnu a jsou od sebe odděleny akceleračním horizontem (v obrázku vyobrazený modře). Nyní však má nekonečno časupodobnou povahu. Navíc, oblast I nad akceleračním horizontem není uzavřena konformním nekonečnem, nýbrž prostoročas zde pokračuje k tzv. *kosmologickému horizontu.*[15] Jím se dostaneme do oblastí O velice podobným prázdnému anti-de Sitterovu vesmíru bez černých děr. Po této 'čistě kosmologické' fázi proletíme opět kosmologickým horizontem do oblasti I, kde do prostoročasu vstoupí další pár černých děr. Obdobným způsobem se situace opakuje znovu a znovu.

V tomto případě je velice názorné připojit i zobrazení s černoděrovými horizonty deformovanými do kapkovitého tvaru (obr. 1.17b). Konformní nekonečno se zde více podobá mírně 'pomačkanému' nekonečnu prázdného anti-de Sitterova vesmíru – viz obr. 13a práce [12]. 'Pomačkání' souvisí opět s tím, že užíváme souřadnice centrované na dírách. Deformace nekonečna tak indikuje urychlený pohyb děr vzhledem k nekonečnu.[16]

Vnoření různých dvoudimenzionálních diagramů z obr. 1.16, jejichž podoba i kvalitativně závisí na konkrétních hodnotách souřadnice ξ, je podrobně diskutována v kapitole IV práce [12] – viz zejména obrázky 8–10, případně také obr. 4–6 v práci [5]. Všechny tyto diagramy jsou také zpracované v digitální příloze způsobem obdobným předchozím případům.

[15] V tomto případě se uplatňují všechny kořeny metrické funkce $\mathcal{F}$.

[16] Viz též související diskuzi týkající se souřadnic urychlených pozorovatelů v anti-de Sitterově vesmíru v kapitole V.B práce [12].

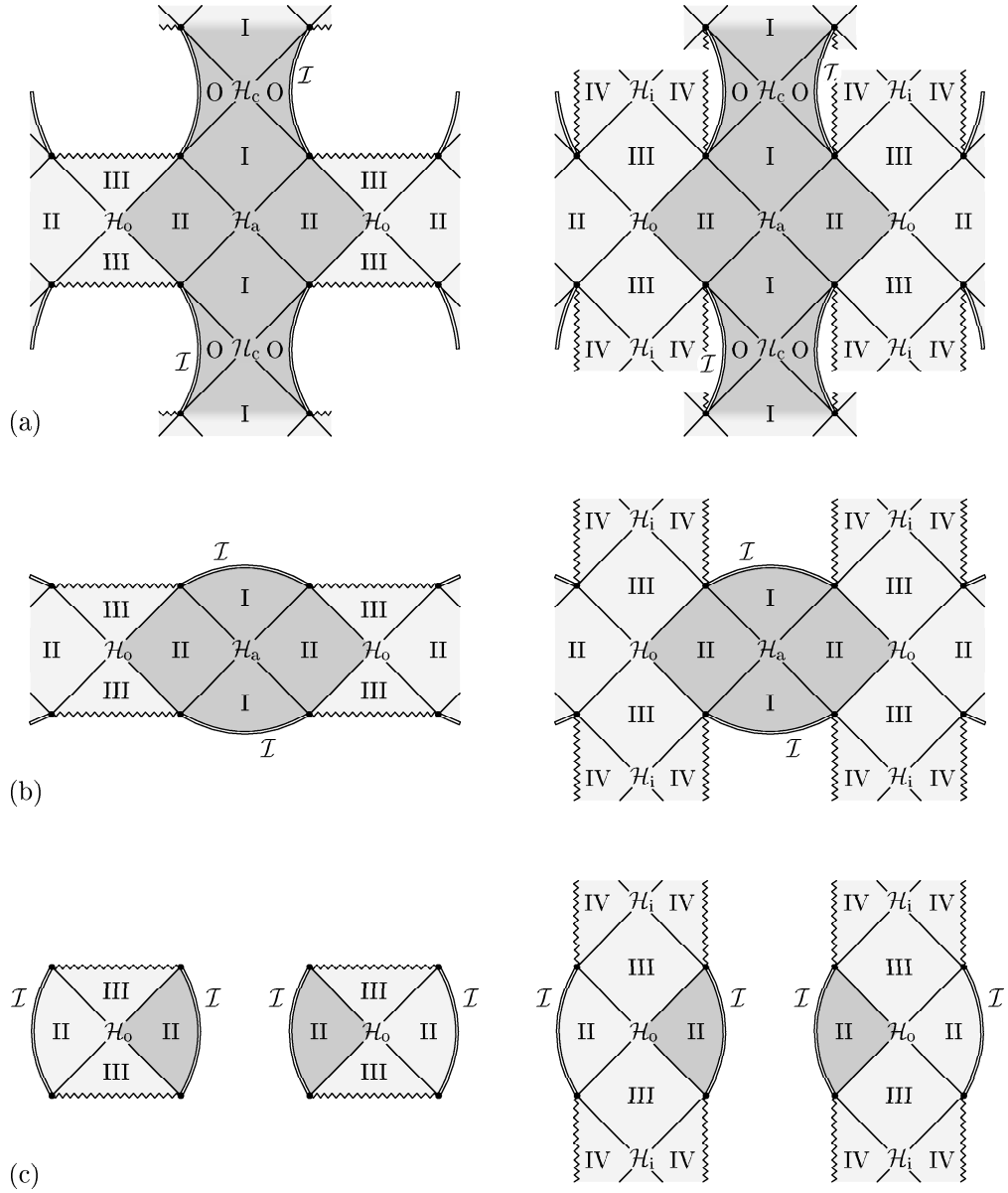

Obrázek 1.16: **Konformní diagramy nadkriticky urychlených děr v anti-de Sitterově vesmíru.** Diagramy nalevo odpovídají nenabitému, diagramy napravo nabitému případu. Značení je stejné jako v obrázcích 1.11, 1.13. Diagramy zobrazují řez $\xi, \varphi = \text{konst.}$. Případ (a) odpovídá řezu v blízkosti osy spojující díry, případ (c) řezu v blízkosti os jdoucích z děr do nekonečna. Vnoření jednotlivých řezů do třídimenzionálního diagramu je zobrazeno v práci [12].

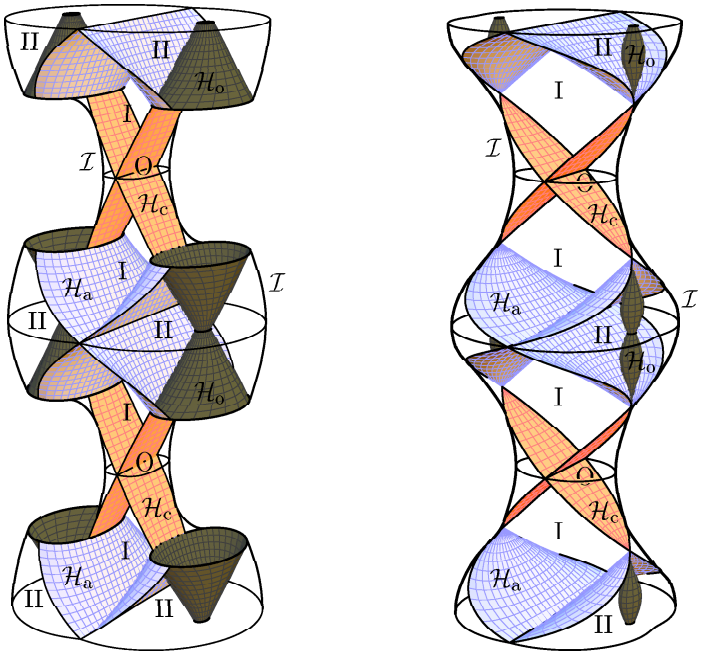

Obrázek 1.17: **Nadkriticky urychlené černé díry v anti-de Sitterově vesmíru.** V diagramu je znázorněna pouze vnější oblast černých děr. Tmavé plochy reprezentují horizont černých děr, obalová plocha konformní nekonečno. Prostoročas v jedné fázi neobsahuje žádné černé díry, ty do něho vstupují v páru časupodobným nekonečnem, pohybují se zpomaleně k sobě až se zastaví a poté odletí od sebe zpět do nekonečna, kde prostoročas opustí. Následuje opět fáze bez černých děr, po které vstoupí do prostoročasu další pár děr. Zobrazení (a) se snaží respektovat kauzální charakter horizontu černých děr a zobrazuje ho jako kónickou plochu připomínající světelný kužel. Diagram (b) deformuje horizont do kapkovité plochy. Toto vyobrazení je výhodnější při zkoumání limity malé hmoty, kdy černé díry přejdou na světočáry rovnoměrně urychlených částic s nadkritickým zrychlením – srovnej s obr. 1.7 napravo.

Kapitola 2

Asymptotické směrová struktura polí

Shrnutí

Jedním ze stále otevřených problémů v obecné teorii relativity je otázka definice záření v asymptoticky netriviálních prostoročasech. Ač tomuto tématu bylo věnováno rozsáhlé úsilí – od pionýrských prací Penrose [32, 81] zavádějících pojem konformního nekonečna, přes dnes již klasické monografie [29, 30, 44] pokrývající znalosti o globálních vlastnostech, koncept asymptotické jednoduchosti či tzv. peeling teorém, až po nedávné výsledky [82–86] o existenci velké třídy asymptoticky de sitterovských a anti-de sitterovských prostoročasů (viz též přehledy [17, 83, 87]) – není doposud vytvořen ucelený obraz kvalitativně i kvantitativně charakterizující záření v blízkosti prostorupodobného a časupodobného nekonečna.

Jednou ze standardních technik ke zkoumání zářivých polí v asymptoticky plochých prostoročasech je zkoumání zářivé komponenty pole z hlediska pozorovatele vzdalujícího se do nekonečna podél nulové geodetiky. V sérii prací [2–8] jsme analyzovali chování této komponenty v případě prostorupodobného a časupodobného nekonečna. V první práci bylo diskutováno testovací elektromagnetické pole v de Sitterově vesmíru, v následujících dvou pracích pole rovnoměrně urychlených černých děr v prostoročasech jak s $\Lambda > 0$, tak $\Lambda < 0$. Tyto výsledky byly následně zobecněny pro obecné pole spinu s v libovolných prostoročasech s lokálně (anti-)de sitterovským nekonečnem. Výsledky byly souhrnně publikovány ve zvaném 'topical review' v časopise Classical and Quantum Gravity [7].

Tato kapitola obsahuje uvedení do kontextu teorie záření v obecné teorii relativity a nastiňuje některé postupy a předkládá hlavní výsledky zmíněných původních prací. Pro podrobný výklad odkazuji čtenáře hlavně na souhrnnou práci [7].

Publikace

Původní výsledky týkající se tématu této kapitoly jsou obsaženy v následujících pracích:

[7] Pavel Krtouš, Jiří Podolský: *Asymptotic directional structure of radiative fields in spacetimes with a cosmological constant*, Class. Quantum Grav. **21**, R233 (2004).

[8] Pavel Krtouš, Jiří Podolský: *Asymptotic directional structure of radiation for fields of algebraic type D*, Czech. J. Phys. **55**, 119 (2005).

[4] Pavel Krtouš, Jiří Podolský, Jiří Bičák: *Gravitational and electromagnetic fields near a de Sitter-like infinity*, Phys. Rev. Lett. **91**, 061101 (2003).

[6] Pavel Krtouš, Jiří Podolský: *Gravitational and electromagnetic fields near an anti-de Sitter-like infinity*, Phys. Rev. D **69**, 084023 (2004).

[3] Pavel Krtouš, Jiří Podolský: *Radiation from accelerated black holes in a de Sitter universe*, Phys. Rev. D 68, 024005 (2003).

[5] Jiří Podolský, Marcello Ortaggio, Pavel Krtouš: *Radiation from accelerated black holes in an anti-de Sitter universe*, Phys. Rev. D **68**, 124004 (2004).

[2] Jiří Bičák, Pavel Krtouš: *The fields of uniformly accelerated charges in de Sitter spacetime*, Phys. Rev. Lett. **88**, 211101 (2002).

Plné znění těchto publikací lze nalézt v druhé části habilitační práce.

2.1 Záření v obecné teorii relativity

Otázka záření a vlastností zářivých polí v obecné teorii relativity je jedním z klíčových problémů matematické relativity, který lze vystopovat až k počátkům této teorie [88,89]. Jelikož je obecná teorie relativity vysoce nelineární a svou povahou geometrická teorie, metody používané v běžných lineárních teoriích (jako např. multipólový rozvoj) mají v tomto případě svá omezení. Gravitační záření od fyzikálních zdrojů (např. binárních systémů) totiž odpovídá deformaci prostoročasu, jistým 'vlnkám' v jeho struktuře, přičemž tato deformace sama ovlivňuje geometrii s jejíž pomocí identifikujeme vzdálené oblasti. Nelinearita Einsteinových rovnic s sebou navíc nese nemožnost lokalizace gravitační energie, což komplikuje analýzu gravitačního záření a určení např. bilanční rovnice pro ztrátu energie zdroje.

Obtížnost Einsteinových rovnic také omezuje 'sortiment' řešení popisujících gravitační pole dostatečně složitých zdrojů, řešení, která mají zářivý charakter. Přesto bylo od padesátých let minulého století nalezeno několik významných příkladů zářivých prostoročasů. S C-metrikou, zástupcem nejdůležitější třídy takovýchto prostoročasů, třídy boost-rotačně symetrických prostoročasů [51, 90], jsme se setkali v minulé kapitole. Ač tyto prostoročasy nepopisují nejtypičtější astrofyzikální situace, jejich studiem bylo získáno mnoho poznatků týkajících se gravitačního záření – viz např. přehledy [69, 70, 91–94].

Vedle hledání a zkoumání přesných řešení bylo velké úsilí věnováno také zkoumání asymptotického chování gravitačního pole. Přelomové práce, vyjasňující povahu gravitačního záření v situacích, kdy se prostoročas daleko od zdrojů podobá prázdnému Minkowského vesmíru, přicházejí v šedesátých letech [95–99]. V těchto pracích se podařilo definovat tzv. *Bondiho hmotu* charakterizující celkovou hmotnost systému z hlediska (budoucího konformního) nekonečna a charakterizovat radiační tok odcházejí do nekonečna pomocí tzv. *informační funkce* (analogie Poyntingova vektoru pro zářivé elektromagnetické pole). Pro tyto veličiny byla ukázána platnost bilanční rovnice.

Tyto práce byly zastřešeny Penrosem [32, 33, 81, 100], který zformuloval geometrický přístup k popisu vzdálených oblastí – metodu konformního nekonečna, kterou jsme krátce nastínili v části 1.1 předchozí kapitoly. V rámci této formulace bylo možné přesně specifikovat třídu asymptoticky plochých prostoročasů, definovat Bondiho hmotu geometrickým způsobem a dokázat tzv. *'peeling' teorém* [32, 97, 101–103] (viz příští podkapitolu).

Zářivá část gravitačního pole se v tomto přístupu charakterizuje jistou komponentou Weylova tenzoru spočtenou vzhledem k tzv. *interpretační tetrádě* – bázi vektorů paralelně přenášených podél nulové geodetiky do konformního nekonečna. Podobným způsobem je možné charakterizovat zářivou komponentu i elektromagnetického pole, případně pole obecného spinu s. Peeling teorém mimo jiné říká, že tato zářivá komponenta má lokálně charakter podobný rovinné vlně.

Penroseův přístup má navíc velkou výhodu, že ho lze alespoň částečně zobecnit i pro prostoročasy, které mají jinou asymptotiku, konkrétně, pro prostoročasy s nenulovou kosmologickou konstantou [29, 32, 81, 86]. Jak jsem již konstatovali v první kapitole, znaménko kosmologické konstanty koreluje s charakterem konformního nekonečna. Pro nenulovou kosmologickou konstantu tak prostoročas

nemůže být asymptoticky plochý, nýbrž bude mít buď prostorupodobné či časupodobné nekonečno. V takovýchto prostoročasech až doposud neumíme zavést veličiny analogické Bondiho hmotě či informační funkci [104, 105]. V Penrosově formalismu alespoň umíme charakterizovat asymptotiku gravitačního pole a definovat zářivou komponentu Weylova tenzoru.

Již Penrose si ale všiml [81, 106], že v případě prostorupodobného či časupodobného konformního nekonečna je zářivá komponenta pole definovaná "méně invariantně" než v případě asymptoticky plochého prostoročasu – závisí totiž na směru, jakým se k nekonečnu přibližujeme.

Toto konstatování zůstalo dlouhou dobu nepovšimnuto a neanalyzováno. Až mnohem později jsme si v práci [2] (v práci analyzující pole rovnoměrně urychlených nábojů v de Sitterově prostoročase) této vlastnosti zářivé složky (zde elektromagnetického pole) povšimli a detailně ji analyzovali. V následných pracích [3, 5] jsme tuto analýzu zobecnili na zajímavější případ gravitačního pole urychlených černých děr v asymptoticky de Sitterově a anti-de Sitterově vesmíru, kde jsme nalezli explicitní směrovou závislost zářivé komponenty jak gravitačního, tak elektromagnetického pole.

Tyto konkrétní směrové závislosti se však ukázaly jako projev mnohem obecnější souvislosti, kterou jsme zformulovali v pracích [4, 6]: asymptotická směrová závislost zářivé komponenty gravitačního pole v blízkosti prostorupodobného a časupodobného nekonečna je zcela determinována algebraickou strukturou Weylova tenzoru v nekonečnu. Penrosem zmíněná nejednoznačnost tak není zcela bezbřehá, nýbrž jasně určitelná pomocí tzv. hlavních nulových směrů pole a jistých normalizačních koeficientů. Tyto výsledky byly shrnuty (a navíc zobecněny na případ obecného pole spinu s) v „topical review" [7]. V práci [8] pak byly rozebrány některé důsledky pro speciální algebraické typy prostoročasů. V příští kapitole se také zmíníme o zobecnění této problematiky do vyšších dimenzí.

Hlavním cílem série publikací zmíněných v předchozích dvou odstavcích (které jsou též součástí této habilitace) bylo alespoň částečně přispět k porozumění charakteru záření v blízkosti prostorupodobného a časupodobného nekonečna. Přestože se na tomto poli podařilo poslední dobou získalo mnoho poznatků v různých směrech, stále nemáme úplný a uspokojivý vhled do tohoto fenoménu. Nadále nejsou k dispozici jasně interpretovatelné globální veličiny, charakterizující tok 'gravitační energie' či nalezena bilanční rovnice. Naše analýza alespoň částečně upřesňuje povahu zářivé komponenty, která se v případě asymptoticky plochých prostoročasů ukázala jako velmi užitečný nástroj. Podobná použití v případě nenulové kosmologické konstanty však zatím zůstává otevřené.

2.2 Použitý formalismus[1]

Jak do nekonečna?

V předchozí kapitole, v podkapitole 1.1, jsme popsali, jakým způsobem lze uchopit pojem nekonečna. Po konformním přeškálování lze fyzikální prostoročas vnořit do pomocné variety, z hlediska které se nekonečno chová jako standardní

[1] V textu této podkapitoly byly použity části práce [20].

nadplocha ohraničující fyzikální prostoročas. Jeho charakter – prostorupodobný, časupodobný či nulový koreluje se znaménkem kosmologické konstanty.

V takovémto pohledu na nekonečno můžeme mluvit o jednotlivých bodech nekonečna a o směrech, ze kterých se k těmto bodům blížíme. Konkrétně nás budou zajímat limity podél nulových geodetik.

Nulové geodetiky – trajektorie nejrychlejšího možného signálu – se mohou do konformního nekonečna přibližovat z minulosti (potom mluvíme o budoucím konformním nekonečnu a o *odcházejících* geodetikách), nebo z něho mohou vycházet směrem do budoucnosti (mluvíme pak o minulém konformním nekonečnu a o *vcházejících* geodetikách). Nekonečno prostorupodobného či nulového charakteru (tj. s normálou časové či nulové povahy) je vždy buď minulé nebo budoucí. Nekonečno časupodobné povahy (s prostorovou normálou) je zároveň minulé i budoucí – viz obr. 1.2.

Nulové geodetiky jsou parametrizované afinním parametrem, který nahrazuje pojem vlastního času či vlastní vzdálenosti podél nich. Pro různé geodetiky mířící do stejného bodu v nekonečnu budeme normalizovat afinní parametr stejným způsobem, a to s pomocí normály k nekonečnu – viz kapitolu 3.3 práce [7].

Zářivá komponenta pole je definována vzhledem k 'pozorovateli' pohybujícímu se podél nulové geodetiky. Konkrétně vzhledem k *interpretační bázi vektorů* paralelně přenášených podél geodetiky.

Tetrády

Při práci s vektory a tenzory v křivém prostoročasu je výhodné tyto objekty reprezentovat jejich složkami vzhledem ke speciálním bázím. Na metrických varietách se typicky používají ortonormální báze vektorů $\boldsymbol{t}$, $\boldsymbol{q}$, $\boldsymbol{r}$, $\boldsymbol{s}$, v prostoročasech dimenze čtyři nazývané též *ortonormální tetrády*. Na varietách s lorentzovskou signaturou lze vedle toho s výhodou využít tzv. *nulové tetrády* $\boldsymbol{k}$, $\boldsymbol{l}$, $\boldsymbol{m}$, $\bar{\boldsymbol{m}}$, ve kterých je časový vektor $\boldsymbol{t}$ a prostorový vektor $\boldsymbol{q}$ nahrazen dvojicí nulových reálných vektorů $\boldsymbol{k}$, $\boldsymbol{l}$, a zbývající dva prostorové vektory dvěma komplexními vektory $\boldsymbol{m}$, $\bar{\boldsymbol{m}}$ nulové velikosti – viz např. (3.1) v práci [7].

V konformním nekonečnu $\mathcal{I}$ je výhodné volit tetrády 'uzpůsobené charakteru' nekonečna. Řekneme, že ortonormální (a s ní asociovaná nulová) tetráda je *přizpůsobená* prostorupodobnému či časupodobnému nekonečnu, pokud normála $\boldsymbol{n}$ k nekonečnu patří do této tetrády. Pro nekonečno nulové povahy požadujeme, aby normála patřila do nulové tetrády. Tetrády splňující tuto podmínku jsou výhodné při popisu jevů blízko nekonečna. S jejich pomocí se jednoduše provádí např. restrikce na nekonečno či parametrizování nulových směrů v nekonečnu.

Typicky se jedna taková tetráda volí jako *referenční* – její nulovou verzi označíme $\boldsymbol{k}_{\mathrm{o}}$, $\boldsymbol{l}_{\mathrm{o}}$, $\boldsymbol{m}_{\mathrm{o}}$, $\bar{\boldsymbol{m}}_{\mathrm{o}}$. Vůči ní se pak parametrizují další fyzikálně zajímavé tetrády. V konkrétních případech může být tato referenční tetráda volena s přihlédnutím ke speciálním geometrickým vlastnostem prostoročasu – pro nás však konkrétní způsob volby není důležitý. Vektor $\boldsymbol{k}_{\mathrm{o}}$ budeme vždy volit orientovaný do budoucnosti. Vzhledem k fyzikálnímu prostoročasu však může být orientován jak směrem ven, tak směrem dovnitř.

Vzhledem k referenční tetrádě budeme parametrizovat i směr $\boldsymbol{k}$, ze kterého se k nekonečnu přibližují nulové geodetiky. Obecně můžeme zavést komplexní

parametr R určující směr $\boldsymbol{k}$ rovnicí

$$\boldsymbol{k} \propto \boldsymbol{k}_{\mathrm{o}} + \bar{R}\,\boldsymbol{m}_{\mathrm{o}} + R\,\bar{\boldsymbol{m}}_{\mathrm{o}} + R\bar{R}\,\boldsymbol{l}_{\mathrm{o}} \,. \tag{2.1}$$

Pro prostorupodobné nekonečno, které má charakter třídimenzionálního riemannovského prostoru, se ke zvolenému bodu v nekonečnu můžeme přiblížit nulovou geodetikou ze všech prostorových stran – nulové směry tedy odpovídají vektorům jednotkové sféry okolo daného bodu. Tyto směry můžeme charakterizovat sférickými úhly θ, ϕ nebo komplexním parametrem (2.1) souvisejícím s úhly vztahem $R = \tan(\theta/2)\exp(-i\phi)$ (viz kapitolu 5.3 v [7]).

V případě časupodobného nekonečna, tvoří $\mathcal{I}$ třídimenzionální lorentzovskou varietu (tj. s indukovanou metrikou signatury $-++$), kterou si můžeme představit jako historii dvoudimenzionální plochy ohraničující náš prostor.[2] K danému bodu v nekonečnu se tak můžeme přiblížit pouze z jedné hemisféry. Stejně tak jedné hemisféře odpovídají všechny nulové směry, které do prostoročasu vcházejí. Tyto směry můžeme parametrizovat opět sférickými úhly nebo alternativně rapiditou ψ a úhlem ϕ projekce nulového směru na nekonečno, viz kapitolu 5.3 v [7]. V každém případě musíme také specifikovat, zda se jedná o směr z prostoročasu vycházející ($\epsilon = +1$) nebo do prostoročasu vcházející ($\epsilon = -1$). Tyto (pseudo)úhly lze nahradit komplexním parametrem (2.1) vztahem $R = \tanh^{\epsilon}\frac{\psi}{2}\,\exp(-i\phi)$.

Jak jsme již řekli, naším cílem je zkoumat pole z hlediska *interpretační tetrády*. Interpretační tetráda $\boldsymbol{k}_{\mathrm{i}}$, $\boldsymbol{l}_{\mathrm{i}}$, $\boldsymbol{m}_{\mathrm{i}}$, $\bar{\boldsymbol{m}}_{\mathrm{i}}$ je tetráda, která je paralelně přenášena podél nulové geodetiky vedoucí do konformního nekonečna, přičemž vektor $\boldsymbol{k}_{\mathrm{i}}$ musí mířit ve směru geodetiky a být vhodně normalizován.

Taková tetráda je podél dané geodetiky dána až na konstantní lorentzovskou transformaci zachovávající vektor $\boldsymbol{k}_{\mathrm{i}}$. Jak je ukázáno v kapitole 3.4 práce [7], při přenášení do nekonečna tato tetráda degeneruje – vektor $\boldsymbol{k}_{\mathrm{i}}$ se vzhledem k referenční tetrádě zvolené v nekonečnu nekonečně zkracuje a vektor $\boldsymbol{l}_{\mathrm{i}}$ nekonečně prodlužuje. Tato degenerace hraje klíčovou roli při odvození peelingu polních komponent spočtených vzhledem k interpretační tetrádě.

Komponenty gravitačního pole a hlavní nulové směry

'Intenzitu' gravitační pole (jeho 'neodtransformovatelnou' složku – např. velikost slapových sil) lze charakterizovat pomocí Riemannova tenzoru křivosti. Ten se rozkládá na část popsanou Einsteinovým tenzorem přímo spojenou s rozložením hmoty a na část popsanou Weylovým tenzorem spojovanou s 'volným' gravitačním polem, tj. s gravitačními vlnami šířícími se prostorem. Jelikož nás zajímá zejména gravitační záření, zaměříme se na část popsanou Weylovým tenzorem. Tento tenzor lze vzhledem k nulové tetrádě $\boldsymbol{k}$, $\boldsymbol{l}$, $\boldsymbol{m}$, $\bar{\boldsymbol{m}}$ charakterizovat pomocí pěti komplexních komponent označovaných Ψ_j – viz standardní reference [91] či kapitolu 4.1 práce [7], konkrétně rovnice (4.1).

Weylův tenzor lze dále algebraicky charakterizovat pomocí zobecněných vlastních vektorů, nazývaných *hlavní nulové směry* (HNuSy). Směr daný vektorem $\boldsymbol{k}$

[2] Samozřejmě ve smyslu konformní geometrie – ve fyzikální geometrii je tato 'hranice' nekonečně daleko.

je HNuS, je-li vzhledem k nulové tetrádě[3] $\boldsymbol{k}$, $\boldsymbol{l}$, $\boldsymbol{m}$, $\bar{\boldsymbol{m}}$ komponenta Ψ_0 nulová. Pokud parametrizujeme směr $\boldsymbol{k}$ pomocí komplexního parametru R (rovnice (2.1)), podmínka na HNuS vede na rovnici

$$R^4\,\Psi_4^{\mathrm{o}} + 4R^3\,\Psi_3^{\mathrm{o}} + 6R^2\,\Psi_2^{\mathrm{o}} + 4R\,\Psi_1^{\mathrm{o}} + \Psi_0^{\mathrm{o}} = 0\,. \tag{2.2}$$

Zde Ψ_j^{o} jsou komponenty pole vzhledem k referenční tetrádě $\boldsymbol{k}_{\mathrm{o}}$, $\boldsymbol{l}_{\mathrm{o}}$, $\boldsymbol{m}_{\mathrm{o}}$, $\bar{\boldsymbol{m}}_{\mathrm{o}}$. Jedná se o rovnici čtvrtého stupně, která má obecně čtyři komplexní kořeny R_1, R_2, R_3, R_4 parametrizující čtyři HNuSy $\boldsymbol{k}_1, \boldsymbol{k}_2, \boldsymbol{k}_3, \boldsymbol{k}_4$. Poznamenejme, že koeficienty Ψ_j^{o}, $j = 0, 1, 2, 3$ mohou být zpětně vyjádřeny pomocí kořenů R_1, R_2, R_3, R_4 a zbývající komponenty Ψ_4^{o} normalizující 'velikost' pole.

HNuSy určují tzv. *algebraickou* strukturu Weylova tenzoru. Říkáme, že algebraická struktura je degenerovaná, pokud některé z HNuSů koincidují. Podle počtu koincidujících HNuSů rozlišujeme následující Petrovovy algebraické typy [91, 107]: N (všechny 4 HNuSy jsou shodné), III (tři HNuSy koincidují), II (právě dva HNuSy koincidují), D (dva a dva HNuSy koincidují), I (obecný algebraický typ s různými HNuSy) a konečně typ 0 pro nulový Weylův tenzor.

Zkušenost z asymptoticky plochých prostoročasů ukazuje, že zářivá pole jsou typicky typu N (např. gravitační *pp*-vlny – analogie rovinných vln v obecné teorii relativity). Vedle toho 'peeling' teorém říká, že z hlediska interpretační tetrády přenášené podél nulové geodetiky do nekonečna se polní komponenty postupně 'odlupují' podle algebraických typů: část pole klesající s převrácenou afinní vzdáleností η^{-1} má strukturu pole typu N, část úměrná η^{-2} má strukturu pole III, komponenta řádu $\eta^{\ 3}$ odpovídá strukturou dvěma koincidujícím HNuSům a konečně komponenta $\sim \eta^{-4}$ odpovídá obecnému typu I. Jinými slovy: komponenty Ψ_j^{i} Weylova tenzoru vzhledem k interpretační tetrádě mají následující asymptotické chování

$$\Psi_j^{\mathrm{i}} \sim \eta^{j-5}\,. \tag{2.3}$$

2.3 Asymptotická směrová charakteristika záření

Zářivá komponenta pole

Vzhledem k právě zmíněnému chování budeme složku pole Ψ_4^{i} v interpretační tetrádě – klesající podél nulové geodetiky jako $1/\eta$ – nazývat *zářivou částí pole.* Tato složka nejenže klesá nejpomaleji, ale má též algebraicky degenerovanou strukturu N očekávanou u zářivých polí. V dalším nás bude zajímat chování této komponenty v závislosti na tom, jakým způsobem se nulová geodetika blíží k nekonečnu, přičemž nekonečno připustíme obecné povahy – prostorupodobné, nulové či časupodobné. Připomeňme, že v podkapitole 1.1 jsme tento charakter parametrizovali znaménkem kvadrátu normály $\sigma = -1, 0, +1$.

Obecné analýzy ukazují [29, 32, 86, 87, 105, 108], že komponenty gravitačního pole Ψ_j^{o} vzhledem k *referenční* tetrádě mají v blízkosti konformního nekonečna

[3] Tetráda musí splňovat normalizační podmínky nulové tetrády, jinak mohou být vektory $\boldsymbol{l}$, $\boldsymbol{m}$, $\bar{\boldsymbol{m}}$ doplněny k vektoru $\boldsymbol{k}$ libovolně.

následující chování:

$$\Psi^{\mathrm{o}}_j \approx \frac{\Psi^{\mathrm{o}}_{j*}}{\eta^3}\,, \qquad \Psi^{\mathrm{o}}_{j*} = \text{konst.} \tag{2.4}$$

Upozorněme znovu, že se jedná o chování vůči *referenční* tetrádě.[4] Jak jsme se však zmínili, interpretační tetráda asymptoticky vůči referenční tetrádě degeneruje. Proto bude chování komponent vůči interpretační tetrádě odlišné. Podrobná analýza provedená v přiložené práci [7] vede k následující závislosti zářivé komponenty Ψ^{i}_4:

$$\Psi^{\mathrm{i}}_4 \approx \frac{\Psi^{\mathrm{o}}_{4*}}{\eta} \frac{\big(1-\sigma R_1\bar R\big)\big(1-\sigma R_2\bar R\big)\big(1-\sigma R_3\bar R\big)\big(1-\sigma R_4\bar R\big)}{\big(1-\sigma R\bar R\big)^2}\,. \tag{2.5}$$

Tato formule plně charakterizuje *asymptotickou směrovou strukturu zářivé komponenty gravitačního pole* – vystihuje její závislost na konstantách Ψ^{o}_{4*}, R_1, R_2, R_3, R_4 charakterizujících pole a jeho HNuSy, na charakteru konformního nekonečna $\sigma = -1, 0, +1$, na afinním parametru η, a hlavně na konkrétním *směru nulové geodetiky*, podél které se do nekonečna blížíme. Tento směr je ve výrazu (2.5) určen komplexním parametrem R ve smyslu rovnice (2.1).

Přesněji řečeno, fyzikální význam má pouze velikost komplexní komponenty Ψ^{i}_4. Její fáze závisí na konkrétní volbě interpretační tetrády. Velikost $\big|\Psi^{\mathrm{i}}_4\big|$ již na volbě interpretační tetrády (podél dané geodetiky) nezávisí. Dává tak invariantní charakteristiku zářivé složky pole.

Záření poblíž nulového nekonečna

Nejjednodušší situace nastává pro konformní nekonečno $\mathcal{I}$ nulové povahy, tedy když $\Lambda = 0$. V tomto případě obecná směrová charakteristika (2.5) degeneruje:

$$|\Psi^{\mathrm{i}}_4| \approx \frac{|\Psi^{\mathrm{o}}_{4*}|}{|\,\eta\,|}\,. \tag{2.6}$$

Vidíme, že závislost na směrovém parametru R zcela vypadla a zářivá složka pole tak nezávisí na směru, jakým se blížíme do nekonečna. V tomto případě je asymptotické chování pole popsáno dostatečně ‘peeling’ teorémem a o směrové struktuře nemá smysl mluvit.

Záření poblíž prostorupodobného nekonečna

V případě prostorupodobného nekonečna ($\Lambda > 0$) je již situace zajímavější. Obecnou směrovou charakteristiku (2.5) lze přepsat do tvaru

$$\Psi^{\mathrm{i}}_4 \approx \frac{\Psi^{\mathrm{o}}_{4*}}{\eta}\big(1+|R|^2\big)^{-2}\left(1-\frac{R_1}{R_{\mathfrak{a}}}\right)\left(1-\frac{R_2}{R_{\mathfrak{a}}}\right)\left(1-\frac{R_3}{R_{\mathfrak{a}}}\right)\left(1-\frac{R_4}{R_{\mathfrak{a}}}\right)\,, \tag{2.7}$$

kde $R_{\mathfrak{a}} = -1/\bar R$ určuje směr *prostorově opačný* ke směru geodetiky. Pomocí úhlových proměnných θ, ϕ dostáváme

$$\big|\Psi^{\mathrm{i}}_4\big| \approx \frac{|\Psi^{\mathrm{o}}_{4*}|}{|\eta|}\,\cos^4\tfrac{\theta}{2}\prod_{n=1,2,3,4}\big|1+\tan\tfrac{\theta_n}{2}\,\tan\tfrac{\theta}{2}\,e^{i(\phi-\phi_n)}\big|\,. \tag{2.8}$$

[4] Přesněji: referenční tetrádě rozšířené hladce do okolí $\mathcal{I}$.

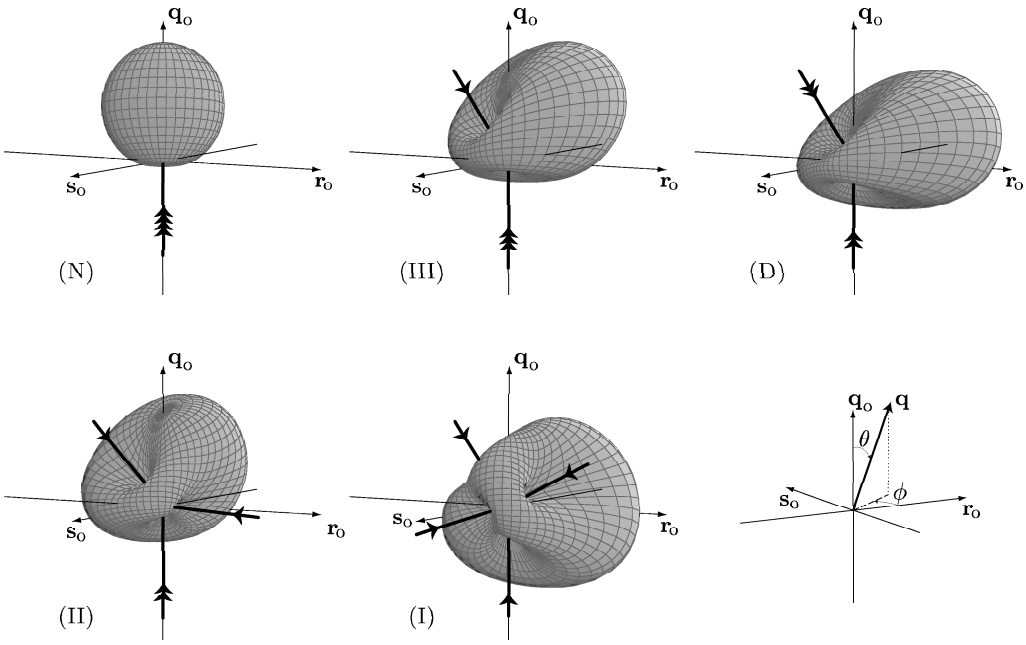

Obrázek 2.1: **Asymptotická směrová struktura záření v prostoročasech s $\Lambda > 0$.** Vyobrazeny jsou konkrétní směrové charakteristiky v prostoročasech různých algebraických typů N, III, D, II a I. Pro každý z možných typů je vykreslena zářivá složka $\left|\Psi_4^{\mathrm{i}}\right|$ měřená podél nulové geodetiky. Směry v diagramech odpovídají prostorovým směrům nulových geodetik v nekonečnu. [Degenerované] hlavní nulové směry (HNuSy) jsou vyznačeny [násobnými] šipkami. Tlusté čáry reprezentují prostorové směry (opačné k HNuSům), podél kterých záření vymizí.

Úhly θ, ϕ popisují směr nulové geodetiky, podél které se blížíme k nekonečnu, úhly θ_n, ϕ_n charakterizují HNuSy gravitačního pole.

Z tvaru (2.7) okamžitě vidíme, že zářivá složka vymizí pro směry splňující $R_{\mathfrak{a}} = R_n$, $n = 1, 2, 3, 4$, tj. pro směry prostorově opačné k HNuSům gravitačního pole. Kvalitativně je tedy směrová charakteristika záření v blízkosti prostorového nekonečna daná HNuSy pole. Pro jednotlivé algebraické typy gravitačního pole proto dostáváme kvalitativně různé zářivé charakteristiky s různým počtem směrů, v nichž záření vymizí – viz obr. 2.1.

Poznamenejme, že v blízkosti budoucího nekonečna $\mathcal{I}^+$ popisuje směrová charakteristika strukturu záření podél geodetik odcházejících z prostoročasu, v blízkosti minulého nekonečna $\mathcal{I}^-$ směrovou strukturu záření podél vycházejících geodetik.

Záření poblíž časupodobného nekonečna

V případě časupodobného nekonečna ($\Lambda < 0$) je směrová struktura záření ještě o něco bohatší. Obecný vztah (2.5) můžeme přepsat do tvaru

$$\Psi_4^{\mathrm{i}} \approx \frac{\Psi_{4*}^{\mathrm{o}}}{\eta}\left(1-|R|^2\right)^{-2}\left(1-\frac{R_1}{R_{\mathfrak{m}}}\right)\left(1-\frac{R_2}{R_{\mathfrak{m}}}\right)\left(1-\frac{R_3}{R_{\mathfrak{m}}}\right)\left(1-\frac{R_4}{R_{\mathfrak{m}}}\right). \quad (2.9)$$

typ	degenerace HNuSů	různé možnosti orientace HNuSů
N	4	o^4 t^4 i^4
III	$3+1$	o^3o o^3t o^3i t^3o t^3t i^3i i^3t i^3o t^3i
D	$2+2$	o^2o^2 o^2t^2 o^2i^2 t^2t^2 i^2i^2 i^2t^2
II	$2+1+1$	o^2oo o^2ot o^2oi o^2ii o^2it o^2tt t^2oo t^2ot t^2oi t^2tt i^2ii i^2it i^2io i^2oo i^2ot i^2tt t^2ii t^2it
I	$1+1+1+1$	$oooo$ $ooot$ $oooi$ $ooit$ $oott$ $ottt$ $ooii$ $oitt$ $tttt$ $iiii$ $iiit$ $iiio$ $iiot$ $iitt$ $ittt$

Tabulka 2.1: **Klasifikace směrové struktury záření v blízkosti časupodobného $\mathcal{I}$.** Tabulka zahrnuje všech 51 kvalitativně odlišných směrových struktur gravitačního záření. Pro daný algebraický typ, určený degenerací HNuSů, závisí konkrétní směrová struktura na orientaci těchto HNuSů vůči $\mathcal{I}$. Odcházející, tečné a vcházející HNuSy označujeme symboly o, t, a i. Jejich degenerace je popsána příslušnou mocninou. Možnosti uvedené ve třetím řádku každého algebraického typu lze získat z prvního řádku pomocí duality mezi odcházejícími a vcházejícími směry, neboli záměnou o za i.

Zde komplexní parametr $R_{\mathfrak{m}} = 1/\bar{R}$ charakterizuje nulový směr *zrcadlově převrácený* ke směru geodetiky podle konformního nekonečna $\mathcal{I}$. Pomocí pseudosférických úhlů ψ, ϕ můžeme (2.5) psát:

$$\left|\Psi_4^{\mathrm{i}}\right| \approx \frac{|\Psi_{4*}^{\mathrm{o}}|}{|\eta|} \left(\frac{\cosh\psi + \epsilon\epsilon_{\mathrm{o}}}{2}\right)^2 \prod_{n=1,2,3,4} \left|1 - \tanh^{\epsilon_n\epsilon_{\mathrm{o}}}\!\left(\tfrac{\psi_n}{2}\right) \tanh^{\epsilon\epsilon_{\mathrm{o}}}\!\left(\tfrac{\psi}{2}\right) e^{i(\phi-\phi_n)}\right| . \tag{2.10}$$

Parametry ψ, ϕ, ϵ udávají směr geodetiky, parametry ψ_n, ϕ_n, ϵ_n HNuSy gravitačního pole a ϵ_{o} charakterizuje orientaci vektoru $\boldsymbol{k}_{\mathrm{o}}$ referenční tetrády.

K danému bodu časupodobného nekonečna se lze přiblížit jak podél odcházející geodetiky tak podél vcházející geodetiky. Dostáváme tak dvě různé směrové charakteristiky, jednu pro $|R| < 1$, druhou pro $|R| > 1$. Pro $|R| = 1$ výraz (2.9) degeneruje, což je dáno použitou normalizací afinního parametru geodetik (viz diskuzi v kapitole 3.3 práce [7]). Směry s $|R| = 1$ jsou však tečné k nekonečnu a neodpovídají tak směrům fyzikálních geodetik.

Z výrazu (2.9) můžeme opět odečíst směry, podél kterých záření vymizí, totiž $R_{\mathfrak{m}} = R_n$, $n = 1, 2, 3, 4$. Jedná se o směry zrcadlově převrácené podle $\mathcal{I}$ k HNuSům pole. Kvalitativní tvar zářivé charakteristiky závisí opět na algebraickém typu gravitačního pole (na počtu degenerovaných HNuSů), vedle toho je však také

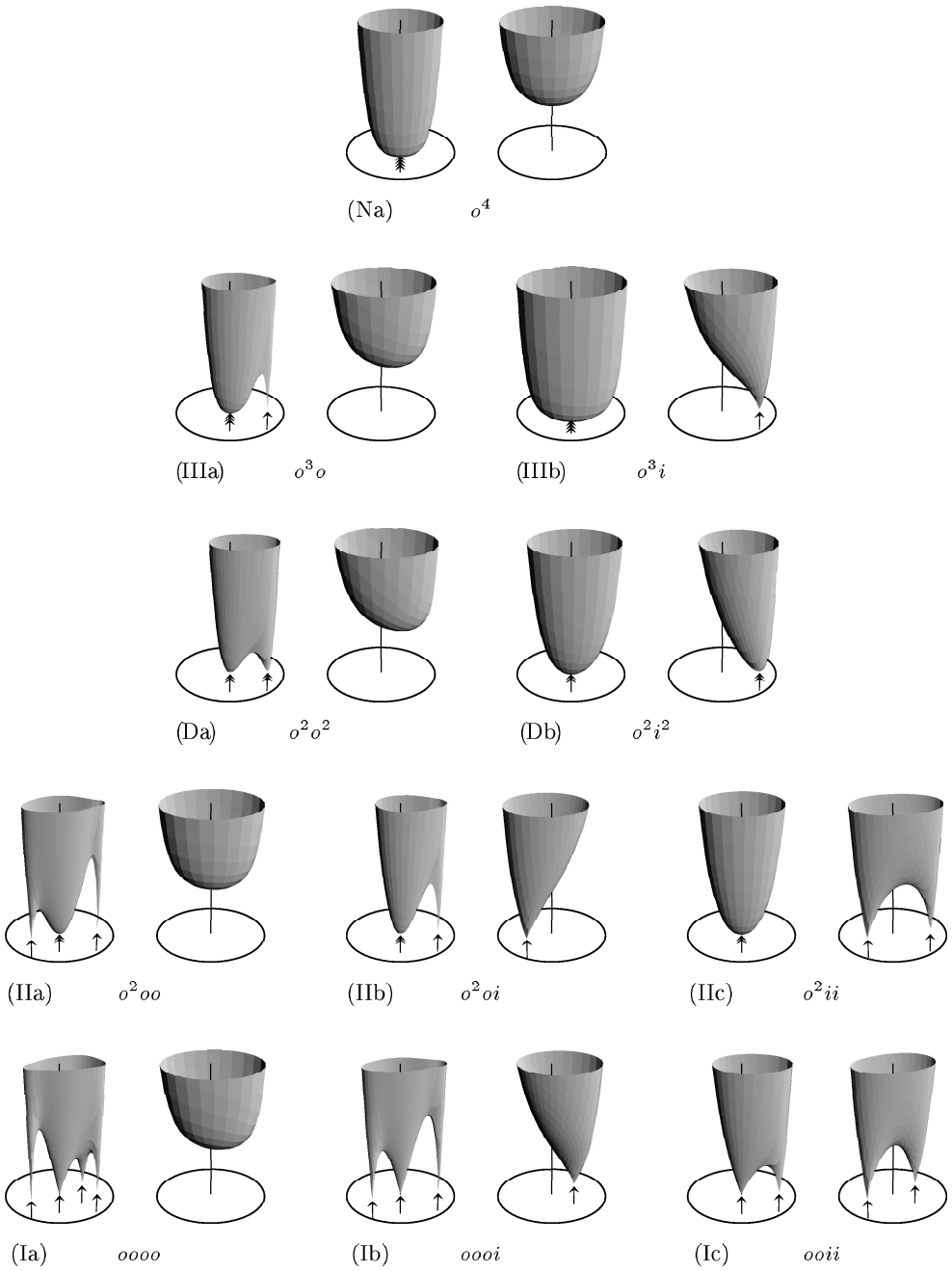

Obrázek 2.2: **Asymptotická směrová struktura zářivé komponenty pole pro $\Lambda < 0$.** V obrázku je zobrazeno všech 11 kvalitativně odlišných typů, kdy HNuSy nejsou tečné k nekonečnu (tedy typy z tabulky 2.1 neobsahující 't'; zbývajících 9 typů se dostane zrcadlením přes $\mathcal{I}$, tj. záměnou 'i' a 'o' směrů). Každý diagram se skládá z charakteristiky pro vcházející (nalevo) a vycházející (napravo) geodetiky. Na vertikální ose se vynáší $\left|\Psi_4^{\mathrm{i}}\right|$, body kruhu v horizontální rovině parametrizují nulové směry v nekonečnu – jedná se o projekce hemisfér prostorových směrů nulových geodetik. Zrcadlové obrazy [degenerovaných] HNuSů jsou vyznačeny [několikanásobnými] šipkami pod kruhy. Pod každým diagramem je vyznačen Petrovův typ (N, III, D, II, I) odpovídající degeneraci HNuSů a kód z tabulky 2.1 charakterizující jejich orientaci.

dán orientací HNuSů vzhledem ke konformnímu nekonečnu. Podle toho, zda jednotlivé HNuSy z prostoročasu odcházejí nebo do něj vcházejí, dostáváme směry nulového záření pro vcházející geodetiky nebo odcházející geodetiky. HNuSům tečným ke konformnímu nekonečnu pak neodpovídá žádný fyzikální směr s nulovým zářením. V závislosti na algebraickém typu pole a orientaci HNuSů můžeme dohromady rozlišit 51 kvalitativně odlišných směrových struktur záření shrnutých v tabulce 2.1. Jejich grafické zobrazení pro případ, kdy HNuSy nejsou tečné k $\mathcal{I}$ je na obr. 2.2.

Příklad – urychlené černé díry

V pracích [3, 5] jsme aplikovali obecnou teorii směrové závislosti záření na konkrétní prostoročasy rovnoměrně urychlených černých děr v asymptoticky de Sitterově a anti-de Sitterově vesmíru, které byly diskutovány v předchozí kapitole. Tyto prostoročasy jsou algebraického typu D – mají dva dvojnásobně degenerované HNuSy. Tyto HNuSy leží právě v řezu $\xi, \varphi = \text{konst.}$, tj. v řezu dvoudimenzionálních konformních diagramů zobrazených v podkapitole 1.4.

V případě $\Lambda > 0$ můžeme tedy usoudit, že zářivá komponenta v daném bodě nekonečna vymizí pro dva speciální směry a to směry v nekonečnu prostorově opačné než směry k černým dírám. Podrobnou diskuzi lze najít v [4]. Analogický rozbor Bornova řešení v de Sitterově vesmíru lze nalézt v [2].

Pro $\Lambda < 0$ závisí kvalitativní tvar směrové závislosti zářivé komponenty také na orientaci HNuSů vzhledem k nekonečnu. U C-metriky s podkritickým zrychlením se uplatňuje pouze jedna možnost – jeden z HNuSů je orientován vždy ven z prostoročasu a druhý dovnitř. Pro nadkritické zrychlení se ale uplatňují všechny alternativy. Pro různé oblasti nekonečna může nastat jak případ, že oba HNuSy směřují dovnitř prostoročasu, ven z prostoročasu či jeden ven a jeden dovnitř. Hranicí mezi těmito oblastmi jsou průsečíky akceleračního a kosmologického horizontu s nekonečnem. Na těchto hranicích se uplatňují i limitní případy, kdy HNuSy mohou být k nekonečnu tečné. Pro podrobnou diskuzi viz [6].

Kapitola 3

Zobecnění do vyšších dimenzí

Shrnutí

V posledních letech se výrazně zvýšil zájem o řešení Einsteinových rovnic ve vyšších dimenzích. Motivace přicházejí zejména ze strunových a bránových teorií a různých verzí kvantové teorie, ať již v rámci 'velkého sjednocení' či kvantové gravitace. Díky tomuto zájmu se začíná rychle rozvíjet i čistě klasická verze obecné teorie relativity ve vyšších dimenzích a postupně se zobecňují různé poznatky z čtyřdimenzionální relativity.

Ač tato oblast výzkumu stojí pouze na okraji autorova zájmu, tři přiložené práce jsou příspěvkem k tomto proudu relativistické fyziky.

Práce [13] je přímé zobecnění výsledků diskutovaných v minulé kapitole na případ prostoročasů vyšších dimenzí. Tato práce využívá nedávných výsledků [109, 110] netriviálně zobecňujících klasickou algebraickou klasifikaci. V práci je odvozena asymptotická směrová charakteristika zářivé komponenty gravitačního pole. Je ukázáno, že ji lze vyjádřit pomocí jistých funkcí charakterizujících algebraickou strukturu. Díky tomu nulové směry zářivé komponenty pole opět souvisejí s algebraicky speciálními směry.

V pracích [9, 11] jsme se zabývali zkoumáním ultrarelativisticky se pohybujícího rotujícího *černého prstence* v pěti prostoročasových dimenzích. Černý prstenec je útvar analogický černým dírám, ale s odlišnou topologií horizontu, s topologií $S^1 \times S^2$. Bylo ukázáno, že prostoročas okolo velmi rychle se pohybujícího prstence má charakter tzv. *pp*-vlny – prototypu rovinné vlny v teorii gravitace. Tento výsledek je zobecněním klasického postupu [111] ze čtyř dimenzí pro rychle pohybující se černou díru. Námi obdržený profil *pp*-vlny je též srovnán s analogickým výsledkem [112] obdrženým pro pětidimenzionální černou díru.

Publikace

Původní výsledky týkající se tématu této kapitoly jsou obsaženy v následujících pracích:

[13] Pavel Krtouš, Jiří Podolský: *Asymptotic structure of radiation in higher dimensions*, předběžně přijato k publikaci v Class. Quantum Grav. (2005).

[9] Marcello Ortaggio, Pavel Krtouš, Jiří Podolský: *Ultrarelativistic boost of the black ring*, Phys. Rev. D **71**, 124031 (2005).

[11] Marcello Ortaggio, Jiří Podolský, Pavel Krtouš: *Ultrarelativistic boost of spinning black rings*, J. High Energy Phys. JHEP12(2005)001.

Plné znění těchto publikací lze nalézt v druhé části habilitační práce.

3.1 Asymptotická směrová charakteristika záření

Algebraická klasifikace Weylova tenzoru gravitačního pole vycházející z práce Petrova [107] a rozpracována Penrosem [113] je založena na zkoumání vztahu tzv. *hlavních nulových směrů* gravitačního pole[1] (viz monografie [29,91] pro přehledný výklad a podkapitolu 2.2 výše pro krátký souhrn). Jedná se o standardní techniku užívanou jako vodítko při hledání a případně identifikaci řešení Einsteinových rovnic. Významnou roli také sehrává při studiu zářivých prostoročasů a je klíčová ve formulaci peeling teorému [32, 97, 101–103]. Jak bylo vyloženo v předchozí kapitole, algebraická struktura vzdáleného pole určuje i směrovou charakteristiku záření.

Definice hlavních nulových směrů v podobě předložené např. Penrosem [29] však podstatně využívá, že prostoročas je čtyřdimenzionální. Hlavní nulové směry nelze stejným způsobem definovat i ve vyšší dimenzi. Teprve nedávno se objevilo zobecnění tohoto konceptu v pracích [109,110] zavádějících namísto hlavních nulových směrů obecnější koncept *nulových směrů přizpůsobených Weylovu tenzoru* (*Weyl tensor aligned null directions*).

Tyto směry jsou definovány způsobem analogickým rovnici (2.2) – nulový směr je přizpůsobený Weylovu tenzoru, pokud jisté komponenty tohoto tenzoru vymizí v bázi vystavěné na tomto nulovém směru. Na rozdíl od standardní situace ve čtyřech dimenzích však přizpůsobené vektory ve vyšší dimenzi nemusí existovat. Jejich definiční rovnice jsou obecně 'přezadané' a typická geometrie tak nemá žádné algebraicky speciální směry. Algebraická klasifikace ve vyšší dimenzi je tak bohatší o generické případy bez přizpůsobených směrů a závisí také na stupni degenerace více přizpůsobených směrů.

Ukázalo se, že tento formalismus lze přímočaře využít ke zobecnění výsledků prací [4, 6, 7]. V práci [13] se analogickým způsobem odvozuje směrová charakteristika zářivých komponent gravitačního pole a vyjadřuje se pomocí funkcí určujících algebraickou strukturu pole. Bylo ukázáno, že podobně jako ve čtyřech dimenzích směry, podél kterých záření vymizí, specifickým způsobem korelují s algebraicky speciálními směry.

3.2 Ultrarelativistický boost černého prstence

Velmi důležitým řešením Einsteinových rovnic z hlediska teorií ve vyšších dimenzích (ale i ve standardních čtyřech dimenzích) je třída *pp*-vln. Tyto prostoročasy hrají v obecné teorii relativity roli rovinných vln s případnými ultrarelativistickými zdroji. Jejich význam ve vyšších dimenzích pramení z toho, že v těchto prostoročasech lze přesně řešit některé strunové teorie [114,115], dále z toho, že v nich vymizí všechny algebraické invarianty [116–118], a v neposlední řadě proto, že popisují i pole rychle se pohybujících zdrojů. To lze nahlédnou např. z faktu, že *pp*-vlny se obecně dostávají při urychlení statických zdrojů (např. černých děr) na rychlost světla [111, 119].

Poslední důvod přispěl k zájmu o *pp*-vlny ve vyšších dimenzích zvláště poté, co některé vícedimenzionální teorie předpověděly, že již v současných či právě

[1] Obdobným způsobem lze studovat i elektromagnetické pole, případně pole obecného spinu.

budovaných urychlovačích by možná mohly být generovány mikroskopické černé díry (viz např. přehled [120]).

Prostoročas popisující rychle pohybující se lehkou Schwarzschildovu černou díru ve čtyřech dimenzích byl obdržený v práci [111]. Předpovědi tvorby černých děr na škálách TeV však fungují pouze ve vícedimenzionálních modelech, a proto je potřebné zkoumat *pp*-vlnovou limitu pro vícedimenzionální černé díry. Obecná rotující černá díra ve vyšší dimenzi byla popsaná Myersem a Perrym ve [121], její zobecnění pro nenulovou kosmologickou konstantu v pracích [122,123]. Ultrarelativistická limita statické díry vedoucí vskutku k *pp*-vlně byla nalezena v práci [119] a zobecněna na rotující případ letos ve [112].

Oproti situaci ve čtyřech dimenzích, ve vyšší dimenzi neplatí teorém o jednoznačnosti černých děr, tj. že nejobecnější stacionární černá díra v asymptoticky plochém vakuovém prostoročase je rotující díra s horizontem topologie S^2 popsaná Kerrovým řešením. Např. v pěti dimenzích je explicitně známo černoděrové řešení s 'toroidální' ($S^1 \times S^3$) topologií horizontu, tzv. *černý prstenec* (*black ring*) [124, 125]. Černý prstenec může být jak statický tak rotující. V obecném případě je k jeho stabilitě nutný membránový zdroj napnutý uvnitř prstence (analogie kosmické struny u C-metriky). Pro speciálně zvolenou rychlost rotace však lze zhruba řečeno vybalancovat gravitační sílu se silou odstředivou a membránu uvnitř prstence eliminovat. (Černý prstenec kupodivu souvisí na formální úrovni s čtyřdimenzionální C-metrikou diskutovanou v podkapitole 1.4: pro nerotující statický prstenec prostorovou část metriky tvoří euklidovská verze čtyřdimenzionální C-metriky.)

V pracích [9, 11] jsme provedli ultrarelativistickou limitu jak statického tak obecně rotujícího prstence v obecném směru vzhledem k ose prstence. Nalezli jsme konkrétní profilové funkce výsledných *pp*-vln a porovnali je s *pp*-vlnou získanou urychlením rotující černé díry [112]. Obě *pp*-vlny jsou pro obecnou volbu parametrů prstence různé. Shodují se pouze ve speciálním případě singulárního prstence, kdy jeho horizont vymizí a zbyde pouze prstencová singularita. Prostoročas singulárního prstence se však shoduje s prostoročasem získaným z Mayersovy-Perryho černé díry degenerovanou volbou parametrů již před ultrarelativistickou limitou a tak shoda výsledných *pp*-vln v tomto případě není překvapením.

Seznam publikací autora

[1]* Jiří Bičák, Pavel Krtouš: *Accelerated sources in de Sitter spacetime and the insufficiency of retarded fields*, Phys. Rev. D **64**, 124020 (2001).

[2]* Jiří Bičák, Pavel Krtouš: *The fields of uniformly accelerated charges in de Sitter spacetime*, Phys. Rev. Lett. **88**, 211101 (2002).

[3]* Pavel Krtouš, Jiří Podolský: *Radiation from accelerated black holes in a de Sitter universe*, Phys. Rev. D **68**, 024005 (2003).

[4]* Pavel Krtouš, Jiří Podolský, Jiří Bičák: *Gravitational and electromagnetic fields near a de Sitter-like infinity*, Phys. Rev. Lett. **91**, 061101 (2003).

[5]* Jiří Podolský, Marcello Ortaggio, Pavel Krtouš: *Radiation from accelerated black holes in an anti-de Sitter universe*, Phys. Rev. D **68**, 124004 (2004).

[6]* Pavel Krtouš, Jiří Podolský: *Gravitational and electromagnetic fields near an anti-de Sitter-like infinity*, Phys. Rev. D **69**, 084023 (2004).

[7]* Pavel Krtouš, Jiří Podolský: *Asymptotic directional structure of radiative fields in spacetimes with a cosmological constant*, Class. Quantum Grav. **21**, R233 (2004).

[8]* Pavel Krtouš, Jiří Podolský: *Asymptotic directional structure of radiation for fields of algebraic type D*, Czech. J. Phys. **55**, 119 (2005).

[9]* Marcello Ortaggio, Pavel Krtouš, Jiří Podolský: *Ultrarelativistic boost of the black ring*, Phys. Rev. D **71**, 124031 (2005).

[10]* Jiří Bičák, Pavel Krtouš: *Fields of accelerated sources: Born in de Sitter*, J. Math. Phys. **46**, 102504 (2005).

[11]* Marcello Ortaggio, Jiří Podolský, Pavel Krtouš: *Ultrarelativistic boost of spinning black rings*, J. High Energy Phys. JHEP12(2005)001 (2005).

[12]* Pavel Krtouš: *Accelerated black holes in an anti-de Sitter universe*, Phys. Rev. D **72**, 124019 (2005).

[13]* Pavel Krtouš, Jiří Podolský: *Asymptotic structure of radiation in higher dimensions*, předběžně přijato k publikaci v Class. Quantum Grav. (2005).

[14] Tomáš Kopf, Pavel Krtouš, Don N. Page: *Too Soon for Doom Gloom?* preprint `gr-qc/9407002` (1994).

[15] Pavel Krtouš. *Relationships between Scalar Field and Relativistic Particle Quantizations*, Ph.D. práce, 194 str. (University of Alberta, Edmonton, 1997).

[16] Pavel Krtouš: *Boundary quantum mechanics*, v Gravitation: Following the Prague Inspiration, Festschrift to J. Bičák, str. 289, ed. O. Semerák, J. Podolský, M. Žofka (World Scientific, Singapore, 2002).

[17] Jiří Bičák, Pavel Krtouš: *Radiative fields in spacetimes with Minkowski and de Sitter asymptotics*, v Recent Developments in Gravity, str. 3, ed. K. D. Kokkotas, N. Stergioulas (World Scientific, Singapore, 2003).

[18] Pavel Krtouš: *Covariant derivative on non-linear fiber bundles*, Czech. J. Phys. **54**, 273 (2004).

[19] Pavel Krtouš: *Sum-over-histories quantization of relativistic particle*, Class. Quantum Grav. **21**, 1519 (2004).

[20] Pavel Krtouš, Jiří Podolský: *Asymptotická struktura prostoročasů s kosmologickou konstantou*, Čs. čas. fyz. **55**, 94 (2005).

Nejdříve jsou uvedeny publikace, které jsou součástí této habilitační práce (označeny hvězdičkou *). Ty lze v plném znění nalézt v druhé části práce. Jinak je řazení chronologické. Většina z prací je též k dispozici na přiloženém CD.

Ostatní literatura

[21] T. Levi-Civita: *ds^2 einsteiniani in campi newtoniani*, Atti Accad. Naz. Lincei, Cl. Sci. Fis., Mat. Nat., Rend. **26**, 307 (1917).

[22] H. Weyl: *Bemerkung uber die axisymmetrischen losungen der Einsteinschen Gravitationsgleinchungen*, Ann. Phys. (Leipzig) **59**, 185 (1918).

[23] W. Kinnersley, M. Walker: *Uniformly accelerating charged mass in general relativity*, Phys. Rev. D **2**, 1359 (1970).

[24] A. Ashtekar, T. Dray: *On the Existence of Solutions to Einstein's Equation With Non-Zero Bondi News*, Commun. Math. Phys. **79**, 581 (1981).

[25] W. B. Bonnor: *The Sources of the Vacuum C-Metric*, Gen. Rel. Grav. **15**, 535 (1983).

[26] J. Plebański, M. Demiański: *Rotating charged and uniformly accelerated mass in general relativity*, Ann. Phys. (N.Y.) **98**, 98 (1976).

[27] B. Carter: *Hamilton-Jacobi and Schrodinger Separable Solutions of Einstein's Equations*, Commun. Math. Phys. **10**, 280 (1968).

[28] R. Debever: *On type D expanding solutions of Einstein-Maxwell equations*, Bull. Soc. Math. Belg. **23**, 360 (1971).

[29] R. Penrose, W. Rindler: *Spinors and Space-Time* (Cambridge University Press, Cambridge, England, 1984, 1986).

[30] R. M. Wald: *General Relativity* (The University of Chicago Press, Chicago and London, 1984).

[31] S. Hawking, R. Penrose: *The nature of space and time* (Princeton University Press, Princeton, 1996); český překlad: *Povaha prostoru a času* (Academia, Praha, 2000).

[32] R. Penrose: *Zero rest-mass fields including gravitation: asymptotic behaviour*, Proc. R. Soc. Lond., Ser A **284**, 159 (1965).

[33] R. Penrose: *Asymptotic properties of fields and space-times*, Phys. Rev. Lett. **10**, 66 (1963).

[34] M. Walker: *Block Diagrams and the Extension of Timelike Two-Surfaces*, J. Math. Phys. **11**, 2280 (1970).

[35] *Modern Cosmology in Retrospect*, edited by B. Bertotti, R. Balbinot, S. Bergia, A. Messina (Cambridge University Press, Cambridge, England, 1990).

[36] P. J. E. Peebles: *Principles of Physical Cosmology* (Princeton University Press, Princeton, 1993).

[37] S. M. Carroll: *The Cosmological Constant*, Living Rev. Rel. **4**, 1 (2001), URL (cited on November 2005):
`http://www.livingreviews.org/lrr-2001-1`.

[38] C. L. Bennett *et al.*: *First-Year Wilkinson Microwave Anisotropy Probe (WMAP) Observations: Preliminary Maps and Basic Results*, Astrophys. J. Suppl. **148**, 1 (2003).

[39] D. N. Spergel *et al.*: *First-Year Wilkinson Microwave Anisotropy Probe (WMAP) Observations: Determination of Cosmological Parameters*, Astrophys. J. Suppl. **148**, 175 (2003).

[40] N. D. Birrell, P. C. W. Davies: *Quantum Fields in Curved Space* (Cambridge University Press, Cambridge, England, 1982).

[41] M. Born: *Die Theorie des starren Elektrons in der Kinematik des Relativitätsprinzips*, Ann. Phys. (Leipzig) **30**, 1 (1909).

[42] E. Eriksen, Ø. Grøn: *Electrodynamics of Hyperbolically Accelerated Charges I, II, III*, Ann. Phys. (N.Y.) **286**, 320 (2000).

[43] C. W. Misner, K. S. Thorne, J. A. Wheeler: *Gravitation* (Freeman, San Francisco, 1973).

[44] S. W. Hawking, G. F. R. Ellis: *The Large Scale Structure of Space-Time* (Cambridge University Press, Cambridge, England, 1973).

[45] K. S. Thorne: *Černé díry a zborcený čas* (Mladá Fronta, Praha, 2004).

[46] A. Hamilton, *Falling Into a Black Hole*, 1998, URL:
`http://casa.colorado.edu/~ajsh/schw.shtml`.

[47] C. T. Bolton: *Identification of Cygnus X-1 with HDE 226868*, Nature **235**, 271 (1972).

[48] C. T. Bolton: *Cygnus X-1-Dimensions of the system*, Nature Phys. Sci. **240**, 124 (1972).

[49] R. Schödel *et al.*: *A star in a 15.2-year orbit around the supermassive black hole at the centre of the Milky Way*, Nature **419**, 694 (2002).

[50] J. Ehlers, W. Kundt: *Exact Solutions of the Gravitational Field Equations*, in *Gravitation: an Introduction to Current Research*, edited by L. Witten (John Wiley, New York, 1962), pp. 49–101.

[51] J. Bičák, B. G. Schmidt: *Asymptotically flat radiative space-times with boost-rotation symmetry: the general structure*, Phys. Rev. D **40**, 1827 (1989).

[52] J. Bičák, V. Pravda: *Spinning C-metric: Radiative specetime with accelerating, rotating black holes*, Phys. Rev. D **60**, 044004 (1999).

[53] P. S. Letelier, S. R. Oliveira: *On Uniformly Accelerated Black Holes*, Phys. Rev. D **64**, 064005 (2001).

[54] V. Pravda, A. Pravdová: *Boost-rotation symmetric spacetimes — review*, Czech. J. Phys. **50**, 333 (2000).

[55] K. Hong, E. Teo: *A new form of the C-metric*, Class. Quantum Grav. **20**, 3269 (2003).

[56] K. Hong, E. Teo: *A new form of the rotating C-metric*, Class. Quantum Grav. **22**, 109 (2005).

[57] J. B. Griffiths, J. Podolsky: *Accelerating and rotating black holes*, Class. Quantum Grav. **22**, 3467 (2005).

[58] J. Podolský, J. B. Griffiths: *Uniformly accelerating black holes in a de Sitter universe*, Phys. Rev. D **63**, 024006 (2001).

[59] O. J. C. Dias, J. P. S. Lemos: *Pair of accelerated black holes in a de Sitter background: The dS C metric*, Phys. Rev. D **67**, 084018 (2003).

[60] J. Podolský: *Accelerating black holes in anti-de Sitter universe*, Czech. J. Phys. **52**, 1 (2002).

[61] O. J. C. Dias, J. P. S. Lemos: *Pair of accelerated black holes in an anti-de Sitter background: The AdS C metric*, Phys. Rev. D **67**, 064001 (2003).

[62] O. J. C. Dias, J. P. S. Lemos: *The extremal limits of the C-metric: Nariai, Bertotti-Robinson and anti-Nariai C-metrics*, Phys. Rev. D **68**, 104010 (2003).

[63] R. Emparan, G. T. Horowitz, R. C. Myers: *Exact description of black holes on branes*, JHEP **01**, 007 (2000).

[64] A. Chamblin: *Capture of bulk geodesics by brane-world black holes*, Class. Quantum Grav. **18**, L17 (2001).

[65] R. Emparan, G. T. Horowitz, R. C. Myers: *Exact description of black holes on branes II: Comparison with BTZ black holes and black strings*, JHEP **01**, 021 (2000).

[66] J. Bičák: *Gravitational radiation from uniformly accelerated particles in general relativity*, Proc. R. Soc. Lond., Ser A **302**, 201 (1968).

[67] J. Bičák, A. Pravdová: *Symmetries of asymptotically flat electrovacuum spacetimes and radiation*, J. Math. Phys. **39**, 6011 (1998).

[68] J. A. Valiente Kroon: *On Killing vector fields and Newman-Penrose constants*, J. Math. Phys. **41**, 898 (2000).

[69] J. Bičák: *Selected Solutions of Einstein's Field Equations: Their Role in General Relativity and Astrophysics*, in *Einstein's Field Equations and Their Physical Implications*, edited by B. G. Schmidt (Springer, Berlin, 2000), Vol. 540, pp. 1–126.

[70] J. Bičák: *Radiative spacetimes: exact approaches*, in *Relativistic Gravitation and Gravitational Radiation, Les Houches 1995*, edited by J. A. Marck, J. P. Lasota (Cambridge University Press, Cambridge, England, 1997), pp. 67–87.

[71] J. Bičák: *Exact radiative spacetimes: some recent developments*, Annalen Phys. **9**, 207 (2000).

[72] J. Frauendiener, M. Hein: *Numerical evolution of axisymmetric, isolated systems in general relativity*, Phys. Rev. D **66**, 124004 (2002).

[73] R. Emparan: *Pair creation of black holes joined by cosmic strings*, Phys. Rev. Lett. **75**, 3386 (1995).

[74] R. B. Mann: *Pair production of topological anti-de Sitter black holes*, Class. Quantum Grav. **14**, L109 (1997).

[75] O. J. C. Dias, J. P. S. Lemos: *Pair creation of de Sitter black holes on a cosmic string background*, Phys. Rev. D **69**, 084006 (2004).

[76] O. J. C. Dias: *Pair creation of anti-de Sitter black holes on a cosmic string background*, Phys. Rev. D **D70**, 024007 (2004).

[77] A. Vilenkin, E. P. S. Shellard: *Cosmic Strings and other Topological Defects* (Cambridge University Press, Cambridge, England, 1994).

[78] F. J. Ernst: *Removal of the nodal singularity of the C-metric*, J. Math. Phys. **17**, 515 (1976).

[79] J. Bičák, C. Hoenselaers, B. Schmidt: *The solutions of the Einstein equations for uniformly accelerated particles without nodal singularities II. Self-accelerating particles*, Proc. R. Soc. Lond., Ser A **390**, 397 (1983).

[80] J. Bičák, C. Hoenselaers, B. Schmidt: *The solutions of the Einstein equations for uniformly accelerated particles without nodal singularities I. Freely falling particles in external fields*, Proc. R. Soc. Lond., Ser A **390**, 411 (1983).

[81] R. Penrose: *Conformal treatment of infinity*, in *Relativity, Groups and Topology, Les Houches 1963*, edited by C. DeWitt, B. DeWitt (Gordon and Breach, New York, 1964), pp. 563–584.

[82] H. Friedrich: *Existence and structure of past asymptotically simple solutions of Einstein's field equations with positive cosmological constant*, J. Geom. Phys. **3**, 101 (1986).

[83] H. Friedrich: *Einstein's Equation and Geometric Asymptotics*, in *Gravitation and Relativity: At the turn of the Millenium (Proceedings of the GR-15 conference)*, edited by N. Dadhich, J. Narlikar (Inter-University Centre for Astronomy and Astrophysics Press, Pune, 1998).

[84] H. Friedrich: *On the global existence and the asymptotic behavior of solutions to the Einstein-Maxwell-Yang-Mills equations*, J. Diff. Geom. **34**, 275 (1991).

[85] H. Friedrich: *Einstein equations and conformal structure: existence of anti-de Sitter-type space-times*, J. Geom. Phys. **17**, 125 (1995).

[86] H. Friedrich: *Conformal Einstein Evolution*, in *The Conformal Structure of Space-Time: Geometry, Analysis, Numerics*, edited by J. Frauendiener, H. Friedrich (Springer, Berlin, 2002), Vol. 604, pp. 1–50.

[87] J. Frauendiener: *Conformal Infinity*, Liv. Rev. Rel. **7**, 2004 (2004), URL (cited on November 2005): http://www.livingreviews.org/lrr-2004-1/.

[88] A. Einstein: *Näherungsweise Integration der Feldgleichungen der Gravitation*, Preuss. Akad. Wiss. Sitz. 688 (1916).

[89] A. Einstein: *Über Gravitationwellen*, Preuss. Akad. Wiss. Sitz. 154 (1918).

[90] J. Bičák: *Radiative properties of spacetimes with the axial and boost symmetries*, in *Gravitation and Geometry (A volume in honour of Ivor Robinson)*, edited by W. Rindler, A. Trautman (Bibliopolis, Naples, 1987), pp. 55–69.

[91] H. Stephani *et al.*: *Exact Solutions of Einstein's Field Equations, Second Edition* (Cambridge University Press, Cambridge, England, 2003).

[92] J. Bičák: *On exact radiative solutions representing finite sources*, in *Galaxies, Axisymmetric Systems and Relativity*, edited by M. A. H. MacCaluum (Cambridge University Press, Cambridge, England, 1985), pp. 91–124.

[93] W. B. Bonnor, J. B. Griffiths, M. A. H. MacCallum: *Physical Interpretation of Vacuum Solutions of Einstein's Equations. Part II. Time-dependent Solutions*, Gen. Rel. Grav. **26**, 687 (1994).

[94] J. Bičák, P. Krtouš: *Radiative fields in spacetimes with Minkowski and de Sitter asymptotics*, in *Recent Developments in Gravity (Proceedings of 10th Greek Relativity Meeting, Chalkidiki, May 2002)*, edited by K. D. Kokkotas, N. Stergioulas (World Scientific, Singapore, 2003), pp. 3–25.

[95] H. Bondi: *Gravitational waves in general relativity*, Nature **186**, 535 (1960).

[96] H. Bondi, M. G. J. van der Burg, A. W. K. Metzner: *Gravitational waves in general relativity: VII. Waves from axi-symmetric isolated systems*, Proc. R. Soc. Lond., Ser A **269**, 21 (1962).

[97] R. K. Sachs: *Gravitational waves in general relativity: VII. Waves in asymptotically flat space-time*, Proc. R. Soc. Lond., Ser A **270**, 103 (1962).

[98] R. K. Sachs: *Aymptotic Symmetries in Gravitational Theory*, Phys. Rev. **128**, 2851 (1962).

[99] F. A. E. Pirani: *Introduction to gravitational radiation theory*, in *Brandeis Lectures on General Relativity*, edited by S. Deser, K. W. Ford (Prentice-Hall, Englewood Cliffs, NJ, 1965), pp. 249–372.

[100] R. Penrose: *Structure of Space-Time*, in *Battelle Recontres*, edited by B. DeWitt, J. A. Wheeler (Benjamin, New York, 1968), pp. 121–235.

[101] R. Sachs: *Gravitational waves in general relativity: VI. The outgoing radiation condition*, Proc. R. Soc. Lond., Ser A **264**, 309 (1961).

[102] E. T. Newman, R. Penrose: *An Approach to Gravitational Radiation by a method of Spin Coefficients*, J. Math. Phys. **3**, 566 (1962).

[103] J. N. Goldberg, R. P. Kerr: *Asymptotic Properties of the Electromagnetic Field*, J. Math. Phys. **5**, 172 (1964).

[104] A. Ashtekar, A. Magnon: *Asymptotically anti-de Sitter space-times*, Class. Quantum Grav. **1**, L39 (1984).

[105] A. Ashtekar, S. Das: *Asymptotically anti-de Sitter spacetimes: conserved quantities*, Class. Quantum Grav. **17**, L17 (2000).

[106] R. Penrose: *Cosmological boundary conditions for zero rest-mass fields*, in *The Nature of Time*, edited by T. Gold (Cornell University Press, Ithaca, New York, 1967), pp. 42–54.

[107] A. Z. Petrov: *Classification of spaces defined by gravitational fields*, Sci. Not. Kazan. State Univ. **114**, 55 (1954).

[108] H. Friedrich: *Einstein's Equation and Conformal Structure*, in *The Geometric Universe: Science, Geometry, and the Work of Roger Penrose*, edited by S. A. Huggett *et al.* (Oxford University Press, Oxford, 1998), pp. 81–98.

[109] A. Coley, R. Milson, V. Pravda, A. Pravdová: *Classification of the Weyl Tensor in Higher Dimensions*, Class. Quantum Grav. **21**, L35 (2004).

[110] R. Milson, A. Coley, V. Pravda, A. Pravdová: *Alignment and algebraically special tensors in Lorentzian geometry*, Int. J. Geom. Meth. Mod. Phys. **2**, 41 (2005).

[111] P. C. Aichelburg1, R. U. Sexl: *On the gravitational field of a massless particle*, Gen. Rel. Grav. **2**, 303 (1971).

[112] H. Yoshino: *Lightlike limit of the boosted Kerr black holes in higher-dimensional spacetimes*, Phys. Rev. D **71**, 044032 (2005).

[113] R. Penrose: *A spinor approach to general relativity*, Ann. Phys. (N.Y.) **10**, 171 (1960).

[114] D. Amati, C. K. k: *Strings in a shock wave background and generation of curved geometry from flat space string theory*, Phys. Lett. **B210**, 92 (1988).

[115] H. J. de Vega, N. Sánchez: *Quantum string scattering in the Aichelburg-Sexl geometry*, Nucl. Phys. **B317**, 706 (1989).

[116] V. Pravda, A. Pravdová, A. Coley, R. Milson: *All spacetimes with vanishing curvature invariants*, Class. Quantum Grav. **19**, 6213 (2002).

[117] A. Coley *et al.*: *Generalizations of pp-wave spacetimes in higher dimensions*, Phys. Rev. D **67**, 104020 (2003).

[118] A. Coley, R. Milson, V. Pravda, A. Pravdová: *Vanishing Scalar Invariant Spacetimes in Higher Dimensions*, Class. Quantum Grav. **21**, 5519 (2004).

[119] C. Loustó, N. Sánchez: *The curved shock wave space-time of ultrarelativistic charged particles and their scattering*, Int. J. Mod. Phys. A **5**, 915 (1990).

[120] V. Cardoso, E. Berti, M. Cavagliá: *What we (dont) know about black hole formation in high-energy collisions*, Class. Quantum Grav. **22**, L61 (2005).

[121] R. C. Myers, M. J. Perry: *Black holes in higher dimensional space-times*, Ann. Phys. (N.Y.) **172**, 304 (1986).

[122] G. W. Gibbons, H. Lü, D. N. Page, C. N. Pope: *Rotating Black Holes in Higher Dimensions with a Cosmological Constant*, Phys. Rev. Lett. **93**, 171102 (2004).

[123] G. W. Gibbons, H. Lü, D. N. Page, C. N. Pope: *The General Kerr-de Sitter Metrics in All Dimensions*, J. Geom. Phys. **53**, 49 (2005).

[124] R. Emparan, H. S. Reall: *A rotating black ring in five dimensions*, Phys. Rev. Lett. **88**, 101101 (2002).

[125] R. Emparan, H. S. Reall: *Generalized Weyl solutions*, Phys. Rev. D **65**, 084025 (2002).

Publikace jsou řazeny v pořadí výskytu v textu.

Obsah přiloženého CD

K habilitační práci je přiloženo CD obsahující některé doplňkové materiály. Výchozím bodem k prohlídce těchto materiálů je soubor `index.html` ve vrchním adresáři disku. Ten obsahuje následující přehled:

Habilitační práce
: Elektronická podoba této práce v několika formátech, včetně 'originálních' elektronických verzí přiložených prací.

Příloha *Černé díry*
: Digitální příloha popisovaná v textu habilitace. Tato příloha obsahuje třídimenzionální obrázky, interaktivní diagramy a animace vizualizující kauzální strukturu prostoročasů s černými dírami.

Publikace
: Elektronická podoba většiny prací uvedených v seznamu na str. 61.

Studijní texty
: Některé studijní texty vypracované k přednáškám „Proseminář teoretické fyziky" a „Geometrické metody teoretické fyziky", které vedu na MFF UK. Zejména se jedná o rozsáhlý text přibližující diferenciální geometrii pro fyziky.

Popularizace
: Dva popularizační a výukové projekty: prezentace objasňující vztah nerelativistického a relativistického chápání prostoru a času, a program sloužící k ilustraci a vysvětlení relativistického paradoxu dvojčat a k diskuzi vztahu červích děr a tzv. strojů času.

Těmto bodům odpovídají na disku i jednotlivé adresáře `habilitace`, `cerne_diry`, `publikace`, `studijni_texty` a `popularizace`.

Pár poznámek k obsahu CD

Příloha *Černé díry*

Příloha *Černé díry* obsahuje odborně nejzajímavější materiál ilustrující mnohé výsledky popsané v kapitole 1. Tento materiál je zde uveřejněn v ucelené formě poprvé – pro svoji interaktivní povahu ho bohužel nelze publikovat v tištěném časopise.

Příloha obsahuje schematické třídimenzionální zobrazení různých prostoročasů s černými dírami. Jedná se o kompaktifikované zobrazení okolí černých děr, naznačující zejména kauzální strukturu těchto oblastí. Je zde zobrazen jak triviální Minkowského prostoročas a asymptoticky plochý prostoročas obsahující statickou černou díru, tak prostoročasy s urychlenými dírami s Minkowského a anti-de Sitterovou asymptotikou. Prezentace umožňuje zobrazovat prostoročas v různých náhledech a ukazuje, jakým způsobem jsou do třídimenzionálních diagramů vnořeny privilegované dvoudimenzionální řezy.

Průvodce ovládáním přílohy je uveden v podkapitole 1.4, v oddíle na str. 36.

Studijní texty

K habilitační práci jsou přiloženy některé studijní texty, které používám při přednáškách vedených na MFF UK. Lze zde nalézt:

- *Přehled vlastností křivočarých souřadnic*
  Jedná se o soubor tabulek shrnujících geometrické vlastnosti ortonormálních systémů v euklidovské rovině a prostoru. Jsou zde tabelovány transformační vztahy, Lamého koeficienty, souřadnicové vektory a tvary vektorových operátorů pro nejběžnější 'rodiny' souřadnic – pro cylindrické, sférické, eliptické, parabolické a bipolární souřadnice. Texty jsou určeny pro „Proseminář teoretické fyziky II" vyučovaný v druhém ročníku studia fyziky.

- *Distribuční kuchařka v* $\mathbb{R}$ *a* E^3
  Text určený pro stejný proseminář, obsahující stručné zavedení distribucí na reálných číslech a v euklidovském prostoru s aplikacemi ve fyzice. V jedné dimenzi se text zaměřuje na zavedení distribucí a operací s nimi, na regularizaci lokálně neintegrovatelných funkcí a na využití distribucí při Fourierově transformaci. Ve třech dimenzích je důraz kladen na popis distribucí se singulárním nosičem, tj. distribucí lokalizovaných v bodě, na křivce či na ploše, a na jejich využití v teorii elektromagnetického pole.

- *Geometrické metody ve fyzice*
  Tento rozsáhlejší text tvoří základ vznikajících skript k výběrové přednášce „Geometrické metody teoretické fyziky" určené pro magisterské studium teoretické fyziky. Jedná se o přehled diferenciální geometrie s důrazem na aplikace v teoretické mechanice, obecné teorii relativity a kalibrační teorii pole. V současnosti text obsahuje pět kapitol a pokrývá tak většinu první části zamýšlených skript týkající se zejména zavedení variet a riemanovské geometrie. (Druhá část skript by měla pokrývat teorii fibrovaných prostorů užívanou v teorii kalibračních polí.)

Popularizace

Tato část obsahuje dva projekty popularizující speciální teorii relativity.

Prezentace *Speciální teorie relativity a žížalí farma* na populární úrovni vysvětluje vztah newtonovského a relativistického chápání prostoru a času. Vztah těchto dvou přístupů je vykládán na smyšleném příkladu žížalího světa - modelu, který využívá pouze středoškolské znalosti euklidovské geometrie a přitom do velké míry vystihuje myšlenkový skok mezi klasickou a relativistickou fyzikou.

Program *Výlet ke hvězdám* obsahuje dvě aplikace: *Paradox dvojčat* a *Stroj času*. Jedná se o program, který byl vytvořen k populární přednášce o 'strojích času'.

Aplikace *Paradox dvojčat* slouží k modelování paradoxu dvojčat na příkladu letu kosmické lodi ze Země k Alfa Centauri A a zpět. Interaktivní formou se zde zájemce může seznámit s různými aspekty relativistického popisu a pomocí různých pohledů na vysvětlovaný jev získat intuici v situacích, se kterými se při běžných rychlostech a rozměrech nesetká.

Aplikace *Stroj času* ukazuje, jak lze pomocí tzv. červí díry a paradoxu dvojčat vytvořit stroj času. Tato část byla připravena jako ilustrace k přednášce jež vysvětluje postoj současné teoretické fyziky k velmi oblíbenému tématu vědeckofantastické literatury, k tzv. strojům času (zařízením umožňujícím návrat do vlastní minulosti). Přednáška ukazuje na koncepční problémy při formulaci takovéto kauzální situace a shrnuje fyzikálně podložené argumenty týkající se její přípustnosti či nepřípustnosti. Přiložený program dokumentuje, že existence červích děr (topologických zkratek v prostoročase) s sebou nevyhnutelně nese i možnost existence strojů času.

Část II

Soubor publikací zahrnutých do habilitační práce

PHYSICAL REVIEW D, VOLUME 64, 124020

Accelerated sources in de Sitter spacetime and the insufficiency of retarded fields

Jiří Bičák* and Pavel Krtouš†
Institute of Theoretical Physics, Faculty of Mathematics and Physics, Charles University, V Holešovičkách 2, 180 00 Prague 8, Czech Republic

(Received 7 June 2001; published 28 November 2001)

The scalar and electromagnetic fields produced by the geodesic and uniformly accelerated discrete charges in de Sitter spacetime are constructed by employing the conformal relation between de Sitter and Minkowski space. Special attention is paid to new effects arising in spacetimes which, like de Sitter space, have *spacelike* conformal infinities. Under the presence of particle and event horizons, purely retarded fields (appropriately defined) become necessarily singular or even cannot be constructed at the ''creation light cones''—future light cones of the ''points'' at which the sources ''enter'' the universe. We construct smooth (outside the sources) fields involving both retarded and advanced effects, and analyze the fields in detail in case of (i) scalar monopoles, (ii) electromagnetic monopoles, and (iii) electromagnetic rigid and geodesic dipoles.

DOI: 10.1103/PhysRevD.64.124020 PACS number(s): 04.20.Cv, 04.40.−b, 98.80.Hw

I. INTRODUCTION

The de Sitter 1917 solution of the vacuum Einstein equations with a positive cosmological constant Λ, in which freely moving test particles accelerate away from one another, played a crucial role in the acceptance of expanding standard cosmological models at the end of the 1920s [1,2]. It reappeared as the basic arena in steady-state cosmology in the 1950s, and it has been resurrected in cosmology again in the context of inflationary theory since the 1980s [2]. de Sitter spacetime represents the ''asymptotic state'' of cosmological models with $\Lambda>0$ [3].

Since de Sitter space shares with Minkowski space the property of being maximally symmetric but has a nonvanishing constant positive curvature and nontrivial global properties, it has been widely used in numerous works studying the effects of curvature in quantum field theory and particle physics (see, e.g., Ref. [4] for references). Recently, its counterpart with a constant negative curvature, anti–de Sitter space, has received much attention again from quantum field and string theorists (e.g., Ref. [5]).

These three maximally symmetric spacetimes of constant curvature also played a most important role in gaining many valuable insights in mathematical relativity. For example, both the particle (cosmological) horizons and the event horizons for geodesic observers occur in de Sitter spacetime, and the Cauchy horizons in anti–de Sitter space (e.g., Ref. [6]). The existence of the past event horizons of the world lines of sources producing fields on de Sitter background is of crucial significance for the structure of the fields.

The existence of the particle and event horizons is intimately related to the fact that de Sitter spacetime has, in contrast with Minkowski spacetime, two *spacelike* infinities—past and future—at which all timelike and null worldlines start and end [6]. Since the pioneering work of Penrose [7,8] it has been well known that Minkowski, de Sitter, and anti–de Sitter spacetimes, being conformally flat, can be represented as parts of the (conformally flat) Einstein static universe. However, the causal structure of these three spaces is globally very different. The causal character of the conformal boundary $\mathcal{I}$ to the physical spacetime that represents the endpoints at infinity reached by infinitely extended null geodesics, depends on the sign of Λ. In Minkowski space, these are *null* hypersurfaces—future and past null infinity, $\mathcal{I}^+$ and $\mathcal{I}^-$. In de Sitter space, both $\mathcal{I}^+$ and $\mathcal{I}^-$ are *spacelike*; in anti–de Sitter space the conformal infinity $\mathcal{I}$ is not the disjoint union of two hypersurfaces, and it is timelike.

Towards the end of his 1963 Les Houches lectures [9], Penrose discusses briefly the zero rest-mass-free fields with spin s in cosmological (not necessarily de Sitter) backgrounds. At a given point P, not too far from $\mathcal{I}^-$, say, the field can be expressed as an integral over quantities defined on the intersection of the past null cone of P and $\mathcal{I}^-$ (''free incoming radiation field'') plus contributions from sources whose worldlines intersect the past null cone. However, the concept of ''incoming radiation field'' at $\mathcal{I}^-$ depends on the position of P if $\mathcal{I}^-$ is spacelike [9,10]. If there should be no incoming radiation at $\mathcal{I}^-$ with respect to all ''origins P,'' all components of the fields must vanish at $\mathcal{I}^-$. Imagine that spacelike $\mathcal{I}^-$ is met by the worldlines of discrete sources. Then there will be points P near $\mathcal{I}^-$ whose past null cones will not cross the worldlines—see Fig. 1. The field at P should vanish if an incoming field is absent. This, however, is not possible since the ''Coulomb-type'' part of the field of the sources cannot vanish there (as follows from Gauss's law). Penrose [9] thus concludes that ''if there is a particle horizon, then purely retarded fields of spin $s>\frac{1}{2}$ do not exist for general source distributions.''[1] (The restriction on s follows from the number of arbitrarily specifiable initial data for the field with spin s—see Ref. [9].) Penrose also emphasized that the result depends on the definition of advanced and retarded fields, and ''the application of the result to actual physical models is not at all clear cut . . . .'' This ob-

*Email address: bicak@mbox.troja.mff.cuni.cz
†Email address: Pavel.Krtous@mff.cuni.cz

[1]The corresponding result holds for spacelike $\mathcal{I}^+$ and advanced fields.

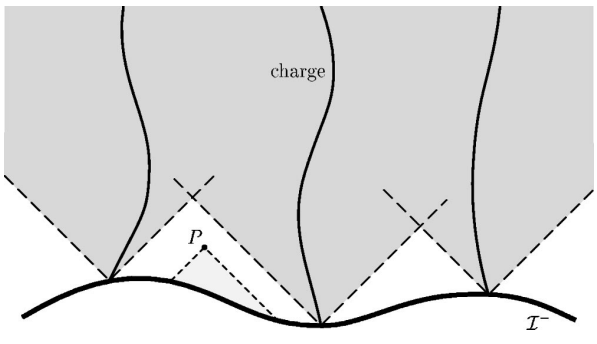

FIG. 1. Fields at spacelike $\mathcal{I}^-$. When past infinity $\mathcal{I}^-$ is spacelike, and some discrete sources ''enter'' the spacetime, then incoming fields must necessarily be present at $\mathcal{I}^-$ and also at such points as *P*, the past null cones of which are not crossed by the worldlines of the sources. If this is not the case, inconsistencies arise. The past null cone of *P* is shaded in light gray, whereas the future domain of influence of sources is shaded in dark gray. (Figure taken after Penrose [9].)

servation was reported in somewhat more detail at the meeting on ''the nature of time'' [11], with an appended discussion (in which, among others, Bondi, Feynman, and Wheeler participated) but technically it was not developed further since 1963. In a much later monograph Penrose and Rindler [10] discuss (see p. 363 in Vol. II) the fact that the radiation field is ''less invariantly'' defined when $\mathcal{I}$ is spacelike than when it is null, but no comments or references are given there on the absence of ''purely retarded fields.''

One of the purposes of this paper is to study the properties of fields of pointlike sources ''entering'' the de Sitter universe across spacelike $\mathcal{I}^-$. We thus provide a specific physical model on which Penrose's observation can be demonstrated and analyzed. We assume the sources and their fields to be weak enough so that they do not change the de Sitter background.

In de Sitter space we identify retarded (advanced) fields of a source as those which are in general nonvanishing only in the future (past) domain of influence of the source. As a consequence, purely retarded (advanced) fields have to vanish at the past (future) infinity. Adopting this definition we shall see that indeed purely retarded fields produced by pointlike sources cannot be smooth or even do not exist. We find this general conclusion to be true not only for charges (monopoles and dipoles) producing electromagnetic fields ($s=1$) but, to some degree, also for scalar fields ($s=0$) produced by scalar charges.

In general, purely retarded fields of monopoles and dipoles become singular on the past horizons (''creation light cones'') of the particle's worldlines. A ''shock-wave-type'' singularity at the particle's creation light cone can be understood similarly to a Cauchy horizon instability inside a black hole (see, e.g., Ref. [12]); an observer crossing the creation light cone sees an infinitely long history of the source in a finite interval of proper time. In the scalar field case (not considered by Penrose) no ''Gaussian-type'' constraints exist and retarded fields can be constructed. However, we shall see that the strength of the retarded field (the gradient of the field) of a scalar monopole has a δ-function character on the creation light cone so that, for example, its energy-momentum tensor cannot be evaluated there. In the electromagnetic case it is not even posible to construct a purely retarded field of a single monopole—one has to allow additional sources on the creation light cone to find a consistent retarded solution vanishing outside the future domain of influence of the sources.

In both our somewhat different explanation of the nonexistence of purely retarded fields of general sources, and in Penrose's original discussion, the main cause of difficulties is the spacelike character of $\mathcal{I}^-$ and the consequential existence of the past horizons, respectively, ''creation light cones.''

It was only after we constructed the various types of fields produced by sources on de Sitter background and analyzed their behavior that we noticed Penrose's general considerations in Ref. [9]. Our original motivation has been to understand fields of accelerated sources, and in particular, the electromagnetic field of uniformly accelerated charges in de Sitter spacetime. The question of electromagnetic field and its radiative properties produced by a charge with hyperbolic motion in Minkowski spacetime has perhaps been one of the most discussed ''perpetual problems'' of classical electrodynamics, if not of all classical physics in the 20th century. Here let us only notice that the December 2000 issue of Annals of Physics contains the series of three papers (covering 80 pp.) by Eriksen and Grøn [13], which study in depth and detail various aspects of ''electrodynamics of hyperbolically accelerated charges''; the papers also contain many (though not all) references on the subject.

The electromagnetic field of a uniformly accelerated charge along the *z* axis, say, is symmetrical not only with respect to the rotations around the axis, but also with respect to the boosts along the axis. Now spacetimes with boost-rotation symmetry play an important role in full general relativity (see, e.g., Ref. [14], and references therein). They represent the only explicitly known exact solutions of the Einstein vacuum field equations, which describe moving ''objects''—accelerated singularities or black holes—emitting gravitational waves, and which are asymptotically flat in the sense that they admit global, though not complete, smooth null infinity $\mathcal{I}^-$. Their radiative character is best manifested in a nonvanishing Bondi's news function, which is an analog of the radiative part of the Poynting vector in electrodynamics. The general structure of all vacuum boost-rotation symmetric spacetimes with hypersurface orthogonal Killing vectors was analyzed in detail in Ref. [15]. One of the best known examples is the *C*-metric, describing uniformly accelerated black holes attached to conical singularities (''cosmic strings'' or ''struts'') along the axis of symmetry.

There exists also the generalization of the *C*-metric including a nonvanishing Λ [16]. It has been used to study the pair creation of black holes [17]; its interpretation as uniformly accelerating black holes in a de Sitter space has been discussed recently [18]. However, no general framework is available to analyze the whole class of boost-rotation symmetric spacetimes, which are asymptotically approaching a

de Sitter (or anti–de Sitter) spacetime as it is given in Ref. [15] for $\Lambda=0$. Before developing such a framework in full general relativity, we wish to gain an understanding of fields produced by (uniformly) accelerated sources in a de Sitter background. This has been our original motivation for this work.

Although it has been widely known and used in various contexts that there exists a conformal transformation between de Sitter and Minkowski spacetimes, this fact does not seem to be employed for constructing the fields of specific sources. In the following we make use of this conformal relation to find scalar and electromagnetic fields of the scalar and electric charges in de Sitter spacetime.

The plan of the paper is as follows. In Sec. II, we will analyze the behavior of scalar and electromagnetic field equations with source terms under general conformal transformations. Few points contained here appear to be new, like the behavior of scalar sources in a general, *n*-dimensional spacetime, but the main purpose of this section is to review results and introduce notation needed in subsequent parts. In Sec. III, the compactification of Minkowski and de Sitter spacetimes and their conformal properties are discussed. Again, all main ideas are known, especially from works of Penrose. But we need the detailed picture of the complete compactification of both spaces and explicit formulas connecting them in various coordinate systems, in order to be able to ''translate'' appropriate motion of the sources and their fields from Minkowski into de Sitter spacetime. The worldlines of uniformly accelerated particles in de Sitter space are defined, found, and their relation to the corresponding worldlines in Minkowski space under the conformal mapping is discussed in Sec. IV. In general, a single worldline in Minkowski space gets transformed into two worldlines in de Sitter space.

In Sec. V, by using the conformal transformation of simple boosted spherically symmetric fields of sources in Minkowski spacetime, we construct the fields of uniformly accelerated monopole sources in de Sitter spacetime. In particular, with both the scalar and electromagnetic fields, we obtain what we call ''symmetric fields.'' They are analytic everywhere outside the sources and can be written as a linear combination of retarded and advanced fields from both particles. From the symmetric fields we wish to construct purely retarded fields that are nonvanishing only in the future domain of influence of particles' worldlines. For the scalar field, this is accomplished in Sec. VI. We do find the retarded field, but its strength contains a δ-function term located on the particle's past horizon (creation light cone). In Sec. VII, the retarded electromagnetic fields are analyzed for free (unaccelerated) monopoles (Sec. VII A), for ''rigid dipoles'' (Sec. VII C), consisting of two close, uniformly accelerated charges of opposite sign, and for ''geodesic dipoles'' (Sec. VII D), made of two free opposite charges moving along geodesics. In Sec. VII B the role of the contraints, which electromagnetic fields and charges have to satisfy on any spacelike hypersurface, is emphasized. These constraints in de Sitter space with compact spatial slicings require the total charge to be zero. As is well known, there can be no net charge in a closed universe (see, e.g., Ref. [19]). However, we find out that the constraints imply even *local* conditions on the charge distribution if $\mathcal{I}^-$ is spacelike and purely retarded fields are only admitted. In the case of an unaccelerated electromagnetic monopole, we discover that the solution resembling retarded field represents not only the monopole charge but also a spherical shell of charges moving with the velocity of light along the creation light cone of the monopole. The total charge of the shell is precisely opposite to that of the monopole. Retarded fields of both rigid and geodesic dipoles blow up along the creation light cone since, by restricting ourselves to the fields nonvanishing in the future domain of influence, we ''squeeze'' the field lines produced by the dipoles into their past horizon (creation light cone).

We do not discuss the radiative character of the fields obtained. The problem of radiation is not a straightforward issue since the conformal transformation does not map an infinity onto an infinity and, thus, one has to analyze carefully the falloff (''the peeling off'') of the fields along appropriate null geodesics going to future, respectively, past spacelike infinity. A detailed discussion of the radiative properties of the solutions found here and of some additional fields will be given in a forthcoming publication [24].

A brief discussion in Sec. VIII concludes the paper. Some details concerning coordinate systems on de Sitter space are relegated to the Appendix.

II. CONFORMAL INVARIANCE OF SCALAR AND ELECTROMAGNETIC FIELD EQUATIONS WITH SOURCES

Conformal rescaling of metric is given by a common spacetime dependent conformal factor $\Omega(x)$:

$$g_{\alpha\beta}\rightarrow\hat{g}_{\alpha\beta}=\Omega^2 g_{\alpha\beta}, \quad g^{\alpha\beta}\rightarrow\hat{g}^{\alpha\beta}=\Omega^{-2}g^{\alpha\beta}. \tag{2.1}$$

An equation for a physical field Ψ is called conformally invariant if there exists a number— *conformal weight*— $p\in\mathbb{R}$ such that $\hat{\Psi}=\Omega^p\Psi$ solves a field equation with metric $\hat{g}$, if and only if Ψ is a solution of the original equation with metric g.

It is well known (see, e.g., Ref. [20]) that (i) the wave equation for a scalar field Φ can be generalized in a conformally invariant way to curved *n*-dimensional spacetime geometry by a suitable coupling with the scalar curvature R, and (ii) the vacuum Maxwell's equations are conformally invariant in four dimensions with conformal weight $p=0$ of covariant components (2-form) of electromagnetic field $F_{\alpha\beta}$, but they fail to be conformally invariant for dimensions $n\neq 4$.

The behavior of the above equations with sources is not so widely known (cf. Ref. [10,21] for the electromagnetic case). It is, however, easy to see that the wave equation for the scalar field Φ with the scalar charge source S,

$$[\Box-\xi R]\Phi=S, \tag{2.2}$$

where in n dimensions $\xi=\frac{1}{4}(n-2)/(n-1)$, R is the scalar curvature, and $\Box=g^{\alpha\beta}\nabla_\alpha\nabla_\beta$ is the d'Alembertian con-

structed from the covariant metric derivative ∇_α, under the conformal rescaling Eq. (2.1) goes over into the equation of the same form

$$[\hat{\Box} - \xi \hat{R}]\hat{\Phi} = \hat{S}, \tag{2.3}$$

provided that

$$\Phi \to \hat{\Phi} = \Omega^{1-(n/2)}\Phi, \tag{2.4}$$

$$S \to \hat{S} = \Omega^{-1-(n/2)}S, \tag{2.5}$$

and $\hat{\nabla}_\alpha$ and $\hat{R}$ are the metric covariant derivative and scalar curvature associated with the rescaled metric $\hat{g}$ [see, e.g., Eqs. (D.1)–(D.14) in Ref. [20]].

Next, it is easy to demonstrate that in four dimensions Maxwell's equations with a source given by a four-current J^α,

$$\nabla_\mu F^{\alpha\mu} = J^\alpha,$$

$$\nabla_{[\alpha} F_{\beta\gamma]} = 0 \quad \text{or} \quad F_{\alpha\beta} = \nabla_\alpha A_\beta - \nabla_\beta A_\alpha, \tag{2.6}$$

are conformally invariant if the vector potential does not change, so that

$$\hat{A}_\alpha = A_\alpha, \quad \hat{F}_{\alpha\beta} = F_{\alpha\beta}, \quad \hat{F}^{\alpha\beta} = \Omega^{-4}F^{\alpha\beta}, \tag{2.7}$$

and the current behaves as follows:

$$\hat{J}^\alpha = \Omega^{-4}J^\alpha, \quad \hat{J}_\alpha = \Omega^{-2}J_\alpha. \tag{2.8}$$

Since the Levi-Civita tensor transforms as

$$\hat{\varepsilon}_{\alpha\beta\gamma\delta} = \Omega^4 \varepsilon_{\alpha\beta\gamma\delta}, \tag{2.9}$$

the following quantities are conformally invariant:

$$*\hat{J}_{\alpha\beta\gamma} = \hat{\varepsilon}_{\alpha\beta\gamma\mu}\hat{J}^\mu = *J_{\alpha\beta\gamma}, \tag{2.10}$$

$$*\hat{F}_{\alpha\beta} = \frac{1}{2!}\hat{\varepsilon}_{\alpha\beta\mu\nu}\hat{F}^{\mu\nu} = *F_{\alpha\beta}. \tag{2.11}$$

Therefore, Maxwell's equations with a source can be written using the external derivative as

$$dF = 0, \quad d*F = -2*J, \tag{2.12}$$

where only conformally invariant quantities appear.

The continuity equation for the electromagnetic current is also conformally invariant:

$$\nabla_\alpha J^\alpha = 0 \to \hat{\nabla}_\alpha \hat{J}^\alpha = \Omega^{-4}\nabla_\alpha J^\alpha = 0 \tag{2.13}$$

thanks to Eq. (2.8) and the conformal property of the four-dimensional volume element $\mathfrak{g}^{1/2} = (-\mathrm{Det}\, g_{\alpha\beta})^{1/2}$:

$$\hat{\mathfrak{g}}^{1/2} = \Omega^4 \mathfrak{g}^{1/2}. \tag{2.14}$$

It is interesting to notice, however, that as a consequence of the invariance (2.7) of the electromagnetic potential under a conformal rescaling, the Lorentz gauge condition is not conformally invariant:

$$\nabla_\alpha A^\alpha = 0 \tag{2.15}$$

implies

$$\hat{\nabla}_\alpha \hat{A}^\alpha - 2\hat{A}^\alpha d_\alpha \log|\Omega| = 0. \tag{2.16}$$

A remarkable property arises in four-dimensional spacetimes: in both the scalar and electromagnetic case the total charge distributed on a three-dimensional spacelike hypersurface is conformally (pseudo)invariant.[2] This follows from the conformal invariance of spatial charge distributions.

Denoting n_α, a future-oriented unit 1-form normal to the hypersurface Σ, we get

$$\hat{n}_\alpha = |\Omega| n_\alpha, \quad \hat{n}^\alpha = |\Omega|^{-1} n^\alpha. \tag{2.17}$$

The three-dimensional volume element is given by $\mathfrak{q}^{1/2} = (\mathrm{Det}\, q_{\alpha\beta})^{1/2}$, where three-metric $q_{\alpha\beta}$ is the restriction of the four-metric $g_{\alpha\beta}$ to the hypersurface Σ. Under the conformal transformation,

$$\mathfrak{q}^{1/2} \to \hat{\mathfrak{q}}^{1/2} = |\Omega|^3 \mathfrak{q}^{1/2}. \tag{2.18}$$

A charge distribution is defined as a charge density multiplied by this volume element. Hence, the scalar charge distribution reads

$$\sigma = S\, \mathfrak{q}^{1/2}, \tag{2.19}$$

and

$$\sigma \to \hat{\sigma} = \mathrm{sign}(\Omega)\sigma. \tag{2.20}$$

We see that it is conformal invariant except for a change of sign if the conformal factor Ω is negative. As seen from Eq. (2.5), this fails to be true for $n \neq 4$. In the following we consider only the case $n = 4$.

The electromagnetic charge distribution is given by

$$\rho = n_\alpha J^\alpha \mathfrak{q}^{1/2}. \tag{2.21}$$

Again, regarding Eqs. (2.8), (2.17), and (2.18), we get

$$\rho \to \hat{\rho} = \rho. \tag{2.22}$$

Thus, the electromagnetic charge is invariant even under conformal transformation with a negative conformal factor Ω.

Similarly, we define the electric field with the three-dimensional volume element included:

$$\mathcal{E}^\alpha = n_\mu F^{\mu\alpha} \mathfrak{q}^{1/2}, \tag{2.23}$$

[2] A quantity is a conformal pseudoinvariant if it is invariant under conformal transformation, except for a change of sign if the conformal factor is negative. See Eq. (2.20).

which represents the momentum conjugated to the potential A_α (cf., e.g., Ref. [19]). With the definition (2.23), $\mathcal{E}^\alpha$ is conformally invariant. Gauss's law simply reads

$$\int_D \nabla^{(3)}_\alpha \mathcal{E}^\alpha = \int_{\partial D} \mathcal{E}^\alpha dS_\alpha , \tag{2.24}$$

where $\nabla^{(3)}$ is three-metric covariant derivative and D is a region in Σ.

III. MINKOWSKI AND de SITTER SPACETIMES: COMPACTIFICATION AND CONFORMAL RELATION

The conformal structure of Minkowski and de Sitter spacetimes and their conformal relation to the regions of the Einstein static universe is well known and has been much used (see, e.g., Refs. [6,20] for basic expositions). However, the complete compactified picture of both spaces and their conformal structure do not appear to be described in detail in the literature, although all main ideas are contained in various writings by Penrose (e.g., Refs. [9,10]). Since we shall need some details in explicit form when analyzing the character of the fields of sources in de Sitter spacetime and their relation to their counterparts in Minkowski spacetime, we shall now discuss the compactification and conformal properties of these spaces.

Recall first that flat Euclidean plane E^2 can be compactified by adding a point at infinity so that the resulting space is a two-sphere S^2 with a regular homogenous metric $g_{\rm sph}$, conformally related to the Euclidean metric:

$$\begin{aligned} g_{\rm sph} &= \alpha^2 (d\vartheta^2 + \sin^2\vartheta\, d\varphi^2) \\ &= \Omega^2 (dr^2 + r^2 d\varphi^2) = \Omega^2 g_{\rm Eucl} , \end{aligned} \tag{3.1}$$

where α is a constant parameter with the dimension of length, $r = \alpha \tan(\vartheta/2)$, and $\Omega = 1 + \cos\vartheta$. Notice that $g_{\rm Eucl}$ is not regular at $r = \infty$, where the conformal factor $\Omega = 0$. The group of conformal transformations of E^2 acts on the compact manifold S^2.

Analogously, one can construct compactified Minkowski space $M^\#$ (see Ref. [10], Sec. 9.2 and references therein) on which the 15-parameter conformal group acts. One starts with the standard Penrose diagram of Minkowski space and makes an identification of $\mathcal{I}^-_{\rm Mink}$ and $\mathcal{I}^+_{\rm Mink}$ by identifying the past and future endpoints of null geodesics as indicated in Fig. 2. The future and past timelike infinities, $i^\pm_{\rm Mink}$, and the spatial infinity, $i^0_{\rm Mink}$, are also identified into one point. The topology of $M^\#$ is $S^3 \times S^1$ (this is not evident from first sight, but see Ref. [10]).

Rescaled Minkowski space (without the identification) can be drawn in a two-dimensional diagram as a part of the Einstein static universe, which is visualized by a cylindrical surface imbedded in E^3—see, e.g., Refs. [6,20]. However, in Fig. 3 we illustrate the compactified Minkowski space $M^\#$ by a *three-dimensional* diagram as a part of the Einstein universe represented by a *solid* cylinder in E^3. This is achieved in the following way: In Fig. 2 the Minkowski spacetime (with one dimension suppressed) is illustrated as a region bounded by two cones joined base to base. Now we take a

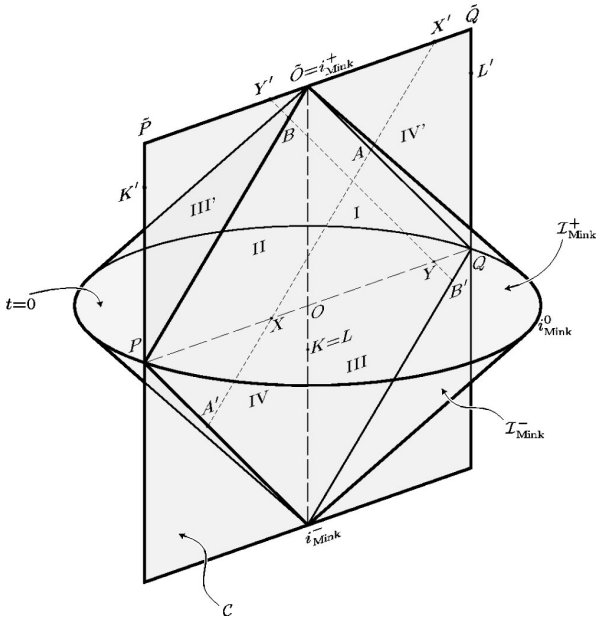

FIG. 2. Three-dimensional Penrose diagram of Minkowski space. The whole spacetime is mapped into the interior of two cones joined base to base along a spacelike (Cauchy) hypersurface $t=0$. The boundary of the two cones consists of past and future null infinities, $\mathcal{I}^-_{\rm Mink}, \mathcal{I}^+_{\rm Mink}$, of the past and future timelike infinities $i^-_{\rm Mink}, i^+_{\rm Mink}$, and of the spacelike infinity, $i^0_{\rm Mink}$. At these infinities, the null, timelike, and spacelike geodesics start and end. A two-dimensional cut $\mathcal{C}$ going through $i^-_{\rm Mink}$, $i^+_{\rm Mink}$, and $P, Q \in i^0_{\rm Mink}$ is considered, with two null geodesics $A'XA$ and $B'YB$ indicated. It is divided into four separate regions, I–IV. Regions III and IV are mapped into regions III' and IV' in the compactified Minkowski space illustrated in Fig. 3.

two-dimensional cut $\mathcal{C}$ and we compactify it by dividing it into four regions, I–IV, as indicated in Fig. 2. We cut out regions III and IV and place them "above" regions II and I so that they are joined along their corresponding null boundaries (e.g., points B,B' and A,A' become identical). Now the segment PO has to be identified with $\tilde{O}\tilde{Q}$ and OQ with $\tilde{P}\tilde{O}$—they correspond to a single segment in Fig. 2. Similarly, boundaries $P\tilde{P}$ and $Q\tilde{Q}$ are identified, and as a result a compact manifold is formed. Consider then all posible cuts $\mathcal{C}$, i.e., "rotate" $\mathcal{C}$ around the "line" $i^-_{\rm Mink} O i^+_{\rm Mink}$, and make the same identifications as we just described. Now all "vertical" boundary lines as $P\tilde{P}$ and $Q\tilde{Q}$ have to be identified (notice that all these points were on the segment $i^-_{\rm Mink} O$ in Fig. 2). The resulting four-dimensional compact manifold is represented in the three-dimensional Fig. 3. From the construction described, it follows that the top and bottom bases of the solid cylinder are identified and each of the circles on the cylindrical surface, as, e.g., k, should be considered as a single point. The "disks" inside these circles are thus two spheres, i.e., without suppressing one dimension—three spheres in $M^\#$.

Now it is important to realize that Fig. 3 can be understood as a part of the Einstein static cylinder, which also

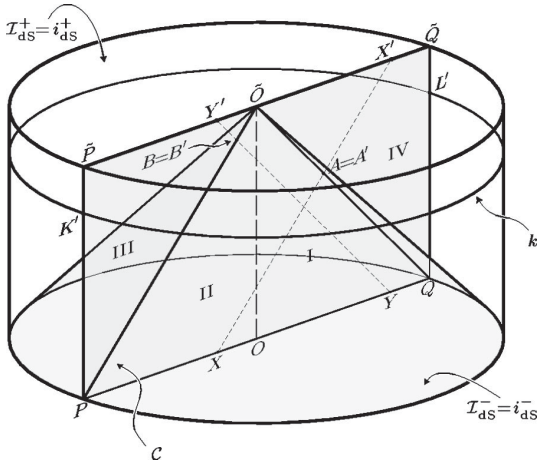

FIG. 3. Compactified Minkowski and de Sitter spaces. The compactified Minkowski and de Sitter space $M^{\#}$, illustrated by the three-dimensional diagram—a part of the Einstein universe represented here as a solid cylinder. The compactification is achieved by considering first the two-dimensional section $\mathcal{C}$ in Fig. 2, cutting out regions III and IV and placing them ''above'' regions II and I so that two-dimensional figure $POQ\tilde{Q}\tilde{O}\tilde{P}$ is formed. PO is identified with $\tilde{O}\tilde{Q}$ (e.g., point X with X'), OQ with $\tilde{P}\tilde{O}$ (e.g., Y with Y'), and $P\tilde{P}$ with $Q\tilde{Q}$. All two-dimensional cuts $\mathcal{C}$ are identified in this way with, in addition, all ''vertical'' boundary lines being identified so that the circle k, for example, is considered as a point. The top and bottom bases of the cylinder, representing the past and the future spacelike infinities of de Sitter space, are identified in the compact manifold $M^{\#}$.

represents the *compactified de Sitter space*. In de Sitter space two bases are future and past spacelike infinities. They are not usually identified in the standard two-dimensional Penrose diagram of de Sitter spacetime (see, e.g., Ref. [6]), as $\mathcal{I}^+_{\rm Mink}$ and $\mathcal{I}^-_{\rm Mink}$ are not identified in the standard Penrose diagram of Minkowski space.

Manifold $M^{\#}$ represents the compactification of both Minkowski and de Sitter space. Similarly as S^2, representing the compactification of E^2, can be equipped with a regular metric $g_{\rm sph}$ mentioned above, $M^{\#}$ can be equipped with the regular metric

$$g_{\rm Eins}=\alpha^2(-d\tilde{t}^{\,2}+d\tilde{r}^{\,2}+\sin^2\tilde{r}\,d\omega^2), \tag{3.2}$$

where dimensionless coordinates $\tilde{t},\tilde{r}\in\langle 0,\pi\rangle$, spacelike hypersurfaces $\tilde{t}=0$, and $\tilde{t}=\pi$ are identified by means of null geodesics, $d\omega^2=d\vartheta^2+\sin^2\vartheta\,d\varphi^2$, and the constant α has dimension of length. The metric (3.2) is the well-known metric of the Einstein universe, in which case

$$\alpha^2=\frac{3}{\Lambda}, \tag{3.3}$$

where Λ is the cosmological constant.

In order to see this explicitly, write the Minkowski metric in standard spherical coordinates,

$$g_{\rm Mink}=-dt^2+dr^2+r^2d\omega^2, \tag{3.4}$$

and introduce coordinates $\tilde{t},\tilde{r}\in\langle 0,\pi\rangle$ by

$$\tilde{t}=\arctan\frac{2\alpha t}{\alpha^2-t^2+r^2},\quad \tilde{r}=\arctan\frac{2\alpha r}{\alpha^2+t^2-r^2}, \tag{3.5}$$

inversely

$$t=\frac{\alpha\sin\tilde{t}}{\cos\tilde{r}+\cos\tilde{t}},\quad r=\frac{\alpha\sin\tilde{r}}{\cos\tilde{r}+\cos\tilde{t}}, \tag{3.6}$$

so that

$$g_{\rm Mink}=\frac{\alpha^2}{(\cos\tilde{r}+\cos\tilde{t})^2}(-d\tilde{t}^{\,2}+d\tilde{r}^{\,2}+\sin^2\tilde{r}\,d\omega^2). \tag{3.7}$$

Let us notice that by requiring the ranges $\tilde{t},\tilde{r}\in\langle 0,\pi\rangle$, we fix the branch of arctan in Eq. (3.5). Further, observe that for $\tilde{t}+\tilde{r}>\pi$, relations (3.6) imply negative r—we shall return to this point in a moment.

In the case of de Sitter space with the metric

$$g_{\rm dS}=-d\tau^2+\alpha^2\cosh^2\frac{\tau}{\alpha}(d\chi^2+\sin^2\chi\,d\omega^2), \tag{3.8}$$

we put

$$\tilde{t}=2\arctan\left(\exp\frac{\tau}{\alpha}\right),\quad \tilde{r}=\chi, \tag{3.9}$$

or

$$\tau=\alpha\log\left(\tan\frac{\tilde{t}}{2}\right),\quad \chi=\tilde{r}, \tag{3.10}$$

so that

$$g_{\rm dS}=\frac{\alpha^2}{\sin^2\tilde{t}}(-d\tilde{t}^{\,2}+d\tilde{r}^{\,2}+\sin^2\tilde{r}\,d\omega^2). \tag{3.11}$$

In this way we obtain explicit forms of the conformal rescaling of both spaces into the metric of the Einstein universe:

$$g_{\rm Eins}=\Omega^2_{\rm Mink}\,g_{\rm Mink},\quad \Omega_{\rm Mink}=\cos\tilde{r}+\cos\tilde{t}, \tag{3.12}$$

$$g_{\rm Eins}=\Omega^2_{\rm dS}\,g_{\rm dS},\quad \Omega_{\rm dS}=\sin\tilde{t}, \tag{3.13}$$

where $g_{\rm Eins}$ is given by Eq. (3.2). As in the simple case of conformal relation of E^2 to S^2, the conformal factors $\Omega_{\rm Mink}$ and $\Omega_{\rm dS}$ vanish at infinities of Minkowski, respectively, de Sitter space.

As a consequence of Eqs. (3.5)–(3.11) we also find the conformal relation between Minkowski and de Sitter space:

$$g_{\rm Mink}=\Omega^2 g_{\rm dS},\quad \Omega=\Omega^{-1}_{\rm Mink}\,\Omega_{\rm dS}, \tag{3.14}$$

where $\Omega_{\rm Mink},\Omega_{\rm dS}$ are given by Eqs. (3.12) and (3.13). The conformal factor Ω has the simplest form when expressed in terms of the Minkowski time t:

$$\Omega=\frac{\sin\tilde{t}}{\cos\tilde{r}+\cos\tilde{t}}=\frac{t}{\alpha}. \tag{3.15}$$

The conformal transformation is not regular at the infinity of Minkowski, respectively, de Sitter space because Ω diverges, respectively, vanishes there. We shall return to this point at the end of this section. First, however, we have to describe the coordinate systems employed in relating particular regions I–IV in Figs. 2 and 3.

Relations (3.5) and (3.6) can be used automatically in region I only. In other regions, ranges of coordinates have to be specified more carefully. In the following we always require $\tilde{t}\in\langle 0,\pi\rangle$. Then, if $\tilde{r}\in\langle 0,\pi\rangle$, we find that relations (3.5) and (3.6) imply negative r in region IV. Also, if we consider events with $t<0$, $r>0$ (region III), we notice that as a consequence of Eqs. (3.5) and (3.6) with $\tilde{t}\in\langle 0,\pi\rangle$, we get $\tilde{r}<0$. Relations (3.5) and (3.6) can be made meaningful in all regions I–IV if we allow negative $r,\tilde{r}$ and adopt the following convention: at a fixed value of time coordinate t, respectively, $\tilde{t}$, the points symmetrical with respect to the origin of spherical coordinates have opposite signs of the radial coordinate, i.e., points with given $\{t,r,\vartheta,\varphi\}$, respectively $\{\tilde{t},\tilde{r},\vartheta,\varphi\}$, are identical with $\{t,-r,\pi-\vartheta,\varphi+\pi\}$, respectively $\{\tilde{t},-\tilde{r},\pi-\vartheta,\varphi+\pi\}$. The way in which regions I–IV are covered by the particular ranges of coordinates is explicitly illustrated in Figs. 5(a)–5(c) in the Appendix, where our convention is described in more detail.

In the Appendix, various useful coordinate systems in de Sitter space are given. First, we shall frequently employ coordinates $\{\tilde{t},\tilde{r},\vartheta,\varphi\}$ which are simply related [by Eqs. (3.9) and (3.10)] to the standard coordinates $\{\tau,\chi,\vartheta,\varphi\}$ covering nicely the whole de Sitter hyperboloid. Next, relations (3.5) and (3.6) can be viewed as the definition of another coordinate system $\{t,r,\vartheta,\varphi\}$ on de Sitter space [with the metric being given by Eq. (A6)]. Let us remind that for fixed ϑ,φ values $\tilde{r}>0$ (commonly assumed in de Sitter space) correspond to $r>0$ for $\tilde{t}+\tilde{r}<\pi$ (region I) and to $r<0$ for $\tilde{t}+\tilde{r}>\pi$ (region IV). Further, one frequently uses static coordinates T,R associated with the static Killing vector of de Sitter spacetime—Eqs. (A8) in the Appendix.

Finally, it will be useful to introduce the null coordinates [cf. Eq. (A12)]

$$u=t-r,\quad v=t+r, \tag{3.16}$$

$$\tilde{u}=\tilde{t}-\tilde{r},\quad \tilde{v}=\tilde{t}+\tilde{r}. \tag{3.17}$$

When employing null coordinates we shall consider only $\tilde{r}>0$ ($\tilde{u},\tilde{v}$ would "exchange their role" if $\tilde{r}<0$); the ranges of $\tilde{u},\tilde{v}$ and u,v are thus given by the choice $\tilde{t},\tilde{r}\in\langle 0,\pi\rangle$. This leaves the standard (Minkowski) meaning of u,v in region I; however, u and v exchange their usual (Minkowski) role in region IV ($\tilde{v}=\tilde{t}+\tilde{r}>\pi$) because here $r<0$. With this choice, the coordinates $\tilde{u}$, $\tilde{v}$ and u cover de Sitter space continuously, in particular the horizon $\tilde{v}=\pi$ [$v\to\pm\infty$ on this horizon—see Fig. 5(e)].

From Eqs. (3.5) and (3.6) we get the simple relations

$$u=\alpha\tan\frac{\tilde{u}}{2},\quad v=\alpha\tan\frac{\tilde{v}}{2}, \tag{3.18}$$

which explicitly verify that local null cones (local causal structure) are unchanged under conformal mapping. Nevertheless, it is well known that the global causal structure of the Minkowski and de Sitter space is different. This is reflected in the fact that, as mentioned above, the conformal transformation between the two spaces is not regular everywhere. In particular, relation (3.18) shows that points at null infinity with $v\to\pm\infty$ in Minkowski space go over into regular points with $\tilde{v}\to\pi$ in de Sitter space, whereas spacelike hypersurface $t=\frac{1}{2}(u+v)=0$ goes into spacelike infinities $\tilde{t}=0,\pi$ in de Sitter space.

In the next sections, when we shall generate solutions for the scalar and electromagnetic fields for given sources in de Sitter space by employing the conformal transformation from Minkowski space, we have to check the behavior of the new solutions at points where the transformation is not regular.

Before turning to the construction of the fields produced by specific sources, let us emphasize that in all the following expressions for fields in de Sitter spacetime only positive $\tilde{r}$ can be considered. However, the results contained in Secs. IV and V are valid also for $\tilde{r}<0$ provided that the convention described above is used.[3]

IV. UNIFORMLY ACCELERATED PARTICLES IN de SITTER SPACETIME

In this section we study the correspondence of the worldlines of uniformly accelerated particles under the conformal mapping (3.5) and (3.6) between Minkowski and de Sitter spacetimes. Let a particle have four-velocity u^α, $u^\mu u_\mu=-1$, so that its acceleration is $a^\alpha=\dot{u}^\alpha=u^\mu\nabla_\mu u^\alpha$, $a^\mu u_\mu=0$. We say that the particle is uniformly accelerated if the projection of $\dot{a}^\alpha=u^\mu\nabla_\mu a^\alpha$ into the three surface orthogonal to u^α vanishes:

$$P^\alpha_\mu\dot{a}^\mu=\dot{a}^\alpha-(a^\mu a_\mu)u^\alpha=0. \tag{4.1}$$

Here the projection tensor $P^\mu_\nu=\delta^\mu_\nu+u^\mu u_\nu$ and $u_\mu\dot{a}^\mu=-a_\mu a^\mu$. Multiplying Eq. (4.1) by a^α, we get $\dot{a}^\mu a_\mu=0$ so that

[3]In Sec. VII, we require $\tilde{r}>0$. The right-hand sides of expressions (7.1), (7.2), (7.12), and (7.19) would have to be multiplied by a factor of $\mathrm{sgn}\,\tilde{r}$ to be also valid for $\tilde{r}<0$. Similar changes would also necessary be in other equations but these contain null coordinates that have not been defined for $\tilde{r}<0$.

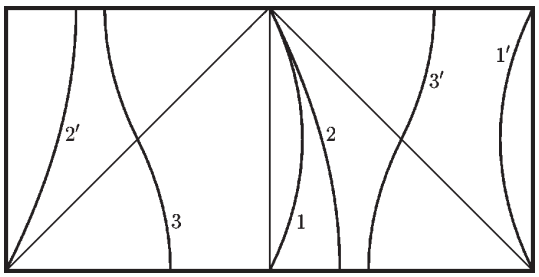

FIG. 4. Worldlines of particles in de Sitter spacetime. The worldlines of geodesics and of uniformly accelerated particles in de Sitter spacetime, obtained by the conformal transformation of appropriate worldlines in Minkowski space: 1,1′ from the worldline of a particle moving uniformly through the origin, 2,2′ from a particle at rest outside the origin, and 3,3′ from two uniformly accelerated particles. In de Sitter space, the worldlines 1 and 1′ describe two uniformly accelerated particles; 2,2′ and 3,3′ are geodesics. Both particles in each pair are causally disconnected.

$$a_\mu a^\mu = \text{constant}. \tag{4.2}$$

This definition of uniform acceleration goes over into the standard definition used in Minkowski space [22]. It implies that the components of a particle's acceleration in its instantaneous rest frames remain constant. Of course, as a special case, a particle may have zero acceleration when it moves along the geodesic.

Consider a particle moving with a constant velocity

$$\frac{R_o}{\alpha} = \tanh\beta = \text{constant} \tag{4.3}$$

along the z axis ($\varphi=0$, $\vartheta=0$) of the inertial frame in Minkowski spacetime with coordinates $\{t,r,\vartheta,\varphi\}$ so that it passes through $r=0$ at $t=0$. Transformations (3.5) and (3.6) map its worldline into *two* worldlines in de Sitter spacetime, given in terms of parameter λ_{Mink}, its proper time in Minkowski space, or in terms of λ_{dS}, its proper time in de Sitter space, as follows:

$$\begin{aligned}\tilde t &= \arctan\left(-2\alpha\frac{\lambda_{\text{Mink}}\cosh\beta}{\lambda_{\text{Mink}}^2-\alpha^2}\right)\\ &= \arctan\left(-\frac{\cosh\beta}{\sinh[(\lambda_{\text{dS}}/\alpha)\cosh\beta]}\right),\\ \tilde r &= \arctan\left(2\alpha\frac{\lambda_{\text{Mink}}\sinh\beta}{\lambda_{\text{Mink}}^2+\alpha^2}\right)\\ &= \arctan\left(\pm\frac{\sinh\beta}{\cosh[(\lambda_{\text{dS}}/\alpha)\cosh\beta]}\right).\end{aligned} \tag{4.4}$$

In these expressions, the arctan has values in[4] $\langle 0,\pi\rangle$; $\lambda_{\text{dS}}\in\mathbb{R}$, and $\lambda_{\text{Mink}}\in(0,\infty)$ for the worldline starting and ending with $\tilde r=0$ [denoted by 1 in Fig. 4; plus sign in the last equation in (4.4)], whereas $\lambda_{\text{Mink}}\in(-\infty,0)$ for the second worldline, starting and ending with $\tilde r=\pi$ [denoted by 1′ in Fig. 4; minus sign in (4.4)]. One thus gets two worldlines in de Sitter space from two "halves" of one worldline in Minkowski space.

These two worldlines are uniformly accelerated with the constant magnitude of the acceleration equal (up to the sign) to

$$a_o = -\frac{1}{\alpha}\sinh\beta. \tag{4.5}$$

An intuitive understanding of the acceleration is gained if we introduce standard *static* coordinates $\{T,R,\vartheta,\varphi\}$ in de Sitter space (see the Appendix). The two worldlines described by Eq. (4.4) in coordinates $\tilde t,\tilde r$ are in the static coordinates simply given by $R=R_o=$constant. [As seen from Eq. (A8), for a given $\tilde t,\tilde r$, the same R corresponds to $\tilde r$ and $\pi-\tilde r$.] Owing to the "cosmic repulsion" caused by the presence of a cosmological constant, fundamental geodesic observers with fixed $\tilde r$ (i.e., fixed χ) are "repelled" one from the other in proportion to their distance. Their initial implosion starting at $\tilde t=0$ ($\tau=-\infty$) is stopped at $\tilde t=\pi/2$ ($\tau=0$—at the "neck" of the de Sitter hyperboloid) and changes into expansion. A particle having constant $R=R_o$, thus a constant proper distance from an observer at $\tilde r=R=0$ (or at $\tilde r=\pi$, $R=0$), has to be accelerated towards that observer. The acceleration of particle 1 points towards the observer at $\tilde r=0$, whereas that of particle 1′ points towards the observer at $\tilde r=\pi$ (Fig. 4). Notice that the two uniformly accelerated worldlines are causally disconnected; no retarded or advanced effects from the particle 1 can reach the particle 1′ and vice versa. This is analogous to two particles symmetrically located along opposite parts of say the z axis and uniformly accelerated in opposite directions in Minkowski space. The worldlines of uniformly accelerated particles in Minkowski space are the orbits of the boost Killing vector. Analogously, in de Sitter space the Killing vector $\partial/\partial T$ also has the character of a boost.

Another type of simple worldline in de Sitter space arises from transforming the worldlines of a particle at rest at $r=r_o$ ($|r_o|<\alpha$), $\vartheta=0$, $\varphi=0$ in Minkowski space. It transforms to two worldlines in de Sitter space given by

$$\begin{aligned}\tilde t &= \arctan\left(\frac{2\alpha\lambda_{\text{Mink}}}{-\lambda_{\text{Mink}}^2+r_o^2+\alpha^2}\right),\\ \tilde r &= \arctan\left(\frac{-2\alpha r_o}{-\lambda_{\text{Mink}}^2+r_o^2-\alpha^2}\right),\\ \vartheta &= 0,\quad \varphi=0,\end{aligned} \tag{4.6}$$

with $\tilde t\in\langle 0,\pi\rangle$, and $\tilde r\,\text{sign}\,r_o\in\langle 0,\pi\rangle$ for $\lambda_{\text{Mink}}>0$ and $\tilde r\,\text{sign}\,r_o\in\langle-\pi,0\rangle$ for $\lambda_{\text{Mink}}<0$. Thus, a geodesic in Minkowski space goes over into two geodesics in de Sitter space. In Fig. 4 these are the worldlines 2 and 2′.

[4] $\tilde r\in\langle-\pi,0\rangle$ for $\beta<0$.

As the last example, let us just mention that the worldlines of two particles uniformly accelerated in Minkowski space get transformed into two geodesics 3,3′ in de Sitter space.

V. SCALAR AND ELECTROMAGNETIC FIELDS FROM UNIFORMLY ACCELERATED PARTICLES: THE SYMMETRIC SOLUTIONS

Two uniformly accelerated particles described by worldlines (4.4) were obtained by the conformal transformation from the worldline of a particle moving with a uniform velocity R_o/α in Minkowski space. Hence, their fields can be constructed by the conformal transformation of a simple boosted spherically symmetric field. In the case of scalar field, Eqs. (2.4), (2.20), and (3.15) then lead to the field

$$\Phi = \frac{s}{4\pi}\frac{t}{\alpha}\frac{1}{|r'|}, \tag{5.1}$$

where r' is spherical coordinate in an inertial frame in which the particle is at rest at the origin.

As emphasized earlier, we have to examine the field at the null hypersurface $\tilde{v}=\pi$, where the conformal transformation fails to be regular. We find that the field (5.1) is indeed not smooth there. The limit of Φ as $\tilde{v}=\pi$ is approached from the region $\tilde{v}<\pi$ differs from the limit from $\tilde{v}>\pi$; Φ has a jump at $\tilde{v}=\pi$, although, as can be checked by a direct calculation, this discontinuous field satisfies the scalar wave equation. However, a field analytic everywhere outside the sources can be obtained by an analytic continuation of the field (5.1) from the domain $\tilde{v}<\pi$ to the domain $\tilde{v}>\pi$. We discover that the new field in $\tilde{v}>\pi$ differs from Eq. (5.1) just by a sign. Therefore it simply corresponds to the charge of the particle in $\tilde{v}>\pi$, which is opposite to that implied by conformal transformation. It is easy to see that, due to the conformal transformation, the sign of the charge on the worldline with $\tilde{v}>\pi$ is opposite to the original charge s because the conformal factor $\Omega = t/\alpha < 0$ for $\tilde{v}>\pi$. Hence, the field which is analytic represents the field of two uniformly accelerated particles with the *same* scalar charge s, which move along two worldlines given by Eq. (4.4). In Sec. VI we shall see that this field can be written as a linear combination of retarded and advanced fields from both particles. We call it the *symmetric field*. Regarding Eq. (5.1), in which r' is first expressed in terms of the original Minkowski coordinates $\{t,r,\vartheta,\varphi\}$, and then using the transformation (3.6), we find the field as a function of $\{\tilde{t},\tilde{r},\vartheta,\varphi\}$:

$$\Phi_{\rm sym} = \frac{s}{4\pi}\frac{\sqrt{\alpha^2-R_o^2}}{\sqrt{(\alpha^2-RR_o\cos\vartheta)^2-(\alpha^2-R^2)(\alpha^2-R_o^2)}}, \tag{5.2}$$

where $R=\alpha(\sin\tilde{r}/\sin\tilde{t})$ is the static radial de Sitter coordinate (see the Appendix). As could have been anticipated, the field is static in the static coordinates since the accelerated particles are at rest at $R=R_o$, $\vartheta=\varphi=0$. (Recall that we need two sets of such coordinates to cover both worldlines but the coordinate R is well defined in the whole de Sitter spacetime—cf. the Appendix.) However, it is dynamical in the coordinates $\{\tilde{t},\tilde{r},\vartheta,\varphi\}$, or in the standard coordinates $\{\tau,\chi,\vartheta,\varphi\}$, covering—in contrast to the static coordinates—the whole de Sitter spacetime.

In order to construct the electromagnetic field produced by uniformly accelerated particles in de Sitter spacetime, we start, analogously to the scalar field case, from the boosted Coulomb field in Minkowski space. The potential 1-form is thus simply

$$A = -\frac{e}{4\pi}\frac{1}{|r'|}dt', \tag{5.3}$$

where the prime again denotes the coordinates in an inertial frame in which the particle is at rest. Since electromagnetic field described by its covariant component is conformally invariant, the field (5.3) *is* automatically a solution of Maxwell's equations in de Sitter space. However, like in the scalar field case, we have to examine its character at $\tilde{v}=\pi$. We discover that the potential (5.3) does *not*, in fact, solve Maxwell's equations there [in contrast to the scalar field (5.1), which is discontinuous on $\tilde{v}=\pi$, but satisfies the scalar wave equation]. This result can be understood when we realize that by the conformal transformation the sign of the electric charge—in contrast to the scalar charge—does *not* change at the worldline with $\tilde{v}>\pi$ so that the total electric charge is $2e$. A nonzero total charge in de Sitter spacetime, however, violates the constraint, as we shall see in Sec. VII B. In fact, it is well-known that in a closed universe the total electric charge must be zero due to Gauss's law (e.g., Ref. [19]).

As with the scalar field, we still can construct a field smooth everywhere outside the sources by analytic continuation of the field obtained in the region $\tilde{v}<\pi$ across $\tilde{v}=\pi$ into whole spacetime. Similar to the scalar case, the resulting field in $\tilde{v}>\pi$ corresponds just to the opposite charge, so that now, in the electromagnetic case, the total charge is indeed zero. The electromagnetic field can be written as a combination of retarded and advanced fields from both charges, as will be shown in Sec. VII. The potential describing this *symmetric field* has a simple form in the static coordinates:

$$A_{\rm sym} = -\frac{e}{4\pi\mathcal{X}}\left[\left(1-\frac{R_oR}{\alpha^2}\cos\vartheta\right)\alpha\,dT + \frac{R-R_o\cos\vartheta}{1-R^2/\alpha^2}dR + RR_o\sin\vartheta\,d\vartheta\right], \tag{5.4}$$

where[5]

$$\mathcal{X}^2 = (\alpha^2-RR_o\cos\vartheta)^2-(\alpha^2-R_o^2)(\alpha^2-R^2). \tag{5.5}$$

As noticed in Sec. II, the Lorentz gauge condition is not conformally invariant, so that the potential (5.4) need not satisfy the condition, although the original Coulomb field does. Expressing the static radial coordinate as

[5]The positive root $\mathcal{X}>0$ is taken here—as in Eq. (5.2).

$R=\alpha(\sin\tilde{r}/\sin\tilde{t})$, and similarly T (see the Appendix) we can find the potential in global coordinates $\{\tilde{t},\tilde{r},\vartheta,\varphi\}$, respectively, $\{\tau,\chi,\vartheta,\varphi\}$. Since the resulting form is not simple, we do not write it here, but we give the electromagnetic field explicitly in both the static and global coordinates. In static coordinates it reads

$$F=dA=-\frac{e}{4\pi}\frac{\alpha(\alpha^2-R_0^2)}{\mathcal{X}^3}\left[(R-R_0\cos\vartheta)dT\wedge dR+\left(1-\frac{R^2}{\alpha^2}\right)RR_0\sin\vartheta\,dT\wedge d\vartheta\right], \tag{5.6}$$

where $\mathcal{X}$ is given by Eq. (5.5). In $\{\tilde{t},\tilde{r},\vartheta,\varphi\}$ coordinates we explicitly find

$$\begin{aligned}F=&-\frac{e}{4\pi}\frac{\alpha^2-R_0^2}{\mathcal{X}^3}\frac{\alpha^3}{\sin^3\tilde{t}}\\&\times[(\alpha\sin\tilde{r}-R_0\sin\tilde{t}\cos\vartheta)d\tilde{t}\wedge d\tilde{r}\\&+R_0\sin\tilde{t}\cos\tilde{r}\sin\tilde{r}\sin\vartheta\,d\tilde{t}\wedge d\vartheta\\&-R_0\cos\tilde{t}\sin\tilde{r}\sin\tilde{r}\sin\vartheta d\tilde{r}\wedge d\vartheta].\end{aligned} \tag{5.7}$$

Summarizing, the field (5.7) represents the time-dependent electromagnetic field of two particles with charges $\pm e$, uniformly accelerated along the worldlines (4.4) with accelerations $\mp\alpha^{-1}\sinh\beta=\mp R_0/(\alpha\sqrt{\alpha^2-R_0^2})$. The field is analytic everywhere outside the charges. In the static coordinates the charges are at rest at $R=R_0$ and their static field is given by Eq. (5.6).

VI. SCALAR FIELD: THE RETARDED SOLUTIONS

The symmetric scalar field solution (5.2), representing two uniformly accelerated scalar charges, is nonvanishing in the whole de Sitter spacetime. As mentioned before, and will be proved at the end of this section [see Eqs. (6.6) and (6.7)], this field is a combination of retarded and advanced effects from both charges. A retarded field of a point particle should in general be nonzero only in the future domain of influence of a particle's worldline, i.e., at those points from which past causal curves exist that intersect the worldline. Hence, the retarded field of the uniformly accelerated charge, which starts and ends at $\tilde{r}=0$ (see Fig. 4), should be nonvanishing only at $\tilde{u}=\tilde{t}-\tilde{r}>0$. It is natural to try to construct such a field by restricting the symmetric field to this region, i.e., to ask whether the field

$$\Phi_{\rm ret}=\Phi_{\rm sym}\theta(\tilde{u}), \tag{6.1}$$

where θ is the usual Heaviside step function, is a solution of the field equation.

The field (6.1) does, of course, satisfy the scalar field wave equation (2.2) at $\tilde{u}>0$ since $\Phi_{\rm sym}$ does, and also at $\tilde{u}<0$ since $\Phi=0$ is a solution of Eq. (2.2) outside a source. Thus we have to examine the field (6.1) only at $\tilde{u}=0$, i.e., at "creation light cone" of the particle's worldline, also referred to as the past event horizon of the worldline [6]. The field strength 1-form implied by Eq. (6.1) becomes

$$d\Phi_{\rm ret}=(d\Phi_{\rm sym})\,\theta(\tilde{u})+\Phi_{\rm sym}\delta(\tilde{u})d\tilde{u}. \tag{6.2}$$

An explicit calculation shows that

$$\Box\Phi_{\rm ret}=(\Box\Phi_{\rm sym})\,\theta(\tilde{u}). \tag{6.3}$$

Therefore, the conformally invariant scalar wave equation (2.2) (with $\xi=1/6$) has the form

$$\begin{aligned}[\Box-\tfrac{1}{6}R]\Phi_{\rm ret}&=([\Box-\tfrac{1}{6}R]\Phi_{\rm sym})\,\theta(\tilde{u})\\&=S_{\rm sym}\theta(\tilde{u})=S_{\rm mon\,1},\end{aligned} \tag{6.4}$$

where $S_{\rm mon\,1}$ denotes the monopole scalar charge starting and ending at $\tilde{r}=0$. Hence, we proved that the field (6.1), where $\Phi_{\rm sym}$ is given by Eq. (5.2), satisfies the field Eq. (6.3) everywhere, including the past event horizon of the particle.

Analogously, we can make sure that

$$\Phi_{\rm adv}=\Phi_{\rm sym}\theta(-\tilde{u}) \tag{6.5}$$

has its support in the future domain of influence of the monopole particle $1'$, starting and ending at $\tilde{r}=\pi$, and is thus the advanced field of source $S_{\rm mon\,1'}=S_{\rm sym}\theta(-\tilde{u})$.

From the results above, it is not difficult to conclude that the symmetric field can be interpreted as arising from the combinations of retarded and advanced potentials due to both particles 1 and $1'$, in which the potentials due to one particle can be taken with arbitrary weights, and the weights due the other particle then determined by

$$\Phi_{\rm sym}=\zeta\Phi_{\rm ret\,1}+(1-\zeta)\Phi_{\rm adv\,1}+(1-\zeta)\Phi_{\rm ret\,1'}+\zeta\Phi_{\rm adv\,1'}, \tag{6.6}$$

where $\zeta\in\mathbb{R}$ is an arbitrary constant factor. In particular, choosing $\zeta=1/2$, the field

$$\Phi_{\rm sym}=\tfrac{1}{2}(\Phi_{\rm ret}+\Phi_{\rm adv}) \tag{6.7}$$

is the symmetric field from both particles. This freedom in the interpretation is exactly the same as with two uniformly accelerated scalar particles in Minkowski spacetime (see Ref. [15], Sec. IV B).

A remarkable property of the retarded field (6.1) is that the field strength (6.2) has a term proportional to $\delta(\tilde{u})$, i.e., it is singular at the past horizon. Since the energy-momentum tensor of the scalar field is quadratic in the field strength, it cannot be evaluated at $\tilde{u}=0$. The "shock wave" at the "creation light cone" can be understood on physical grounds similarly as the instability of Cauchy horizons inside black holes (e.g., Ref. [12]); an observer crossing the pulse along a timelike worldline will see an infinitely long history of the source within a finite proper time. The character of the shock is given by the pointlike nature of the source. If, for example, a scalar charge has typical extension l at $\tilde{t}=\pi/2$, i.e., at the moment of the minimal size of the de Sitter universe ($\tau=0$), and the extension of the charge in the $\tilde{r}$ coordinate

would be roughly the same at $\mathcal{I}^-_{\rm dS}$, the corresponding shock would be smoothed around $\tilde{u}=0$ with a width $\sim l$. However, the *proper* extension of the charge at $\mathcal{I}^-_{\rm dS}$ would be infinite in that case.

Let us note that the retarded field (6.1) could also be computed by means of the retarded Green's function. In our case of the conformally invariant equation for a scalar field, the retarded Green's function in de Sitter space is localized on the future null cone, as it is in the ''original'' Minkowski space. (It is interesting to note that in the case of a minimal, or more general coupling, the scalar field does not vanish inside the null cone.) Thanks to this property we can understand a ''jump'' in the field on the creation light cone: the creation light cone is precisely the future light cone of the point at which the source ''enters'' the spacetime, i.e., it is the boundary of a domain where we can obtain a contribution from the retarded Green's function integrated over sources.

VII. ELECTROMAGNETIC FIELDS: THE RETARDED SOLUTIONS

In this section we shall analyze the electromagnetic fields of free or accelerated charges with monopole and also with a dipole structure. We shall pay attention to the constraints which the electromagnetic field, in contrast to the scalar field, has to satisfy on any spacelike hypersurface.

A. Free monopole

Let us start with an unaccelerated monopole at rest at the origin of both coordinate systems used, i.e., at $\tilde{r}=R=0$. With $R_{\rm o}=0$, the potential (5.4) and the field (5.6) simplify to

$$A_{\rm sym}=-\frac{e}{4\pi}\frac{\sin\tilde{t}}{\cos\tilde{t}+\cos\tilde{r}}\left(\frac{1+\cos\tilde{t}\cos\tilde{r}}{\sin\tilde{t}\sin\tilde{r}}d\tilde{t}+d\tilde{r}\right) \tag{7.1}$$

and

$$F_{\rm sym}=-\frac{e}{4\pi}\frac{1}{\sin^2\tilde{r}}d\tilde{t}\wedge d\tilde{r}. \tag{7.2}$$

Let us restrict the potential to the ''creation light cone'' and its interior by defining

$$A_{\rm o}=A_{\rm sym}\theta(\tilde{u}). \tag{7.3}$$

The field in null coordinates $\tilde{u},\tilde{v}$ then reads

$$F_{\rm o}=dA_{\rm o}=F_{\rm sym}\theta(\tilde{u})-\frac{e}{4\pi}\frac{1}{\sin\tilde{v}}\delta(\tilde{u})d\tilde{u}\wedge d\tilde{v}, \tag{7.4}$$

so that the left-hand side of Maxwell's equations becomes

$$\begin{aligned}\nabla_\mu F^{\alpha\mu}_{\rm o}=&J^\alpha_{\rm mon}\\&+\frac{e}{4\pi\alpha^4}\left[\frac{1-\cos\tilde{v}}{1+\cos\tilde{v}}\frac{\partial^\alpha}{\partial\tilde{u}}+2(1-\cos\tilde{v})\frac{\partial^\alpha}{\partial\tilde{v}}\right]\delta(\tilde{u})\\&-\frac{e}{4\pi\alpha^4}\frac{\partial^\alpha}{\partial\tilde{v}}\delta'(\tilde{u}).\end{aligned} \tag{7.5}$$

Here $J^\alpha_{\rm mon}=(\nabla_\mu F^{\alpha\mu}_{\rm sym})\theta(\tilde{u})$ is the current produced by the charge at $\tilde{r}=0$. Additional terms on the right-hand side of Eq. (7.5), localized on the null hypersurface $\tilde{u}=0$, clearly show that the restricted field (7.3) does not correspond to a single point source. The terms of this type did not arise in the case of the scalar field discussed in the previous section.

We can try to add a field localized on $\tilde{u}=0$, which would cancel the additional terms. Although we shall see in the following section that this cannot be achieved, it is instructive to add, for example, the field

$$A_*=-\frac{e}{4\pi}\ln\left(\tan\frac{\tilde{v}}{2}\right)\delta(\tilde{u})d\tilde{u}, \tag{7.6}$$

which cancels the second term on the right-hand side of the field (7.4). Thus, denoting

$$\begin{aligned}A_{\rm mon}&=A_{\rm o}+A_*,\\F_{\rm mon}&=dA_{\rm mon}=F_{\rm sym}\theta(\tilde{u}),\end{aligned} \tag{7.7}$$

we find that with $F_{\rm mon}$, Maxwell's equations become

$$\nabla_\mu F^{\alpha\mu}_{\rm mon}=J^\alpha_{\rm mon}-\frac{e}{4\pi\alpha^4}(1-\cos\tilde{v})\delta(\tilde{u})\frac{\partial^\alpha}{\partial\tilde{v}}. \tag{7.8}$$

Hence, the field $A_{\rm mon}$ does not represent only the unaccelerated monopole charge but also a spherical shell of charges moving outwards from the monopole with the velocity of light along the ''creation light cone'' $\tilde{u}=0$. The total charge of the shell is precisely opposite to the monopole charge so that the total charge of the system is zero.

We shall return to this point in the following section; now let us add yet two comments. It is interesting that, in contrast to the scalar field strength (6.2), the electromagnetic field $F_{\rm mon}$ is not singular at $\tilde{u}=0$. Apparently, the effects of the monopole and the charged shell compensate along $\tilde{u}=0$ in such a way that even the energy-momentum tensor of the field is finite there.

Second, if the field $A_{\rm mon}$, corresponding to the retarded field from the charge e at $\tilde{r}=0$ and the outgoing charged shell is superposed with the analogous field corresponding to the advanced field from the charge $-e$ at $\tilde{r}=\pi$ and the ingoing charged shell, the fields corresponding to charged shells localized on $\tilde{u}=0$ cancel each other and the field $A_{\rm sym}$ [Eq. (5.4)] with $R_{\rm o}=0$ is obtained. The same compensation occurs for two uniformly accelerated charges ($R_{\rm o}\neq 0$) considered in Sec. V, as it follows from the symmetry. Therefore, the symmetric electromagnetic field (5.4) can be interpreted as arising from the combinations of retarded and advanced

potentials due to both charges 1 and $1'$ in the same way as was the case for the symmetric scalar field; relation (6.6) remains true if Φ's are replaced by A's.

B. Constraints

The appearance of a shell with the total charge exactly opposite to that of the monopole discussed above has deeper reasons. It is a consequence of the constraints, which any electromagnetic field and charge distributions have to satisfy on a spatial hypersurface, and of the fact that spatial hypersurfaces, including past and future infinities, in de Sitter spacetime, are compact. Integrating the constraint equation

$$\nabla^{(3)}_{\mu}\mathcal{E}^{\mu}=\rho \tag{7.9}$$

[see Eq. (2.23) for the definition of $\mathcal{E}^{\alpha}$] over a compact Cauchy hypersurface Σ, we convert the integral of the divergence on the left-hand side to the integral over a ''boundary'' which, however, does not exist for a compact Σ. Hence, as it is well-known, the total charge on a compact hypersurface (in any spacetime, not only de Sitter) must vanish:

$$Q_{\rm tot}=0. \tag{7.10}$$

Therefore, the field $F_{\rm mon}$ constructed in Eq. (7.7) represents the monopole field plus the ''simplest'' additional source localized on the past horizon of the monopole that leads to the total zero charge. This enables the monopole electric-field lines to end on this horizon.

A stronger, even *local* condition on the charge distribution in de Sitter spacetime (or, indeed, in any spacetime with spacelike past infinity $\mathcal{I}^-$) arises if we admit purely retarded fields only. Here we define *purely retarded fields* as those that *vanish at* $\mathcal{I}^-$. Then, however, the constraint (7.9) directly implies that at $\mathcal{I}^-$ the charge distribution vanishes:

$$\rho|_{\tilde{t}=0}=0. \tag{7.11}$$

In the Les Houches lectures in 1963 Penrose [9] gave a general argument showing that if $\mathcal{I}^-$ is spacelike and the charges meet it in a discrete set of points, then there will be inconsistencies if an incoming field is absent (see in particular Fig. 16 in Ref. [9], cf. Fig. 1, see also Ref. [11]). Penrose also remarked that an alternative definition of advanced and retarded fields might be found that leads to different results, and that the application of the result to physical models is not clear. We found nothing more on this problem in the literature since Penrose's observation in 1963. Our work appears to give the first explicit model in which this issue can be analyzed.

C. Rigid dipole

As the first example of a simple source satisfying both the constraint (7.10) and the local condition (7.11) required by the absence of incoming radiation, we consider a rigid dipole. To construct an elementary rigid dipole, we place point charges e/ε and $-e/\varepsilon$ on the worldlines with $R_{\rm o}=\frac{1}{2}\varepsilon\alpha$ and $\vartheta=0,\pi$, fixed in the static coordinates, and take the limit $\varepsilon\to 0$. The constant dipole moment is thus given by $p=e\alpha$. The resulting symmetric field can easily be deduced from the symmetric fields (5.4)–(5.7) of electric monopoles:[6]

$$A_{\rm sym}=-\frac{p}{4\pi\alpha}\frac{\cos\vartheta}{\sin^2\tilde{r}}(\sin\tilde{t}\cos\tilde{r}\,d\tilde{t}-\cos\tilde{t}\sin\tilde{r}\,d\tilde{r}),$$

$$\begin{aligned}F_{\rm sym}=-\frac{p}{4\pi\alpha}\Bigg[&2\cos\vartheta\frac{\sin\tilde{t}}{\sin^3\tilde{r}}d\tilde{t}\wedge d\tilde{r}\\&-\frac{\sin\vartheta}{\sin^2\tilde{r}}(\sin\tilde{t}\cos\tilde{r}\,d\vartheta\wedge d\tilde{t}\\&-\cos\tilde{t}\sin\tilde{r}\,d\vartheta\wedge d\tilde{r})\Bigg].\end{aligned} \tag{7.12}$$

As in Sec. V, $R_{\rm o}=0$ corresponds to two worldlines and the symmetric solution (7.12) describes the fields of *two* dipoles, one at rest at $\tilde{r}=0$, the other at $\tilde{r}=\pi$.

To construct a purely retarded field of the dipole at $\tilde{r}=0$, we first restrict the symmetric field (7.12) to the inside of the ''creation light cone'' of the dipole, analogously as we did with the monopole charge in Sec. VII A. Writing [cf. Eq. (7.3)]

$$A_{\rm o}=A_{\rm sym}\theta(\tilde{u}), \tag{7.13}$$

we now get

$$F_{\rm o}=F_{\rm sym}\theta(\tilde{u}), \tag{7.14}$$

so that no additional term like that in Eq. (7.4) arises; however, expressing the left-hand side of Maxwell's equations as in Eq. (7.5), we find

$$\nabla_{\mu}F^{\alpha\mu}_{\rm o}=J^{\alpha}_{\rm rdip}-\frac{p}{4\pi\alpha}\,2\cos\vartheta(1-\cos\tilde{v})\,\delta(\tilde{u})\frac{\partial^{\alpha}}{\partial\tilde{v}}. \tag{7.15}$$

Here $J^{\alpha}_{\rm rdip}=(\nabla_{\mu}F^{\alpha\mu}_{\rm sym})\,\theta(\tilde{u})$ is the current corresponding to the rigid dipole at $\tilde{r}=0$. Similarly to the case of the monopole, there is an additional term on the right-hand side of Eq. (7.15), localized on the null cone $\tilde{u}=0$, indicating that the field (7.13) represents, in addition to the dipole, an additional source located on the horizon $\tilde{u}=0$. In contrast to the monopole case, however, this source can be compensated by adding to the potential (7.13) the term

$$A_{*}=-\frac{p}{4\pi\alpha}\cos\vartheta\,\delta(\tilde{u})d\tilde{u}. \tag{7.16}$$

In this way we finally obtain the purely retarded field of the dipole with dipole moment p, located at $\tilde{r}=R=0$, in the form

[6]Here in the potential we ignore a trivial gauge term proportional to $d\cos\vartheta$.

$$A_{\rm rdip}=A_{\rm o}+A_{*},$$
$$F_{\rm rdip}=F_{\rm sym}\theta(\tilde{u})+\frac{p}{4\pi\alpha}\sin\vartheta\,\delta(\tilde{u})\,d\vartheta\wedge d\tilde{u}, \tag{7.17}$$

where $A_{\rm o}$, A_{*}, $F_{\rm sym}$ are given by Eqs. (7.13), (7.16), and (7.12). It is easy to check that $\nabla_\mu F^{\alpha\mu}_{\rm rdip}=J^{\alpha}_{\rm rdip}$ is satisfied.

Regarding the retarded field (7.17), we see that it is, in contrast to the symmetric field (7.12), singular on the ''creation light cone'' (past event horizon) $\tilde{u}=0$. This is not suprising; in order to obtain a purely retarded field, we ''squeezed'' the field lines produced by the dipole into the horizon.

D. Geodesic dipole

Next we consider dipoles consisting of two free charges moving along the geodesic[7] $r=$constant, $\vartheta=$constant, $\varphi=$constant in the Minkowski space which, as discussed at the end of Sec. IV [see Eq. (4.6) and the worldlines 2,2′ in Fig. 4] transforms into geodesics of the conformally related de Sitter space. We call two free opposite charges a *geodesic dipole*.

We start again by constructing first the symmetric field. Two elementary geodesic dipoles located at $\tilde{r}=0$ and $\tilde{r}=\pi$ can be obtained by placing point charges $\pm e/\varepsilon$ on the worldlines $r=\frac{1}{2}\varepsilon\alpha$, $\vartheta=0,\pi$ and taking the limit $\varepsilon\to 0$. As with monopoles, to find the symmetric field we conformally transform the field of a standard rigid Minkowski dipole (bewaring the signs for $t>0$ and $t<0$ so that the field is analytic outside the sources). The dipole moment in Minkowski space $\hat{p}=e\alpha$ is constant, the corresponding value in de Sitter spacetime, however, depends now on time:

$$p=\frac{\alpha}{t}\,\hat{p}=\frac{\pm 1+\cos\tilde{t}}{\sin\tilde{t}}\,e\alpha, \tag{7.18}$$

as it follows from the transformation relations (2.22) and (3.6). In terms of $\hat{p}$ we find the symmetric field of geodesic dipoles located at $\tilde{r}=0$ and $\tilde{r}=\pi$ to read

$$A_{\rm sym}=-\frac{\hat{p}}{4\pi}\frac{\cos\vartheta}{r^2}dt$$
$$=-\frac{\hat{p}}{4\pi\alpha^2}\frac{\cos\vartheta}{\sin^2\tilde{r}}[(1+\cos\tilde{t}\cos\tilde{r})d\tilde{t}+\sin\tilde{t}\sin\tilde{r}\,d\tilde{r}],$$
$$F_{\rm sym}=-\frac{\hat{p}}{4\pi\alpha^2}\left\{2\frac{\cos\vartheta}{\sin^3\tilde{r}}(\cos\tilde{t}+\cos\tilde{r})d\tilde{t}\wedge d\tilde{r}\right.$$
$$-\frac{\sin\vartheta}{\sin^2\tilde{r}}[(1+\cos\tilde{t}\cos\tilde{r})d\vartheta\wedge d\tilde{t}$$
$$\left.+\sin\tilde{t}\sin\tilde{r}\,d\vartheta\wedge d\tilde{r}]\right\}. \tag{7.19}$$

Proceeding as with the rigid dipole, we generate the retarded field of only one geodesic dipole at $\tilde{r}=0$ by restricting the symmetric field by the step function:

$$A_{\rm o}=A_{\rm sym}\theta(\tilde{u}),$$
$$F_{\rm o}=F_{\rm sym}\theta(\tilde{u})-\frac{\hat{p}}{4\pi\alpha^2}\frac{2\cos\vartheta}{1-\cos\tilde{v}}\delta(\tilde{u})d\tilde{v}\wedge d\tilde{u}. \tag{7.20}$$

Since

$$\nabla_\mu F^{\alpha\mu}_{\rm o}=J^{\alpha}_{\rm gdip}+\frac{2\hat{p}}{4\pi\alpha^6}\delta(\tilde{u})\left(-\sin\vartheta\frac{\partial^\alpha}{\partial\vartheta}+\cos\vartheta\sin\tilde{v}\frac{\partial^\alpha}{\partial\tilde{v}}\right)$$
$$-\frac{2\hat{p}}{4\pi\alpha^6}\cos\vartheta(1-\cos\tilde{v})\,\delta'(\tilde{u})\frac{\partial^\alpha}{\partial\tilde{v}}, \tag{7.21}$$

where $J^{\alpha}_{\rm gdip}=(\nabla_\mu F^{\alpha\mu}_{\rm sym})\,\theta(\tilde{u})$, an additional source is present at the horizon $\tilde{u}=0$; it can be compensated by adding an additional field with potential, for example, given by

$$A_{*}=-\frac{2\hat{p}}{4\pi\alpha^2}\delta(\tilde{u})\left(\cos\vartheta\frac{\sin\tilde{v}}{1-\cos\tilde{v}}d\tilde{u}+\sin\vartheta d\vartheta\right). \tag{7.22}$$

The total retarded field of the geodesic dipole is then given as follows:

$$A_{\rm gdip}=A_{\rm o}+A_{*},$$
$$F_{\rm gdip}=F_{\rm sym}\theta(\tilde{u})+\frac{2\hat{p}}{4\pi\alpha^2}\,\delta(\tilde{u})\left(\frac{2\cos\vartheta}{1-\cos\tilde{v}}\,d\tilde{v}\wedge d\tilde{u}\right.$$
$$\left.+\sin\vartheta\frac{\sin\tilde{v}}{1-\cos\tilde{v}}\,d\vartheta\wedge d\tilde{u}\right)$$
$$-\frac{2\hat{p}}{4\pi\alpha^2}\sin\vartheta\,\delta'(\tilde{u})d\vartheta\wedge d\tilde{u}. \tag{7.23}$$

It indeed satisfies Maxwell's equations:

$$\nabla_\mu F^{\alpha\mu}_{\rm gdip}=J^{\alpha}_{\rm gdip}. \tag{7.24}$$

VIII. CONCLUSION

By using the conformal relation between de Sitter and Minkowski space, we constructed various types of fields pro-

[7]Charges are called free in the sense that they are assumed to be moving along geodesics. Of course, there is an electromagnetic interaction between them, which is neglected or has to be compensated.

duced by scalar and electromagnetic charges moving with a uniform (possibly zero) acceleration in de Sitter background. One of our main conclusions has been the explicit confirmation and elucidation of the observation by Penrose that in spacetimes with a spacelike past infinity, which implies the existence of a particle horizon, purely retarded fields do not exist for general source distributions.

In Sec. VII D we constructed the field (7.23) of the geodesic dipole which, at first sight, appears as being a purely retarded field. Can thus purely retarded fields of, for example, two opposite monopoles, be constructed by distributing the elementary geodesic dipoles along a segment $\tilde{r} \in \langle 0,a\rangle$, $\vartheta=\varphi=0$, so that neighboring opposite charges cancel out, and only two monopoles, at $\tilde{r}=0$ and $\tilde{r}=a$, remain? Then, however, the local constraint (7.11) on the charge distribution would clearly be violated!

The solution of this paradox is in the fact that the field (7.23) *is not a purely* retarded field; if we calculate (by using distributions) the initial data leading to the field strength (7.23), we discover that the electric-field strength contains terms proportional to the δ-function at $\tilde{t}=0$, $\tilde{r}=0$ so that the field does not vanish at $\mathcal{I}^-$. Hence the field of the dipoles distributed along the segment does *not* vanish at $\mathcal{I}^-$ and thus cannot be considered as a purely retarded field of the two monopoles at $\tilde{r}=0$ and $\tilde{r}=a$.

We thus arrive at the conclusion that a purely retarded field of even two opposite charges (so that the global constraint of a zero net charge *is* satisfied) cannot be constructed in the de Sitter spacetime unless the charges ''enter'' the universe at the same point at $\mathcal{I}^-$ and the *local* constraint (7.11) is satisfied. If we allow nonvanishing initial data at $\mathcal{I}^-$, the resulting fields can hardly be considered as ''purely retarded.''

By applying the superposition principle we can consider a greater number of sources, and our arguments of the insufficiency of purely retarded fields (based on the global and local constraints) can clearly be generalized also to infinitely many discrete sources. Our discussion of the fields of dipoles indicates that interesting situations may arise.

The absence of purely retarded fields in de Sitter spacetime or, in fact, in any spacetime with spacelike $\mathcal{I}^-$ is, of course, to be expected to occur for higher-spin fields as well. In particular, there has been much interest in the primordial gravitational radiation. Since de Sitter spacetime is a standard arena for inflationary models, the generation of gravitational waves by (test) sources in de Sitter spacetime has been studied in recent literature (see Ref. [23], and references therein). We plan to analyze the linearized gravity on de Sitter background in light of the results described above. The fact that particles are expected to have only positive gravitational mass will apparently prevent any purely retarded field to exist.

First, however, we shall present the generalization of the well-known Born solution for uniformly accelerated charges in Minkowski spacetime to the generalized Born solution representing uniformly accelerated charges in de Sitter spacetime [24]. As demonstrated in the present paper, to be ''born in de Sitter'' is quite a different matter than to be ''born in Minkowski.''

ACKNOWLEDGMENTS

The authors would like to thank the Albert-Einstein Institute, Golm, where part of this work was done, for its kind hospitality. J.B. also acknowledges the Sackler Fellowship at the Institute of Astronomy in Cambridge, where this work was finished. We were supported in part by Grant Nos. GAČR 202/99/026 and GAUK 141/2000 of the Czech Republic and Charles University.

APPENDIX: COORDINATE SYSTEMS IN de SITTER SPACE

We describe here coordinate systems employed in the main text. There exists extensive literature on various useful coordinates in de Sitter spacetime—for standard reference see Ref. [6], for more recent reviews, containing also many references, see, for example, Refs. [25,26].

de Sitter spacetime has topology $S^3\times\mathbb{R}$. It is best visualized as the four-dimensional hyperboloid imbedded in flat five-dimensional Minkowski space; it is the homogeneous space of constant curvature spherically symmetric about any point. The following coordinate systems are constructed around any fixed (though arbitrary) point. Two of the coordinates are just standard spherical angular coordinates $\vartheta\in\langle 0,\pi\rangle$ and $\varphi\in\langle -\pi,\pi\rangle$ on the orbits of the Killing vectors of spherical symmetry with the homogeneous metric

$$d\omega^2 = d\vartheta^2 + \sin^2\theta\, d\varphi^2. \tag{A1}$$

In the transformations considered below, these coordinates remain unchanged and are thus are not written down. The axis is fixed by $\vartheta=0,\pi$.

Next, we have to introduce time and radial coordinates labeling the orbits of spherical symmetry. The coordinate systems defined below differ only in these time and radial coordinates and, therefore, we essentially work with a two-dimensional system. Radial coordinates commonly take positive values and coordinate systems are degenerate for their value zero.

As discussed in Sec. III below Eq. (3.15), the relations between various regions I–IV of Minkowski and de Sitter spaces are conveniently described if we allow radial coordinates to attain negative values. We adopt the convention that at a fixed time the points symmetrical with respect to the origin of spherical coordinates have the opposite sign of the radial coordinate. Hence, the points with $\{t,r,\vartheta,\varphi\}$ are identical with $\{t,-r,\pi-\vartheta,\varphi+\pi\}$, analogously for the coordinates $\{\tilde{t},\tilde{r},\vartheta,\varphi\}$ introduced below.

Let us characterize this convention in more detail. Imagine that on our manifold (either compactified Minkowski space or de Sitter space) two coordinate maps $\{t_-,r_-,\vartheta_-,\varphi_-\}$ and $\{t_+,r_+,\vartheta_+,\varphi_+\}$ are introduced, which for any fixed point are connected by the relations

$$t_- = t_+, \quad r_- = -r_+,$$
$$\vartheta_- = \pi - \vartheta_+, \quad \varphi_- = \varphi_+ + \pi \bmod 2\pi, \tag{A2}$$

where $r_+ \in \mathbb{R}^+$ and $r_- \in \mathbb{R}^-$. *Both* maps cover the *whole* spacetime manifold. Now we consider a two-dimensional cut given by $\vartheta_+ = \vartheta_o$, $\varphi_+ = \varphi_o$, with t_+, r_+ changing. This represents the history of a half-line l_+ in Fig. 2, illustrated by regions I and III, say. The history of a half-line l_-, obtained by the smooth extension of l_+ through the origin, illustrated by regions II and IV, is covered by the coordinates $\{t_-, r_-, \vartheta_-, \varphi_-\}$ with the *same* angular coordinates $\vartheta_- = \vartheta_o$, $\varphi_- = \varphi_o$ but $r_- < 0$ (which, in our convention, is identical to $r_+ > 0$, $\vartheta_+ = \pi - \vartheta_o$, $\varphi_+ = \varphi_o + \pi$).

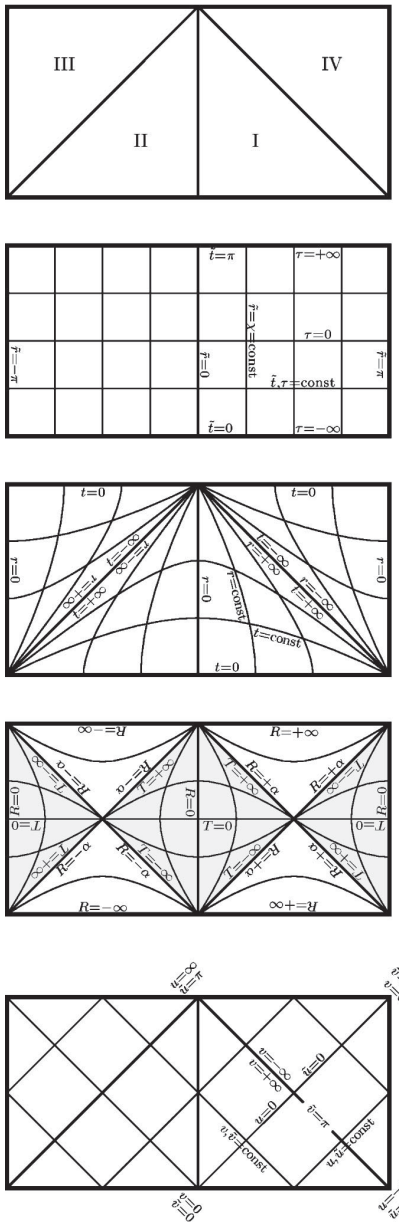

FIG. 5. Coordinates in de Sitter space. (a) Regions I–IV are specified. They correspond to the same regions as in the cut $\mathcal{C}$ in Fig. 3. Coordinate lines of the conformally Einstein coordinates (b), of the conformally flat coordinates (c), of the static coordinates (d), and of the null coordinates (e), are indicated. For the definition of all these coordinate systems, see Eqs. (A4)–(A14). All the figures describe the same cut of de Sitter space. The ranges of coordinates covering the cut, as well as directions in which they grow, can be seen from the figures.

In exactly the same way we may introduce coordinates $\{\tilde{t}_\pm, \tilde{r}_\pm, \vartheta, \varphi\}$, with $\{\tilde{t}_+, \tilde{r}_+\}$ covering regions I and IV in Fig. 3, whereas $\{\tilde{t}_-, \tilde{r}_-\}$ cover regions II and III. In Fig. 5, the two-dimensional cuts (with angular coordinates fixed) through de Sitter space (or through the compactified space $M^\#$) are illustrated. Both regions covered by $\{\tilde{t}_+, \tilde{r}_+\}$ and by $\{\tilde{t}_-, \tilde{r}_-\}$ are included (the right and left parts of the diagrams). However, in the figures, as well as in the main text, we do not write down subscripts "+" and "−" at the coordinates, since the sign of the radial coordinate specifies which map is used.

de Sitter spacetime can be covered by *standard* coordinates τ, χ ($\tau \in \mathbb{R}$, $\chi \in \mathbb{R}^+$) in which the metric has the form [6]:

$$g = -d\tau^2 + \alpha^2 \cosh^2 \frac{\tau}{\alpha} (d\chi^2 + \sin^2 \chi \, d\omega^2). \tag{A3}$$

It is useful to rescale the coordinate τ to obtain *conformally Einstein* coordinates $\{\tilde{t}, \tilde{r}\}$:

$$\tilde{t} = 2 \arctan\left(\exp \frac{\tau}{\alpha} \right), \quad \tilde{t} \in \langle 0, \pi \rangle,$$
$$\tilde{r} = \chi, \quad \tilde{r} \in \langle 0, \pi \rangle, \tag{A4}$$
$$g = \frac{\alpha^2}{\sin^2 \tilde{t}} (-d\tilde{t}^2 + d\tilde{r}^2 + \sin^2 \tilde{r} \, d\omega^2). \tag{A5}$$

In these coordinates, de Sitter space is explicitly seen to be conformal to the part of the Einstein static universe. Coordinate lines are drawn in Fig. 5(b).

Another coordinate system used in our work are inertial coordinates t, r of conformally related Minkowski space. We call them *conformally flat* coordinates:

$$t = \frac{\alpha \sin \tilde{t}}{\cos \tilde{r} + \cos \tilde{t}}, \quad \tilde{t} = \arctan \frac{2t\alpha}{\alpha^2 - t^2 + r^2}, \quad t \in \mathbb{R}, \tag{A6}$$
$$r = \frac{\alpha \sin \tilde{r}}{\cos \tilde{r} + \cos \tilde{t}}, \quad \tilde{r} = \arctan \frac{2r\alpha}{\alpha^2 + t^2 - r^2}, \quad r \in \mathbb{R}^+,$$
$$g = \frac{\alpha^2}{t^2} (-dt^2 + dr^2 + r^2 d\omega^2). \tag{A7}$$

Coordinate lines are drawn in Fig. 5(c).

Commonly used are *static* coordinates T,R, related to the timelike Killing vector $\partial/\partial T$ of de Sitter spacetime:

$$T=\frac{\alpha}{2}\log\frac{t^2-r^2}{\alpha^2}=\frac{\alpha}{2}\log\frac{\cos\tilde r-\cos\tilde t}{\cos\tilde r+\cos\tilde t},\quad T\in\mathbb{R},$$
$$R=\alpha\frac{r}{t}=\alpha\frac{\sin\tilde r}{\sin\tilde t},\quad R\in\langle 0,\alpha\rangle, \tag{A8}$$
$$g=-\left(1-\frac{R^2}{\alpha^2}\right)dT^2+\left(1-\frac{R^2}{\alpha^2}\right)^{-1}dR^2+R^2d\omega^2. \tag{A9}$$

As it is well known, these coordinates do not cover the whole spacetime but only the domain with $\tilde t+\tilde r<\pi$ and $\tilde t-\tilde r>0$. The boundary of this domain is the Killing horizon. The coordinate R can be extended smoothly to the whole spacetime but it is not unique globally. It is also useful to rescale coordinate R to obtain the *expanded static* coordinates $\overline{t}$, $\overline{r}$:

$$\overline{t}=T,\quad \overline{t}\in\mathbb{R},$$
$$\overline{r}=\alpha\,\mathrm{arctanh}\frac{R}{\alpha},\quad \overline{r}\in\mathbb{R}, \tag{A10}$$
$$g=\left(\cosh\frac{\overline{r}}{\alpha}\right)^{-2}\left(-d\overline{t}^2+d\overline{r}^2+\alpha^2\sinh^2\frac{\overline{r}}{\alpha}d\omega^2\right). \tag{A11}$$

Coordinate lines for the static coordinates are drawn in Fig. 5(d).

Finally, three sets of *null* coordinates $\{u,v\}$, $\{\overline{u},\overline{v}\}$, and $\{\tilde u,\tilde v\}$ are defined by

$$\begin{aligned} u&=t-r,\quad \tilde u=\tilde t-\tilde r,\quad \overline{u}=\overline{t}-\overline{r},\\ v&=t+r,\quad \tilde v=\tilde t+\tilde r,\quad \overline{v}=\overline{t}+\overline{r}.\end{aligned} \tag{A12}$$

From here we find

$$u=\alpha\tan\frac{\tilde u}{2}=\alpha\exp\frac{\overline{u}}{\alpha},\quad v=\alpha\tan\frac{\tilde v}{2}=\alpha\exp\frac{\overline{v}}{\alpha}. \tag{A13}$$

The metric in these coordinates reads

$$\begin{aligned} g&=\frac{\alpha^2}{(u+v)^2}[-2\,du\vee dv+(u-v)^2d\omega^2]\\ &=\frac{\alpha^2}{1-\cos(\tilde v+\tilde u)}[-d\tilde v\vee d\tilde u+(1-\cos(\tilde v-\tilde u))d\omega^2]\\ &=(e^{\overline{u}/\alpha}+e^{\overline{v}/\alpha})^{-2}[-2\,e^{(\overline{u}+\overline{v})/\alpha}d\overline{u}\vee d\overline{v}\\ &\quad+\alpha^2(e^{\overline{u}/\alpha}-e^{\overline{v}/\alpha})^2d\omega^2].\end{aligned} \tag{A14}$$

The corresponding coordinate lines are illustrated in Fig. 5(e).

[1] *Modern Cosmology in Retrospect*, edited by B. Bertotti, R. Balbinot, S. Bergia, and A. Messina (Cambridge University Press, Cambridge, England, 1990).
[2] P. J. E. Peebles, *Principles of Physical Cosmology* (Princeton University Press, Princeton, NJ, 1993).
[3] K. Maeda, in *Proceedings of the Fifth M. Grossman Meeting on General Relativity*, Perth, Australia, 1988, edited by D. G. Blair, M. J. Buckingham, and R. Ruffini (World Scientific, Singapore, 1989).
[4] N. D. Birrell and P. C. W. Davies, *Quantum Fields in Curved Space* (Cambridge University Press, Cambridge, England, 1982).
[5] B. de Wit and I. Herger, in *Towards Quantum Gravity*, Lecture Notes in Physics Vol. 541 (Springer-Verlag, New York, 2000), p. 79.
[6] S. W. Hawking and G. F. R. Ellis, *The Large Scale Structure of Space-Time* (Cambridge University Press, Cambridge, England, 1973).
[7] R. Penrose, Phys. Rev. Lett. **10**, 66 (1963).
[8] R. Penrose, Proc. R. Soc. London **A284**, 159 (1965).
[9] R. Penrose, in *Relativity, Groups and Topology, Les Houches 1963*, edited by C. DeWitt and B. DeWitt (Gordon and Breach, New York, 1964).
[10] R. Penrose and W. Rindler, *Spinors and Space-Time* (Cambridge University Press, Cambridge, England, 1984).
[11] R. Penrose, in *The Nature of Time*, edited by T. Gold (Cornell University Press, Ithaca, NY, 1967), pp. 42–54.
[12] *Internal Structure of Black Holes and Spacetime Singularities*, edited by L. Burko and A. Ori (Institute of Physics, and The Israel Physical Society, Bristol, Jerusalem, 1997).
[13] E. Eriksen and Ø. Grøn, Ann. Phys. (N.Y.) **286**, 320 (2000).
[14] J. Bičák, in *Einstein's Field Equations and Their Physical Implications*, Lecture Notes in Physics Vol. 540, edited by B. G. Schmidt (Springer-Verlag, Berlin, 2000), pp. 1–126; gr-qc/0004016.
[15] J. Bičák and B. G. Schmidt, Phys. Rev. D **40**, 1827 (1989).
[16] J. Plebański and M. Demiański, Ann. Phys. (N.Y.) **98**, 98 (1976).
[17] R. B. Mann and S. F. Ross, Phys. Rev. D **52**, 2254 (1995).
[18] J. Podolský and J. B. Griffiths, Phys. Rev. D **63**, 024006 (2001).
[19] C. W. Misner, K. S. Thorne, and J. A. Wheeler, *Gravitation* (Freeman, San Francisco, 1973).
[20] R. M. Wald, *General Relativity* (The University of Chicago Press, Chicago, 1984).
[21] T. Fulton, F. Rohrlich, and L. Witten, Rev. Mod. Phys. **34**, 442 (1962).
[22] F. Rohrlich, *Classical Charged Particles* (Addison-Wesley, Reading, MA, 1965).
[23] H. J. Vega, J. Ramirez, and N. Sanchez, Phys. Rev. D **60**, 044007 (1999).
[24] J. Bičák and P. Krtouš (unpublished).
[25] H. J. Schmidt, Fortschr. Phys. **41**, 179 (1993).
[26] E. Eriksen and Ø. Grøn, Int. J. Mod. Phys. D **4**, 115 (1995).

VOLUME 88, NUMBER 21 PHYSICAL REVIEW LETTERS 27 MAY 2002

The Fields of Uniformly Accelerated Charges in de Sitter Spacetime

Jiří Bičák* and Pavel Krtouš†

Institute of Theoretical Physics, Faculty of Mathematics and Physics, Charles University, V Holešovičkách 2, 180 00 Prague 8, Czech Republic

(Received 15 November 2001; published 8 May 2002)

The scalar and electromagnetic fields of charges uniformly accelerated in de Sitter spacetime are constructed. They represent the generalization of the Born solutions describing fields of two particles with hyperbolic motion in flat spacetime. In the limit $\Lambda \to 0$, the Born solutions are retrieved. Since in the de Sitter universe the infinities $\mathcal{I}^{\pm}$ are spacelike, the radiative properties of the fields depend on the way in which a given point of $\mathcal{I}^{\pm}$ is approached. The fields must involve both retarded and advanced effects: Purely retarded fields do not satisfy the constraints at the past infinity $\mathcal{I}^{-}$.

DOI: 10.1103/PhysRevLett.88.211101 PACS numbers: 04.20.–q, 03.50.–z, 04.40.–b, 98.80.Hw

The question of the electromagnetic field and associated radiation from uniformly accelerated charges has been one of the best known "perpetual problems" in classical physics from the beginning of the past century. In the pioneering work in 1909, Born gave the time-symmetric solution for the field of two point particles with opposite charges, uniformly accelerated in opposite directions in Minkowski space. In the 1920s, Sommerfeld, von Laue, Pauli, Schott, and others discussed the properties of the field. The controversial point that the field exhibits radiative features but that the radiation reaction force vanishes for the hyperbolic motion, and related questions, was discussed in many articles from the 1960s onward. Even the December 2000 issue of Annals of Physics contains three papers [1] with numerous references on "electrodynamics of hyperbolically accelerated charges."

In general relativity, solutions of Einstein's equations, representing "uniformly accelerated particles or black holes," are the *only* explicitly known exact *radiative* spacetimes describing *finite* sources. They are asymptotically flat at null infinity [2] (except for some special points) and have been used in gravitational radiation theory, quantum gravity, and numerical relativity (cf. review [3]). One of the best known examples is the C-metric, describing uniformly accelerated black holes. There exists also the C-metric for a nonvanishing cosmological constant Λ. However, no general framework is available to analyze these spacetimes for $\Lambda \neq 0$ as that given in Ref. [2] for $\Lambda = 0$.

In this Letter, we present the generalization of the Born solutions for scalar and electromagnetic fields to the case of two charges uniformly accelerated in a de Sitter universe, and explicitly show how in the limit $\Lambda \to 0$ the Born solutions are retrieved. We also study the asymptotic expansions of the fields in the neighborhood of future infinity $\mathcal{I}^{+}$. In de Sitter spacetime, conformal infinities, $\mathcal{I}^{\pm}$, are *spacelike,* which implies the presence of particle and event horizons. It is known [4] that the radiation field is "less invariantly" defined when $\mathcal{I}^{+}$ is spacelike (it depends on the direction in which $\mathcal{I}^{+}$ is approached), but no explicit model appears to be available thus far. Our solutions can serve as prototypes for studying these issues.

In recent work [5], we analyzed fields of accelerated sources to show the *insufficiency of purely retarded fields in de Sitter spacetime*. Consider a point P near $\mathcal{I}^{-}$ whose past null cone will not cross the particles' world lines (Fig. 1). The field at P should vanish if an incoming field is absent. However, the "Coulomb-type" field of particles cannot vanish there because of Gauss law [6]. The requirement that the field be purely retarded leads, in general, to a bad behavior of the field along the "creation light cone" of the "point" at which a source enters the universe (see Ref. [5] for detailed discussion).

It is natural to use de Sitter space for studying radiating sources in spacetimes which are not asymptotically flat and possess spacelike infinities: It is the space of constant curvature, conformal to Minkowski space, and with the Huygens principle satisfied for conformally invariant fields. The de Sitter universe also plays an important role in cosmology — not only in the context of inflationary theories but also as the "asymptotic state" of standard cosmological models with $\Lambda > 0$, which has been indeed suggested by recent observations. In addition, the Born fields generalized to de Sitter space should be relevant from quantum perspectives: for example, for studying particle production in strong fields, or accelerating detectors in the presence of a cosmological horizon.

The de Sitter universe has topology $S^3 \times \mathbb{R}$. The metric in standard "spherical" coordinates (note [7]) is

$$g_{\mathrm{dS}} = -d\tau^2 + \alpha^2 \cosh^2(\tau/\alpha)(d\chi^2 + \sin^2\chi\, d\omega^2), \tag{1}$$

where $d\omega^2 = d\vartheta^2 + \sin^2\vartheta\, d\varphi^2$, $\tau \in \mathbb{R}$, and $\alpha^2 = 3/\Lambda$. Putting $\chi = \tilde{r}$, $\tau = \alpha \log\tan(\tilde{t}/2)$, $\tilde{t} \in \langle 0, \pi\rangle$, in Eq. (1), the de Sitter metric can be written in the form

$$g_{\mathrm{dS}} = \alpha^2 \sin^{-2}\tilde{t}(-d\tilde{t}^2 + d\tilde{r}^2 + \sin^2\tilde{r}\, d\omega^2). \tag{2}$$

The lines $\tilde{r} = \pi$ and $\tilde{r} = -\pi$ are identified, the spacelike hypersurfaces $\tilde{t} = 0, \pi$ represent $\mathcal{I}^{-}$ and $\mathcal{I}^{+}$ (Fig. 1).

By employing conformal techniques, we recently studied [5] two particles moving with uniform acceleration

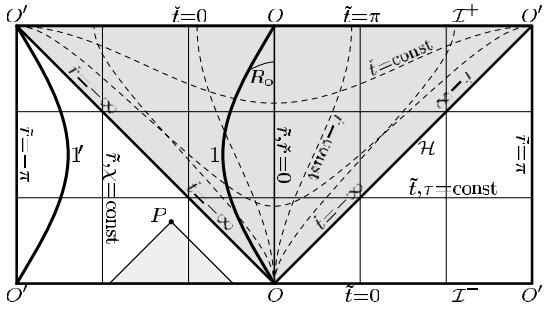

FIG. 1. The conformal diagram of de Sitter spacetime. Uniformly accelerated particles move along world lines 1 and $1'$. The shaded region is the domain of influence of 1, its boundary $\mathcal{H}$ is the "creation light cone" of this particle "born" at $\tilde{t} = 0$ at "point" O. Retarded fields of 1 and $1'$ cannot affect point P; a Coulomb-type field, however, cannot vanish there.

(note [8]) in de Sitter space. Their world lines are plotted in Fig. 1 as 1, $1'$ [for explicit formulas see Ref. [5], Eq. (4.4); see also Eqs. (6) and (10) below]. Both particles start at antipodes of the spatial section of de Sitter space at $\mathcal{I}^-$ and move one towards the other until $\tilde{t} = \pi/2$, the moment of the maximal contraction of de Sitter space. Then they move, in a time-symmetric manner, apart from each other until they reach future infinity at the antipodes from which they started. Their physical velocities, as measured in the "comoving" coordinates $\{\tau, \chi, \vartheta, \varphi\}$, have simple forms $v_\chi = \sqrt{g_{\chi\chi}}\, d\chi/d\tau = \mp a_o \alpha \tanh(\tau/\alpha) \times [1 + a_o^2 \alpha^2 \tanh^2(\tau/\alpha)]^{-1/2}$, where $|a_o|$ is the magnitude of their acceleration. In contrast to the flat space case, the particles do not approach the velocity of light in the "natural" global coordinate system. They are causally disconnected (Fig. 1) as in the flat space case: No signal from one particle can reach the other particle.

Two charges moving along the orbits of the boost Killing vector in flat space are *at rest* in the Rindler coordinate system and have a constant distance from the spacetime origin, as measured along the slices orthogonal to the Killing vector. Similarly, the world lines 1 and $1'$ are the orbits of the "static" Killing vector $\partial/\partial T$ of de Sitter space. In static coordinates $\{T, R, \vartheta, \varphi\}$, $T = \frac{\alpha}{2} \log[(\cos\tilde{r} - \cos\tilde{t})/(\cos\tilde{r} + \cos\tilde{t})]$, $R = \alpha \sin\tilde{r}/\sin\tilde{t}$, the particles 1, $1'$ are at rest at $R = \pm R_o = \mp a_o \alpha^2/\sqrt{1 + a_o^2 \alpha^2}$, with four accelerations $-(R_o/\alpha^2)\partial/\partial R$. The particle 1 ($1'$) has, as measured at fixed T, a constant proper distance from the origin $\tilde{t} = \pi/2$, $\tilde{r} = 0$ ($\tilde{r} = \pi$). As with Rindler coordinates in Minkowski space, the static coordinates cover only a "half" of de Sitter space; in the other half the Killing vector $\partial/\partial T$ becomes spacelike.

By the conformal transformation of the boosted Coulomb fields in Minkowski space, we constructed [5] test scalar and electromagnetic fields produced by charges moving along the world lines 1, $1'$ in de Sitter space. The scalar field from two *identical* scalar charges s is given by

$$\Phi_{\text{sym}} = (s/4\pi)\mathcal{Q}^{-1}, \tag{3}$$

$$\mathcal{Q} = [\alpha^2(\sqrt{1 + a_o^2\alpha^2} + a_o R \cos\vartheta)^2 - \alpha^2 + R^2]^{1/2} \tag{4}$$

[Ref. [5], Eq. (5.4)], whereas the electromagnetic field due to *opposite* charges $+e$ and $-e$ is [Ref. [5], Eq. (5.7)]

$$F_{\text{sym}} = -\frac{e}{4\pi}\frac{1}{\mathcal{Q}^3}\frac{a_o\alpha^4}{\sin^3\tilde{t}}[\cos\tilde{t}\sin^2\tilde{r}\sin\vartheta\, d\tilde{r}\wedge d\vartheta + (a_o^{-1}\sqrt{a_o^2 + \alpha^{-2}}\sin\tilde{r} + \sin\tilde{t}\cos\vartheta) d\tilde{t}\wedge d\tilde{r} - \sin\tilde{t}\cos\tilde{r}\sin\tilde{r}\sin\vartheta\, d\tilde{t}\wedge d\vartheta]. \tag{5}$$

We call these smooth (outside the sources) fields symmetric because they can be written as a symmetric combination of retarded and advanced effects from both charges.

Although Eqs. (3) and (5) represent fields due to uniformly accelerated charges in de Sitter space, their relation to the Born solutions is not transparent because the sources are not located symmetrically with respect to $\tilde{r} = 0$. Hence, we consider the world lines 2 and $2'$ (Fig. 2) which, due to homogeneity and isotropy of de Sitter space, also represent uniformly accelerated particles. These world lines and the resulting fields can be obtained from Eqs. (3)–(5) by a spatial rotation by $\pi/2$. We find the world lines 2, $2'$ to be given by

$$\begin{aligned}\cot\tilde{t} &= -\sinh(\lambda_{\text{dS}}\alpha^{-1}\sqrt{1 + a_o^2\alpha^2})/\sqrt{1 + a_o^2\alpha^2}\,,\\ \tan\tilde{r} &= \pm\cosh(\lambda_{\text{dS}}\alpha^{-1}\sqrt{1 + a_o^2\alpha^2})/(a_o\alpha)\,,\end{aligned} \tag{6}$$

$\vartheta = 0$, $\varphi = 0$. The scalar and electromagnetic fields are

$$\Phi_{\text{BdS}} = (s/4\pi)\sin\tilde{t}(\sin\tilde{t} + \cos\tilde{r})^{-1}\mathcal{R}^{-1}, \tag{7}$$

$$F_{\text{BdS}} = -\frac{e}{4\pi}\frac{\alpha^3}{\mathcal{R}^3}\frac{a_o\alpha\sin\vartheta}{(\sin\tilde{t} + \cos\tilde{r})^3}[\sin^2\tilde{r}\cos\tilde{t}\, d\tilde{r}\wedge d\vartheta - (a_o^{-1}\sqrt{a_o^2 + \alpha^{-2}}\cos\tilde{r} - \sin\tilde{t})\cot\vartheta\, d\tilde{t}\wedge d\tilde{r} + (a_o^{-1}\sqrt{a_o^2 + \alpha^{-2}} - \cos\tilde{r}\sin\tilde{t})\sin\tilde{r}\, d\tilde{t}\wedge d\vartheta], \tag{8}$$

$$\frac{\mathcal{R}}{\alpha} = \frac{[(a_o\alpha\sin\tilde{t} - \sqrt{1 + a_o^2\alpha^2}\cos\tilde{r})^2 + \sin^2\tilde{r}\sin^2\vartheta]^{1/2}}{\sin\tilde{t} + \cos\tilde{r}}.$$

In order to understand explicitly the relation of these fields to the classical Born solutions, consider Minkowski spacetime with spherical coordinates $\{t, r, \vartheta, \varphi\}$ with metric $g_{\text{M}} = -dt^2 + dr^2 + r^2 d\omega^2$. If we set

$$\begin{aligned}t &= -\alpha\cos\tilde{t}/(\cos\tilde{r} + \sin\tilde{t})\,,\\ r &= \alpha\sin\tilde{r}/(\cos\tilde{r} + \sin\tilde{t})\,,\end{aligned}$$

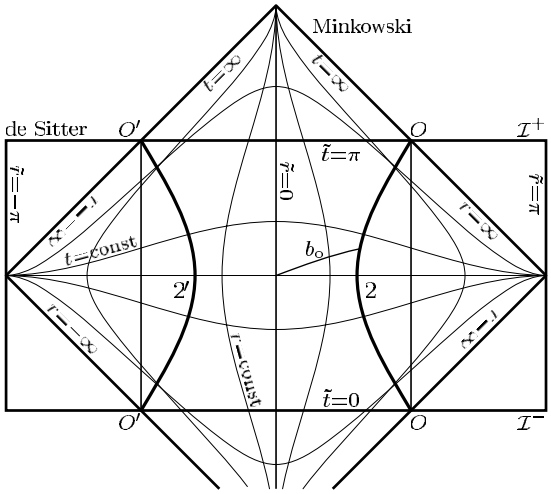

FIG. 2. The world lines 2, 2′ of uniformly accelerated charges symmetrically located with respect to the origins of both de Sitter and conformally related Minkowski spacetimes.

with ϑ, φ unchanged, we find that this Minkowski space is conformally related to de Sitter space as follows (Fig. 2):

$$g_{\mathrm{dS}} = \Omega^2 g_{\mathrm{M}}, \qquad \Omega = \frac{\cos\tilde{r} + \sin\tilde{t}}{\sin\tilde{t}} = \frac{2\alpha^2}{\alpha^2 - t^2 + r^2}. \tag{9}$$

In coordinates $\{t, r, \vartheta, \varphi\}$, which can also be used in de Sitter space (note [9]), the world lines 2, 2′, Eqs. (6), acquire the simple form: $\vartheta = 0$, $\varphi = 0$, and

$$t = b_{\mathrm{o}} \sinh(\lambda_{\mathrm{M}}/b_{\mathrm{o}}), \qquad r = \pm b_{\mathrm{o}} \cosh(\lambda_{\mathrm{M}}/b_{\mathrm{o}}), \tag{10}$$

where λ_{M} is the proper time as measured by g_{M}, and $b_{\mathrm{o}}/\alpha = \sqrt{1 + a_{\mathrm{o}}^2\alpha^2} - a_{\mathrm{o}}\alpha$. The world lines (10) are just two hyperbolas (Fig. 2), representing particles with uniform acceleration $1/b_{\mathrm{o}}$ as measured in Minkowski space.

Transforming the fields (7) and (8) into conformally flat coordinates $\{t, r, \vartheta, \varphi\}$, we obtain

$$\Phi_{\mathrm{BdS}} = (s/4\pi)\Omega^{-1}\mathcal{R}^{-1}, \tag{11}$$

$$F_{\mathrm{BdS}} = -\frac{e}{4\pi}\frac{\alpha^3}{2b_{\mathrm{o}}}\frac{\sin\vartheta}{\mathcal{R}^3} \times [r(b_{\mathrm{o}}^2 + t^2 + r^2)dt \wedge d\vartheta - (b_{\mathrm{o}}^2 + t^2 - r^2) \times \cot\vartheta dt \wedge dr - 2tr^2 dr \wedge d\vartheta], \tag{12}$$

the factor $\mathcal{R}$ now being given by

$$\mathcal{R} = [(b_{\mathrm{o}}^2 + t^2 - r^2)^2 + 4b_{\mathrm{o}}^2 r^2 \sin^2\vartheta]^{1/2}/(2b_{\mathrm{o}}). \tag{13}$$

Expressions (7), (8), (11), and (12) represent *the generalized Born scalar and electromagnetic fields from the sources moving with constant acceleration a_{o} along the world lines (6), respectively (10), in de Sitter universe.*

To connect these fields with their counterparts in flat space, note that they are conformally related by transformation (9). Under the conformal transformation, the field Φ_{BdS} in (11) has to be multiplied by factor Ω, which gives $\Phi_{\mathrm{BdS}} = (s/4\pi)\mathcal{R}^{-1}$, and F_{BdS} in (12) remains unchanged. The transformed fields then precisely coincide with the classical Born fields; see, e.g., Refs. [1,2,10].

In order to see the limit for $\Lambda \to 0$, we parametrize the sequence of de Sitter spaces by Λ, identifying them in terms of coordinates $\{t, r, \vartheta, \varphi\}$. As $\Lambda = 3/\alpha^2 \to 0$, Eq. (9) implies $\Omega_\Lambda \to 2$, $g_{\mathrm{dS}\,\Lambda} \to 4g_{\mathrm{M}}$. After the trivial rescaling of t, r by factor 2, the standard Minkowski metric is obtained. The limit of the fields (11) and (12), in which b_{o} is kept constant [cf. $a_{\mathrm{o}} = (1 - b_{\mathrm{o}}^2\alpha^{-2})/(2b_{\mathrm{o}})$], leads to the scalar and electromagnetic Born fields in flat space. Because of the rescaling of coordinates by factor 2, we get the physical acceleration $1/b_{\mathrm{o}} = 2a_{\mathrm{o}}$, and the scalar field rescaled by $1/2$.

What is the character of the generalized Born fields? Focusing on the electromagnetic case, we first decompose the field (8) into the orthonormal tetrad $\{e_\mu\}$ tied to coordinates $\{\tilde{t}, \tilde{r}, \vartheta, \varphi\}$; for example, $e_{\tilde{t}} = (\alpha^{-1}\sin\tilde{t})\partial/\partial\tilde{t}$, etc., the dual tetrad $e^{\tilde{t}} = (\alpha/\sin\tilde{t})d\tilde{t}$, etc. Splitting the field into the electric and the magnetic parts, $F_{\mathrm{BdS}} = E \wedge e^{\tilde{t}} + B \cdot e^{\check{r}} \wedge e^{\vartheta} \wedge e^{\varphi}$, we get

$$E = \frac{e}{4\pi}\frac{\alpha\sin^2\tilde{t}}{\mathcal{R}^3(\sin\tilde{t} + \cos\tilde{r})^3} \times [-(\sqrt{1 + a_{\mathrm{o}}^2\alpha^2}\cos\tilde{r} - a_{\mathrm{o}}\alpha\sin\tilde{t})\cos\vartheta e_{\check{r}} + (\sqrt{1 + a_{\mathrm{o}}^2\alpha^2} - a_{\mathrm{o}}\alpha\sin\tilde{t}\cos\tilde{r})\sin\vartheta e_{\vartheta}],$$
$$B = -\frac{e}{4\pi}\frac{a_{\mathrm{o}}\alpha^2\sin^2\tilde{t}}{\mathcal{R}^3(\sin\tilde{t} + \cos\tilde{r})^3}\cos\tilde{t}\sin\tilde{r}\sin\vartheta e_{\varphi}. \tag{14}$$

The fields exhibit some features typical for the classical Born solution. The toroidal electric field, E_φ, vanishes; only B_φ is nonvanishing. At $\tilde{t} = \pi/2$, the moment of time symmetry, $B_\varphi = 0$. It vanishes also for $\vartheta = 0$—there is no Poynting flux along the axis of symmetry.

The classical Born field decays rapidly ($E \sim r^{-4}$, $B \sim r^{-5}$) at spatial infinity, but it is "radiative" ($E, B \sim r^{-1}$) if we expand it along null geodesics $t - r = \text{const}$, approaching thus null infinity. In de Sitter spacetime with standard slicing, the space is finite (S^3). However, we can approach infinity along spacelike hypersurfaces if, for example, we consider the "steady-state" half of the de Sitter universe (cf. Fig. 1) with flat-space slices, i.e., if we take the "conformally flat" time $\check{t} = \text{const}$ (note [9]). Introducing the orthogonal tetrad tied to conformally flat coordinates $\{\check{t}, \check{r}, \vartheta, \varphi\}$, the tetrad components of the fields decay as $\check{r}^{-2}$ at $\check{t} = \text{const}$, $\check{r} \to \infty$, so that the Poynting flux falls off as $\check{r}^{-4}$.

The fields decay very rapidly along *timelike* world lines as $\mathcal{I}^+$ is approached. This is caused by the exponential expansion of slices $\tau = \text{const}$ [cf. Eq. (1)]. As $\tau \to \infty$, the electric field (14) becomes radial, $E_{\check{r}} \sim \exp(-2\tau/\alpha)$, and $B_\varphi \sim \exp(-2\tau/\alpha)$. The energy density, $u = \frac{1}{2}(E^2 + B^2)$, decays as (expansion factor)$^{-4}$—as energy density in the radiation dominated standard cosmologies. The

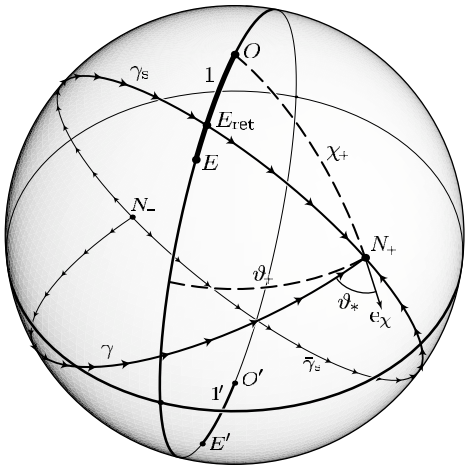

FIG. 3. Space trajectories of null geodesics γ, γ_s, and $\bar\gamma_s$ indicated on the slice $\tilde t = \text{const}$ ($\varphi = 0$). Charges 1, 1′ move along $\vartheta = 0$ from poles O, O' to points E, E' and back. γ, γ_s, and $\bar\gamma_s$ start at N_- at $\tilde t = 0$ and arrive at N_+ (with coordinates χ_+, ϑ_+) at $\tilde t = \pi$. The direction of γ at N_+ is specified by angles ϑ_*, φ_* (φ_* describes rotation around e_χ in the dimension not seen). γ_s crosses the world line of particle 1 at E_{ret}; $\bar\gamma_s$ reaches N_+ from the opposite direction.

density of the conserved energy $u_{conf} = (\alpha/\sin\tilde t)u \sim \exp(-3\tau/\alpha)$ (determined by a timelike conformal Killing vector $\partial/\partial\tilde t$) gets rarified at the same rate that the volume increases.

Will a slower decay occur if $\mathcal{I}^+$ is approached along null geodesics? To study the asymptotic behavior of a field along a null geodesic (see, e.g., Ref. [4]), we have to (i) find a geodesic and parametrize it by an affine parameter ζ, (ii) construct a tetrad parallelly propagated along the geodesic, and (iii) study the asymptotic expansion of the tetrad components of the field. We find that along null geodesics lying in the axis $\vartheta = 0$ (thus crossing the particles' world lines) the "radiation field," i.e., the coefficient of the leading term in $1/\zeta$, vanishes, as could have been anticipated—particles do not radiate in the direction of their acceleration. The radiation field also vanishes along null geodesics reaching infinity along directions *opposite* to those of geodesics emanating from the particles (see Fig. 3). Along all other geodesics, the field *has* radiative character. Along a null geodesic coming from a general direction to a general point on $\mathcal{I}^+$, we find the electric and magnetic fields (in a parallelly transported tetrad $\{f_\mu\}$) to be perpendicular one to the other, equal in magnitude, and proportional to ζ^{-1}. The magnitude of Poynting flux, $|S_{(f)}| = |E_{(f)}|^2 = |B_{(f)}|^2$, is

$$|S_{(f)}| = \frac{e^2}{(4\pi)^2}\,\frac{a_o^2 \sin^2\vartheta_+ \csc^4\chi_+}{4(1 + a_o^2\alpha^2\cos^2\vartheta_+)^3}\,[\cos^2\vartheta_* \sin^2\varphi_* + (\cos\varphi_* + a_o^{-1}\sqrt{a_o^2 + \alpha^{-2}}\sin\vartheta_* \csc\vartheta_+)^2]\zeta^{-2} \qquad (15)$$

(see Fig. 3 for the definition of angles χ_+, ϑ_+, ϑ_*, φ_*). These results are typical for a *radiative* field. Most interestingly, this radiative aspect depends on the specific geodesic along which a given point on *spacelike* $\mathcal{I}^+$ is approached (cf. [4]). Moreover, the radiative character does not disappear even for static sources but it does along null geodesics emanating from such sources.

Since the field can be interpreted as the combination of retarded and advanced effects, similarly to the flat space case [2], the radiation reaction force also vanishes.

In summary, we have constructed the fields of uniformly accelerated charges in a de Sitter universe which go over to classical Born fields in the limit $\Lambda \to 0$. Aside from some similarities found, the generalized fields provide the models showing how a positive cosmological constant implies essential differences from physics in flat spacetime: Advanced effects occur inevitably, and the character of the far fields depends substantially on the way in which future (spacelike) infinity is approached. Since vacuum energy seems to be dominant in the universe, it is of interest to understand fundamental physics in the vacuum dominated de Sitter spacetime.

The authors thank the Albert-Einstein-Institute, Golm, for hospitality, and Jeff Winicour for very helpful comments on the manuscript. We have been supported by Grants No. GAČR 202/99/026 and No. GAUK 141/2000.

*Electronic address: bicak@mbox.troja.mff.cuni.cz

†Electronic address: Pavel.Krtous@mff.cuni.cz

[1] E. Eriksen and Ø. Grøn, Ann. Phys. (N.Y.) **286**, 320 (2000); **286**, 343 (2000); **286**, 373 (2000).

[2] J. Bičák and B. Schmidt, Phys. Rev. D **40**, 1827 (1989).

[3] J. Bičák, in *Einstein's Field Equations and Their Physical Implications,* edited by B. Schmidt, Lecture Notes in Physics Vol. 540 (Springer, Berlin, 2000), pp. 1–126.

[4] R. Penrose and W. Rindler, *Spinors and Space-time* (Cambridge University Press, Cambridge, England, 1984).

[5] J. Bičák and P. Krtouš, Phys. Rev. D **64**, 124020 (2001).

[6] R. Penrose, in *The Nature of Time,* edited by T. Gold (Cornell University, Ithaca, New York, 1967), pp. 42–54.

[7] It is convenient to allow the angular coordinates χ, ϑ, φ on S^3 to attain values in $\mathbb{R}$ and use the identifications "mod2π," and $\{\chi, \vartheta, \varphi\} \cong \{-\chi, \pi - \vartheta, \varphi + \pi\}$, $\{\chi, \vartheta, \varphi\} \cong \{\chi, -\vartheta, \varphi + \pi\}$. Thus, the "radial" coordinate χ can be negative, the points with $\chi < 0$ being identical to those with $|\chi| > 0$, located "symmetrically" with respect to the origin $\chi = 0$. The same convention is used for $\check r$, r, $\check r$, and R (see Appendix in [5] for details).

[8] "A uniform acceleration" means that the (proper) time derivative $\dot a^\alpha$ of the acceleration, projected into the hypersurface orthogonal to the four-velocity, vanishes. The magnitude of the acceleration is constant.

[9] $\{t, r, \vartheta, \varphi\}$ differ from the standard conformally flat coordinates $\{\check t, \check r, \vartheta, \varphi\}$ by the shift in $\tilde t$ direction by $\pi/2$ (Figs. 1 and 2). $\{\check t, \check r, \vartheta, \varphi\}$ are related to the usual "steady-state" coordinates $\{\check\eta, \check r, \vartheta, \varphi\}$ of exponentially expanding $k = 0$ cosmologies by $\check t = -\alpha \exp(-\check\eta/\alpha)$.

[10] F. Rohrlich, *Classical Charged Particles* (Addison-Wesley, Reading, MA, 1965).

PHYSICAL REVIEW D **68**, 024005 (2003)

Radiation from accelerated black holes in a de Sitter universe

Pavel Krtouš* and Jiří Podolský†
Institute of Theoretical Physics, Faculty of Mathematics and Physics, Charles University in Prague, V Holešovičkách 2, 180 00 Prague 8, Czech Republic

(Received 27 January 2003; published 2 July 2003)

Radiative properties of gravitational and electromagnetic fields generated by uniformly accelerated charged black holes in asymptotically de Sitter spacetime are studied by analyzing the *C*-metric exact solution of the Einstein-Maxwell equations with a positive cosmological constant Λ. Its global structure and physical properties are thoroughly discussed. We explicitly find and describe the specific pattern of radiation which exhibits the dependence of the fields on a null direction along which the (spacelike) conformal infinity is approached. This directional characteristic of radiation supplements the peeling behavior of the fields near infinity. The interpretation of the solution is achieved by means of various coordinate systems, and suitable tetrads. The relation to the Robinson-Trautman framework is also presented.

DOI: 10.1103/PhysRevD.68.024005 PACS number(s): 04.20.Ha, 04.20.Jb, 04.40.Nr

I. INTRODUCTION

There has been great effort in general relativity devoted to investigation of gravitational radiation in asymptotically flat spacetimes. Some of the now classical works, which date back to the 1960s, set up rigorous frameworks within which a general asymptotic character of radiative fields near infinity could be elucidated [1–11]. Also, particular examples of explicit exact radiative spacetimes have been found and analyzed, e.g., Refs. [12–15], for a review of these important contributions to the theory of radiation see, for example, Refs. [16–20].

One of the fundamental approaches to investigate the radiative properties of a gravitational field at large distances from a bounded source is based on introducing a suitable Bondi-Sachs coordinate system adapted to outgoing null hypersurfaces, and expanding the metric functions in negative powers of the luminosity distance [1–4]. In the case of asymptotically flat spacetimes this framework enables one to define the Bondi mass (total mass of the system as measured at future null infinity $\mathcal{I}^+$), and characterize the time evolution including radiation in terms of the news functions. Using these concepts it is possible to formulate a balance between the amount of energy radiated by gravitational waves and the decrease of the Bondi mass of an isolated system. Unfortunately, this standard explicit approach is not directly applicable to spacetimes whose conformal infinity $\mathcal{I}^+$ has a spacelike character as is the case of an asymptotically de Sitter universe which we wish to study here.

Alternatively, in accordance with the Newman-Penrose formalism [5,6], information about the character of radiation in asymptotically flat spacetimes can be extracted from the tetrad components of fields measured along a family of null geodesics approaching $\mathcal{I}^+$. The gravitational field is radiative if the dominant components of the Weyl tensor $\mathbf{C}_{\alpha\beta\gamma\delta}$ (or of the Maxwell tensor $\mathbf{F}_{\alpha\beta}$ in the electromagnetic case) fall off as $1/\eta$, where η is an affine parameter along the null geodesics. The rate of approach to zero of the Weyl and electromagnetic tensor is generally given by the ''peeling off'' theorem of Sachs [3,7,8]. In analogy to this well-known behavior it is natural to expect that those components of the fields in parallelly transported tetrad which are proportional to $1/\eta$ characterize gravitational and electromagnetic radiation also in more general cases of spacetimes not asymptotically flat. We shall adopt such a definition of radiation below.

In the presence of a positive cosmological constant Λ, however, the conformal infinity $\mathcal{I}^+$ has a *spacelike* character, and for principal reasons the rigorous concept of gravitational and electromagnetic radiation is much less clear. As Penrose noted in the 1960s [9,10] already, following his geometrical formalization of the idea of asymptotical flatness based of the conformal technique [8,11], radiation is defined ''less invariantly'' when $\mathcal{I}$ is spacelike than when it has a null character.

One of the difficulties related to the spacelike character of the infinity is that initial data on $\mathcal{I}^-$ (or final data on $\mathcal{I}^+$) for, e.g., electromagnetic field with sources cannot be prescribed freely because the Gauss constraint has to be satisfied at $\mathcal{I}^-$ (or $\mathcal{I}^+$). This results in the insufficiency of purely retarded solutions in case of a spacelike $\mathcal{I}^-$—advanced effects must also be presented. This phenomenon has been demonstrated explicitly recently [21] by analyzing test electromagnetic fields of uniformly accelerated charges in de Sitter background.

We will concentrate on another crucial difference in behavior of radiative fields near null versus spacelike infinity. In the case of asymptotically flat spacetimes, any point N_+ at null infinity $\mathcal{I}^+$ can be approached essentially only along *one* null direction. However, if future infinity $\mathcal{I}^+$ has a spacelike character, one can approach the point N_+ from *infinitely many different* null directions. It is not a priori clear how the radiation components of the fields depend on a direction along which N_+ is approached. In this paper such dependence will be thoroughly investigated.

In fact, radiative properties of a test electromagnetic field of two uniformly accelerated pointlike charges in the de Sitter background has recently been studied [22,23]. Within this context, the above mentioned directional dependence has

*Electronic address: Pavel.Krtous@mff.cuni.cz
†Electronic address: Jiri.Podolsky@mff.cuni.cz

been explicitly found. In particular, it has been demonstrated that there are always exactly two special directions—those opposite to the direction from the sources—along which the radiation vanishes. For all other directions the radiation is nonvanishing and it is described by an explicit formula which completely characterizes its angular dependence.

In the present paper, these results will be considerably generalized to both gravitational and electromagnetic field which are not just test fields in the de Sitter background. Interestingly, it will be demonstrated that the gravitational and electromagnetic fields of the *C*-metric with $\Lambda>0$, which is an *exact* solution representing a pair of uniformly accelerated possibly charged black holes in the de Sitter–like universe, exhibits exactly the *same* asymptotic radiative behavior as the test fields [22,23]. We are thus able to supplement the information about the peeling behavior of the fields near $\mathcal{I}^+$ with an additional general property of radiation, namely, with the specific *directional pattern of the radiation* at conformal infinity.

The *C*-metric with $\Lambda=0$ is a well-known solution of the Einstein (-Maxwell) equations which, together with the famous Bonnor-Swaminarayan solutions [15], belongs to a large class of asymptotically flat spacetimes with boost and rotational symmetry [24] representing accelerated sources. It was discovered already in 1917 by Levi-Civita [25] and Weyl [26], and named by Ehlers and Kundt [13]. Physical interpretation and understanding of the global structure of the *C*-metric as a spacetime with radiation generated by a pair of accelerated black holes came with the fundamental papers by Kinnersley and Walker [27] and Bonnor [28]. Consequently, a great number of works analyzed various aspects and properties of this solution, including its generalization which admits a rotation of the black holes. References and summary of the results can be found e.g., in Refs. [24,29–31]. Another possible generalization of the standard *C*-metric exists, namely, that to a nonvanishing value of the cosmological constant Λ [32], cf. [33,34]. However, in this case a complete understanding of global properties, mainly a character of radiation, is still missing despite a successful application of this solution to the problem of cosmological production of black holes [35], and its recent analysis and interpretation [36–38].

There exists a strong motivation to investigate the *C*-metric solution with $\Lambda>0$. As will be demonstrated below, it may serve as an interesting exact model of gravitational and electromagnetic radiation of bounded sources in the asymptotically de Sitter universe (in contrast to $\Lambda=0$, in which case the system is not permanently bounded). The character of radiation, in particular the above mentioned dependence of the asymptotic fields on directions, along which points on the de Sitter–like infinity $\mathcal{I}^+$ are approached, can explicitly be found and studied. These results may provide an important clue to formulation of a general theory of radiation in spacetimes which are not asymptotically flat. In addition to this purely theoretical motivation, understanding the behavior of accelerated black holes in the universe with a positive value of the cosmological constant can also be interesting from perspective of contemporary cosmology.

The paper is organized as follows. First, in Sec. II we present the *C*-metric solution with a positive cosmological constant in various coordinates which will be necessary for the subsequent analysis. The global structure of the spacetime is described in detail in Sec. III. Next, in Sec. IV we introduce and discuss various privileged orthonormal and null tetrads near the de Sitter–like infinity $\mathcal{I}^+$ together with their mutual relations, and we give corresponding components of the gravitational and electromagnetic *C*-metric fields. Section V contains the core of our analysis. We carefully define interpretation tetrad parallelly transported along all null geodesics approaching asymptotically a given point on spacelike $\mathcal{I}^+$ from different spatial directions. The magnitude of the leading terms of gravitational and electromagnetic fields in such a tetrad then provides us with a specific directional pattern of radiation which is described and analyzed. This result is subsequently rederived in Sec. VI using the Robinson-Trautman framework which also reveals some other aspects of the radiative properties. Particular behavior of radiation along the algebraically special null directions is studied in Sec. VII. For these privileged geodesics the results are obtained explicitly without performing asymptotic expansions of the physical quantities near $\mathcal{I}^+$. In this case we also study a specific dependence of the field components on a choice of initial conditions on horizons.

The paper contains four appendixes. Appendix A summarizes known and also several new coordinates for the *C*-metric with $\Lambda>0$. The properties of the specific metric functions are described in Appendix B. In Appendix C useful relations between the various coordinate one-form and vector frames are presented, together with the relations between the different privileged null tetrads. Appendix D contains general Lorentz transformations of the null-tetrad components of the gravitational and electromagnetic fields.

II. THE *C*-METRIC WITH A COSMOLOGICAL CONSTANT IN SUITABLE COORDINATES

The generalization of the *C*-metric which admits a nonvanishing cosmological constant $\Lambda>0$, representing a pair of uniformly accelerated black holes in a ''de Sitter background,'' has the form

$$\boldsymbol{g}=\frac{1}{A^2(x+y)^2}\left(-F\mathbf{d}t^2+\frac{1}{F}\mathbf{d}y^2+\frac{1}{G}\mathbf{d}x^2+G\mathbf{d}\varphi^2\right), \tag{2.1}$$

where

$$\begin{aligned} F&=-\frac{1}{a_\Lambda^2A^2}-1+y^2-2mAy^3+e^2A^2y^4,\\ G&=1-x^2-2mAx^3-e^2A^2x^4, \end{aligned} \tag{2.2}$$

see Eqs. (A1), (A2). Here $t\in\mathbb{R}$, $\varphi\in(-\pi C,\pi C)$, m, e, A, C are constants, and ranges of the coordinates x, y [or, more precisely, of the related coordinates ξ, ν defined below by Eq. (2.7)] will be discussed in detail in the next section. For convenience, we have parameterized the cosmological constant Λ by the ''de Sitter radius'' as

$$a_\Lambda = \sqrt{\frac{3}{\Lambda}}. \tag{2.3}$$

The metric (2.1) is a solution of the Einstein-Maxwell equations with the electromagnetic field given by (see [39,40])

$$\mathbf{F} = e\,\mathbf{d}y \wedge \mathbf{d}t. \tag{2.4}$$

The constants m, e, A, and C parametrize *mass*, *charge*, *acceleration*, and *conicity* of the black holes, although their relation to physical quantities is not, in general, direct. For example, the total charge Q on a timelike hypersurface $t=\text{const}$ localized inside a surface $y=\text{const}$, defined using the Gauss law, is given by $Q=\frac{1}{2}(\xi_2-\xi_1)Ce$, where the constants ξ_1, ξ_2 are introduced at the beginning of the next section. Obviously, Q depends not only on the charge parameter e. Similarly, physical conicity is proportional to the parameter C, but it also depends on other parameters, see Eq. (3.4) below. The concept of mass (outside the context of asymptotically flat spacetimes) and of physical acceleration of black holes is even more complicated. We will return to this point at the end of the next section. For satisfactory interpretation of the parameters m, e, and A in the limit of their small values see, e.g., Ref. [36].

In the following we will always assume

$$m>0, \quad e^2<m^2, \quad A>0, \tag{2.5}$$

and F, as a polynomial in y, to have only distinct real roots. Also, instead of the acceleration constant A we will conveniently use the dimensionless *acceleration parameter* α defined as

$$\sinh\alpha = a_\Lambda A, \quad \cosh\alpha = \sqrt{1+a_\Lambda^2 A^2}. \tag{2.6}$$

We will also use other suitable coordinates which are introduced and discussed in more detail in Appendix A. Here we list only the basic definitions and the corresponding forms of metric.

The rescaled coordinates τ, υ, ξ, φ are defined

$$\begin{aligned} \tau &= t\coth\alpha, \quad \varphi=\varphi, \\ \upsilon &= y\tanh\alpha, \quad \xi=-x, \end{aligned} \tag{2.7}$$

cf. Eq. (A5), in which the metric takes the form (A6),

$$\boldsymbol{g} = r^2\left(-\mathcal{F}\mathbf{d}\tau^2 + \frac{1}{\mathcal{F}}\mathbf{d}\upsilon^2 + \frac{1}{\mathcal{G}}\mathbf{d}\xi^2 + \mathcal{G}\mathbf{d}\varphi^2\right), \tag{2.8}$$

where

$$r = \frac{1}{A(x+y)} = \frac{a_\Lambda}{\upsilon\cosh\alpha - \xi\sinh\alpha} \tag{2.9}$$

and

$$-\mathcal{F} = 1-\upsilon^2+\cosh\alpha\,\frac{2m}{a_\Lambda}\upsilon^3 - \cosh^2\alpha\,\frac{e^2}{a_\Lambda^2}\upsilon^4, \tag{2.10}$$

$$\mathcal{G} = 1-\xi^2+\sinh\alpha\,\frac{2m}{a_\Lambda}\xi^3 - \sinh^2\alpha\,\frac{e^2}{a_\Lambda^2}\xi^4.$$

The coordinates ω, τ, σ, φ adapted to the Killing vectors $\boldsymbol{\partial}_\tau$, $\boldsymbol{\partial}_\varphi$ and the conformal infinity $\mathcal{I}$ ($\omega=0$) are defined by

$$\begin{aligned} \omega &= -\upsilon\cosh\alpha + \xi\sinh\alpha, \\ \mathbf{d}\sigma &= \frac{\sinh\alpha}{\mathcal{F}}\mathbf{d}\upsilon + \frac{\cosh\alpha}{\mathcal{G}}\mathbf{d}\xi, \end{aligned} \tag{2.11}$$

see Eqs. (A21), (A22), and the metric (A23),

$$\boldsymbol{g} = \frac{a_\Lambda^2}{\omega^2}\left(-\mathcal{F}\mathbf{d}\tau^2 + \frac{1}{\mathcal{E}}\mathbf{d}\omega^2 + \frac{\mathcal{F}\mathcal{G}}{\mathcal{E}}\mathbf{d}\sigma^2 + \mathcal{G}\mathbf{d}\varphi^2\right), \tag{2.12}$$

where

$$\mathcal{E} = \mathcal{F}\cosh^2\alpha + \mathcal{G}\sinh^2\alpha. \tag{2.13}$$

Finally, we will also use the C-metric expressed in the Robinson-Trautman coordinates ζ, $\bar{\zeta}$, u, r which has the form (A29) (see [41] for a definition of the symmetric product $\vee$)

$$\boldsymbol{g} = \frac{r^2}{P^2}\mathbf{d}\zeta\vee\mathbf{d}\bar{\zeta} - \mathbf{d}u\vee\mathbf{d}r - H\mathbf{d}u^2, \tag{2.14}$$

with

$$\frac{1}{P^2} = \mathcal{G}, \quad H = \frac{r^2}{a_\Lambda^2}\mathcal{E}. \tag{2.15}$$

It follows immediately from Eqs. (2.9) and (2.11) that

$$r = -\frac{a_\Lambda}{\omega}. \tag{2.16}$$

For explicit definitions of the coordinates u, ζ and further details see Eqs. (A25), (A28), and related text in Appendix A.

III. THE GLOBAL STRUCTURE

In this section we shall describe the global structure of the C-metric with $\Lambda>0$. In particular, we shall analyze the character of infinity, singularities, and possible horizons. (See recent work [38] for similar discussions that also cover cases not studied here.) From the form (2.8) of the metric we observe that it is necessary to investigate zeros of the metric functions $\mathcal{F}$ and $\mathcal{G}$ given by Eq. (2.10). We will only discuss the particular case when the function $\mathcal{F}$ has n distinct real roots, where n is the degree of polynomial dependence of $\mathcal{F}$ on υ ($n=4$ for $e\neq 0$). Let us denote these roots as υ_i, υ_o, υ_c, and υ_m in a descending order (the meaning of the subscripts will be explained below). In the case $e=0$, the value of υ_i is not defined, etc. Analogously, we denote the roots of $\mathcal{G}$ as ξ_1, ξ_2, ξ_3, and ξ_4 in an ascending order. Similarly to discussion of the C-metric with vanishing Λ [27,29,30], the zeros of the function $\mathcal{F}$ correspond to *horizons*, and the zeros

of $\mathcal{G}$ to *axes* of φ symmetry. Following these works and Ref. [36] for $\Lambda>0$ in particular, the qualitative diagrams of the ξ-υ slice (i.e., τ, $\varphi=$const) are drawn in Fig. 1. In this diagram we use relations

$$\upsilon_{\mathrm{m}}\coth\alpha<\xi_1<0<\xi_2<\upsilon_{\mathrm{c}}\coth\alpha, \tag{3.1}$$

which are obvious from Fig. 9 in Appendix B. Different columns and rows in the diagrams in Fig. 1 correspond to different signs of the functions $\mathcal{G}$ and $\mathcal{F}$. The metric has a physical signature $(-+++)$ for $\xi_1<\xi<\xi_2$ and $\xi_3<\xi<\xi_4$. We will be interested only in the first region.

Infinity $\mathcal{I}$ of the spacetime corresponds to $r=\infty$, or equivalently to

$$\omega=0, \quad \text{i.e.,} \quad \upsilon=\xi\tanh\alpha, \tag{3.2}$$

(double line in Fig. 1). We will restrict to the region $\upsilon>\xi\tanh\alpha$ (i.e. $r>0$) which describes both interior and exterior of accelerated black holes in de Sitter–like spacetime (the shaded areas in Fig. 1). The metric has an unbounded curvature for $r=0$ which corresponds to a physical singularity inside the black holes, a zigzag line on the boundary of the diagrams in Fig. 1, in particular of the column $\xi_1<\xi<\xi_2$.

For a further discussion of the global structure we employ the double null coordinates $\tilde{u}$, $\tilde{v}$, ξ, φ defined by Eqs. (A38), (A33), (A34) in which the metric is (A39),

$$\boldsymbol{g}=r^2\left(\frac{2\delta^2\mathcal{F}}{\sin\tilde{u}\sin\tilde{v}}\,\mathbf{d}\tilde{u}\vee\mathbf{d}\tilde{v}+\frac{1}{\mathcal{G}}\mathbf{d}\xi^2+\mathcal{G}\mathbf{d}\varphi^2\right). \tag{3.3}$$

Using these coordinates we can draw the conformal diagram of the spacetime section τ-υ, i.e., for ξ, $\varphi=$const—see Fig. 2. The domains I–IV in this figure correspond to the regions I–IV in Fig. 1.

The region I describes the domain of spacetime above the cosmological horizons given by $\upsilon=\upsilon_{\mathrm{c}}$, which has a similar structure as an analogous domain in the de Sitter spacetime. The region II corresponds to a static spacetime domain between the cosmological horizon and the (outer) horizon of the black hole. If the black hole is charged ($e\neq0$), region III corresponds to a spacetime domain between the outer horizon $\upsilon=\upsilon_{\mathrm{o}}$ and the inner horizon $\upsilon=\upsilon_{\mathrm{i}}$, and region IV to a domain below the inner horizon of the black hole (similar to the analogous domains of the Reissner-Nordström spacetime). The domain IV contains a timelike singularity at $\upsilon=\infty$ ($r=0$). In the uncharged case ($e=0$, $m\neq0$) there is only region III which corresponds to a domain below the single black hole horizon $\upsilon=\upsilon_{\mathrm{o}}$. In this case the singularity at $\upsilon=\infty$ has a spacelike character, similarly as for the Schwarzschild black hole. If both $e=0$, $m=0$, we obtain de Sitter spacetime expressed in accelerated coordinates. In this case there is no black hole horizon, and region II (the domain below the cosmological horizon υ_{c}) is ''cut off'' by nonsingular poles $\upsilon=\infty$. We will return to this particular case at the end of this section.

Before we proceed to discuss further properties in detail let us note that (as will be explicitly demonstrated in the next section) the *C*-metric is the Petrov type *D* spacetime, i.e., it admits two double principal null directions. These directions lie exactly in the section τ-υ depicted in Fig. 2.

In this paper we are mainly interested in a behavior of fields near the infinity. Therefore, we will concentrate mostly on the region I. This region has similar properties for all possible values of the parameters *m*, *e*, and α. Its more precise diagrams are drawn in Fig. 3. Observers in one of the regions I (near the future infinity $\mathcal{I}^+$) will consider themselves to live in an asymptotically de Sitter–like universe ''containing'' two causally disconnected black holes (for $m\neq0$). Here by *two* black holes we understand those black holes (i.e., regions III and IV) immediately ''visible'' from the given asymptotical region I, although the geodesically complete spacetime can, of course, contain an infinite number of black holes. As we have said, the conformal infinity $\mathcal{I}$ is given by the condition (3.2), $\omega=0$. Thanks to a timelike character of $\mathbf{d}\omega$ at $\omega=0$ [see Eq. (2.12)] the infinity has indeed a spacelike character as for de Sitter universe (see Refs. [8,9,42] for a general discussion of conformal infinity). In Fig. 1 the infinity corresponds to the diagonal line, in Fig. 2, however, it obtains a richer structure. It comprises of two parts—*future infinity* $\mathcal{I}^+$ and the *past infinity* $\mathcal{I}^-$—both possibly consisting of several disjoint parts (depending on the global topology) in different asymptotically de Sitter domains I. Because the conformal diagrams in Fig. 2 are slices with a fixed coordinate ξ, and the condition (3.2) depends on ξ, the conformal infinity $\mathcal{I}$ would have a different position in diagrams with different values of ξ. We shall return to this fact at the end of this section. Note, that for values of the coordinate υ smaller than $\xi_2\tanh\alpha$, the hypersurface $\upsilon=$const reaches $\mathcal{I}$. Clearly, the coordinate υ is not well adapted to the region near the conformal infinity $\mathcal{I}$. Near the infinity it is more convenient to use the coordinates ω, τ, σ, φ defined by Eqs. (2.11) [see Eqs. (A21), (A22); see also Fig. 3].

The coordinate τ is a coordinate along the ''boost'' Killing vector $\boldsymbol{\partial}_\tau$, and in region I it can be understood simply as a translational spatial coordinate. The coordinates ξ, φ play roles of longitudinal and latitudinal coordinates of a suitably defined hypersurface at an ''instant of time.'' For example, in region I the spacelike hypersurface $\upsilon=$const has topology $\mathbb{R}\times S^2$ (if it does not cross infinity $\mathcal{I}$) with the coordinate τ along the $\mathbb{R}$ direction, and ξ, φ on the sphere S^2. To justify the ''longitudinal'' character of the coordinate ξ, we introduce, instead of ξ, an angular coordinate ϑ by the relation $\sin\vartheta=\sqrt{\mathcal{G}}$ [cf. Eq. (A10)]. This is a longitudinal angle measured by a circumference of the φ circle [see the metric (2.8)]. Alternatively, we can introduce the angle Θ, defined by Eq. (A12), measured by the length of a ''meridian.'' At infinity $\mathcal{I}$ or, in general, on any hypersurface $\omega=$const, the coordinate lines $\sigma=$const coincide with the lines of constant ξ. The coordinate σ thus also parameterizes the longitudinal direction near the infinity, similarly to the coordinate ξ.

In Sec. II we mentioned that the coordinate φ along the second Killing vector $\boldsymbol{\partial}_\varphi$ takes values in the interval $(-\pi C,\pi C)$. Here $C>0$ is the parameter which allows us to change the conicity on the axis of the φ symmetry, i.e., it allows us to choose a deficit (or excess) angle around the axis arbitrarily. Such a change of the range of the coordinate

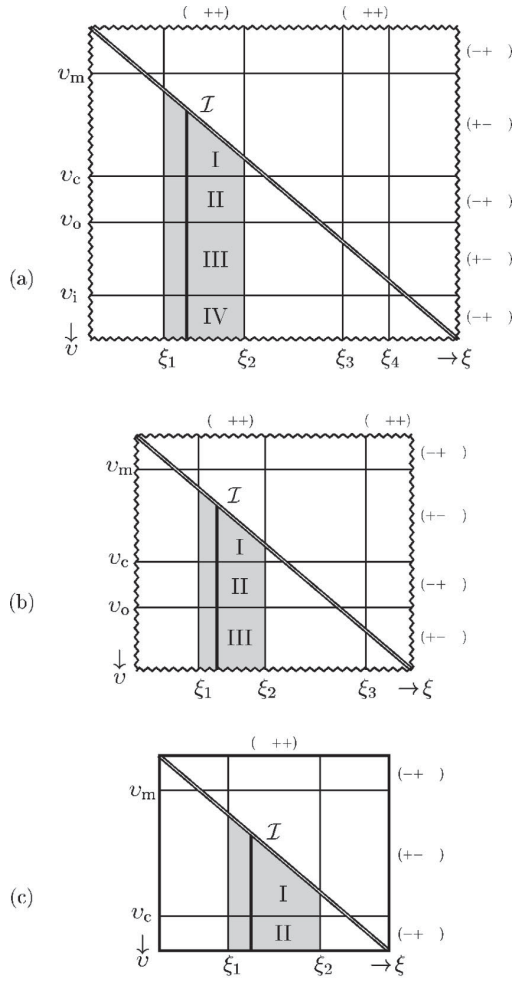

FIG. 1. A qualitative diagram of the ξ-v section (τ, φ = constant) of the studied spacetime. The three cases correspond to (a) charged accelerated black holes in asymptotically de Sitter universe ($e \neq 0$, $m \neq 0$), (b) uncharged black holes ($e = 0$, $m \neq 0$), and (c) de Sitter universe ($e = 0$, $m = 0$). Horizontal lines indicate the horizons, vertical lines are axes of φ symmetry. The diagonal double line $v = \xi \tanh \alpha$ corresponds to infinity $\mathcal{I}$. Singularities are depicted by ''zigzag'' lines. The boundary of each diagram corresponds to ξ, $v = \pm\infty$. Mutual intersections of different lines are governed by relations (3.1). Different columns and rows correspond to different signs of the functions $\mathcal{G}$ and $\mathcal{F}$, respectively, and thus to different signatures of the metric, which are indicated on the sides of the diagrams. The metric (2.8) describes, in general, four distinct spacetimes—the domains in columns $\xi_1 < \xi < \xi_2$ and $\xi_3 < \xi < \xi_4$, separated in addition by infinity (the diagonal line). In this paper we discuss only the physically most reasonable spacetime with the coordinates ξ, v in the ranges $\xi_1 < \xi < \xi_2$ and $v > \xi \tanh \alpha$ (the shaded areas). Sections ξ = const which correspond to the conformal diagrams in Fig. 2 are indicated by thick lines.

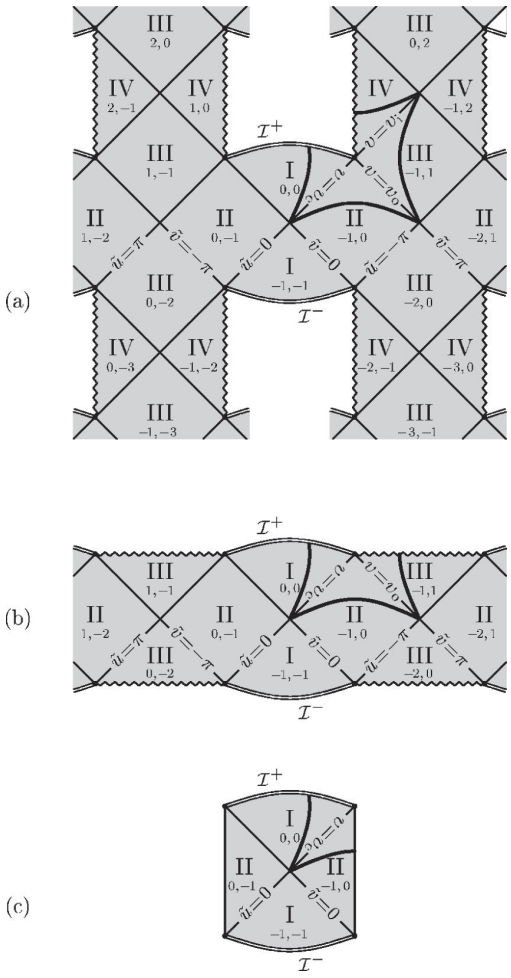

FIG. 2. The conformal diagrams of the τ-v section (ξ, φ = const). Similarly to Fig. 1, the three diagrams correspond to the cases of (a) charged accelerated black holes, (b) uncharged black holes, and (c) de Sitter universe (in accelerated coordinates). The conformal infinities $\mathcal{I}$ are indicated by double lines, the singularities are drawn by ''zigzag'' lines, and horizons by thin lines. The horizons $v = v_c$, v_o, v_i correspond to the values $\tilde{u} = m\pi$ or $\tilde{v} = n\pi$, m, $n \in \mathbb{Z}$. Thus, the integers (m, n), indicated in the figure, label different blocks $\tilde{u} \in (m\pi, (m+1)\pi)$, $\tilde{v} \in (n\pi, (n+1)\pi)$ of the conformal diagrams. There are four types of these blocks, labeled by I–IV, which correspond to the regions I–IV in Fig. 1. The sections τ = const (drawn in Fig. 1) are indicated by thick lines. Similar lines could, of course, be drawn also in other blocks. Only a part of the complete conformal diagram is shown in the cases (a) and (b), however, the rest of the diagram would have a similar structure as the part shown. The complete diagram depends on a freedom in the choice of a global topology of the spacetime given by identifications of different blocks of the conformal diagram. In the case (c), the diagram does not contain any black hole—it is ''closed on its sides'' by poles of a spacelike section S^3 of de Sitter universe (see the discussion at the end of Sec. III).

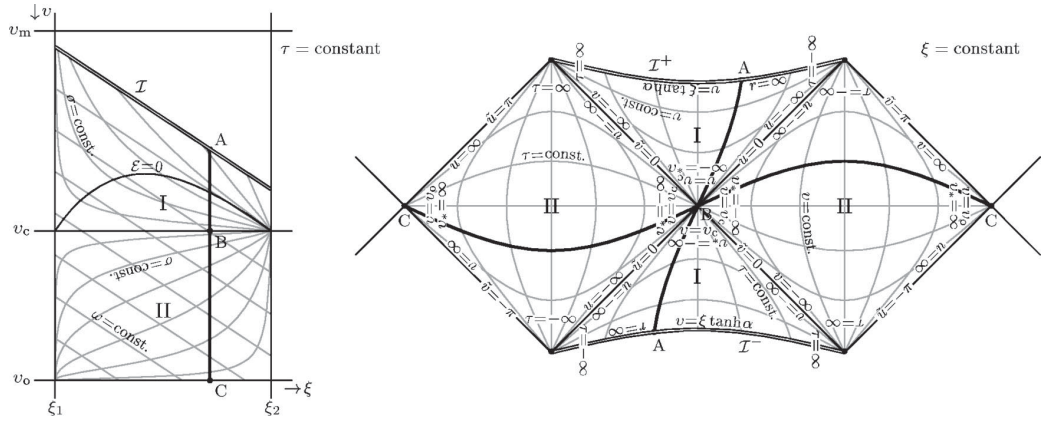

FIG. 3. The ξ-v (left) and the conformal (right) diagrams near infinity $\mathcal{I}$. Only one asymptotically de Sitter–like region of the spacetime (domains I and II of Figs. 1 and 2) is shown. Ranges of various coordinates introduced in the paper are indicated (orientation of the coordinate labels suggests a direction in which the coordinates increase). The thick line in the conformal diagram corresponds to the ξ-v diagram and vice versa. In the ξ-v diagram the lines of constant ω and σ are also drawn. The coordinates ω, σ are not unambiguous in the full domain I, however, they are invertible near $\mathcal{I}$, in the domain $\mathcal{E}<0$. On the boundary $\mathcal{E}=0$ (shown in diagram) the coordinates ω, σ change their timelike/spacelike character. [Notice the difference between the null coordinate v (''v''; diagonal straight lines) and the ''radial'' coordinate v (''upsilon''; curved lines) in the τ-v conformal diagram.]

φ is allowed for any axially symmetric spacetime. The range is usually chosen in such a way that the axis of the φ symmetry is regular. However, for the *C*-metric such a choice is not globally possible. In this case the axis consists of two parts $\xi=\xi_1$ and $\xi=\xi_2$—one of them joins the ''north'' poles of the black holes, the other one joins the ''south'' poles. The physical *conicity* (defined as a limiting ratio of ''circumference'' and $2\pi\times$''radius'' of a small circle around the axis) calculated at the axes ξ_1 and ξ_2 is

$$\kappa_1=\frac{1}{2}C\mathcal{G}'|_{\xi=\xi_1},\quad \kappa_2=-\frac{1}{2}C\mathcal{G}'|_{\xi=\xi_2}, \tag{3.4}$$

respectively, see, e.g., Ref. [36]. In general, the values of $|\mathcal{G}'|$ at ξ_1 and ξ_2 are not the same, see Eq. (3.5) below. Therefore we can set $\kappa=1$ (zero deficit of angle, i.e., a regular axis) by a suitable choice of the parameter C only at *one* part of the axis.

This fact has a clear physical interpretation. The axis with nonregular conicity corresponds to a cosmic string which causes the ''accelerated motion'' of the black holes. The cosmic string [43] is a one-dimensional object, sort of a ''rod'' or a ''spring,'' which is characterized by its mass density equal to its linear tension. These parameters are proportional to the deficit angle, namely, a string with a deficit angle ($\kappa<1$) has a positive mass density and it is stretched, a string with an excess angle ($\kappa>1$) has negative mass density and is squeezed. In Appendix B, Eq. (B7), we prove for $m\neq0$, $A\neq0$ that

$$\kappa_2<\kappa_1. \tag{3.5}$$

Using this fact, we may conclude that by eliminating a nontrivial conicity at the axis $\xi=\xi_2$ (so that $\kappa_2=1$) we obtain $\kappa_1>1$, i.e., a squeezed cosmic string at the axis $\xi=\xi_1$. Alternatively, if we set the physical conicity $\kappa_1=1$ at $\xi=\xi_1$, we obtain $\kappa_2<1$, i.e., a stretched cosmic string at the axis $\xi=\xi_2$. In both these cases, as well as in the general cases of cosmic strings on both parts of the axis, the system of black holes with string(s) between them is not in an equilibrium. The string(s) acts on both black holes and cause what we usually call an ''accelerated motion'' of black holes. However, the precise interpretation of acceleration is not so straightforward.

The problem here is that we consider a fully self-gravitating system, not just a motion of test particles on a fixed background. The motion of black holes is actually realized through a nonstatic, nonspherical deformation of geometry of the spacetime in a direction of motion, i.e., along the axis of φ symmetry. Moving black holes together with the cosmic string(s) curve the spacetime in such a way that, strictly speaking, it is not justified to use the term *acceleration* in a rigorous sense. This has several reasons. First, black holes are nonlocal objects and one can hardly expect a uniquely defined acceleration for such extended objects. Secondly, thanks to the equivalence principle we cannot distinguish between acceleration of the black holes with respect to the universe, and acceleration due to the gravitational field of each hole. Finally, one has to expect a gravitational dragging of local inertial frames by moving black holes, i.e., it is not obvious how to define an acceleration of black holes with respect to these frames. A plausible definition could be given if some privileged cosmological coordinate system playing a role of ''nonmoving'' background is available. Unfortunately, we are not aware of such a system applicable in a general case. In the next paragraph we shall demonstrate this approach just for a simple case of empty de Sitter spacetime. Summarizing, it is not straightforward to define the acceleration of black holes in the general case. One usually identifies the acceleration only in an appropriate limiting regime. The usage of the term *acceleration* for the parameter A in the *C*-metric (see Refs. [28–30] for the case $\Lambda=0$, and, e.g.,

Ref. [36] for the case $\Lambda \neq 0$) has been justified exactly in this way.

Of course, the situation extremely simplifies in the case of vanishing mass and charge ($m=0$, $e=0$). In this case there are no black holes, and the spacetime reduces to de Sitter universe. However, if we still keep $A \neq 0$, a trace of (now vanished) ''accelerated'' sources remains in the metric (2.8) through the parameter α. By a simple transformation (A12),

$$T = a_\Lambda \tau, \quad R = \frac{a_\Lambda}{\upsilon}, \quad \cos\Theta = -\xi, \quad \Phi = \varphi, \qquad (3.6)$$

we obtain the metric (A17) of the de Sitter space in *accelerated coordinates T, R,* Θ, Φ introduced in Ref. [36] and discussed in Ref. [23]. These coordinates are an analogue of the Rindler coordinates in Minkowski space generalized to the case of the de Sitter universe. They are adapted to accelerated observers: the origins $R=0$ represent two uniformly accelerated observers which are decelerating from antipodal poles of the spherical space section of the de Sitter universe towards each other until the moment of minimal contraction of the universe, and then accelerate away back to the antipodal poles (see Fig. 4). In the standard de Sitter static coordinates $T_{\rm dS}$, $R_{\rm dS}$, $\Theta_{\rm dS}$, $\Phi_{\rm dS}$ of the metric (A19), related to Eq. (3.6) by Eq. (A20), these observers are characterized by $R_{\rm dS}=R_{\rm o}$, $\Theta_{\rm dS}=0$. Thus, they are static observers staying at constant distance $R_{\rm o}=a_\Lambda \tanh\alpha$ [see Eq. (A18)] from the poles $R_{\rm dS}=0$ of de Sitter space, measured in their instantaneous rest frame (or, equivalently, in the de Sitter static frame). They are uniformly accelerated with acceleration $A=a_\Lambda^{-1}\sinh\alpha$ toward these poles—in fact, this acceleration exactly compensates the acceleration due to cosmological contraction and subsequent expansion of de Sitter universe.

We can consider the above accelerated observers as ''remnants'' of accelerated black holes of the full *C*-metric universe. Of course, in the oversimplified case of de Sitter space these ''sources'' just move along the worldlines and we are able to measure their acceleration explicitly. It is thus natural to draw the conformal diagram [Fig. 4(a)] of de Sitter universe, based on the standard global cosmological coordinates, in which the remnants of sources are obviously depicted as moving ''objects.'' On other hand, we can draw an alternative conformal diagram based on the accelerated coordinates [Fig. 4(b)], in which the remnants of the sources are located at the ''fixed'' poles of the space sections of the universe. The diagram in Fig. 4(a) is adapted to global cosmological structure of the universe and explicitly visualizes the motion of the sources, whereas the diagram in Fig. 4(b) is adapted to sources and thus ''hides'' their motion.

This intuition can be carried on to the general case with nontrivial sources. The coordinates τ, υ, ξ, φ [or alternatively the accelerated coordinates defined in the general case by Eq. (A12)] are adapted to sources and thus the conformal diagrams in Fig. 2 ''hide'' the motion of the black holes. Therefore, it would be very useful to find an analogue of the coordinates of Fig. 4(a) for the general case $m\neq 0$, $e\neq 0$, to be able to explicitly identify the accelerated motion of the black holes. However, as was already mentioned, we are not aware of such coordinates.

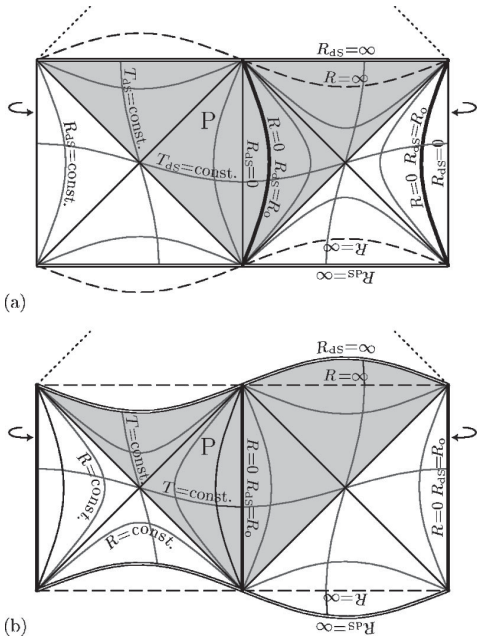

FIG. 4. Conformal diagrams of de Sitter universe (a) in the standard cosmological coordinates (A20), and (b) based on the accelerated coordinates (3.6) [cf. Eq. (A12)]. In contrast to Fig. 2(c), the diagram (b) depicts two sections of constant ξ, namely, $\xi=\xi_1$ ($\Theta=0$) at the right half of the diagram, and $\xi=\xi_2$ ($\Theta=\pi$) at the left half. We can see that the position of infinity (double line) is different for these two values of ξ. For intermediate values of ξ infinity $\mathcal{I}$ would attain an intermediate position at $R=a_\Lambda/\xi\coth\alpha$, according to Eq. (3.2). The infinity has a simple shape in diagram (a), where it is indicated by the horizontal lines $R_{\rm dS}=\infty$. In both diagrams the left and right boundaries are identified—they correspond to one of the two poles of the appropriate coordinates (the other pole is located in the center of the diagram). A horizontal line thus corresponds to the main circle of a spatial S^3 section of de Sitter universe. Bold lines corresponds to the origins of the accelerated coordinates ($R=0$) which have been employed in the paper as ''remnants'' of the sources. In diagram (a) they move with respect to the cosmological frame. Diagram (b) is adapted to their accelerated motion and therefore the sources are located at origins. Dashed line corresponds to value $R=\infty$, i.e., $\upsilon=0$, where the accelerated coordinates are not well defined. Relative position of the hypersurface $R=\infty$ and of infinity $R_{\rm dS}=\infty$ can be visualized with help of a conformally related Minkowski space (lower half indicated by the shaded domain *P*, the upper half indicated by dotted line). In this space the infinity corresponds to hypersurface $\mathrm{t}=0$, the coordinate singularity $R=\infty$ corresponds to $\mathrm{t}'=0$, where t and t' are Minkowski time coordinates in inertial frames moving with relative velocity $\tanh\alpha$—see Appendix A for a related discussion.

Using the insight obtained from the de Sitter case, we also observe that the ''changing of shape'' of infinity $\mathcal{I}$ in the conformal diagrams for different values of the coordinate ξ, as discussed above, is actually an *evidence* of nonvanishing acceleration of the sources. In the case of pure de Sitter space we have obtained this ''changing of position'' of $\mathcal{I}$ when we

have used the coordinates adapted to the accelerated observers. We expect that the analogous ''changing of shape'' of the infinity in a general case also indicates accelerated motion of the sources.

IV. PRIVILEGED ORTHONORMAL AND NULL TETRADS NEAR $\mathcal{I}^+$

We wish to investigate properties of null geodesics and the character of fields near infinity $\mathcal{I}$ (domain I in Figs. 1, 2). Therefore, we will assume $\mathcal{F}<0$, $\mathcal{G}>0$, and $\mathcal{E}<0$. Before we discuss the geodesics and behavior of the fields we first introduce some privileged tetrads which will be used for physical interpretation. In the following, we will denote a normalized vector tangent to the coordinate x^α, i.e., the unit vector proportional to the coordinate vector $\boldsymbol{\partial}_\alpha$, by $\mathbf{e}_\alpha$.

We will employ several types of orthonormal and null tetrads which will be distinguished by specific labels in subscript. We denote the vectors of an orthonormal tetrad as **n**, **q**, **r**, **s**. Here **n** is a unit timelike vector and the remaining three are spacelike. With this normalized tetrad we associate a null tetrad of null vectors **k**, **l**, **m**, $\overline{\mathbf{m}}$, such that

$$\mathbf{k}=\frac{1}{\sqrt{2}}(\mathbf{n}+\mathbf{q}),\quad \mathbf{l}=\frac{1}{\sqrt{2}}(\mathbf{n}-\mathbf{q}),$$
$$\mathbf{m}=\frac{1}{\sqrt{2}}(\mathbf{r}-i\mathbf{s}),\quad \overline{\mathbf{m}}=\frac{1}{\sqrt{2}}(\mathbf{r}+i\mathbf{s}). \tag{4.1}$$

Using the associated tetrad of null one-forms $\boldsymbol{\kappa}$, $\boldsymbol{\lambda}$, $\boldsymbol{\mu}$, $\overline{\boldsymbol{\mu}}$ dual to the null tetrad **k**, **l**, **m**, $\overline{\mathbf{m}}$, the metric can be written as

$$\boldsymbol{g}=-\boldsymbol{\kappa}\vee\boldsymbol{\lambda}+\boldsymbol{\mu}\vee\overline{\boldsymbol{\mu}}, \tag{4.2}$$

which implies

$$\mathbf{k}\cdot\mathbf{l}=-1,\quad \mathbf{m}\cdot\overline{\mathbf{m}}=1, \tag{4.3}$$

all other scalar products being zero. From this it follows that

$$\boldsymbol{\kappa}_\alpha=-g_{\alpha\beta}\mathbf{l}^\beta,\quad \boldsymbol{\lambda}_\alpha=-g_{\alpha\beta}\mathbf{k}^\beta,$$
$$\boldsymbol{\mu}_\alpha=g_{\alpha\beta}\overline{\mathbf{m}}^\beta,\quad \overline{\boldsymbol{\mu}}_\alpha=g_{\alpha\beta}\mathbf{m}^\beta. \tag{4.4}$$

The Weyl tensor $\mathbf{C}_{\alpha\beta\gamma\delta}$ has ten independent real components which can be parametrized by five standard complex coefficients defined as its components with respect to the above null tetrad (see, e.g., Refs. [42,44]):

$$\Psi_0=\mathbf{C}_{\alpha\beta\gamma\delta}\,\mathbf{k}^\alpha\mathbf{m}^\beta\mathbf{k}^\gamma\mathbf{m}^\delta,$$
$$\Psi_1=\mathbf{C}_{\alpha\beta\gamma\delta}\,\mathbf{k}^\alpha\mathbf{l}^\beta\mathbf{k}^\gamma\mathbf{m}^\delta,$$
$$\Psi_2=-\mathbf{C}_{\alpha\beta\gamma\delta}\,\mathbf{k}^\alpha\mathbf{m}^\beta\mathbf{l}^\gamma\overline{\mathbf{m}}^\delta, \tag{4.5}$$
$$\Psi_3=\mathbf{C}_{\alpha\beta\gamma\delta}\mathbf{l}^\alpha\mathbf{k}^\beta\mathbf{l}^\gamma\overline{\mathbf{m}}^\delta,$$
$$\Psi_4=\mathbf{C}_{\alpha\beta\gamma\delta}\mathbf{l}^\alpha\overline{\mathbf{m}}^\beta\mathbf{l}^\gamma\overline{\mathbf{m}}^\delta.$$

The coefficients Ψ_n transform in a simple way under special Lorentz transformations of the null tetrad **k**, **l**, **m**, $\overline{\mathbf{m}}$, namely, under null rotation around null vectors **k** or **l**, under a boost in the **k-l** plane, and a spatial rotation in the **m**-$\overline{\mathbf{m}}$ plane [44]. These transformation are summarized in Appendix D. The tensor of electromagnetic field $\mathbf{F}_{\alpha\beta}$ has six independent real components which can be parametrized, similarly to the Weyl tensor, as

$$\Phi_0=\mathbf{F}_{\alpha\beta}\,\mathbf{k}^\alpha\mathbf{m}^\beta,$$
$$\Phi_1=\frac{1}{2}\mathbf{F}_{\alpha\beta}\,(\mathbf{k}^\alpha\mathbf{l}^\beta-\mathbf{m}^\alpha\overline{\mathbf{m}}^\beta), \tag{4.6}$$
$$\Phi_2=\mathbf{F}_{\alpha\beta}\,\overline{\mathbf{m}}^\alpha\mathbf{l}^\beta.$$

The transformation properties of coefficients Φ_n under the null rotations, special boost, and spatial rotation can also be found in Appendix D.

Now, we first introduce an *algebraically special tetrad* $\mathbf{n}_\mathrm{s}$, $\mathbf{q}_\mathrm{s}$, $\mathbf{r}_\mathrm{s}$, $\mathbf{s}_\mathrm{s}$ which is associated with the *principal null directions* of the *C*-metric spacetime. We define

$$\mathbf{n}_\mathrm{s}=-\mathbf{e}_v=-\frac{\sqrt{-\mathcal{F}}}{r}\boldsymbol{\partial}_v,\quad \mathbf{r}_\mathrm{s}=\mathbf{e}_{\tilde\xi}=\frac{\sqrt{\mathcal{G}}}{r}\boldsymbol{\partial}_{\tilde\xi},$$
$$\mathbf{q}_\mathrm{s}=-\mathbf{e}_\tau=-\frac{1}{r\sqrt{-\mathcal{F}}}\boldsymbol{\partial}_\tau,\quad \mathbf{s}_\mathrm{s}=\mathbf{e}_\varphi=\frac{1}{r\sqrt{\mathcal{G}}}\boldsymbol{\partial}_\varphi, \tag{4.7}$$

and the corresponding null tetrad $\mathbf{k}_\mathrm{s}$, $\mathbf{l}_\mathrm{s}$, $\mathbf{m}_\mathrm{s}$, $\overline{\mathbf{m}}_\mathrm{s}$ by Eqs. (4.1). It is straightforward to check that these null directions $\mathbf{k}_\mathrm{s}$, $\mathbf{l}_\mathrm{s}$ can be expressed as

$$\mathbf{k}_\mathrm{s}=\frac{\sin\tilde v}{\sqrt{2}r|\delta|}\,\frac{1}{\sqrt{-\mathcal{F}}}\boldsymbol{\partial}_{\tilde v},\quad \mathbf{l}_\mathrm{s}=\frac{\sin\tilde u}{\sqrt{2}r|\delta|}\,\frac{1}{\sqrt{-\mathcal{F}}}\boldsymbol{\partial}_{\tilde u}, \tag{4.8}$$

where the global null coordinates $\tilde u$, $\tilde v$, parametrized by a constant δ, are introduced in Eq. (A38). It turns out that the Weyl tensor has the simplest form in this tetrad. It can be expressed as

$$\mathbf{C}=\frac{1}{12}(\mathcal{F}''+\mathcal{G}'')r^2$$
$$\times\Big(\frac{1}{\mathcal{F}\mathcal{G}}\mathbf{d}v\wedge\mathbf{d}\xi\,\mathbf{d}v\wedge\mathbf{d}\xi-\mathcal{F}\mathcal{G}\,\mathbf{d}\tau\wedge\mathbf{d}\varphi\mathbf{d}\tau\wedge\mathbf{d}\varphi$$
$$+\frac{\mathcal{G}}{\mathcal{F}}\mathbf{d}v\wedge\mathbf{d}\varphi\,\mathbf{d}v\wedge\mathbf{d}\varphi-\frac{\mathcal{F}}{\mathcal{G}}\mathbf{d}\tau\wedge\mathbf{d}\xi\,\mathbf{d}\tau\wedge\mathbf{d}\xi$$
$$+2\,\mathbf{d}\tau\wedge\mathbf{d}v\,\mathbf{d}\tau\wedge\mathbf{d}v-2\,\mathbf{d}\xi\wedge\mathbf{d}\varphi\,\mathbf{d}\xi\wedge\mathbf{d}\varphi\Big). \tag{4.9}$$

Transforming this into the null tetrad $\boldsymbol{\kappa}_\mathrm{s}$, $\boldsymbol{\lambda}_\mathrm{s}$, $\boldsymbol{\mu}_\mathrm{s}$, $\overline{\boldsymbol{\mu}}_\mathrm{s}$ we find that the only nonvanishing component is Ψ_2^s, namely,

$$\Psi_2^{\rm s}=\frac{1}{12}(\mathcal{F}''+\mathcal{G}'')r^{-2}$$
$$=-\left(\frac{m}{a_\Lambda}-\frac{e^2}{a_\Lambda^2}(v\cosh\alpha+\xi\sinh\alpha)\right)\frac{a_\Lambda}{r^3}$$
$$=-\left(m-2e^2A\xi-\frac{e^2}{r}\right)\frac{1}{r^3},$$
$$\Psi_0^{\rm s}=\Psi_1^{\rm s}=\Psi_3^{\rm s}=\Psi_4^{\rm s}=0. \tag{4.10}$$

This exhibits explicitly that $\mathbf{k}_{\rm s}$, $\mathbf{l}_{\rm s}$ are the double principal null directions [44], which lie in the τ-v plane.

Similarly, the electromagnetic field tensor (2.4) in coordinates τ, v, ξ, φ reads

$$\mathbf{F}=e\,\mathbf{d}v\wedge\mathbf{d}\tau. \tag{4.11}$$

Using relations (4.1), (4.7), we find that the only nonvanishing coefficient of electromagnetic field is $\Phi_1^{\rm s}$,

$$\Phi_1^{\rm s}=-\frac{e}{2r^2},\quad \Phi_0^{\rm s}=\Phi_2^{\rm s}=0. \tag{4.12}$$

The special null tetrad defined above is appropriate for discussion of algebraic properties of the fields. However, near future infinity $\mathcal{I}^+$ we will also have to use a different tetrad $\mathbf{n}_{\rm o}$, $\mathbf{q}_{\rm o}$, $\mathbf{r}_{\rm o}$, $\mathbf{s}_{\rm o}$ and the related null tetrad $\mathbf{k}_{\rm o}$, $\mathbf{l}_{\rm o}$, $\mathbf{m}_{\rm o}$, $\overline{\mathbf{m}}_{\rm o}$. These will serve as *reference tetrads* with respect to which we will parametrize a general asymptotic direction. These tetrads are adapted to the Killing vectors $\boldsymbol{\partial}_\tau$, $\boldsymbol{\partial}_\varphi$ and to de Sitter–like infinity $\mathcal{I}^+$. Namely, the timelike vector $\mathbf{n}_{\rm o}$ is asymptotically orthogonal to $\mathcal{I}^+$, and $\mathbf{q}_{\rm o}$, $\mathbf{r}_{\rm o}$, $\mathbf{s}_{\rm o}$ are tangent to $\mathcal{I}^+$. We define

$$\mathbf{n}_{\rm o}=\mathbf{e}_\omega=\frac{\sqrt{-\mathcal{E}}}{r}\boldsymbol{\partial}_\omega,\quad \mathbf{r}_{\rm o}=\mathbf{e}_\sigma=\frac{1}{r}\sqrt{\frac{\mathcal{E}}{\mathcal{F}\mathcal{G}}}\boldsymbol{\partial}_\sigma,$$
$$\mathbf{q}_{\rm o}=-\mathbf{e}_\tau=-\frac{1}{r\sqrt{-\mathcal{F}}}\boldsymbol{\partial}_\tau,\quad \mathbf{s}_{\rm o}=\mathbf{e}_\varphi=\frac{1}{r\sqrt{\mathcal{G}}}\boldsymbol{\partial}_\varphi, \tag{4.13}$$

the corresponding null tetrad $\mathbf{k}_{\rm o}$, $\mathbf{l}_{\rm o}$, $\mathbf{m}_{\rm o}$, $\overline{\mathbf{m}}_{\rm o}$ is given by Eqs. (4.1).

Relations between the tetrads $\mathbf{n}_{\rm s}$, $\mathbf{q}_{\rm s}$, $\mathbf{r}_{\rm s}$, $\mathbf{s}_{\rm s}$ and $\mathbf{n}_{\rm o}$, $\mathbf{q}_{\rm o}$, $\mathbf{r}_{\rm o}$, $\mathbf{s}_{\rm o}$ immediately follow from the definitions (4.7), (4.13) and from relations of coordinates (2.11) [cf. Eqs. (C2b), (C2c)],

$$\mathbf{n}_{\rm s}=\sqrt{\frac{\mathcal{F}}{\mathcal{E}}}\cosh\alpha\ \ \mathbf{n}_{\rm o}+\sqrt{\frac{\mathcal{G}}{-\mathcal{E}}}\sinh\alpha\ \ \mathbf{r}_{\rm o},$$
$$\mathbf{r}_{\rm s}=\sqrt{\frac{\mathcal{G}}{-\mathcal{E}}}\sinh\alpha\ \ \mathbf{n}_{\rm o}+\sqrt{\frac{\mathcal{F}}{\mathcal{E}}}\cosh\alpha\ \ \mathbf{r}_{\rm o}, \tag{4.14}$$
$$\mathbf{q}_{\rm s}=\mathbf{q}_{\rm o},\quad \mathbf{s}_{\rm s}=\mathbf{s}_{\rm o}.$$

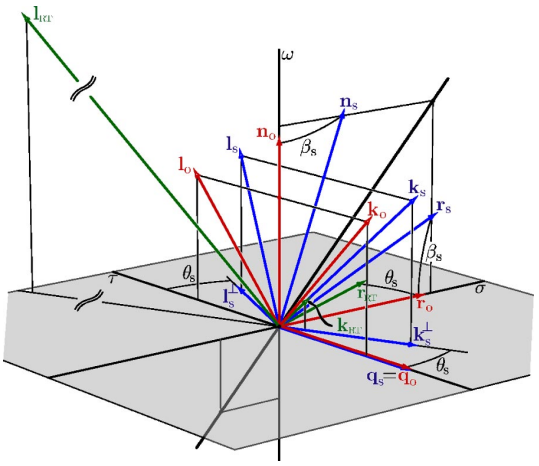

FIG. 5. A spacetime diagram (φ direction is suppressed) that depicts relations between the reference tetrad $\mathbf{n}_{\rm o}$, $\mathbf{q}_{\rm o}$, $\mathbf{r}_{\rm o}$, $\mathbf{s}_{\rm o}$ (or $\mathbf{k}_{\rm o}$, $\mathbf{l}_{\rm o}$, $\mathbf{m}_{\rm o}$, $\overline{\mathbf{m}}_{\rm o}$), the algebraically special tetrad $\mathbf{n}_{\rm s}$, $\mathbf{q}_{\rm s}$, $\mathbf{r}_{\rm s}$, $\mathbf{s}_{\rm s}$ (or $\mathbf{k}_{\rm s}$, $\mathbf{l}_{\rm s}$, $\mathbf{m}_{\rm s}$, $\overline{\mathbf{m}}_{\rm s}$), and the Robinson-Trautman tetrad $\mathbf{k}_{\rm RT}$, $\mathbf{l}_{\rm RT}$, $\mathbf{m}_{\rm RT}$, $\overline{\mathbf{m}}_{\rm RT}$. The reference tetrad is naturally adapted to the infinity ($\mathbf{n}_{\rm o}$ is normal to $\mathcal{I}^+$) and the Killing vectors ($\mathbf{q}_{\rm o}$ and $\mathbf{s}_{\rm o}$ are tangent to them), while the algebraically special tetrad is adapted to both double principal null directions $\mathbf{k}_{\rm s}$ and $\mathbf{l}_{\rm s}$. These two are related by a boost in the $\mathbf{n}_{\rm o}-\mathbf{r}_{\rm o}$ plane, with the boost parameter $\beta_{\rm s}$ given by Eq. (4.15). The vectors $\mathbf{q}_{\rm o}$ and $\mathbf{q}_{\rm s}$ are identical, similarly $\mathbf{s}_{\rm o}=\mathbf{s}_{\rm s}$. Orthogonal projections $\mathbf{k}_{\rm s}^{\perp}$, $\mathbf{l}_{\rm s}^{\perp}$ of the principal null directions onto $\omega=$const hyperplane (shaded) define the angle $\theta_{\rm s}$ [Eq. (4.18)] that, similarly to $\beta_{\rm s}$, characterizes the relation between the reference and the special tetrads. The vector $\mathbf{k}_{\rm RT}$ of the Robinson-Trautman tetrad points into the principal null direction $\mathbf{k}_{\rm s}$ with the coefficient of proportionality approaching zero on $\mathcal{I}^+$, cf. Eq. (4.28). The other null direction $\mathbf{l}_{\rm RT}$ belongs to the $\mathbf{n}_{\rm o}$-$\mathbf{k}_{\rm s}$ plane and it becomes "infinitely long" on $\mathcal{I}^+$.

A geometrical meaning of these transformations is seen in Fig. 5. Both tetrads are related by a simple boost in the $\mathbf{n}_{\rm o}$-$\mathbf{r}_{\rm o}$ plane with a boost parameter $\beta_{\rm s}$ given by

$$\tanh\beta_{\rm s}=\sqrt{\frac{\mathcal{G}}{-\mathcal{F}}}\tanh\alpha. \tag{4.15}$$

This boost is described by relations similar to Eq. (D10), with the vectors $\mathbf{q}$ and $\mathbf{r}$ interchanged.

We obtain even a better visualization if we perform a projection of the principal null directions $\mathbf{k}_{\rm s}$, $\mathbf{l}_{\rm s}$ to a three-dimensional hyperplane orthogonal to the timelike vector $\mathbf{n}_{\rm o}$. We thus obtain "spatial" directions $\mathbf{k}_{\rm s}^{\perp}$, $\mathbf{l}_{\rm s}^{\perp}$,

$$\mathbf{k}_{\rm s}^{\perp}=\mathbf{k}_{\rm s}+(\mathbf{k}_{\rm s}\cdot\mathbf{n}_{\rm o})\mathbf{n}_{\rm o},\quad \text{etc.}, \tag{4.16}$$

of the null vectors $\mathbf{k}_{\rm s}$, $\mathbf{l}_{\rm s}$ which lie in the $\mathbf{q}_{\rm o}$-$\mathbf{r}_{\rm o}$ plane, symmetrically with respect to the vector $\mathbf{r}_{\rm o}$ (see Fig. 5). If we denote by $\theta_{\rm s}$ the angle between $\mathbf{q}_{\rm o}$ and $\mathbf{k}_{\rm s}^{\perp}$, we can write $\mathbf{k}_{\rm s}^{\perp}\propto\sin\theta_{\rm s}\,\mathbf{r}_{\rm o}+\cos\theta_{\rm s}\,\mathbf{q}_{\rm o}$, and taking into account the normalization (4.3) we obtain

$$\mathbf{k}_{\mathrm{s}}=\frac{1}{\sqrt{2}\cos\theta_{\mathrm{s}}}(\mathbf{n}_{\mathrm{o}}+\sin\theta_{\mathrm{s}}\ \mathbf{r}_{\mathrm{o}}+\cos\theta_{\mathrm{s}}\ \mathbf{q}_{\mathrm{o}}),$$
$$\mathbf{l}_{\mathrm{s}}=\frac{1}{\sqrt{2}\cos\theta_{\mathrm{s}}}(\mathbf{n}_{\mathrm{o}}+\sin\theta_{\mathrm{s}}\ \mathbf{r}_{\mathrm{o}}-\cos\theta_{\mathrm{s}}\ \mathbf{q}_{\mathrm{o}}), \tag{4.17}$$

see also Eq. (C3). Comparing this with relations (4.14) and using Eq. (4.1), we find that the angle θ_{s} is given in terms of the metric functions $\mathcal{F}$, $\mathcal{G}$, $\mathcal{E}$ as

$$\sin\theta_{\mathrm{s}}=\sqrt{\frac{\mathcal{G}}{-\mathcal{F}}}\tanh\alpha,\quad \cos\theta_{\mathrm{s}}=\left(\sqrt{\frac{\mathcal{F}}{\mathcal{E}}}\cosh\alpha\right)^{-1}, \tag{4.18}$$

i.e., $\tanh\beta_{\mathrm{s}}=\sin\theta_{\mathrm{s}}$.

We will be interested mainly in the tetrads at the conformal infinity $\mathcal{I}^+$, i.e., for $\omega=0$, where $v=\xi\tanh\alpha$ and $\mathcal{E}=-1$, see Eqs. (3.2), (A24). From the definitions (4.15), (4.18) and using Eqs. (A10), (A11) we find that the boost parameter β_{s} and the angle θ_{s} (which both characterize directions "from the sources") may on the $\mathcal{I}^+$ have values in the ranges

$$\beta_{\mathrm{s}}\in[0,\alpha],\quad \sin\theta_{\mathrm{s}}\in[0,\tanh\alpha]. \tag{4.19}$$

The zero values occur on the axis of φ symmetry (points "between" the moving black holes; $\xi=\xi_1,\xi_2$), the maximal values occur on the "equator"—the φ circle of maximal circumference ($\xi=0$, $v=0$).

Transformation formulas (C3) allow us to find components of the Weyl tensor and tensor of electromagnetic field in the reference null tetrad $\mathbf{k}_{\mathrm{o}}$, $\mathbf{l}_{\mathrm{o}}$, $\mathbf{m}_{\mathrm{o}}$, $\overline{\mathbf{m}}_{\mathrm{o}}$, namely,

$$\Psi_2^{\mathrm{o}}=\frac{1}{2}\Psi_2^{\mathrm{s}}(3\cos^{-2}\theta_{\mathrm{s}}-1),$$
$$\Psi_1^{\mathrm{o}}=\Psi_3^{\mathrm{o}}=-\frac{3}{2}\Psi_2^{\mathrm{s}}\sin\theta_{\mathrm{s}}\cos^{-2}\theta_{\mathrm{s}},$$
$$\Psi_0^{\mathrm{o}}=\Psi_4^{\mathrm{o}}=\frac{3}{2}\Psi_2^{\mathrm{s}}\sin^2\theta_{\mathrm{s}}\cos^{-2}\theta_{\mathrm{s}},$$
$$\Phi_0^{\mathrm{o}}=\Phi_2^{\mathrm{o}}=-\tan\theta_{\mathrm{s}}\Phi_1^{\mathrm{s}},\quad \Phi_1^{\mathrm{o}}=\cos^{-1}\theta_{\mathrm{s}}\Phi_1^{\mathrm{s}}, \tag{4.20, 4.21}$$

or, more explicitly [using Eqs. (4.10), (4.12), and (4.18)]

$$\Psi_2^{\mathrm{o}}=\frac{\mathcal{F}''+\mathcal{G}''}{8\mathcal{E}r^2}\frac{1}{3}(2\mathcal{F}\cosh^2\alpha-\mathcal{G}\sinh^2\alpha),$$
$$\Psi_1^{\mathrm{o}}=\Psi_3^{\mathrm{o}}=\frac{\mathcal{F}''+\mathcal{G}''}{8\mathcal{E}r^2}\sqrt{-\mathcal{F}\mathcal{G}}\cosh\alpha\sinh\alpha,$$
$$\Psi_0^{\mathrm{o}}=\Psi_4^{\mathrm{o}}=-\frac{\mathcal{F}''+\mathcal{G}''}{8\mathcal{E}r^2}\mathcal{G}\sinh^2\alpha, \tag{4.22}$$

$$\Phi_1^{\mathrm{o}}=-\frac{e}{2r^2}\sqrt{\frac{\mathcal{F}}{\mathcal{E}}}\cosh\alpha,$$
$$\Phi_0^{\mathrm{o}}=\Phi_2^{\mathrm{o}}=\frac{e}{2r^2}\sqrt{\frac{\mathcal{G}}{-\mathcal{E}}}\sinh\alpha. \tag{4.23}$$

As we have already mentioned, the tetrad $\mathbf{n}_{\mathrm{o}}$, $\mathbf{q}_{\mathrm{o}}$, $\mathbf{r}_{\mathrm{o}}$, $\mathbf{s}_{\mathrm{o}}$ serves as the reference tetrad with respect to which we characterize an arbitrarily *rotated tetrad* $\mathbf{n}_{\mathrm{r}}$, $\mathbf{q}_{\mathrm{r}}$, $\mathbf{r}_{\mathrm{r}}$, $\mathbf{s}_{\mathrm{r}}$. The tetrad $\mathbf{n}_{\mathrm{r}}$, $\mathbf{q}_{\mathrm{r}}$, $\mathbf{r}_{\mathrm{r}}$, $\mathbf{s}_{\mathrm{r}}$ is obtained from the reference tetrad by a spatial rotation given by angles θ, ϕ,

$$\mathbf{n}_{\mathrm{r}}=\mathbf{n}_{\mathrm{o}},$$
$$\mathbf{q}_{\mathrm{r}}=\cos\theta\mathbf{q}_{\mathrm{o}}+\sin\theta\cos\phi\mathbf{r}_{\mathrm{o}}+\sin\theta\sin\phi\mathbf{s}_{\mathrm{o}},$$
$$\mathbf{r}_{\mathrm{r}}=-\sin\theta\mathbf{q}_{\mathrm{o}}+\cos\theta\cos\phi\mathbf{r}_{\mathrm{o}}+\cos\theta\sin\phi\mathbf{s}_{\mathrm{o}},$$
$$\mathbf{s}_{\mathrm{r}}=-\sin\phi\mathbf{r}_{\mathrm{o}}+\cos\phi\mathbf{s}_{\mathrm{o}}. \tag{4.24}$$

Let us note that the angles θ, ϕ, understood as standard spherical coordinates spanned on the axes $\mathbf{q}_{\mathrm{o}}$, $\mathbf{r}_{\mathrm{o}}$, $\mathbf{s}_{\mathrm{o}}$, describe exactly the spatial direction $\mathbf{k}_{\mathrm{r}}^{\perp}=(1/\sqrt{2})\mathbf{q}_{\mathrm{r}}$ of the null vector $\mathbf{k}_{\mathrm{r}}$, where the *spatial direction* means projection orthogonal to the vector $\mathbf{n}_{\mathrm{o}}$. The relation between null tetrads following from Eq. (4.24) can be found in Eq. (C5). This transformation is obtained as a consecutive composition of null rotation with fixed $\mathbf{k}$ [Eq. (D3)], null rotation with fixed $\mathbf{l}$ [Eq. (D6)], and of special boost and spatial rotation (D9) with parameters

$$L=-\tan\frac{\theta}{2}\exp(-i\phi),$$
$$K=\sin\frac{\theta}{2}\cos\frac{\theta}{2}\exp(-i\phi),$$
$$B=\cos^{-2}\frac{\theta}{2},\quad \Phi=\phi. \tag{4.25}$$

Finally, we also introduce the *Robinson-Trautman tetrad* $\mathbf{k}_{\mathrm{RT}}$, $\mathbf{l}_{\mathrm{RT}}$, $\mathbf{m}_{\mathrm{RT}}$, $\overline{\mathbf{m}}_{\mathrm{RT}}$ (see, e.g., Ref. [44]) naturally connected with the Robinson-Trautman coordinates ζ, $\overline{\zeta}$, u, r [see Eqs. (2.9) and (A25), (A28)]

$$\mathbf{k}_{\mathrm{RT}}=\boldsymbol{\partial}_r,$$
$$\mathbf{l}_{\mathrm{RT}}=-\frac{1}{2}H\boldsymbol{\partial}_r+\boldsymbol{\partial}_u=-\frac{r^2\mathcal{E}}{2a_\Lambda^2}\boldsymbol{\partial}_r+\boldsymbol{\partial}_u,$$
$$\mathbf{m}_{\mathrm{RT}}=\frac{P}{r}\boldsymbol{\partial}_{\bar\zeta}=\frac{1}{\sqrt{\mathcal{G}}r}\boldsymbol{\partial}_{\bar\zeta},$$
$$\overline{\mathbf{m}}_{\mathrm{RT}}=\frac{P}{r}\boldsymbol{\partial}_{\zeta}=\frac{1}{\sqrt{\mathcal{G}}r}\boldsymbol{\partial}_{\zeta}. \tag{4.26}$$

Here we have written down equivalent expressions using both metric functions *H, P* commonly used in the Robinson-Trautman framework, and the metric functions $\mathcal{G}$, $\mathcal{E}$ of the *C*-metric [see Eqs. (2.14), (2.15)]. The vector $\mathbf{k}_{\mathrm{RT}}$ of this tetrad is oriented along the principal null direction $\mathbf{k}_{\mathrm{s}}$, and it will be demonstrated in Sec. VII that this tetrad is parallelly transported along the geodesics tangent to principal null directions.

The tetrad (4.26) is simply related to the particularly rotated tetrad $\mathbf{k}_{\mathrm{r}}$, $\mathbf{l}_{\mathrm{r}}$, $\mathbf{m}_{\mathrm{r}}$, $\overline{\mathbf{m}}_{\mathrm{r}}$ [Eq. (C5)] with $\theta=\theta_{\mathrm{s}}$, $\phi=0$, θ_{s} given by Eq. (4.18):

$$\mathbf{k}_{\mathrm{RT}}=\exp(\beta_{\mathrm{RT}})\mathbf{k}_{\mathrm{r}}, \quad \mathbf{l}_{\mathrm{RT}}=\exp(-\beta_{\mathrm{RT}})\mathbf{l}_{\mathrm{r}}, \qquad \mathbf{m}_{\mathrm{RT}}=\mathbf{m}_{\mathrm{r}}, \quad \overline{\mathbf{m}}_{\mathrm{RT}}=\overline{\mathbf{m}}_{\mathrm{r}}, \tag{4.27}$$

i.e., the Robinson-Trautman tetrad can be obtained from the reference tetrad $\mathbf{k}_{\mathrm{o}}$, $\mathbf{l}_{\mathrm{o}}$, $\mathbf{m}_{\mathrm{o}}$, $\overline{\mathbf{m}}_{\mathrm{o}}$ by the spatial rotation (C5) with $\theta=\theta_{\mathrm{s}}$, $\phi=0$, followed by the boost (D9) with parameter

$$B=\exp\beta_{\mathrm{RT}}=-\frac{\sqrt{2}\omega}{\sqrt{-\mathcal{E}}}=\sqrt{-\frac{2}{H}}. \tag{4.28}$$

We also give the relation between the Robinson-Trautman and the algebraically special tetrad. Because the vectors $\mathbf{k}_{\mathrm{RT}}$ and $\mathbf{k}_{\mathrm{s}}$ are proportional, the Robinson-Trautman tetrad is obtained from the special tetrad by the null rotation (D3) followed by the boost (D9) with the parameters

$$L=-\sin\theta_{\mathrm{s}}=-\sqrt{\frac{\mathcal{G}}{-\mathcal{F}}}\tanh\alpha, \qquad B=\exp\beta_{\mathrm{RT}}\cos\theta_{\mathrm{s}}=\frac{\sqrt{2}a_{\Lambda}}{r\sqrt{-\mathcal{F}}\cosh\alpha}. \tag{4.29}$$

The explicit relation of both tetrads can be found in Eqs. (C3) and (C4).

Using the transformations (D4), (D11) and (D5), (D12) with these parameters *L*, *B*, we find that the only nonvanishing components of the gravitational and electromagnetic fields in the Robinson-Trautman tetrad are

$$\Psi_2^{\mathrm{RT}}=\Psi_2^{\mathrm{s}}=-\left(m-2e^2A\xi-\frac{e^2}{r}\right)\frac{1}{r^3}, \tag{4.30}$$

$$\Psi_3^{\mathrm{RT}}=-\frac{3}{\sqrt{2}}\frac{Ar}{P}\Psi_2^{\mathrm{s}}, \quad \Psi_4^{\mathrm{RT}}=3\frac{A^2r^2}{P^2}\Psi_2^{\mathrm{s}},$$

$$\Phi_1^{\mathrm{RT}}=\Phi_1^{\mathrm{s}}=-\frac{e}{2r^2}, \quad \Phi_2^{\mathrm{RT}}=-\sqrt{2}\frac{Ar}{P}\Phi_1^{\mathrm{s}}, \tag{4.31}$$

with Ψ_2^{s} and Φ_1^{s} also given by Eqs. (4.10) and (4.12), see Ref. [44].

V. GRAVITATIONAL AND ELECTROMAGNETIC FIELDS NEAR $\mathcal{I}^+$

Now we are prepared to discuss radiative properties of the *C*-metric fields near the de Sitter–like infinity $\mathcal{I}^+$. As we have already explained in Sec. I, by the *radiative field* we understand a field with a dominant component having the $1/\eta$ fall-off, calculated in a tetrad parallelly transported along a null geodesic $z(\eta)$. We will in particular concentrate on investigation of a directional dependence of the gravitational and electromagnetic radiation.

To study the dependence of the fields on the directions along which the spacelike infinity $\mathcal{I}^+$ is approached, it is crucial to find a parallelly transported tetrad along all null geodesics. However, it is difficult to find a general geodesic and the corresponding tetrad in an explicit form, except for the case of very special geodesics along the privileged principal null directions, which will be discussed in Sec. VII. Fortunately, it is not, in fact, necessary to find an explicit form of the geodesics and tetrads because we are interested only in the dominant terms of the fields close to $\mathcal{I}^+$. It is fully sufficient to study only their *asymptotic forms*.

Near infinity $\mathcal{I}^+$, null geodesics $z(\eta)$ can be expanded in the inverse powers of the affine parameter $\eta\to\infty$. In particular, in coordinates τ, ω, σ, φ introduced in Eq. (2.11), the null geodesics $z(\eta)$ can be expanded as

$$\begin{aligned}\omega(\eta)&\approx\omega_*\frac{a_\Lambda}{\eta}+\cdots,\\ \tau(\eta)&\approx\tau_+ +\tau_*\frac{a_\Lambda}{\eta}+\cdots,\\ \sigma(\eta)&\approx\sigma_+ +\sigma_*\frac{a_\Lambda}{\eta}+\cdots,\\ \varphi(\eta)&\approx\varphi_+ +\varphi_*\frac{a_\Lambda}{\eta}+\cdots,\end{aligned} \tag{5.1}$$

where the affine parameter η has the dimension of length. There is no absolute term in the expansion of the coordinate ω because $\omega=0$ at $\mathcal{I}^+$. The constant parameters τ_+, σ_+, φ_+ [and the corresponding values v_+ and ξ_+ given by Eq. (2.11)] label the *point* N_+ at $\mathcal{I}^+$ which is approached by the geodesic $z(\eta)$. The parameters τ_*, σ_*, φ_* characterize the *direction* along which this point N_+ is approached. The remaining coefficient ω_* can be determined from the normalization of the tangent vector which must be null. The tangent vector has the form

$$\frac{Dz}{d\eta}\approx-\frac{a_\Lambda}{\eta^2}(\omega_*\boldsymbol{\partial}_\omega+\tau_*\boldsymbol{\partial}_\tau+\sigma_*\boldsymbol{\partial}_\sigma+\varphi_*\boldsymbol{\partial}_\varphi). \tag{5.2}$$

The asymptotic form of the metric (2.12) along the null geodesic is

$$\boldsymbol{g}\approx\frac{\eta^2}{\omega_*^2}(-\mathbf{d}\omega^2-\mathcal{F}_+\mathbf{d}\tau^2-\mathcal{F}_+\mathcal{G}_+\mathbf{d}\sigma^2+\mathcal{G}_+\mathbf{d}\varphi^2), \tag{5.3}$$

where $\mathcal{F}_+$ and $\mathcal{G}_+$ are the functions $\mathcal{F}$ and $\mathcal{G}$ evaluated at the point N_+ at infinity $\mathcal{I}^+$, and we used $\mathcal{E}_+=-1$. Therefore, the condition that the tangent vector is a null vector implies

$$\omega_*^2=-\mathcal{F}_+\tau_*^2-\mathcal{F}_+\mathcal{G}_+\sigma_*^2+\mathcal{G}_+\varphi_*^2. \tag{5.4}$$

Notice that $\omega_*<0$ since $\omega<0$, and

$$r(\eta)\approx\gamma\eta+\cdots, \quad \text{where} \quad \gamma=-\frac{1}{\omega_*}, \tag{5.5}$$

which follows from Eq. (2.16).

We wish to compare geodesics approaching the given point N_+ along different directions. We thus need to ensure "the same" universal choice of the affine parameter η for all geodesics. It is natural to require that the energy (or, equivalently, the frequency) of the ray represented by the null geodesic

$$E_{\mathrm{o}}=-\mathbf{p}\cdot\mathbf{n}_{\mathrm{o}}=-a_\Lambda\frac{Dz}{d\eta}\cdot\mathbf{n}_{\mathrm{o}} \tag{5.6}$$

(see [45]), is *the same* independently of the direction of the geodesic, i.e., that the component of the tangent vector to the normal direction $\mathbf{n}_{\mathrm{o}}$ is fixed. From Eqs. (5.6), (5.2), and (4.13) it immediately follows that

$$E_{\mathrm{o}}\approx\frac{a_\Lambda^2}{\eta}=\gamma\frac{a_\Lambda^2}{r}. \tag{5.7}$$

The value of the energy E_{o} with respect to any asymptotic observer characterized by the four-velocity $\mathbf{n}_{\mathrm{o}}$ thus obviously approaches zero as $\eta\to\infty$. This behavior is caused by the de Sitter–like character of $\mathcal{I}^+$. Therefore, we have to compare the values of E_{o} at the same "proximity" to $\mathcal{I}^+$, i.e., at some fixed large but *finite* value of the coordinate r (see [46]). We conclude from Eq. (5.7) that fixing the energy at a given prescribed value of r is equivalent to fixing the value of the constant parameter γ independently of a direction of the geodesic. Let us note that this approach is fully equivalent to fixing a finite value of *conformal energy*, i.e., of the energy defined with respect to a vector normal to $\mathcal{I}^+$ normalized using a conformal metric $\tilde{\mathbf{g}}=\omega^2\mathbf{g}$.

Next, it is necessary to find an *interpretation tetrad* $\mathbf{k}_{\mathrm{i}}$, $\mathbf{l}_{\mathrm{i}}$, $\mathbf{m}_{\mathrm{i}}$, $\overline{\mathbf{m}}_{\mathrm{i}}$ which is parallelly transported along the geodesic $z(\eta)$. However, using only an asymptotic expansion of the tetrad at infinity $\mathcal{I}^+$, we cannot determine unique initial conditions which define this tetrad somewhere in a finite region of the spacetime. But without specifying these initial conditions, the parallelly transported tetrad at $\mathcal{I}^+$ is given only up to an arbitrary (finite) Lorentz transformation. It thus seems that we are losing all information because of this nonuniqueness. However, it is not so. It will be demonstrated that the crucial information about the behavior of the fields at infinity $\mathcal{I}^+$ is hidden in an "infinite" Lorentz transformation corresponding to the parallel transport from a finite region of the spacetime up to infinity. It will thus be sufficient to find only the leading term of this transformation.

To be more specific, we naturally choose the vector $\mathbf{k}_{\mathrm{i}}$ of the parallelly transported interpretation null tetrad to be proportional to the (parallelly transported) tangent vector of the geodesic. This ensures that $\mathbf{k}_{\mathrm{i}}$ is finite in finite regions of spacetime (see [47]). However, we still have a freedom in the normalization of $\mathbf{k}_{\mathrm{i}}$ which can be multiplied by an arbitrary finite factor, constant along the geodesic. Similarly to the choice of the "universal" affine parameter for different geodesics, we have to choose the parallelly transported tetrads in some suitable "comparable" way for various geodesics approaching the same point N_+ at infinity from different directions. Not having an explicit form of the geodesics (except for those special ones discussed in Sec. VII), we have to eliminate the dependence on initial conditions by fixing final conditions for the tetrad at infinity $\mathcal{I}^+$. Namely, we will require that the normalization of the vector $\mathbf{k}_{\mathrm{i}}$ is specified independently of the direction of the geodesics. This is achieved, for example, by the condition

$$\mathbf{k}_{\mathrm{i}}\cdot\mathbf{d}r=1. \tag{5.8}$$

Thanks to Eq. (5.5) we thus have

$$\mathbf{k}_{\mathrm{i}}=\frac{1}{\gamma}\frac{Dz}{d\eta}. \tag{5.9}$$

Concerning vectors $\mathbf{m}_{\mathrm{i}}$, $\overline{\mathbf{m}}_{\mathrm{i}}$ of the parallelly transported interpretation tetrad, there is a priori no "canonical" prescription how to choose these in a universal way for different geodesics. The only constraint is the correct normalization (4.3). Therefore, we have to find such physical quantities which are invariant under this freedom. It will be shown below [see Eq. (5.18) and discussion therein] that the *magnitude of the leading term* of the fields at $\mathcal{I}^+$ is, in fact, independent of the specific choice of the vectors $\mathbf{m}_{\mathrm{i}}$, $\overline{\mathbf{m}}_{\mathrm{i}}$.

However, there is a natural possibility to fix the null vector $\mathbf{l}_{\mathrm{i}}$ of the tetrad by the condition that the timelike unit vector $\mathbf{n}_{\mathrm{o}}$, orthogonal to infinity $\mathcal{I}^+$, lies in the $\mathbf{k}_{\mathrm{i}}$-$\mathbf{l}_{\mathrm{i}}$ plane. In this case the parallelly transported tetrad can be obtained by a boost in the $\mathbf{k}_{\mathrm{i}}$-$\mathbf{l}_{\mathrm{i}}$ plane from the rotated tetrad $\mathbf{k}_{\mathrm{r}}$, $\mathbf{l}_{\mathrm{r}}$, $\mathbf{m}_{\mathrm{r}}$, $\overline{\mathbf{m}}_{\mathrm{r}}$ [see Eqs. (4.24) or (C5)] with properly chosen angles θ, ϕ. Clearly, the vector $\mathbf{k}_{\mathrm{r}}$ has to point exactly in the direction of the geodesic or, equivalently, the spatial vector $\mathbf{q}_{\mathrm{r}}$ has to point in the spatial direction of the geodesic (here again by *spatial vectors* we mean those orthogonal to $\mathbf{n}_{\mathrm{o}}=\mathbf{n}_{\mathrm{r}}$, i.e., tangent to $\mathcal{I}^+$). Using Eqs. (5.9), (5.2), and (4.13) we obtain

$$\mathbf{k}_{\mathrm{i}}\approx\frac{a_\Lambda}{\gamma\eta}\left(\mathbf{n}_{\mathrm{o}}-\frac{1}{\eta}(\tau_*\boldsymbol{\partial}_\tau+\sigma_*\boldsymbol{\partial}_\sigma+\varphi_*\boldsymbol{\partial}_\varphi)\right). \tag{5.10}$$

The unit vector $\mathbf{q}_{\mathrm{r}}$ in the spatial direction of the geodesic is thus

$$\begin{aligned}\mathbf{q}_{\mathrm{r}}&\approx-\frac{1}{\eta}(\tau_*\boldsymbol{\partial}_\tau+\sigma_*\boldsymbol{\partial}_\sigma+\varphi_*\boldsymbol{\partial}_\varphi)\\&=-\sqrt{-\mathcal{F}_+}\frac{\tau_*}{\omega_*}\mathbf{q}_{\mathrm{o}}+\sqrt{-\mathcal{F}_+\mathcal{G}_+}\frac{\sigma_*}{\omega_*}\mathbf{r}_{\mathrm{o}}+\sqrt{\mathcal{G}_+}\frac{\varphi_*}{\omega_*}\mathbf{s}_{\mathrm{o}}.\end{aligned} \tag{5.11}$$

The leading term of the expansion of the parallelly transported tetrad near the infinity then can be written as

$$\mathbf{k}_{\mathrm{i}} \approx \frac{\sqrt{2}a_\Lambda}{\gamma\eta}\mathbf{k}_{\mathrm{r}} = \frac{a_\Lambda}{\gamma\eta}(\mathbf{n}_{\mathrm{o}} + \mathbf{q}_{\mathrm{r}}), \quad \mathbf{m}_{\mathrm{i}} \approx \mathbf{m}_{\mathrm{r}},$$
$$\mathbf{l}_{\mathrm{i}} \approx \frac{\gamma\eta}{\sqrt{2}a_\Lambda}\mathbf{l}_{\mathrm{r}} = \frac{\gamma\eta}{2a_\Lambda}(\mathbf{n}_{\mathrm{o}} - \mathbf{q}_{\mathrm{r}}), \quad \overline{\mathbf{m}}_{\mathrm{i}} \approx \overline{\mathbf{m}}_{\mathrm{r}}. \tag{5.12}$$

Here, we have made a particular choice of the vectors $\mathbf{m}_{\mathrm{i}}$, $\overline{\mathbf{m}}_{\mathrm{i}}$. In general, $\mathbf{m}_{\mathrm{i}}$ could differ from $\mathbf{m}_{\mathrm{r}}$ by a phase factor (a rotation in the $\mathbf{m}_{\mathrm{i}}$-$\overline{\mathbf{m}}_{\mathrm{i}}$ plane) which, as we mentioned, cannot be fixed in a canonical way. Our choice $\mathbf{m}_{\mathrm{i}} \approx \mathbf{m}_{\mathrm{r}}$ is ''natural'' for the approach presented here. However, in the next section we will encounter another ''suitable'' choice of the vector $\mathbf{m}_{\mathrm{i}}$.

Now we have to identify the angles θ, ϕ. Let us recall that these angles are just spherical coordinates of the spatial direction $\mathbf{q}_{\mathrm{r}} \propto \mathbf{k}_{\mathrm{i}}^{\perp}$ with respect to the reference frame $\mathbf{q}_{\mathrm{o}}$, $\mathbf{r}_{\mathrm{o}}$, $\mathbf{s}_{\mathrm{o}}$. Comparing Eqs. (5.11) and (4.24) we find that the parameters τ_*, σ_*, φ_*, characterizing the asymptotic spatial direction of the geodesic (5.1), fix the angles θ, ϕ as

$$\tau_* = \frac{1}{\gamma\sqrt{-\mathcal{F}_+}}\cos\theta,$$
$$\sigma_* = -\frac{1}{\gamma\sqrt{-\mathcal{F}_+\mathcal{G}_+}}\sin\theta\cos\phi, \tag{5.13}$$
$$\varphi_* = -\frac{1}{\gamma\sqrt{\mathcal{G}_+}}\sin\theta\sin\phi.$$

In the following we will use these angles θ, ϕ to parametrize the direction along which a null geodesic approaches the point N_+ on $\mathcal{I}^+$.

Now we are ready to calculate the leading terms of the components Ψ_n^{i} of the Weyl tensor in the parallelly transported tetrad given above. First we find the components Ψ_n^{r} in the rotated tetrad $\mathbf{k}_{\mathrm{r}}$, $\mathbf{l}_{\mathrm{r}}$, $\mathbf{m}_{\mathrm{r}}$, $\overline{\mathbf{m}}_{\mathrm{r}}$. These can easily be obtained from Eq. (4.22) using relations (D4), (D7), and (D11) with the parameters (4.25). Notice that all these components are of the same order in η, namely, $\sim\eta^{-3}$ [cf. also Eq. (5.17) below]. To obtain the components Ψ_n^{i} in the parallelly transported tetrad we perform an additional boost (5.12) in the $\mathbf{k}_{\mathrm{r}}$-$\mathbf{l}_{\mathrm{r}}$ plane with the boost parameter given by

$$B = \frac{\sqrt{2}a_\Lambda}{\gamma\eta}. \tag{5.14}$$

Using relations (D11) we immediately observe that it rescales Ψ_n^{i} by different powers of η, namely,

$$\Psi_n^{\mathrm{i}} \sim \frac{1}{\eta^{5-n}}, \quad n = 0,1,2,3,4. \tag{5.15}$$

The field thus clearly exhibits the *peeling behavior*. The leading term of the gravitational field representing radiation near infinity $\mathcal{I}^+$ is $\Psi_4^{\mathrm{i}} \sim 1/\eta$. Explicitly, this term asymptotically takes the form

$$\Psi_4^{\mathrm{i}} \approx \frac{1}{16a_\Lambda^2\cos^2\theta_{\mathrm{s}}}(\mathcal{F}'' + \mathcal{G}'') \times(\sin\theta + \sin\theta_{\mathrm{s}}\cos\phi - i\sin\theta_{\mathrm{s}}\cos\theta\sin\phi)^2. \tag{5.16}$$

Here we should note that [see Eq. (4.10)]

$$\frac{1}{12}(\mathcal{F}'' + \mathcal{G}'') \approx -(m - 2e^2A\xi_+)\frac{1}{\gamma\eta}. \tag{5.17}$$

The phase of the component Ψ_4^{i} depends on the choice of the vector $\overline{\mathbf{m}}_{\mathrm{i}}$ [see Eq. (4.5)]. Because the vector $\overline{\mathbf{m}}_{\mathrm{i}}$ was chosen arbitrarily, only the modulus $|\Psi_4^{\mathrm{i}}|$ can have a physical meaning. Using the peeling behavior (5.15) we can even justify that the magnitude $|\Psi_4^{\mathrm{i}}|$ does not depend on any change of the null vectors $\mathbf{l}_{\mathrm{i}}$, $\mathbf{m}_{\mathrm{i}}$, $\overline{\mathbf{m}}_{\mathrm{i}}$ at infinity. Indeed, we may perform an arbitrary *finite* Lorentz transformation which leaves the vector $\mathbf{k}_{\mathrm{i}}$ fixed. Such a transformation can be generated by a combination of the discussed spatial rotation in the $\mathbf{m}_{\mathrm{i}}$-$\overline{\mathbf{m}}_{\mathrm{i}}$ plane (D9) which change only a phase of Ψ_4^{i}, and of a null rotation (D3). Under this transformation, the component Ψ_4^{i} transforms according to Eq. (D4) as

$$\Psi_4^{\mathrm{i}'} = \Psi_4^{\mathrm{i}} + 4\overline{L}\Psi_3^{\mathrm{i}} + 6\overline{L}^2\Psi_2^{\mathrm{i}} + 4\overline{L}^3\Psi_1^{\mathrm{i}} + \overline{L}^4\Psi_0^{\mathrm{i}}. \tag{5.18}$$

Since L is finite and the components $\Psi_n^{\mathrm{i}} \sim \eta^{n-5}$, $n = 0, 1, 2, 3$ are of the higher order in $1/\eta$ than $\Psi_4^{\mathrm{i}} \sim \eta^{-1}$, they do not change the leading term of the field, i.e., Ψ_4^{i} remains invariant. (Let us note that the same is obviously not true for leading terms of other components of the Weyl tensor.)

The invariant physical quantity $|\Psi_4^{\mathrm{i}}|$ is thus

$$|\Psi_4^{\mathrm{i}}| \approx \frac{3}{4}\frac{(m - 2e^2A\xi_+)}{\gamma a_\Lambda^2\cos^2\theta_{\mathrm{s}}}\frac{1}{\eta} \times[(\sin\theta + \sin\theta_{\mathrm{s}}\cos\phi)^2 + \sin^2\theta_{\mathrm{s}}\cos^2\theta\sin^2\phi], \tag{5.19}$$

where the angle θ_{s} identifying the principal null directions at infinity is, thanks to Eqs. (4.18), (2.6), (2.13) and $\mathcal{E}_+ = -1$, given by

$$\sin\theta_{\mathrm{s}} = \sqrt{\frac{\mathcal{G}_+a_\Lambda^2A^2}{1 + \mathcal{G}_+a_\Lambda^2A^2}}, \quad \frac{1}{\cos^2\theta_{\mathrm{s}}} = 1 + \mathcal{G}_+a_\Lambda^2A^2. \tag{5.20}$$

Note that the term $(m - 2e^2A\xi_+)$ in Eq. (5.19) is positive, which follows (although not immediately, see Appendix B) from the conditions (2.5).

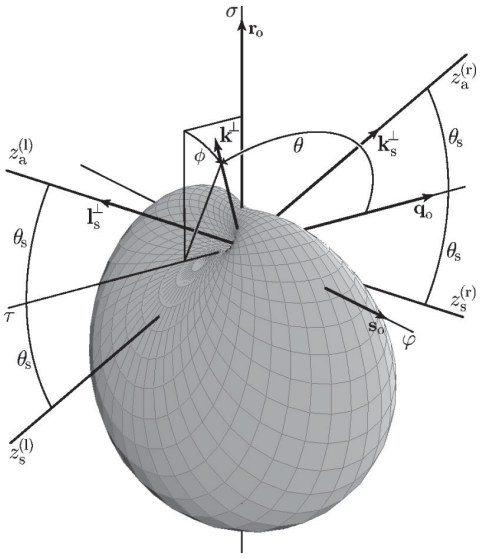

FIG. 6. The magnitude of the leading terms of gravitational and electromagnetic fields, given by Eqs. (5.19) and (5.23), as a function of a direction from which the point N_+ at infinity is approached—the *directional pattern of radiation*. The directions from the origin N_+ of the diagram correspond to spatial directions in spacelike conformal infinity $\mathcal{I}^+$. The magnitude of the fields measured along a null geodesic with a tangent vector $\mathbf{k}$ is drawn in the spatial direction $-\mathbf{k}^\perp$ *from* which the geodesic arrives (i.e., the geodesic points into the spatial direction $\mathbf{k}^\perp$). The angles θ, ϕ parametrizing the spatial direction $\mathbf{k}^\perp$ are measured from the axis $\mathbf{q}_o$ and around the axis $\mathbf{q}_o$ starting from the $\mathbf{r}_o$-$\mathbf{q}_o$ plane, respectively. The special geodesics in principal null directions $\mathbf{k}_s$ and $\mathbf{l}_s$, i.e., the null geodesics coming from the ''left'' black hole and the ''right'' black hole (pointing ''from the sources''), are denoted by $z_s^{(1)}$ and $z_s^{(r)}$. They approach the point N_+ at infinity along the spatial directions $\mathbf{k}_s^\perp$ and $\mathbf{l}_s^\perp$. On the other hand, $z_a^{(r)}$ and $z_a^{(l)}$ are ''antipodal'' null geodesics approaching the infinity along the spatial directions $-\mathbf{k}_s^\perp$, $-\mathbf{l}_s^\perp$, opposite to that of $z_s^{(l)}$ and $z_s^{(r)}$, respectively. The leading radiative term of the fields completely vanishes along these antipodal geodesics.

Analogously, we obtain the components Φ_n^{i} of the electromagnetic field in the parallelly transported null tetrad in the form

$$\Phi_n^{\mathrm{i}} \sim \frac{1}{\eta^{3-n}}, \quad n=0,1,2, \tag{5.21}$$

which also exhibits the peeling behavior. The leading term of the radiative component Φ_2^{i} is asymptotically

$$\Phi_2^{\mathrm{i}} \approx \frac{1}{2\sqrt{2}} \frac{e}{\gamma a_\Lambda \cos\theta_s} \frac{1}{\eta} \times (\sin\theta + \sin\theta_s \cos\phi - i \sin\theta_s \cos\theta \sin\phi). \tag{5.22}$$

Similarly to the Ψ_4^{i} component, only the modulus of this expression is independent of a choice of the interpretation tetrad. Moreover, the square of modulus now has a clear physical meaning—it is exactly the leading term of the magnitude of the Poynting vector $\mathbf{S}_{\mathrm{i}}$ in the parallelly transported frame defined with respect to the timelike vector $\mathbf{n}_{\mathrm{i}}$. Thus, we obtain

$$4\pi|\mathbf{S}_{\mathrm{i}}| \approx |\Phi_2^{\mathrm{i}}|^2 \approx \frac{1}{8} \frac{e^2}{\gamma^2 a_\Lambda^2 \cos^2\theta_s} \frac{1}{\eta^2} \times [(\sin\theta + \sin\theta_s \cos\phi)^2 + \sin^2\theta_s \cos^2\theta \sin^2\phi]. \tag{5.23}$$

The direction of the Poynting vector $\mathbf{S}_{\mathrm{i}}$ is asymptotically given by the vector $\mathbf{q}_{\mathrm{i}}$. Interestingly, the dependence of $|\Psi_4^{\mathrm{i}}|$ and $|\Phi_2^{\mathrm{i}}|^2$ on the direction along which a point N_+ at infinity $\mathcal{I}^+$ is approached (i.e., the dependence on angles θ and ϕ) is *exactly the same*, namely,

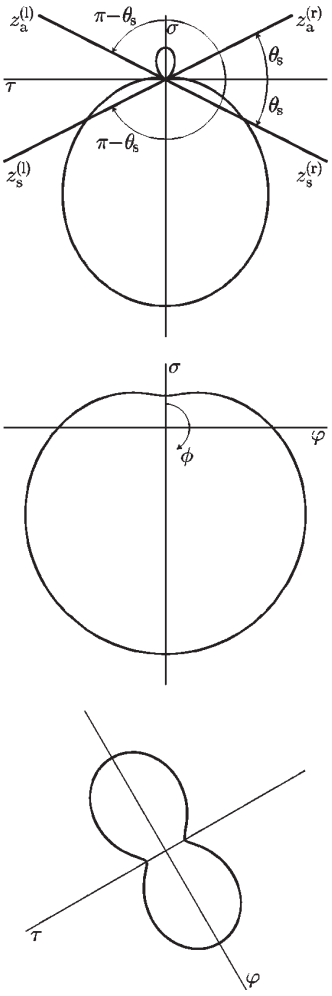

FIG. 7. The particular sections τ-σ, σ-φ, and τ-φ of the directional pattern of radiation shown in Fig. 6. The *oriented* angles θ of the spatial directions of the geodesics from sources ($\theta=\theta_s$ and $\theta=\pi-\theta_s$, $\phi=0$) and of the antipodal geodesics ($\theta=\theta_s$ and $\theta=\pi-\theta_s$, $\phi=\pi$) are indicated.

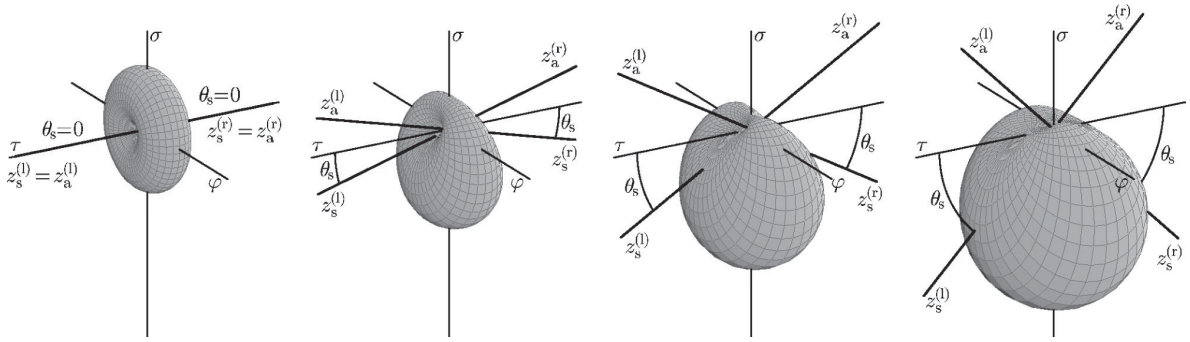

FIG. 8. The directional pattern of radiation from Fig. 6 for different values of the angular parameter θ_s. Because the directional dependence (5.24) of the gravitational and electromagnetic radiation depends only on this single parameter θ_s given by Eq. (4.18), both changes of a position N_+ at infinity $\mathcal{I}^+$ and changes of the physical parameters *m*, *e*, *A*, and Λ manifest only through a change of the angle θ_s. The diagrams with different values of θ_s can thus be interpreted either as the directional patterns at different points of infinity $\mathcal{I}^+$, or as the directional characteristics at "the same" point (with fixed values of the metric functions $\mathcal{F}$ and $\mathcal{G}$), but in spacetimes with, for example, different acceleration of the black holes.

$$\mathcal{A}(\theta,\phi)=(\sin\theta+\sin\theta_s\cos\phi)^2+\sin^2\theta_s\cos^2\theta\sin^2\phi. \tag{5.24}$$

The angular dependence (5.24) for a fixed value of θ_s which characterize the *directional pattern of radiation* at a given point of $\mathcal{I}^+$ is shown in Figs. 6 and 7, and for various θ_s in Fig. 8.

Let us now discuss the main results (5.19) and (5.23). These expressions can be understood as a more detailed characterization of radiative fields near the spacelike conformal infinity, supplementing thus the peeling behavior (5.15), (5.21). It follows from Eqs. (5.19), (5.22) that the dominant components of both fields decay asymptotically near $\mathcal{I}^+$, corresponding to $r=\infty$, as $(\gamma\eta)^{-1}=r^{-1}$. The electromagnetic field is proportional to the charge parameter *e* whereas the gravitational field is proportional to the mass parameter *m* modified, interestingly, by the term $-2e^2A\xi_+$ which is a combination of electric charge and acceleration parameters, and the constant ξ_+ denoting a specific point at infinity $\mathcal{I}^+$. Both the gravitational field $|\Psi_4^{\rm i}|$ and the electromagnetic Poynting vector $4\pi\,|\mathbf{S}_{\rm i}|\approx|\Phi_2^{\rm i}|^2$ are proportional to $a_\Lambda^{-2}=\frac{1}{3}\Lambda$ [but they also depend implicitly on Λ through the parameter θ_s, see Eq. (5.20)]. The radiation at $\mathcal{I}^+$ thus increases with a growing value of the cosmological constant Λ.

The angular dependence of the magnitude of radiation $\mathcal{A}(\theta,\phi)$ is presented in Figs. 6 and 8. Their grid is given by the coordinate lines $\theta=$const and $\phi=$const, respectively. It is straightforward to investigate the behavior of the function $\mathcal{A}(\theta,\phi)$ for a fixed θ. The minimal value is $\mathcal{A}(\theta,\pi)=(\sin\theta-\sin\theta_s)^2$, and the maximum is $\mathcal{A}(\theta,0)=(\sin\theta+\sin\theta_s)^2$. The *global maximum* $\mathcal{A}=(1+\sin\theta)^2$ occurs for $\theta=\pi/2$, $\phi=0$. The greatest magnitude of radiation thus arrives at infinity from the direction of $\mathbf{r}_o$. On the other hand, the minimal value $\mathcal{A}=0$ is obtained for $\theta=\theta_s$, $\phi=\pi$ and $\theta=\pi-\theta_s$, $\phi=\pi$. These are exactly the spatial directions $-\mathbf{l}_s^\perp$, $-\mathbf{k}_s^\perp$ of *antipodal null geodesics* $z_a^{(l)}$ and $z_a^{(r)}$, along which the radiation completely vanishes. The value of $\mathcal{A}$ along the geodesics $z_s^{(l)}$ and $z_s^{(r)}$ coming from the black holes in the directions $\mathbf{k}_s^\perp$ $(\theta=\theta_s,\phi=0)$ and $\mathbf{l}_s^\perp$ $(\theta=\pi-\theta_s,\phi=0)$ is $\mathcal{A}=4\sin^2\theta_s$. The value along the direction $\mathbf{q}_o$ (corresponding to $\theta=0$) is $\mathcal{A}=\sin^2\theta_s$, and along $\mathbf{s}_o$ $(\theta=\pi/2,\phi=\pi/2)$ is $\mathcal{A}=1$.

Finally, it is interesting to observe that for a vanishing acceleration of the black holes, i.e., for $A=0$ which implies $\theta_s=0$, we obtain

$$|\Psi_4^{\rm i}|\approx\frac{3}{4}\frac{m}{\gamma a_\Lambda^2}\frac{1}{\eta}\sin^2\theta,$$
$$|\Phi_2^{\rm i}|\approx\frac{1}{2\sqrt{2}}\frac{e}{\gamma a_\Lambda}\frac{1}{\eta}\sin\theta. \tag{5.25}$$

The angular dependence $\mathcal{A}=\sin^2\theta$ is now independent of ϕ so that the directional pattern is axially symmetric (see the diagram on the very left of Fig. 8). Moreover, the gravitational and electromagnetic fields decay as $1/\eta$ even in this case of *nonaccelerated* black holes if the fields are measured along a nonradial null geodesic $(\theta\neq0,\pi)$. A generic observer thus detects radiation. This effect is intuitively caused by observer's asymptotic motion relative to the "static" black holes. Only for special observers moving along null geodesics radially from the black holes $(\theta=0,\pi)$ the radiation vanishes as one would expect for "static" sources.

Interestingly, the angular dependence $\mathcal{A}(\theta,\phi)$ is exactly the same as that obtained in Ref. [22] for test electromagnetic field of two accelerated charges in de Sitter space (see [48]).

VI. THE RADIATION IN THE ROBINSON-TRAUTMAN FRAMEWORK

In this part we rederive the above results using the framework naturally adapted to the Robinson-Trautman coordinate system (2.14). This will not only provide us with an independent way of deriving the characteristic directional pattern of radiation generated by accelerated charged black holes in the asymptotically de Sitter universe, but opens a possibility to investigate even more general exact radiative solutions from

the large and important Robinson-Trautman family.

We start again with investigation of *asymptotic null geodesics* approaching infinity $\mathcal{I}^+$, i.e., those for which $r\to\infty$. Assuming a natural expansion of these geodesics in powers of $1/r$ (rather than in the affine parameter $1/\eta$ as was done in the previous section),

$$\begin{aligned} \zeta &\approx \zeta_+ + \frac{c}{r} + \cdots, \\ u &\approx u_+ + \frac{d}{r} + \cdots, \\ r(\eta) &\to \infty \quad \text{as} \quad \eta\to\infty, \end{aligned} \tag{6.1}$$

where ζ_+, u_+, c, d are constants, the derivatives with respect to the affine parameter η are

$$\begin{aligned} \dot\zeta &\approx -\frac{\dot r}{r^2}c + \cdots, \\ \ddot\zeta &\approx -\frac{\ddot r}{r^2}(c+\cdots) + \frac{\dot r^2}{r^3}(2c+\cdots). \end{aligned} \tag{6.2}$$

The expressions for $\dot u$, $\ddot u$ are obtained from Eq. (6.2) by replacing c with d. Similarly, we may expand the metric functions and other quantities. Using Eqs. (6.1) and (6.2) and the Christoffel symbols (A32), the geodesic equations in the highest order read

$$c\frac{\ddot r}{r}=0, \quad d\frac{\ddot r}{r}=\mathcal{N}\frac{\dot r^2}{r^2}, \quad a_\Lambda^2\frac{\ddot r}{r}=-\mathcal{N}\frac{\dot r^2}{r^2}, \tag{6.3}$$

where

$$\mathcal{N}=2P_+^{-2}c\bar c+2d+a_\Lambda^{-2}d^2, \tag{6.4}$$

P_+ being the asymptotic value of P at the point N_+ at infinity. However, a normalization of the tangent vector for *null* geodesics requires

$$\mathcal{N}=0. \tag{6.5}$$

Consequently, the asymptotic form of the null geodesics approaching $\mathcal{I}^+$ is

$$\begin{aligned} &r\approx\gamma\eta, \quad \zeta\approx\zeta_+ + \frac{c}{r}, \quad u\approx u_+ + \frac{d}{r}, \\ &\frac{Dz}{d\eta}=\gamma\left(\boldsymbol\partial_r - \frac{c}{r^2}\boldsymbol\partial_\zeta - \frac{\bar c}{r^2}\boldsymbol\partial_{\bar\zeta} - \frac{d}{r^2}\boldsymbol\partial_u\right), \end{aligned} \tag{6.6}$$

where the constant γ can be identified with that introduced in Eq. (5.5), ζ_+, u_+ specify the *point* N_+ on $\mathcal{I}^+$ towards which the particular geodesic is approaching, and c, d are parameters representing the *direction* along which N_+ is reached. In fact, this direction is basically parameterized just by the complex constant c since, using relations (6.5), (6.4), d is then given as $d=-a_\Lambda^2(1\pm\sqrt{1-2a_\Lambda^{-2}P_+^{-2}c\bar c})$. For a particular c, there are thus only two real values of d which represent two possible different *orientations* with which the null geodesics may approach $\mathcal{I}^+$ in the given spatial direction. In particular, for the special choice $c=0$ we obtain $d=0$ and $d=-2a_\Lambda^2$. The first corresponds exactly to the privileged principal null direction along $\mathbf{k}_{\rm s}$ "from the source" (i.e., the null geodesic $z_{\rm s}^{(l)}$ along the spatial direction $\mathbf{k}_{\rm s}^\perp$), the second to an opposite orientation of this direction "away from the source" (the "antipodal" null geodesic $z_{\rm a}^{(r)}$ along $-\mathbf{k}_{\rm s}^\perp$), see Fig. 6.

In order to find the behavior of radiation near $\mathcal{I}^+$ we again have to set up the interpretation tetrad transported parallelly along a general asymptotic null geodesic, and project the Weyl tensor and the tensor of electromagnetic field onto this tetrad. We start with the Robinson-Trautman null tetrad (4.26), naturally adapted to the Robinson-Trautman coordinate system (2.14). We have seen in Sec. IV that the vector $\mathbf{k}_{\rm RT}$ is oriented along one of the principal null direction, namely, $\mathbf{k}_{\rm s}$, and (as we will see in Sec. VII) the tetrad (4.26) is parallelly transported along the algebraically special geodesics. In this standard tetrad the only nontrivial components $\Psi_n^{\rm RT}$ and $\Phi_n^{\rm RT}$, which represent the gravitational and electromagnetic field, are given by Eqs. (4.30) and (4.31). Let us now perform two subsequent null rotations and a boost of this Robinson-Trautman null tetrad (4.26). We first apply Eq. (D6), then (D3), and finally (D9) with the parameters

$$\begin{aligned} K &= -\frac{c}{\left(1+\frac12 a_\Lambda^{-2}d\right)Pr}, \\ L &= \frac{cr}{2a_\Lambda^2 P}, \\ B &= 1+\tfrac12 a_\Lambda^{-2}d, \quad \Phi=0. \end{aligned} \tag{6.7}$$

The resulting null tetrad, using relation (6.5), then takes the following asymptotic form as $r\to\infty$:

$$\begin{aligned} \mathbf{k}_{\rm i} &\approx \left(\boldsymbol\partial_r - \frac{c}{r^2}\boldsymbol\partial_\zeta - \frac{\bar c}{r^2}\boldsymbol\partial_{\bar\zeta} - \frac{d}{r^2}\boldsymbol\partial_u\right), \\ \mathbf{l}_{\rm i} &\approx \frac{r^2}{2a_\Lambda^2}\left(\boldsymbol\partial_r + \frac{c}{r^2}\boldsymbol\partial_\zeta + \frac{\bar c}{r^2}\boldsymbol\partial_{\bar\zeta} + \frac{d+2a_\Lambda^2}{r^2}\boldsymbol\partial_u\right), \\ \mathbf{m}_{\rm i} &\approx \frac{P}{r}\left(\frac{cd}{2a_\Lambda^2\bar c}\boldsymbol\partial_\zeta + \left(1+\frac12 a_\Lambda^{-2}d\right)\boldsymbol\partial_{\bar\zeta} - \frac{c}{P^2}\boldsymbol\partial_u\right), \\ \bar{\mathbf{m}}_{\rm i} &\approx \frac{P}{r}\left(\left(1+\frac12 a_\Lambda^{-2}d\right)\boldsymbol\partial_\zeta + \frac{\bar c d}{2a_\Lambda^2 c}\boldsymbol\partial_{\bar\zeta} - \frac{\bar c}{P^2}\boldsymbol\partial_u\right). \end{aligned} \tag{6.8}$$

Obviously, the above vector $\mathbf{k}_{\rm i}$ is tangent to a general asymptotic null geodesics (6.6). Moreover, the tetrad is chosen in such a way that the timelike unit vector orthogonal to $\mathcal{I}^+$

$$\mathbf{n}_{\rm o}=\frac{1}{\sqrt{-H}}(-H\boldsymbol\partial_r+\boldsymbol\partial_u)\approx\frac{r}{a_\Lambda}\boldsymbol\partial_r+\frac{a_\Lambda}{r}\boldsymbol\partial_u, \tag{6.9}$$

introduced in Eq. (4.13), belongs to the plane spanned by the two null vectors $\mathbf{k}_{\rm i}$ and $\mathbf{l}_{\rm i}$. Indeed,

$$\mathbf{n}_{\rm o}\approx\frac{1}{\sqrt{2}}\left(\frac{r}{\sqrt{2}a_\Lambda}\mathbf{k}_{\rm i}+\frac{\sqrt{2}a_\Lambda}{r}\mathbf{l}_{\rm i}\right). \tag{6.10}$$

Note that this choice corresponds to a boost Eq. (D9) which becomes unbounded as $r\to\infty$.

As discussed in the previous section, in order to *compare* the radiation for all null geodesics approaching the given point at de Sitter–like infinity $\mathcal{I}^+$, it is necessary to introduce a unique and universal normalization of the affine parameter η and of the vector $\mathbf{k}_{\rm i}$. We concluded that a natural and also the most convenient choice is to keep the parameter γ fixed [see discussion near Eq. (5.6)] and to require Eq. (5.9). These conditions are obviously satisfied by Eq. (6.8), cf. Eq. (6.6). Therefore, the tetrad (6.8) is exactly the interpretation tetrad suitable for analysis of behavior of fields on $\mathcal{I}^+$.

Now we perform a projection of the above null tetrad onto the spacelike infinity $\mathcal{I}^+$. These projections $\mathbf{k}_{\rm i}^\perp$, $\mathbf{l}_{\rm i}^\perp$, $\mathbf{m}_{\rm i}^\perp$ [cf. Eq. (4.16)] are

$$\begin{aligned}\mathbf{k}_{\rm i}^\perp&\approx-\frac{1}{r^2}[c\boldsymbol{\partial}_\zeta+\overline{c}\overline{\boldsymbol{\partial}_\zeta}+(d+a_\Lambda^2)\boldsymbol{\partial}_u],\\ \mathbf{l}_{\rm i}^\perp&\approx-\frac{r^2}{2a_\Lambda^2}\mathbf{k}_{\rm i}^\perp,\quad \mathbf{m}_{\rm i}^\perp=\mathbf{m}_{\rm i},\quad \overline{\mathbf{m}}_{\rm i}^\perp=\overline{\mathbf{m}}_{\rm i}.\end{aligned} \tag{6.11}$$

The radiation approaching $\mathcal{I}^+$ along the null vector $\mathbf{k}_{\rm i}$ propagates in the spatial direction $\mathbf{k}_{\rm i}^\perp\propto\mathbf{q}_{\rm r}$. Imposing the normalization condition $\mathbf{q}_{\rm r}\cdot\mathbf{q}_{\rm r}=1$, the unit vector of the radiation direction thus takes the form

$$\mathbf{q}_{\rm r}\approx-\frac{1}{a_\Lambda r}[c\boldsymbol{\partial}_\zeta+\overline{c}\overline{\boldsymbol{\partial}_\zeta}+(d+a_\Lambda^2)\boldsymbol{\partial}_u]. \tag{6.12}$$

Of course, this vector is identical to the vector $\mathbf{q}_{\rm r}$ introduced previously in Eq. (4.24). Using Eqs. (C2f)–(C2h), (4.13), and (4.18) we obtain

$$\begin{aligned}\boldsymbol{\partial}_\zeta&=\frac{1}{\sqrt{2}}\frac{r}{P}(-\sin\theta_{\rm s}\mathbf{q}_{\rm o}+\cos\theta_{\rm s}\mathbf{r}_{\rm o}+i\mathbf{s}_{\rm o}),\\ \boldsymbol{\partial}_u&=-\sqrt{-H}(\cos\theta_{\rm s}\mathbf{q}_{\rm o}+\sin\theta_{\rm s}\mathbf{r}_{\rm o}),\\ \boldsymbol{\partial}_r&=\frac{1}{\sqrt{-H}}(\mathbf{n}_{\rm o}+\cos\theta_{\rm s}\mathbf{q}_{\rm o}+\sin\theta_{\rm s}\mathbf{r}_{\rm o}).\end{aligned} \tag{6.13}$$

Substituting this into Eq. (6.12), using $\mathcal{E}_+=-1$, and comparing with the expression (4.24), we obtain the following relation between the Robinson-Trautman parameters c, d and the angles θ, ϕ

$$\begin{aligned}\frac{c+\overline{c}}{\sqrt{2}a_\Lambda P_+}&=\sin\theta_{\rm s}\cos\theta-\cos\theta_{\rm s}\sin\theta\cos\phi,\\ i\frac{c-\overline{c}}{\sqrt{2}a_\Lambda P_+}&=-\sin\theta\sin\phi,\\ 1+a_\Lambda^{-2}d&=\cos\theta_{\rm s}\cos\theta+\sin\theta_{\rm s}\sin\theta\cos\phi.\end{aligned} \tag{6.14}$$

Of course, this parametrization identically satisfies the normalization condition (6.5). Moreover, it can now be demonstrated that the above null tetrad (6.8) is in fact identical to the parallelly transported tetrad (5.12), except for the transverse vector $\mathbf{m}_{\rm i}$, which was previously defined as $\mathbf{m}_{\rm i}\approx\mathbf{m}_{\rm r}$, $\mathbf{m}_{\rm r}$ given by Eq. (C5) [cf. Eqs. (4.24), (4.1)]. Such a vector is related to the vector $\mathbf{m}_{\rm i}$ adapted to the Robinson-Trautman framework (6.8) by the spatial rotation (D9), $\mathbf{m}_{\rm i}=\exp(-i\phi_{\rm i})\mathbf{m}_{\rm r}$, where the rotation angle $\phi_{\rm i}$ is given by

$$\begin{aligned}\sin\phi_{\rm i}&=\frac{(\cos\theta_{\rm s}+\cos\theta)\sin\phi}{1+\cos\theta_{\rm s}\cos\theta+\sin\theta_{\rm s}\sin\theta\cos\phi},\\ \cos\phi_{\rm i}&=\frac{\sin\theta_{\rm s}\sin\theta+(1+\cos\theta_{\rm s}\cos\theta)\cos\phi}{1+\cos\theta_{\rm s}\cos\theta+\sin\theta_{\rm s}\sin\theta\cos\phi},\\ \exp(i\phi_{\rm i})&=\frac{\exp(i\phi)\cos\frac{\theta_{\rm s}}{2}\cos\frac{\theta}{2}+\sin\frac{\theta_{\rm s}}{2}\sin\frac{\theta}{2}}{\cos\frac{\theta_{\rm s}}{2}\cos\frac{\theta}{2}+\exp(i\phi)\sin\frac{\theta_{\rm s}}{2}\sin\frac{\theta}{2}}.\end{aligned} \tag{6.15}$$

Finally, we calculate the leading components of the gravitational and electromagnetic fields in the interpretation frame (6.8) asymptotically close to infinity $\mathcal{I}^+$. As we have said, the Lorentz transformation from the tetrad (4.26) to the tetrad (6.8) is given by two subsequent null rotations and the boost with the parameters given by Eq. (6.7). Starting with the components (4.30) in the standard Robinson-Trautman frame, using Eqs. (D7), (D4), (D11) and (D8), (D5), (D12), we obtain after somewhat lengthy calculation

$$\begin{aligned}\Psi_4^{\rm i}&\approx-\frac{3A^2(m-2e^2A\xi_+)}{rP_+^2}\left(1-\frac{1}{\sqrt{2}a_\Lambda^2A}\overline{c}+\frac{1}{2a_\Lambda^2}d\right)^2,\\ \Phi_2^{\rm i}&\approx\frac{eA}{\sqrt{2}rP_+}\left(1-\frac{1}{\sqrt{2}a_\Lambda^2A}\overline{c}+\frac{1}{2a_\Lambda^2}d\right).\end{aligned} \tag{6.16}$$

Substituting from Eq. (6.14) for the parameters c and d, and using Eqs. (5.20) and (2.15) we get

$$\begin{aligned}\Psi_4^{\rm i}&\approx-\frac{3}{4}\frac{(m-2e^2A\xi_+)}{a_\Lambda^2r\cos^2\theta_{\rm s}}\\ &\quad\times(\sin\theta_{\rm s}+\sin\theta\cos\phi+i\cos\theta_{\rm s}\sin\theta\sin\phi)^2,\\ \Phi_2^{\rm i}&\approx\frac{1}{2\sqrt{2}}\frac{e}{a_\Lambda r\cos\theta_{\rm s}}\\ &\quad\times(\sin\theta_{\rm s}+\sin\theta\cos\phi+i\cos\theta_{\rm s}\sin\theta\sin\phi).\end{aligned} \tag{6.17}$$

We should have recovered the previous results (5.16) and (5.22). Comparing them we find that the expressions differ in the angular part. However, this is a consequence of the difference of interpretation tetrads used in the previous and in this sections. The results are, in fact, identical after performing a spatial rotation (D9) with the angular parameter $\phi_{\rm i}$ given by Eq. (6.15). This changes the phase of the components according to Eqs. (D11), (D12), and we obtain $\Psi^{\rm i}_4 = \exp(2i\phi_{\rm i})\Psi^{\rm i}_4$, $\Phi^{\rm i}_2 = \exp(i\phi_{\rm i})\Phi^{\rm i}_2$, where the left hand side is given by Eq. (6.17), and the right-hand side by Eqs. (5.16), (5.22). Both results are thus equivalent.

The tetrads (5.12) and (6.8) have been introduced in a way natural to each specific approach. The fact that they differ in definitions of the vector $\mathbf{m}_{\rm i}$ documents what we have already discussed above: there is no canonical way how to choose the interpretation tetrad. It also means that the *phase* of the results (5.16), (5.22), or (6.17) is not physical. Invariant information, independent of a choice of the interpretation tetrad, is contained in the *modulus* of the tetrad components of the fields. Obviously, the magnitudes of the field components (6.17) are the same as the results (5.19) and (5.23) derived previously.

VII. RADIATION ALONG THE ALGEBRAICALLY SPECIAL NULL DIRECTIONS

In the final section we concentrate on a family of special geodesics $z^{(l)}_{\rm s}$ approaching infinity $\mathcal{I}^+$ along principal null direction $\mathbf{k}_{\rm s}$, and investigate the fields with respect to the corresponding interpretation tetrad. Using Eqs. (A32) it is straightforward to observe that the coordinate lines

$$u = u_+ = \text{const}, \quad \zeta = \zeta_+ = \text{const} \tag{7.1}$$

(i.e., also $\xi = \text{const}$, $\varphi = \text{const}$) are null geodesics, r is their affine parameter, and the tangent vector is $\mathbf{k}_{\rm RT} = \boldsymbol{\partial}_r$. [For simplicity, in this section we use the affine parameter r, a general affine parameter η can be introduced by a trivial rescaling $r = \gamma\eta$, cf. Eq. (5.5).] The geodesics $z^{(l)}_{\rm s}(r)$ emanate ''radially'' from the ''left'' black hole up to the infinity (similarly we could investigate analogous geodesics $z^{(r)}_{\rm s}$ along $\mathbf{l}_{\rm s}$ from the ''right'' black hole). As we have seen in Sec. IV [cf. Eq. (4.27) and the subsequent discussion], the tangent vector $\mathbf{k}_{\rm RT}$ is oriented along the principal null direction $\mathbf{k}_{\rm s}$. These geodesics thus approach the infinity from the specific spatial direction characterized by the angles

$$\theta = \theta_{\rm s}, \quad \phi = 0 \tag{7.2}$$

or by the parameters $c = 0$, $d = 0$ [see Eq. (6.14)].

Moreover, in such a case we can identify explicitly the parallelly transported interpretation tetrad—it can easily be shown using Eqs. (A32) that the Robinson-Trautman tetrad (4.26) is parallelly transported along $z^{(l)}_{\rm s}(r)$, i.e.,

$$\mathbf{k}_{\rm RT}\cdot\nabla\mathbf{k}_{\rm RT} = 0, \quad \mathbf{k}_{\rm RT}\cdot\nabla\mathbf{l}_{\rm RT} = 0, \quad \mathbf{k}_{\rm RT}\cdot\nabla\mathbf{m}_{\rm RT} = 0. \tag{7.3}$$

We can thus set the interpretation tetrad

$$(\mathbf{k}_{\rm i}, \mathbf{l}_{\rm i}, \mathbf{m}_{\rm i}, \overline{\mathbf{m}}_{\rm i}) \equiv (\mathbf{k}_{\rm RT}, \mathbf{l}_{\rm RT}, \mathbf{m}_{\rm RT}, \overline{\mathbf{m}}_{\rm RT}) \tag{7.4}$$

in the *whole* spacetime, not only asymptotically near $\mathcal{I}^+$, as in Eq. (6.8) for $c = 0$, $d = 0$. As follows from Eqs. (4.30) and (4.31), all components of gravitational and electromagnetic fields are explicitly

$$\begin{aligned}
\Psi^{\rm i}_4 &= -3\left(m - 2e^2A\xi - \frac{e^2}{r}\right)A^2\mathcal{G}\frac{1}{r},\\
\Psi^{\rm i}_3 &= \frac{3}{\sqrt{2}}\left(m - 2e^2A\xi - \frac{e^2}{r}\right)A\sqrt{\mathcal{G}}\frac{1}{r^2},\\
\Psi^{\rm i}_2 &= -\left(m - 2e^2A\xi - \frac{e^2}{r}\right)\frac{1}{r^3}, \quad \Psi^{\rm i}_1 = \Psi^{\rm i}_0 = 0,
\end{aligned} \tag{7.5}$$

and

$$\Phi^{\rm i}_2 = \frac{eA\sqrt{\mathcal{G}}}{\sqrt{2}}\frac{1}{r}, \quad \Phi^{\rm i}_1 = -\frac{e}{2}\frac{1}{r^2}, \quad \Phi^{\rm i}_0 = 0. \tag{7.6}$$

Clearly, the leading terms in the $1/r$ expansion give the previous general asymptotical results (5.19) and (5.23) with θ, ϕ specified by Eq. (7.2), and $r = \gamma\eta$. In the case of de Sitter spacetime ($m = 0, e = 0$) the field components identically vanish, in the general case the fields have a radiative character ($\sim 1/r$) except for a vanishing acceleration A and/or for $\mathcal{G}_+ = 0$. The ''static'' case $A = 0$ has been already discussed after Eq. (5.25). The case $\mathcal{G}_+ = 0$ corresponds to observers located at the privileged position—on the axes $\xi = \xi_1$ and $\xi = \xi_2$. This is analogous to the well-known situation of an electromagnetic field of accelerated test charges in flat spacetime which is also not radiative along the axis of symmetry.

Let us note that in this case the affine parameter r coincides, in fact, both with the *luminosity distance* and the *parallax distance* for the congurence of the above null geodesics—as for any Robinson-Trautman spacetime described by the metric (2.14). Indeed, the luminosity distance $r_{\rm L}$ is related to the affine parameter r by the relation [3]

$$\frac{dr_{\rm L}}{dr} = \frac{1}{2}r_{\rm L}\nabla\cdot\mathbf{k}_{\rm RT}. \tag{7.7}$$

Thanks to Eqs. (A32) one obtains $(1/2)\nabla\cdot\mathbf{k}_{\rm RT} = 1/r$, and thus $r_{\rm L} = r$. This means that the radiative $1/r$ fall-off of the fields is naturally measurable (even locally) by observers moving radially to infinity, using both the parallax and the luminosity methods for determining the distance.

In the previous sections, when we studied the radiation along general geodesics, we have been able to fix the interpretation tetrad only asymptotically, by specifying appropriate final conditions at infinity [see Eqs. (5.8), (5.12) and the discussion nearby]. For the special family of geodesics (7.1) discussed here we can specify the interpretation tetrad by setting the initial conditions anywhere in the *finite* region inside the spacetime. Because any point at infinity $\mathcal{I}^+$ is only reached by one algebraically special geodesic $z^{(1)}_{\rm s}$ from the ''left'' black hole, this does not allow us to study the *directional* pattern of radiation with respect to the interpretation tetrad fixed by these explicit initial conditions. However, we

can study the standard *positional* pattern of radiation along these special geodesics—the dependence of radiation on the position of asymptotic point N_+ in the infinity.

The initial conditions for interpretation tetrad inside a finite region of the spacetime can be chosen in many different ways, e.g., using some natural tetrad on a spacelike hypersurface (''initial instant of time,'' cf. [49]), on a ''surface of sources,'' on a special null hypersurface, etc. Obviously, geometrically privileged locations where we can specify such initial conditions are *horizons*, in particular the cosmological horizon $v=v_c$, or the outer horizon $v=v_o$ of the ''left'' black hole. The former one (its ''future'' half) forms a (past) boundary of the domain in which any observer has to reach the future infinity $\mathcal{I}^+$ (the domain I containing $\mathcal{I}^+$ in Fig. 2). The latter one forms the ''surface'' of black hole and can thus be understood as a ''surface of sources'' (the boundary between regions II and III). Although we have in mind mainly these two cases, the following discussion can be applied to any horizon $v=v_h$. The special geodesics cross such horizon at null hypersurface $\tilde{v}=n\pi$, the global null coordinates $\tilde{u}$, $\tilde{v}$ being defined in Eq. (A38), and the integer n fixed by the horizon under consideration (in particular $n=0$ and $n=-1$ in Fig. 2).

First, we observe that the choice (7.4) is the most natural one. The Robinson-Trautman tetrads in the whole spacetime—and thus the corresponding initial conditions on any horizon $v=v_h$—are actually invariant under a shift along the Killing vector $\boldsymbol{\partial}_\tau$. Indeed, expressing the Robinson-Trautman tetrad in terms of the coordinate vectors $\boldsymbol{\partial}_\tau, \boldsymbol{\partial}_\omega, \boldsymbol{\partial}_\sigma, \boldsymbol{\partial}_\varphi$ [using Eqs. (4.26), and (C2f)-(C2h)] we find that the coefficients are independent of τ, i.e., the Lie derivatives vanish,

$$\mathcal{L}_{\boldsymbol{\partial}_\tau}\mathbf{k}_{\mathrm{RT}}=0, \quad \mathcal{L}_{\boldsymbol{\partial}_\tau}\mathbf{l}_{\mathrm{RT}}=0, \quad \mathcal{L}_{\boldsymbol{\partial}_\tau}\mathbf{m}_{\mathrm{RT}}=0. \tag{7.8}$$

The definition of the interpretation tetrad (7.4) thus respects the symmetry of spacetime.

There is also another possibility to fix the interpretation tetrad $\mathbf{k}_{\mathrm{i}'}, \mathbf{l}_{\mathrm{i}'}, \mathbf{m}_{\mathrm{i}'}, \overline{\mathbf{m}}_{\mathrm{i}'}$ on the horizon $v=v_h$. We choose the null vector $\mathbf{k}_{\mathrm{i}'} \propto \mathbf{k}_{\mathrm{RT}}$ tangent to the geodesic, and the null vector $\mathbf{l}_{\mathrm{i}'}$ tangent to the horizon. Now we have to specify the length of one of these vectors, length of the other one is then fixed by the normalization (4.3). It will be achieved by requiring that the vector $\mathbf{l}_{\mathrm{i}'}$ is parallelly transported along the null geodesic generator of the horizon (note, however, that this condition cannot be satisfied for the vector $\mathbf{k}_{\mathrm{i}'}$). Finally, we should fix the remaining vectors $\mathbf{m}_{\mathrm{i}'}, \overline{\mathbf{m}}_{\mathrm{i}'}$. However, we will be interested only in the magnitude of the leading terms of the field components (as in the previous sections) and therefore a specific choice of the vectors $\mathbf{m}_{\mathrm{i}'}, \overline{\mathbf{m}}_{\mathrm{i}'}$, is irrelevant—see the discussion before Eq. (5.18). The interpretation tetrad defined in this way is a natural choice for observers localized on the horizon—its definition remains ''the same'' (is parallelly transported) along the generators of the horizon.

To follow explicitly the procedure described above, we use the global null coordinates $\tilde{u}$, $\tilde{v}$. The definition of these coordinates depends on a choice of parameter δ. As explained in Appendix A, the metric (A39) is regular with respect of these coordinates on the horizon $v=v_h$ if we set

$$\delta=\delta_h, \tag{7.9}$$

where δ_h is given by Eq. (A36). In the following we assume such a choice. We also introduce the sign of δ_h:

$$\pm 1=\mathrm{sgn}\,\delta_h, \tag{7.10}$$

then

$$\cos\tilde{u}\Big|_{\substack{v=v_h\\ \tilde{u}=m\pi}}=\cos\tilde{v}\Big|_{\substack{v=v_h\\ \tilde{v}=n\pi}}=\pm 1. \tag{7.11}$$

For the cosmological horizon $\mathrm{sgn}\delta_c=1$, whereas for the outer horizon $\mathrm{sgn}\delta_o=-1$. With these definitions the metric coefficient $\boldsymbol{g}_{\tilde{u}\tilde{v}}$ evaluated on the horizon $v=v_h$ reads

$$\boldsymbol{g}_{\tilde{u}\tilde{v}}\Big|_{\substack{v=v_h\\ \tilde{v}=n\pi}}=-r_h^2\frac{|\delta_h|}{\tilde{\delta}_h}(1\pm\cos\tilde{u})^{-1}, \tag{7.12}$$

where $\tilde{\delta}_h$ is defined in Eq. (A42), and

$$r_h=r|_{v=v_h}=\frac{a_\Lambda}{v_h\cosh\alpha-\xi\sinh\alpha}. \tag{7.13}$$

Here and in the following we repeatedly use relation (A41).

Now, we fix the vectors $\mathbf{k}_{\mathrm{i}'}, \mathbf{l}_{\mathrm{i}'}$ at the bifurcation two-surface $\tilde{u}=m\pi$, $\tilde{v}=n\pi$ of the horizon in a ''symmetric way,'' namely,

$$\mathbf{l}_{\mathrm{i}'}\Big|_{\substack{v=v_h\\ \tilde{v}=n\pi\\ \tilde{u}=m\pi}}=\frac{\sqrt{2}}{r_h}\sqrt{\frac{\tilde{\delta}_h}{|\delta_h|}}\boldsymbol{\partial}_{\tilde{u}}, \quad \mathbf{k}_{\mathrm{i}'}\Big|_{\substack{v=v_h\\ \tilde{u}=m\pi\\ \tilde{v}=n\pi}}=\frac{\sqrt{2}}{r_h}\sqrt{\frac{\tilde{\delta}_h}{|\delta_h|}}\boldsymbol{\partial}_{\tilde{v}}. \tag{7.14}$$

Using the fact that the only nonvanishing Christoffel coefficient $\Gamma^{\alpha}_{\tilde{u}\tilde{u}}$ is

$$\Gamma^{\tilde{u}}_{\tilde{u}\tilde{u}}|_{v=v_h}=\pm\left(\tan\frac{\tilde{u}}{2}\right)^{\pm 1}, \tag{7.15}$$

we find that the vector $\mathbf{l}_{\mathrm{i}'}$ defined by

$$\mathbf{l}_{\mathrm{i}'}\Big|_{\substack{v=v_h\\ \tilde{v}=n\pi}}=\frac{1}{\sqrt{2}r_h}\sqrt{\frac{\tilde{\delta}_h}{|\delta_h|}}(1\pm\cos\tilde{u})\boldsymbol{\partial}_{\tilde{u}}, \tag{7.16}$$

is parallelly transported along the geodesic null generators of the horizon $\tilde{v}=\mathrm{const}$, $\xi=\mathrm{const}$, $\varphi=\mathrm{const}$, with the initial condition (7.14). Obviously, $\mathbf{l}_{\mathrm{i}'}$ is tangent to the generator, and $\mathbf{l}_{\mathrm{i}'}\cdot\nabla\mathbf{l}_{\mathrm{i}'}\big|_{\substack{v=v_h\\ \tilde{v}=n\pi}}=0$. Taking into account the normalization (4.3) and the metric coefficient (7.12) we find the normalization of the null vector $\mathbf{k}_{\mathrm{i}'}$,

$$\mathbf{k}_{\mathrm{i}'}\Big|_{\substack{v=v_h\\ \tilde{v}=n\pi}}=\frac{\sqrt{2}}{r_h}\sqrt{\frac{\tilde{\delta}_h}{|\delta_h|}}\boldsymbol{\partial}_{\tilde{v}}. \tag{7.17}$$

The null vectors $\mathbf{k}_{\mathrm{i}'}, \mathbf{l}_{\mathrm{i}'}$ do *not* coincide on the horizon with the Robinson-Trautman null vectors $\mathbf{k}_{\mathrm{i}}$, $\mathbf{l}_{\mathrm{i}}$ given by

Eq. (7.4). Expressing the tetrad (4.26) in the $\tilde{u}$, $\tilde{v}$ coordinates [cf. Eqs. (C4), (4.8)] we find

$$\mathbf{k}_{\mathrm{i}}|_{\substack{v=v_h \\ \tilde{v}=n\pi}} = \frac{2a_\Lambda \widetilde{\delta}_h}{r_h^2 \cosh\alpha}\left(\cot\frac{\tilde{u}}{2}\right)^{\pm 1} \boldsymbol{\partial}_{\tilde{v}}, \tag{7.18}$$

i.e., the vectors $\mathbf{k}_{\mathrm{i}'}$ and $\mathbf{k}_{\mathrm{i}}$ are proportional. The vectors $\mathbf{l}_{\mathrm{i}'}$ and $\mathbf{l}_{\mathrm{i}}$ do not even point into the same null direction. We could explicitly relate the interpretation tetrad $\mathbf{k}_{\mathrm{i}'}, \mathbf{l}_{\mathrm{i}'}, \mathbf{m}_{\mathrm{i}'}, \overline{\mathbf{m}}_{\mathrm{i}'}$ to the tetrad (7.4) by a combination of a boost in the **k**-**l** plane (D9) followed by a transformation (D3) leaving **k** fixed. Of course, this relation obtained on the horizon is propagated by a parallel transport up to infinity $\mathcal{I}^+$. The parameter B of the boost transformation simply follows from relation $\mathbf{k}_{\mathrm{i}'} = B\mathbf{k}_{\mathrm{i}}$ between the vectors $\mathbf{k}_{\mathrm{i}'}$ and $\mathbf{k}_{\mathrm{i}}$ [see Eqs. (7.17), (7.18)],

$$B = \frac{r_h \cosh\alpha}{a_\Lambda \sqrt{2|\delta_h|\widetilde{\delta}_h}}\left(\tan\frac{\tilde{u}}{2}\right)^{\pm 1}. \tag{7.19}$$

As we discussed in Sec. V [see Eq. (5.18)] the magnitude of the leading term of the fields is independent of the transformation with **k** fixed, so we do not need to identify the second transformation (D3) explicitly.

Using the transformation properties (D11) and (D12) of the fields we finally derive the magnitude of the leading term of the fields with respect to the interpretation tetrad $\mathbf{k}_{\mathrm{i}'}, \mathbf{l}_{\mathrm{i}'}, \mathbf{m}_{\mathrm{i}'}, \overline{\mathbf{m}}_{\mathrm{i}'}$ specified on the horizon $v = v_h$. We obtain

$$|\Psi_4^{\mathrm{i}'}| \approx B^{-2}|\Psi_4^{\mathrm{i}}|, \quad |\Phi_2^{\mathrm{i}'}|^2 \approx B^{-2}|\Phi_2^{\mathrm{i}}|^2, \tag{7.20}$$

$$B^{-2} = 2|\delta_h|\widetilde{\delta}_h(v_h - \xi_+ \tanh\alpha)^2 \exp\left(-\frac{\cosh\alpha}{a_\Lambda}\frac{u_+}{\delta_h}\right),$$

where ξ_+ and u_+ denote the coordinates of the point N_+ on $\mathcal{I}^+$, and we have used relations (7.13) and (A38).

As expected, such a different choice of the interpretation tetrad does not change the radiative character of the fields (the $1/r$ fall-off), it only modifies the field components by a finite factor. Nevertheless, such modification can be substantial—we have obtained an additional factor which is exponential in the Robinson-Trautman coordinate u, namely, $\exp[-\sqrt{(\Lambda/3)+A^2}\, u_+/\delta_h]$. This expresses the dependence of the magnitude of gravitational and electro-magnetic radiation on position of the asymptotic point N_+ at de Sitter–like infinity $\mathcal{I}^+$. Notice that the exponential ''damping'' of radiation depends not only on the cosmological constant Λ but also on the acceleration A of the black holes. Interestingly, the factor $\sqrt{(\Lambda/3)+A^2}$ is exactly the Hawking temperature $2\pi T$ recently discussed, e.g., in Ref. [50].

VIII. SUMMARY

In the present paper we have thoroughly investigated the C-metric with a positive cosmological constant $\Lambda > 0$. This exact solution of the Einstein-Maxwell equations represents a radiative spacetime in which the radiation is generated by a pair of (charged) black holes uniformly accelerated in asymptotically de Sitter universe. By introducing new convenient coordinates and suitable interpretation tetrads near the conformal light infinity $\mathcal{I}^+$ we were able to analyze the asymptotic behavior of gravitational and electromagnetic fields. The peeling off property has been demonstrated, the leading components of the fields in the parallelly transported tetrad are inversely proportional to the affine parameter of the corresponding null geodesic.

In addition, as a main result of our investigation, an explicit formula which describes the directional pattern of radiation has been derived: it expresses the dependence of the fields on directions along which a given point N_+ at conformal infinity $\mathcal{I}^+$ is approached. This specific directional characteristic supplements the peeling property, thus completing the asymptotic behavior of gravitational and electromagnetic fields near infinity $\mathcal{I}^+$ with a spacelike character.

It was already observed in the 1960s by Penrose [9,10] that radiation is defined ''less invariantly'' when $\mathcal{I}^+$ is spacelike than in the case when it is null (asymptotically flat spacetimes in particular). Our results can thus be understood as an investigation of this ''nonuniqueness.'' In fact, the peeling off property supplemented by the directional pattern of radiation (5.19), (5.23) characterize *fully* the radiation near the de Sitter–like infinity $\mathcal{I}^+$.

The specific pattern of radiation has been obtained here by analyzing the exact model of uniformly accelerated black holes in de Sitter universe. It is in agreement with the analogous recent result for the test electromagnetic field generated by accelerated charges in the de Sitter background [22,23]. We are convinced that the directional pattern of radiation derived has a ''universal'' validity and applies to *all* radiative fields of a given Petrov algebraic type near the spacelike conformal infinity $\mathcal{I}^+$. The proof of this statement will be presented elsewhere [51].

ACKNOWLEDGMENTS

We are very grateful to Jiří Bičák who brought our attention to the problem of radiation in the de Sitter–like universes, the C-metric in particular. Thanks are also due to him for reading the manuscript, for his comments and suggestions. The work has been supported in part by the Grants No. GACR 202/02/0735 and GAUK 141/2000 of the Czech Republic and the Charles University in Prague.

APPENDIX A: VARIOUS COORDINATES FOR THE C-METRIC WITH Λ

The C-metric with possibly nonvanishing cosmological constant $\Lambda = 3/a_\Lambda^2$ can be written as

$$\boldsymbol{g} = \frac{1}{A^2(x+y)^2}\left(-F\mathbf{d}t^2 + \frac{1}{F}\mathbf{d}y^2 + \frac{1}{G}\mathbf{d}x^2 + G\mathbf{d}\varphi^2\right) \tag{A1}$$

with

$$F = -\frac{1}{a_\Lambda^2 A^2} - 1 + y^2 - 2mAy^3 + e^2A^2y^4,$$
$$G = 1 - x^2 - 2mAx^3 - e^2A^2x^4. \tag{A2}$$

The functions F and G are polynomials of the coordinates y and x, respectively, and are mutually related by

$$F=-Q(y)-\frac{1}{a_\Lambda^2 A^2},\quad G=Q(-x), \tag{A3}$$

where $Q(w)$ denotes the polynomial

$$Q(w)=1-w^2+2mAw^3-e^2A^2w^4. \tag{A4}$$

The constants A, m, e, and C [such that $\varphi\in(-\pi C,\pi C)$] parametrize acceleration, mass, charge of the black holes, and conicity of the φ-symmetry axis, respectively.

The metric (A1), (A2) is an ordinary form of the C-metric in the case when the cosmological constant Λ vanishes, i.e., when $F=-Q(y)$. This has been extensively used for investigation of uniformly accelerated (pair) of black holes in asymptotically flat spacetime, see, e.g., Refs. [13,27,28,30,31]. However, for $\Lambda\neq 0$ the form of the generalization is not so obvious and unique. For example, in Ref. [35] the term with the cosmological constant was included in the metric function G rather than in F. Also, the parametrization of the metric (A1) is not unique. A simple rescaling of the coordinates can be performed which removes the acceleration parameter A from the conformal factor. These related metric forms, which allow an explicit limit $A\to 0$, were introduced, e.g., in Refs. [32,36,44].

Throughout this paper we use the particularly rescaled coordinates τ, υ, ξ, φ given by

$$\begin{aligned}\tau&=t\coth\alpha,\quad \varphi=\varphi,\\ \upsilon&=y\tanh\alpha,\quad \xi=-x,\end{aligned} \tag{A5}$$

where the dimensionless acceleration parameter α is introduced in Eq. (2.6). In these convenient coordinates the C-metric (A1), (A2) takes the form

$$\boldsymbol{g}=r^2\left(-\mathcal{F}\mathbf{d}\tau^2+\frac{1}{\mathcal{F}}\mathbf{d}\upsilon^2+\frac{1}{\mathcal{G}}\mathbf{d}\xi^2+\mathcal{G}\mathbf{d}\varphi^2\right), \tag{A6}$$

with the function r given by

$$r=\frac{1}{A(x+y)}=\frac{a_\Lambda}{\upsilon\cosh\alpha-\xi\sinh\alpha} \tag{A7}$$

and

$$\begin{aligned}-\mathcal{F}&=1-\upsilon^2+\cosh\alpha\,\frac{2m}{a_\Lambda}\upsilon^3-\cosh^2\alpha\,\frac{e^2}{a_\Lambda^2}\upsilon^4,\\ \mathcal{G}&=1-\xi^2+\sinh\alpha\,\frac{2m}{a_\Lambda}\xi^3-\sinh^2\alpha\,\frac{e^2}{a_\Lambda^2}\xi^4.\end{aligned} \tag{A8}$$

These coordinates have the following ranges: $\tau\in\mathbb{R}$, $\varphi\in(-\pi C,\pi C)$, $\xi\in(\xi_1,\xi_2)$, and $\upsilon\in(\xi\tanh\alpha,\infty)$, with ξ_1,ξ_2 being the two smallest roots of $\mathcal{G}$—see discussion in Sec. III.

The metric functions F, G and $\mathcal{F}$, $\mathcal{G}$ as functions on the spacetime manifold are related by

$$\mathcal{F}=F\tanh^2\alpha,\quad \mathcal{G}=G, \tag{A9}$$

but they are usually understood as functions of different arguments, namely, $F(y)$, $G(x)$ and $\mathcal{F}(\upsilon)$, $\mathcal{G}(\xi)$. In this sense we will also use a notation for differentiation of these functions $F'=dF/dy$ and $\mathcal{F}'=d\mathcal{F}/d\upsilon$ or $G'=dG/dx$ and $\mathcal{G}'=d\mathcal{F}/d\xi$. The metric function $\mathcal{G}$ takes the values

$$\mathcal{G}\in[0,1], \tag{A10}$$

$\mathcal{G}=0$ for $\xi=\xi_1,\xi_2$ (axes of φ symmetry), and $\mathcal{G}=1$ for $\xi=0$ (on "equator," i.e., a φ circle of maximum circumference). At infinity $\mathcal{I}$ the metric function $\mathcal{F}$ takes the values

$$-\mathcal{F}\in[\cosh^{-2}\alpha,1], \tag{A11}$$

with $\mathcal{F}=-\cosh^{-2}\alpha$ on the axes of φ symmetry, and $\mathcal{F}=-1$ on the equator $(\xi,\upsilon=0)$.

The above coordinates τ, υ, ξ, φ are closely related to the *accelerated coordinates* T, R, Θ, Φ introduced and discussed in Refs. [36,52]. If we define

$$T=a_\Lambda\tau,\quad R=\frac{a_\Lambda}{\upsilon},\quad \mathbf{d}\Theta=\frac{1}{\sqrt{\mathcal{G}}}\mathbf{d}\xi,\quad \Phi=\varphi, \tag{A12}$$

the metric (A6) takes the form

$$\boldsymbol{g}=\frac{r^2}{R^2}\left[-\mathcal{H}\mathbf{d}T^2+\frac{1}{\mathcal{H}}\mathbf{d}R^2+R^2(\mathbf{d}\Theta^2+\mathcal{G}\mathbf{d}\Phi^2)\right], \tag{A13}$$

where

$$\mathcal{H}=\frac{1}{\upsilon^2}\mathcal{F}=1-\frac{R^2}{a_\Lambda^2}-\cosh\alpha\,\frac{2m}{R}+\cosh^2\alpha\,\frac{e^2}{R^2}. \tag{A14}$$

These coordinates have an obvious physical interpretation in two particular cases—in the case of a vanishing acceleration of the black holes ($A=0$), and for empty de Sitter spacetime ($m=0$, $e=0$). In both these cases the metric function $\mathcal{G}$ reduces to a simple form $\mathcal{G}=1-\xi^2$, so the definition (A12) of the angle Θ gives

$$\cos\Theta=-\xi,\quad \sin\Theta=\sqrt{1-\xi^2}. \tag{A15}$$

For vanishing acceleration $A=0$, i.e., by setting $\alpha=0$, we obtain $R=r$, and the metric (A13) reduces to the well-known metric for the Reissner-Nordström black hole in Minkowski or de Sitter universe [36,53],

$$\boldsymbol{g}|_{\alpha=0}=-\mathcal{H}\mathbf{d}T^2+\frac{1}{\mathcal{H}}\mathbf{d}R^2+R^2(\mathbf{d}\Theta^2+\sin^2\Theta\mathbf{d}\Phi^2), \tag{A16}$$

with the metric function (A14) simplified by $\cosh\alpha=1$.

In the case of empty de Sitter space ($m=0$, $e=0$), but with generally nonvanishing acceleration, the metric function $\mathcal{F}$ also simplifies to $\mathcal{F}=\upsilon^2-1$. The de Sitter metric in accelerated coordinates thus takes the form (cf. Ref. [36])

$$\boldsymbol{g}_{\mathrm{dS}}=\frac{1-a_\Lambda^{-2}R_\mathrm{o}^2}{(1+a_\Lambda^{-2}R_\mathrm{o}R\cos\Theta)^2}\left(-\left(1-\frac{R^2}{a_\Lambda^2}\right)\mathbf{d}T^2+\left(1-\frac{R^2}{a_\Lambda^2}\right)^{-1}\mathrm{d}R^2+R^2(\mathbf{d}\Theta^2+\sin^2\Theta\,\mathbf{d}\Phi^2)\right), \tag{A17}$$

where we introduced the constant

$$R_\mathrm{o}=a_\Lambda\tanh\alpha. \tag{A18}$$

An explicit relation to the standard de Sitter static coordinates T_{dS}, R_{dS}, Θ_{dS}, Φ_{dS}, in which

$$\boldsymbol{g}_{\mathrm{dS}}=-\left(1-\frac{R_{\mathrm{dS}}^2}{a_\Lambda^2}\right)\mathrm{d}T_{\mathrm{dS}}^2+\left(1-\frac{R_{\mathrm{dS}}^2}{a_\Lambda^2}\right)^{-1}\mathbf{d}R_{\mathrm{dS}}^2+R_{\mathrm{dS}}^2(\mathbf{d}\Theta_{\mathrm{dS}}^2+\sin^2\Theta_{\mathrm{dS}}\mathbf{d}\Phi_{\mathrm{dS}}^2) \tag{A19}$$

is

$$R_{\mathrm{dS}}\cos\Theta_{\mathrm{dS}}=\frac{R\cos\Theta+R_\mathrm{o}}{1+a_\Lambda^{-2}R_\mathrm{o}R\cos\Theta},\quad T_{\mathrm{dS}}=T,$$
$$R_{\mathrm{dS}}\sin\Theta_{\mathrm{dS}}=\frac{R\sin\Theta\sqrt{1-a_\Lambda^{-2}R_\mathrm{o}^2}}{1+a_\Lambda^{-2}R_\mathrm{o}R\cos\Theta},\quad \Phi_{\mathrm{dS}}=\Phi. \tag{A20}$$

The origin $R=0$ clearly corresponds to worldlines of two static observers $R_{\mathrm{dS}}=R_\mathrm{o}$, $\Theta_{\mathrm{dS}}=0$ which move with a uniform acceleration A. Further details concerning the interpretation of the accelerated coordinates in de Sitter space were discussed at the end of Sec. III (see also Ref. [23]).

It is also instructive to elucidate a geometrical relation between these two coordinate systems (A17) and (A19). It is well known that the de Sitter spacetime is conformally related to Minkowski space (see Refs. [8,11], or recently Ref. [21]). Specifically, the (shaded) domain P of de Sitter spacetime depicted in Fig. 4 corresponds to the $\mathfrak{t}<0$ region of Minkowski spacetime in standard spherical coordinates $\mathfrak{t}$, $\mathfrak{r}$, ϑ, φ, the metrics being related by $\mathbf{g}_{\mathrm{dS}}=(a_\Lambda/\mathfrak{t})^2\mathbf{g}_{\mathrm{Mink}}$. The de Sitter static coordinates T_{dS}, R_{dS}, Θ_{dS}, Φ_{dS} can be obtained from the spherical coordinates of Minkowski space by a "spherical Rindler" transformation, i.e., $R_{\mathrm{dS}}=a_\Lambda\mathfrak{r}/\mathfrak{t}$, $T_{\mathrm{dS}}/a_\Lambda=(1/2)\log|(\mathfrak{t}^2-\mathfrak{r}^2)/a_\Lambda^2|$, $\Theta_{\mathrm{dS}}=\vartheta$, $\Phi_{\mathrm{dS}}=\varphi$. On the other hand, the accelerated coordinates T, R, Θ, Φ are also obtained from conformally related Minkowski space by the same construction, however, starting from a different spherical coordinates $\mathfrak{t}'$, $\mathfrak{r}'$, ϑ', φ' which are defined in the inertial frame boosted along the $\vartheta=0$ direction with the boost given exactly by the acceleration parameter α (i.e., with the relative velocity $\tanh\alpha$). Using this insight we can easily visualize the relation between the hypersurface $R_{\mathrm{dS}}=\infty$ (the conformal infinity $\mathcal{I}$ of de Sitter universe; the $\mathfrak{t}=0$ hypersurface of conformally related Minkowski space) and the hypersurface $R=\infty$ (the coordinate singularity of accelerated coordinates in de Sitter space, which is easily removable, for example, by the coordinate $v=a_\Lambda/R$; the hypersurface $\mathfrak{t}'=0$ of Minkowski space), as indicated in Fig. 4. For more details see Ref. [23].

It is particularly useful to introduce also new coordinates τ, ω, σ, φ for the C-metric naturally adapted both to the Killings vectors $\boldsymbol{\partial}_\tau$, $\boldsymbol{\partial}_\varphi$ and to infinity $\mathcal{I}$. In terms of the new coordinate

$$\omega=-v\cosh\alpha+\xi\sinh\alpha=-\frac{a_\Lambda}{r}, \tag{A21}$$

infinity $\mathcal{I}$ is given by a simple condition $\omega=0$. The coordinate σ is introduced by requiring an orthogonality of the coordinates. Indeed, if we define σ by the differential form

$$\mathbf{d}\sigma=\frac{\sinh\alpha}{\mathcal{F}}\mathbf{d}v+\frac{\cosh\alpha}{\mathcal{G}}\mathbf{d}\xi,\qquad \sigma=0\quad\text{for}\quad \xi,v=0, \tag{A22}$$

[which, thanks to Eq. (A8), is integrable] the C-metric takes the form

$$\mathbf{g}=\frac{a_\Lambda^2}{\omega^2}\left(-\mathcal{F}\mathbf{d}\tau^2+\frac{1}{\mathcal{E}}\mathbf{d}\omega^2+\frac{\mathcal{F}\mathcal{G}}{\mathcal{E}}\mathbf{d}\sigma^2+\mathcal{G}\mathbf{d}\varphi^2\right), \tag{A23}$$

where

$$\begin{aligned}\mathcal{E}&=\mathcal{F}\cosh^2\alpha+\mathcal{G}\sinh^2\alpha\\&=-1-\omega\Big[v\cosh\alpha+\xi\sinh\alpha-\frac{2m}{a_\Lambda}(v^2\cosh^2\alpha\\&\quad+v\xi\cosh\alpha\sinh\alpha+\xi^2\sinh^2\alpha)+\frac{e^2}{a_\Lambda^2}(v^3\cosh^3\alpha\\&\quad+v^2\xi\cosh^2\alpha\sinh\alpha+v\xi^2\cosh\alpha\sinh^2\alpha+\xi^3\sinh^3\alpha)\Big].\end{aligned} \tag{A24}$$

Obviously, on $\mathcal{I}$, where $\omega=0$, we obtain $\mathcal{E}=-1$. Thanks to relation $\mathcal{F}<0$ in region I of Fig. 3, we observe from metric (A23) that near infinity $\mathcal{I}^+$, the coordinate ω plays the role of a time if $\mathcal{E}<0$. It can be shown that for $\mathcal{E}<0$ the coordinate transformation (A21), (A22) from v, ξ to ω, σ is invertible. We will use the coordinate σ only in this region. The hypersurface $\mathcal{E}=0$ is always located above the cosmological horizon and it touches the horizon on the axes $\xi=\xi_1$, ξ_2, see the left part of Fig. 3.

The C-metric can also be put into the Robinson-Trautman form (see Ref. [54]). Introducing the coordinates r and u,

$$Ar=(x+y)^{-1},\qquad A\mathbf{d}u=\frac{\mathbf{d}y}{F}+\mathbf{d}t, \tag{A25}$$

we obtain from Eq. (A1) the metric

$$\boldsymbol{g}=r^2\left(\frac{1}{G}\mathbf{d}x^2+G\mathbf{d}\varphi^2\right)-\mathbf{d}u\vee\mathbf{d}r-Ar^2\mathbf{d}u\vee\mathbf{d}x-A^2r^2F\mathbf{d}u^2, \tag{A26}$$

where the function A^2r^2F, expressed in the coordinates x, r using $y=(Ar)^{-1}-x$, reads

$$A^2r^2F=-\frac{r^2}{a_\Lambda^2}-A^2r^2G+ArG'-\frac{1}{2}G''+\frac{1}{6}(Ar)^{-1}G'''-\frac{1}{24}(Ar)^{-2}G''''. \tag{A27}$$

This is the generalization of the Kinnersley-Walker coordinates [27] to $\Lambda\neq0$. Introducing the complex coordinates ζ, $\overline{\zeta}$ [or real coordinates ψ, φ, related by $\zeta=(1/\sqrt{2})(\psi-i\varphi)$] instead of the coordinates x, φ,

$$\frac{1}{\sqrt{2}}(\mathbf{d}\zeta+\mathbf{d}\overline{\zeta})=\mathbf{d}\psi=A\mathbf{d}u-\frac{\mathbf{d}x}{G},\qquad \frac{i}{\sqrt{2}}(\mathbf{d}\zeta-\mathbf{d}\overline{\zeta})=\mathbf{d}\varphi, \tag{A28}$$

(notice that $\psi=\tau\tanh\alpha+\sigma\,\mathrm{sech}\,\alpha$), we put the C-metric into the Robinson-Trautman form

$$\boldsymbol{g}=\frac{r^2}{P^2}\mathbf{d}\zeta\vee\mathbf{d}\overline{\zeta}-\mathbf{d}u\vee\mathbf{d}r-H\mathbf{d}u^2 \tag{A29}$$

(or, alternatively, with $\mathbf{d}\boldsymbol{\zeta}\vee\mathbf{d}\overline{\zeta}$ replaced by $\mathbf{d}\psi^2+\mathbf{d}\varphi^2$), where the metric functions are

$$P^{-2}=G=\mathcal{G},\qquad H=A^2r^2(F+G)=\frac{r^2}{a_\Lambda^2}\mathcal{E}. \tag{A30}$$

Using Eqs. (A27), (A30), and (A28), which for $P=G^{-1/2}$ imply $AG'=-2(\ln P)_{,u}$ and $G''=-2\Delta\ln P$ with $\Delta=2P^2\partial_\zeta\partial_{\overline{\zeta}}$, we recover that

$$H=-\frac{r^2}{a_\Lambda^2}-2r(\ln P)_{,u}+\Delta\ln P-\frac{2}{r}(m-2e^2A\xi)+\frac{e^2}{r^2}. \tag{A31}$$

This is the standard general expression for the metric function of the Robinson-Trautman solution [44]. Let us finally note that the Christoffel coefficients for the metric (A29) are

$$\Gamma^\zeta_{r\zeta}=\frac{1}{r},\quad \Gamma^\zeta_{u\zeta}=-\frac{P_{,u}}{P},\quad \Gamma^\zeta_{\zeta\zeta}=-\frac{2P_{,\zeta}}{P},\quad \Gamma^\zeta_{uu}=\frac{P^2H_{,\overline{\zeta}}}{2r^2},$$

$$\Gamma^u_{\zeta\overline{\zeta}}=\frac{r}{P^2},\quad \Gamma^u_{uu}=-\frac{1}{2}H_{,r},\quad \Gamma^r_{uu}=\frac{1}{2}HH_{,r}+\frac{1}{2}H_{,u}, \tag{A32}$$

$$\Gamma^r_{\zeta\overline{\zeta}}=-\frac{rPH+r^2P_{,u}}{P^3},\quad \Gamma^r_{u\zeta}=\frac{1}{2}H_{,\zeta},\quad \Gamma^r_{ur}=\frac{1}{2}H_{,r}.$$

Finally, for a discussion of the global structure of the spacetime it is necessary, following the general approach [55,56], to introduce global double null coordinates $\tilde{u}$, $\tilde{v}$, ξ, φ. For this, we supplement the above defined null coordinate u with the complementary null coordinate v (see [57]). In terms of the coordinates τ, v these are [cf. Eq. (A25), (A5)]

$$u=\frac{a_\Lambda}{\cosh\alpha}(v_*+\tau),\quad v=\frac{a_\Lambda}{\cosh\alpha}(v_*-\tau), \tag{A33}$$

where the tortoise coordinate v_* is defined by the differential relation

$$\mathbf{d}v_*=\frac{1}{\mathcal{F}}\mathbf{d}v. \tag{A34}$$

Taking into account the polynomial structure (A8) of the function $\mathcal{F}$,

$$\mathcal{F}=\gamma_{\mathrm{o}}\prod_h(v-v_h), \tag{A35}$$

where $\gamma_{\mathrm{o}}=\mathrm{const}$ and v_h ($h=\mathrm{i,o,c,m}$) are the values of the coordinate v at the horizons (the roots of $\mathcal{F}$), we obtain

$$v_*=\sum_h\delta_h\log|v-v_h|,\quad \delta_h=(\mathcal{F}'|_{v=v_h})^{-1}. \tag{A36}$$

In these coordinates the C-metric with $\Lambda>0$ takes the form

$$\boldsymbol{g}=r^2\left(\frac{\mathcal{F}\cosh^2\alpha}{2a_\Lambda^2}\mathbf{d}u\vee\mathbf{d}v+\frac{1}{\mathcal{G}}\mathbf{d}\xi^2+\mathcal{G}\mathbf{d}\varphi^2\right). \tag{A37}$$

Now, we can define the global null coordinates $\tilde{u}$, $\tilde{v}$, ξ, φ parametrized by a constant coefficient δ, covering, for suitable values of δ, the horizons smoothly,

$$\left|\tan\frac{\tilde{u}}{2}\right|=\exp\left(\frac{u\cosh\alpha}{2|\delta|a_\Lambda}\right),\quad \mathrm{sgn}\left(\tan\frac{\tilde{u}}{2}\right)=(-1)^m,$$
$$\left|\tan\frac{\tilde{v}}{2}\right|=\exp\left(\frac{v\cosh\alpha}{2|\delta|a_\Lambda}\right),\quad \mathrm{sgn}\left(\tan\frac{\tilde{v}}{2}\right)=(-1)^n. \tag{A38}$$

The C-metric in these coordinates then takes the form

$$\boldsymbol{g}=r^2\left(\frac{2\delta^2\mathcal{F}}{\sin\tilde{u}\sin\tilde{v}}\mathbf{d}\tilde{u}\vee\mathbf{d}\tilde{v}+\frac{1}{\mathcal{G}}\mathbf{d}\xi^2+\mathcal{G}\mathbf{d}\varphi^2\right). \tag{A39}$$

The horizons $v=v_{\mathrm{i}}$, v_{o}, v_{c} now correspond to the values $\tilde{u}=m\pi$ or $\tilde{v}=n\pi$, with $m,n\in\mathbb{Z}$ (see Fig. 2).

Notice, that it follows from Eqs. (A38), (A36) that

$$\left|\tan\frac{\tilde{u}}{2}\tan\frac{\tilde{v}}{2}\right|^{\mathrm{sgn}\,\delta}=\prod_k|v-v_k|^{\delta_k/\delta}. \tag{A40}$$

Evaluating this expression on the particular horizon $v=v_h$ and comparing with Eq. (A35) we find that with the choice $\delta=\delta_h$ the expression

$$-\mathcal{F}\left(\tan\frac{\tilde u}{2}\tan\frac{\tilde v}{2}\right)^{-\operatorname{sgn}\delta}\Big|_{v=v_h} = \gamma_o\prod_{k\neq h}|v_h-v_k|^{1-\delta_k/\delta_h}=\frac{1}{|\delta_h|\tilde\delta_h} \qquad \text{(A41)}$$

is finite and nonvanishing. Here we introduced the constant

$$\tilde\delta_h=\prod_{k\neq h}|v_h-v_k|^{\delta_k/\delta_h}. \qquad \text{(A42)}$$

Using this fact it is possible to guarantee a regularity of the metric coefficient $\delta^2\mathcal{F}/(\sin\tilde u\sin\tilde v)$ in Eq. (A39) (including smoothness and that it is finite and nonzero) and smoothness of the coordinates r and v near the horizon v_h by the choice $\delta=\delta_h$ of the coefficient δ in Eqs. (A38), assuming that $\tilde u$, $\tilde v$ forms a smooth coordinate map in the neighborhood of this horizon. However, such an appropriate factor δ cannot be chosen for all horizons simultaneously—a different smooth map $\tilde u$, $\tilde v$ parametrized by different coefficients δ has to be used near the different horizons to demonstrate the smoothness of the metric in the whole spacetime (see, e.g., Refs. [55,56] for a general discussion).

APPENDIX B: PROPERTIES OF THE METRIC FUNCTIONS $\mathcal{F}$ AND $\mathcal{G}$

First, let us note that $\mathcal{F}$ and $\mathcal{G}$ can be represented in terms of polynomial $S(w)$

$$-\frac{\cosh^2\alpha}{a_\Lambda^2}\mathcal{F}=S\left(\frac{\cosh\alpha}{a_\Lambda}v\right)+\frac{\cosh^2\alpha}{a_\Lambda^2},$$
$$\frac{\sinh^2\alpha}{a_\Lambda^2}\mathcal{G}=S\left(\frac{\sinh\alpha}{a_\Lambda}\xi\right)+\frac{\sinh^2\alpha}{a_\Lambda^2}, \qquad \text{(B1)}$$

where

$$S(w)=-w^2(1-2mw+e^2w^2). \qquad \text{(B2)}$$

A typical graph of the polynomial $S(w)$ is drawn in Fig. 9. By inspecting the graph we obtain, e.g., relations (3.1) between the roots of the metric functions $\mathcal{F}$ and $\mathcal{G}$.

We may also prove some interesting properties, including Eq. (3.5), of the metric function $\mathcal{G}$ in the case of charged accelerated black holes. [Similar properties—in particular the inequality (B7)—can be also proved for uncharged accelerated black holes, i.e., for $e=0$, $m\neq0$, $A\neq0$.] In the case $e\neq0$, $A\neq0$, the metric function $\mathcal{G}$ is a polynomial of the fourth order in ξ and its zeros have been denoted in the ascending order as ξ_1, ξ_2, ξ_3, ξ_4. The extremes of $\mathcal{G}$ (zeros of $\mathcal{G}'$) are $\xi_0^{(1)}=0$, $\xi_\pm^{(1)}=(3m\pm\sqrt{9m^2-8e^2})/(4Ae^2)$. The zero of $\mathcal{G}'''=12(Am-2e^2A^2\xi)$ is $\xi^{(3)}=m/(2Ae^2)$, and $\mathcal{G}'''>0$ for $\xi<\xi^{(3)}$. Using the conditions (2.5), a straightforward calculation leads to an inequality $\mathcal{G}|_{\xi_+^{(1)}}>0$. The condition that $\mathcal{G}$ has four real roots requires $\mathcal{G}|_{\xi_-^{(1)}}<0$. This confirms that the graph of $\mathcal{G}$ has always a qualitative shape shown on Fig. 9. The extremes of $\mathcal{G}$ are located between its zeros, so that $\xi_1<0<\xi_2<\xi_-^{(1)}$. Expressing the vanishing linear coefficient in $\mathcal{G}$ in terms of the roots we obtain $(\xi_1+\xi_2)\xi_3\xi_4=-\xi_1\xi_2(\xi_3+\xi_4)$, the right-hand side is clearly positive, as well as $\xi_3\xi_4$, so we obtain

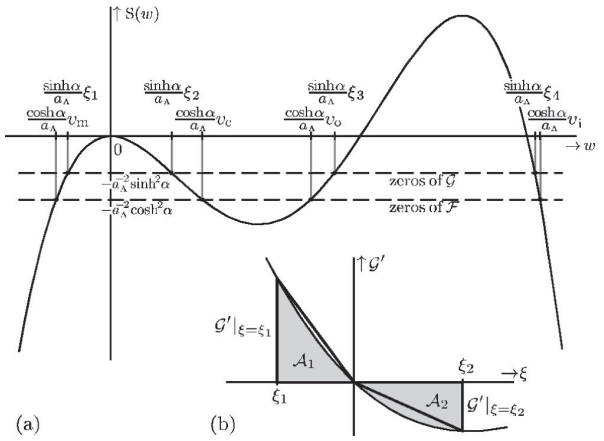

FIG. 9. (a) A qualitative shape of the metric functions $\mathcal{F}$ and $\mathcal{G}$ (in the case $m\neq0$, $e\neq0$) which are polynomials in v and ξ, respectively. It follows from the representation (B1) that both functions $\mathcal{F}$ and $\mathcal{G}$ are, up to the specific rescaling and the constant term, given by the same polynomial $S(w)$, the graph of which is presented here. The zeros of $\mathcal{F}$ and $\mathcal{G}$ are thus given by intersections of the graph of S with the horizontal lines $-a_\Lambda^{-2}\cosh^2\alpha$ and $-a_\Lambda^{-2}\sinh^2\alpha$, respectively. Relations (3.1) between the zeros of $\mathcal{F}$ and $\mathcal{G}$ follows immediately from this fact. (b) A graphical representation of the triangular estimate (B6) for the areas $\mathcal{A}_1$, $\mathcal{A}_2$ under the graph of $\mathcal{G}'$.

$$-\xi_1<\xi_2. \qquad \text{(B3)}$$

From the conditions (2.5) it also follows that $\xi_-^{(1)}<\xi^{(3)}$ and thus we have

$$\xi_1<0<\xi_2<\xi_-^{(1)}<\xi^{(3)}. \qquad \text{(B4)}$$

This means that $\mathcal{G}'$ is convex on the relevant interval (ξ_1,ξ_2), it is positive on the interval $(\xi_1,0)$ and negative on $(0,\xi_2)$. The positivity of $\mathcal{G}'''$ on the interval (ξ_1,ξ_2) also implies $m-2e^2A\xi_+>0$, which is the relation used in the discussion following the result (5.19). Clearly, $\int_{\xi_1}^{\xi_2}\mathcal{G}'\,d\xi=0$, i.e., the areas

$$\mathcal{A}_1=\int_{\xi_1}^{0}\mathcal{G}'\,d\xi,\quad \mathcal{A}_2=-\int_{0}^{\xi_2}\mathcal{G}'\,d\xi \qquad \text{(B5)}$$

are the same. Thanks to the convexity of $\mathcal{G}'$, we can estimate $\mathcal{A}_1$ and $\mathcal{A}_2$ by simpler triangular areas [see Fig. 9(b)], and we obtain

$$-\frac{1}{2}\xi_2\mathcal{G}'|_{\xi=\xi_2}<\mathcal{A}_2=\mathcal{A}_1<-\frac{1}{2}\xi_1\mathcal{G}'|_{\xi=\xi_1}. \qquad \text{(B6)}$$

Using Eq. (B3) this implies

$$-\mathcal{G}'|_{\xi=\xi_2}<\mathcal{G}'|_{\xi=\xi_1}. \tag{B7}$$

Considering Eq. (3.4) we obtain the important relation (3.5) which is necessary for the discussion of conicity in Sec. III.

APPENDIX C: RELATIONS BETWEEN THE COORDINATE FRAMES

In this appendix we summarize for convenience the relations between different coordinate one-form and vector frames. For coordinate one-form frames $(\mathbf{d}\tau,\mathbf{d}\upsilon,\mathbf{d}\xi,\mathbf{d}\varphi)$, $(\mathbf{d}\tau,\mathbf{d}\omega,\mathbf{d}\sigma,\mathbf{d}\varphi)$, and $(\mathbf{d}\zeta,\mathbf{d}\bar{\zeta},\mathbf{d}r,\mathbf{d}u)$ we obtain

$$\mathbf{d}\tau=\mathbf{d}\tau \qquad =\frac{\mathcal{E}}{\mathcal{F}\cosh\alpha}\frac{1}{a_\Lambda}\mathbf{d}u+\frac{1}{\mathcal{F}\cosh\alpha}\frac{a_\Lambda}{r^2}\mathbf{d}r-\frac{\mathcal{G}}{\mathcal{F}}\tanh\alpha\mathbf{d}\psi, \tag{C1a}$$

$$\mathbf{d}\upsilon=-\frac{\mathcal{F}}{\mathcal{E}}\cosh\alpha\mathbf{d}\omega+\frac{\mathcal{F}\mathcal{G}}{\mathcal{E}}\sinh\alpha\mathbf{d}\sigma \qquad =-\mathcal{G}\frac{\sinh^2\alpha}{\cosh\alpha}\frac{1}{a_\Lambda}\mathbf{d}u-\frac{1}{\cosh\alpha}\frac{a_\Lambda}{r^2}\mathbf{d}r+\mathcal{G}\tanh\alpha\mathbf{d}\psi, \tag{C1b}$$

$$\mathbf{d}\xi=\frac{\mathcal{G}}{\mathcal{E}}\sinh\alpha\mathbf{d}\omega+\frac{\mathcal{F}\mathcal{G}}{\mathcal{E}}\cosh\alpha\mathbf{d}\sigma \qquad =-\mathcal{G}\sinh\alpha\frac{1}{a_\Lambda}\mathbf{d}u+\mathcal{G}\mathbf{d}\psi, \tag{C1c}$$

$$\mathbf{d}\omega=-\cosh\alpha\mathbf{d}\upsilon+\sinh\alpha\mathbf{d}\xi \qquad =\frac{a_\Lambda}{r^2}\mathbf{d}r, \tag{C1d}$$

$$\mathbf{d}\sigma=\frac{\sinh\alpha}{\mathcal{F}}\mathbf{d}\upsilon+\frac{\cosh\alpha}{\mathcal{G}}\mathbf{d}\xi \qquad =-\frac{\mathcal{E}}{\mathcal{F}}\tanh\alpha\frac{1}{a_\Lambda}\mathbf{d}u-\frac{\tanh\alpha}{\mathcal{F}}\frac{a_\Lambda}{r^2}\mathbf{d}r+\frac{\mathcal{E}}{\mathcal{F}\cosh\alpha}\mathbf{d}\psi, \tag{C1e}$$

$$\frac{1}{a_\Lambda}\mathbf{d}u=\frac{1}{\cosh\alpha}\mathbf{d}\tau+\frac{1}{\mathcal{F}\cosh\alpha}\mathbf{d}\upsilon \qquad =\frac{1}{\cosh\alpha}\mathbf{d}\tau-\frac{1}{\mathcal{E}}\mathbf{d}\omega+\frac{\mathcal{G}}{\mathcal{E}}\tanh\alpha\mathbf{d}\sigma, \tag{C1f}$$

$$\frac{1}{a_\Lambda}\mathbf{d}r=-\frac{\cosh\alpha}{\omega^2}\mathbf{d}\upsilon+\frac{\sinh\alpha}{\omega^2}\mathbf{d}\xi \qquad =\frac{1}{\omega^2}\mathbf{d}\omega, \tag{C1g}$$

$$\sqrt{2}\mathbf{d}\zeta=\tanh\alpha\mathbf{d}\tau+\frac{\tanh\alpha}{\mathcal{F}}\mathbf{d}\upsilon+\frac{1}{\mathcal{G}}\mathbf{d}\xi-i\mathbf{d}\varphi \quad =\tanh\alpha\mathbf{d}\tau+\frac{1}{\cosh\alpha}\mathbf{d}\sigma-i\mathbf{d}\varphi, \tag{C1h}$$

where

$$\mathbf{d}\psi=\frac{1}{\sqrt{2}}(\mathbf{d}\zeta+\mathbf{d}\bar{\zeta}),\quad \mathbf{d}\varphi=\frac{i}{\sqrt{2}}(\mathbf{d}\zeta-\mathbf{d}\bar{\zeta}),\quad \mathbf{d}\zeta=\frac{1}{\sqrt{2}}(\mathbf{d}\psi-i\mathbf{d}\varphi),\quad \mathbf{d}\bar{\zeta}=\overline{\mathbf{d}\zeta}. \tag{C1i}$$

Coordinate vector frames $(\boldsymbol{\partial}_\tau,\boldsymbol{\partial}_\upsilon,\boldsymbol{\partial}_\xi,\boldsymbol{\partial}_\varphi)$, $(\boldsymbol{\partial}_\tau,\boldsymbol{\partial}_\omega,\boldsymbol{\partial}_\sigma,\boldsymbol{\partial}_\varphi)$, and $(\boldsymbol{\partial}_\zeta,\boldsymbol{\partial}_{\bar{\zeta}},\boldsymbol{\partial}_r,\boldsymbol{\partial}_u)$ are related by

$$\boldsymbol{\partial}_\tau=\boldsymbol{\partial}_\tau \qquad =\frac{1}{\cosh\alpha}a_\Lambda\boldsymbol{\partial}_u+\tanh\alpha\boldsymbol{\partial}_\psi, \tag{C2a}$$

$$\boldsymbol{\partial}_\upsilon=-\cosh\alpha\boldsymbol{\partial}_\omega+\frac{\sinh\alpha}{\mathcal{F}}\boldsymbol{\partial}_\sigma \qquad =\frac{1}{\mathcal{F}\cosh\alpha}a_\Lambda\boldsymbol{\partial}_u-\cosh\alpha\frac{r^2}{a_\Lambda}\boldsymbol{\partial}_r+\frac{\tanh\alpha}{\mathcal{F}}\boldsymbol{\partial}_\psi, \tag{C2b}$$

$$\boldsymbol{\partial}_\xi=\sinh\alpha\boldsymbol{\partial}_\omega+\frac{\cosh\alpha}{\mathcal{G}}\boldsymbol{\partial}_\sigma \qquad =\sinh\alpha\frac{r^2}{a_\Lambda}\boldsymbol{\partial}_r+\frac{1}{\mathcal{G}}\boldsymbol{\partial}_\psi, \tag{C2c}$$

$$\boldsymbol{\partial}_\omega=-\frac{\mathcal{F}}{\mathcal{E}}\cosh\alpha\boldsymbol{\partial}_\upsilon+\frac{\mathcal{G}}{\mathcal{E}}\sinh\alpha\boldsymbol{\partial}_\xi \qquad =-\frac{1}{\mathcal{E}}a_\Lambda\boldsymbol{\partial}_u+\frac{r^2}{a_\Lambda}\boldsymbol{\partial}_r, \tag{C2d}$$

$$\boldsymbol{\partial}_\sigma=\frac{\mathcal{F}\mathcal{G}}{\mathcal{E}}\sinh\alpha\boldsymbol{\partial}_\upsilon+\frac{\mathcal{F}\mathcal{G}}{\mathcal{E}}\cosh\alpha\boldsymbol{\partial}_\xi \qquad =\frac{\mathcal{G}}{\mathcal{E}}\tanh\alpha a_\Lambda\boldsymbol{\partial}_u+\frac{1}{\cosh\alpha}\boldsymbol{\partial}_\psi, \tag{C2e}$$

$$a_\Lambda\boldsymbol{\partial}_u=\frac{\mathcal{E}}{\mathcal{F}\cosh\alpha}\boldsymbol{\partial}_\tau-\mathcal{G}\frac{\sinh^2\alpha}{\cosh\alpha}\boldsymbol{\partial}_\upsilon-\mathcal{G}\sinh\alpha\boldsymbol{\partial}_\xi \quad =\frac{\mathcal{E}}{\mathcal{F}\cosh\alpha}\boldsymbol{\partial}_\tau-\frac{\mathcal{E}}{\mathcal{F}}\tanh\alpha\boldsymbol{\partial}_\sigma, \tag{C2f}$$

$$a_\Lambda\boldsymbol{\partial}_r=\frac{\omega^2}{\mathcal{F}\cosh\alpha}\boldsymbol{\partial}_\tau-\frac{\omega^2}{\cosh\alpha}\boldsymbol{\partial}_\upsilon \qquad =\frac{\omega^2}{\mathcal{F}\cosh\alpha}\boldsymbol{\partial}_\tau+\omega^2\boldsymbol{\partial}_\omega-\frac{\tanh\alpha}{\mathcal{F}}\omega^2\boldsymbol{\partial}_\sigma, \tag{C2g}$$

$$\sqrt{2}\boldsymbol{\partial}_\zeta=-\frac{\mathcal{G}}{\mathcal{F}}\tanh\alpha\boldsymbol{\partial}_\tau+\mathcal{G}\tanh\alpha\boldsymbol{\partial}_\upsilon+\mathcal{G}\boldsymbol{\partial}_\xi+i\boldsymbol{\partial}_\varphi \quad =-\frac{\mathcal{G}}{\mathcal{F}}\tanh\alpha\boldsymbol{\partial}_\tau+\frac{\mathcal{E}}{\mathcal{F}\cosh\alpha}\boldsymbol{\partial}_\sigma+i\boldsymbol{\partial}_\varphi, \tag{C2h}$$

where

$$\boldsymbol{\partial}_\psi=\frac{1}{\sqrt{2}}(\boldsymbol{\partial}_\zeta+\boldsymbol{\partial}_{\bar\zeta}),\quad \boldsymbol{\partial}_\varphi=-\frac{i}{\sqrt{2}}(\boldsymbol{\partial}_\zeta-\boldsymbol{\partial}_{\bar\zeta}),\quad \boldsymbol{\partial}_\zeta=\frac{1}{\sqrt{2}}(\boldsymbol{\partial}_\psi+i\boldsymbol{\partial}_\varphi),\quad \boldsymbol{\partial}_{\bar\zeta}=\overline{\boldsymbol{\partial}_\zeta}. \tag{C2i}$$

It is also useful to express the relations between different null tetrads introduced in the paper. The special null tetrad [defined by Eq. (4.7), using Eq. (4.1)] the reference null tetrad [see Eq. (4.13)], and the Robinson-Trautman tetrad (4.26) are related by

$$\begin{aligned}
\mathbf{k}_{\rm s}&=\frac{1}{2}\tan\theta_{\rm s}\Big(\cot\frac{\theta_{\rm s}}{2}\mathbf{k}_{\rm o}+\tan\frac{\theta_{\rm s}}{2}\mathbf{l}_{\rm o}+\mathbf{m}_{\rm o}+\overline{\mathbf{m}}_{\rm o}\Big)=\exp(-\beta_{\rm RT})\sec\theta_{\rm s}\mathbf{k}_{\rm RT},\\
\mathbf{l}_{\rm s}&=\frac{1}{2}\tan\theta_{\rm s}\Big(\tan\frac{\theta_{\rm s}}{2}\mathbf{k}_{\rm o}+\cot\frac{\theta_{\rm s}}{2}\mathbf{l}_{\rm o}+\mathbf{m}_{\rm o}+\overline{\mathbf{m}}_{\rm o}\Big)=\sin\theta_{\rm s}[\exp(-\beta_{\rm RT})\tan\theta_{\rm s}\mathbf{k}_{\rm RT}+\exp(\beta_{\rm RT})\cot\theta_{\rm s}\mathbf{l}_{\rm RT}+\mathbf{m}_{\rm RT}+\overline{\mathbf{m}}_{\rm RT}],\\
\mathbf{m}_{\rm s}&=\frac{1}{2}\tan\theta_{\rm s}\Big(\mathbf{k}_{\rm o}+\mathbf{l}_{\rm o}+\cot\frac{\theta_{\rm s}}{2}\mathbf{m}_{\rm o}+\tan\frac{\theta_{\rm s}}{2}\overline{\mathbf{m}}_{\rm o}\Big)=\mathbf{m}_{\rm RT}+\exp(-\beta_{\rm RT})\tan\theta_{\rm s}\mathbf{k}_{\rm RT},\\
\overline{\mathbf{m}}_{\rm s}&=\frac{1}{2}\tan\theta_{\rm s}\Big(\mathbf{k}_{\rm o}+\mathbf{l}_{\rm o}+\tan\frac{\theta_{\rm s}}{2}\mathbf{m}_{\rm o}+\cot\frac{\theta_{\rm s}}{2}\overline{\mathbf{m}}_{\rm o}\Big)=\overline{\mathbf{m}}_{\rm RT}+\exp(-\beta_{\rm RT})\tan\theta_{\rm s}\mathbf{k}_{\rm RT},
\end{aligned} \tag{C3}$$

$$\begin{aligned}
\mathbf{k}_{\rm RT}&=\frac{1}{2}\exp(\beta_{\rm RT})\sin\theta_{\rm s}\Big(\cot\frac{\theta_{\rm s}}{2}\mathbf{k}_{\rm o}+\tan\frac{\theta_{\rm s}}{2}\mathbf{l}_{\rm o}+\mathbf{m}_{\rm o}+\overline{\mathbf{m}}_{\rm o}\Big)=\exp(\beta_{\rm RT})\cos\theta_{\rm s}\mathbf{k}_{\rm s},\\
\mathbf{l}_{\rm RT}&=\frac{1}{2}\exp(-\beta_{\rm RT})\sin\theta_{\rm s}\Big(\tan\frac{\theta_{\rm s}}{2}\mathbf{k}_{\rm o}+\cot\frac{\theta_{\rm s}}{2}\mathbf{l}_{\rm o}-\mathbf{m}_{\rm o}-\overline{\mathbf{m}}_{\rm o}\Big)=\exp(-\beta_{\rm RT})\tan\theta_{\rm s}(\sin\theta_{\rm s}\mathbf{k}_{\rm s}+\csc\theta_{\rm s}\mathbf{l}_{\rm s}-\mathbf{m}_{\rm s}-\overline{\mathbf{m}}_{\rm s}),\\
\mathbf{m}_{\rm RT}&=\frac{1}{2}\sin\theta_{\rm s}\Big(-\mathbf{k}_{\rm o}+\mathbf{l}_{\rm o}+\cot\frac{\theta_{\rm s}}{2}\mathbf{m}_{\rm o}-\tan\frac{\theta_{\rm s}}{2}\overline{\mathbf{m}}_{\rm o}\Big)=\mathbf{m}_{\rm s}-\sin\theta_{\rm s}\mathbf{k}_{\rm s},\\
\overline{\mathbf{m}}_{\rm RT}&=\frac{1}{2}\sin\theta_{\rm s}\Big(-\mathbf{k}_{\rm o}+\mathbf{l}_{\rm o}-\tan\frac{\theta_{\rm s}}{2}\mathbf{m}_{\rm o}+\cot\frac{\theta_{\rm s}}{2}\overline{\mathbf{m}}_{\rm o}\Big)=\overline{\mathbf{m}}_{\rm s}-\sin\theta_{\rm s}\mathbf{k}_{\rm s}.
\end{aligned} \tag{C4}$$

The factor $\beta_{\rm RT}$ is defined in Eq. (4.28). The rotated null tetrad [cf. Eq. (4.24)] is related to the reference tetrad as

$$\begin{aligned}
\mathbf{k}_{\rm r}&=\frac{1}{2}\sin\theta\Big(\cot\frac{\theta}{2}\mathbf{k}_{\rm o}+\tan\frac{\theta}{2}\mathbf{l}_{\rm o}+\exp(i\phi)\mathbf{m}_{\rm o}+\exp(-i\phi)\overline{\mathbf{m}}_{\rm o}\Big),\\
\mathbf{l}_{\rm r}&=\frac{1}{2}\sin\theta\Big(\tan\frac{\theta}{2}\mathbf{k}_{\rm o}+\cot\frac{\theta}{2}\mathbf{l}_{\rm o}-\exp(i\phi)\mathbf{m}_{\rm o}-\exp(-i\phi)\overline{\mathbf{m}}_{\rm o}\Big),\\
\mathbf{m}_{\rm r}&=\frac{1}{2}\sin\theta\Big(-\mathbf{k}_{\rm o}+\mathbf{l}_{\rm o}+\cot\frac{\theta}{2}\exp(i\phi)\mathbf{m}_{\rm o}-\tan\frac{\theta}{2}\exp(-i\phi)\overline{\mathbf{m}}_{\rm o}\Big),\\
\overline{\mathbf{m}}_{\rm r}&=\frac{1}{2}\sin\theta\Big(-\mathbf{k}_{\rm o}+\mathbf{l}_{\rm o}-\tan\frac{\theta}{2}\exp(i\phi)\mathbf{m}_{\rm o}+\cot\frac{\theta}{2}\exp(-i\phi)\overline{\mathbf{m}}_{\rm o}\Big).
\end{aligned} \tag{C5}$$

Here, the angle $\theta_{\rm s}$ is defined by Eq. (4.18).

APPENDIX D: TRANSFORMATIONS OF THE COMPONENTS Ψ_n AND Φ_n

The components Ψ_n of the Weyl tensor (see [58])

$$\Psi_0=\mathbf{C}_{\kappa\mu\kappa\mu},\quad \Psi_4=\mathbf{C}_{\lambda\bar\mu\lambda\bar\mu},$$

$$\begin{aligned}
\Psi_1&=-\mathbf{C}_{\kappa\mu\mu\bar\mu}=-\mathbf{C}_{\mu\bar\mu\kappa\mu}=\mathbf{C}_{\kappa\lambda\kappa\mu}=\mathbf{C}_{\kappa\mu\kappa\lambda},\\
\Psi_3&=-\mathbf{C}_{\kappa\lambda\lambda\bar\mu}=-\mathbf{C}_{\lambda\bar\mu\kappa\lambda}=\mathbf{C}_{\lambda\bar\mu\mu\bar\mu}=\mathbf{C}_{\mu\bar\mu\lambda\bar\mu},\\
\Psi_2&=-\mathbf{C}_{\kappa\mu\lambda\bar\mu}=-\mathbf{C}_{\lambda\bar\mu\kappa\mu},\\
2\,\mathrm{Re}\,\Psi_2&=\mathbf{C}_{\kappa\lambda\kappa\lambda}=\mathbf{C}_{\mu\bar\mu\mu\bar\mu},\\
2\,\mathrm{Im}\,\Psi_2&=i\mathbf{C}_{\kappa\lambda\mu\bar\mu}=i\mathbf{C}_{\mu\bar\mu\kappa\lambda},
\end{aligned} \tag{D1}$$

and the components Φ_n of tensor of electromagnetic field

$$\Phi_0 = \mathbf{F}_{\kappa\mu}, \quad 2\,\mathrm{Re}\,\Phi_1 = \mathbf{F}_{\kappa\lambda}, \qquad \Phi_2 = \mathbf{F}_{\bar{\mu}\bar{\lambda}}, \quad 2\,\mathrm{Im}\,\Phi_1 = i\mathbf{F}_{\mu\bar{\mu}}, \tag{D2}$$

transform in the well-known way under special Lorentz transformations, see, e.g., Ref. [44].

For a null rotation with **k** fixed,

$$\mathbf{k} = \mathbf{k}_o, \qquad \mathbf{l} = \mathbf{l}_o + \bar{L}\mathbf{m}_o + L\bar{\mathbf{m}}_o + L\bar{L}\mathbf{k}_o, \qquad \mathbf{m} = \mathbf{m}_o + L\mathbf{k}_o, \qquad \bar{\mathbf{m}} = \bar{\mathbf{m}}_o + \bar{L}\mathbf{k}_o, \tag{D3}$$

L being a complex number which parametrize the rotation, the components of the Weyl tensor transform as

$$\Psi_0 = \Psi_0^o,$$
$$\Psi_1 = \bar{L}\Psi_0^o + \Psi_1^o,$$
$$\Psi_2 = \bar{L}^2\Psi_0^o + 2\bar{L}\Psi_1^o + \Psi_2^o, \tag{D4}$$
$$\Psi_3 = \bar{L}^3\Psi_0^o + 3\bar{L}^2\Psi_1^o + 3\bar{L}\Psi_2^o + \Psi_3^o,$$
$$\Psi_4 = \bar{L}^4\Psi_0^o + 4\bar{L}^3\Psi_1^o + 6\bar{L}^2\Psi_2^o + 4\bar{L}\Psi_3^o + \Psi_4^o,$$

and the components of tensor of electromagnetic field transform according to

$$\Phi_0 = \Phi_0^o,$$
$$\Phi_1 = \bar{L}\Phi_0^o + \Phi_1^o, \tag{D5}$$
$$\Phi_2 = \bar{L}^2\Phi_0^o + 2\bar{L}\Phi_1^o + \Phi_2^o.$$

Under a null rotation with **l** fixed,

$$\mathbf{k} = \mathbf{k}_o + \bar{K}\mathbf{m}_o + K\bar{\mathbf{m}}_o + K\bar{K}\mathbf{l}_o, \qquad \mathbf{l} = \mathbf{l}_o, \qquad \mathbf{m} = \mathbf{m}_o + K\mathbf{l}_o, \qquad \bar{\mathbf{m}} = \bar{\mathbf{m}}_o + \bar{K}\mathbf{l}_o, \tag{D6}$$

K being a complex number which parameterize the rotation, the components of the Weyl tensor transform as

$$\Psi_0 = K^4\Psi_4^o + 4K^3\Psi_3^o + 6K^2\Psi_2^o + 4K\Psi_1^o + \Psi_0^o,$$
$$\Psi_1 = K^3\Psi_4^o + 3K^2\Psi_3^o + 3K\Psi_2^o + \Psi_1^o,$$
$$\Psi_2 = K^2\Psi_4^o + 2K\Psi_3^o + \Psi_2^o, \tag{D7}$$
$$\Psi_3 = K\Psi_4^o + \Psi_3^o,$$
$$\Psi_4 = \Psi_4^o,$$

and for electromagnetic field we have

$$\Phi_0 = K^2\Phi_2^o + 2K\Phi_1^o + \Phi_0^o,$$
$$\Phi_1 = K\Phi_2^o + \Phi_1^o, \tag{D8}$$
$$\Phi_2 = \Phi_2^o.$$

A boost in the **n-q**$\equiv$**k-l** plane and a spatial rotation in the **r-s**$\equiv$**m-**$\bar{\mathbf{m}}$ plane is given by

$$\mathbf{k} = B\mathbf{k}_o, \quad \mathbf{l} = B^{-1}\mathbf{l}_o, \qquad \mathbf{m} = \exp(i\Phi)\mathbf{m}_o, \quad \bar{\mathbf{m}} = \exp(-i\Phi)\bar{\mathbf{m}}_o \tag{D9}$$

or, introducing $B = \exp\beta$,

$$\mathbf{n} = \cosh\beta\mathbf{n}_o + \sinh\beta\mathbf{q}_o, \qquad \mathbf{q} = \sinh\beta\mathbf{n}_o + \cosh\beta\mathbf{q}_o, \qquad \mathbf{r} = \cos\Phi\mathbf{r}_o + \sin\Phi\mathbf{s}_o, \qquad \mathbf{s} = -\sin\Phi\mathbf{r}_o + \cos\Phi\mathbf{s}_o, \tag{D10}$$

B, β being real numbers which parametrize the boost, Φ parametrizing an angle of the rotation. The components Ψ_n now transform

$$\Psi_0 = B^2\exp(2i\Phi)\Psi_0^o,$$
$$\Psi_1 = B\exp(i\Phi)\Psi_1^o,$$
$$\Psi_2 = \Psi_2^o, \tag{D11}$$
$$\Psi_3 = B^{-1}\exp(-i\Phi)\Psi_3^o,$$
$$\Psi_4 = B^{-2}\exp(-2i\Phi)\Psi_4^o,$$

and Φ_n transform as

$$\Phi_0 = B\exp(i\Phi)\Phi_0^o,$$
$$\Phi_1 = \Phi_1^o, \tag{D12}$$
$$\Phi_2 = B^{-1}\exp(-i\Phi)\Phi_2^o.$$

[1] H. Bondi, Nature (London) **186**, 535 (1960).
[2] H. Bondi, M. G. J. van der Burg, and A. W. K. Metzner, Proc. R. Soc. London **A269**, 21 (1962).
[3] R. K. Sachs, Proc. R. Soc. London **A270**, 103 (1962).
[4] M. G. J. van der Burg, Proc. R. Soc. London **A310**, 221 (1969).
[5] E. Newman and R. Penrose, J. Math. Phys. **3**, 566 (1962).
[6] E. T. Newman and T. W. J. Unti, J. Math. Phys. **3**, 891 (1962).
[7] R. Sachs, Proc. R. Soc. London **A264**, 309 (1961).
[8] R. Penrose, Proc. R. Soc. London **A284**, 159 (1965).
[9] R. Penrose, in *Relativity, Groups and Topology, Les Houches 1963*, edited by C. DeWitt and B. DeWitt (Gordon and Breach, New York, 1964).
[10] R. Penrose, in *The Nature of Time*, edited by T. Gold (Cornell University Press, Ithaca, NY, 1967), pp. 42–54.
[11] R. Penrose, Phys. Rev. Lett. **10**, 66 (1963).
[12] H. Bondi, F. A. E. Pirani, and I. Robinson, Proc. R. Soc. London **A251**, 519 (1959).
[13] J. Ehlers and W. Kundt, in *Gravitation: an Introduction to Current Research*, edited by L. Witten (John Wiley, New York, 1962), pp. 49–101.
[14] I. Robinson and A. Trautman, Proc. R. Soc. London **A265**, 463 (1962).
[15] W. B. Bonnor and N. S. Swaminarayan, Z. Phys. **177**, 240 (1964).
[16] F. A. E. Pirani, in *Brandeis Lectures on General Relativity*, edited by S. Deser and K. W. Ford (Prentice-Hall, New Jersey, 1965), pp. 249–372.
[17] W. B. Bonnor, J. B. Griffiths, and M. A. H. MacCallum, Gen. Relativ. Gravit. **26**, 687 (1994).
[18] J. Bičák, in *Galaxies, Axisymmetric Systems and Relativity*, edited by M. A. H. MacCallum (Cambridge University Press, Cambridge, 1985), pp. 91–124.
[19] J. Bičák, in *Relativistic Gravitation and Gravitational Radiation, Les Louches 1995*, edited by J.-A. Marck and J.-P. Lasota (Cambridge University Press, Cambridge, 1997), pp. 67–87.
[20] J. Bičák, in *Einstein's Field Equations and Their Physical Implications*, edited by B. G. Schmidt, Vol. 540 (Springer, Berlin, 2000), pp. 1–126.
[21] J. Bičák and P. Krtouš, Phys. Rev. D **64**, 124020 (2001).
[22] J. Bičák and P. Krtouš, Phys. Rev. Lett. **88**, 211101 (2002).
[23] J. Bičák and P. Krtouš (unpublished).
[24] J. Bičák and B. G. Schmidt, Phys. Rev. D **40**, 1827 (1989).
[25] T. Levi-Civita, Rend. Acc. Lincei **26**, 307 (1917).
[26] H. Weyl, Ann. Phys. (Leipzig) **59**, 185 (1918).
[27] W. Kinnersley and M. Walker, Phys. Rev. D **2**, 1359 (1970).
[28] W. B. Bonnor, Gen. Relativ. Gravit. **15**, 535 (1983).
[29] J. Bičák and V. Pravda, Phys. Rev. D **60**, 044004 (1999).
[30] P. S. Letelier and S. R. Oliveira, Phys. Rev. D **64**, 064005 (2001).
[31] V. Pravda and A. Pravdová, Czech. J. Phys. **50**, 333 (2000).
[32] J. Plebański and M. Demiański, Ann. Phys. (N.Y.) **98**, 98 (1976).
[33] B. Carter, Commun. Math. Phys. **10**, 280 (1968).
[34] R. Debever, Bull. Soc. Math. Belg. **23**, 360 (1971).
[35] R. B. Mann and S. F. Ross, Phys. Rev. D **52**, 2254 (1995).
[36] J. Podolský and J. B. Griffiths, Phys. Rev. D **63**, 024006 (2001).
[37] O. J. C. Dias and J. P. S. Lemos, Phys. Rev. D **67**, 064001 (2003).
[38] O. J. C. Dias and J. P. S. Lemos, Phys. Rev. D **67**, 084018 (2003).
[39] We use here the unit conventions of Ref. [40] (which is somewhat different from Ref. [44], namely, we assume "geometrical" values of the gravitational constant $\varkappa=8\pi$, and of the electric permittivity $\varepsilon=1/(4\pi)$. These constants are fixed by the Einstein equation $\mathrm{Ein}=\varkappa\mathbf{T}$, and the Maxwell equation $\nabla\cdot\mathbf{F}=(1/\varepsilon)\mathbf{J}$. Both the mass and the charge thus have the dimension of length. The constants $\varkappa$, ε can be explicitly reinserted into the expressions using a dimensional analysis with the help of relations $1\,\mathrm{m}=\varkappa/(8\pi)\times 1\,\mathrm{kg}$, and $1\,\mathrm{m}=\sqrt{\varkappa/(32\pi^2\varepsilon)}\times 1\,\mathrm{C}$. For example, $G=1-x^2-\varkappa m/(4\pi)Ax^3+\varkappa e^2/(32\pi^2\varepsilon)A^2x^4$, with the mass m measured in kg and the charge e in C. Note, however, that because the tensor of electromagnetic field $\mathbf{F}_{\alpha\beta}$ is not dimensionless, we, in fact, obtain $\mathbf{F}=e/(4\pi\varepsilon)\mathbf{d}y\wedge\mathbf{d}t$. (Of course, $c=1$ is always assumed here.)
[40] C. W. Misner, K. S. Thorne, and J. A. Wheeler, *Gravitation* (Freeman, San Francisco, 1973).
[41] A *symmetric product* $\vee$ of two one-forms is defined as $\mathbf{a}\vee\mathbf{b}=\mathbf{ab}+\mathbf{ba}$. For example, the metric (2.14) written in a more common (but less precise) notation would read $\boldsymbol{g}=2(r^2/P^2)\mathbf{d}\zeta\mathbf{d}\bar{\zeta}-2\mathbf{d}u\mathbf{d}r-H\mathbf{d}u^2$.
[42] R. Penrose and W. Rindler, *Spinors and Space-time* (Cambridge University Press, Cambridge, England, 1984).
[43] A. Vilenkin and E. P. S. Shellard, *Cosmic Strings and other Topological Defects* (Cambridge University Press, Cambridge, 1994).
[44] D. Kramer, H. Stephani, E. Herlt, and M. MacCallum, *Exact Solutions of Einstein's Field Equation* (Cambridge University Press, Cambridge, 1980).
[45] The four-momentum $\mathbf{p}=Dz/d\tilde{\eta}$ of the ray is a tangent vector with respect to a physical dimensionless affine parameter $\tilde{\eta}$. Since we are not interested in dynamical properties of the rays but rather in behavior of fields at "large distances," we are using the affine parameter η which has the dimension of length. The relation between this "distance" parameter η and the physical parameter $\tilde{\eta}$ which determines energy can conventionally be chosen as $\eta=a_\Lambda\tilde{\eta}$. Therefore, $\mathbf{p}=a_\Lambda(Dz/d\eta)$.
[46] We cannot define here "the same proximity to $\mathcal{I}^+$" using some fixed value of the affine parameter η, since we wish to use this procedure to determine the specific normalization of the affine parameter.
[47] A general choice of final conditions at infinity might cause a degenerated values of the vector $\mathbf{k}_i$ in finite domains of the spacetime.
[48] In fact, Ref. [22] use a different notation for quantities defined in the present paper. When comparing the angular dependence of Eq. (15) of Ref. [22] with Eq. (5.23) it is necessary to use the following dictionary: $\alpha\to a_\Lambda$, $a_o\to A$, $\vartheta_*\to\theta$, $\varphi\to\phi$, and $a_o\alpha/\sqrt{1+a_o^2\alpha^2}\sin\vartheta_+\to\sin\theta_s$. In the case $m=0$, $e=0$ we can also identify $\vartheta_+\to\Theta_{dS}$ and express χ_+ of Ref. [22] in terms of R_{dS} and T_{dS}. The normalization of Eq. (5.23) and of the result of Ref. [22] does not coincide due to different choice of initial conditions for the interpretation tetrads here and in Ref. [22] (cf. Sec. VII). Let us also note that Ref. [22] uses the

unit convention $\varepsilon=1$ in the sense of [39] instead of $\varepsilon=1/(4\pi)$ used here.
[49] This method has been used in Ref. [22].
[50] S. Deser and O. Levin, Phys. Rev. D **59**, 064004 (1999).
[51] P. Krtouš, J. Podolský, and J. Bičák, Phys. Rev. Lett. (to be published).
[52] J. Podolský, Czech. J. Phys. **52**, 1 (2002).
[53] D. R. Brill and S. A. Hayward, Class. Quantum Grav. **11**, 359 (1994).
[54] J. Podolský, Ph.D. thesis, Charles University, Prague, Czech Republic, 1993.
[55] S. W. Hawking and G. F. R. Ellis, *The Large Scale Structure of Space-time* (Cambridge University Press, Cambridge, 1973).
[56] M. Walker, J. Math. Phys. **11**, 2280 (1970).
[57] Notice the difference between υ (v) and $\boldsymbol{\upsilon}$ (upsilon). Fortunately, υ is used only here, as an intermediate step, and in Fig. 3 where the ranges of null coordinates are indicated.
[58] Here, e.g., $\mathbf{C}_{\kappa\lambda\mu\bar{\mu}}=\mathbf{C}_{\alpha\beta\gamma\delta}\mathbf{k}^{\alpha}\mathbf{l}^{\beta}\mathbf{m}^{\gamma}\bar{\mathbf{m}}^{\delta}$.

VOLUME 91, NUMBER 6 PHYSICAL REVIEW LETTERS week ending 8 AUGUST 2003

Gravitational and Electromagnetic Fields near a de Sitter–Like Infinity

Pavel Krtouš, Jiří Podolský, and Jiří Bičák

Institute of Theoretical Physics, Faculty of Mathematics and Physics, Charles University in Prague, V Holešovičkách 2, 180 00 Prague 8, Czech Republic

(Received 30 May 2003; published 8 August 2003)

We present a characterization of general gravitational and electromagnetic fields near de Sitter–like conformal infinity which supplements the standard peeling behavior. This is based on an explicit evaluation of the dependence of the radiative component of the fields on the null direction from which infinity is approached. It is shown that the directional pattern of radiation has a universal character that is determined by the algebraic (Petrov) type of the spacetime. Specifically, the radiation field vanishes along directions opposite to principal null directions.

DOI: 10.1103/PhysRevLett.91.061101 PACS numbers: 04.20.Ha, 04.40.Nr, 98.80.Jk

A direct observation of gravitational waves will be properly understood only when it can be compared with reliable predictions supplied by numerical relativity. To make such predictions is difficult since, among other things, no rigorous statements are available which relate the properties of sufficiently general strong sources to the radiation fields produced. Only a few explicit radiative solutions of Einstein's equations are known which can be used as test beds for numerical codes (see, e.g., [1,2]), in particular, spacetimes representing "uniformly accelerated particles or black holes." These have also been the main inspiration for our present analysis of the general asymptotic properties of radiation in spacetimes with a positive cosmological constant Λ. The motivation for considering de Sitter–like universes arises not only by their role in inflationary theories but also by the fact that many *nonvacuum* cosmological models with $\Lambda > 0$ (as suggested by recent observations) approach the de Sitter universe asymptotically in time ("cosmic no-hair conjecture") and hence have a de Sitter–like infinity.

We have recently constructed the test fields of uniformly accelerated charges in de Sitter spacetime (the Born solutions generalized for $\Lambda > 0$) and investigated how their radiative properties depend on the way in which infinity is approached [3]. Somewhat surprisingly, we have found analogous results [4] in the case of the exact solution of the Einstein-Maxwell equations with $\Lambda > 0$, namely, the "charged C-metric" describing a pair of charged accelerated black holes in a de Sitter universe.

In the following, we shall demonstrate that the directional pattern of radiation near an infinity of de Sitter type has a universal character that is determined by the algebraic (Petrov) type of the spacetime. In spacetimes which are asymptotically de Sitter, there are two disjoint past and future (conformal) infinities $\mathcal{I}^-$ and $\mathcal{I}^+$, both spacelike [5,6]. In such spacetimes both cosmological horizons and event horizons for geodesic observers occur and, consequently, advanced effects have to be present if the fields are smooth [7]. Curiously enough, with $\Lambda > 0$ the global existence has been established of asymptotically simple vacuum solutions which differ on an arbitrary given Cauchy surface by a finite but sufficiently small amount from de Sitter data [8], while an analogous result for data close to Minkowski ($\Lambda = 0$) is still under investigation [2,8]. Thus, many vacuum asymptotically simple spacetimes with de Sitter–like $\mathcal{I}^+$ do exist. Assuming their existence, Penrose proved already in 1965 [5,6] that both the gravitational and the electromagnetic fields satisfy the peeling-off property with respect to null geodesics reaching any point of $\mathcal{I}^+$. This means that along a null geodesic parametrized by an affine parameter η, the part of any spin-s zero rest-mass field proportional to $\eta^{-(k+1)}$, $k = 0, 1, \ldots, 2s$, has, in general, $2s - k$ coincident principal null directions. In particular, the part of the field that falls off as η^{-1} is a *radiation* ("null") *field*. The peeling-off property is easier to prove with $\Lambda > 0$ than in asymptotically Minkowskian spacetimes when $\mathcal{I}^+$ is a null hypersurface [5]. With a spacelike $\mathcal{I}^+$, however, one can approach any point on $\mathcal{I}^+$ from infinitely many different null directions and, consequently, the radiation field becomes mixed up with other components of the field when the null geodesic is changed. This fact of the "origin dependence" of the radiation field in the case of a spacelike $\mathcal{I}^+$ has been repeatedly emphasized by Penrose [5,6]. Exactly this *directional radiation pattern*, i.e., the dependence of fields (with respect to appropriate tetrad) on the direction along which the null geodesic reaches a point on a spacelike $\mathcal{I}^+$, is analyzed in the present work.

Following general formalism [5,6], a spacetime $\mathcal{M}$ with physical metric $\boldsymbol{g}$ can be embedded into a larger *conformal manifold* $\widetilde{\mathcal{M}}$ with *conformal metric* $\tilde{\boldsymbol{g}}$ related to $\boldsymbol{g}$ by $\tilde{\boldsymbol{g}} = \omega^2 \boldsymbol{g}$. Here, the conformal factor ω, negative in $\mathcal{M}$, vanishes on the boundary of $\mathcal{M}$ in $\widetilde{\mathcal{M}}$ called conformal infinity $\mathcal{I}$. It is *spacelike* if the gradient $\mathbf{d}\omega$ on $\mathcal{I}$ has timelike character. This may be either future infinity $\mathcal{I}^+$ or past infinity $\mathcal{I}^-$. Near $\mathcal{I}^+$ we decompose $\tilde{\boldsymbol{g}}$ into a spatial 3-metric ${}^{\mathcal{I}}\tilde{\boldsymbol{g}}$ tangent to $\mathcal{I}^+$ and a part orthogonal to $\mathcal{I}^+$:

$$\boldsymbol{g} = \omega^{-2}(-\tilde{N}^2 \mathbf{d}\omega^2 + {}^{\mathcal{I}}\tilde{\boldsymbol{g}}). \tag{1}$$

The conformal lapse function $\tilde{N}$ can be chosen to be constant on $\mathcal{I}^+$, e.g., equal to $\ell = \sqrt{3/\Lambda}$. The form (1) allows us to define a timelike unit vector $\mathbf{n}$ normal to $\mathcal{I}^+$,

 0031-9007/03/91(6)/061101(4)$20.00

$$\mathbf{n}^{\mu} = \omega^{-1}\tilde{N}\boldsymbol{g}^{\mu\nu}\mathbf{d}_{\nu}\omega. \tag{2}$$

Next, we denote the vectors of an *orthonormal* tetrad as $\mathbf{t}$, $\mathbf{q}$, $\mathbf{r}$, $\mathbf{s}$, where $\mathbf{t}$ is a unit timelike vector and the remaining three are unit spacelike vectors. With this tetrad we associate a *null* tetrad $\mathbf{k}$, $\mathbf{l}$, $\mathbf{m}$, $\bar{\mathbf{m}}$, such that $\mathbf{k}\cdot\mathbf{l} = -1$, $\mathbf{m}\cdot\bar{\mathbf{m}} = 1$,

$$\begin{aligned} \mathbf{k} &= (\mathbf{t}+\mathbf{q})/\sqrt{2}, & \mathbf{l} &= (\mathbf{t}-\mathbf{q})/\sqrt{2}, \\ \mathbf{m} &= (\mathbf{r}-i\,\mathbf{s})/\sqrt{2}, & \bar{\mathbf{m}} &= (\mathbf{r}+i\,\mathbf{s})/\sqrt{2}. \end{aligned} \tag{3}$$

Various specific tetrads introduced below will be distinguished by an additional label in subscript.

As usual, we parametrize the Weyl tensor $\mathbf{C}_{\alpha\beta\gamma\delta}$ (representing the gravitational field) by five complex coefficients

$$\begin{aligned} \Psi_0 &= \mathbf{C}_{\alpha\beta\gamma\delta}\mathbf{k}^{\alpha}\mathbf{m}^{\beta}\mathbf{k}^{\gamma}\mathbf{m}^{\delta}, & \Psi_1 &= \mathbf{C}_{\alpha\beta\gamma\delta}\mathbf{k}^{\alpha}\mathbf{l}^{\beta}\mathbf{k}^{\gamma}\mathbf{m}^{\delta}, \\ \Psi_2 &= -\mathbf{C}_{\alpha\beta\gamma\delta}\mathbf{k}^{\alpha}\mathbf{m}^{\beta}\mathbf{l}^{\gamma}\bar{\mathbf{m}}^{\delta}, & \Psi_3 &= \mathbf{C}_{\alpha\beta\gamma\delta}\mathbf{l}^{\alpha}\mathbf{k}^{\beta}\mathbf{l}^{\gamma}\bar{\mathbf{m}}^{\delta}, \\ & & \Psi_4 &= \mathbf{C}_{\alpha\beta\gamma\delta}\mathbf{l}^{\alpha}\bar{\mathbf{m}}^{\beta}\mathbf{l}^{\gamma}\bar{\mathbf{m}}^{\delta}, \end{aligned} \tag{4}$$

and the electromagnetic field $\mathbf{F}_{\alpha\beta}$ by three coefficients

$$\begin{aligned} \Phi_0 &= \mathbf{F}_{\alpha\beta}\mathbf{k}^{\alpha}\mathbf{m}^{\beta}, & \Phi_2 &= \mathbf{F}_{\alpha\beta}\bar{\mathbf{m}}^{\alpha}\mathbf{l}^{\beta}, \\ & & \Phi_1 &= \frac{1}{2}\mathbf{F}_{\alpha\beta}(\mathbf{k}^{\alpha}\mathbf{l}^{\beta} - \mathbf{m}^{\alpha}\bar{\mathbf{m}}^{\beta}). \end{aligned} \tag{5}$$

These simply transform under special Lorentz transformations — null rotations with $\mathbf{k}$ or $\mathbf{l}$ fixed, boosts in $\mathbf{k}$-$\mathbf{l}$ plane, and spatial rotations in $\mathbf{m}$-$\bar{\mathbf{m}}$ plane. For instance, under a null rotation with $\mathbf{l}$ fixed, parametrized by $K \in \mathbb{C}$:

$$\begin{aligned} \mathbf{l} &= \mathbf{l}_{\mathrm{o}}, & \mathbf{k} &= \mathbf{k}_{\mathrm{o}} + \bar{K}\,\mathbf{m}_{\mathrm{o}} + K\,\bar{\mathbf{m}}_{\mathrm{o}} + K\bar{K}\,\mathbf{l}_{\mathrm{o}}, \\ & & \mathbf{m} &= \mathbf{m}_{\mathrm{o}} + K\,\mathbf{l}_{\mathrm{o}}, & \bar{\mathbf{m}} &= \bar{\mathbf{m}}_{\mathrm{o}} + \bar{K}\,\mathbf{l}_{\mathrm{o}}, \end{aligned} \tag{6}$$

$$\begin{aligned} \Psi_0 &= K^4\Psi_4^{\mathrm{o}} + 4K^3\Psi_3^{\mathrm{o}} + 6K^2\Psi_2^{\mathrm{o}} + 4K\Psi_1^{\mathrm{o}} + \Psi_0^{\mathrm{o}}, \\ \Phi_0 &= K^2\Phi_2^{\mathrm{o}} + 2K\Phi_1^{\mathrm{o}} + \Phi_0^{\mathrm{o}}. \end{aligned} \tag{7}$$

Similarly, null rotations with $\mathbf{k}$ fixed can be parametrized by $L \in \mathbb{C}$. For boosts in $\mathbf{k}$-$\mathbf{l}$ plane, cf. Eqs. (12) and (13). For details and notation, see, e.g., Refs. [4,9].

Our goal is to investigate the field components in an appropriate interpretation tetrad parallelly transported along all null geodesics $z(\eta)$ which terminate at $\mathcal{I}^+$ at a point P_+. A geodesic reaches $\mathcal{I}^+$ at an infinite value of the affine parameter η. The conformal factor ω and lapse $\tilde{N}$ can be expanded along the geodesic in powers of $1/\eta$:

$$\omega \approx \omega_* \eta^{-1} + \cdots, \qquad \tilde{N} \approx \tilde{N}_+ + \ldots. \tag{8}$$

The value $\tilde{N}_+ = \tilde{N}\,|_{P_+}$ is the same for all geodesics ending at point P_+. We require that the approach of geodesics to $\mathcal{I}^+$ is "comparable," independent of their *direction,* so we assume also ω_* to be constant. This is equivalent to fixing the energy $E_{\mathrm{o}} = -\mathbf{p}\cdot\mathbf{n}$ ($\mathbf{p} = \frac{Dz}{d\eta}$ being 4-momentum) at a given small value of ω, i.e., at a given proximity from the conformal infinity [4].

To define an *interpretation null tetrad* $\mathbf{k}_{\mathrm{i}}$, $\mathbf{l}_{\mathrm{i}}$, $\mathbf{m}_{\mathrm{i}}$, $\bar{\mathbf{m}}_{\mathrm{i}}$, we have to specify it in a comparable way for all geodesics along different directions. The geodesics reach the same point P_+ and we prescribe its form there. We require the null vector $\mathbf{k}_{\mathrm{i}}$ to be proportional to the tangent vector of the geodesic,

$$\mathbf{k}_{\mathrm{i}} = \frac{1}{\sqrt{2}\tilde{N}_+}\,\frac{Dz}{d\eta}; \tag{9}$$

the factor is again chosen independent of the direction. The null vector $\mathbf{l}_{\mathrm{i}}$ is fixed by $\mathbf{k}_{\mathrm{i}}\cdot\mathbf{l}_{\mathrm{i}} = -1$ and by the requirement that the normal vector $\mathbf{n}$ belongs to the $\mathbf{k}_{\mathrm{i}}$-$\mathbf{l}_{\mathrm{i}}$ plane. The vectors $\mathbf{m}_{\mathrm{i}}$, $\bar{\mathbf{m}}_{\mathrm{i}}$ (or, $\mathbf{r}_{\mathrm{i}}$, $\mathbf{s}_{\mathrm{i}}$) cannot be specified canonically—they will be chosen by Eqs. (12) and (16).

Now, the projection of $\mathbf{k}_{\mathrm{i}}$ on the normal $\mathbf{n}$ is

$$-\mathbf{k}_{\mathrm{i}}\cdot\mathbf{n} \approx (1/\sqrt{2})\eta^{-1}, \tag{10}$$

so that, as $\eta \to \infty$, the interpretation tetrad is "infinitely boosted" with respect to an observer with 4-velocity $\mathbf{n}$. To see this explicitly, we introduce an auxiliary tetrad $\mathbf{t}_{\mathrm{r}}$, $\mathbf{q}_{\mathrm{r}}$, $\mathbf{r}_{\mathrm{r}}$, $\mathbf{s}_{\mathrm{r}}$ adapted to the conformal infinity, $\mathbf{t}_{\mathrm{r}} = \mathbf{n}$, with $\mathbf{q}_{\mathrm{r}}$ oriented along the spatial direction of the geodesic,

$$\mathbf{q}_{\mathrm{r}} \propto \mathbf{k}_{\mathrm{i}}^{\perp} = (\mathbf{k}_{\mathrm{i}}\cdot\mathbf{n})\,\mathbf{n} + \mathbf{k}_{\mathrm{i}}, \tag{11}$$

and we choose the remaining spatial vectors $\mathbf{r}_{\mathrm{r}}$, $\mathbf{s}_{\mathrm{r}}$ to coincide with those of the interpretation tetrad. Using Eqs. (8) and (9) and the definition of $\mathbf{l}_{\mathrm{i}}$, we get

$$\begin{aligned} \mathbf{k}_{\mathrm{i}} &= B_{\mathrm{i}}\,\mathbf{k}_{\mathrm{r}} = \eta^{-1}(\mathbf{n}+\mathbf{q}_{\mathrm{r}})/\sqrt{2}, & \mathbf{m}_{\mathrm{i}} &= \mathbf{m}_{\mathrm{r}}, \\ \mathbf{l}_{\mathrm{i}} &= B_{\mathrm{i}}^{-1}\,\mathbf{l}_{\mathrm{r}} = \eta(\mathbf{n}-\mathbf{q}_{\mathrm{r}})/\sqrt{2}, & \bar{\mathbf{m}}_{\mathrm{i}} &= \bar{\mathbf{m}}_{\mathrm{r}}, \end{aligned} \tag{12}$$

$B_{\mathrm{i}} = 1/\eta$ being the boost parameter. Under such a boost the field components (4) and (5) transform as [4,9]

$$\Psi_j^{\mathrm{i}} = B_{\mathrm{i}}^{2-j}\,\Psi_j^{\mathrm{r}}, \qquad \Phi_j^{\mathrm{i}} = B_{\mathrm{i}}^{1-j}\,\Phi_j^{\mathrm{r}}. \tag{13}$$

Together with behavior (22) of the field components in a tetrad adapted to $\mathcal{I}^+$ we obtain the *peeling-off property.*

We shall now derive the directional dependence of radiation near a point P_+ at $\mathcal{I}^+$. It is necessary to parametrize the direction of the null geodesic reaching P_+. This can be done with respect to a suitable *reference tetrad* $\mathbf{t}_{\mathrm{o}}$, $\mathbf{q}_{\mathrm{o}}$, $\mathbf{r}_{\mathrm{o}}$, $\mathbf{s}_{\mathrm{o}}$, with the time vector $\mathbf{t}_{\mathrm{o}}$ adapted to the conformal infinity, $\mathbf{t}_{\mathrm{o}} = \mathbf{n}$, and spatial directions chosen arbitrarily. It is convenient to choose them in accordance with the spacetime geometry. Privileged choices will be discussed later (cf. Fig. 1).

The unit spatial direction $\mathbf{q}_{\mathrm{r}}$ of a general null geodesic near $\mathcal{I}^+$ can be expressed in terms of *spherical angles* θ, ϕ, with respect to the reference tetrad,

$$\mathbf{q}_{\mathrm{r}} = \cos\theta\;\mathbf{q}_{\mathrm{o}} + \sin\theta\cos\phi\;\mathbf{r}_{\mathrm{o}} + \sin\theta\sin\phi\;\mathbf{s}_{\mathrm{o}}. \tag{14}$$

It is useful to introduce the *stereographic representation* of the angles θ, ϕ

$$R = \tan(\theta/2)\exp(-i\phi). \tag{15}$$

VOLUME 91, NUMBER 6 PHYSICAL REVIEW LETTERS week ending 8 AUGUST 2003

Then the null rotation (6) with $K = R$ transforms $\mathbf{k}_o$ into $\mathbf{k}$ with its spatial direction $\mathbf{k}^\perp \propto \mathbf{q}_r$ specified by θ, ϕ.

Now, the interpretation tetrad is related by boost (12) to the tetrad $\mathbf{t}_r$, $\mathbf{q}_r$, $\mathbf{r}_r$, $\mathbf{s}_r$, which is a spatial rotation of the reference tetrad. If we choose

$$\mathbf{r}_r = -\sin\theta\cos\phi\left[\mathbf{q}_o + \tan\frac{\theta}{2}(\cos\phi\ \mathbf{r}_o + \sin\phi\ \mathbf{s}_o)\right] + \mathbf{r}_o,$$
$$\mathbf{s}_r = -\sin\theta\cos\phi\left[\mathbf{q}_o + \tan\frac{\theta}{2}(\cos\phi\ \mathbf{r}_o + \sin\phi\ \mathbf{s}_o)\right] + \mathbf{s}_o, \tag{16}$$

the spatial rotation is a composition of the null rotations with $\mathbf{l}$ fixed, $\mathbf{k}$ fixed, and the boost, given by parameters $K = R$, $L = -R/(1 + |R|^2)$, $B = (1 + |R|^2)^{-1}$. This decomposition into elementary Lorentz transformations enables us to calculate the field components in the interpretation tetrad. We start with Ψ_j^o, or Φ_j^o in the reference tetrad and we characterize these in terms of algebraically privileged *principal null directions* (PNDs).

Principal null directions of the gravitational (or electromagnetic) field are null directions $\mathbf{k}$ such that $\Psi_0 = 0$ (or $\Phi_0 = 0$) in a null tetrad $\mathbf{k}, \mathbf{l}, \mathbf{m}, \bar{\mathbf{m}}$ (a choice of $\mathbf{l}, \mathbf{m}, \bar{\mathbf{m}}$ is irrelevant). In the tetrad related to the reference tetrad by null rotation (6), such a condition for Ψ_0 takes the form of a quartic (or quadratic for Φ_0) equation for K, cf. Eqs. (7). The roots $K = R_n$, $n = 1, 2, 3, 4$ (or $K = R_n^E$, $n = 1, 2$) of this equation thus parametrize PNDs $\mathbf{k}_n$ (or $\mathbf{k}_n^E$). As follows from the note after Eq. (15), the angles θ_n, ϕ_n of these PNDs are related to R_n exactly by Eq. (15).

In a generic situation we have $\Psi_4^o \neq 0$ (or $\Phi_2^o \neq 0$), and we can express the remaining components of the Weyl (or electromagnetic) tensor in terms of roots R_n (or R_n^E)

$$\Psi_3^o = -\tfrac{1}{4}\Psi_4^o(R_1 + R_2 + R_3 + R_4),$$
$$\Psi_2^o = \tfrac{1}{6}\Psi_4^o(R_1R_2 + R_1R_3 + R_1R_4 + R_2R_3 + R_2R_4 + R_3R_4),$$
$$\Psi_1^o = -\tfrac{1}{4}\Psi_4^o(R_1R_2R_3 + R_1R_2R_4 + R_1R_3R_4 + R_2R_3R_4),$$
$$\Psi_0^o = \Psi_4^o R_1R_2R_3R_4, \tag{17}$$

$$\Phi_1^o = -\tfrac{1}{2}\Phi_2^o(R_1^E + R_2^E), \qquad \Phi_0^o = \Phi_2^o R_1^E R_2^E. \tag{18}$$

Transforming these to tetrad $\mathbf{k}_r$, $\mathbf{l}_r$, $\mathbf{m}_r$, $\bar{\mathbf{m}}_r$, we obtain

$$\Psi_4^r = \Psi_4^o(1 + |R|^2)^{-2} \times \left(1 - \frac{R_1}{R_a}\right)\left(1 - \frac{R_2}{R_a}\right)\left(1 - \frac{R_3}{R_a}\right)\left(1 - \frac{R_4}{R_a}\right), \tag{19}$$

$$\Phi_2^r = \Phi_2^o(1 + |R|^2)^{-1}\left(1 - \frac{R_1^E}{R_a}\right)\left(1 - \frac{R_2^E}{R_a}\right). \tag{20}$$

Here, the complex number R_a,

$$R_a = -\bar{R}^{-1} = -\cot(\theta/2)\ \exp(-i\phi), \tag{21}$$

characterizes a spatial direction *opposite* to the direction given by R, i.e., the *antipodal* direction with $\theta_a = \pi - \theta$ and $\phi_a = \phi + \pi$. Finally, we express the leading term of the field components in the interpretation tetrad. The freedom in the choice of the vectors $\mathbf{m}_i$, $\bar{\mathbf{m}}_i$ changes just a phase of the field components, so only their modulus has a physical meaning. It is also known [5,6] that as a consequence of field equations, field components in a reference tetrad near $\mathcal{I}^+$ behave as

$$\Psi_j^o \approx \Psi_{j*}^o \eta^{-3}, \qquad \Phi_j^o \approx \Phi_{j*}^o \eta^{-2}. \tag{22}$$

Combining Eqs. (13), (20), and (19), we thus obtain

$$|\Psi_4^i| \approx |\Psi_{4*}^o|\eta^{-1}\cos^4(\theta/2) \times \left|1 - \frac{R_1}{R_a}\right|\left|1 - \frac{R_2}{R_a}\right|\left|1 - \frac{R_3}{R_a}\right|\left|1 - \frac{R_4}{R_a}\right|, \tag{23}$$

$$|\Phi_2^i| \approx |\Phi_{2*}^o|\eta^{-1}\cos^4(\theta/2)\left|1 - \frac{R_1^E}{R_a}\right|\left|1 - \frac{R_2^E}{R_a}\right|. \tag{24}$$

These expressions characterize the asymptotic behavior of fields near de Sitter–like infinity. In a general spacetime there are *four* spatial directions along which the radiative component of the gravitational field Ψ_4^i vanishes, namely, directions $R_a = R_n$, $n = 1, 2, 3, 4$ (or *two* such directions for electromagnetic field Φ_2^i). In fact, their spatial parts $-\mathbf{k}_n^\perp$ are exactly *opposite to the projections of the principal null directions* $\mathbf{k}_n^\perp$ *onto* $\mathcal{I}^+$.

In algebraically special spacetimes, some PNDs coincide and Eq. (23) simplifies. Moreover, it is always possible to choose the "canonical" reference tetrad: (i) the vector $\mathbf{q}_o$ oriented along the spatial projection of the *degenerate* (multiple) PND, say $\mathbf{k}_4^\perp$ (i.e., $\mathbf{k}_o \propto \mathbf{k}_4$); (ii) the $\mathbf{q}_o$-$\mathbf{r}_o$ plane oriented so that it contains the spatial projection of one of the remaining PNDs (for type N spacetimes this choice is arbitrary). Using such a reference tetrad, the degenerate PND $\mathbf{k}_4^\perp$ is given by $\theta_4 = 0$, i.e., $R_4 = 0$ [cf. Eq. (15)], whereas one of the remaining PNDs, say $\mathbf{k}_1^\perp$, has $\phi_1 = 0$, i.e., $R_1 = \tan\frac{\theta_1}{2}$ is real.

Thus, for Petrov type N spacetimes (with quadruple PND) $R_1 = R_2 = R_3 = R_4 = 0$, so the asymptotic behavior of gravitational field (23) becomes

$$|\Psi_4^i| = |\Psi_{4*}^o|\eta^{-1}\cos^4\frac{\theta}{2}. \tag{25}$$

The corresponding directional pattern of radiation is illustrated in Fig. 1(N). It is axisymmetric, with a maximum value at $\theta = 0$ along the spatial projection of the quadruple PND onto $\mathcal{I}^+$. Along the opposite direction, $\theta = \pi$, the field vanishes.

In the Petrov type III spacetimes, $R_1 = \tan\frac{\theta_1}{2}$, $R_2 = R_3 = R_4 = 0$, so (23) implies

$$|\Psi_4^i| = |\Psi_{4*}^o|\eta^{-1}\cos^4\frac{\theta}{2}\left|1 + \tan\frac{\theta_1}{2}\ \tan\frac{\theta}{2}\ e^{i\phi}\right|. \tag{26}$$

The directional pattern of radiation is shown in Fig. 1(III). The field vanishes along $\theta = \pi$ and along $\theta = \pi - \theta_1$, $\phi = \pi$ which are spatial directions opposite to the PNDs.

VOLUME 91, NUMBER 6 PHYSICAL REVIEW LETTERS week ending 8 AUGUST 2003

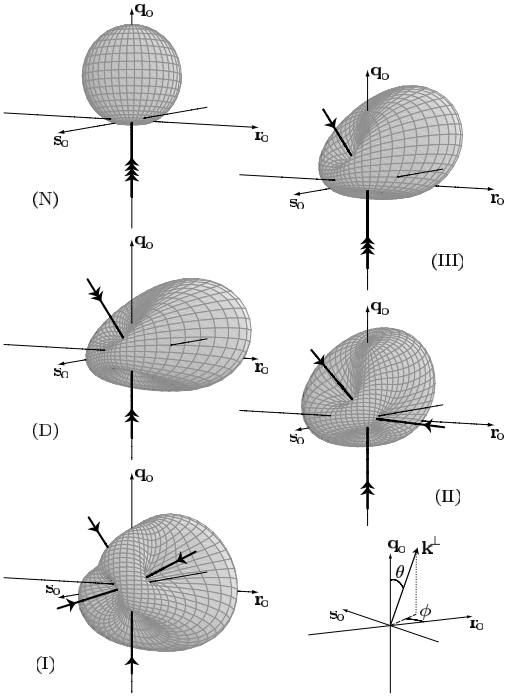

FIG. 1. Specific directional patterns of radiation for spacetimes of Petrov types N, III, D, II, and I. Directions in the diagrams represent all spatial directions tangent to $\mathcal{I}^+$. For each type, the radiative component $|\Psi_4^i|$ along a null geodesic is depicted in the corresponding spatial direction $\mathbf{k}^\perp$ parametrized by spherical angles θ, ϕ. [Degenerate] principal null directions (PNDs) are indicated by [multiple] bold arrows. Thick lines represent spatial directions (opposite to PNDs) along which the radiation vanishes.

The type D spacetimes admit two double degenerate PNDs, $R_1 = R_2 = \tan\frac{\theta_1}{2}$ and $R_3 = R_4 = 0$. The gravitational field near $\mathcal{I}^+$ thus takes the form

$$|\Psi_4^{\mathrm{i}}| = |\Psi_{4*}^{\mathrm{o}}|\eta^{-1}\cos^4\frac{\theta}{2}\left|1 + \tan\frac{\theta_1}{2}\ \tan\frac{\theta}{2}\ e^{i\phi}\right|^2, \quad (27)$$

with two planes of symmetry, see Fig. 1(D). This directional dependence agrees with the radiation pattern for the C metric with $\Lambda > 0$ derived recently [4].

For Petrov type II spacetimes only two PNDs coincide so that $R_1 = \tan\frac{\theta_1}{2}$, $R_2 = \tan\frac{\theta_2}{2}\exp(-i\phi_2)$, $R_3 = R_4 = 0$. The directional pattern of radiation is in Fig. 1(II). Finally, in the case of algebraically general spacetimes one needs five real parameters to characterize the directional dependence Fig. 1(I) of the gravitational field.

An analogous discussion can be presented for the electromagnetic field. The square of expression (24) is, in fact, the Poynting vector with respect to the interpretation tetrad, $|\mathbf{S}_{\mathrm{i}}| \approx \frac{1}{4\pi}|\Phi_2^{\mathrm{i}}|^2$. If the two PNDs coincide ($R_1^E = R_2^E = 0$) the directional dependence of the Poynting vector at $\mathcal{I}^+$ is the same as in Eq. (25) [Fig. 1(N)]; if they differ ($R_1^E = \tan\frac{\theta_1}{2}$, $R_2^E = 0$), the angular dependence of $|\mathbf{S}_{\mathrm{i}}|$ is given by Eq. (27) [Fig. 1(D)]. The latter has already been obtained for the test field of uniformly accelerated charges in de Sitter spacetime [3].

To summarize: it is well known that for *null* $\mathcal{I}^+$ the null direction $\mathbf{l}_{\mathrm{i}}$, which is complementary to the tangent vector $\mathbf{k}_{\mathrm{i}}$ of the null geodesic $z(\eta)$ reaching $\mathcal{I}^+$, is tangent to $\mathcal{I}^+$ and does not depend on the choice of $z(\eta)$. This is not the case when $\mathcal{I}^+$ is spacelike. The radiation field (η^{-1} term) is thus "less invariant" [6]. We have shown that the dependence of this field on the choice of $z(\eta)$ has a universal character that is determined by the algebraic (Petrov) type of the fields. In particular, we have proved that the radiation vanishes along directions opposite to PNDs. In a *generic* direction the radiative component of the fields generated by *any* source is *nonvanishing*. Thus, unlike in asymptotically flat spacetimes, the absence of η^{-1} component cannot be used to distinguish nonradiative sources: for a de Sitter–like infinity the radiative component reflects not only properties of the sources but also their "kinematic" relation to an observer at infinity. Intuitively, near spacelike $\mathcal{I}^+$ our observer is, in general, moving "nonradially" from sources and thus measures infinitely boosted fields. Some important questions, such as how energy is radiated away in asymptotically de Sitter spacetimes, still remain open. Since vacuum energy seems to be dominant in our Universe, these appear to be of considerable interest.

The work was supported by GAČR 202/02/0735 and GAUK 166/2003. We thank J. B. Griffiths for comments.

[1] J. Bičák, in *Einstein's Field Equations and Their Physical Implications*, edited by B. G. Schmidt (Springer, Berlin, 2000), Vol. 540, pp. 1–126.
[2] J. Bičák and P. Krtouš, in Proceedings of the 10th Greek Relativity Meeting (World Scientific, Singapore, to be published).
[3] J. Bičák and P. Krtouš, Phys. Rev. Lett. **88**, 211101 (2002).
[4] P. Krtouš and J. Podolský, Phys. Rev. D **68**, 024005 (2003). Notice a different choice of the reference tetrad, and thus of θ, ϕ. For another recent work on "de Sitter C-metric" see O. J. C. Dias and J. P. S. Lemos, Phys. Rev. D **67**, 084018 (2003).
[5] R. Penrose, Proc. R. Soc. London A **284**, 159 (1965).
[6] R. Penrose and W. Rindler, *Spinors and Space-Time* (Cambridge University Press, Cambridge, 1984).
[7] J. Bičák and P. Krtouš, Phys. Rev. D **64**, 124020 (2001).
[8] H. Friedrich, in *Gravitation and Relativity: At the Turn of the Millenium (Proceedings of the GR-15)*, edited by N. Dadhich and J. Narlikar (IUCAA Press, Pune, 1998).
[9] D. Kramer, H. Stephani, E. Herlt, and M. MacCallum, *Exact Solutions of Einstein's Field Equation* (Cambridge University Press, Cambridge, 1980).

PHYSICAL REVIEW D **68**, 124004 (2003)

Radiation from accelerated black holes in an anti–de Sitter universe

Jiří Podolský,* Marcello Ortaggio,† and Pavel Krtouš‡
Institute of Theoretical Physics, Faculty of Mathematics and Physics, Charles University in Prague, V Holešovičkách 2, 180 00 Prague 8, Czech Republic
(Received 23 July 2003; published 5 December 2003)

We study gravitational and electromagnetic radiation generated by uniformly accelerated charged black holes in anti–de Sitter spacetime. This is described by the *C*-metric exact solution of the Einstein-Maxwell equations with a negative cosmological constant Λ. We explicitly find and interpret the pattern of radiation that characterizes the dependence of the fields on a null direction from which the (timelike) conformal infinity is approached. This directional pattern exhibits specific properties which are more complicated if compared with recent analogous results obtained for asymptotic behavior of fields near a de Sitter–like infinity. In particular, for large acceleration the anti–de Sitter–like infinity is divided by Killing horizons into several distinct domains with a different structure of principal null directions, in which the patterns of radiation differ.

DOI: 10.1103/PhysRevD.68.124004 PACS number(s): 04.20.Ha, 04.20.Jb, 04.40.Nr

I. INTRODUCTION

In the context of exact solutions of Einstein's field equations, gravitational radiation has been studied for decades. In particular, various techniques have been developed to rigorously characterize asymptotic properties of the gravitational field, i.e., the geometry of spacetime at ''large distance'' from bounded sources.

In the fundamental work [1] gravitational waves emitted by axisymmetric systems were analyzed by considering an expansion of metric functions in inverse powers of an appropriate ''radial'' coordinate r parametrizing outgoing null geodesics. In particular, the news function was defined that characterizes radiation, and which is related to a decreasing (Bondi) mass of the source. Generalizations and refinement of this method, with a deeper understanding of its relation to the Petrov types (such as the peeling-off behavior of the Weyl tensor) were subsequently achieved in [2–6], see, e.g., [7–10] for reviews. Nevertheless, in these works the analysis of radiative fields remained confined to *asymptotically flat* spacetimes thus ruling out, for instance, the presence of a nonvanishing cosmological constant Λ. In addition, it was based on the use of privileged coordinate systems.

It was Penrose [11–13], see [14] for a comprehensive overview, who introduced a *covariant* approach to the definition of radiation for massless fields, which is based on the conformal treatment of infinity (a comparison of the Bondi-Sachs and Penrose approaches was recently presented in [15]). This enables one to apply methods of local differential geometry ''at infinity,'' and thus to define in a rigorous geometric way such basic concepts as the Bondi mass, the peeling-off property, and the Bondi-Metzner-Sachs group of asymptotic symmetries. In particular, gravitational radiation propagating along a given null geodesic is described by the Ψ_4 component of the Weyl tensor projected on a parallelly transported complex null tetrad at infinity. The crucial point is that such a tetrad is (essentially) determined *uniquely* by the conformal geometry [14]. Moreover, an advantage of the Penrose method is that it can be naturally applied also to asymptotically simple spacetimes which *include the cosmological constant* [12–14]. This is quite remarkable since there is no analogue of the news function in the presence of Λ [16,17].

However, specific new features appear in the case of asymptotically de Sitter ($\Lambda>0$) or anti–de Sitter ($\Lambda<0$) spacetimes, for which the conformal infinity $\mathcal{I}$ is, respectively, spacelike or timelike [12–14,18]. First of all, the concept of radiation for a massless field is ''less invariant'' in cases when $\mathcal{I}$ is not null. Namely, it emerges as necessarily direction dependent since the choice of the above-mentioned null tetrad, and thus the radiative component Ψ_4 of the field, turns out to be *different* for different null geodesics reaching the same point on $\mathcal{I}$. This is related to the fact that with nonvanishing Λ even fields of *nonaccelerated* sources are *radiative* along a *generic* direction, as it has been shown for test charges [19] or for Reissner-Nordström black holes [20] in a de Sitter universe, and it will be shown here for a negative Λ (Sec. V C). In addition, the character of infinity plays a crucial role in the formulation of the initial value problem. A spacelike $\mathcal{I}$ implies the insufficiency of purely retarded massless fields so that, for example, in de Sitter space purely retarded solutions of the Maxwell equations are impossible for generic charge distributions [21]. On the other hand, it is well known that a timelike $\mathcal{I}$ prevents the existence of a Cauchy surface, and one is necessarily led to a kind of ''mixed initial value boundary problem,'' see, e.g., [22–24]. For all the above reasons, the definition of radiation is much less obvious when $\Lambda\neq 0$.

Any explicit exact example of a source which generates gravitational waves in an (anti–)de Sitter universe is thus of paramount importance since this may provide us with insight into the character of radiation in spacetimes which are not asymptotically flat. Exact solutions with boost-rotation symmetry [25–27], which represent radiative spacetimes with uniformly accelerating sources, play a unique role when $\Lambda=0$. Among these the *C*-metric, which describes accelerated black holes, admits a natural generalization to a nonva-

*Electronic address: Jiri.Podolsky@mff.cuni.cz
†Electronic address: Marcello.Ortaggio@comune.re.it
‡Electronic address: Pavel.Krtous@mff.cuni.cz

nishing value of the cosmological constant, and it will thus be considered in the present paper.

The *C*-metric [28–31] is a classic solution of the Einstein(-Maxwell) equations which has been physically interpreted and analyzed in fundamental papers [32–35] and in many other works, see, e.g., [25,27,36–38] for references and summary of the results. A generalization of the standard *C*-metric to admit a nonvanishing value of Λ has also been known for a long time [39], cf. [40,41] (also, related solutions have been obtained by considering extremal limits of the *C*-metric with an arbitrary Λ [42]). These spacetimes have found successful application to the problem of cosmological pair creation of black holes [43–46]. However, a deeper understanding of their physical and global properties, including the character of radiation, has been missing until recently. The interpretation of the *C*-metric solutions with $\Lambda>0$, in particular the meaning of parameters in the metric and the relation to the ''background'' de Sitter universe, was clarified in [47] by introducing an appropriate coordinate system adapted to uniformly accelerated observers. The causal structure was further studied in [48] for various choices of the physical parameters. Very recently [20], we have carefully analyzed the *C*-metric with $\Lambda>0$ and, among other results, we have demonstrated that gravitational and electromagnetic fields of this exact solution exhibit asymptotically a *specific directional pattern of radiation at* $\mathcal{I}$. Interestingly, this directional dependence of fields on null directions from which the conformal infinity is approached is the same as for the test fields of uniformly accelerated charges in a de Sitter universe [19].

In the present work we wish to investigate an analogous asymptotic behavior of fields of the *C*-metric with $\Lambda<0$, i.e., the directional dependence at conformal infinity $\mathcal{I}$ of radiation generated by uniformly accelerated (possibly charged) black holes in an anti–de Sitter universe. Some fundamental differences from the cases $\Lambda\geqslant 0$ appear since $\mathcal{I}$ now has a *timelike* character. In fact, the whole structure of the ''anti–de Sitter *C*-metric'' is much more complex and new peculiar phenomena thus occur. As observed in [49] and thoroughly studied in the recent work [38], for a small value of acceleration, $A<\sqrt{-\Lambda/3}$, the metric describes a *single* uniformly accelerated black hole in an anti–de Sitter universe [50] whereas for $A>\sqrt{-\Lambda/3}$ this represents *a pair* of accelerated black holes. The ''limiting case'' given by $A=\sqrt{-\Lambda/3}$, previously investigated in [51,52], plays a special important role in the context of the Randall-Sundrum model since it describes a black hole bound to a two-brane in four dimensions. However, this case is not investigated in the present work.

Our paper is organized as follows. First, in Sec. II we present the *C*-metric solution with a negative cosmological constant, in particular the Robinson-Trautman coordinates which will be used in the subsequent analysis. Basic properties of the solution are also summarized, including a description of the global structure. Sections III–V contain the core of our analysis. First we define a suitable interpretation tetrad parallelly transported along null geodesics approaching asymptotically a given point on conformal infinity $\mathcal{I}$ from all possible spacetime directions. The magnitude of the leading terms of gravitational and electromagnetic fields in such a tetrad then provides us with a specific directional pattern of radiation. Convenient parametrizations of null directions approaching $\mathcal{I}$ are introduced in Sec. IV, and the results are subsequently described and analyzed in Sec. V. This is done for both the cases of a single black hole and a pair of black holes accelerating in an anti–de Sitter universe (and for vanishing acceleration). The paper also contains two appendixes. In Appendix A the behavior of radiation along special null directions is studied. In particular, for geodesics along principal null directions the results are obtained in closed explicit form without performing asymptotic expansions of the physical quantities near $\mathcal{I}$. Appendix B summarizes the Lorentz transformations of the null-tetrad components of the gravitational and electromagnetic fields.

II. THE *C*-METRIC WITH A NEGATIVE COSMOLOGICAL CONSTANT

The *C*-metric with a cosmological constant $\Lambda<0$, contained in the family of solutions [39], can be written as

$$\boldsymbol{g}=\frac{1}{A^2(x+y)^2}\left(-F\mathbf{d}t^2+\frac{1}{F}\mathbf{d}y^2+\frac{1}{G}\mathbf{d}x^2+G\mathbf{d}\varphi^2\right), \tag{2.1}$$

where F and G are, respectively, polynomials of y and x,

$$F=\frac{-\Lambda}{3A^2}-1+y^2-2mAy^3+e^2A^2y^4,$$

$$G=1-x^2-2mAx^3-e^2A^2x^4. \tag{2.2}$$

These functions are mutually related by

$$F=-Q(y)+\frac{-\Lambda}{3A^2},\quad G=Q(-x), \tag{2.3}$$

where $Q(w)=1-w^2+2mAw^3-e^2A^2w^4$. The metric (2.1) is a solution of the Einstein-Maxwell equations with a non-null electromagnetic field given by

$$\mathbf{F}=e\mathbf{d}y\wedge\mathbf{d}t, \tag{2.4}$$

or related expressions which can be obtained by a constant duality rotation. There exist two double-degenerate principal null directions (PNDs)

$$\mathbf{k}_1\propto\boldsymbol{\partial}_t-F\boldsymbol{\partial}_y,\quad \mathbf{k}_2\propto\boldsymbol{\partial}_t+F\boldsymbol{\partial}_y, \tag{2.5}$$

so that the spacetime is of the Petrov type *D*. It admits two *Killing vectors* $\boldsymbol{\partial}_t$, $\boldsymbol{\partial}_\varphi$, and one *conformal Killing tensor* $\mathbf{Q}$ (cf. Refs. [14,53,54]),

$$\mathbf{Q}=\frac{1}{A^4(x+y)^4}\left(F\mathbf{d}t^2-\frac{1}{F}\mathbf{d}y^2+\frac{1}{G}\mathbf{d}x^2+G\mathbf{d}\varphi^2\right). \tag{2.6}$$

The metric (2.1) can describe different spacetimes, depending on the choice of parameters and of ranges of coordinates. We are interested in the physically most relevant

case when the metric describes one black hole or pairs of black holes uniformly accelerated in anti–de Sitter universe. In this case the constants A, m, e, and C, such that $\varphi\in(-\pi C,\pi C)$, characterize acceleration, mass, charge of the black holes, and conicity of the φ symmetry axis, respectively. They have to satisfy $m\geqslant 0$, $e^2<m^2$, A, $C>0$, and they have to be such that the function G has four real roots in the charged case $(e,m\neq 0)$ or three real roots in the uncharged case $(e=0,m\neq 0)$. The coordinates x, y have to satisfy $y>-x$ and $x\in[x_{\rm f},x_{\rm b}]$, where $x_{\rm f}<0<x_{\rm b}$ are two roots of G, namely those closest to zero [see [20,38,44,50] for details and discussion of other cases, cf. also Figs. 1(d) and 3 below]. From these conditions we obtain $0\leqslant G\leqslant 1$, and $m+2e^2Ax>0$. The spacetime (2.1) reduces to the anti–de Sitter universe for $m=0$, $e=0$.

The coordinates x and φ are longitudinal and latitudinal angular coordinates, $x_{\rm f}$ denotes the axis of φ symmetry extending from the ''forward'' pole of the black hole (in the direction of acceleration) to infinity, whereas $x_{\rm b}$ denotes the axis from the opposite ''backward'' pole. For nonvanishing acceleration the axis cannot be regular everywhere—at least one part of it has to have a nontrivial conicity, depending on the choice of the parameter C. This corresponds to the presence of cosmic strings (or struts) which are responsible for the acceleration of the black holes, see the references above for more details.

The spacetime metric (2.1) can be put into various forms. In this paper we concentrate on investigation of radiation near infinity, for which the Robinson-Trautman form seems to be a convenient one. Introducing real coordinates r, u and complex coordinates ζ, $\overline{\zeta}$ by

$$Ar=(x+y)^{-1},$$

$$A\mathbf{d}u=\frac{\mathbf{d}y}{F}+\mathbf{d}t,$$

$$\frac{1}{\sqrt{2}}(\mathbf{d}\zeta+\mathbf{d}\overline{\zeta})=\frac{\mathbf{d}y}{F}-\frac{\mathbf{d}x}{G}+\mathbf{d}t,$$

$$\frac{i}{\sqrt{2}}(\mathbf{d}\zeta-\mathbf{d}\overline{\zeta})=\mathbf{d}\varphi, \tag{2.7}$$

we put the C-metric (2.1) into the form [55]

$$\boldsymbol{g}=\frac{r^2}{P^2}\mathbf{d}\zeta\vee\mathbf{d}\overline{\zeta}-\mathbf{d}u\vee\mathbf{d}r-H\mathbf{d}u^2. \tag{2.8}$$

The metric functions are

$$P^{-2}=G,\quad H=A^2r^2(F+G), \tag{2.9}$$

or explicitly

$$H=-\frac{\Lambda}{3}r^2-2r(\ln P)_{,u}+\Delta\ln P-\frac{2}{r}(m+2e^2Ax)+\frac{e^2}{r^2}, \tag{2.10}$$

with $\Delta=2P^2\partial_\zeta\partial_{\overline{\zeta}}$, where x is expressed using the relation

$$\int\frac{dx}{G(x)}=Au-\frac{1}{\sqrt{2}}(\zeta+\overline{\zeta}). \tag{2.11}$$

The functions (2.9), (2.10) represent a particular case, corresponding to the C-metric, of the standard general expression for the Robinson-Trautman spacetimes [31]. As opposed to the metric form (2.1), the Robinson-Trautman coordinates allow an explicit limit $A=0$. The coordinates are not defined globally but it is possible to cover the whole universe by many coordinate patches of the same type. Therefore, it is sufficient to study the spacetime only in just one Robinson-Trautman coordinate map; such a patch is indicated by a shaded domain in Figs. 4–6. We additionally assume there that the coordinate u is increasing from the past to the future.

The global causal structure of the C-metric with $\Lambda<0$ has recently been analyzed in [38]. In particular, the character of infinity, singularities, and possible horizons has been described in detail.

Infinity $\mathcal{I}$ of the spacetime is given by

$$r=\infty,\quad \text{or equivalently}\quad x+y=0, \tag{2.12}$$

where the conformal factor

$$\Omega=\frac{1}{r}=A(x+y) \tag{2.13}$$

vanishes. The conformal (unphysical) metric $\tilde{\boldsymbol{g}}=\Omega^2\boldsymbol{g}$,

$$\tilde{\boldsymbol{g}}=\frac{1}{P^2}\mathbf{d}\zeta\vee\mathbf{d}\overline{\zeta}+\mathbf{d}u\vee\mathbf{d}\Omega-H\Omega^2\mathbf{d}u^2, \tag{2.14}$$

is regular at infinity, given by $\Omega=0$. Moreover, it follows from Eq. (2.10) that at $\mathcal{I}$ the metric function reads

$$H\Omega^2\Big|_{\mathcal{I}}=-\frac{\Lambda}{3}, \tag{2.15}$$

i.e., it is independent of the parameters m, e, and A. The vector $\mathbf{n}_{\rm P}=-(H\Omega^2\boldsymbol{\partial}_\Omega+\boldsymbol{\partial}_u)$ is orthogonal to each hypersurface $\Omega=$const. In particular, it is outgoing and normal to infinity $\mathcal{I}$ at any of its point, with the norm $\tilde{\boldsymbol{g}}(\mathbf{n}_{\rm P},\mathbf{n}_{\rm P})=H\Omega^2=-\Lambda/3>0$. The universe is thus weakly asymptotically anti–de Sitter [16], at least locally, with the conformal infinity $\mathcal{I}$ having a timelike character (in general, it is not asymptotically anti–de Sitter according to the definition based on the ''reflective boundary condition'' [16,17,23,56]: the $(2+1)$-metric induced on $\mathcal{I}$ by $\tilde{\boldsymbol{g}}$ is not conformally flat since the associated Bach tensor is nonvanishing). Throughout the paper, however, it will be more convenient to employ the spacelike outward vector $\mathbf{n}=\mathbf{n}_{\rm P}/\sqrt{H}$ orthogonal to $\mathcal{I}$,

$$\mathbf{n}=\sqrt{H}\boldsymbol{\partial}_r-\frac{1}{\sqrt{H}}\boldsymbol{\partial}_u, \tag{2.16}$$

which has a unit norm $\mathbf{n}\cdot\mathbf{n}=\boldsymbol{g}(\mathbf{n},\mathbf{n})=1$ with respect to the *physical* metric.

At $r=0$ the metric has unbounded curvature which corresponds to a physical singularity hidden behind the black hole

horizon. Similarly to the *C*-metric with vanishing Λ [32–37] or the *C*-metric with $\Lambda>0$ [20,47,48], the zeros of the function F correspond to *Killing horizons* associated with $\boldsymbol{\partial}_t$. Interestingly, unlike in the $\Lambda\geqslant 0$ case, the anti–de Sitter *C*-metric describes either a single uniformly accelerated black hole (for $A<\sqrt{-\Lambda/3}$), or a pair of uniformly accelerated black holes (when $A>\sqrt{-\Lambda/3}$).

A. A single accelerated black hole

Indeed, as described in [38,50], when the acceleration parameter A is *small*, namely $A<\sqrt{-\Lambda/3}$, and $m\neq 0$, the metric (2.1), (2.2) describes a *single* uniformly accelerated black hole. The condition of small acceleration guarantees that the function F has only two zeros $y_{\rm o}, y_{\rm i}$ in the charged case, or only one zero $y_{\rm o}$ for the uncharged black hole. These zeros define *outer* and, if applicable, *inner* horizons of the black hole. The relevant ranges of coordinates x, y representing the spacetime outside the black hole are depicted in Fig. 1(d).

In [38] the causal structure of this spacetime was represented by the Penrose-Carter conformal diagram of a two-dimensional *t*-*y* section (i.e., the section of constant angular coordinates x, φ). This section is, in fact, spanned by the PNDs $\mathbf{k}_1$ and $\mathbf{k}_2$, cf. Eq. (2.5). A part of such a conformal diagram representing an exterior of the black hole is depicted in Fig. 1(c). The conformal infinity $\mathcal{I}$ is indicated here by a double line. The outer horizons $\mathcal{H}_{\rm o}$, given by $y=y_{\rm o}$, separate region II outside the black hole from an interior of the black hole, denoted as III [57]. A more detailed structure of the interior of the black hole depends on whether the hole is charged or not, and its causal structure is analogous to the Schwarzschild or Reissner-Nordström black holes. Because we are mainly interested in region II near the infinity, we will not discuss the interior of the hole here.

It seems to be more instructive to combine the *t*-*y* sections for different values of x into a unifying three-dimensional picture in which just the coordinate φ is suppressed, as it is done in Fig. 1(a). Despite the fact that this is not a complete and rigorous conformal diagram, it helps to visualize and understand the global causal structure of the spacetime. The outer horizon $\mathcal{H}_{\rm o}$ of the black hole is here indicated by two joined conical surfaces, and the conformal timelike infinity $\mathcal{I}$ is depicted as a deformed outer boundary. It has a ''simple'' topology $\mathbb{R}\times S^2$ if we include ''nonsmooth'' points on the φ axis where the string is located. For a vanishing acceleration the timelike infinity would be rotationally symmetric around the vertical axis, and smooth everywhere. Its deformation for $A\neq 0$ indicates that the coordinates are adapted to the accelerated source (for an analogous discussion in the $\Lambda>0$ case see [20]) and that there is a string (a conical singularity) on the φ axis. Particular surfaces $\mathcal{S}$ of a constant x, corresponding to the two-dimensional conformal diagram 1(c), are also indicated. The section $\mathcal{S}_S$ with $x=x_{\rm f}$ corresponds to the axis from the ''forward'' pole of the black hole, the value $x=x_{\rm b}$ to the axis from the opposite ''backward'' pole. In Fig. 1(a) the conicity parameter C is chosen in such a way that the string is located only on the axis $x=x_{\rm f}$, and the conical singularity is indicated by nonsmooth embedding of the t, $y=$const surface into the three-dimensional diagram, i.e., by a nonsmooth

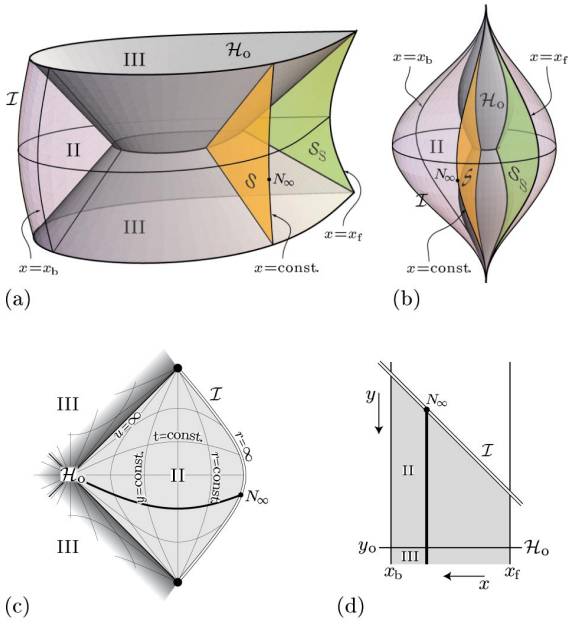

FIG. 1. Spacetime outside a single accelerated black hole moving in an anti–de Sitter universe with acceleration $A<\sqrt{-\Lambda/3}$. Diagrams (a) and (b) depict a three-dimensional section $\varphi=$const, diagram (c) is a conformal diagram of the *t*-*y* section, and diagram (d) shows relevant ranges of coordinates x and y. The diagrams focus on region II between the outer black hole horizon $\mathcal{H}_{\rm o}$ ($y=y_{\rm o}$) and timelike infinity $\mathcal{I}$, $y=-x$. Therefore, only a small part of an interior of the black hole near the horizon $\mathcal{H}_{\rm o}$ is shown (region III). In diagram (a) the horizon $\mathcal{H}_{\rm o}$ is represented by two conical surfaces which intersect on a bifurcation surface of the Killing vector $\boldsymbol{\partial}_t$ (a continuation of cones inside the black hole to another asymptotic domain is not shown). The outer deformed boundary of domain II corresponds to infinity $\mathcal{I}$. A particular section $\mathcal{S}$ given by $x=$const is shown, and the axes $x=x_{\rm b}$ and $x=x_{\rm f}$ are indicated. It is assumed in diagram (a) that the string causing acceleration of the black hole is located on the ''forward'' axis $x=x_{\rm f}$ and the corresponding conical singularity is represented by nonsmooth behavior at $\mathcal{S}_S$ (the edge at $x=x_{\rm f}$). Diagram (b) is a deformation of diagram (a) in which both the top and the bottom of the diagram are squeezed to single points, and the longitudinal x direction is embedded smoothly at both axes. The black hole horizon $\mathcal{H}_{\rm o}$ has thus a droplike shape, symmetrical around the vertical axis. Diagram (c) is the Penrose-Carter conformal diagram of the *t*-*y* section $\mathcal{S}$ ($x,\varphi=$const). Both principal null directions lie in this section. The precise shape of infinity $\mathcal{I}$ (double line) depends on the value of coordinate x, cf. Eq. (2.12) [and this dependence is the reason for the deformed shape of $\mathcal{I}$ in diagram (a)]. Lines $t=$const, and $y=$const (coinciding with $r=$const in $\mathcal{S}$) are drawn with labels oriented in the direction of an increasing coordinate. A small part of the interior of the black hole is indicated by the dark area at the left of the diagram. Finally, diagram (d) depicts the *x*-*y* section for relevant ranges of coordinates (shaded area). The infinity is again represented by the double line, and the horizon $\mathcal{H}_{\rm o}$ is shown. The thick line $x=$const corresponds to the *t*-*y* section of diagram (c); similarly the thick line $t=$const in diagram (c) corresponds to the *x*-*y* section from diagram (d).

gluing of $x=\text{const}$ sections at x_f. Notice that since $F>0$ for $y<y_o$, region II near infinity $\mathcal{I}$ is everywhere *static*, and there are no Killing horizons which extend up to $\mathcal{I}$ [cf. also Eqs. (5.6), (5.7)]. We can thus interpret the spacetime as a universe having *global* anti–de Sitter–like infinity (except the nonsmoothness at the string) with the black hole moving ''inside'' it (in contrast to the case discussed below, where pairs of black holes ''enter'' and ''exit'' the spacetime ''through'' the infinity).

The diagram 1(b) is a deformed version of the diagram 1(a): gluing of the angular coordinate x is now done smoothly even on the axis where the string is located, and the top and the bottom of the diagram are ''squeezed'' to single points. The horizon $\mathcal{H}_o$ thus has a shape of two joined ''drops,'' and sections $x=\text{const}$ are deformed accordingly. Here we can see that coordinates t, y, x, φ used to construct this diagram are adapted to the source, not to the infinity—the horizon $\mathcal{H}_o$ is symmetric around the vertical axis in contrast to infinity $\mathcal{I}$ which is deformed in the direction of acceleration. Diagram 1(b) is not so crucial in the present case of a single black hole but an analogous representation of the black hole horizon will be used in the case of two accelerated holes which we are going to discuss now.

B. A pair of accelerated black holes

A more complicated situation occurs when $A>\sqrt{-\Lambda/3}$, $m\neq 0$. For such large values of acceleration the metric (2.1), (2.2) describes an infinite number of *pairs* of accelerated black holes in anti–de Sitter universe. In Fig. 2, representing a part of the section $\varphi=\text{const}$, one pair of black holes is indicated by the (outer) horizons $\mathcal{H}_o$ which have droplike shapes analogous to the horizon in diagram 1(b). The main difference from the previous case is that both black holes ''simultaneously enter'' the universe at infinity $\mathcal{I}$, approach each other with an opposite deceleration until they stop, and start to move apart, again up to the infinity $\mathcal{I}$. The same situation repeats infinitely many times both in the past and in the future—the diagrams in Fig. 2 should be infinitely long, composed of parts isomorphic to the part shown there. In the following we study only one such part of the whole universe. Relevant ranges of coordinates x and y are drawn in Fig. 3.

Clearly, both the global causal structure of the spacetime and the algebraic structure are now more complex. The metric function F has two more zeros, y_a and y_c, which correspond to the two additional Killing horizons *outside* of the black holes. We shall refer to these as *acceleration* horizons $\mathcal{H}_a$, and *cosmological* horizons $\mathcal{H}_c$ [58]. In contrast to the black hole horizons, spatial sections of these horizons are noncompact. The horizons are represented by inclined planes in Fig. 2(a) or as corresponding horizontal lines in Fig. 3. They separate static and nonstatic regions of the spacetime outside of the black holes: the domains O and II are static, whereas the domains I^+ and I^- are nonstatic. Regions II enclose the black holes, the regions O are ''as far as possible away'' from the black holes. Two black holes of a given pair are separated by the acceleration horizons $\mathcal{H}_a$, and they are thus causally disconnected. Different pairs of black holes are separated by the cosmological horizons $\mathcal{H}_c$.

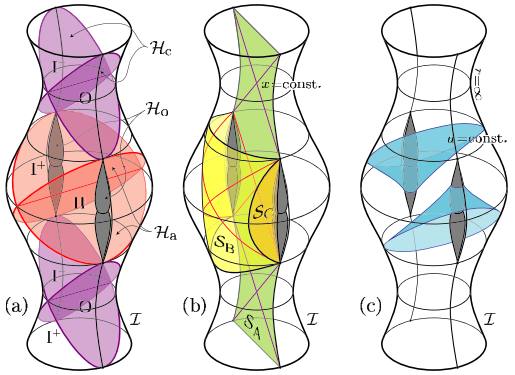

FIG. 2. Schematic diagrams of a part of spacetime outside accelerated black holes moving in an anti–de Sitter universe with acceleration $A>\sqrt{-\Lambda/3}$. Diagrams represent a three-dimensional section $\varphi=\text{const}$. They depict a domain near one pair of black holes. However, they should continue periodically in the vertical direction, featuring thus an infinite chain of pairs of black holes entering and later exiting the spacetime through timelike infinity $\mathcal{I}$. Only regions of spacetime *outside* the outer black hole horizons $\mathcal{H}_o$ are drawn. Interiors of black holes and continuations of the spacetime into other asymptotically anti–de Sitter universes (through the Einstein-Rosen bridge or through charged black hole) are hidden under the horizons $\mathcal{H}_o$ and not studied in the paper. The outer black hole horizons $\mathcal{H}_o$ are represented by droplike gray shapes analogous to that of Fig. 1(b), the timelike infinity $\mathcal{I}$ is depicted as a deformed cylindrical boundary of the diagrams. Diagram (a) shows the Killing horizons outside the black holes: *acceleration horizons* $\mathcal{H}_a$ separating two black holes, and *cosmological horizons* $\mathcal{H}_c$ separating different pairs of black holes (only one pair of holes is drawn in the diagram). These horizons divide spacetime into several regions: static domains O and II, nonstatic domains I^+ and I^-, and domains inside the holes hidden under $\mathcal{H}_o$. Diagram (b) indicates embedding of t-y sections for different constant values of the coordinate x, which are spanned by principal null directions. Three qualitatively different sections $\mathcal{S}_A$, $\mathcal{S}_B$, and $\mathcal{S}_C$ are shown. Exact conformal diagrams corresponding to these sections can be found in Figs. 4–6. Diagram (c) shows hypersurfaces $u=\text{const}$ which are generated by null geodesics along the principal null directions $\mathbf{k}_1$ that are discussed in Appendix A.

Figure 2(b) shows the foliation of the spacetime by the t-y surfaces $x=\text{const}$, the surfaces spanned by the PNDs. These are of three different types, namely $\mathcal{S}_A$, $\mathcal{S}_B$, and $\mathcal{S}_C$. Classification of these types is seen from the x-y diagram in Fig. 3, where the t-y sections are represented by vertical lines. These different types of t-y sections are distinguished by the number of horizons which they intersect.

For $x\in(-y_c,x_b]$ the section denoted as $\mathcal{S}_A$ passes through *all* regions O, I, II (and regions inside black holes), and intersects all horizons $\mathcal{H}_c$, $\mathcal{H}_a$, $\mathcal{H}_o$. Such a section corresponds to the conformal diagram drawn in Fig. 4. The *intersection* of such a section with the conformal infinity $\mathcal{I}$ is *timelike*. We denote as $\mathcal{I}_O$ a part of the infinity with $x\in(-y_c,x_b]$, i.e., the part which can be reached by the sections $\mathcal{S}_A$, cf. also Fig. 10.

The situation is different for section $\mathcal{S}_B$ of a constant $x\in(-y_a,-y_c)$ which goes only through regions I, II (and

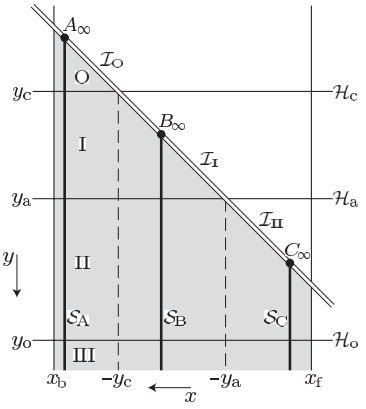

FIG. 3. A qualitative *x*-*y* diagram in the case of large acceleration $A>\sqrt{-\Lambda/3}$ [cf. Fig. 1(d) for small acceleration]. The relevant domain of coordinates *x* and *y* is indicated by the shaded area. It is given by the coordinate *x* between the axes x_f and x_b, and the coordinate *y* between the infinity $\mathcal{I}$, $y=-x$, and the outer black hole horizon $\mathcal{H}_o$, $y=y_o$ (the interior of black holes, $y>y_o$, is not studied here). The infinity is represented by a double line, the horizons by horizontal lines. The *t*-*y* sections of constant *x* are represented by vertical lines. Three such typical sections $\mathcal{S}_A$, $\mathcal{S}_B$ and $\mathcal{S}_C$ are shown. They are distinguished by the number of horizons which they intersect. These sections correspond to the conformal diagrams in Figs. 4–6. A_∞, B_∞, C_∞ are points at the infinity which belong to these three sections, respectively. They can be found also in Figs. 4–6.

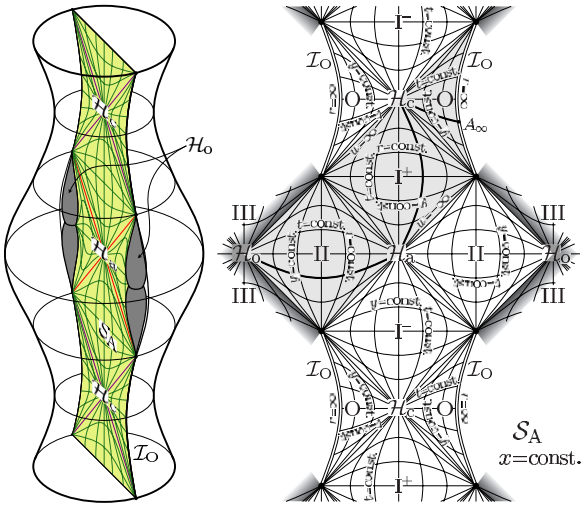

FIG. 4. Conformal diagram of the *t*-*y* section $\mathcal{S}_A$ intersecting both the horizons $\mathcal{H}_a$, $\mathcal{H}_c$ outside black holes (right), and its embedding into three-dimensional diagram $\varphi=$const (left). Each of sections of constant *x* (and φ) with $x\in(-y_c,x_b]$ intersects all horizons and extends through the whole spacetime. Both three-dimensional and two-dimensional diagrams should continue periodically in the vertical direction. In the two-dimensional conformal diagram the infinity $\mathcal{I}$ is depicted by double lines. Section $\mathcal{S}_A$ intersects the infinity in a timelike surface belonging to domain $\mathcal{I}_O$, cf. Fig. 10. Cosmological horizons $\mathcal{H}_c$, acceleration horizons $\mathcal{H}_a$, and outer black hole horizons $\mathcal{H}_o$ are represented by diagonal lines. Domains between the horizons are labeled as O, $I^\pm$, II, and III, cf. Fig. 2(a). Interiors of black holes are indicated only partially, by the dark area behind the horizon $\mathcal{H}_o$. Lines of coordinates *t* and *y* are shown with labels oriented in direction of an increasing coordinate. An area covered by one Robinson-Trautman coordinate map (coordinates *u*, *r*) is indicated by the shaded background. Without the loss of a typical behavior, the special section $x=x_b$ has been chosen for this diagram; other sections with $x>-y_c$ look qualitatively the same, only with embedding not lying in the plane of symmetry of the three-dimensional diagram.

regions inside black holes), and does not intersect the horizon $\mathcal{H}_c$. This section corresponds to the conformal diagram presented in Fig. 5. The intersection of such a section with infinity is *spacelike*, and consists of two disjoint parts, one in the future and another in the past of the section. A part of the infinity which can be reached in this way will be labeled as $\mathcal{I}_{I^+}$ and $\mathcal{I}_{I^-}$, respectively, cf. Fig. 10.

Finally, for $x\in[x_f,-y_a)$ the section $\mathcal{S}_C$ of constant *x* extends only to the region II (and regions inside the black hole), and it does not intersect the horizons $\mathcal{H}_a$ and $\mathcal{H}_c$. The conformal diagram of this type is given in Fig. 6. Section $\mathcal{S}_C$ *intersects* the infinity in a *timelike* surface, and a part of the infinity which can be reached by these sections will be denoted by $\mathcal{I}_{II}$, cf. also Fig. 10.

The above described three types of conformal diagrams depicted in Figs. 4–6 have been drawn recently in [38] (together with special limiting cases $x=-y_c$ and $x=-y_a$ which we do not discuss here). Their qualitative dependence on the value of coordinate *x* has been already noted there but not discussed in more details. Putting all these conformal diagrams together to the single three-dimensional picture shown in Fig. 2(b) elucidates the character of this dependence. Moreover, it clarifies how the timelike infinity $\mathcal{I}$ can form a *spacelike* boundary of a conformal diagram as for section $\mathcal{S}_B$, Fig. 5—this spacelike boundary is the intersection of the two timelike hypersurfaces $\mathcal{I}$ and $\mathcal{S}_B$.

In Fig. 2(c) the surfaces $u=$const are shown. These null surfaces are formed by null geodesics *u*, $\zeta=$const tangent to PND (see Appendix A), and they indicate how the spacetime is covered by Robinson-Trautman coordinates. A surface of constant *u* reduces to a horizon $\mathcal{H}_a$ for $u=-\infty$, and to a horizon $\mathcal{H}_o$ and $\mathcal{H}_c$ for $u=\infty$. A connected domain covered by finite values of coordinate *u* is indicated in Figs. 4–6 by the shaded background. Remaining parts of spacetime have to be covered by different patches of Robinson-Trautman coordinates defined analogously. The domain indicated in figures by a shaded background, covered by a single Robinson-Trautman map, thus reaches up to all types of infinity except to the part $\mathcal{I}_{I^-}$, which is, however, related to the part $\mathcal{I}_{I^+}$ by a simple time reversion. Therefore, we do not loose any substantial information using only this Robinson-Trautman coordinate map.

III. GRAVITATIONAL AND ELECTROMAGNETIC FIELDS NEAR $\mathcal{I}$

Now we are prepared to discuss radiative properties of the *C*-metric fields near the timelike infinity $\mathcal{I}$. As we have already mentioned in Sec. I, following [14], by *radiative field* we understand a field with the dominant component having

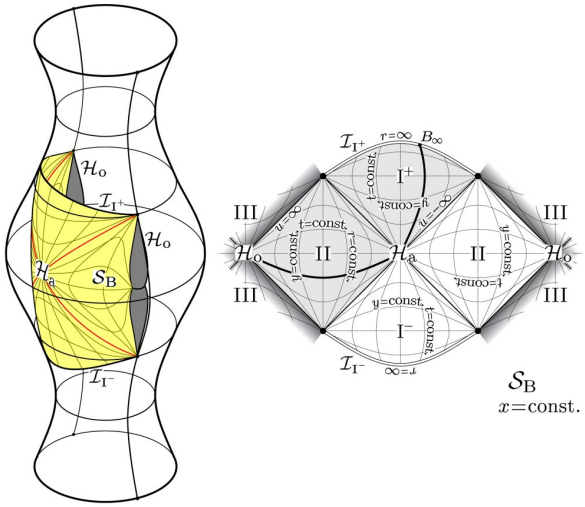

FIG. 5. Conformal diagram of the *t-y* section $\mathcal{S}_B$ intersecting only the horizons $\mathcal{H}_a$ outside black holes, and its embedding into three-dimensional diagram $\varphi=\text{const}$. Such a section of constant x (and φ) with $x\in(-y_a,-y_c)$ intersects all horizons except the cosmological ones. In contrast to section $\mathcal{S}_A$ of Fig. 4, section $\mathcal{S}_B$ does not extend through the whole spacetime, but it can be found near all pairs of black holes. The section still extends between both holes of a given pair. Section $\mathcal{S}_B$ intersects the infinity in two *spacelike* surfaces, one forming a future boundary of $\mathcal{S}_B$ belonging to domain $\mathcal{I}_{I^+}$, the other forming a past boundary belonging to domain $\mathcal{I}_{I^-}$, cf. Fig. 10. Notation for infinity, horizons, etc., is the same as in Fig. 4. The shaded area again indicates Robinson-Trautman coordinate patch.

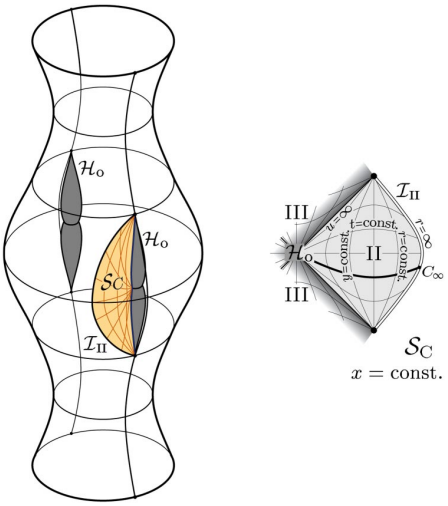

FIG. 6. Conformal diagram of the *t-y* section $\mathcal{S}_C$ not intersecting any horizons outside black holes, and its embedding into the three-dimensional diagram $\varphi=\text{const}$. Such a section of constant x (and φ) with $x\in[x_f,-y_a)$ does not intersect cosmological and acceleration horizons. In contrast to section $\mathcal{S}_A$ of Fig. 4, section $\mathcal{S}_C$ does not extend through the whole spacetime, but it can be found near any black hole. Unlike section $\mathcal{S}_B$ from Fig. 5, it even does not extend between holes of a given pair of black holes. Section $\mathcal{S}_C$ intersects the infinity in a timelike surface which belongs to domain $\mathcal{I}_{II}$ of the conformal infinity, cf. Fig. 10. Notation for infinity, horizons, etc., and the meaning of the shaded area are the same as in Fig. 4.

the $1/\eta$ fall-off, calculated in a tetrad parallelly transported along a null geodesic $z(\eta)$, η being the affine parameter. In the following we derive the characteristic *directional pattern of radiation*, i.e., the dependence of the radiative component of the fields on the *direction* along which a *given* point at the infinity is approached.

We start with a general *null geodesics* $z(\eta)$ approaching a fixed point N_∞ at infinity $\mathcal{I}$ as $\eta\to+\infty$ (or $\eta\to-\infty$). We observe that coordinates x, y, and u, ζ, as well as metric functions F, G, and P, are finite at the point N_∞, whereas the affine parameter η and the Robinson-Trautman coordinate r go to infinity as the geodesic approaches $\mathcal{I}$, cf. Sec. II. We denote the limiting values on $\mathcal{I}$ of the coordinates and the metric functions by a subscript "∞."

To obtain a more detailed description how N_∞ is reached, we have to find the tangent vector of the geodesic,

$$\frac{Dz}{d\eta}=\dot{t}\,\boldsymbol{\partial}_t+\dot{y}\,\boldsymbol{\partial}_y+\dot{x}\,\boldsymbol{\partial}_x+\dot{\varphi}\,\boldsymbol{\partial}_\varphi. \tag{3.1}$$

As mentioned in [32], an explicit form of the tangent vector can be obtained using specific geometrical properties of the *C*-metric (2.1). The presence of two Killing vectors $\boldsymbol{\partial}_t$, $\boldsymbol{\partial}_\varphi$, and of one conformal Killing tensor $\mathbf{Q}$ (cf. Sec. II) implies that there exist three constants of motion $E=-\boldsymbol{\partial}_t\cdot\frac{Dz}{d\eta}$, $J=\boldsymbol{\partial}_\varphi\cdot\frac{Dz}{d\eta}$, and $Q=\frac{1}{2}\mathbf{Q}(\frac{Dz}{d\eta},\frac{Dz}{d\eta})$, respectively, for any null geodesic. Namely, we have

$$E=\frac{F\dot{t}}{A^2(x+y)^2},\quad J=\frac{G\dot{\varphi}}{A^2(x+y)^2},$$

$$Q=\frac{F\dot{t}^2-F^{-1}\dot{y}^2+G^{-1}\dot{x}^2+G\dot{\varphi}^2}{2A^4(x+y)^4}. \tag{3.2}$$

In addition, $Dz/d\eta$ has a null norm

$$-F\dot{t}^2+F^{-1}\dot{y}^2+G^{-1}\dot{x}^2+G\dot{\varphi}^2=0. \tag{3.3}$$

The above four equations imply

$$\dot{t}=EA^2(x+y)^2F^{-1},\quad \dot{y}=\epsilon_yA^2(x+y)^2\sqrt{E^2-QF},$$
$$\dot{\varphi}=JA^2(x+y)^2G^{-1},\quad \dot{x}=\epsilon_xA^2(x+y)^2\sqrt{QG-J^2}, \tag{3.4}$$

where ϵ_y, $\epsilon_x=\pm1$ are the signs of $\dot{y}$ and $\dot{x}$, respectively. The components of the tangent vector $Dz/d\eta$ in the Robinson-Trautman coordinates (2.7) are thus given by

$$\dot{r}=-\epsilon_xA\sqrt{QG-J^2}-\epsilon_yA\sqrt{E^2-QF},$$

$$\dot{u}=\frac{1}{Ar^2F}(\epsilon_y\sqrt{E^2-QF}+E),$$

$$\dot{\zeta}=\frac{1}{\sqrt{2}r^2}(\epsilon_y\sqrt{E^2-QF}F^{-1}+EF^{-1}$$
$$-\epsilon_x\sqrt{QG-J^2}G^{-1}-iJG^{-1}). \tag{3.5}$$

We immediately observe that there exists a family of simple null geodesics $\dot r = AE$, $\dot\zeta = 0 = \dot u$, corresponding to the special choice of the constants $J=0=Q$, $\epsilon_y = -\operatorname{sgn} E$. These lie in the planes x, $\varphi = \text{const}$, cf. Eq. (3.4), and they are considered in Appendix A.

Now, we notice that $\dot r$ remains finite at infinity $\mathcal{I}$,

$$\dot r \approx -\epsilon_x A\sqrt{QG_\infty - J^2} - \epsilon_y A\sqrt{E^2 - QF_\infty} \equiv \gamma. \tag{3.6}$$

This means that r and η are asymptotically proportional,

$$r \approx \gamma\eta. \tag{3.7}$$

We can thus easily obtain the *asymptotic behavior* of the above tangent vector by expanding expressions (3.5) in powers of $1/\eta$ (assuming $\gamma \neq 0$ because the geodesic approaches infinity). We get [59]

$$\frac{Dz}{d\eta} \approx \frac{1}{\gamma\eta^2}(r^2\boldsymbol{\partial}_r - c\,\boldsymbol{\partial}_\zeta - \bar c\,\bar{\boldsymbol{\partial}}_\zeta - d\,\boldsymbol{\partial}_u), \tag{3.8}$$

with the constants $c \in \mathbb{C}$ and $d \in \mathbb{R}$ related to the conserved quantities E, J, Q by

$$\begin{aligned} c = &-\frac{1}{\gamma\sqrt{2}}(\epsilon_y\sqrt{E^2 - QF_\infty}F_\infty^{-1} + EF_\infty^{-1} \\ &- \epsilon_x\sqrt{QG_\infty - J^2}G_\infty^{-1} - iJG_\infty^{-1}), \\ d = &-\frac{1}{\gamma A F_\infty}(\epsilon_y\sqrt{E^2 - QF_\infty} + E). \end{aligned} \tag{3.9}$$

These constants are not independent. In fact, they satisfy the normalization condition (3.3) which in Robinson-Trautman coordinates asymptotically reads [recall Eqs. (2.9) and (2.15)]

$$2P_\infty^{-2}c\bar c + 2d + \frac{\Lambda}{3}d^2 = 0. \tag{3.10}$$

The expansion (3.8) of the tangent vector corresponds to the asymptotic form of null geodesics $z(\eta)$ near $\mathcal{I}$ given by Eq. (3.7) and

$$\zeta = \zeta_\infty + \frac{c}{\gamma\eta} + \cdots, \quad u = u_\infty + \frac{d}{\gamma\eta} + \cdots. \tag{3.11}$$

The constants ζ_∞, u_∞ specify the *position* at $\mathcal{I}$ which particular geodesic (3.11) is approaching (or from which it is receding), whereas c, d represent the (spacetime) *direction* along which N_∞ is reached. The constant γ fixes the affine parameter η. From Eq. (3.7) we see that if $\gamma > 0$ then r is growing and geodesics are approaching the infinity for $\eta \to +\infty$—we will denote these as outgoing. On the other hand, when $\gamma < 0$ then the geodesics approach $\mathcal{I}$ ($r \to \infty$) as $\eta \to -\infty$, i.e., the coordinate r is decreasing with a growing η. The corresponding geodesics are ingoing: they ''start'' on $\mathcal{I}$ and recede from this into finite regions of the spacetime.

Solving the normalization condition (3.10) we obtain

$$d + \frac{3}{\Lambda} = \epsilon\frac{3}{\Lambda}\sqrt{1 - \frac{\Lambda}{3}\frac{2c\bar c}{P_\infty^2}}, \tag{3.12}$$

where $\epsilon = \pm 1$. For any given c there are thus two real values of d, according to the sign of ϵ. In fact, the above parameter ϵ identifies whether the geodesic is future or past oriented. To see this explicitly, let us consider the future-oriented timelike vector $\boldsymbol{\partial}_u$ near infinity [$\boldsymbol{\partial}_u \cdot \boldsymbol{\partial}_u = -H \approx (\Lambda/3)r^2 < 0$]. The projection of tangent vector (3.8) onto $\boldsymbol{\partial}_u$ is, using Eq. (3.12),

$$\frac{Dz}{d\eta}\cdot\boldsymbol{\partial}_u \approx -\gamma\left(1 + \frac{\Lambda}{3}d\right) = -\epsilon\gamma\sqrt{1 - \frac{\Lambda}{3}\frac{2c\bar c}{P_\infty^2}}. \tag{3.13}$$

The geodesic is thus future or past oriented when $\epsilon\gamma > 0$ or $\epsilon\gamma < 0$, respectively. Of course, it is physically natural to *restrict ourselves to future-oriented* geodesics only. Without loss of generality we thus assume the identification

$$\operatorname{sgn}\gamma = \epsilon. \tag{3.14}$$

Consequently, geodesics with $\epsilon = +1$ are *outgoing* (reaching $\mathcal{I}$ for $\eta \to +\infty$) whereas those with $\epsilon = -1$ are *ingoing* (starting at $\mathcal{I}$ for $\eta \to -\infty$).

In order to find the radiative behavior of fields near $\mathcal{I}$ we have to set up an interpretation tetrad transported parallelly along a general asymptotic null geodesic, and project the Weyl tensor and the tensor of electromagnetic field onto this tetrad. In fact, in the following we will employ several orthonormal and null tetrads which will be distinguished by specific labels in subscript. We denote the vectors of a generic orthonormal tetrad as **t**, **q**, **r**, **s**, where **t** is a unit timelike vector and the remaining three are spacelike. With this normalized tetrad we associate a null tetrad **k**, **l**, **m**, $\bar{\mathbf{m}}$,

$$\begin{aligned} \mathbf{k} &= \frac{1}{\sqrt2}(\mathbf{t} + \mathbf{q}), \quad \mathbf{l} = \frac{1}{\sqrt2}(\mathbf{t} - \mathbf{q}), \\ \mathbf{m} &= \frac{1}{\sqrt2}(\mathbf{r} - i\mathbf{s}), \quad \bar{\mathbf{m}} = \frac{1}{\sqrt2}(\mathbf{r} + i\mathbf{s}), \end{aligned} \tag{3.15}$$

such that

$$\mathbf{k}\cdot\mathbf{l} = -1, \quad \mathbf{m}\cdot\bar{\mathbf{m}} = 1, \tag{3.16}$$

all other scalar products being zero.

The Weyl tensor is parametrized by five standard complex coefficients Ψ_n, $n = 0,1,2,3,4$, defined as its specific components with respect to the above null tetrad, see Eq. (B1). Similarly, the tensor of electromagnetic field is parametrized by Φ_n, $n = 0,1,2$, see Eq. (B2). The well-known transformation properties of coefficients Ψ_n and Φ_n under null rotations, boost, and spatial rotation of the tetrad are summarized in Appendix B.

To define a suitable *interpretation tetrad* $\mathbf{k}_\mathrm{i}$, $\mathbf{l}_\mathrm{i}$, $\mathbf{m}_\mathrm{i}$, $\bar{\mathbf{m}}_\mathrm{i}$ we need to specify either its initial condition inside the spacetime, or its final condition at timelike infinity $\mathcal{I}$, in a comparable way for all geodesics approaching infinity along differ-

ent directions. We consider geodesics which reach the same point N_∞ at $\mathcal{I}$, and thus we prescribe the final condition there. We naturally require that the null vector $\mathbf{k}_\mathrm{i}$ is *proportional to the tangent vector* (3.8) of the asymptotic null geodesic (3.11),

$$\mathbf{k}_\mathrm{i} \approx \frac{\epsilon}{\gamma}\frac{Dz}{d\eta}. \tag{3.17}$$

We wish to *compare* the radiation for all such null geodesics approaching the given point at $\mathcal{I}$, and it is thus necessary to consider a unique and universal normalization of the affine parameter η, and of the vector $\mathbf{k}_\mathrm{i}$. A natural and also the most convenient choice is to *keep the parameter* γ *fixed*—see an analogous discussion in [20] near Eqs. (5.6) and (5.9). In fact, this is equivalent to fixing the component $\mathbf{p}\cdot\mathbf{n}$ of the 4-momentum $\mathbf{p}=Dz/d\eta$ at some large value of r, i.e., at the given proximity of the conformal infinity.

Following a general framework introduced in [14], the null vector $\mathbf{l}_\mathrm{i}$ of the interpretation tetrad now can be fixed asymptotically by normalization (3.16) and the requirement that on $\mathcal{I}$ the *vector* $\mathbf{n}$ *normal to the infinity belongs to* $\mathbf{k}_\mathrm{i}$-$\mathbf{l}_\mathrm{i}$ *plane*. Obviously, the direction of $\mathbf{l}_\mathrm{i}$ at a point N_∞ on $\mathcal{I}$ thus uniquely depends on the choice of the particular null geodesic (3.11) approaching infinity, i.e., on the specific vector $\mathbf{k}_\mathrm{i}$. Remaining vectors $\mathbf{m}_\mathrm{i}$, $\overline{\mathbf{m}}_\mathrm{i}$ cannot be prescribed canonically—there is a freedom in choice of their phase factor (a rotation in the transverse $\mathbf{m}_\mathrm{i}$-$\overline{\mathbf{m}}_\mathrm{i}$ plane). Therefore, we have to find such physical quantities which are invariant under this freedom. Obviously, the *moduli* $|\Psi_n|$ and $|\Phi_n|$ of the fields at $\mathcal{I}$ are independent of the specific choice of the vectors $\mathbf{m}_\mathrm{i}$, $\overline{\mathbf{m}}_\mathrm{i}$.

To derive the field components in the above-defined interpretation tetrad we start with the simple Robinson-Trautman null tetrad $\mathbf{k}_\mathrm{RT}$, $\mathbf{l}_\mathrm{RT}$, $\mathbf{m}_\mathrm{RT}$, $\overline{\mathbf{m}}_\mathrm{RT}$ (see, e.g., [31]) naturally adapted to the Robinson-Trautman coordinates (2.8)

$$\mathbf{k}_\mathrm{RT}=\boldsymbol{\partial}_r,\quad \mathbf{l}_\mathrm{RT}=-\tfrac{1}{2}H\boldsymbol{\partial}_r+\boldsymbol{\partial}_u,$$

$$\mathbf{m}_\mathrm{RT}=\frac{P}{r}\boldsymbol{\partial}_{\bar\zeta},\quad \overline{\mathbf{m}}_\mathrm{RT}=\frac{P}{r}\boldsymbol{\partial}_\zeta. \tag{3.18}$$

Note that the vector $\mathbf{k}_\mathrm{RT}$ is oriented along the double degenerate principal null direction $\mathbf{k}_1$, cf. Eq. (5.4). In this tetrad the only nontrivial components Ψ_n^RT and Φ_n^RT, which represent the gravitational and electromagnetic fields, are

$$\Psi_2^\mathrm{RT}=-\left(m+2e^2Ax-\frac{e^2}{r}\right)\frac{1}{r^3},$$

$$\Psi_3^\mathrm{RT}=-\frac{3}{\sqrt{2}}\frac{Ar}{P}\Psi_2^\mathrm{RT},\quad \Psi_4^\mathrm{RT}=3\frac{A^2r^2}{P^2}\Psi_2^\mathrm{RT},$$

$$\Phi_1^\mathrm{RT}=-\frac{e}{2r^2},\quad \Phi_2^\mathrm{RT}=-\sqrt{2}\frac{Ar}{P}\Phi_1^\mathrm{RT}. \tag{3.19}$$

The interpretation tetrad $\mathbf{k}_\mathrm{i}$, $\mathbf{l}_\mathrm{i}$, $\mathbf{m}_\mathrm{i}$, $\overline{\mathbf{m}}_\mathrm{i}$ can be obtained by performing two subsequent null rotations and a boost of this Robinson-Trautman null tetrad (3.18). We first apply Eq. (B6), then Eq. (B3), and finally Eq. (B9) of Appendix B with the parameters [60]

$$K=-\left(1+\frac{\Lambda}{6}d\right)^{-1}\frac{c}{Pr},$$

$$L=\frac{\Lambda}{6}\frac{cr}{P},$$

$$B=\epsilon\left(1+\frac{\Lambda}{6}d\right),\quad \Phi=0. \tag{3.20}$$

The resulting null tetrad, using relation (3.10), then takes the following asymptotic form as $\eta\to\epsilon\infty$:

$$\mathbf{k}_\mathrm{i}\approx\epsilon\frac{1}{\gamma^2\eta^2}(r^2\boldsymbol{\partial}_r-c\boldsymbol{\partial}_\zeta-\bar c\boldsymbol{\partial}_{\bar\zeta}-d\boldsymbol{\partial}_u),$$

$$\mathbf{l}_\mathrm{i}\approx\epsilon\frac{\Lambda}{6}\left[r^2\boldsymbol{\partial}_r+c\boldsymbol{\partial}_\zeta+\bar c\boldsymbol{\partial}_{\bar\zeta}+\left(d+\frac{6}{\Lambda}\right)\boldsymbol{\partial}_u\right],$$

$$\mathbf{m}_\mathrm{i}\approx\frac{P_\infty}{\gamma\eta}\left[\frac{\Lambda}{6}\frac{cd}{\bar c}\boldsymbol{\partial}_\zeta+\left(1+\frac{\Lambda}{6}d\right)\boldsymbol{\partial}_{\bar\zeta}-\frac{c}{P_\infty^2}\boldsymbol{\partial}_u\right],$$

$$\overline{\mathbf{m}}_\mathrm{i}\approx\frac{P_\infty}{\gamma\eta}\left[\left(1+\frac{\Lambda}{6}d\right)\boldsymbol{\partial}_\zeta+\frac{\Lambda}{6}\frac{\bar c d}{c}\boldsymbol{\partial}_{\bar\zeta}-\frac{\bar c}{P_\infty^2}\boldsymbol{\partial}_u\right]. \tag{3.21}$$

The above vector $\mathbf{k}_\mathrm{i}$ is indeed obviously tangent to a general asymptotic null geodesics (3.11), and satisfies the condition (3.17). Moreover, the normal $\mathbf{n}$ to $\mathcal{I}$, cf. Eq. (2.16), belongs to the plane spanned by the two null vectors $\mathbf{k}_\mathrm{i}$ and $\mathbf{l}_\mathrm{i}$, as required,

$$\mathbf{n}\approx\frac{\epsilon}{\sqrt{2}}\left(\sqrt{-\frac{\Lambda}{6}}\,\gamma\eta\,\mathbf{k}_\mathrm{i}-\sqrt{-\frac{6}{\Lambda}}\,\frac{1}{\gamma\eta}\mathbf{l}_\mathrm{i}\right). \tag{3.22}$$

Notice that the projection of $\mathbf{k}_\mathrm{i}$ on $\mathbf{n}$ is

$$\mathbf{k}_\mathrm{i}\cdot\mathbf{n}\approx\frac{\epsilon}{\gamma\eta}\sqrt{-\frac{3}{\Lambda}}. \tag{3.23}$$

For outgoing geodesics ($\epsilon=+1,\eta\to+\infty$) we indeed obtain $\mathbf{k}_\mathrm{i}\cdot\mathbf{n}>0$, whereas for ingoing ones ($\epsilon=-1,\eta\to-\infty$) there is $\mathbf{k}_\mathrm{i}\cdot\mathbf{n}<0$.

Therefore, the tetrad (3.21) is exactly the interpretation tetrad suitable for analysis of the behavior of fields close to infinity $\mathcal{I}$. As seen above, the Lorentz transformations from the tetrad (3.18) to (3.21) are given by two subsequent null rotations and the boost with the parameters (3.20). Starting with the components (3.19) in the Robinson-Trautman frame we thus obtain, using Eqs. (B7), (B4), (B10) and (B8), (B5), (B11), the asymptotic form of the leading terms of gravitational and electromagnetic fields

$$\Psi_4^\mathrm{i}\approx-\frac{3(m+2e^2Ax_\infty)}{\gamma\eta P_\infty^2}\left[A\left(1+\frac{\Lambda}{6}d\right)-\frac{\Lambda\bar c}{3\sqrt{2}}\right]^2,$$

$$\Phi_2^{\mathrm{i}} \approx \frac{\epsilon e}{\sqrt{2}\,\gamma\eta P_\infty}\left[A\left(1+\frac{\Lambda}{6}d\right)-\frac{\Lambda\bar{c}}{3\sqrt{2}}\right], \tag{3.24}$$

where x_∞ is the coordinate of the point N_∞ related to the coordinates ζ_∞, u_∞ by Eq. (2.11). The other terms decrease faster in accordance with the well-known *peeling behavior*, which is a consequence of the boost contained in Eq. (3.22) that is infinite on $\mathcal{I}$, cf. [14]. Notice also that the square of Φ_2^{i} gives the modulus of the Poynting vector, $4\pi|\mathbf{S}_{\mathrm{i}}| \approx |\Phi_2^{\mathrm{i}}|^2$, defined in the interpretation tetrad (3.21). Interestingly, the dependence of $|\Psi_4^{\mathrm{i}}|$ and $|\Phi_2^{\mathrm{i}}|^2$ on the direction along which the point N_∞ at infinity $\mathcal{I}$ is approached is *exactly the same*.

Expressions (3.24) are (formally) identical to Eqs. (6.16) of [20] in which radiation in the *C*-metric spacetime with $\Lambda>0$ was investigated. Interestingly enough, one can also directly set $\Lambda=0$. The directional dependence given by the parameters c and d vanishes in this limit (since $\mathbf{l}_{\mathrm{i}}$ becomes independent of $\mathbf{k}_{\mathrm{i}}$) and formulas (3.24) can be compared with the results obtained in classic work [32] (see also [33]) for accelerated black holes in asymptotically flat spacetime.

Nevertheless, the physical and geometrical meanings of Eqs. (3.24) is very different now since new interesting and specific features occur for the $\Lambda<0$ case. The following sections will be devoted to deeper description and analysis of the above result.

IV. PARAMETRIZATIONS OF THE NULL DIRECTION AT $\mathcal{I}$

For a physical understanding of expressions (3.24), as well as for explicit demonstration of fundamental differences between radiation generated by accelerated black holes in spacetimes with $\Lambda>0$ and $\Lambda<0$, we introduce more convenient parameterizations of the direction $\mathbf{k}_{\mathrm{i}}$ along which the infinity $\mathcal{I}$—now timelike—is approached. To parametrize this radiation direction we first choose a suitable *reference tetrad* $\mathbf{t}_{\mathrm{o}}$, $\mathbf{q}_{\mathrm{o}}$, $\mathbf{r}_{\mathrm{o}}$, $\mathbf{s}_{\mathrm{o}}$ on $\mathcal{I}$ which is orthonormal, adapted to the infinity,

$$\mathbf{q}_{\mathrm{o}}=\mathbf{n}, \tag{4.1}$$

and with $\mathbf{t}_{\mathrm{o}}$ future oriented. Otherwise the tetrad can be chosen arbitrarily. A natural choice is to consider a tetrad closely related to the Robinson-Trautman tetrad (3.18), namely,

$$\mathbf{k}_{\mathrm{o}}=\sqrt{\frac{H}{2}}\,\mathbf{k}_{\mathrm{RT}}, \quad \mathbf{l}_{\mathrm{o}}=\sqrt{\frac{2}{H}}\,\mathbf{l}_{\mathrm{RT}}, \quad \mathbf{m}_{\mathrm{o}}=\mathbf{m}_{\mathrm{RT}}, \tag{4.2}$$

so that [cf. Eq. (3.15)]

$$\begin{aligned}
\boldsymbol{\partial}_u &= \sqrt{H}\;\mathbf{t}_{\mathrm{o}},\\
\boldsymbol{\partial}_r &= \frac{1}{\sqrt{H}}(\mathbf{t}_{\mathrm{o}}+\mathbf{q}_{\mathrm{o}}),\\
\boldsymbol{\partial}_{\zeta} &= \frac{1}{\sqrt{2}}\,\frac{r}{P}(\mathbf{r}_{\mathrm{o}}+i\mathbf{s}_{\mathrm{o}}).
\end{aligned} \tag{4.3}$$

The null direction $\mathbf{k}_{\mathrm{i}}$ can be obtained (up to normalization) from the above reference vector $\mathbf{k}_{\mathrm{o}}$ by a null rotation (B6), and thus it can be parametrized by a complex parameter R as [61]

$$\mathbf{k}_{\mathrm{i}} \propto \mathbf{k}_{\mathrm{o}}+\bar{R}\mathbf{m}_{\mathrm{o}}+R\bar{\mathbf{m}}_{\mathrm{o}}+R\bar{R}\mathbf{l}_{\mathrm{o}}. \tag{4.4}$$

Comparing this expression with Eq. (3.21) we can relate R to the parameters c and d,

$$\begin{aligned}
c &= -\sqrt{-\frac{6}{\Lambda}}\,P_\infty\frac{R}{1-|R|^2},\\
d &= \frac{6}{\Lambda}\,\frac{|R|^2}{1-|R|^2}.
\end{aligned} \tag{4.5}$$

Now we may rewrite the directional pattern (3.24) in terms of the parameter R. First, recall that there is no canonical way how to choose the phase of the transverse null vectors $\mathbf{m}_{\mathrm{i}}$, $\bar{\mathbf{m}}_{\mathrm{i}}$. Therefore, invariant information independent of a choice of the interpretation tetrad is contained only in the *moduli* of fields components. Substituting relations (4.5) into expressions (3.24) we obtain

$$\begin{aligned}
|\Psi_4^{\mathrm{i}}| &\approx \frac{3A^2(m+2e^2Ax_\infty)}{\gamma\eta P_\infty^2}\,\frac{|1-R_1\bar{R}|^2|1-R_2\bar{R}|^2}{(1-|R|^2)^2},\\
|\Phi_2^{\mathrm{i}}| &\approx \frac{|e|A}{\sqrt{2}\,\gamma\eta P_\infty}\,\frac{|1-R_1\bar{R}||1-R_2\bar{R}|}{|1-|R|^2|},
\end{aligned} \tag{4.6}$$

where

$$R_1=0, \quad R_2=\sqrt{-\frac{\Lambda}{3}}\,\frac{P_\infty}{A}. \tag{4.7}$$

We have introduced here not only R_2 but also a "superfluous" parameter $R_1=0$. This is motivated by a general result [62] concerning an asymptotic structure of the fields when $\Lambda<0$. In fact, the real parameters R_1, R_2 have an important physical meaning—they represent double-degenerate *principal null directions* (PNDs) $\mathbf{k}_1$ and $\mathbf{k}_2$ [cf. Eq. (2.5)] at the infinity $\mathcal{I}$. Indeed, the specific complex parameter R representing a PND with respect to the reference tetrad has to satisfy quartic equation $\Psi_0=0$ (see, e.g., [31]), i.e., using Eq. (B7),

$$R^4\Psi_4^{\mathrm{o}}+4R^3\Psi_3^{\mathrm{o}}+6R^2\Psi_2^{\mathrm{o}}+4R\Psi_1^{\mathrm{o}}+\Psi_0^{\mathrm{o}}=0. \tag{4.8}$$

This, in view of Eqs. (4.2), (B10), and (3.19), asymptotically reduces exactly to

$$(R-R_1)^2(R-R_2)^2=0. \tag{4.9}$$

Therefore, the first double-degenerate PND $\mathbf{k}_1$ is indeed given by $R=R_1$, whereas the second one, $\mathbf{k}_2$, is given by $R=R_2$.

Instead of using the complex parameter R for identification of the null direction $\mathbf{k}_i$ we can introduce two real parameters with an obvious geometrical meaning. First, we perform a normalized projection of the null vector $\mathbf{k}_i$ onto $\mathcal{I}$, defining thus the unit timelike vector $\mathbf{t}_b$ tangent to the infinity:

$$\mathbf{t}_b = \frac{\mathbf{k}_i - (\mathbf{k}_i \cdot \mathbf{n})\mathbf{n}}{|\mathbf{k}_i \cdot \mathbf{n}|}. \tag{4.10}$$

Then $\mathbf{t}_b$ represents the radiation direction along $\mathcal{I}$ corresponding to the null vector $\mathbf{k}_i \propto \mathbf{t}_b + \epsilon\mathbf{n}$. We can characterize $\mathbf{t}_b$ (and thus $\mathbf{k}_i$) with respect to the reference tetrad as

$$\mathbf{t}_b = \cosh\psi\ \mathbf{t}_o + \sinh\psi(\cos\phi\ \mathbf{r}_o + \sin\phi\ \ \mathbf{s}_o). \tag{4.11}$$

The parameters ψ, ϕ are *pseudo-spherical* coordinates, $\psi \in [0,\infty)$ corresponding to a *boost*, and $\phi \in [0,2\pi)$ being an *angle*. Their geometric meaning is visualized in Fig. 7. However, these parameters do not specify the null direction $\mathbf{k}_i$ uniquely—there always exists *one ingoing* and *one outgoing* null direction with the same parameters ψ and ϕ, which are distinguished by ϵ.

Substituting Eq. (4.4) into Eq. (4.10) and comparing with Eq. (4.11) we can express ψ and ϕ in terms of R as

$$\tanh\psi = \frac{2|R|}{1+|R|^2}, \quad \phi = -\arg R. \tag{4.12}$$

Observing that the sign of the expression $1-|R|^2 \propto \mathbf{k}_i \cdot \mathbf{n}$ determines whether $\mathbf{k}_i$ is ingoing or outgoing, i.e.,

$$\epsilon = \mathrm{sgn}(1-|R|^2), \tag{4.13}$$

we can write down the inverse relations,

$$R = \begin{cases} \tanh\dfrac{\psi}{2}\exp(-i\phi) & \text{for } \mathbf{k}_i \text{ outgoing } (\epsilon = +1), \\ \coth\dfrac{\psi}{2}\exp(-i\phi) & \text{for } \mathbf{k}_i \text{ ingoing } (\epsilon = -1), \end{cases} \tag{4.14}$$

and also the relations to the parameters c and d,

$$-\epsilon\sqrt{-\frac{\Lambda}{6}}\,\frac{2\overline{c}}{P_\infty} = \sinh\psi\exp(i\phi), \quad \epsilon\left(1+\frac{\Lambda}{3}d\right) = \cosh\psi. \tag{4.15}$$

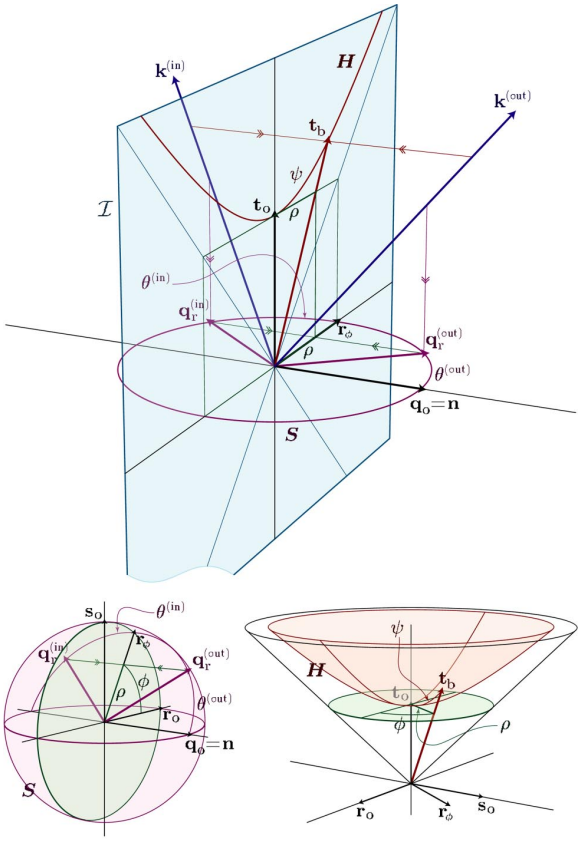

FIG. 7. Parametrizations of a null direction at timelike infinity $\mathcal{I}$. All null directions at a point $N_\infty \in \mathcal{I}$ can be characterized by a future oriented null vector $\mathbf{k}$. According to their orientation $\epsilon = \mathrm{sgn}(\mathbf{k}\cdot\mathbf{n})$ with respect to $\mathcal{I}$, these can be divided into *outgoing* and *ingoing* families—see, e.g., vectors $\mathbf{k}^{(\mathrm{out})}$ and $\mathbf{k}^{(\mathrm{in})}$ in the figure. (Special null directions *tangent* to $\mathcal{I}$ will not be discussed here.) The null direction is parametrized by a boost ψ and an angle ϕ, or alternatively by spherical angles θ, ϕ. These parametrizations are defined with respect to the reference tetrad $\mathbf{t}_o$, $\mathbf{q}_o$, $\mathbf{r}_o$, $\mathbf{s}_o$. In the top diagram the vectors $\mathbf{t}_o$, $\mathbf{q}_o$, $\mathbf{r}_\phi$ (where $\mathbf{r}_\phi = \cos\phi\,\mathbf{r}_o + \sin\phi\,\mathbf{s}_o$) are depicted, the remaining spatial direction $\mathbf{s}_\phi$ is suppressed. In the bottom left diagram the timelike direction $\mathbf{t}_o$ is suppressed and all spatial directions are drawn. Finally, in the bottom right diagram the spatial direction $\mathbf{q}_o = \mathbf{n}$ normal to $\mathcal{I}$ is omitted. The parameters ψ, ϕ specify the normalized orthogonal projection $\mathbf{t}_b$ [Eq. (4.10)] of the null vector $\mathbf{k}$ onto $\mathcal{I}$ by Eq. (4.11). All possible $\mathbf{t}_b$ form a two-dimensional hyperboloid $\boldsymbol{H}$ drawn in the bottom right diagram. This hyperboloid can be radially projected onto a two-dimensional disk tangent to the vertex of the hyperboloid given by $\mathbf{t}_o$. The disk can be parametrized by radial coordinate $\rho = \tanh\psi$, and angle ϕ. Alternatively, the null direction can be characterized by the normalized *spatial* projection $\mathbf{q}_r$ [Eq. (4.17)] of the null vector $\mathbf{k}$ into the 3-space orthogonal to $\mathbf{t}_o$. The projection $\mathbf{q}_r$ can be parametrized by spherical angles θ, ϕ with respect to the reference tetrad, see Eq. (4.18). All spatial projections $\mathbf{q}_r$ form a two-dimensional sphere $\boldsymbol{S}$ shown in the bottom left. This sphere can be orthogonally projected onto $\mathcal{I}$, where it again forms a two-dimensional disk parametrized by $\rho = \sin\theta$, and ϕ, cf. Eq. (4.19).

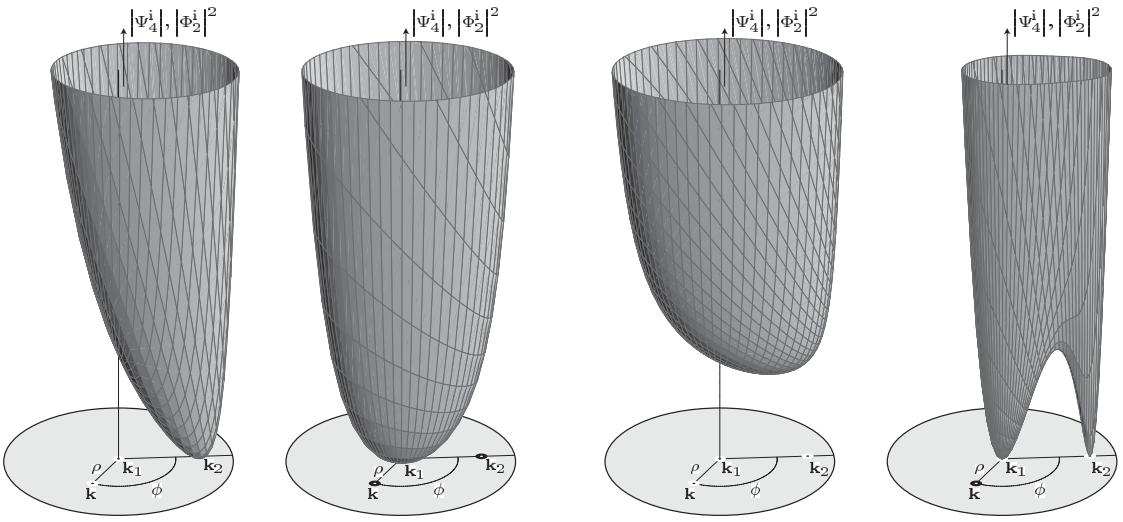

FIG. 8. Possible directional patterns of radiation (4.16) [or, equivalently, (4.6), (4.21)] which express the magnitude of the leading terms of gravitational or electromagnetic fields as a function of a direction from which the point N_∞ at infinity $\mathcal{I}$ is approached. The corresponding outgoing ($\epsilon=+1$, small white spot) or ingoing ($\epsilon=-1$, black spot) null geodesic with a tangent vector $\mathbf{k}$ are parametrized by $\rho=\tanh\psi$ and ϕ, cf. Fig. 7. The patterns (a) apply to points N_∞ in which the double degenerate PND $\mathbf{k}_1$ (white spot) is oriented outwards from the universe whereas $\mathbf{k}_2$ (black spot) inside it. The patterns (b) apply to points in which both the PNDs are outgoing. The pattern (b) would also apply for points where both PNDs are ingoing, only with exchanged words ''ingoing'' and ''outgoing.'' The radiation completely vanishes along directions which are exactly mirrored of the PNDs, with respect to $\mathcal{I}$.

Substituting from Eq. (4.15) into Eq. (3.24) we obtain

$$|\Psi_4^i| \approx \frac{|\Lambda|}{4}\frac{(m+2e^2Ax_\infty)}{\gamma\eta} \times|R_2^{-1}(1+\epsilon\cosh\psi)-\epsilon\sinh\psi\exp(i\phi)|^2,$$

$$|\Phi_2^i| \approx \sqrt{\frac{|\Lambda|}{24}}\frac{|e|}{\gamma\eta} \times|R_2^{-1}(1+\epsilon\cosh\psi)-\epsilon\sinh\psi\exp(i\phi)|. \tag{4.16}$$

The dependence of the fields on the parameters ψ and ϕ is shown in Fig. 8.

There exists yet another natural possibility how to characterize the null direction at the infinity. Instead of decomposing the propagation vector $\mathbf{k}_i$ into the component normal to $\mathcal{I}$ and the transverse timelike vector $\mathbf{t}_b$ tangent to $\mathcal{I}$, we may alternatively consider its normalized *spatial* projection $\mathbf{q}_r$, where by the spatial projection we mean a projection to a suitable three-dimensional space, say that orthogonal to $\mathbf{t}_o$ (see Fig. 7). This spatial propagation vector

$$\mathbf{q}_r=\frac{\mathbf{k}_i+(\mathbf{k}_i\cdot\mathbf{t}_o)\mathbf{t}_o}{|\mathbf{k}_i\cdot\mathbf{t}_o|}, \tag{4.17}$$

such that $\mathbf{k}_i\propto\mathbf{t}_o+\mathbf{q}_r$, is naturally characterized by *spherical* angles θ and ϕ with respect to the spatial vectors $\mathbf{q}_o$, $\mathbf{r}_o$, $\mathbf{s}_o$ of the reference tetrad, namely,

$$\mathbf{q}_r=\cos\theta\ \mathbf{q}_o+\sin\theta(\cos\phi\ \mathbf{r}_o+\sin\phi\ \mathbf{s}_o). \tag{4.18}$$

Obviously, this is more convenient for a unified description of both outgoing ($\epsilon=+1$) and ingoing ($\epsilon=-1$) null geodesics. The former are parametrized by $\theta\in[0,\pi/2)$, the latter by $\theta\in(\pi/2,\pi]$. Comparing with the previous parametrizations of the null direction $\mathbf{k}_i$ we obtain

$$\sin\theta=\tanh\psi=\frac{2|R|}{1+|R|^2}\equiv\rho,$$

$$\cos\theta=\epsilon\,\mathrm{sech}\,\psi=\frac{1-|R|^2}{1+|R|^2},$$

$$\tan\theta=\epsilon\sinh\psi=\frac{2|R|}{1-|R|^2}. \tag{4.19}$$

The parameter ρ is used in Figs. 7, 8, and 11. The inverse relation

$$R=\tan\frac{\theta}{2}\exp(-i\phi), \tag{4.20}$$

and analogous expression Eq. (4.14), show that R is actually a *stereographic* parametrization of $\mathbf{q}_{\rm r}$, and *Lorentzian stereographic* parametrization of $\mathbf{t}_{\rm b}$.

Expressing the fields (4.16) using θ and ϕ we get

$$|\Psi_4^{\rm i}| \approx \frac{|\Lambda|}{4}\,\frac{(m+2e^2Ax_\infty)}{\gamma\eta\cos^2\theta}\,|R_2^{-1}(1+\cos\theta)-\sin\theta\exp(i\phi)|^2,$$

$$|\Phi_2^{\rm i}| \approx \sqrt{\frac{|\Lambda|}{24}}\,\frac{|e|}{\gamma\eta|\cos\theta|}\,|R_2^{-1}(1+\cos\theta)-\sin\theta\exp(i\phi)|. \tag{4.21}$$

We have thus presented the directional radiation pattern at the anti–de Sitter infinity using three suitable parametrizations of the null direction along which the infinity is approached, namely Eqs. (4.6), (4.16), and (4.21). The pattern is depicted in Fig. 8. Now we can proceed with its physical interpretation.

V. ANALYSIS OF THE RADIATION PATTERN

First, we observe that the radiation ''blows up'' for directions with $|R|=1$, i.e., $\psi\to\infty$, $\theta=\pi/2$, $\rho=1$. These are null directions *tangent* to the infinity $\mathcal{I}$, and thus they do not represent a direction of any outgoing or ingoing geodesic approaching the infinity from the ''interior'' of the spacetime. The reason for this divergent behavior of the radiation is purely kinematic: by imposing the ''comparable'' final conditions for the interpretation tetrad [cf. the discussion after Eq. (3.17)] we have fixed the projection of the 4-momentum $\mathbf{p}\propto\mathbf{k}_{\rm i}$ onto the normal $\mathbf{n}$. Clearly, this condition leads to an ''infinite'' rescaling of $\mathbf{k}_{\rm i}$ if $\mathbf{k}_{\rm i}$ is tangent to $\mathcal{I}$, i.e., orthogonal to $\mathbf{n}$. Such rescaling results in the above divergence of $|\Psi_4^{\rm i}|$ and $|\Phi_2^{\rm i}|$.

This divergence at $|R|=1$ actually splits the radiation pattern into two components—the radiation pattern for *outgoing* geodesics, $|R|<1$, and to the pattern for *ingoing* geodesics, $|R|>1$, cf. Eq. (4.13). These two different patterns correspond to Eq. (4.16) with $\epsilon=+1$ and $\epsilon=-1$, respectively. They are depicted in Fig. 8 as separate diagrams.

From Eqs. (4.6) it can immediately be observed that radiation completely vanishes, $|\Psi_4^{\rm i}|=0=|\Phi_2^{\rm i}|$, along specific null directions with $R=R_{\rm m}$ satisfying

$$R_{\rm m}=\frac{1}{R_1} \quad \text{or} \quad R_{\rm m}=\frac{1}{R_2}. \tag{5.1}$$

In fact, the direction given by $1/R_n$, $n=1,2$ is the *mirrored reflection* of the PND $\mathbf{k}_n$ with respect to $\mathcal{I}$: using Eqs. (4.13), (4.14) we find that both $1/R_n$ and R_n correspond to the same $\psi=\psi_n$ (and $\phi=0$) but with the opposite ϵ. *The radiation thus vanishes along mirrored reflections of the PNDs* [63].

In terms of pseudo-spherical parameters ψ, ϕ we find, cf. also Eqs. (4.16), that the radiation vanishes along outgoing ($\epsilon=+1$) null geodesics such that

$$\coth\frac{\psi_{\rm m}}{2}=R_2, \quad \phi_{\rm m}=0, \tag{5.2}$$

or along ingoing ($\epsilon=-1$) geodesics given by

$$\tanh\frac{\psi_{\rm m}}{2}=R_1\Rightarrow\psi_{\rm m}=0, \quad \text{or}$$

$$\tanh\frac{\psi_{\rm m}}{2}=R_2, \quad \phi_{\rm m}=0. \tag{5.3}$$

Clearly, only one of the conditions (5.2), (5.3) involving R_2 can be satisfied for a given value of R_2. Therefore, further description of the radiation pattern necessarily depends on the *specific algebraic structure of the spacetime at a given point N_∞ at $\mathcal{I}$*, in particular on the *orientation* of PNDs.

The PNDs have explicit form, cf. Eqs. (4.4), (4.7),

$$\mathbf{k}_1\propto\frac{1}{\sqrt{2}}(\mathbf{t}_{\rm o}+\mathbf{q}_{\rm o})=\mathbf{k}_{\rm o}\propto\mathbf{k}_{\rm RT},$$

$$\mathbf{k}_2\propto\frac{1}{\sqrt{2}}\left(\mathbf{t}_{\rm o}+\frac{1-R_2^2}{1+R_2^2}\mathbf{q}_{\rm o}+\frac{2R_2}{1+R_2^2}\mathbf{r}_{\rm o}\right). \tag{5.4}$$

Using the relation (4.14) they can be parametrized as

$$\psi_1=0,$$

$$\tanh\frac{\psi_2}{2}=\begin{cases} R_2 & \text{for } R_2\leqslant 1 \\ 1/R_2 & \text{for } R_2\geqslant 1 \end{cases}, \quad \phi_2=0. \tag{5.5}$$

By inspecting Eqs. (5.4) we observe that the first PND $\mathbf{k}_1$ always points along the normal $\mathbf{n}=\mathbf{q}_{\rm o}$, i.e., *outside the universe*. However, for the second PND $\mathbf{k}_2$ there are distinct possibilities according to whether $R_2\lessgtr 1$. At points on $\mathcal{I}$ where $R_2<1$ the vector $\mathbf{k}_2$ is *outgoing* ($\epsilon_2=+1$), i.e., oriented *outside* the universe. In the regions where $R_2>1$ it is *ingoing* ($\epsilon_2=-1$), oriented *inside* the universe. At special points where $R_2=1$ the PND $\mathbf{k}_2\propto(\mathbf{t}_{\rm o}+\mathbf{r}_{\rm o})$ has no component along $\mathbf{n}$; it is *tangent to* $\mathcal{I}$.

Which of these three alternatives can occur depends on values of the parameters describing the spacetime. Before we continue with a discussion of the different possibilities, let us note that the three possible regions of $\mathcal{I}$ with the distinct structure of PNDs *exactly coincide* with regions of different *characters of the Killing vector field* $\boldsymbol{\partial}_t$. Recalling (2.12), the value of the metric function F at a given point N_∞ on $\mathcal{I}$ is $F_\infty=F|_{y=-x_\infty}$. Considering Eqs. (2.3), (2.9), and (4.7) we obtain

$$F_\infty=\frac{R_2^2-1}{P_\infty^2}=(R_2^2-1)G_\infty, \tag{5.6}$$

which demonstrates the relation between the structure of PNDs and the character of the spacetime near infinity. If $R_2<1$ then $F_\infty<0$ and the Killing vector $\boldsymbol{\partial}_t$ near $\mathcal{I}$ is spacelike. If, instead, $R_2>1$ then $F_\infty>0$ and $\boldsymbol{\partial}_t$ is a timelike Killing vector field—the region near $\mathcal{I}$ is thus *static*. The above two domains of infinity are separated by the *Killing horizon* consisting of points for which $R_2=1$, where the Killing vector is null. Note that the Killing horizons may indeed extend

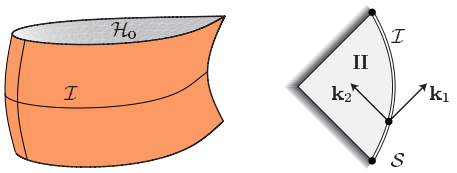

FIG. 9. When $A<\sqrt{-\Lambda/3}$, the *C*-metric represents a single, uniformly accelerated black hole. The region near infinity $\mathcal{I}$ is everywhere static. The first PND $\mathbf{k}_1$ is oriented outside the universe, whereas the second one $\mathbf{k}_2$ points inside it.

(for sufficiently large acceleration) to the conformal infinity, which is a specific property of anti–de Sitter *C*-metric.

A. A single accelerated black hole

We now discuss the case when the acceleration parameter A is small, $A<\sqrt{-\Lambda/3}$. As explained in Sec. II A, the *C*-metric then describes a single uniformly accelerated black hole in an anti–de Sitter universe. Its global structure for a constant φ is visualized in Fig. 1. There are *no* Killing horizons extending to $\mathcal{I}$ (which would correspond to $F_\infty=0$, i.e., $R_2=1$) since using Eq. (4.7), (2.10), and $0\leqslant G\leqslant 1$ there is

$$R_2>P_\infty=\frac{1}{\sqrt{G_\infty}}\geqslant 1, \tag{5.7}$$

for all $x\in[x_f,x_b]$. Accordingly, the region near infinity $\mathcal{I}$ is *everywhere static*. We thus find that the first PND $\mathbf{k}_1$ is always oriented *outside*, whereas the second one $\mathbf{k}_2$ is always oriented *inside* the universe, see Eq. (5.4) and Fig. 9.

The corresponding radiation pattern is shown in Fig. 8(a). There exists *just one* direction along which the *outgoing* radiation ($\epsilon=+1, |R|<1$) vanishes, namely the direction $R_m=1/R_2$. It is the mirrored reflection of the ingoing PND $\mathbf{k}_2$ [see the left part of Fig. 8(a)]. In terms of pseudospherical parameters the direction is described by Eq. (5.2), i.e., $\psi_m=\psi_2$ and $\phi_m=\phi_2=0$, where ψ_2—the boost parameter characterizing $\mathbf{k}_2$—is given by Eq. (5.5). The radiation pattern for *ingoing* radiation ($\epsilon=-1, |R|>1$) is visualized in the right part of Fig. 8(a). Again, there exists just one direction of vanishing radiation given by $R_m=1/R_1=\infty$ [i.e., $\psi_m=\psi_1=0$, cf. Eq. (5.3)], which is also the mirrored reflection of a PND, this time of the outgoing $\mathbf{k}_1$.

B. A pair of accelerated black holes

A more interesting but also more complicated situation occurs when $A>\sqrt{-\Lambda/3}$. In this case the *C*-metric represents pairs of uniformly accelerated black holes in an anti–de Sitter universe, as indicated in Figs. 2–6; see Sec. II B. There are (outer) black-hole horizons $\mathcal{H}_o$, acceleration horizons $\mathcal{H}_a$, and cosmological horizons $\mathcal{H}_c$; see Fig. 2(a). At $\mathcal{I}$, the horizons $\mathcal{H}_a$ and $\mathcal{H}_c$ can be identified by $R_2=1$. They separate various static and nonstatic regions of $\mathcal{I}$, and simultaneously the domains of infinity with different structure of the PNDs, as shown in Fig. 10. The vector $\mathbf{k}_1$ is always oriented outside the universe. In the static domains of $\mathcal{I}$ where

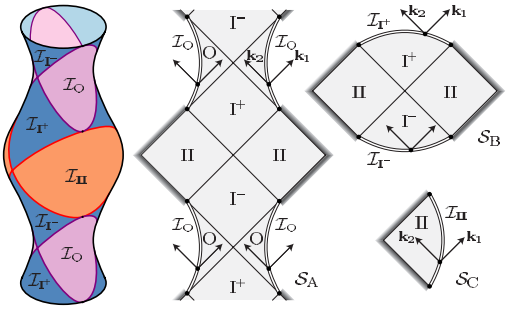

FIG. 10. For large values of $A>\sqrt{-\Lambda/3}$ the *C*-metric represents pairs of accelerated black holes. The conformal infinity $\mathcal{I}$ shown on the left is divided by horizons $\mathcal{H}_c$ and $\mathcal{H}_a$ into several distinct domains: $\mathcal{I}_O$ and $\mathcal{I}_{II}$ are static, whereas $\mathcal{I}_{I^+}$ and $\mathcal{I}_{I^-}$ are nonstatic. Moreover, in the regions $\mathcal{I}_O$ (corresponding to sections $\mathcal{S}_A$) and $\mathcal{I}_{II}$ (corresponding to $\mathcal{S}_C$) the PND $\mathbf{k}_1$ is oriented outwards, whereas the PND $\mathbf{k}_2$ is oriented inwards. In $\mathcal{I}_{I^+}$ (sections $\mathcal{S}_B$) both $\mathbf{k}_1$ and $\mathbf{k}_2$ point outside the universe, in $\mathcal{I}_{I^-}$ both the PNDs point inside it.

$R_2>1$, denoted as $\mathcal{I}_O$ and $\mathcal{I}_{II}$, $\mathbf{k}_2$ is oriented inside it; see Eq. (5.4). These domains of the infinity can be reached through the sections $\mathcal{S}_A$ and $\mathcal{S}_C$, cf. Figs. 4, 6. On the other hand, in the domain where $R_2<1$, denoted as $\mathcal{I}_{I^+}$ (accessible through $\mathcal{S}_B$, Fig. 5), both PNDs are oriented outside the spacetime.

In each of these regions the radiation pattern (4.16) is thus different. In particular, it admits a different number of directions along which the radiation vanishes. Recalling that the radiation vanishes along mirrored reflections of PNDs, we see that in the static regions $\mathcal{I}_O$ and $\mathcal{I}_{II}$ there is just one *outgoing* ($\epsilon=+1$) direction along which the radiation vanishes, as in the previous case of a single black hole. This is the mirrored reflection of $\mathbf{k}_2$, $R_m=1/R_2$ [$\psi_m=\psi_2$, $\phi_m=\phi_2=0$, cf. Eq. (5.2)]. The corresponding directional pattern is again given by the left part of Fig. 8(a). However, in the nonstatic region $\mathcal{I}_{I^+}$ there is no *outgoing* direction along which the radiation vanishes because mirrored reflections of both PNDs are ingoing. In other words, the condition (5.2) cannot be satisfied because $R_2<1$. The radiation pattern for outgoing directions for this case is shown in the left part of Fig. 8(b).

Of course, the number of null directions with vanishing radiation in the pattern for *ingoing* geodesics ($\epsilon=-1$) is complementary. In the domains $\mathcal{I}_O$ and $\mathcal{I}_{II}$ with $R_2>1$ there is again just one zero, now given by the mirrored reflection of $\mathbf{k}_1$ ($R_m=\infty$, $\psi_m=\psi_1=0$); see the right part of Fig. 8(a). On the other hand, in the domain $\mathcal{I}_{I^+}$ there are exactly two zeros for ingoing radiation given by mirrored reflections of both PNDs [$R_m=\infty$, $\psi_m=0$, and $R_m=1/R_2$, $\psi_m=\psi_2$, $\phi_m=0$, cf. Eq. (5.3)] as shown in the right part of Fig. 8(b).

In addition, there is also another domain with $R_2<1$, namely the domain $\mathcal{I}_{I^-}$; see Fig. 10. Here both PNDs are oriented inside the spacetime. However, the region I^- of the spacetime and its infinity $\mathcal{I}_{I^-}$ are *not covered* by the same map of Robinson-Trautman coordinates as that used above. We have to introduce another ''time-reversed'' map to cover the white domain in Fig. 5. Still, the directions of vanishing radiation are given by *mirrored directions* of the PNDs at the

infinity, similarly to the cases discussed above. The mirrored directions of the PNDs are both outgoing so that the radiation pattern for outgoing geodesics contains *two* zeros [cf. the right part of Fig. 8(b)], whereas the pattern for ingoing geodesics does not have any zero directions, cf. the left part of Fig. 8(b).

To summarize, the directional patterns of outgoing radiation [Eqs. (4.16) with $\epsilon=+1$, or Eqs. (4.6) with $|R|<1$] in the domains $\mathcal{I}_{\rm O}$, $\mathcal{I}_{\rm I^+}$, $\mathcal{I}_{\rm I^-}$, and $\mathcal{I}_{\rm II}$ of the conformal infinity are given by the left (a), left (b), right (b), and left (a) parts of Fig. 8, respectively. For ingoing radiation [Eqs. (4.16) with $\epsilon=-1$, or Eqs. (4.6) with $|R|>1$] these are given by the right (a), right (b), left (b), and right (a) parts of Fig. 8, respectively.

C. Vanishing acceleration

Finally, we briefly describe the character of radiation when the *acceleration vanishes*, in which case the spacetime describes a single nonaccelerating black hole in an anti–de Sitter universe (''Reissner-Nordström–anti–de Sitter solution''). It is thus spherically symmetric with surfaces t, $y=$const being the orbits of the rotational group, and radial directions being contained in sections x, $\varphi=$const. From $A=0$ it follows $R_2=\infty$, cf. Eq. (4.7), and the above general expressions simplify. In particular for $A=0$ not only $\mathbf{k}_{\rm RT}\propto\mathbf{k}_1\propto(1/\sqrt{2})(\mathbf{t}_{\rm o}+\mathbf{q}_{\rm o})$, but also $\mathbf{l}_{\rm RT}\propto\mathbf{k}_2\propto(1/\sqrt{2})(\mathbf{t}_{\rm o}-\mathbf{q}_{\rm o})$ is a PND, see Eq. (5.4); this is consistent with relations (3.19) in which only the components $\Psi_2^{\rm RT}$ and $\Phi_1^{\rm RT}$ remain nonvanishing. At the infinity $\mathcal{I}$ the PNDs are mutually mirrored reflections, $\mathbf{k}_1$ oriented outside the universe and $\mathbf{k}_2$ inside it, parametrized by $\psi_1=0=\psi_2$; see Eqs. (5.4), (4.12). Both the PNDs point in radial directions of the spherical symmetry. Moreover, since $R_2>1$, it follows from relation (5.6) that the region near $\mathcal{I}$ is always static, without the Killing horizon extending there.

For vanishing acceleration the expressions (4.16) and (4.21) reduce to

$$|\Psi_4^{\rm i}|\approx\frac{|\Lambda|}{4}\,\frac{m}{\gamma\eta}\sinh^2\psi=\frac{|\Lambda|}{4}\,\frac{m}{\gamma\eta}\tan^2\theta,$$

$$|\Phi_2^{\rm i}|\approx\sqrt{\frac{|\Lambda|}{24}}\,\frac{|e|}{\gamma\eta}\sinh\psi=\sqrt{\frac{|\Lambda|}{24}}\,\frac{|e|}{\gamma\eta}|\tan\theta|. \quad (5.8)$$

The corresponding directional pattern of radiation, shown in Fig. 11, is axially symmetric and independent of ϵ, i.e., it is the same both for ingoing and outgoing null geodesics. Interestingly, even for a nonaccelerated black hole there is thus radiation on $\mathcal{I}$ along *any nonradial* null direction, i.e., except for $\psi=0$, $\epsilon=\pm1$, which corresponds to both PNDs. This may seem quite surprising since the region near infinity is *static*. It is a completely new specific feature: for $\Lambda>0$ a generic, *nonradial* observer near $\mathcal{I}^+$ would also detect radiation generated by nonaccelerated black holes [20], but the region near infinity is nonstatic. In asymptotically flat spacetimes ($\Lambda=0$) there is no radiation on $\mathcal{I}^+$ from black holes with $A=0$ [32], which, remarkably, also follows from expression (3.24).

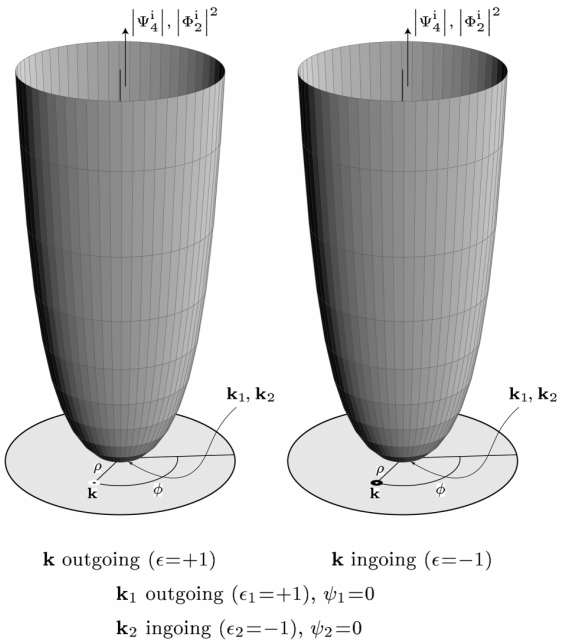

FIG. 11. The directional patterns of outgoing/ingoing radiation are the same and axially symmetric when $A=0$. In such a case the PNDs $\mathbf{k}_1$ and $\mathbf{k}_2$ are mutual mirror images under reflection with respect to $\mathcal{I}$. Therefore, there is exactly one direction given by $\psi=0$ along which the radiation vanishes, both for outgoing and ingoing null geodesics.

VI. SUMMARY

It was observed already in the 1960s by Penrose [12,13,18] that radiation is defined ''less invariantly'' in spacetimes with a non-null $\mathcal{I}$. Recently we have analyzed the C-metric solution with $\Lambda>0$ [20] and found an explicit directional pattern of radiation. This fully characterizes the radiation from uniformly accelerated black holes near the de Sitter–like conformal infinity $\mathcal{I}^+$, which has a spacelike character. Here we have completed the picture by investigating the radiative properties of the C-metric with a negative cosmological constant. This exact solution of the Einstein-Maxwell equations with $\Lambda<0$ represents a spacetime in which the radiation is generated either by a (possibly charged) single black hole or pairs of black holes uniformly accelerated in an anti–de Sitter universe.

We have analyzed the asymptotic behavior of the gravitational and electromagnetic fields near the conformal infinity $\mathcal{I}$, which has a timelike character. The leading components of the fields have been expressed in a suitable parallelly transported interpretation tetrad. These components are inversely proportional to the affine parameter of the corresponding null geodesic. In addition, an explicit formula (4.16) [or, equivalently, Eqs. (4.6) and (4.21)] which describes the directional pattern of radiation has been derived: it expresses the dependence of the field magnitudes on spacetime directions from which a given point N_∞ at infinity $\mathcal{I}$ is approached. This specific directional characteristic supplements the peeling property, completing thus the asymptotic behavior of gravi-

tational and electromagnetic fields near infinity $\mathcal{I}$ with a timelike character.

We have demonstrated that the situation is much more complicated in the anti–de Sitter case than in the case $\Lambda>0$. The new specific feature is that timelike conformal infinity $\mathcal{I}$ is, in general, divided by Killing horizons into several static and nonstatic regions with a different structure of (double degenerate) principal null directions. In these distinct domains of infinity the directional patterns of radiation differ. For example, there are different numbers of geometrically privileged directions (namely one, two, or none) in which the radiation vanishes completely. These exactly correspond to mirrored directions of principal null direction, with respect to $\mathcal{I}$. Accordingly, there exists an asymmetry between outgoing and ingoing radiation patterns in all the domains.

As in the $\Lambda>0$ case [64], it seems plausible that a general structure of the radiation pattern at conformal infinity depends only on the PNDs there, i.e., it is given by the algebraic (Petrov) type of the spacetime. This hypothesis will be proven elsewhere [62].

ACKNOWLEDGMENTS

The work was supported in part by the grants GAČR 202/02/0735 and GAUK 166/2003 of the Czech Republic and Charles University in Prague. The stay of M.O. at the Institute of Theoretical Physics in Prague was enabled by financial support from Fondazione Angelo Della Riccia (Firenze).

APPENDIX A: RADIATION ALONG SOME PARTICULAR NULL GEODESICS

Here we concentrate on a geometrically privileged family of special geodesics which asymptotically take the form (3.11) with $c=0$. It follows from Eq. (3.12) that this corresponds either to outgoing null geodesics with $d=0$ or ingoing ones with $d=-6/\Lambda$.

In fact, the geodesics $c=0=d$ are *exact null geodesics*

$$u=u_\infty=\text{const}, \quad \zeta=\zeta_\infty=\text{const}, \tag{A1}$$

in the whole spacetime, with r being their affine parameter. They approach infinity $\mathcal{I}$ along the (double degenerate) principal null direction $\mathbf{k}_{\mathrm{RT}}=\boldsymbol{\partial}_r$, which is characterized by the parameter $\psi=0$, see Eq. (4.15) (or by $\theta=0$). It can be shown that the Robinson-Trautman tetrad (3.18) is parallelly transported along these geodesics,

$$\mathbf{k}_{\mathrm{RT}}\cdot\nabla\mathbf{k}_{\mathrm{RT}}=0, \quad \mathbf{k}_{\mathrm{RT}}\cdot\nabla\mathbf{l}_{\mathrm{RT}}=0, \quad \mathbf{k}_{\mathrm{RT}}\cdot\nabla\mathbf{m}_{\mathrm{RT}}=0, \tag{A2}$$

and it is also invariant under a shift along the Killing vector $\boldsymbol{\partial}_t$, i.e., $\mathcal{L}_{\boldsymbol{\partial}_t}\mathbf{k}_{\mathrm{RT}}=0$, $\mathcal{L}_{\boldsymbol{\partial}_t}\mathbf{l}_{\mathrm{RT}}=0$, $\mathcal{L}_{\boldsymbol{\partial}_t}\mathbf{m}_{\mathrm{RT}}=0$, respecting thus a symmetry of the spacetime. Consequently, we can naturally set the interpretation tetrad $(\mathbf{k}_{\mathrm{i}},\mathbf{l}_{\mathrm{i}},\mathbf{m}_{\mathrm{i}},\overline{\mathbf{m}}_{\mathrm{i}})\equiv(\mathbf{k}_{\mathrm{RT}},\mathbf{l}_{\mathrm{RT}},\mathbf{m}_{\mathrm{RT}},\overline{\mathbf{m}}_{\mathrm{RT}})$ in the *whole* spacetime, not only asymptotically near $\mathcal{I}$, as in Eq. (3.21) for $c=0$, $d=0$. As follows from Eqs. (3.19), all components of gravitational and electromagnetic fields are explicitly given by

$$\Psi^{\mathrm{i}}_4=-\frac{3A^2}{P}\left(m+2e^2Ax-\frac{e^2}{r}\right)\frac{1}{r},$$

$$\Psi^{\mathrm{i}}_3=\frac{3A}{\sqrt{2}P}\left(m+2e^2Ax-\frac{e^2}{r}\right)\frac{1}{r^2},$$

$$\Psi^{\mathrm{i}}_2=-\left(m+2e^2Ax-\frac{e^2}{r}\right)\frac{1}{r^3}, \quad \Psi^{\mathrm{i}}_1=\Psi^{\mathrm{i}}_0=0, \tag{A3}$$

and

$$\Phi^{\mathrm{i}}_2=\frac{eA}{\sqrt{2}P}\,\frac{1}{r}, \quad \Phi^{\mathrm{i}}_1=-\frac{e}{2}\,\frac{1}{r^2}, \quad \Phi^{\mathrm{i}}_0=0. \tag{A4}$$

Clearly, the leading terms in the $1/r$ expansion give the previous general asymptotical results (3.24) with $c=0=d$. In the case of anti–de Sitter spacetime ($m=0,e=0$) the field components obviously identically vanish. In the general case the fields have a radiative character ($\sim 1/r$) except for a vanishing acceleration A and/or for $P=\infty$. The interesting "static" limiting case $A=0$ has been already discussed in Sec. V C. The case $P=\infty$ corresponds to observers located at the privileged position where $G=0$, i.e., on the axes $x=x_{\mathrm{b}}$ and $x=x_{\mathrm{f}}$ where the strings/struts are localized. This is analogous to the situation when $\Lambda>0$ [20], and an electromagnetic field of accelerated test charges in flat spacetime: this is also not radiative along the axis of symmetry, which is the direction of acceleration.

Let us also recall (see [20]) that the affine parameter r coincides both with the luminosity and the parallax distance for the congruence of the above null geodesics. The radiative $1/r$ fall-off of the fields is naturally measurable (even locally) by observers moving radially to infinity, using both the luminosity and the parallax methods for determining the distance.

Concerning the other special family of ingoing null geodesics, $c=0$, $d=-6/\Lambda$, $\epsilon=-1$, it can be observed that the transformation given by Eq. (3.20) becomes singular and Eq. (3.21) is not thus justified. However, from Eqs. (3.8), (3.17), and (3.18), with the condition (3.22) for fixing $\mathbf{l}_{\mathrm{i}}$, it follows that in this case

$$\mathbf{k}_{\mathrm{i}}\approx-\frac{1}{\gamma^2\eta^2}\left(r^2\boldsymbol{\partial}_r+\frac{6}{\Lambda}\boldsymbol{\partial}_u\right)\approx-\frac{6}{\Lambda}\,\frac{1}{\gamma^2\eta^2}\,\mathbf{l}_{\mathrm{RT}},$$

$$\mathbf{l}_{\mathrm{i}}\approx-\frac{\Lambda}{6}r^2\boldsymbol{\partial}_r\approx-\frac{\Lambda}{6}\,\gamma^2\eta^2\mathbf{k}_{\mathrm{RT}}, \tag{A5}$$

which—somewhat surprisingly—fully agrees with expressions (3.21) for the special case $c=0$, $d=-6/\Lambda$. Thus the interpretation tetrad along these geodesics is equivalent to the tetrad (3.21) along the PND given by $c=0$, $d=0$ [which itself agrees with the Robinson-Trautman tetrad (3.18)] after interchanging $\mathbf{k}_{\mathrm{i}}\leftrightarrow\mathbf{l}_{\mathrm{i}}$ and $\mathbf{m}_{\mathrm{i}}\leftrightarrow-\overline{\mathbf{m}}_{\mathrm{i}}$, accompanied by a boost (B9) with $B=-6/(\Lambda r^2)$. Components of the gravitational

and electromagnetic fields can thus easily be obtained from Eq. (A3),(A4). In particular, it follows that $\Psi_4^{\mathrm{i}} \approx 0 \approx \Psi_3^{\mathrm{i}}$, $\Psi_2^{\mathrm{i}} \sim \eta^{-3}$, $\Psi_1^{\mathrm{i}} \sim \eta^{-4}$, $\Psi_0^{\mathrm{i}} \sim \eta^{-5}$, and $\Phi_2^{\mathrm{i}} \approx 0$, $\Phi_1^{\mathrm{i}} \sim \eta^{-2}$, $\Phi_0^{\mathrm{i}} \sim \eta^{-3}$. Obviously, the radiative parts of the fields vanish along these special ingoing geodesics, which agrees with the expression $\psi_{\mathrm{m}}=0$ in Eq. (5.3), cf. Eq. (4.15). Indeed, this direction is just the reflection of the PND $\mathbf{k}_1$.

APPENDIX B: TRANSFORMATIONS OF THE COMPONENTS Ψ_n AND Φ_n

The Weyl tensor can be parametrized by five standard complex coefficients defined as components with respect to a null tetrad (see, e.g., [31]):

$$\begin{aligned}
\Psi_0 &= \mathbf{C}_{\alpha\beta\gamma\delta}\mathbf{k}^\alpha\mathbf{m}^\beta\mathbf{k}^\gamma\mathbf{m}^\delta,\\
\Psi_1 &= \mathbf{C}_{\alpha\beta\gamma\delta}\mathbf{k}^\alpha\mathbf{l}^\beta\mathbf{k}^\gamma\mathbf{m}^\delta,\\
\Psi_2 &= -\mathbf{C}_{\alpha\beta\gamma\delta}\mathbf{k}^\alpha\mathbf{m}^\beta\mathbf{l}^\gamma\overline{\mathbf{m}}^\delta,\\
\Psi_3 &= \mathbf{C}_{\alpha\beta\gamma\delta}\mathbf{l}^\alpha\mathbf{k}^\beta\mathbf{l}^\gamma\overline{\mathbf{m}}^\delta,\\
\Psi_4 &= \mathbf{C}_{\alpha\beta\gamma\delta}\mathbf{l}^\alpha\overline{\mathbf{m}}^\beta\mathbf{l}^\gamma\overline{\mathbf{m}}^\delta.
\end{aligned} \tag{B1}$$

Similarly, the tensor of electromagnetic field is parametrized as

$$\begin{aligned}
\Phi_0 &= \mathbf{F}_{\alpha\beta}\mathbf{k}^\alpha\mathbf{m}^\beta,\\
\Phi_1 &= \tfrac{1}{2}\mathbf{F}_{\alpha\beta}(\mathbf{k}^\alpha\mathbf{l}^\beta - \mathbf{m}^\alpha\overline{\mathbf{m}}^\beta),\\
\Phi_2 &= \mathbf{F}_{\alpha\beta}\overline{\mathbf{m}}^\alpha\mathbf{l}^\beta.
\end{aligned} \tag{B2}$$

These transform in a well-known way under the following particular Lorentz transformations. For a null rotation with $\mathbf{k}$ fixed, $L \in \mathbb{C}$,

$$\begin{aligned}
\mathbf{k} &= \mathbf{k}_{\mathrm{o}},\\
\mathbf{l} &= \mathbf{l}_{\mathrm{o}} + \overline{L}\mathbf{m}_{\mathrm{o}} + L\overline{\mathbf{m}}_{\mathrm{o}} + L\overline{L}\mathbf{k}_{\mathrm{o}},\\
\mathbf{m} &= \mathbf{m}_{\mathrm{o}} + L\mathbf{k}_{\mathrm{o}},
\end{aligned} \tag{B3}$$

$$\begin{aligned}
\Psi_0 &= \Psi_0^{\mathrm{o}},\\
\Psi_1 &= \overline{L}\Psi_0^{\mathrm{o}} + \Psi_1^{\mathrm{o}},\\
\Psi_2 &= \overline{L}^2\Psi_0^{\mathrm{o}} + 2\overline{L}\Psi_1^{\mathrm{o}} + \Psi_2^{\mathrm{o}},\\
\Psi_3 &= \overline{L}^3\Psi_0^{\mathrm{o}} + 3\overline{L}^2\Psi_1^{\mathrm{o}} + 3\overline{L}\Psi_2^{\mathrm{o}} + \Psi_3^{\mathrm{o}},\\
\Psi_4 &= \overline{L}^4\Psi_0^{\mathrm{o}} + 4\overline{L}^3\Psi_1^{\mathrm{o}} + 6\overline{L}^2\Psi_2^{\mathrm{o}} + 4\overline{L}\Psi_3^{\mathrm{o}} + \Psi_4^{\mathrm{o}},
\end{aligned} \tag{B4}$$

$$\begin{aligned}
\Phi_0 &= \Phi_0^{\mathrm{o}},\\
\Phi_1 &= \overline{L}\Phi_0^{\mathrm{o}} + \Phi_1^{\mathrm{o}},\\
\Phi_2 &= \overline{L}^2\Phi_0^{\mathrm{o}} + 2\overline{L}\Phi_1^{\mathrm{o}} + \Phi_2^{\mathrm{o}}.
\end{aligned} \tag{B5}$$

Under a null rotation with $\mathbf{l}$ fixed, $K \in \mathbb{C}$,

$$\begin{aligned}
\mathbf{k} &= \mathbf{k}_{\mathrm{o}} + \overline{K}\mathbf{m}_{\mathrm{o}} + K\overline{\mathbf{m}}_{\mathrm{o}} + K\overline{K}\mathbf{l}_{\mathrm{o}},\\
\mathbf{l} &= \mathbf{l}_{\mathrm{o}},\\
\mathbf{m} &= \mathbf{m}_{\mathrm{o}} + K\mathbf{l}_{\mathrm{o}},
\end{aligned} \tag{B6}$$

$$\begin{aligned}
\Psi_0 &= K^4\Psi_4^{\mathrm{o}} + 4K^3\Psi_3^{\mathrm{o}} + 6K^2\Psi_2^{\mathrm{o}} + 4K\Psi_1^{\mathrm{o}} + \Psi_0^{\mathrm{o}},\\
\Psi_1 &= K^3\Psi_4^{\mathrm{o}} + 3K^2\Psi_3^{\mathrm{o}} + 3K\Psi_2^{\mathrm{o}} + \Psi_1^{\mathrm{o}},\\
\Psi_2 &= K^2\Psi_4^{\mathrm{o}} + 2K\Psi_3^{\mathrm{o}} + \Psi_2^{\mathrm{o}},\\
\Psi_3 &= K\Psi_4^{\mathrm{o}} + \Psi_3^{\mathrm{o}},\\
\Psi_4 &= \Psi_4^{\mathrm{o}},
\end{aligned} \tag{B7}$$

$$\begin{aligned}
\Phi_0 &= K^2\Phi_2^{\mathrm{o}} + 2K\Phi_1^{\mathrm{o}} + \Phi_0^{\mathrm{o}},\\
\Phi_1 &= K\Phi_2^{\mathrm{o}} + \Phi_1^{\mathrm{o}},\\
\Phi_2 &= \Phi_2^{\mathrm{o}}.
\end{aligned} \tag{B8}$$

Under a boost in the **k-l** plane and a spatial rotation in the **m-$\overline{\mathbf{m}}$** plane given by

$$\begin{aligned}
\mathbf{k} &= B\mathbf{k}_{\mathrm{o}}, \quad \mathbf{l} = B^{-1}\mathbf{l}_{\mathrm{o}},\\
\mathbf{m} &= \exp(i\Phi)\mathbf{m}_{\mathrm{o}},
\end{aligned} \tag{B9}$$

$B, \Phi \in \mathbb{R}$, the components Ψ_n and Φ_n transform as

$$\begin{aligned}
\Psi_0 &= B^2\exp(2i\Phi)\Psi_0^{\mathrm{o}},\\
\Psi_1 &= B\exp(i\Phi)\Psi_1^{\mathrm{o}},\\
\Psi_2 &= \Psi_2^{\mathrm{o}},\\
\Psi_3 &= B^{-1}\exp(-i\Phi)\Psi_3^{\mathrm{o}},\\
\Psi_4 &= B^{-2}\exp(-2i\Phi)\Psi_4^{\mathrm{o}},
\end{aligned} \tag{B10}$$

$$\begin{aligned}
\Phi_0 &= B\exp(i\Phi)\Phi_0^{\mathrm{o}},\\
\Phi_1 &= \Phi_1^{\mathrm{o}},\\
\Phi_2 &= B^{-1}\exp(-i\Phi)\Phi_2^{\mathrm{o}}.
\end{aligned} \tag{B11}$$

[1] H. Bondi, M. G. J. van der Burg, and A. W. K. Metzner, Proc. R. Soc. London **A269**, 21 (1962).
[2] R. K. Sachs, Proc. R. Soc. London **A270**, 103 (1962).
[3] E. T. Newman and R. Penrose, J. Math. Phys. **3**, 566 (1962).
[4] E. T. Newman and T. W. J. Unti, J. Math. Phys. **3**, 891 (1962).
[5] M. G. J. van der Burg, Proc. R. Soc. London **A310**, 221 (1969).
[6] J. Bičák and A. Pravdová, J. Math. Phys. **39**, 6011 (1998).
[7] F. A. E. Pirani, in *Brandeis Lectures on General Relativity*, edited by S. Deser and K. W. Ford (Prentice-Hall, Englewood Cliffs, NJ, 1965), pp. 249–372.
[8] J. Bičák, in *Galaxies, Axisymmetric Systems and Relativity*, edited by M. A. H. MacCaluum (Cambridge University Press, Cambridge, England, 1985), pp. 91–124.
[9] J. Bičák, in *Relativistic Gravitation and Gravitational Radiation, Les Houches 1995*, edited by J.-A. Marck and J.-P. Lasota (Cambridge University Press, Cambridge, England, 1997), pp. 67–87.
[10] J. Bičák, in *Einstein's Field Equations and Their Physical Implications*, edited by B. G. Schmidt (Springer, Berlin, 2000), Vol. 540, pp. 1–126.
[11] R. Penrose, Phys. Rev. Lett. **10**, 66 (1963).
[12] R. Penrose, in *Relativity, Groups and Topology, Les Houches 1963*, edited by C. DeWitt and B. DeWitt (Gordon and Breach, New York, 1964), pp. 563–584.
[13] R. Penrose, Proc. R. Soc. London **A284**, 159 (1965).
[14] R. Penrose and W. Rindler, *Spinors and Space-Time* (Cambridge University Press, Cambridge, England, 1986), Vol. 2.
[15] J. Tafel and S. Pukas, Class. Quantum Grav. **17**, 1559 (2000).
[16] A. Ashtekar and A. Magnon, Class. Quantum Grav. **1**, L39 (1984).
[17] A. Ashtekar and S. Das, Class. Quantum Grav. **17**, L17 (2000).
[18] R. Penrose, in *The Nature of Time*, edited by T. Gold (Cornell University Press, Ithaca, NY, 1967), pp. 42–54.
[19] J. Bičák and P. Krtouš, Phys. Rev. Lett. **88**, 211101 (2002).
[20] P. Krtouš and J. Podolský, Phys. Rev. D **68**, 024005 (2003).
[21] J. Bičák and P. Krtouš, Phys. Rev. D **64**, 124020 (2001).
[22] S. J. Avis, C. J. Isham, and D. Storey, Phys. Rev. D **18**, 3565 (1978).
[23] S. W. Hawking, Phys. Lett. **126B**, 175 (1983).
[24] H. Friedrich, J. Geom. Phys. **17**, 125 (1995).
[25] J. Bičák and B. G. Schmidt, Phys. Rev. D **40**, 1827 (1989).
[26] J. Bičák, Proc. R. Soc. London **A302**, 201 (1968).
[27] V. Pravda and A. Pravdová, Czech. J. Phys. **50**, 333 (2000).
[28] T. Levi-Civita, Atti Accad. Naz. Lincei, Cl. Sci. Fis., Mat. Nat., Rend. **26**, 307 (1917).
[29] H. Weyl, Ann. Phys. (Leipzig) **59**, 185 (1918).
[30] J. Ehlers and W. Kundt, in *Gravitation: An Introduction to Current Research*, edited by L. Witten (Wiley, New York, 1962), pp. 49–101.
[31] D. Kramer, H. Stephani, E. Herlt, and M. MacCallum, *Exact Solutions of Einstein's Field Equations* (Cambridge University Press, Cambridge, England, 1980).
[32] W. Kinnersley and M. Walker, Phys. Rev. D **2**, 1359 (1970).
[33] H. Farhoosh and R. L. Zimmerman, J. Math. Phys. **20**, 2272 (1979).
[34] A. Ashtekar and T. Dray, Commun. Math. Phys. **79**, 581 (1981).
[35] W. B. Bonnor, Gen. Relativ. Gravit. **15**, 535 (1983).
[36] J. Bičák and V. Pravda, Phys. Rev. D **60**, 044004 (1999).
[37] P. S. Letelier and S. R. Oliveira, Phys. Rev. D **64**, 064005 (2001).
[38] O. J. C. Dias and J. P. S. Lemos, Phys. Rev. D **67**, 064001 (2003).
[39] J. Plebański and M. Demiański, Ann. Phys. (N.Y.) **98**, 98 (1976).
[40] B. Carter, Commun. Math. Phys. **10**, 280 (1968).
[41] R. Debever, Bull. Soc. Math. Belg. **23**, 360 (1971).
[42] O. J. C. Dias and J. P. S. Lemos, Phys. Rev. D **68**, 104010 (2003).
[43] R. B. Mann and S. F. Ross, Phys. Rev. D **52**, 2254 (1995).
[44] R. B. Mann, Class. Quantum Grav. **14**, L109 (1997).
[45] R. B. Mann, Nucl. Phys. **B516**, 357 (1998).
[46] I. S. Booth and R. B. Mann, Nucl. Phys. **B539**, 267 (1999).
[47] J. Podolský and J. B. Griffiths, Phys. Rev. D **63**, 024006 (2001).
[48] O. J. C. Dias and J. P. S. Lemos, Phys. Rev. D **67**, 084018 (2003).
[49] R. Emparan, G. T. Horowitz, and R. C. Myers, J. High Energy Phys. **01**, 021 (2000).
[50] J. Podolský, Czech. J. Phys. **52**, 1 (2002).
[51] R. Emparan, G. T. Horowitz, and R. C. Myers, J. High Energy Phys. **01**, 007 (2000).
[52] A. Chamblin, Class. Quantum Grav. **18**, L17 (2001).
[53] M. Walker and R. Penrose, Commun. Math. Phys. **18**, 265 (1970).
[54] L. P. Hughston, R. Penrose, P. Sommers, and M. Walker, Commun. Math. Phys. **27**, 303 (1972).
[55] The symmetric product $\vee$ of two 1-forms is defined as $\mathbf{a}\vee\mathbf{b}=\mathbf{ab}+\mathbf{ba}$.
[56] M. Henneaux and C. Teitelboim, Commun. Math. Phys. **98**, 391 (1985).
[57] There is no region I in this case. The numbering of regions, starting with II, has been chosen to be consistent with the case of two black holes (cf. Figs. 4–6) and with the *C*-metric with $\Lambda>0$ [20].
[58] The terms *acceleration* and *cosmological* horizons are rather arbitrary. Both horizons $y=y_{\rm a}$ and $y=y_{\rm c}$ could actually qualify for the name acceleration (Rindler) horizon, cf. [38]. For convenience, to distinguish them we use the name *cosmological* horizon for the horizon $y=y_{\rm c}$ which separates domains containing different pairs of black holes, cf. Fig. 2(a).
[59] Let us note here that the vector $r^2\boldsymbol{\partial}_r=-\boldsymbol{\partial}_\Omega$ is ''of the same order'' as other coordinate vectors in the sense of expansion in $1/r$, i.e., $r^2\boldsymbol{\partial}_r\sim\boldsymbol{\partial}_\zeta\sim\boldsymbol{\partial}_u$. More precisely, the vectors $\boldsymbol{\partial}_\Omega$, $\boldsymbol{\partial}_u$, $\boldsymbol{\partial}_\zeta$ are regular at $\mathcal{I}$ in the sense of the tangent space of the conformal manifold with metric (2.14), cf. Ref. [14].
[60] For the particular case of geodesics with $c=0$ see Appendix A.
[61] The special case $\mathbf{k}_{\rm i}\propto\mathbf{l}_{\rm o}$ formally corresponds to $R=\infty$. Here and in the following the symbol $\propto$ means a proportionality with a *positive* factor. Thanks to this convention we do not lose information about the orientation of related vectors.
[62] P. Krtouš and J. Podolský, ''Gravitational and electromagnetic fields near anti-de Sitter-like infinity,'' gr-qc/0310089.
[63] In general, a mirrored reflection of the direction R is $1/\overline{R}$, but the PNDs R_1 and R_2 are real, see Eq. (4.7).
[64] P. Krtouš, J. Podolský, and J. Bičák, Phys. Rev. Lett. **91**, 061101 (2003).

PHYSICAL REVIEW D **69**, 084023 (2004)

Gravitational and electromagnetic fields near an anti–de Sitter–like infinity

Pavel Krtouš and Jiří Podolský
Institute of Theoretical Physics, Faculty of Mathematics and Physics, Charles University in Prague, V Holešovičkách 2, 180 00 Prague 8, Czech Republic

(Received 17 October 2003; published 27 April 2004)

We analyze the asymptotic structure of general gravitational and electromagnetic fields near an anti–de Sitter–like conformal infinity. The dependence of the radiative component of the fields on a null direction along which the infinity is approached is obtained. The directional pattern of outgoing and ingoing radiation, which supplements standard peeling property, is determined by the algebraic (Petrov) type of the fields and also by the orientation of the principal null directions with respect to timelike infinity. The dependence on the orientation is a new feature if compared to spacelike infinity.

DOI: 10.1103/PhysRevD.69.084023 PACS number(s): 04.20.Ha, 04.40.Nr, 98.80.Jk

In spacetimes which are asymptotically flat the behavior of radiative gravitational and electromagnetic fields near infinity has been rigorously analyzed by means of now classical techniques, such as those in Refs. [1–3]. However, it still remains an open problem to fully characterize the asymptotic properties of more general exact solutions of the Einstein-Maxwell equations. Even in spacetimes which admit a smooth infinity $\mathcal{I}$ the concept of radiation is not obvious when the cosmological constant Λ is nonvanishing. If we define the *radiative component of a field* as the η^{-1} term of the field with respect to a parallelly transported tetrad along a null geodesic (η being affine parameter), then for $\Lambda\neq 0$ the radiation depends on the direction along which the geodesics approach a given point at $\mathcal{I}$ [2,3].

It is natural to analyze and describe such dependence. Recently, we studied [4] this behavior of fields near $\mathcal{I}$ in the case $\Lambda>0$ and demonstrated that the directional pattern of radiation close to de Sitter–like infinity has a universal character that is determined by the algebraic type of the fields. In the present work we investigate the complementary situation when $\Lambda<0$. Interestingly, although the method is similar to the previous case, the results turn out to be more complicated, and completely new phenomena occur. This stems from the fundamental difference that the anti–de Sitter–like infinity $\mathcal{I}$ is *timelike*, and thus admits a ''richer structure'' of radiative patterns. This fact was recently demonstrated by analyzing radiation generated by accelerating black holes in an anti–de Sitter (AdS) universe [5]: $\mathcal{I}$ is divided by the Killing horizons into several domains with a different structure of principal null directions, in which the patterns of radiation differ. Moreover, ingoing and outgoing radiation have to be treated separately. It is the purpose of our work to generalize these results and to describe all the possible radiative patterns for gravitational and electromagnetic fields near an anti–de Sitter–like infinity.

A study of spacetimes with $\Lambda\neq 0$ is motivated also by the fact that they have now become commonly used in various branches of physical research, e.g., in inflationary models brane cosmologies, supergravity or string theories, in particular due to the AdS conformal field theory (CFT) correspondence. Although branes and strings are typically studied in higher-dimensional spacetimes, four-dimensional models have also been considered (see, e.g., Refs. [6], [7]). Our contribution analyzes only standard $3+1$ universes with $\Lambda<0$; generalization to higher dimensions does not seem to be straightforward.

I. SPACETIME INFINITY, FIELDS, AND TETRADS

The *conformal infinity* $\mathcal{I}$ can be introduced [2,3] as a boundary of physical spacetime $\mathcal{M}$ with physical metric $\mathbf{g}$, when embedded into a larger conformal manifold $\tilde{\mathcal{M}}$ with conformal metric $\tilde{\mathbf{g}}=\omega^2\mathbf{g}$; the *conformal factor* ω (negative in $\mathcal{M}$) vanishes on $\mathcal{I}$. Assuming $\tilde{\mathbf{g}}$ is regular there, the metric $\mathbf{g}$ is ''infinite'' on $\mathcal{I}$, and $\mathcal{I}$ is thus *infinitely* distant from the interior of spacetime $\mathcal{M}$. We will be interested here in a *timelike* conformal infinity which is characterized by a spacelike gradient $\mathbf{d}\omega$ on $\mathcal{I}$. The conformal metric $\tilde{\mathbf{g}}$ near such an anti–de Sitter–like infinity can always be decomposed into Lorentzian three-metric ${}^{\mathcal{I}}\tilde{\mathbf{g}}$ tangent to $\mathcal{I}$, and a part orthogonal to it,

$$\mathbf{g}=\omega^{-2}({}^{\mathcal{I}}\tilde{\mathbf{g}}+\tilde{N}^2\mathbf{d}\omega^2). \tag{1}$$

The spacelike unit vector $\mathbf{n}$ normal to the infinity is then

$$\mathbf{n}^\mu=-\omega^{-1}\tilde{N}\mathbf{g}^{\mu\nu}\mathbf{d}_\nu\omega. \tag{2}$$

We denote the vectors of an *orthonormal tetrad* as $\mathbf{t}$, $\mathbf{q}$, $\mathbf{r}$, $\mathbf{s}$ ($\mathbf{t}$ timelike) and the associated null tetrad as

$$\mathbf{k}=\frac{1}{\sqrt{2}}(\mathbf{t}+\mathbf{q}),\quad \mathbf{l}=\frac{1}{\sqrt{2}}(\mathbf{t}-\mathbf{q}),$$

$$\mathbf{m}=\frac{1}{\sqrt{2}}(\mathbf{r}-i\mathbf{s}),\quad \overline{\mathbf{m}}=\frac{1}{\sqrt{2}}(\mathbf{r}+i\mathbf{s}), \tag{3}$$

so that $\mathbf{k}\cdot\mathbf{l}=-1$, $\mathbf{m}\cdot\overline{\mathbf{m}}=1$. In the null tetrad the Weyl tensor $\mathbf{C}_{\alpha\beta\gamma\delta}$ can be parametrized by five complex coefficients Ψ_j, $j=0,1,2,3,4$, and the electromagnetic tensor $\mathbf{F}_{\alpha\beta}$ by three coefficients Φ_j, $j=0,1,2$; see Refs. [8], [9].

We wish to investigate the behavior of these field components in an appropriate interpretation tetrad parallelly transported along future oriented null geodesics $z(\eta)$ which reach a given point P_∞ at $\mathcal{I}$. Such geodesics form two distinct

families which are distinguished by their *orientation* ϵ: geodesics *outgoing* to $\mathcal{I}$ which *end* at P_∞ ($\epsilon=+1$) and geodesics *ingoing* from $\mathcal{I}$ which *start* at P_∞ ($\epsilon=-1$). A geodesic thus reaches the point P_∞ for the affine parameter $\eta\to\epsilon\infty$. The lapse-like function $\tilde{N}>0$ and the conformal factor $\omega<0$ can be expanded along the geodesic in powers of $1/\eta$ as $\tilde{N}\approx\tilde{N}_\infty+\cdots$, $\omega\approx\epsilon\omega_*\eta^{-1}+\cdots$. Here, $\tilde{N}_\infty=\tilde{N}|_{P_\infty}$ is the same for all geodesics reaching P_∞. Moreover, we require that the approach of all geodesics to the infinity is "comparable," independent of their *direction*, so we assume ω_* to be a (negative) constant. It is equivalent to fixing the momentum $p_o=\mathbf{p}\cdot\mathbf{n}$ ($\mathbf{p}=Dz/d\eta$ being the four-momentum) at a given small value of ω. This choice of the "comparable" approach to $\mathcal{I}$ is the only one we can apply unless there are additional geometrical structures (as, e.g., a Killing vector) which would allow us to fix a different quantity (e.g., the energy). We will see that this choice has significant consequences for the character of the radiation pattern.

The *interpretation tetrad* $\mathbf{k}_i$, $\mathbf{l}_i$, $\mathbf{m}_i$, $\overline{\mathbf{m}}_i$ also has to be specified "comparably" for all geodesics having different directions. We require that (i) the null vector $\mathbf{k}_i$ is proportional to the tangent vector of the geodesic

$$\mathbf{k}_i=\frac{1}{\sqrt{2}\tilde{N}_\infty}\frac{Dz}{d\eta}, \tag{4}$$

the factor being independent of the direction, and (ii) the null vector $\mathbf{l}_i$ is fixed by normalization $\mathbf{k}_i\cdot\mathbf{l}_i=-1$ and the requirement that normal vector $\mathbf{n}$ belongs to $\mathbf{k}_i$-$\mathbf{l}_i$ plane [3]. The remaining vectors $\mathbf{m}_i$, $\overline{\mathbf{m}}_i$ cannot be specified canonically. Below, these vectors will be chosen arbitrarily and we will only study moduli $|\Psi^i_4|$ and $|\Phi^i_2|$ of the radiative field components which are independent of such a choice.

As $\eta\to\epsilon\infty$, the interpretation tetrad is "infinitely" boosted with respect to an observer with four-velocity tangent to $\mathcal{I}$. To see this explicitly, we introduce an auxiliary tetrad $\mathbf{t}_b$, $\mathbf{q}_b$, $\mathbf{r}_b$, $\mathbf{s}_b$ adapted to the infinity, $\mathbf{q}_b=\epsilon\mathbf{n}$, with timelike vector $\mathbf{t}_b$ given by the projection of $\mathbf{k}_i$ to $\mathcal{I}$,

$$\mathbf{t}_b\propto\mathbf{k}_i-(\mathbf{k}_i\cdot\mathbf{n})\mathbf{n}, \tag{5}$$

and the spatial vectors $\mathbf{r}_b$, $\mathbf{s}_b$ being identical to $\mathbf{r}_i$, $\mathbf{s}_i$. Checking that $\mathbf{k}_i\cdot\mathbf{n}\approx\epsilon(1/\sqrt{2})\eta^{-1}$ we obtain

$$\mathbf{k}_i=B_i\mathbf{k}_b=\eta^{-1}\frac{1}{\sqrt{2}}(\mathbf{t}_b+\epsilon\mathbf{n}),\quad \mathbf{m}_i=\mathbf{m}_b,$$

$$\mathbf{l}_i=B_i^{-1}\mathbf{l}_b=\eta\frac{1}{\sqrt{2}}(\mathbf{t}_b-\epsilon\mathbf{n}),\quad \overline{\mathbf{m}}_i=\overline{\mathbf{m}}_b, \tag{6}$$

$B_i=1/\eta$ being a boost parameter which approaches zero on $\mathcal{I}$, i.e., it represents an "infinite" boost. Under this the fields transform as $\Psi^i_j=B_i^{2-j}\Psi^b_j$, $\Phi^i_j=B_i^{1-j}\Phi^b_j$. Considering the behavior (10) in a tetrad adapted to $\mathcal{I}$ this implies standard peeling-off property.

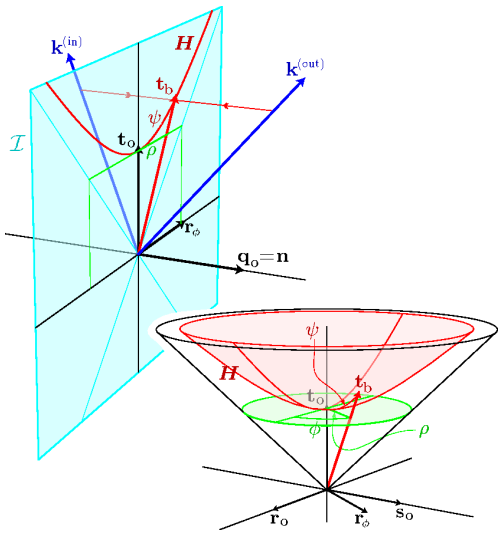

FIG. 1. Parametrization of a null direction $\mathbf{k}$ near timelike infinity $\mathcal{I}$. All null directions form three families: *outgoing* directions ($\mathbf{k}\cdot\mathbf{n}>0$, vector $\mathbf{k}^{(\mathrm{out})}$ in the figure), *ingoing* directions ($\mathbf{k}\cdot\mathbf{n}<0$, vector $\mathbf{k}^{(\mathrm{in})}$), and directions tangent to $\mathcal{I}$. With respect to a reference tetrad $\mathbf{t}_o$, $\mathbf{q}_o$, $\mathbf{r}_o$, $\mathbf{s}_o$, a direction $\mathbf{k}$ can be parameterized by boost ψ, angle ϕ, and orientation ϵ, or by parameters ρ, ϕ, or by a complex number R. In the upper diagram, the vectors $\mathbf{t}_o$, $\mathbf{q}_o$, $\mathbf{r}_\phi$ are depicted, the remaining spatial direction $\mathbf{s}_\phi$ is suppressed; in the bottom the direction $\mathbf{q}_o=\mathbf{n}$ is omitted. The parameters ψ, ϕ specify the normalized orthogonal projection $\mathbf{t}_b$ of $\mathbf{k}$ into $\mathcal{I}$ [cf. Eqs. (5) and (7)]. To parametrize $\mathbf{k}$ uniquely, we have to specify also its orientation $\epsilon=\mathrm{sgn}(\mathbf{k}\cdot\mathbf{n})$ with respect to $\mathcal{I}$. Vectors $\mathbf{t}_b$ corresponding to all outgoing (or ingoing) null directions form a hyperbolic surface $\mathbf{H}$. This can be radially mapped onto a two-dimensional disk tangent to the hyperboloid at $\mathbf{t}_o$, which can be parametrized by an angle ϕ and a radial coordinate $\rho=\tanh\psi$. In the exceptional case $\epsilon=0$ the boost $\psi\to\infty$, and $\mathbf{k}\propto\mathbf{t}_b+\mathbf{r}_\phi$ is tangent to $\mathcal{I}$. Finally, the parameter R is the Lorentzian stereographic representation of ψ, ϕ, ϵ [cf. Eq. (8)].

II. DIRECTIONAL PATTERN OF RADIATION

Now we explicitly derive the dependence of the radiation on the direction of a null geodesic along which the infinity is approached. First, we parametrize this direction with respect to a suitable *reference tetrad* $\mathbf{t}_o$, $\mathbf{q}_o$, $\mathbf{r}_o$, $\mathbf{s}_o$ adapted to the conformal infinity, namely $\mathbf{q}_o=\mathbf{n}$. The vectors $\mathbf{t}_o$, $\mathbf{r}_o$, $\mathbf{s}_o$ can be fixed conveniently with the help of the particular geometry of the spacetime. The timelike vector $\mathbf{t}_b$ is related to the vector $\mathbf{t}_o$ by a boost (cf. Fig. 1)

$$\mathbf{t}_b=(\cosh\psi)\mathbf{t}_o+(\sinh\psi)\mathbf{r}_\phi, \tag{7}$$

with $\mathbf{r}_\phi=(\cos\phi)\mathbf{r}_o+(\sin\phi)\mathbf{s}_o$ [and $\mathbf{s}_\phi=(-\sin\phi)\mathbf{r}_o+(\cos\phi)\mathbf{s}_o$]. Because the vector $\mathbf{t}_b$ is related to the projection of $\mathbf{k}_i$ we can use the "Lorentzian angles" ψ, ϕ and the orientation ϵ to parameterize the direction of the null geodesic. Instead of these parameters it is also convenient to use their *Lorentzian stereographic representation* R,

$$R=\begin{cases}\tanh(\psi/2)\exp(-i\phi) & \text{for } \epsilon=+1,\\ \coth(\psi/2)\exp(-i\phi) & \text{for } \epsilon=-1.\end{cases} \tag{8}$$

We allow also the infinite value $R=\infty$ corresponding to $\psi=0$, $\epsilon=-1$, i.e., $\mathbf{k}\propto(1/\sqrt{2})(\mathbf{t}_o-\mathbf{q}_o)$.

Next, we express the field components Ψ_j^o (and Φ_j^o) with respect to the reference tetrad using algebraically privileged *principal null directions* (PNDs). The PNDs of the gravitational (or electromagnetic, respectively) field are the null directions $\mathbf{k}$ such that $\Psi_0=0$ (or $\Phi_0=0$) in a null tetrad $\mathbf{k}$, $\mathbf{l}$, $\mathbf{m}$, $\overline{\mathbf{m}}$ (the choice of $\mathbf{l}$, $\mathbf{m}$, $\overline{\mathbf{m}}$ being irrelevant). If we parametrize $\mathbf{k}$ by the above stereographic parameter R, the condition on PND with respect to the reference tetrad takes the form [8,9]

$$R^4\Psi_4^o+4R^3\Psi_3^o+6R^2\Psi_2^o+4R\Psi_1^o+\Psi_0^o=0,$$

$$R^2\Phi_2^o+2R\Phi_1^o+\Phi_0^o=0, \qquad (9)$$

respectively. There are thus four (or two) PNDs characterized by the roots $R=R_n$, $n=1, 2, 3, 4$ (or $R=R_n^{\mathrm{EM}}$, $n=1,2$). In a generic situation we have $\Psi_4^o\neq 0$, and the remaining components Ψ_j^o, $j=0, 1, 2, 3$, can be expressed in terms of R_n (analogously for Φ_j^o, $j=0, 1$); see Ref. [4].

Using the conditions (i) and (ii) above and Eqs. (6)–(8), we can now find the Lorentz transformation from the reference tetrad to the interpretation tetrad (up to a nonunique rotation in the $\mathbf{m}_i-\overline{\mathbf{m}}_i$ plane). We can thus express the field components Ψ_4^i (or Φ_2^i) with respect to the interpretation tetrad in terms of Ψ_j^o (or Φ_j^o), and consequently in terms of the parameters R_n of PNDs and Ψ_4^o (or R_n^{EM} and Φ_2^o); cf. Ref. [4]. Taking into account a typical behavior of the fields in a tetrad adapted to $\mathcal{I}$ (e.g., Ref. [3]),

$$\Psi_n^o\approx\Psi_{n*}^o\eta^{-3}, \quad \Phi_n^o\approx\Phi_{n*}^o\eta^{-2}, \qquad (10)$$

we finally obtain the *directional pattern of radiation*—the dependence of radiative components of gravitational and electromagnetic fields on the null direction (given by R) along which the timelike infinity is approached:

$$|\Psi_4^i|\approx|\Psi_{4*}^o|\,\eta^{-1}|1-|R|^2|^{-2}\times\left|1-\frac{R_1}{R_m}\right|\left|1-\frac{R_2}{R_m}\right|\left|1-\frac{R_3}{R_m}\right|\left|1-\frac{R_4}{R_m}\right|, \qquad (11)$$

$$|\Phi_2^i|\approx|\Phi_{2*}^o|\,\eta^{-1}|1-|R|^2|^{-1}\left|1-\frac{R_1^{\mathrm{EM}}}{R_m}\right|\left|1-\frac{R_2^{\mathrm{EM}}}{R_m}\right|. \qquad (12)$$

Here, the complex number R_m,

$$R_m=\overline{R}^{-1}=\coth^{\epsilon}(\psi/2)\exp(-i\phi), \qquad (13)$$

characterizes a direction obtained from the direction R by a *reflection with respect to* $\mathcal{I}$, i.e., the *mirrored* direction with $\psi_m=\psi$, $\phi_m=\phi$ but opposite orientation $\epsilon_m=-\epsilon$.

The expression (11) has been derived assuming $\Psi_4^o\neq 0$, i.e., $R_n\neq\infty$. However, to describe PND oriented along $\mathbf{l}_o$ it is necessary to use a different component Ψ_j^o as a normalization factor. For example, with Ψ_0^o we obtain

$$|\Psi_4^i|\approx|\Psi_{0*}^o|\,\eta^{-1}|1-|R_m|^2|^{-2}\times\left|1-\frac{R_{1m}}{R}\right|\left|1-\frac{R_{2m}}{R}\right|\left|1-\frac{R_{3m}}{R}\right|\left|1-\frac{R_{4m}}{R}\right|. \qquad (14)$$

Interestingly, the radiation pattern thus has the same form if we reflect all PNDs, $R_n\to(R_n)_m$, and switch ingoing and outgoing directions, $R\to R_m$.

III. DISCUSSION

Expressions (11) and (12) characterize the asymptotic behavior of the fields near anti–de Sitter–like infinity. We will analyze here only the gravitational field, the discussion of the electromagnetic field being analogous. First, we observe that the radiation "blows up" for directions with $|R|=1$ (i.e., $\psi\to\infty$). These are null directions *tangent* to the infinity $\mathcal{I}$, and thus they do not represent a direction of any geodesic approaching the infinity from the "interior" of the spacetime. The reason for this divergent behavior is purely kinematic: when we required the "comparable" approach of geodesics to the infinity we had fixed the component of the four-momentum $\mathbf{p}\propto\mathbf{k}_i$ normal to $\mathcal{I}$. Clearly, such a condition implies an "infinite" rescaling if $\mathbf{k}_i$ is tangent to $\mathcal{I}$, which results in the divergence of $|\Psi_4^i|$.

The divergence at $|R|=1$ splits the radiation pattern into two components—the pattern for *outgoing* geodesics ($|R|<1, \epsilon=+1$) and that for *ingoing* geodesics ($|R|>1$, $\epsilon=-1$). These two different patterns are depicted in diagrams in Fig. 2 separately.

From Eq. (11) it is obvious that there are, in general, *four* directions along which the radiation *vanishes*, namely PNDs reflected with respect to $\mathcal{I}$, given by $R=(R_n)_m$. Outgoing PNDs give rise to zeros in the radiation pattern for ingoing geodesics, and vice versa. A qualitative shape of the radiation pattern thus depends on (i) *orientation* of PNDs with respect to $\mathcal{I}$ (i.e., the number of outgoing, ingoing, or tangent PNDs), and (ii) *degeneracy* of PNDs (Petrov type of the spacetime). Depending on these factors, there are 51 qualitatively different shapes of the radiation patterns (3 for Petrov type N spacetimes, 9 for type III, 6 for D, 18 for II, and 15 for type I spacetimes); 21 pairs of them are related by the duality of Eqs. (11) and (14). The most typical are shown in Fig. 2.

The reference tetrad can be chosen to capture a geometry of the spacetime. To simplify the radiation pattern we can also adapt it to the algebraic structure, i.e., to correlate the tetrad with PNDs. For example, we can always orient $\mathbf{t}_o$ along the orthogonal projection to $\mathcal{I}$ of the most degenerate PND, say $\mathbf{k}_4$. For the outgoing $\mathbf{k}_4$ we then obtain $\mathbf{k}_4\propto\mathbf{k}_o$, $R_4=0$ ($\psi_4=0, \epsilon_4=+1$); for the ingoing $\mathbf{k}_4$ we get $\mathbf{k}_4\propto\mathbf{l}_o$, $R_4=\infty$ ($\psi_4=0, \epsilon_4=-1$) and we have to employ the pattern (14). Thus, for spacetime of the Petrov type N we get $\psi_n=0$, $n=1,2,3,4$, and the directional dependence

$$|\Psi_4^i|\propto(\cosh\psi+\epsilon_1\epsilon)^2 \qquad (15)$$

illustrated in Fig. 2 (Na). Similarly, the radiation pattern simplifies for other algebraically special spacetimes.

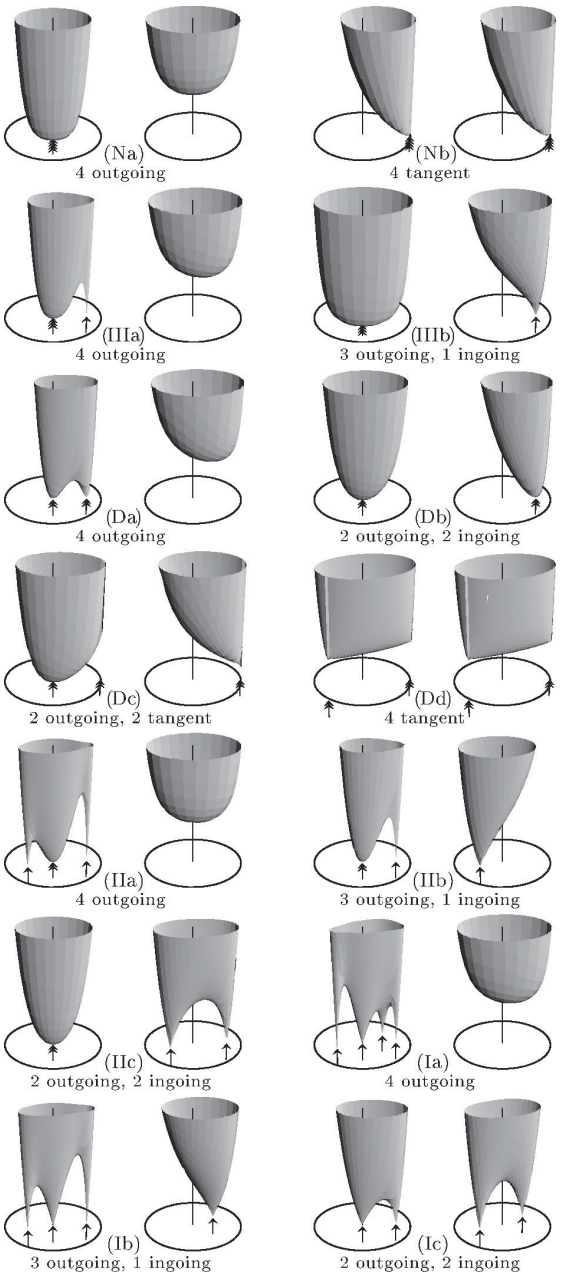

FIG. 2. Directional patterns of radiation near a timelike $\mathcal{I}$. All 11 qualitatively different shapes of the pattern when PNDs are not tangent to $\mathcal{I}$ are shown (the remaining 9 are related by a simple reflection with respect to $\mathcal{I}$). Patterns (Nb), (Dc), (Dd) are just a few examples with PNDs tangent to $\mathcal{I}$. Each diagram consists of patterns for ingoing (left) and outgoing geodesics (right). $|\Psi_4^{\mathrm{i}}|$ is drawn on the vertical axis, and the directions of the geodesics are represented on the horizontal disk by coordinates ρ, ϕ introduced in Fig. 1. *Reflected* (degenerate) PNDs are indicated by (multiple) arrows under the discs. For PNDs that are not tangent to $\mathcal{I}$ these are directions of vanishing radiation. The Petrov type (N, III, D, II, I) corresponding to the degeneracy of PNDs is indicated by the labels of diagrams; the number of ingoing and outgoing PNDs is also displayed.

At generic points the PNDs are not tangent to $\mathcal{I}$. However, they can be tangent on some lower-dimensional subspace such as the intersection of $\mathcal{I}$ with Killing horizons—cf. the anti–de Sitter *C*-metric [5]. These subspaces are important, e.g., in the context of a lower-dimensional version of the Randall-Sundrum model: a two-brane moving in a *C*-metric reaches the infinity with PNDs tangent both to it and to $\mathcal{I}$ [6].

In the case when the PND $\mathbf{k}_1$ *is tangent* to $\mathcal{I}$, the reference tetrad has to be chosen differently, e.g., in such a way that $R_4=1$. For the type N spacetime we then obtain the directional dependence [see Fig. 2 (Nb)]

$$|\Psi_4^{\mathrm{i}}| \propto \frac{|1-R|^4}{|1-|R|^2|^2} = (\cosh\psi - \sinh\psi\cos\phi)^2. \qquad (16)$$

The only zero of this expression is for $R=1$ ($\psi\to\infty, \phi=0$; limit considered through directions with $|R|\neq 1$) which does not correspond to any outgoing or ingoing geodesic. For type D spacetime ($R_1=R_2, R_3=R_4=1$) the directional dependence becomes [Figs. 2 (Dc), (Dd)]

$$|\Psi_4^{\mathrm{i}}| \propto \frac{|1-R|^2|1-R_1/R_{\mathrm{m}}|^2}{|1-|R|^2|^2}. \qquad (17)$$

This has zero at $R=(R_1)_{\mathrm{m}}$ (if $|R_1|\neq 1$), and it does *not* diverge for $R=1$, with a directionally dependent limit there. If *all PNDs are tangent* to $\mathcal{I}$, $R_n=\exp(-i\phi_n)$, (not necessary degenerate) the pattern can be written

$$|\Psi_4^{\mathrm{i}}| \approx |\Psi_{4*}^{\mathrm{o}}|\,\eta^{-1} \prod_{n=1,2,3,4} [\cosh\psi - \sinh\psi\cos(\phi-\phi_n)]^{1/2}. \qquad (18)$$

There are no outgoing or ingoing directions along which radiation vanishes in this case—see, e.g., Fig. 2 (Dd).

To summarize, when $\mathcal{I}$ is timelike the radiation fields depend on the direction along which the infinity is approached. Analogously to the $\Lambda>0$ case [4] the radiation pattern has a universal character determined by the *algebraic type* of the fields. However, new features occur when $\Lambda<0$: both *outgoing* and *ingoing* patterns have to be studied; their shapes depend also on the *orientation of PNDs* with respect to the infinity, and an interesting possibility of PNDs *tangent to* $\mathcal{I}$ appears. Radiation vanishes only along directions which are reflections of PNDs with respect to $\mathcal{I}$, in a *generic* direction it is *nonvanishing*. The absence of η^{-1} term thus cannot be used to distinguish nonradiative sources: near an anti–de Sitter–like infinity the radiative component reflects not only properties of the sources but also their relation to the observer.

ACKNOWLEDGMENTS

This work has been supported by the grants GAČR 202/02/0735 and GAUK 166/2003.

[1] H. Bondi, M. G. J. van der Burg, and A. W. K. Metzner, Proc. R. Soc. London **A269**, 21 (1962).
[2] R. Penrose, Proc. R. Soc. London **A284**, 159 (1965).
[3] R. Penrose and W. Rindler, *Spinors and Space-Time*, Vol. 2 (Cambridge University Press, Cambridge, 1986).
[4] P. Krtouš, J. Podolský, and J. Bičák, Phys. Rev. Lett. **91**, 061101 (2003).
[5] J. Podolský, M. Ortaggio, and P. Krtouš, Phys. Rev. D **68**, 124004 (2003).
[6] R. Emparan, G. T. Horowitz, and R. C. Myers, J. High Energy Phys. **01**, 007 (2000).
[7] A. Chamblin, Class. Quantum Grav. **18**, L17 (2001).
[8] D. Kramer, H. Stephani, E. Herlt, and M. MacCallum, *Exact Solutions of Einstein's Field Equations* (Cambridge University Press, Cambridge, 1980).
[9] P. Krtouš and J. Podolský, Phys. Rev. D **68**, 024005 (2003).

INSTITUTE OF PHYSICS PUBLISHING CLASSICAL AND QUANTUM GRAVITY

Class. Quantum Grav. **21** (2004) R233–R273 PII: S0264-9381(04)68912-X

TOPICAL REVIEW

Asymptotic directional structure of radiative fields in spacetimes with a cosmological constant

Pavel Krtouš and Jiří Podolský

Institute of Theoretical Physics, Charles University in Prague, V Holešovičkách 2, 180 00 Prague 8, Czech Republic

E-mail: Pavel.Krtous@mff.cuni.cz and Jiri.Podolsky@mff.cuni.cz

Received 14 July 2004, in final form 4 October 2004
Published 25 November 2004
Online at stacks.iop.org/CQG/21/R233
doi:10.1088/0264-9381/21/24/R01

Abstract

We analyse the directional properties of general gravitational, electromagnetic and spin-s fields near conformal infinity $\mathcal{I}$. The fields are evaluated in normalized tetrads which are parallelly propagated along null geodesics which approach a point P of $\mathcal{I}$. The standard peeling-off property is recovered and its meaning is discussed and refined. When the (local) character of the conformal infinity is null, such as in asymptotically flat spacetimes, the dominant term which is identified with radiation is unique. However, for spacetimes with a non-vanishing cosmological constant the conformal infinity is spacelike (for $\Lambda > 0$) or timelike (for $\Lambda < 0$), and the radiative component of each field depends substantially on the null direction along which P is approached.

The directional dependence of asymptotic fields near such de Sitter-like or anti-de Sitter-like $\mathcal{I}$ is explicitly found and described. We demonstrate that the corresponding directional structure of radiation has a universal character that is determined by the algebraic (Petrov) type of the field. In particular, when $\Lambda > 0$ the radiation vanishes only along directions which are opposite to principal null directions. For $\Lambda < 0$ the directional dependence is more complicated because it is necessary to distinguish outgoing and ingoing radiation. Near such anti-de Sitter-like conformal infinity the corresponding directional structures differ, depending not only on the number and degeneracy of the principal null directions at P but also on their specific orientation with respect to $\mathcal{I}$.

The directional structure of radiation near (anti-)de Sitter-like infinities supplements the standard peeling-off property of spin-s fields. This characterization offers a better understanding of the asymptotic behaviour of the fields near conformal infinity under the presence of a cosmological constant.

PACS numbers: 04.20.Ha, 98.80.Jk, 04.40.Nr

Contents

1. Introduction

Many studies have been devoted to theoretical investigations of gravitational waves. The first—by Einstein himself—appeared immediately after the formulation of general relativity [1, 2], and was soon followed by other papers [3, 4]. Since then numerous works on gravitational radiation have concentrated on specific *approximate* (analytic or numerical) analyses of various spatially isolated gravitating sources, most recently binary systems, collision and merger of black holes or neutron stars, supernova explosions and other possible astrophysical sources.

In *rigorous* treatments within the full Einstein theory, several interesting classes of exact radiative solutions were found and investigated in the late 1950s and the early 1960s—for example [5–11]. For reviews of these contributions to the theory of gravitational radiation see, e.g., [12–19]. Although most of such spacetimes seem to be physically not very realistic, they serve as useful explicit models and test beds for numerical relativity and other approximations. Almost simultaneously, general frameworks which allow one to study asymptotic properties of radiative fields were also developed and applied in now classical works [20–29] and elsewhere (see, e.g., [30–35] for reviews and many references).

Despite this long-standing effort, however, there still remain open fundamental problems concerning the very concept of gravitational radiation in the context of the *full* nonlinear Einstein theory. No rigorous statements are available which would relate the properties of sufficiently *general* strong sources to the radiation fields produced. Also, the presence of a *non-vanishing cosmological constant* Λ is not mathematically compatible with asymptotic flatness that is naturally assumed in many of the existing analyses. Although important results on the existence of vacuum solutions with $\Lambda \neq 0$ have already been obtained [36], in order to fully understand the properties of gravitational and electromagnetic radiation in such 'de Sitter-type' or 'anti-de Sitter-type' spacetimes, further studies are necessary.

As a particular contribution to this task we will here describe the asymptotic directional behaviour of general fields in spacetimes which admit any value of the cosmological constant.

1.1. On studies of asymptotic behaviour of radiative fields in general relativity

First, we briefly summarize the main methods which have been developed to characterize rigorously the asymptotic properties of fields in general relativity. It is not our intention to present an exhaustive and thorough review of previous works. We only wish to set up a context in which we could place our present analysis and results.

One fundamental technique for investigating radiative properties of gravitational and electromagnetic fields at 'large distance' from a spatially bounded source is based on introducing a suitable *Bondi–Sachs coordinate system* adapted to *null hypersurfaces*, and expanding the metric functions in inverse powers of the luminosity distance r which plays the role of an appropriate 'radial' coordinate parametrizing outgoing null geodesics [20, 21, 23, 37]. In the case of asymptotically flat spacetimes this framework allows one to introduce the Bondi mass (the total mass of a system as measured at future null infinity $\mathcal{I}$) and momentum, and characterize the time evolution including radiation in terms of the news functions which are the analogue of the radiative part of the Poynting vector in electrodynamics. Using these concepts, it is possible to formulate a balance between the amount of energy radiated by gravitational waves and the decrease of the Bondi mass of an isolated system. These pioneering contributions were subsequently refined and generalized [24, 38, 39], and also extended after the development of the complex null tetrad formalism and the associated spin coefficient formalism [25, 26] which lead to great simplifications in the expressions, see, e.g., [13, 17, 18, 30, 32] for reviews. Nevertheless, in these works the analysis of radiative fields assumed that spacetime is asymptotically flat. This ruled out, for instance, a non-vanishing cosmological constant Λ. These methods generally are based on privileged coordinate systems which are not automatically possible to generalize to the cases when $\Lambda \neq 0$.

Alternatively, information about the character of radiation can be extracted from the tetrad components of fields measured along a family of null geodesics approaching $\mathcal{I}$. One can consider only a bundle of such geodesics, as $\mathcal{I}$ need not exist globally. The rate of approach to zero of the Weyl or Maxwell tensor is given by the celebrated *peeling-off theorem* [22, 23, 25, 29, 33, 40]. The component of a spin-s zero-rest-mass field (with respect to a parallelly transported and suitably normalized interpretation tetrad) proportional to $\eta^{-(j+1)}$, where η is an affine parameter along the null geodesics, $j = 0, 1, \ldots, 2s$, appears to have in general $2s - j$ coincident principal null directions. Consequently, the part of the field that falls off as η^{-1} exhibits $2s$-degeneracy of principal null directions. It is thus considered as the *radiation field* because its asymptotic algebraic 'null' structure [12, 33, 41–44] locally resembles that of standard plane waves [5]. The gravitational or electromagnetic field thus represents outgoing radiation if the dominant component of the Weyl or Maxwell tensor, conveniently expressed in the Newman–Penrose formalism [25, 26, 45] as quantity Ψ_4 or Φ_2, respectively, is

non-vanishing. This component manifests itself through typical transverse effects on nearby test particles [23, 46, 47]. Such a characterization of the radiative field remains valid also in more general spacetimes because the peeling-off property holds even for a non-vanishing Λ (the precise meaning of the peeling-off behaviour of fields will be discussed below in the main text, see sections 5.2 and 6).

Another major step made by Penrose [27–29, 48] (see [33] for a comprehensive overview) was his *coordinate-independent* (geometric) approach to the definition of radiation for massless fields based on the *conformal treatment of infinity*. The Penrose technique enables one to apply methods of local differential geometry near conformal infinity $\mathcal{I}$ (also referred to as 'scri') which is defined as the boundary $\Omega = 0$ of the physical spacetime manifold $(\mathcal{M}, \mathbf{g})$ in the conformally related 'unphysical' spacetime manifold $(\tilde{\mathcal{M}}, \tilde{\mathbf{g}})$, $\tilde{\mathbf{g}} = \Omega^2\mathbf{g}$ (see section 2). Properties of radiation fields in $\mathcal{M}$ can thus be studied by analysing conformally (i.e., isotropically) rescaled fields on $\mathcal{I}$ in the compactified manifold $\tilde{\mathcal{M}}$. For asymptotically flat spacetimes, $\mathcal{I}$ is a smooth null hypersurface in $\tilde{\mathcal{M}}$ generated by the endpoints of null geodesics. In this case it is possible to define in a geometric way the Bondi mass, to derive the peeling-off property, or to characterize the Bondi–Metzner–Sachs group of asymptotic symmetries [21, 27, 37, 49, 50]. In particular, one can evaluate gravitational radiation propagating along a given null geodesic which is described by the Ψ_4 component of the Weyl tensor projected on a parallelly transported complex null tetrad. The crucial point is that such a tetrad is (essentially) *determined uniquely* by the conformal geometry, see [33]. Moreover, the Penrose covariant approach can be naturally applied also to spacetimes which include the cosmological constant [28, 29, 33, 51]. This is quite remarkable, since there is no analogue of the news function in the presence of Λ [52, 53] (for a comparison of the Bondi–Sachs and Penrose approaches, see, e.g., [50, 54–59]).

The above mentioned analysis led Penrose to the elegant idea of *(weakly) asymptotically simple spacetimes*—those having a *smooth* $\tilde{\mathbf{g}}$ and Ω on $\mathcal{I}$ (see, e.g., [27, 29 , 33–35, 60–62] and references therein for the precise definition). Because it entails a certain fall-off behaviour of the physical metric near $\mathcal{I}$, this is a fruitful rigorous concept for studying asymptotic radiation properties of isolated systems in general relativity. It follows from the important recent works [63–69], and also [70–80], that there indeed *exist* large classes of exact—though not given in explicit forms—solutions to Einstein's field equations which globally satisfy the required regularity conditions on $\mathcal{I}$ (see [19, 36, 62, 81, 82] for a review). Let us emphasize that, until now, the only *explicitly* known exact metrics satisfying Penrose's asymptotic conditions (although not globally since there are at least four 'points' at $\mathcal{I}$ which are singular) are boost-rotation symmetric spacetimes representing uniformly accelerated 'sources' or black holes [11, 13–15, 17, 18, 39, 83, 84]. Nevertheless, the original Penrose conjecture of asymptotic simplicity may appear to be too restrictive in general. More recent studies have indicated that *generic* Cauchy data fail to be smoothly extendable to the conformal boundary [74, 75, 85, 86], see also [71, 80, 87–89]. More general spacetimes with *polyhomogeneous* $\mathcal{I}$ were thus studied in [57, 90, 91] and in other works, for which the metric $\tilde{\mathbf{g}}$ admits an asymptotic expansion in terms of $r^{-j}\log^i r$ rather than r^{-j}. This new setup naturally extends the Bondi–Sachs–Penrose approach. For example, when $\Lambda = 0$ the Bondi mass still remains well defined at polyhomogeneous $\mathcal{I}$, and it is a non-increasing function of retarded time as in [21, 23, 92]. For the class of polyhomogeneous vacuum metrics the asymptotic symmetry group is the standard BMS group, and the peeling-off property of the curvature tensor is the same as that for smooth metrics [23] *up to the terms of order* $r^{-(2+\epsilon)}$, $0 \leqslant \epsilon < 1$, but the term $\sim r^{-3}\log r$ also appears. Further studies of polyhomogeneity for zero-rest-mass fields, such as the existence of conserved quantities (NP constants) at $\mathcal{I}$ [33, 93–97], can be found, e.g., in [98, 99].

Let us now concentrate on the main *differences* between the asymptotically flat spacetimes and those with a non-vanishing cosmological constant Λ. Interestingly, specific new features appear in the case of asymptotically 'de Sitter-like' ($\Lambda > 0$) or 'anti-de Sitter-like' ($\Lambda < 0$) solutions for which the conformal infinity $\mathcal{I}$ is, respectively, spacelike or timelike. As Penrose observed and repeatedly emphasized in his early works [28, 29, 100], the concept of radiation for massless fields turns out to be 'less invariant' in cases when $\mathcal{I}$ does not have a null character, see section 9.7 of [33]. Namely, it emerges as necessarily *direction dependent* since the choice of the appropriate null tetrad, and thus the radiative component Ψ_4 of the field, may differ for different null geodesics reaching the same point on $\mathcal{I}$. This is, for example, demonstrated by the fact that with a non-vanishing Λ even fields of 'static', non-accelerated sources have a non-vanishing radiative component along a *generic* ('non-radial') direction, as was shown for test charges in [101] or for Reissner–Nordström black holes in [102, 103] in a (anti-)de Sitter universe.

For $\Lambda \neq 0$, the non-null character of conformal infinity $\mathcal{I}$ also plays a fundamental role in the formulation of the initial value problem. As mentioned above, quite surprisingly the *global* existence has been established of asymptotically simple vacuum solutions (with a smooth $\mathcal{I}$) which differ on an arbitrary given Cauchy surface by a finite but sufficiently small amount from de Sitter data [36, 64], while an analogous result for data close to Minkowski ($\Lambda = 0$) is still under investigation (see [19, 36, 81] for more details). Thus, many vacuum asymptotically simple spacetimes with de Sitter-like $\mathcal{I}$ do exist. However, a spacelike $\mathcal{I}$ as occurs in this case implies the existence of cosmological and particle horizons for geodesic observers, which results in insufficiency of purely retarded massless fields—advanced effects must necessarily be present. For example, the electromagnetic field produced by sources cannot be prescribed freely because the Gauss constraint has to be satisfied at $\mathcal{I}^-$ (or $\mathcal{I}^+$). This phenomenon has been demonstrated explicitly [104] by analysing test electromagnetic fields of uniformly accelerated charges on a de Sitter background. On the other hand, it is well-known that for a timelike $\mathcal{I}$, which occurs when $\Lambda < 0$, the spacetimes are not globally hyperbolic, and one is necessarily led to a kind of 'mixed initial boundary value problem', see, e.g., [68, 105–107]. The data need to be given on a spacetime slice extending to $\mathcal{I}$ and also on $\mathcal{I}$ itself. The rigorous concept of gravitational and electromagnetic radiation is thus much less clear in situations when $\Lambda \neq 0$.

Here we will analyse mainly the *directional structure* of radiative fields. This structure is significantly different for null and spacelike/timelike conformal infinities. In the case of asymptotically flat spacetimes, the dominant radiative component of the field at any point P at null infinity $\mathcal{I}$ is essentially *unique*. One can however approach a point P from *infinitely many different* null directions, and if $\mathcal{I}$ has a spacelike or timelike character it is not *a priori* clear how the radiation components of the fields in the corresponding interpretation tetrads depend on a specific direction.

Such a directional dependence was explicitly found and described for the first time in the context of the *test electromagnetic field* generated by a pair of uniformly accelerated point-like charges in the de Sitter background [101, 108]. In particular, it was demonstrated that there always exist two special directions—those opposite to the direction from the sources—along which the radiation vanishes. For all other directions the radiation field is non-vanishing. This is described by an explicit formula which completely characterizes its angular dependence (see [101]).

Subsequently, we have carefully analysed the *exact* solution of the Einstein–Maxwell equations which generalizes the classic C-metric (see, e.g., [7, 83, 109, 110] for reviews and references) to admit a cosmological constant [111–115]. For $\Lambda > 0$ it represents a pair of uniformly accelerated possibly charged black holes in a de Sitter-like universe.

In [102] we demonstrated that the corresponding electromagnetic field exhibits exactly the *same* asymptotic radiative behaviour at the spacelike conformal infinity $\mathcal{I}$ as for the test fields [101] of accelerated charges. Moreover, we found and explicitly described the specific analogous directional structure of the *gravitational radiation field*, and we proved that the directional pattern of radiation is adapted to the principal null directions of this Petrov type D spacetime.

Elsewhere [103] we investigated the asymptotic behaviour of fields corresponding to the *C*-metric with $\Lambda < 0$, i.e. the directional dependence of radiation generated by accelerated black holes in an anti-de Sitter universe. Some fundamental differences from the case $\Lambda > 0$ occur since the conformal infinity $\mathcal{I}$ now has a timelike character. In fact, the whole structure of the spacetime is more complex and new phenomena also arise: $\mathcal{I}$ is divided by Killing horizons into several domains with a different structure of principal null directions—in these domains the directional structure of radiation is thus different. The radiative field vanishes along directions which are mirror images of the principal null directions with respect to $\mathcal{I}$. Moreover, ingoing and outgoing radiation has to be treated separately.

These studies of particular exact radiative models with a non-vanishing Λ gave us a sufficient insight necessary to understand the asymptotic behaviour of *general* fields near spacelike or timelike conformal infinities. The directional dependence of gravitational and electromagnetic radiation is given mainly by *spacetime geometry*, namely by the character of $\mathcal{I}$ and by the specific orientation and degeneracy of principal null directions at infinity.

In [116] we demonstrated that the directional structure of radiation close to a de Sitter-like infinity has a *universal character* that is determined by the *algebraic type* of the fields. For example, the radiation completely vanishes along spatial directions on $\mathcal{I}$ which are antipodal to principal null directions. In the following work [117] we investigated the complementary situation when $\Lambda < 0$. Although the idea is similar to the previous case, the asymptotic behaviour of fields turns out to be more complicated because $\mathcal{I}$ is timelike, and thus admits a 'richer structure' of possible radiative patterns.

1.2. Outline of the present work

It is the purpose of this review to present these results—concerning the asymptotic directional structure of general fields near conformal infinity $\mathcal{I}$ of any type—in a synoptic, compact and unified form. The paper is organized as follows. First, in section 2 we summarize basic concepts of conformal geometry and their relation to quantities in a physical spacetime. In particular, we introduce the conformal infinity $\mathcal{I}$, correlate its character with the sign of the cosmological constant Λ and investigate the correspondence between null geodesics in physical and conformal spacetimes. Section 3 is devoted to careful analysis of various orthonormal and null tetrads which are key ingredients in our subsequent study of the asymptotic behaviour of fields. We define an interpretation tetrad which is parallelly propagated along a null geodesic, and we demonstrate that—after performing a specific boost—it becomes asymptotically adjusted to $\mathcal{I}$ (i.e., naturally normalized and adapted to normal and tangent directions at a given point of conformal infinity). This fact becomes crucial in section 4 in which we explicitly evaluate the components of general gravitational, electromagnetic or any spin-s field in the interpretation tetrad near conformal infinity. For zero-rest-mass fields the dominant component decays as η^{-1} (where η is the affine parameter of a null geodesic) and thus represents radiation.

The complete expression (4.19) fully chracterizes the asymptotic behaviour of the field near any $\mathcal{I}$, including the directional structure, i.e. the dependence on the direction of the geodesic along which a point $P \in \mathcal{I}$ is approached as $\eta \to \infty$. The final section 5 contains

a detailed discussion of the result. In asymptotically Minkowskian spacetimes with $\Lambda = 0$ for which $\mathcal{I}$ has a null character, the directional dependence completely vanishes. The presence or absence of the η^{-1} component of the field can thus be used as an invariant characterization of radiation. In this context we also elucidate the precise meaning of the peeling-off behaviour. For $\Lambda \neq 0$ the asymptotic structure of fields is more complicated because the dominant component depends substantially on the direction of a null geodesic along which P is approached. We introduce a convenient parametrization of such directions near a spacelike or timelike $\mathcal{I}$ which occur in spacetimes with $\Lambda > 0$ or $\Lambda < 0$, respectively. Finally, we describe in detail the asymptotic directional structure of radiative fields near such de Sitter-like or anti-de Sitter-like conformal infinities. It is proved to be essentially determined by the algebraic type of the field, namely by the number, degeneracy and specific orientation of the principal null directions at point $P \in \mathcal{I}$.

Two appendices are included. In appendix A we present expansions of the conformal factor Ω and the conformal affine parameter $\tilde{\eta}$ in terms of the physical affine parameter η of a null geodesic. We demonstrate their polyhomogeneous character. We also investigate the conditions under which the two main vectors of the interpretation tetrad become coplanar with the normal to $\mathcal{I}$. Appendix B summarizes the description of spin-s fields, tetrads and their Lorentz transformations in spinor formalism.

2. Conformal infinity and null geodesics

In this section we recall some basic concepts and properties concerning the geometry of a physical spacetime and its conformally related counterpart which will be necessary for our subsequent analysis. Many of these concepts can be found in standard literature, e.g., in [12, 33, 61]. However, we summarize them for convenience and to introduce our notation.

2.1. Conformal geometry

We wish to study spacetimes which locally admit conformal infinity. According to the general formalism [27, 29, 31, 33, 61], such an n-dimensional manifold $\mathcal{M}$ with physical metric $\mathbf{g}$ can be embedded into a larger *conformal manifold* $\tilde{\mathcal{M}}$ with *conformal metric* $\tilde{\mathbf{g}}$ via a conformal transformation

$$\tilde{\mathbf{g}} = \Omega^2 \mathbf{g}. \tag{2.1}$$

Obviously, the spacetimes $(\mathcal{M}, \mathbf{g})$ and $(\tilde{\mathcal{M}}, \tilde{\mathbf{g}})$ have identical local causal structure (the same light cones). The conformal factor Ω is assumed to be positive in $\mathcal{M}$, and vanishes on the boundary of $\mathcal{M}$ in $\tilde{\mathcal{M}}$. Such a boundary $\Omega = 0$ is called *conformal infinity* $\mathcal{I}$. Let us note that in the following it is not necessary to require global existence of $\mathcal{I}$. However, we assume that Ω is smooth near $\mathcal{I}$, and we impose suitable regularity conditions for the conformal metric. Specifically, we assume that the conformal factor is sufficiently smooth along null geodesics approaching $\mathcal{I}$ in $(\tilde{\mathcal{M}}, \tilde{\mathbf{g}})$, cf equation (2.16) in this section.

To indicate explicitly which of the above metrics is used for raising indices, we introduce $\mathbf{g}^{ab}$ as the inverse of $\mathbf{g}_{ab}$ and $\tilde{\mathbf{g}}^{ab}$ as the inverse of $\tilde{\mathbf{g}}_{ab}$.

The derivative operator of $\tilde{\mathbf{g}}$ is related to that of $\mathbf{g}$. The relation between the derivative $\tilde{\nabla}$ associated with $\tilde{\mathbf{g}}$ and ∇ associated with $\mathbf{g}$ is (see, e.g., [61])

$$\tilde{\nabla}_a \mathbf{v}^c = \nabla_a \mathbf{v}^c + \gamma^c_{ab} \mathbf{v}^b, \qquad \gamma^c_{ab} = \Omega^{-1}\big(\delta^c_a \mathbf{d}_b\Omega + \delta^c_b \mathbf{d}_a\Omega - \mathbf{g}_{ab}\mathbf{g}^{cd}\mathbf{d}_d\Omega\big). \tag{2.2}$$

This implies relations between the curvature associated with $\tilde{\nabla}$, and the curvature associated with ∇. By contracting the formula for the Riemann tensor we obtain relations between the

conformal and physical Ricci tensors,

$$\tilde{\mathbf{Ric}}_{ab} = \mathbf{Ric}_{ab} - (n-2)\Omega^{-1}\nabla_a \mathbf{d}_b\Omega - \Omega^{-1}\mathbf{g}_{ab}\Box\Omega + 2(n-2)\Omega^{-2}\mathbf{d}_a\Omega\,\mathbf{d}_b\Omega - (n-3)\Omega^{-2}\mathbf{g}_{ab}\mathbf{g}^{cd}\mathbf{d}_c\Omega\,\mathbf{d}_d\Omega, \tag{2.3}$$

where $\Box = \mathbf{g}^{ab}\nabla_a\nabla_b$, and the scalar curvatures,

$$\tilde{R} = \Omega^{-2}R - 2(n-1)\Omega^{-3}\Box\Omega - (n-1)(n-4)\Omega^{-4}\mathbf{g}^{ab}\mathbf{d}_a\Omega\,\mathbf{d}_b\Omega. \tag{2.4}$$

The Weyl tensor is unchanged by a conformal transformation,

$$\tilde{\mathbf{C}}_{abc}{}^{d} = \mathbf{C}_{abc}{}^{d}. \tag{2.5}$$

2.2. Conformal infinity $\mathcal{I}$ and its character

The conformal infinity is localized by the condition $\Omega = 0$. Its character is determined by the gradient $\mathbf{d}\Omega$ on $\mathcal{I}$—it can be timelike, null or spacelike. We introduce a normalized vector $\tilde{\mathbf{n}}$ which is *normal to the conformal infinity* $\mathcal{I}$,

$$\tilde{\mathbf{n}}^a = \tilde{N}\tilde{\mathbf{g}}^{ab}\mathbf{d}_b\Omega, \qquad \tilde{\mathbf{g}}_{ab}\tilde{\mathbf{n}}^a\tilde{\mathbf{n}}^b = \sigma, \qquad \sigma = -1, 0, +1. \tag{2.6}$$

For $\sigma = \pm 1$ the conformal 'lapse' function $\tilde{N} > 0$ is given by $\tilde{N} = |\tilde{\mathbf{g}}^{ab}\mathbf{d}_a\Omega\,\mathbf{d}_b\Omega|^{-1/2}$, and $\tilde{\mathbf{g}} = \sigma\tilde{N}^2\mathbf{d}\Omega^2 + {}^{\mathcal{I}}\tilde{\mathbf{g}}$, where ${}^{\mathcal{I}}\tilde{\mathbf{g}}$ is a restriction of $\tilde{\mathbf{g}}$ on $\mathcal{I}$. For $\sigma = 0$ the 'lapse' $\tilde{N}$ is chosen arbitrarily. The normalization factor σ determines the character of the conformal infinity, namely

$$\sigma = \begin{cases} -1: & \mathcal{I}\ \textit{is spacelike}, \\ 0: & \mathcal{I}\ \text{is } \textit{null}, \\ +1: & \mathcal{I}\ \text{is } \textit{timelike}. \end{cases} \tag{2.7}$$

This is illustrated in figure 1.

In fact, we can explicitly evaluate the 'lapse' $\tilde{N}$. Transforming $\Box$ into $\tilde{\Box} = \tilde{\mathbf{g}}^{ab}\tilde{\nabla}_a\tilde{\nabla}_b$ in (2.4) using relation (2.2), we obtain

$$\tilde{\mathbf{g}}^{ab}\mathbf{d}_a\Omega\,\mathbf{d}_b\Omega = -\frac{R}{n(n-1)} + \Omega\left(\frac{2}{n}\tilde{\Box}\Omega + \frac{\Omega\tilde{R}}{n(n-1)}\right). \tag{2.8}$$

By contracting the Einstein field equations

$$\mathbf{Ric} - \tfrac{1}{2}R\mathbf{g} + \Lambda\mathbf{g} = \varkappa\mathbf{T}, \tag{2.9}$$

we get $R = \frac{2}{n-2}(n\Lambda - \varkappa T)$. Assuming a vanishing trace T of the energy–momentum tensor, which is valid in vacuum, pure radiation or electrovacuum ($n = 4$) spacetimes, equation (2.8) on $\mathcal{I}$ implies

$$\sigma\tilde{N}|_{\mathcal{I}}^{-2} = \tilde{\mathbf{g}}^{ab}\mathbf{d}_a\Omega\mathbf{d}_b\Omega|_{\mathcal{I}} = -\frac{2\Lambda}{(n-1)(n-2)}, \qquad \text{i.e.,} \quad \sigma = -\operatorname{sign}\Lambda. \tag{2.10}$$

The character of the conformal infinity is thus correlated with the sign of the cosmological constant. For $\sigma \neq 0$ we also obtain that the '*lapse' is constant on* $\mathcal{I}$, $\tilde{N}|_{\mathcal{I}} = \ell > 0$, where ℓ is a typical length, which for spacetime dimension $n = 4$ is $\ell = \sqrt{|3/\Lambda|}$. For (anti-)de Sitter spacetime, the scale ℓ represents its characteristic radius. When $\sigma = 0$ ($\Lambda = 0$) we choose $\tilde{N}$ to be an arbitrary constant on $\mathcal{I}$. The normalized timelike/null/spacelike vector $\tilde{\mathbf{n}}$ given by (2.6) which is normal to conformal infinity $\mathcal{I}$ is thus set uniquely.

Analogously we introduce a vector $\mathbf{n}$ normal to $\Omega = \text{const}$ in the physical spacetime $(\mathcal{M}, \mathbf{g})$ such that

$$\mathbf{g}_{ab}\mathbf{n}^a\mathbf{n}^b = \sigma, \tag{2.11}$$

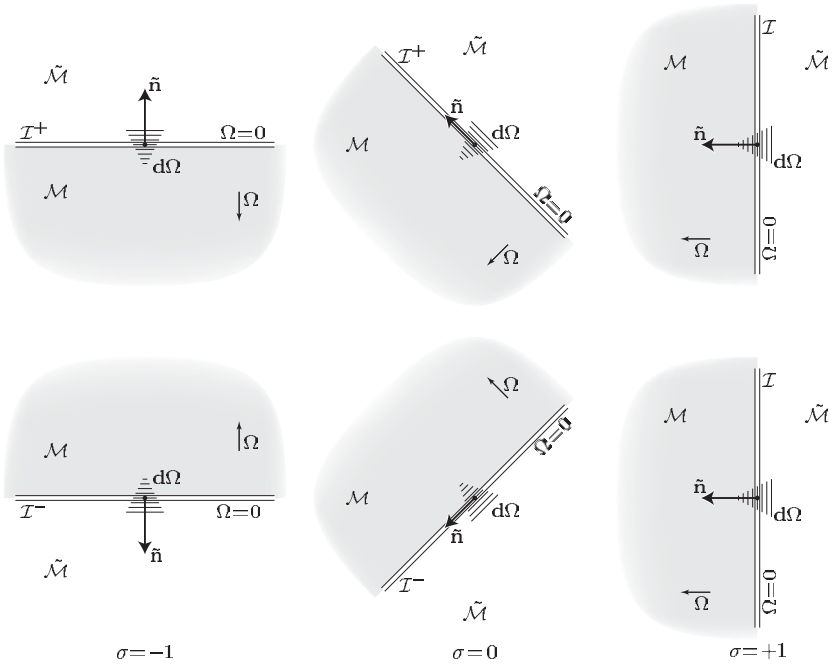

Figure 1. The local character of the conformal infinity $\mathcal{I}$ (situated on the boundary $\Omega = 0$ of $\mathcal{M}$ in $\tilde{\mathcal{M}}$) is determined by the norm σ of vector $\tilde{\mathbf{n}}$ normal to $\mathcal{I}$. For $\sigma = -1, 0$ or $+1$ the infinity $\mathcal{I}$ is spacelike, null or timelike, respectively. When $\sigma = -1$ or $\sigma = 0$, the future conformal infinity $\mathcal{I}^+$ and the past conformal infinity $\mathcal{I}^-$ can be distinguished; the corresponding diagrams are drawn in the upper and lower parts of the figure. For $\sigma = +1$ the future and past infinities of null geodesics are the same, and therefore the diagrams are identical.

which implies the relation

$$\mathbf{n} = \Omega\tilde{\mathbf{n}}. \tag{2.12}$$

Strictly speaking, it is not possible to introduce the vector $\mathbf{n}$ normalized in the physical geometry $(\mathcal{M}, \mathbf{g})$ at $\mathcal{I}$ directly. The conformal infinity *does not* belong to the physical spacetime, and even if we extend the manifold $\mathcal{M}$ into the conformal manifold $\tilde{\mathcal{M}}$, the physical metric $\mathbf{g}$ is not well defined on $\mathcal{I}$: it is related to the conformal metric $\tilde{\mathbf{g}}$ by the factor Ω^{-2}, see (2.1), which becomes infinite.

We could try to extend the definition of the physical metric (and other tensors related to physical spacetime) up to the infinity $\mathcal{I}$ using some limiting procedure, e.g., using its expansion along curves approaching $\mathcal{I}$. However, the 'infinite ratio' between $\mathbf{g}$ and $\tilde{\mathbf{g}}$ still poses problems. Physically defined vectors transported in a natural way to $\mathcal{I}$ are rescaled to zero when measured in conformal geometry and vectors from the conformal tangent space at $\mathcal{I}$ have an infinite length if measured using the physical metric. The tangent space of the conformal manifold at $\mathcal{I}$ is infinitely 'blown up' with respect to the tangent space of the physical manifold defined at the conformal infinity by a suitable limiting procedure. Nevertheless, one can deal with such infinite scaling using the conformal technique: its important feature is that the conformal rescaling is *isotropic*—it rescales all directions in the same way. If the rescaling enters expansions of physical tensor quantities only as a common factor which is some power of Ω, it is 'well controlled': we can associate with any physical quantity a conformal quantity

rescaled by a proper power of Ω which is correctly defined at conformal infinity, independent of the direction along which $\mathcal{I}$ is approached.

The conformal geometry and the definition of the conformal infinity can thus be understood as a convenient way to deal with tensors at infinity—any physical quantity can be 'translated' into its conformal counterpart which is well defined at $\mathcal{I}$. However, it can be convenient sometimes to speak directly about physical quantities at $\mathcal{I}$ and we will do so if the 'translation' to the conformal picture is clear. Exactly in this sense, we can speak about the physical normal vector $\mathbf{n}$ at $\mathcal{I}$, even if it is related to the well defined conformal normal $\tilde{\mathbf{n}}$ by relation (2.12) which is degenerate on $\mathcal{I}$. Similarly, in the next section we use a null tetrad adjusted to the infinity $\mathcal{I}$ normalized in the physical geometry.

Let us note however that one has to be careful with asymptotic expansions if these are not isotropic, i.e., if they rescale one direction by an 'infinite amount' as compared with other directions. This will be the case of, for example, interpretation null tetrads parallelly transported to $\mathcal{I}$ as discussed in section 3.4. Various components of physical tensors with respect to the interpretation tetrad thus will not rescale in the same way and their behaviour has to be studied more carefully, cf section 4.3.

2.3. Null geodesics

Now we consider geodesics in the physical spacetime $(\mathcal{M}, \mathbf{g})$ and we relate them to geodesics in the conformal spacetime $(\tilde{\mathcal{M}}, \tilde{\mathbf{g}})$. It follows from (2.2) that *null geodesics are conformally invariant*, i.e., null geodesics $z(\eta)$ with respect to ∇ coincide with null geodesics $\tilde{z}(\tilde{\eta})$ with respect to $\tilde{\nabla}$. The affine parameter $\tilde{\eta}$ for geodesics in conformal spacetime is related to the affine parameter η for geodesics in physical spacetime by

$$\frac{\mathrm{d}\tilde{\eta}}{\mathrm{d}\eta} = \Omega^2, \qquad \text{i.e.,} \quad \frac{\mathrm{D}z}{\mathrm{d}\eta} = \Omega^2 \frac{\mathrm{D}\tilde{z}}{\mathrm{d}\tilde{\eta}} \tag{2.13}$$

(we fix a trivial factor corresponding to constant rescaling of $\tilde{\eta}$ to unity).

Without loss of generality we take the affine parameter $\tilde{\eta}$ such that $\tilde{\eta} = 0$ at conformal infinity $\mathcal{I}$. Therefore, as $\tilde{\eta} \to 0$ the null geodesic $\tilde{z}(\tilde{\eta})$ in conformal spacetime approaches a specific point $P \in \mathcal{I}$, i.e., $\tilde{z}(0) = P$. Such a geodesic can be either *outgoing* or *ingoing* with respect to physical spacetime $\mathcal{M}$:

$$\frac{\mathrm{D}\tilde{z}^a}{\mathrm{d}\tilde{\eta}} \mathbf{d}_a \Omega \bigg|_{\mathcal{I}} \equiv \frac{\mathrm{d}\Omega}{\mathrm{d}\tilde{\eta}} \bigg|_{\mathcal{I}} = -\epsilon, \tag{2.14}$$

where

$$\epsilon = \begin{cases} +1: & \text{for } \textit{outgoing geodesics}, \quad \tilde{\eta} < 0 \text{ in } \mathcal{M}, \\ -1: & \text{for } \textit{ingoing geodesics}, \quad \tilde{\eta} > 0 \text{ in } \mathcal{M}. \end{cases} \tag{2.15}$$

By this condition, the normalization of the affine parameter $\tilde{\eta}$ is fixed uniquely, including the orientation of the null geodesic $\tilde{z}(\tilde{\eta})$. As we have already mentioned, we assume smoothness of the conformal factor along $\tilde{z}(\tilde{\eta})$, hence we may expand Ω in powers of $\tilde{\eta}$ near $\mathcal{I}$. Taking into account that $\tilde{\eta}|_{\mathcal{I}} = 0$, and equation (2.14), we have

$$\Omega = -\epsilon\tilde{\eta} + \Omega_2 \tilde{\eta}^2 + \cdots, \tag{2.16}$$

with Ω_2 constant. Substituting into equation (2.13), straightforward integration leads to the relation between the physical and conformal affine parameters

$$\eta = -\frac{1}{\tilde{\eta}}(1 - 2\epsilon\Omega_2\tilde{\eta}\ln|\tilde{\eta}| - \eta_0\tilde{\eta} + \cdots). \tag{2.17}$$

Here η_0 is a constant of integration. Consequently, near $\mathcal{I}$ we obtain in the leading order that $\tilde{\eta} \approx -\eta^{-1}$ and $\Omega \approx \epsilon\eta^{-1}$. The null geodesic $z(\eta)$ thus reaches the point $P \in \mathcal{I}$ for an *infinite* value of the affine parameter η, namely $z(\epsilon\infty) = P$.

The leading term in the expansions (2.16) and (2.17) is sufficient for all calculations throughout this paper. However, for other purposes it can be useful to express these expansions up to the next order. It is not simple to invert expansion (2.17) due to the presence of the logarithmic term. In appendix A we demonstrate that (cf equation (A.6))

$$\tilde{\eta} = -\frac{1}{\eta}(1 - 2\epsilon\Omega_2\eta^{-1}\ln|\eta| + \eta_0\eta^{-1} + \cdots), \tag{2.18}$$

and (cf equation (A.7))

$$\Omega = \epsilon\eta^{-1} + (-2\Omega_2\ln|\eta| + \epsilon\eta_0 + \Omega_2)\eta^{-2} + \cdots. \tag{2.19}$$

Nevertheless, the logarithmic terms in these expansions disappear provided Penrose's *asymptotic Einstein condition* (cf equation 9.6.21 of [33]),

$$\tilde{\nabla}_b\mathbf{d}_a\Omega \approx \tfrac{1}{4}\tilde{\mathbf{g}}_{ab}\tilde{\Box}\Omega, \tag{2.20}$$

is satisfied, cf equation (A.16).

3. Various null tetrads

We now wish to investigate the behaviour of fields near conformal infinity in standard general relativity in four dimensions ($n = 4$). For this purpose we introduce the normalized 'interpretation' tetrad which is parallelly transported along null geodesics $z(\eta)$ approaching $\mathcal{I}$. To achieve this we will employ several orthonormal and null tetrads which will be distinguished by specific labels in subscripts.

3.1. Tetrads and their transformations

We denote the vectors of an *orthonormal tetrad* as $\mathbf{t}$, $\mathbf{q}$, $\mathbf{r}$, $\mathbf{s}$, where $\mathbf{t}$ is a unit timelike vector, typically chosen to be future oriented, and the remaining three are spacelike unit vectors. With this tetrad we associate a *null tetrad* of null vectors $\mathbf{k}$, $\mathbf{l}$, $\mathbf{m}$, $\bar{\mathbf{m}}$, such that

$$\begin{aligned} \mathbf{k} &= \tfrac{1}{\sqrt{2}}(\mathbf{t}+\mathbf{q}), & \mathbf{l} &= \tfrac{1}{\sqrt{2}}(\mathbf{t}-\mathbf{q}), \\ \mathbf{m} &= \tfrac{1}{\sqrt{2}}(\mathbf{r}-\mathrm{i}\mathbf{s}), & \bar{\mathbf{m}} &= \tfrac{1}{\sqrt{2}}(\mathbf{r}+\mathrm{i}\mathbf{s}), \end{aligned} \tag{3.1}$$

where the only non-vanishing scalar products are

$$\mathbf{g}_{ab}\mathbf{k}^a\mathbf{l}^b = -1, \qquad \mathbf{g}_{ab}\mathbf{m}^a\bar{\mathbf{m}}^b = 1. \tag{3.2}$$

Similarly, we introduce a *conformal null tetrad* $\tilde{\mathbf{k}}, \tilde{\mathbf{l}}, \tilde{\mathbf{m}}, \bar{\tilde{\mathbf{m}}}$ in conformal spacetime $\tilde{\mathcal{M}}$ normalized by the conformal metric $\tilde{\mathbf{g}}$ as $\tilde{\mathbf{g}}_{ab}\tilde{\mathbf{k}}^a\tilde{\mathbf{l}}^b = -1$, $\tilde{\mathbf{g}}_{ab}\tilde{\mathbf{m}}^a\bar{\tilde{\mathbf{m}}}^b = 1$, which is associated with *conformal orthonormal tetrad* $\tilde{\mathbf{t}}$, $\tilde{\mathbf{q}}$, $\tilde{\mathbf{r}}$, $\tilde{\mathbf{s}}$.

Transformations between orthonormal tetrads (and corresponding null tetrads) form the Lorentz group. In the context of null tetrads it is convenient to consider four simple transformations from which any Lorentz transformation can be generated [12]: *null rotation with* $\mathbf{k}$ fixed, parametrized by $L \in \mathbb{C}$,

$$\mathbf{k} = \mathbf{k}_\mathrm{o}, \quad \mathbf{l} = \mathbf{l}_\mathrm{o} + \bar{L}\mathbf{m}_\mathrm{o} + L\bar{\mathbf{m}}_\mathrm{o} + L\bar{L}\mathbf{k}_\mathrm{o}, \qquad \mathbf{m} = \mathbf{m}_\mathrm{o} + L\mathbf{k}_\mathrm{o}, \tag{3.3}$$

null rotation with $\mathbf{l}$ *fixed*, given by $K \in \mathbb{C}$,

$$\mathbf{k} = \mathbf{k}_\mathrm{o} + \bar{K}\mathbf{m}_\mathrm{o} + K\bar{\mathbf{m}}_\mathrm{o} + K\bar{K}\mathbf{l}_\mathrm{o}, \quad \mathbf{l} = \mathbf{l}_\mathrm{o}, \quad \mathbf{m} = \mathbf{m}_\mathrm{o} + K\mathbf{l}_\mathrm{o}, \tag{3.4}$$

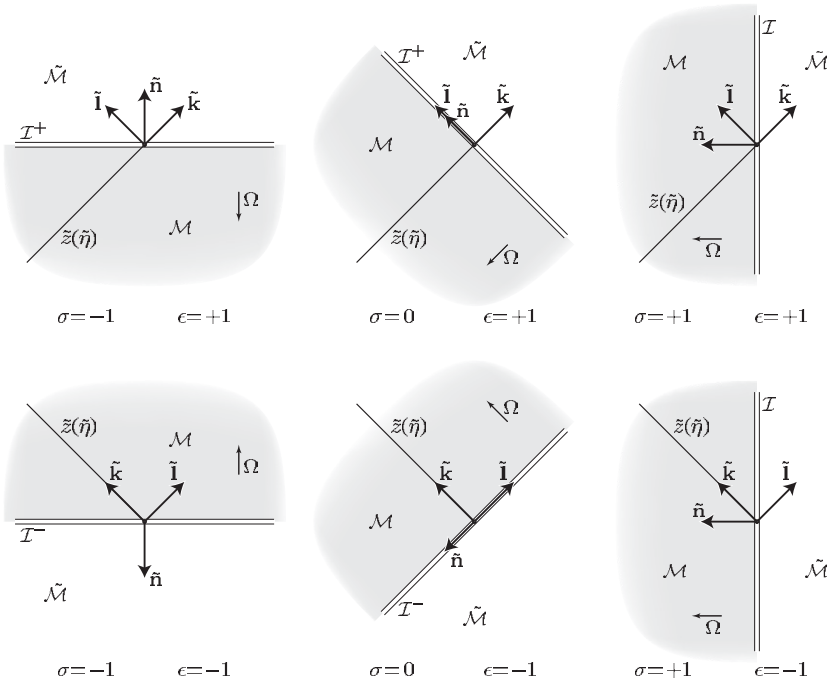

Figure 2. Tetrads adjusted to conformal infinity $\mathcal{I}$ of various characters, determined by σ, cf figure 1. If the vector $\tilde{\mathbf{k}}$ is oriented along the tangent vector of the null geodesic $\tilde{z}(\tilde{\eta})$ it is either outgoing ($\epsilon = +1$) or ingoing ($\epsilon = -1$).

boost in the **k**–**l** *plane*, $B \in \mathbb{R}$, and a *spatial rotation in the* **m**–$\bar{\mathbf{m}}$ *plane*, $\phi \in \mathbb{R}$,

$$\mathbf{k} = B\mathbf{k}_{\mathrm{o}}, \qquad \mathbf{l} = B^{-1}\mathbf{l}_{\mathrm{o}}, \qquad \mathbf{m} = \exp(\mathrm{i}\phi)\mathbf{m}_{\mathrm{o}}. \tag{3.5}$$

The transformations of the corresponding normalized spinor frames are listed in appendix B, relations (B.4)–(B.6).

3.2. The tetrad adjusted to $\mathcal{I}$

We say that a conformal null tetrad is *adjusted to conformal infinity* if the vectors $\tilde{\mathbf{k}}$ and $\tilde{\mathbf{l}}$ on $\mathcal{I}$ are coplanar with $\tilde{\mathbf{n}}$ (the vector (2.6) normal to conformal infinity), and satisfy the relation

$$\tilde{\mathbf{n}} = \epsilon\tfrac{1}{\sqrt{2}}(-\sigma\tilde{\mathbf{k}} + \tilde{\mathbf{l}}), \tag{3.6}$$

where $\epsilon = \pm 1$. As shown in figure 2, for a 'de Sitter type' spacelike infinity ($\sigma = -1$) there is $\tilde{\mathbf{n}} = \epsilon\tilde{\mathbf{t}} = \epsilon(\tilde{\mathbf{k}} + \tilde{\mathbf{l}})/\sqrt{2}$, for an 'anti-de Sitter type' timelike $\mathcal{I}$ ($\sigma = +1$) $\tilde{\mathbf{n}} = -\epsilon\tilde{\mathbf{q}} = -\epsilon(\tilde{\mathbf{k}} - \tilde{\mathbf{l}})/\sqrt{2}$, and $\tilde{\mathbf{n}} = \epsilon\tilde{\mathbf{l}}/\sqrt{2}$ for null 'Minkowskian' $\mathcal{I}$ ($\sigma = 0$). If the null vector $\tilde{\mathbf{k}}$ is chosen to be oriented along the tangent vector of the null geodesic $\tilde{z}(\tilde{\eta})$, the parameter ϵ then identifies whether the geodesic is outgoing ($\epsilon = +1$) or ingoing ($\epsilon = -1$), see (2.15). Note that the condition (3.6) also implies $\tilde{\mathbf{g}}_{ab}\tilde{\mathbf{m}}^a\tilde{\mathbf{n}}^b = 0 = \tilde{\mathbf{g}}_{ab}\bar{\tilde{\mathbf{m}}}^a\tilde{\mathbf{n}}^b$, so that the vectors $\tilde{\mathbf{m}}$, $\bar{\tilde{\mathbf{m}}}$ of the tetrad adjusted to conformal infinity are always *tangent to* $\mathcal{I}$.

Analogously we define a tetrad in the physical spacetime adjusted to conformal infinity by the condition

$$\mathbf{n} = \epsilon\tfrac{1}{\sqrt{2}}(-\sigma\mathbf{k} + \mathbf{l}), \tag{3.7}$$

where the vector **n** normal to $\mathcal{I}$ in $(\mathcal{M}, \mathbf{g})$ is normalized by (2.11) (cf discussion at the end of section 2.2).

3.3. The interpretation tetrad

Let us introduce an *interpretation* null tetrad $\mathbf{k}_{\mathrm{i}}, \mathbf{l}_{\mathrm{i}}, \mathbf{m}_{\mathrm{i}}, \bar{\mathbf{m}}_{\mathrm{i}}$. It is any tetrad which is *parallelly transported along a null geodesic* $z(\eta)$ *in the physical spacetime* $\mathcal{M}$, with $\mathbf{k}_{\mathrm{i}}$ tangent to $z(\eta)$. We thus require

$$\mathbf{k}_{\mathrm{i}} = \frac{\gamma}{\sqrt{2}\ell}\frac{\mathrm{D}z}{\mathrm{d}\eta}, \qquad \gamma = \text{constant}, \tag{3.8}$$

and

$$\mathbf{k}_{\mathrm{i}}^a \nabla_a \mathbf{k}_{\mathrm{i}}^b = 0, \qquad \mathbf{k}_{\mathrm{i}}^a \nabla_a \mathbf{l}_{\mathrm{i}}^b = 0, \qquad \mathbf{k}_{\mathrm{i}}^a \nabla_a \mathbf{m}_{\mathrm{i}}^b = 0, \qquad \mathbf{k}_{\mathrm{i}}^a \nabla_a \bar{\mathbf{m}}_{\mathrm{i}}^b = 0. \tag{3.9}$$

Here, ℓ is a constant scale parameter introduced below equation (2.10). For a geodesic the first equation in (3.9) is satisfied automatically. It only remains to investigate the remaining three conditions for parallel transport of the vectors $\mathbf{l}_{\mathrm{i}}$, $\mathbf{m}_{\mathrm{i}}$ and $\bar{\mathbf{m}}_{\mathrm{i}}$.

The interpretation tetrad is not unique—there is a freedom in its particular initial or final specification. It is possible to scale the vector $\mathbf{k}_{\mathrm{i}}$ by fixing the constant γ in (3.8). By such a choice we fix the 'physical wavelength' of the associated null ray. The initial scale of the vector $\mathbf{k}_{\mathrm{i}}$ can be fixed somewhere in the spacetime, e.g., with respect to a Killing vector or with respect to worldlines of sources, etc. Unfortunately, on a general level, we do not know how to specify privileged initial conditions for the interpretation tetrad. However, our goal here is to *compare* the field measured in interpretation tetrads transported along *different* null geodesics approaching the same point at $\mathcal{I}$. It is thus natural to choose the *final* conditions for tetrads in a 'comparable' way independently of the geodesics. Observing that the normalization of the tangent vector $\mathrm{D}z/\mathrm{d}\eta$ was chosen naturally with respect to the asymptotic structure of the spacetime by equations (2.13) and (2.14), we require that the vector $\mathbf{k}_{\mathrm{i}}$ is proportional to $\mathrm{D}z/\mathrm{d}\eta$ by the *same* factor. Namely, we require that the constant γ in (3.8) is independent of the choice of the geodesics. In the following we will set

$$\gamma = 1. \tag{3.10}$$

This is equivalent to the condition that the component of the vector $\mathbf{k}_{\mathrm{i}}$ normal to the conformal infinity is the same for *all* interpretation tetrads approaching a given point on $\mathcal{I}$, cf equation (3.16).

There is a remaining freedom in the choice of the interpretation tetrad which corresponds to a null rotation with $\mathbf{k}_{\mathrm{i}}$ fixed, and to a spatial $\mathbf{m}_{\mathrm{i}}$–$\bar{\mathbf{m}}_{\mathrm{i}}$ rotation. However, we will find that the asymptotic characterization of the field components derived in section 4.5 does not, in fact, depend on such freedom. To demonstrate this property, we now analyse an explicit relation between the interpretation tetrad and a conformal tetrad adjusted to $\mathcal{I}$.

3.4. Asymptotic behaviour of the interpretation tetrad

We consider a particular null tetrad $\tilde{\mathbf{k}}_{\mathrm{a}}, \tilde{\mathbf{l}}_{\mathrm{a}}, \tilde{\mathbf{m}}_{\mathrm{a}}, \bar{\tilde{\mathbf{m}}}_{\mathrm{a}}$, where $\tilde{\mathbf{k}}_{\mathrm{a}}$ is *tangent to a null geodesic* $\tilde{z}(\tilde{\eta})$,

$$\tilde{\mathbf{k}}_{\mathrm{a}} = \frac{1}{\sqrt{2}\ell}\frac{\mathrm{D}\tilde{z}}{\mathrm{d}\tilde{\eta}}, \tag{3.11}$$

$\tilde{\mathbf{l}}_{\mathrm{a}}$ is *coplanar* with $\tilde{\mathbf{k}}_{\mathrm{a}}$ and $\tilde{\mathbf{n}}$ on $\mathcal{I}$, and such that the vectors of the tetrad are *parallelly transported* along $\tilde{z}(\tilde{\eta})$ in conformal geometry,

$$\tilde{\mathbf{k}}_{\mathrm{a}}^a \tilde{\nabla}_a \tilde{\mathbf{k}}_{\mathrm{a}}^b = 0, \qquad \tilde{\mathbf{k}}_{\mathrm{a}}^a \tilde{\nabla}_a \tilde{\mathbf{l}}_{\mathrm{a}}^b = 0, \qquad \tilde{\mathbf{k}}_{\mathrm{a}}^a \tilde{\nabla}_a \tilde{\mathbf{m}}_{\mathrm{a}}^b = 0, \qquad \tilde{\mathbf{k}}_{\mathrm{a}}^a \tilde{\nabla}_a \bar{\tilde{\mathbf{m}}}_{\mathrm{a}}^b = 0. \tag{3.12}$$

Using expressions (3.11), (2.14), and (2.6) we immediately derive the relation $-\sigma\tilde{\mathbf{k}}_{\mathrm{a}} + \tilde{\mathbf{l}}_{\mathrm{a}} = \epsilon\sqrt{2}\tilde{\mathbf{n}}$ on conformal infinity, which demonstrates that the tetrad considered *becomes adjusted to* $\mathcal{I}$ for $\tilde{\eta} = 0$ at the point $\tilde{z}(0) = P \in \mathcal{I}$.

On the other hand, from (3.8), (3.11), (2.13) we obtain

$$\mathbf{k}_{\mathrm{i}} = \Omega^2\tilde{\mathbf{k}}_{\mathrm{a}}, \tag{3.13}$$

so that using (2.12), $\mathbf{g}_{ab}\mathbf{k}_{\mathrm{i}}^a\mathbf{n}^b = -\epsilon\frac{1}{\sqrt{2}}\Omega$. The interpretation tetrad is thus *not* adjusted to $\mathcal{I}$ since it does not satisfy equation (3.7).

To find an explicit relation between the tetrads $\mathbf{k}_{\mathrm{i}}, \mathbf{l}_{\mathrm{i}}, \mathbf{m}_{\mathrm{i}}, \bar{\mathbf{m}}_{\mathrm{i}}$ and $\tilde{\mathbf{k}}_{\mathrm{a}}, \tilde{\mathbf{l}}_{\mathrm{a}}, \tilde{\mathbf{m}}_{\mathrm{a}}, \bar{\tilde{\mathbf{m}}}_{\mathrm{a}}$, we first introduce an *auxiliary null tetrad* $\mathbf{k}_{\mathrm{a}}, \mathbf{l}_{\mathrm{a}}, \mathbf{m}_{\mathrm{a}}, \bar{\mathbf{m}}_{\mathrm{a}}$ by conformal rescaling of the tetrad $\tilde{\mathbf{k}}_{\mathrm{a}}, \tilde{\mathbf{l}}_{\mathrm{a}}, \tilde{\mathbf{m}}_{\mathrm{a}}, \bar{\tilde{\mathbf{m}}}_{\mathrm{a}}$,

$$\mathbf{k}_{\mathrm{a}} = \Omega\tilde{\mathbf{k}}_{\mathrm{a}}, \qquad \mathbf{l}_{\mathrm{a}} = \Omega\tilde{\mathbf{l}}_{\mathrm{a}}, \qquad \mathbf{m}_{\mathrm{a}} = \Omega\tilde{\mathbf{m}}_{\mathrm{a}}, \qquad \bar{\mathbf{m}}_{\mathrm{a}} = \Omega\bar{\tilde{\mathbf{m}}}_{\mathrm{a}}. \tag{3.14}$$

The auxiliary tetrad is normalized with respect to the physical metric $\mathbf{g}$, it is adjusted to $\mathcal{I}$ but its vectors are no longer parellelly transported along the geodesics $z(\eta)$ in $\mathcal{M}$.

Secondly, we perform a specific boost of the interpretation tetrad such that the boost parameter is given by the conformal factor, introducing thus the tetrad $\mathbf{k}_{\mathrm{b}}, \mathbf{l}_{\mathrm{b}}, \mathbf{m}_{\mathrm{b}}, \bar{\mathbf{m}}_{\mathrm{b}}$,

$$\mathbf{k}_{\mathrm{b}} = \Omega^{-1}\mathbf{k}_{\mathrm{i}}, \qquad \mathbf{l}_{\mathrm{b}} = \Omega\mathbf{l}_{\mathrm{i}}, \qquad \mathbf{m}_{\mathrm{b}} = \mathbf{m}_{\mathrm{i}}, \qquad \bar{\mathbf{m}}_{\mathrm{b}} = \bar{\mathbf{m}}_{\mathrm{i}}. \tag{3.15}$$

The vector $\mathbf{k}_{\mathrm{b}}$ is then normalized on $\mathcal{I}$ in the same way as $\mathbf{k}_{\mathrm{a}}$, namely

$$\mathbf{g}_{ab}\mathbf{k}_{\mathrm{b}}^a\mathbf{n}^b = -\epsilon\tfrac{1}{\sqrt{2}}. \tag{3.16}$$

Considering (3.13), the tetrad (3.15) has to be related to the auxiliary tetrad (3.14) by a null rotation with fixed $\mathbf{k}$ and a possible spatial rotation in the $\mathbf{m}$–$\bar{\mathbf{m}}$ plane,

$$\mathbf{k}_{\mathrm{b}} = \mathbf{k}_{\mathrm{a}}, \qquad \mathbf{l}_{\mathrm{b}} = \mathbf{l}_{\mathrm{a}} + \bar{\tilde{L}}\mathbf{m}_{\mathrm{a}} + \tilde{L}\bar{\mathbf{m}}_{\mathrm{a}} + \tilde{L}\bar{\tilde{L}}\mathbf{k}_{\mathrm{a}}, \qquad \mathbf{m}_{\mathrm{b}} = \exp(\mathrm{i}\phi)(\mathbf{m}_{\mathrm{a}} + \tilde{L}\mathbf{k}_{\mathrm{a}}), \tag{3.17}$$

with parameters $\tilde{L} \in \mathbb{C}$, $\phi \in \mathbb{R}$, cf (3.3), (3.5). For the interpretation tetrad it implies

$$\mathbf{k}_{\mathrm{i}} = \Omega\mathbf{k}_{\mathrm{a}}, \qquad \mathbf{l}_{\mathrm{i}} = \Omega^{-1}\mathbf{l}_{\mathrm{a}} + \bar{L}\mathbf{m}_{\mathrm{a}} + L\bar{\mathbf{m}}_{\mathrm{a}} + L\bar{L}\Omega\mathbf{k}_{\mathrm{a}}, \qquad \mathbf{m}_{\mathrm{i}} = \exp(\mathrm{i}\phi)(\mathbf{m}_{\mathrm{a}} + L\Omega\mathbf{k}_{\mathrm{a}}), \tag{3.18}$$

with $L = \Omega^{-1}\tilde{L}$. Now, substituting these expressions into the conditions (3.9) for parallel transport of the interpretation tetrad, and using (2.2), (3.12) and (3.13) we obtain

$$\tilde{\mathbf{k}}_{\mathrm{a}}^a\mathbf{d}_a\phi = 0, \qquad \tilde{\mathbf{k}}_{\mathrm{a}}^a\mathbf{d}_a L = \Omega^{-2}\tilde{\mathbf{m}}_{\mathrm{a}}^a\mathbf{d}_a\Omega. \tag{3.19}$$

The first equation implies $\phi = \phi_0 = \mathrm{const}$, see equation (3.11). Assuming again the regularity of conformal geometry near infinity, the term on the right-hand side of the second equation can be expanded in powers of $\tilde{\eta}$. Moreover, for $\tilde{\eta} = 0$ the vector $\tilde{\mathbf{m}}_{\mathrm{a}}$ is tangent to $\mathcal{I}$, see the text below equation (3.6), so that the expansion has the form

$$\sqrt{2}\ell\tilde{\mathbf{m}}_{\mathrm{a}}^a\mathbf{d}_a\Omega = M_1\tilde{\eta} + M_2\tilde{\eta}^2 + \cdots, \tag{3.20}$$

where M_1, M_2 are constants which depend on derivatives of Ω. Using (2.16) we thus integrate (3.19) to get

$$L = M_1\ln|\tilde{\eta}| + L_0 + \cdots, \qquad \text{i.e.,} \quad \tilde{L} = -\epsilon M_1\tilde{\eta}\ln|\tilde{\eta}| - \epsilon L_0\tilde{\eta} + \cdots, \tag{3.21}$$

where L_0 is a constant of integration. Using (2.18) we obtain the expansion in physical affine parameter η,

$$\begin{aligned}&\phi = \phi_0,\\ &L = -M_1\ln|\eta| + L_0 + \cdots, \qquad \text{i.e.,} \quad \tilde{L} = -\epsilon M_1\eta^{-1}\ln|\eta| + \epsilon L_0\eta^{-1} + \cdots.\end{aligned} \tag{3.22}$$

Calculations to the next order in the affine parameter are presented in appendix A.

We observe that $\tilde{L}$ *approaches zero near* $\mathcal{I}$. Inspecting relations (3.17) we thus obtain an important result: *the tetrad* $\mathbf{k}_b, \mathbf{l}_b, \mathbf{m}_b, \bar{\mathbf{m}}_b$, associated with *any interpretation tetrad* by the boost (3.15), *becomes asymptotically adjusted to conformal infinity* $\mathcal{I}$. Asymptotically it may differ from the chosen auxiliary tetrad $\mathbf{k}_a, \mathbf{l}_a, \mathbf{m}_a, \bar{\mathbf{m}}_a$ only by a trivial rotation in the $\mathbf{m}_a$–$\bar{\mathbf{m}}_a$ plane by a fixed angle ϕ_0, and in this sense it is 'essentially unique'.

Let us note that in general the vectors $\mathbf{k}_i, \mathbf{l}_i$ of the interpretation tetrad are not asymptotically coplanar with the normal $\mathbf{n}$ to $\mathcal{I}$. From equations (3.18) with L given by (3.21) we see that the vector $\mathbf{l}_i$ has components in the $\mathbf{m}_a$–$\bar{\mathbf{m}}_a$ directions which are perpendicular to $\mathbf{n}$. Fortunately, these components grow only logarithmically and, as we shall see later, they do not influence the leading term of the fields evaluated with respect to the interpretation tetrad. Moreover, it is demonstrated in appendix A (see equation (A.17)) that

$$M_1 \sim \left(\tilde{\eta}^{-1}\Phi^a_{01}\right)\big|_{\tilde{\eta}=0} \sim \left(\eta\Phi^a_{01}\right)\big|_{\eta=\epsilon\infty}, \tag{3.23}$$

where Φ^a_{01} is the specific component of the energy–momentum tensor evaluated in the auxiliary tetrad (3.14). This vanishes for a vacuum spacetime. It also disappears in non-vacuum cases when the asymptotic Einstein condition (2.20) holds—it is satisfied provided that matter fields decay faster then $\sim\tilde{\eta}$ near conformal infinity. For such spacetimes, the $\ln|\tilde{\eta}|$ term in expansion (3.21) of the parameter L near $\mathcal{I}$ is absent, so that

$$L \approx L_0, \qquad \text{i.e.,} \quad \tilde{L} \approx -\epsilon L_0\tilde{\eta}, \tag{3.24}$$

and, by the proper choice $L_0 = 0$, the vectors $\mathbf{k}_i, \mathbf{l}_i$ of the interpretation tetrad *can be arranged* to become asymptotically *coplanar* with the normal $\mathbf{n}$. This coplanarity was assumed previously in [33] (see discussion concerning figure 9-20 therein), and in [116, 117].

Let us also discuss the geometrical meaning of the integration constants L_0 and ϕ_0. In the above derivation we have represented the transformation (3.18) from the auxiliary tetrad to the interpretation tetrad as an application of null rotation with fixed $\mathbf{k}$ given by the parameter $\tilde{L} = \tilde{L}_* + \Omega L_0$ ($\tilde{L}_*$ independent of L_0, cf equation (3.21)), spatial rotation with the parameter $\phi = \phi_0$, and finally boost with the parameter $B = \Omega$. This can be rearranged as the sequence of $\mathbf{k}$-fixed null rotation given by the parameter $\tilde{L}_*$, boost with $B = \Omega$, then $\mathbf{k}$-fixed null rotation given by the parameter L_0, and finally spatial rotation with $\phi = \phi_0$. The last two transformations exactly correspond to the freedom in the choice of the interpretation tetrad—the condition (3.8) determines the interpretation tetrad exactly up to such null rotation with $\mathbf{k}$ fixed, and a spatial rotation in the $\mathbf{m}$–$\bar{\mathbf{m}}$ plane. The parameters L_0 and ϕ_0 thus determine a *specific choice* of the interpretation tetrad which is usually given by some physical prescription in a finite domain of the spacetime.

It will be demonstrated below that the *asymptotic directional behaviour of the fields* (see section 4.3) *is independent of the parameter* L_0. It will depend on the parameter ϕ_0 only through a *phase* of the complex component of the field, and such dependence can be eliminated by considering just the magnitude of the field. We will return to the corresponding question of the phase ('polarization') dependence of the fields in the discussion of the results.

3.5. The reference tetrad and parametrization of null directions

In the following, we will need to identify the direction $\mathbf{k}_i$ of the null geodesic and orientation of the associated interpretation tetrad near conformal infinity using suitable directional parameters. For this purpose we set up a reference tetrad. The *reference tetrad* $\mathbf{k}_o, \mathbf{l}_o, \mathbf{m}_o, \bar{\mathbf{m}}_o$ is any tetrad adjusted to $\mathcal{I}$ which satisfies the coplanarity and normalization condition (3.7),

$$\mathbf{n} = \epsilon_o \tfrac{1}{\sqrt{2}}(-\sigma\mathbf{k}_o + \mathbf{l}_o). \tag{3.25}$$

Otherwise, the reference tetrad can be chosen *arbitrarily*, ergo conveniently. It may thus either respect the symmetry of the spacetime (by adapting the reference tetrad to the Killing vectors) or its specific algebraic structure (in which case it can be oriented along the principal null directions). The parameter $\epsilon_o = \pm 1$ in (3.25) will be chosen in such a way that the vectors $\mathbf{k}_o$ and $\mathbf{l}_o$ are *future oriented*. For $\sigma = -1, 0$ this means that $\epsilon_o = +1$ on $\mathcal{I}^+$ and $\epsilon_o = -1$ on $\mathcal{I}^-$. For $\sigma = +1$ the parameter ϵ_o can be chosen either $+1$ or -1: it corresponds to $\mathbf{k}_o$ oriented outside or inside $\mathcal{M}$, cf figure 2.

We use the given reference tetrad $\mathbf{k}_o, \mathbf{l}_o, \mathbf{m}_o, \bar{\mathbf{m}}_o$ as a fixed basis with respect to which it is possible to define uniquely other directions, for example asymptotic directions along which various null geodesics approach a point P at $\mathcal{I}$, or the principal null directions, see section 4.2. It is natural to characterize such a general null direction $\mathbf{k}$ by a *complex parameter* R in the following way: the direction $\mathbf{k}$ is obtained (up to a rescaling) from $\mathbf{k}_o$ by the null rotation (3.4) with the parameter $K = R$,

$$\mathbf{k} \propto \mathbf{k}_o + \bar{R}\mathbf{m}_o + R\bar{\mathbf{m}}_o + R\bar{R}\mathbf{l}_o. \tag{3.26}$$

The value $R = \infty$ is also permitted—this corresponds to $\mathbf{k}$ being oriented along $\mathbf{l}_o$.

Let us mention that the reference tetrad introduced above is not well defined in conformal geometry—it is normalized using the physical metric. However, it could be rescaled *isotropically* by the *common* factor Ω^{-1} to obtain the associated *conformal reference tetrad* which is well defined in the conformal geometry. For convenience, in the following we will use the physically normalized reference tetrad instead of the conformally normalized one—see discussion at the end of section 2.2.

4. The fields and their asymptotic structure

Now we have all 'prerequisites' needed to analyse the asymptotic properties of the fields. We are mainly interested in gravitational and electromagnetic fields. However, the principal result—the asymptotic directional structure of the fields—can be derived for general fields of spin s. In all these cases we will study the dominant (radiative) component of the field as one approaches conformal infinity. For this purpose, it is useful to parametrize the fields using complex tetrad components which have special transformation properties.

4.1. The field components and their transformation properties

Following the notation of [12], gravitational field is characterized by the Weyl tensor $\mathbf{C}_{abcd}$ and can be parametrized by five complex coefficients

$$\begin{aligned}
\Psi_0 &= \mathbf{C}_{abcd}\mathbf{k}^a\mathbf{m}^b\mathbf{k}^c\mathbf{m}^d,\\
\Psi_1 &= \mathbf{C}_{abcd}\mathbf{k}^a\mathbf{l}^b\mathbf{k}^c\mathbf{m}^d,\\
\Psi_2 &= \mathbf{C}_{abcd}\mathbf{k}^a\mathbf{m}^b\bar{\mathbf{m}}^c\mathbf{l}^d,\\
\Psi_3 &= \mathbf{C}_{abcd}\mathbf{l}^a\mathbf{k}^b\mathbf{l}^c\bar{\mathbf{m}}^d,\\
\Psi_4 &= \mathbf{C}_{abcd}\mathbf{l}^a\bar{\mathbf{m}}^b\mathbf{l}^c\bar{\mathbf{m}}^d,
\end{aligned} \tag{4.1}$$

whereas electromagnetic field is described by the tensor $\mathbf{F}_{ab}$ which is parametrized by three complex coefficients

$$\begin{aligned}
\Phi_0 &= \mathbf{F}_{ab}\mathbf{k}^a\mathbf{m}^b,\\
\Phi_1 &= \tfrac{1}{2}\mathbf{F}_{ab}(\mathbf{k}^a\mathbf{l}^b - \mathbf{m}^a\bar{\mathbf{m}}^b),\\
\Phi_2 &= \mathbf{F}_{ab}\bar{\mathbf{m}}^a\mathbf{l}^b.
\end{aligned} \tag{4.2}$$

By a field of spin s we understand field which transforms according to spin-s representation of the Lorentz group. It can be characterized by $(2s + 1)$ complex components

$$\Upsilon_j, \qquad j = 0, 1, \ldots, 2s. \tag{4.3}$$

A more detailed (spinor) description of such fields can be found in appendix B. The gravitational field Ψ_j or electromagnetic field Φ_j are special cases of (4.3) for $s = 2, 1$, cf (B.8)–(B.10).

These field components transform in a well-known way under special Lorentz transformations introduced above (see, e.g., [12] or appendix B). For a null rotation with $\mathbf{k}$ fixed, cf equation (3.3), the field transforms as

$$\Upsilon_j = \Upsilon_j^{\mathrm{o}} + j\bar{L}\Upsilon_{j-1}^{\mathrm{o}} + \binom{j}{2}\bar{L}^2\Upsilon_{j-2}^{\mathrm{o}} + \binom{j}{3}\bar{L}^3\Upsilon_{j-3}^{\mathrm{o}} + \cdots + \bar{L}^j\Upsilon_0^{\mathrm{o}}. \tag{4.4}$$

Under a null rotation with $\mathbf{l}$ fixed, see equation (3.4), the transformation reads

$$\Upsilon_j = \Upsilon_j^{\mathrm{o}} + (2s - j)K\Upsilon_{j+1}^{\mathrm{o}} + \binom{2s-j}{2}K^2\Upsilon_{j+2}^{\mathrm{o}} + \cdots + K^{2s-j}\Upsilon_{2s}^{\mathrm{o}}. \tag{4.5}$$

Under a boost in the $\mathbf{k}$–$\mathbf{l}$ plane, and a spatial rotation in the $\mathbf{m}$–$\bar{\mathbf{m}}$ plane, given by equation (3.5), the components Υ_j transform as

$$\Upsilon_j = B^{s-j}\exp(\mathrm{i}(s - j)\phi)\Upsilon_j^{\mathrm{o}}. \tag{4.6}$$

4.2. Principal null directions and algebraic classification

For gravitational, electromagnetic or any spin-s field there exist *principal null directions* (PNDs) which are privileged null directions $\mathbf{k}$ such that $\Upsilon_0 = 0$ in a null tetrad $\mathbf{k}, \mathbf{l}, \mathbf{m}, \bar{\mathbf{m}}$ (a choice of $\mathbf{l}, \mathbf{m}, \bar{\mathbf{m}}$ is irrelevant). The PND $\mathbf{k}$ can be obtained from a reference tetrad $\mathbf{k}_{\mathrm{o}}, \mathbf{l}_{\mathrm{o}}, \mathbf{m}_{\mathrm{o}}, \bar{\mathbf{m}}_{\mathrm{o}}$ by a null rotation (3.26) given by a directional parameter $R \in \mathbb{C}$. We choose the remaining vectors $\mathbf{l}, \mathbf{m}, \bar{\mathbf{m}}$ to be given by the same null rotation, i.e., by (3.4) with $K = R$. The condition $\Upsilon_0 = 0$ thus takes the form of an algebraic equation of the order $2s$ for the directional parameter R, see equation (4.5),

$$R^{2s}\Upsilon_{2s}^{\mathrm{o}} + \binom{2s}{2s-1}R^{2s-1}\Upsilon_{2s-1}^{\mathrm{o}} + \cdots + \binom{2s}{1}R\Upsilon_1^{\mathrm{o}} + \Upsilon_0^{\mathrm{o}} = 0. \tag{4.7}$$

In particular, for gravitational field it reduces to a quartic

$$R^4\Psi_4^{\mathrm{o}} + 4R^3\Psi_3^{\mathrm{o}} + 6R^2\Psi_2^{\mathrm{o}} + 4R\Psi_1^{\mathrm{o}} + \Psi_0^{\mathrm{o}} = 0. \tag{4.8}$$

The complex roots R_n, $n = 1, 2, \ldots, 2s$, of equation (4.7) parametrize PNDs $\mathbf{k}_n$ with respect to the reference tetrad $\mathbf{k}_{\mathrm{o}}, \mathbf{l}_{\mathrm{o}}, \mathbf{m}_{\mathrm{o}}, \bar{\mathbf{m}}_{\mathrm{o}}$. The situation when $\Upsilon_{2s}^{\mathrm{o}} = 0$ formally corresponds to an infinite value of one of the roots, say $R_1 = \infty$, in which case $\mathbf{k}_1 = \mathbf{l}_{\mathrm{o}}$. There are four principal null directions for gravitational field, two for electromagnetic field, and $2s$ for spin-s field. According to whether some of these PNDs coincide, the fields are algebraically special and can be classified into various (Petrov) algebraic types [12, 33, 44].

In a generic situation $\Upsilon_{2s}^{\mathrm{o}}$ is non-vanishing and the polynomial on the left-hand side of equation (4.7) can be decomposed as

$$\begin{aligned} R^{2s}\Upsilon_{2s}^{\mathrm{o}} + \binom{2s}{1}R^{2s-1}\Upsilon_{2s-1}^{\mathrm{o}} + \cdots + \binom{2s}{2s-1}R\Upsilon_1^{\mathrm{o}} + \Upsilon_0^{\mathrm{o}} \\ = \Upsilon_{2s}^{\mathrm{o}}(R - R_1)(R - R_2)\cdots(R - R_{2s}). \end{aligned} \tag{4.9}$$

By comparing the coefficients of various powers of R it is possible to express all Υ^{o}_j components in terms of $\Upsilon^{\mathrm{o}}_{2s}$ and the algebraically privileged principal null directions characterized by R_n. For example, the components of gravitational field can be written

$$\begin{aligned}
\Psi^{\mathrm{o}}_3 &= -\tfrac{1}{4}\Psi^{\mathrm{o}}_4(R_1+R_2+R_3+R_4),\\
\Psi^{\mathrm{o}}_2 &= \tfrac{1}{6}\Psi^{\mathrm{o}}_4(R_1R_2+R_1R_3+R_1R_4+R_2R_3+R_2R_4+R_3R_4),\\
\Psi^{\mathrm{o}}_1 &= -\tfrac{1}{4}\Psi^{\mathrm{o}}_4(R_1R_2R_3+R_1R_2R_4+R_1R_3R_4+R_2R_3R_4),\\
\Psi^{\mathrm{o}}_0 &= \Psi^{\mathrm{o}}_4 R_1R_2R_3R_4.
\end{aligned} \tag{4.10}$$

Similar expressions apply to other fields; we write only the expression for the Υ^{o}_0 component,

$$\Upsilon^{\mathrm{o}}_0 = (-1)^{2s}\Upsilon^{\mathrm{o}}_{2s}\prod_{j=1}^{2s} R_j. \tag{4.11}$$

Finally, let us note that a rescaling of all field components by a common factor does not change the algebraic structure, i.e., the PNDs remain unchanged. This observation is useful when we study the algebraic structure of the fields near conformal infinity. As we will discuss in section 4.4, the field components Υ^{o}_j decay to zero near conformal infinity, see equation (4.18). However, the leading term of the field still carries information about its algebraic structure. In other words, asymptotically we define PNDs in terms of the leading order of the field.

4.3. Field components in the interpretation tetrad

Using the above quantities and relations we may now analyse the asymptotic behaviour of a general gravitational, electromagnetic or any spin-s field with respect to the interpretation tetrad near conformal infinity. To evaluate the field components Υ^{i}_j in the interpretation tetrad $\mathbf{k}_{\mathrm{i}}, \mathbf{l}_{\mathrm{i}}, \mathbf{m}_{\mathrm{i}}, \bar{\mathbf{m}}_{\mathrm{i}}$ we employ its relation to the tetrad $\mathbf{k}_{\mathrm{b}}, \mathbf{l}_{\mathrm{b}}, \mathbf{m}_{\mathrm{b}}, \bar{\mathbf{m}}_{\mathrm{b}}$ which is asymptotically adjusted to $\mathcal{I}$, then the relation between this tetrad and the auxiliary tetrad $\mathbf{k}_{\mathrm{a}}, \mathbf{l}_{\mathrm{a}}, \mathbf{m}_{\mathrm{a}}, \bar{\mathbf{m}}_{\mathrm{a}}$, and finally we perform the transformation to the reference tetrad $\mathbf{k}_{\mathrm{o}}, \mathbf{l}_{\mathrm{o}}, \mathbf{m}_{\mathrm{o}}, \bar{\mathbf{m}}_{\mathrm{o}}$. We thus express Υ^{i}_j in terms of Υ^{o}_j.

The tetrads $\mathbf{k}_{\mathrm{i}}, \mathbf{l}_{\mathrm{i}}, \mathbf{m}_{\mathrm{i}}, \bar{\mathbf{m}}_{\mathrm{i}}$ and $\mathbf{k}_{\mathrm{b}}, \mathbf{l}_{\mathrm{b}}, \mathbf{m}_{\mathrm{b}}, \bar{\mathbf{m}}_{\mathrm{b}}$ are related by the boost (3.15), i.e., $\mathbf{k}_{\mathrm{i}} = \Omega\mathbf{k}_{\mathrm{b}}, \mathbf{l}_{\mathrm{i}} = \Omega^{-1}\mathbf{l}_{\mathrm{b}}$, where $\Omega = B \approx \epsilon\eta^{-1}$, see equation (2.19). The next transformation to the auxiliary tetrad is given by the $\mathbf{l}$-fixed null rotation and spatial rotation (3.17), with the parameters $\tilde{L}$ and ϕ given by (3.22). As we have already demonstrated above, with $\phi_0 = 0$ these two tetrads asymptotically coincide. Using (4.6) and (4.4) we thus obtain

$$\Upsilon^{\mathrm{i}}_j \approx (\epsilon\eta)^{j-s}\exp(\mathrm{i}(s-j)\phi_0)\Upsilon^{\mathrm{a}}_j. \tag{4.12}$$

We observe that the field components are asymptotically independent of the parameter L_0 and they depend on the parameter ϕ_0 only through the phase. Because these parameters L_0 and ϕ_0 specify the choice of the interpretation tetrad, we have thus explicitly demonstrated that the *magnitude of the leading term of field components is independent of a particular choice of the interpretation tetrad*.

The specific phase behaviour of Υ^{i}_j under spatial rotations indicates that different field components have different polarization properties. The polarization can carry important physical data. However, to retrieve such information it would be necessary to fix the initial conditions for the interpretation tetrad somewhere in a finite domain of the physical spacetime. In the general situation which we study here, we are not able to fix the interpretation tetrad in such a complete way, and thus the polarization information contained in the phase of the field components is not accessible. Therefore, in the following we will concentrate on the magnitude of the field components, and for simplicity we choose $\phi_0 = 0$.

Considering that all Υ^{a}_j for $j = 0, 1, \ldots, 2s$ are of the same order, cf equation (4.18), the expression (4.12) demonstrates the well-known *peeling-off property* of the fields according to which various tetrad components are proportional to different powers of the affine parameter η as one approaches conformal infinity along a null geodesic. The *dominant component* is $j = 2s$. Such a term $\Upsilon^{\mathrm{i}}_{2s}$ represents the radiative part of the field. In particular, the dominant component of the gravitational field is characterized by $\Psi^{\mathrm{i}}_4 \approx \eta^2 \Psi^{\mathrm{a}}_4$, the electromagnetic field by $\Phi^{\mathrm{i}}_2 \approx \epsilon\eta\Phi^{\mathrm{a}}_4$, etc.

Finally, we express $\Upsilon^{\mathrm{a}}_{2s}$ in terms of components Υ^{o}_j. Both the reference and the auxiliary tetrads are adjusted to $\mathcal{I}$ and thus they only differ by a transformation which leaves the normal vector $\mathbf{n}$ fixed. Such a transformation can be obtained, e.g., by the null rotation (3.3) of the reference tetrad, followed by the null rotation (3.4), and the boost (3.5) with the parameters

$$L = \sigma R, \qquad K = \frac{R}{1 - \sigma R\bar{R}}, \qquad B = \epsilon\epsilon_{\mathrm{o}}(1 - \sigma R\bar{R}). \tag{4.13}$$

(For a general transformation between two tetrads adjusted to $\mathcal{I}$ we should also admit a spatial rotation but this only changes a phase of the field components which was discussed above.) It has an explicit form

$$\begin{aligned}
\mathbf{k}_{\mathrm{a}} &= \frac{\epsilon\epsilon_{\mathrm{o}}}{1 - \sigma R\bar{R}}(\mathbf{k}_{\mathrm{o}} + \bar{R}\mathbf{m}_{\mathrm{o}} + R\bar{\mathbf{m}}_{\mathrm{o}} + R\bar{R}\mathbf{l}_{\mathrm{o}}),\\
\mathbf{l}_{\mathrm{a}} &= \frac{\epsilon\epsilon_{\mathrm{o}}}{1 - \sigma R\bar{R}}(\sigma^2 R\bar{R}\mathbf{k}_{\mathrm{o}} + \sigma\bar{R}\mathbf{m}_{\mathrm{o}} + \sigma R\bar{\mathbf{m}}_{\mathrm{o}} + \mathbf{l}_{\mathrm{o}}),\\
\mathbf{m}_{\mathrm{a}} &= \frac{1}{1 - \sigma R\bar{R}}(\sigma R\mathbf{k}_{\mathrm{o}} + \mathbf{m}_{\mathrm{o}} + \sigma R^2\bar{\mathbf{m}}_{\mathrm{o}} + R\mathbf{l}_{\mathrm{o}}).
\end{aligned} \tag{4.14}$$

Using (3.14) and (3.25) we easily check that $\epsilon\frac{1}{\sqrt{2}}(-\sigma\tilde{\mathbf{k}}_{\mathrm{a}} + \tilde{\mathbf{l}}_{\mathrm{a}}) = \tilde{\mathbf{n}}$, which is the condition (3.6). Moreover, the vector $\mathbf{k}_{\mathrm{a}}$ satisfies (3.26), and represents the direction along which the null geodesic approaches conformal infinity: this direction is characterized by the complex directional parameter R.

It only remains to perform the transformation of the leading field component corresponding to (4.13). Using (4.4)–(4.6) we obtain

$$\Upsilon^{\mathrm{a}}_{2s} = B^{-s}\bar{L}^{2s}\left[\bar{L}^{-2s}\Upsilon^{\mathrm{o}}_{2s} + \binom{2s}{1}\bar{L}^{-2s+1}\Upsilon^{\mathrm{o}}_{2s-1} + \binom{2s}{2}\bar{L}^{-2s+2}\Upsilon^{\mathrm{o}}_{2s-2} + \cdots + \Upsilon^{\mathrm{o}}_0\right]. \tag{4.15}$$

Applying now the identity (4.9), the expression in the bracket can be written as $\Upsilon^{\mathrm{o}}_{2s}(\bar{L}^{-1} - R_1)(\bar{L}^{-1} - R_2)\cdots(\bar{L}^{-1} - R_{2s})$, so that

$$\Upsilon^{\mathrm{a}}_{2s} = \Upsilon^{\mathrm{o}}_{2s}B^{-s}(1 - R_1\bar{L})(1 - R_2\bar{L})\cdots(1 - R_{2s}\bar{L}). \tag{4.16}$$

Using (4.12), (4.13) we thus obtain explicitly

$$\Upsilon^{\mathrm{i}}_{2s} \approx \Upsilon^{\mathrm{o}}_{2s}\left(\frac{\epsilon_{\mathrm{o}}\eta}{1 - \sigma R\bar{R}}\right)^s (1 - \sigma R_1\bar{R})(1 - \sigma R_2\bar{R})\cdots(1 - \sigma R_{2s}\bar{R}). \tag{4.17}$$

4.4. Asymptotic behaviour of the field components in the reference tetrad

For a complete analysis of radiation it is important to identify the specific 'fall-off' of the field. The correct asymptotic behaviour can only be obtained by a detailed study of the field equations. There exists a wide spectrum of various results concerning this topic in the literature. As mentioned in the introduction, the decay behaviour of the fields is well understood in asymptotically flat spacetimes and there are some important results also in the case of a non-vanishing cosmological constant.

However, our goal in this work is to study the *directional dependence* of the leading term of the fields, not its *decay behaviour*. We will thus only assume the fall-off typical for *zero-rest-mass fields*, without engaging in a study of the field equations. Motivated by discussion of behaviour of fields with a consistent field equation ($s \leqslant 2$) in asymptotically flat spacetimes ([29, 33] or, e.g., [51, 62] for a gravitational field), we will assume

$$\Upsilon^{\mathrm{o}}_{j} \approx \frac{\Upsilon^{\mathrm{o}}_{j*}}{\eta^{s+1}}, \qquad \Upsilon^{\mathrm{o}}_{j*} = \text{constant}. \tag{4.18}$$

For gravitational and electromagnetic fields this means that $\Psi^{\mathrm{o}}_{j} \approx \Psi^{\mathrm{o}}_{j*}\eta^{-3}$, $\Phi^{\mathrm{o}}_{j} \approx \Phi^{\mathrm{o}}_{j*}\eta^{-2}$. Recalling the behaviour (2.19) of the conformal factor and the fact that the tensor of an electromagnetic field and the Weyl tensor are conformally invariant, $\tilde{\mathbf{F}}_{ab} = \mathbf{F}_{ab}$, $\tilde{\mathbf{C}}_{abc}{}^{d} = \mathbf{C}_{abc}{}^{d}$, the fall-off (4.18) follows from the condition that the conformal quantities $\tilde{\mathbf{F}}_{ab}$ and $\mathbf{d}_{abc}{}^{d} = \Omega^{-1}\tilde{\mathbf{C}}_{abc}{}^{d}$ are regular at infinity. For $\Lambda \neq 0$ such behaviour of a gravitational field can be obtained rigorously, see, e.g., [36, 51], and it is plausible also for asymptotically flat spacetimes. Inspired by these observations, in the following we will assume the behaviour (4.18) in a general situation.

Of course, some of the field components may decay faster even if the fall-off (4.18) is valid for a generic component. This happens when the reference tetrad is aligned along PNDs, as we will discuss in the next section. If at least one of the field components $\Upsilon^{\mathrm{o}}_{j}$ falls off as in (4.18) (i.e., at least one $\Upsilon^{\mathrm{o}}_{j*}$ is non-vanishing) it is always possible to change the reference tetrad in such a way that all $\Upsilon^{\mathrm{o}}_{j*} \neq 0$. When all field components $\Upsilon^{\mathrm{o}}_{j}$ decay faster than (4.18) we call such a field asymptotically of type 0, i.e., the field with a trivial algebraic structure.

Let us however emphasize again that the assumption (4.18) *is not crucial* for the asymptotic directional structure of the field. It influences the decay of the field, not its directional dependence. Because we are mainly interested in the analysis of the directional structure we will not study the behaviour (4.18) in more detail.

4.5. Asymptotic directional structure of radiation

Substituting (4.18) into equation (4.17) we finally obtain

$$\Upsilon^{\mathrm{i}}_{2s} \approx \frac{1}{\eta}\epsilon^{s}_{\mathrm{o}}\Upsilon^{\mathrm{o}}_{2s*}\frac{(1-\sigma R_1\bar{R})(1-\sigma R_2\bar{R})\cdots(1-\sigma R_{2s}\bar{R})}{(1-\sigma R\bar{R})^{s}}. \tag{4.19}$$

This expression fully characterizes the asymptotic behaviour on $\mathcal{I}$ of the dominant component of any massless field of spin s in the normalized interpretation tetrad $\mathbf{k}_{\mathrm{i}}$, $\mathbf{l}_{\mathrm{i}}$, $\mathbf{m}_{\mathrm{i}}$, $\bar{\mathbf{m}}_{\mathrm{i}}$ which is parallelly propagated along a null geodesic $z(\eta)$. Due to the remaining freedom corresponding to a spatial rotation (3.5) in the transverse $\mathbf{m}_{\mathrm{i}}$–$\bar{\mathbf{m}}_{\mathrm{i}}$ plane, only the modulus $\left|\Upsilon^{\mathrm{i}}_{2s}\right|$ has an invariant meaning, the phase of $\Upsilon^{\mathrm{i}}_{2s}$ describes a polarization. The field decays as η^{-1}, where η is the affine parameter, so we call expression (4.19) the *radiative part of the field*.

The complex parameter R represents the *direction* of the null geodesic along which a given point $P \in \mathcal{I}$ of conformal infinity is approached as $\eta \to \epsilon\infty$. Let us recall that the constants R_n characterize the *principal null directions*, i.e. the algebraic structure of the field at P. The directional structure of radiation is thus completely determined by the algebraic (Petrov) type of the field. However, the dependence of $\Upsilon^{\mathrm{i}}_{2s}$ on the direction R along which $P \in \mathcal{I}$ is approached occurs only if $\sigma \neq 0$, i.e., at a 'de Sitter-like' or 'anti-de Sitter-like' conformal infinity. For $\mathcal{I}$ of 'Minkowskian' type which has a null character, $\sigma = 0$, this directional dependence completely vanishes.

The directional pattern of radiation (4.19) has been derived assuming that the field component $\Upsilon^{\mathrm{o}}_{2s}$ is non-vanishing, cf (4.9). More precisely, we assume that this component does not vanish asymptotically faster than a typical field component, namely that $\Upsilon^{\mathrm{o}}_{2s*} \neq 0$,

see (4.18). The vanishing coefficient $\Upsilon^{\mathrm{o}}_{2s*}$ indicates that the reference tetrad is asymptotically aligned along some PND. Indeed, considering the fact that by interchanging $\mathbf{k}_{\mathrm{o}}$ with $\mathbf{l}_{\mathrm{o}}$ the component $\Upsilon^{\mathrm{o}}_{0}$ goes to $\bar{\Upsilon}^{\mathrm{o}}_{2s}$, the condition $\Upsilon^{\mathrm{o}}_{2s*} = 0$ implies that the vector $\mathbf{l}_{\mathrm{o}}$ of the reference tetrad is the PND, say $\mathbf{k}_1$. In terms of the directional parameter this means that $R_1 = \infty$. In such a case we have to use a different normalization factor to express the field components. With the help of relation (4.11), for $\Upsilon^{\mathrm{o}}_{0} \neq 0$ we can write

$$\Upsilon^{\mathrm{i}}_{2s} \approx \frac{1}{\eta}\epsilon^{s}_{\mathrm{o}}\Upsilon^{\mathrm{o}}_{0*}\frac{\left(\sigma\bar{R} - R_1^{-1}\right)\left(\sigma\bar{R} - R_2^{-1}\right)\cdots\left(\sigma\bar{R} - R_{2s}^{-1}\right)}{(1-\sigma R\bar{R})^{s}}. \tag{4.20}$$

This expression describes the same directional dependence as expression (4.19), it is only normalized using a different field component.

Expression (4.19) is useful if $\Upsilon^{\mathrm{o}}_{2s*} \neq 0$, expression (4.20) is applicable when $\Upsilon^{\mathrm{o}}_{0*} \neq 0$. In situations when $\Upsilon^{\mathrm{o}}_{0*} = \Upsilon^{\mathrm{o}}_{2s*} = 0$, so that *both* the vectors $\mathbf{k}_{\mathrm{o}}$ and $\mathbf{l}_{\mathrm{o}}$ are PNDs, another non-vanishing component $\Upsilon^{\mathrm{o}}_{j*}$ has to be used for the normalization. A particular example of normalization using a different field component for the gravitational Petrov type D field will be discussed in section 5.4, see equation (5.23).

5. Discussion of the directional structure of radiation on $\mathcal{I}$

In this section we will discuss the general expression (4.19) for different values of $\sigma = -\mathrm{sign}\,\Lambda$ in detail. For practical purposes, we will restrict the description to gravitational and electromagnetic fields; general spin-s field will be mentioned only for maximally degenerate field of algebraic type N.

5.1. Radiation on null $\mathcal{I}$

For 'Minkowskian' conformal infinity we have $\sigma = 0$, $\mathbf{l}_{\mathrm{o}} \propto \mathbf{n}$, and the field thus has *no directional structure*. In such a case the radiative parts of the gravitational and electromagnetic fields (4.19) are uniquely given by

$$\left|\Psi^{\mathrm{i}}_{4}\right| \approx \frac{\left|\Psi^{\mathrm{o}}_{4*}\right|}{|\eta|}, \qquad \left|\Phi^{\mathrm{i}}_{2}\right| \approx \frac{\left|\Phi^{\mathrm{o}}_{2*}\right|}{|\eta|}, \tag{5.1}$$

i.e., they are *the same for all null geodesics approaching a given point $P \in \mathcal{I}$*. For (locally) asymptotically flat spacetimes it is thus possible to distinguish between the radiative and non-radiative fields. Radiation is absent at those points of null conformal infinity where the constants Ψ^{o}_{4*} or Φ^{o}_{2*} vanish. As we discussed, this occurs when *the principal null direction is oriented along the vector* $\mathbf{l}_{\mathrm{o}} \propto \mathbf{n}$. This can be viewed as an invariant characterization of the absence of radiation near $\mathcal{I}$.

In section 4.5 we suggested that for $\Psi^{\mathrm{o}}_{4*} = 0$ we should use the alternative form of the directional pattern of radiation (4.20). However, in the case $\sigma = 0$ it reduces to

$$\left|\Psi^{\mathrm{i}}_{4}\right| \approx \frac{\left|\Psi^{\mathrm{o}}_{0*}\right|}{|\eta|}\,|R_1R_2R_3R_4|^{-1} \tag{5.2}$$

with one of the R_n infinite. We thus again obtain $\Psi^{\mathrm{i}}_{4} = 0$ in the order η^{-1}.

5.2. On the meaning of the peeling-off behaviour

Let us give here some general comments concerning the character of the fields near infinity which apply also to spacelike and timelike $\mathcal{I}$. Because for the Minkowskian infinity the leading term of the field is independent of the direction along which the infinity is approached,

one tends to attribute the invariant meaning to the components of the field with respect to the interpretation tetrad, say, to the components Ψ^{i}_j of the gravitational field. The peeling-off behaviour $\Psi^{\mathrm{i}}_j \sim \eta^{j-5}$ could thus be rephrased that the Weyl tensor becomes asymptotically of type N—only the component Ψ^{i}_4 'survives' when one is approaching infinity. However, as pointed out in [33], such an interpretation can be misleading. The peeling-off property is a consequence of a delicate interplay between the decay behaviour (4.18) of the field and of the different asymptotic scaling of the vectors of the interpretation tetrad. Consequently, the asymptotic type N characterization of the Weyl tensor *is not invariant*—the Weyl tensor of type N should have one quadruply degenerate PND which should coincide with the vector $\mathbf{k}_{\mathrm{i}}$ of the interpretation tetrad, i.e., with the vector tangent to the geodesic along which the infinity is approached. But this vector obviously depends on our choice and cannot thus be an invariant characterization of the Weyl tensor.

The invariant asymptotic algebraic characterization of the field (asymptotic PNDs of the field) can be obtained by the conformal technique. As discussed already in section 4.2, PNDs do not depend on isotropic rescaling of the field and they can thus be defined using the leading term of the field tensor, i.e., using the field components with respect to the reference tetrad (or any other tetrad) which is related by an *isotropic* rescaling to a tetrad well defined in the sense of the conformal manifold $\tilde{\mathcal{M}}$. Defining PNDs in this way, the field can be of a *general* type up to infinity. The PNDs defined at infinity can be used to define canonical reference tetrads as will be done in sections 5.4 and 5.5. For example, the C-metric spacetime is of Petrov type D everywhere, including at infinity, and its double degenerate PNDs at $\mathcal{I}$ have been used to define the reference tetrad in [102].

Because the interpretation tetrad is *not* of the type described above (the vectors $\mathbf{k}_{\mathrm{i}}$ and $\mathbf{l}_{\mathrm{i}}$ scale differently with respect to the conformal manifold), the field components in this tetrad can exhibit apparent degeneracy typical for type N fields.

As we have found, the asymptotic algebraic structure of the field allows us to give a clear unambiguous characterization of the field near Minkowskian (null) infinity. The leading radiative term (along any null geodesic approaching $\mathcal{I}$) disappears if a PND is tangent to infinity. For spacelike and timelike infinities the leading term depends on a direction along which $\mathcal{I}$ is approached, and it is absent only along some specific directions, given again by the orientation of PNDs as described in detail in the following sections.

The invariant characterization of the absence of radiation using PNDs raises a question of the relation between the algebraic structure of fields (orientation of PNDs on $\mathcal{I}$) and the structure of sources. For example, in the case of two accelerated black holes (the C-metric) the two (double degenerate) PNDs play the role of 'radial' directions from the holes, cf [102, 109]. It would be interesting to discover a similar relation between PNDs and sources in a more general situation. We will analyse this question in another work.

5.3. Parametrization of directions by (pseudo-)spherical angles

In order to characterize more lucidly the directions on spacelike or timelike $\mathcal{I}$, it is convenient to express the complex directional parameter R in terms of (pseudo-)spherical parameters.

At any point $P \in \mathcal{I}$ we have a reference null tetrad $\mathbf{k}_{\mathrm{o}}, \mathbf{l}_{\mathrm{o}}, \mathbf{m}_{\mathrm{o}}, \bar{\mathbf{m}}_{\mathrm{o}}$ which is adjusted to conformal infinity. Such a tetrad is associated with an orthonormal adjusted tetrad $\mathbf{t}_{\mathrm{o}}, \mathbf{q}_{\mathrm{o}}, \mathbf{r}_{\mathrm{o}}, \mathbf{s}_{\mathrm{o}}$, where $\mathbf{t}_{\mathrm{o}}$ is a unit timelike vector and $\mathbf{q}_{\mathrm{o}}, \mathbf{r}_{\mathrm{o}}, \mathbf{s}_{\mathrm{o}}$ are perpendicular spacelike unit vectors,

$$\begin{aligned} \mathbf{t}_{\mathrm{o}} &= \frac{1}{\sqrt{2}}(\mathbf{k}_{\mathrm{o}} + \mathbf{l}_{\mathrm{o}}), & \mathbf{q}_{\mathrm{o}} &= \frac{1}{\sqrt{2}}(\mathbf{k}_{\mathrm{o}} - \mathbf{l}_{\mathrm{o}}), \\ \mathbf{r}_{\mathrm{o}} &= \frac{1}{\sqrt{2}}(\mathbf{m}_{\mathrm{o}} + \bar{\mathbf{m}}_{\mathrm{o}}), & \mathbf{s}_{\mathrm{o}} &= \frac{i}{\sqrt{2}}(\mathbf{m}_{\mathrm{o}} - \bar{\mathbf{m}}_{\mathrm{o}}), \end{aligned} \tag{5.3}$$

see (3.1). From the coplanarity and normalization condition (3.25) it follows that

$$\begin{cases} \mathbf{t}_{\mathrm{o}} = \epsilon_{\mathrm{o}}\mathbf{n} & \text{when } \mathcal{I} \text{ is spacelike} \quad (\sigma = -1), \\ \mathbf{q}_{\mathrm{o}} = -\epsilon_{\mathrm{o}}\mathbf{n} & \text{when } \mathcal{I} \text{ is timelike} \quad (\sigma = +1), \end{cases} \tag{5.4}$$

where $\mathbf{n}$ is the normal to $\mathcal{I}$, cf figure 2. We can now project a null vector $\mathbf{k}$, whose direction is represented by the parameter R by (3.26), onto the corresponding conformal infinity.

In spacetimes with $\Lambda > 0$, for which $\mathcal{I}$ is spacelike, we perform a normalized spatial projection to a three-dimensional space orthogonal to $\mathbf{t}_{\mathrm{o}}$,

$$\mathbf{q} = \frac{\mathbf{k} + (\mathbf{k}\cdot\mathbf{t}_{\mathrm{o}})\mathbf{t}_{\mathrm{o}}}{|\mathbf{k}\cdot\mathbf{t}_{\mathrm{o}}|}, \tag{5.5}$$

where $\mathbf{k}\cdot\mathbf{t}_{\mathrm{o}} = \mathbf{g}_{ab}\mathbf{k}^a\mathbf{t}_{\mathrm{o}}^b$. The unit spatial direction $\mathbf{q}$ corresponding to $\mathbf{k}$ can be expressed in terms of standard *spherical angles* θ, ϕ, with respect to the reference tetrad,

$$\mathbf{q} = \cos\theta\,\mathbf{q}_{\mathrm{o}} + \sin\theta(\cos\phi\,\mathbf{r}_{\mathrm{o}} + \sin\phi\,\mathbf{s}_{\mathrm{o}}). \tag{5.6}$$

Substituting (3.26) into (5.5), and comparing with (5.6) we obtain

$$R = \tan\frac{\theta}{2}\exp(-\mathrm{i}\phi). \tag{5.7}$$

Therefore, R is exactly the *stereographic representation* of the angles θ, ϕ. Additionally, for $\sigma = -1$ the orientation of the null vector $\mathbf{k}$ with respect to $\mathcal{I}$ coincides with the orientation of $\mathbf{k}_{\mathrm{o}}$, $\epsilon = \epsilon_{\mathrm{o}}$, cf figure 2.

Alternatively, in spacetimes with $\Lambda < 0$ for which $\mathcal{I}$ is timelike the normalized projection of $\mathbf{k}$ onto $\mathcal{I}$ is

$$\mathbf{t} = \frac{\mathbf{k} - (\mathbf{k}\cdot\mathbf{q}_{\mathrm{o}})\mathbf{q}_{\mathrm{o}}}{|\mathbf{k}\cdot\mathbf{q}_{\mathrm{o}}|}. \tag{5.8}$$

The resulting unit timelike vector $\mathbf{t}$ is tangent to the Lorentzian (1 + 2) conformal infinity. We can analogously characterize $\mathbf{t}$ (and thus $\mathbf{k}$) with respect to the reference tetrad as

$$\mathbf{t} = \cosh\psi\,\mathbf{t}_{\mathrm{o}} + \sinh\psi(\cos\phi\,\mathbf{r}_{\mathrm{o}} + \sin\phi\,\mathbf{s}_{\mathrm{o}}). \tag{5.9}$$

The parameters ψ, ϕ are *pseudo-spherical* parameters, $\psi \in (0, \infty)$ corresponding to a boost, and $\phi \in (-\pi, +\pi)$ being an angle. Their geometrical meaning is visualized in figure 3. However, these parameters do not specify the null direction $\mathbf{k}$ uniquely—there always exist *one ingoing* and *one outgoing* null direction with the same parameters ψ and ϕ, which are distinguished by $\epsilon = \pm 1$. Substituting equation (3.26) into (5.8), and comparing with equation (5.9) we express ψ and ϕ in terms of R as

$$\tanh\psi = \frac{2\,|R|}{1 + |R|^2}, \qquad \phi = -\arg R. \tag{5.10}$$

Observing that $\mathrm{sign}(1 - |R|^2)$ characterizes a difference in orientations of the vectors $\mathbf{k}$ and $\mathbf{k}_{\mathrm{o}}$ with respect to infinity, $\epsilon = \epsilon_{\mathrm{o}}\,\mathrm{sign}\,(1 - |R|^2)$, we can write down the inverse relations,

$$R = \begin{cases} \tanh\dfrac{\psi}{2}\exp(-\mathrm{i}\phi) & \text{for} \quad \epsilon = +\epsilon_{\mathrm{o}}, \\ \coth\dfrac{\psi}{2}\exp(-\mathrm{i}\phi) & \text{for} \quad \epsilon = -\epsilon_{\mathrm{o}}. \end{cases} \tag{5.11}$$

We also allow an infinite value $R = \infty$ which corresponds to $\psi = 0, \epsilon = -\epsilon_{\mathrm{o}}$, i.e., $\mathbf{k} \propto (\mathbf{t}_{\mathrm{o}} - \mathbf{q}_{\mathrm{o}})/\sqrt{2}$.

Of course such a parametrization can be applied to any null direction $\mathbf{k}$. In particular, it may characterize the direction $\mathbf{k}_{\mathrm{i}}$ of a null geodesic along which the infinity is approached, and also describe the principal null directions. The PNDs on a 'de Sitter-like' $\mathcal{I}$ are thus given by the spherical angles θ_n, ϕ_n related to R_n by equation (5.7), whereas on an 'anti-de Sitter-like' $\mathcal{I}$ by $\psi_n, \phi_n, \epsilon_n$ which are given by (5.11).

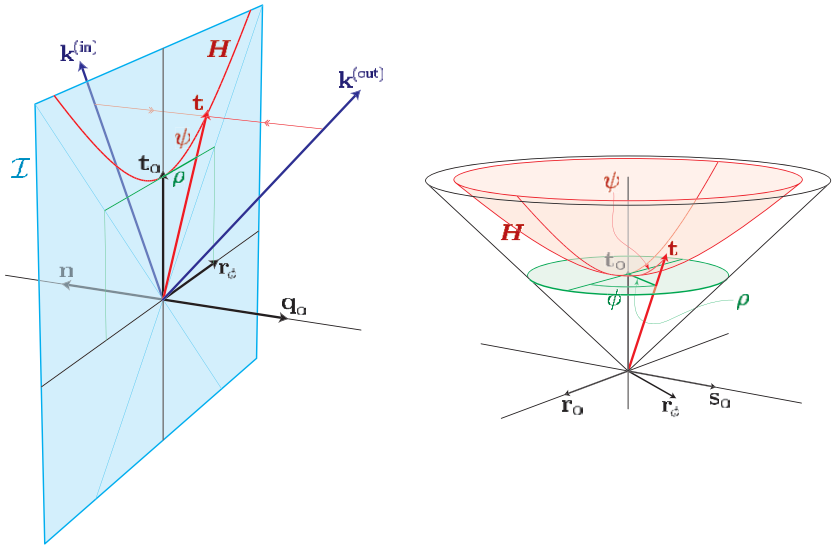

Figure 3. Parametrization of null directions $\mathbf{k}$ near timelike infinity $\mathcal{I}$. All null directions form three families: *outgoing* ($\epsilon = +1$, vector $\mathbf{k}^{(\mathrm{out})}$ in the figure), *ingoing* ($\epsilon = -1$, vector $\mathbf{k}^{(\mathrm{in})}$) and directions *tangent* to $\mathcal{I}$. The direction $\mathbf{k}$ can be parametrized with respect to a reference tetrad $\mathbf{t}_\mathrm{o}$, $\mathbf{q}_\mathrm{o}$, $\mathbf{r}_\mathrm{o}$, $\mathbf{s}_\mathrm{o}$ by the boost ψ, angle ϕ and orientation ϵ, or by a complex number R, or by parameters ρ, ϕ. In the left diagram, the vectors $\mathbf{t}_\mathrm{o}$, $\mathbf{q}_\mathrm{o}$, $\mathbf{r}_\phi$, where $\mathbf{r}_\phi = \cos\phi\,\mathbf{r}_\mathrm{o} + \sin\phi\,\mathbf{s}_\mathrm{o}$, are depicted; in the right the direction $\mathbf{q}_\mathrm{o} = -\epsilon_\mathrm{o}\mathbf{n}$ is omitted. The parameters ψ, ϕ specify the normalized orthogonal projection $\mathbf{t}$ of $\mathbf{k}$ into $\mathcal{I}$, cf equations (5.8), (5.9). To parametrize $\mathbf{k}$ uniquely, we have to specify also its orientation ϵ with respect to $\mathcal{I}$. The parameter R is the Lorentzian stereographic representation of ψ, ϕ, ϵ, cf equations (5.11). Vectors $\mathbf{t}$ corresponding to all outgoing (or ingoing) null directions form a hyperbolic surface $\boldsymbol{H}$. This can be radially mapped onto a two-dimensional disc tangent to the hyperboloid at $\mathbf{t}_\mathrm{o}$, which can be parametrized by an angle ϕ and a radial coordinate $\rho = \tanh\psi$. In the exceptional case $\rho = 1$, i.e. $\psi \to \infty$, the vector $\mathbf{k} \propto \mathbf{t} + \mathbf{r}_\phi$ is tangent to $\mathcal{I}$.

(This figure is in colour only in the electronic version)

5.4. Radiation on spacelike $\mathcal{I}$

The asymptotic structure of gravitational and electromagnetic fields evaluated in the interpretation tetrad near a *de Sitter-like conformal infinity*, $\sigma = -1$ with $\mathbf{n} = \epsilon_\mathrm{o}\mathbf{t}_\mathrm{o}$, is given by (4.19) for $s = 2$ and $s = 1$, respectively,

$$\Psi_4^\mathrm{i} \approx \frac{\Psi_{4*}^\mathrm{o}}{\eta}(1+|R|^2)^{-2}\left(1-\frac{R_1}{R_\mathfrak{a}}\right)\left(1-\frac{R_2}{R_\mathfrak{a}}\right)\left(1-\frac{R_3}{R_\mathfrak{a}}\right)\left(1-\frac{R_4}{R_\mathfrak{a}}\right), \tag{5.12}$$

$$\Phi_2^\mathrm{i} \approx \epsilon_0\frac{\Phi_{2*}^\mathrm{o}}{\eta}(1+|R|^2)^{-1}\left(1-\frac{R_1}{R_\mathfrak{a}}\right)\left(1-\frac{R_2}{R_\mathfrak{a}}\right), \tag{5.13}$$

where, using (5.7),

$$(1+|R|^2)^{-1} = \cos^2\left(\frac{\theta}{2}\right), \tag{5.14}$$

and the complex number $R_\mathfrak{a}$ is

$$R_\mathfrak{a} = -\frac{1}{\bar{R}} = -\cot\left(\frac{\theta}{2}\right)\exp(-\mathrm{i}\phi). \tag{5.15}$$

It characterizes a spatial direction *opposite* to the direction given by R, i.e., the *antipodal* direction with $\theta_{\mathfrak{a}} = \pi - \theta$ and $\phi_{\mathfrak{a}} = \phi + \pi$. The remaining freedom in the choice of the vectors $\mathbf{m}_{\mathrm{i}}$, $\bar{\mathbf{m}}_{\mathrm{i}}$ changes just a phase of the field components, so that only their modulus $\left|\Psi_4^{\mathrm{i}}\right|$ or $\left|\Phi_2^{\mathrm{i}}\right|$ has an invariant meaning.

In a general spacetime there exist *four* spatial directions at $P \in \mathcal{I}$ along which the radiative component of the gravitational field (5.12) *vanishes*, namely the directions satisfying $R_{\mathfrak{a}} = R_n, n = 1, 2, 3, 4$ (or *two* such directions for electromagnetic field (5.13)). These privileged null directions $\mathbf{k}$ are given by (3.26) with $R = (R_n)_{\mathfrak{a}}$. Spatial parts of them are thus exactly *opposite to the projections of the principal null directions onto* $\mathcal{I}$.

In *algebraically special* spacetimes some PNDs coincide, and expressions (5.12), (5.13) simplify. Moreover, it is always possible to choose the *canonical reference tetrad* aligned to the algebraic structure:

(i) the vector $\mathbf{q}_{\mathrm{o}}$ is oriented along the spatial projection of the *degenerate* (multiple) PND onto $\mathcal{I}$, say $\mathbf{k}_4$, i.e. $\mathbf{k}_{\mathrm{o}} = \mathbf{k}_4$,

(ii) the $\mathbf{q}_{\mathrm{o}}$–$\mathbf{r}_{\mathrm{o}}$ plane is oriented so that it contains the spatial projection of one of the remaining PNDs, say $\mathbf{k}_1$ (for type N spacetimes this choice is arbitrary).

Using such a canonical reference tetrad, the degenerate PND $\mathbf{k}_4$ is parametrized by $\theta_4 = 0$, i.e. $R_4 = 0$, see equations (5.6) and (5.7). The PND $\mathbf{k}_1$ has $\phi_1 = 0$, i.e. $R_1 = \tan(\theta_1/2)$ is a real constant.

Consequently, for the Petrov *type N* spacetimes (which have a quadruply degenerate PND), in the canonical reference tetrad there is $R_1 = R_2 = R_3 = R_4 = 0$, so that the asymptotic behaviour of gravitational field (5.12) becomes

$$\left|\Psi_4^{\mathrm{i}}\right| \approx \left|\Psi_{4*}^{\mathrm{o}}\right| |\eta|^{-1} \cos^4 \frac{\theta}{2}. \tag{5.16}$$

The corresponding directional structure of radiation is illustrated in figure 4(N). It is axisymmetric, with maximum value at $\theta = 0$ along the spatial projection of the quadruple PND onto $\mathcal{I}$. Along the opposite direction, $\theta = \pi$, the field vanishes. Analogously, for a spin-s field of type N (with all PNDs coinciding) we obtain

$$\left|\Upsilon_{2s}^{\mathrm{i}}\right| \approx \left|\Upsilon_{2s*}^{\mathrm{o}}\right| |\eta|^{-1} \left|\cos \frac{\theta}{2}\right|^{2s}. \tag{5.17}$$

In Petrov *type III* spacetimes, $R_1 = \tan \frac{\theta_1}{2}$, $R_2 = R_3 = R_4 = 0$, and (5.12) implies

$$\left|\Psi_4^{\mathrm{i}}\right| \approx \left|\Psi_{4*}^{\mathrm{o}}\right| |\eta|^{-1} \cos^4 \frac{\theta}{2} \left|1 + \tan \frac{\theta_1}{2} \tan \frac{\theta}{2} \mathrm{e}^{\mathrm{i}\phi}\right|. \tag{5.18}$$

This directional pattern is shown in figure 4(III). The field vanishes along $\theta = \pi$ and along $\theta = \pi - \theta_1, \phi = \pi$ which are spatial directions opposite to the PNDs.

The *type D* spacetimes admit two double degenerate PNDs, $R_1 = R_2 = \tan \frac{\theta_1}{2}$ and $R_3 = R_4 = 0$. The gravitational field near spacelike $\mathcal{I}$ thus takes the form

$$\left|\Psi_4^{\mathrm{i}}\right| \approx \left|\Psi_{4*}^{\mathrm{o}}\right| |\eta|^{-1} \cos^4 \frac{\theta}{2} \left|1 + \tan \frac{\theta_1}{2} \tan \frac{\theta}{2} \mathrm{e}^{\mathrm{i}\phi}\right|^2, \tag{5.19}$$

with two planes of symmetry, see figure 4(D). This directional dependence agrees with that for the C-metric spacetime with $\Lambda > 0$ derived recently in [102].

For Petrov *type II* spacetimes, only two PNDs coincide so that $R_1 = \tan \frac{\theta_1}{2}$, $R_2 = \tan \frac{\theta_2}{2} \exp(-\mathrm{i}\phi_2)$, $R_3 = R_4 = 0$. Asymptotic directional structure of the field,

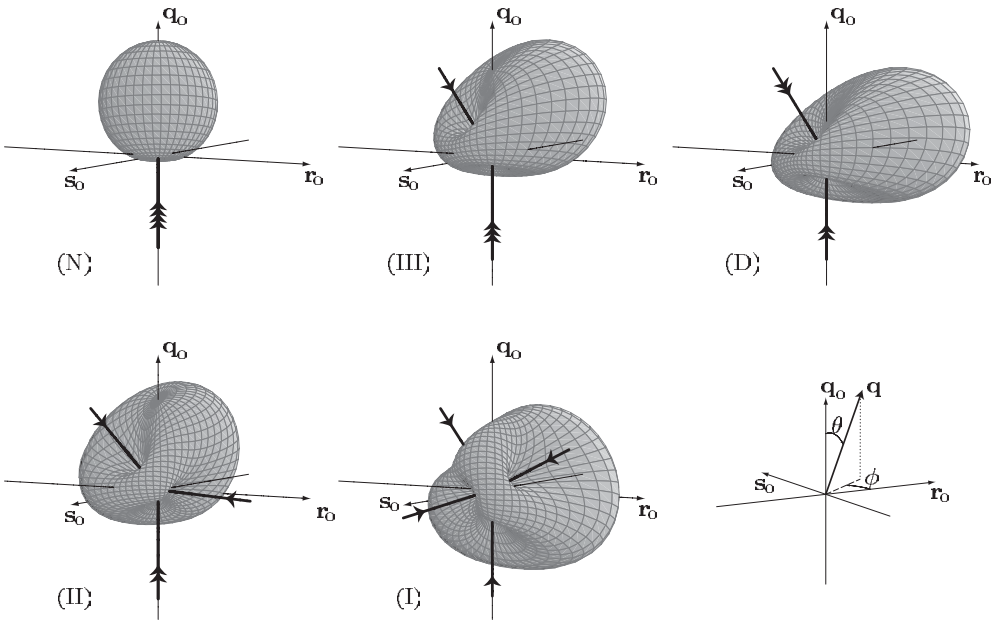

Figure 4. Specific directional structure of radiation for spacetimes of Petrov types N, III, D, II and I. Directions in the diagrams are spatial directions tangent to a spacelike $\mathcal{I}$. For each type, the radiative component $|\Psi_4^{\mathrm{i}}|$ along a null geodesic is depicted in the corresponding spatial direction $\mathbf{q}$ parametrized by spherical angles θ, ϕ, see (5.6). [Degenerate] principal null directions (PNDs) are indicated by [multiple] bold arrows. Thick lines represent spatial directions (opposite to PNDs) along which the radiation vanishes.

$$|\Psi_4^{\mathrm{i}}| \approx |\Psi_{4*}^{\mathrm{o}}||\eta|^{-1} \cos^4\frac{\theta}{2} \left|1 + \tan\frac{\theta_1}{2}\tan\frac{\theta}{2}\,\mathrm{e}^{\mathrm{i}\phi}\right| \left|1 + \tan\frac{\theta_2}{2}\tan\frac{\theta}{2}\,\mathrm{e}^{\mathrm{i}(\phi-\phi_2)}\right|, \tag{5.20}$$

is drawn in figure 4(II).

Finally, in the case of algebraically general *type I* spacetimes one needs five real parameters $\theta_1, \theta_2, \phi_2, \theta_3, \phi_3$ to characterize the directional dependence

$$\begin{aligned}|\Psi_4^{\mathrm{i}}| \approx |\Psi_{4*}^{\mathrm{o}}||\eta|^{-1} \cos^4\frac{\theta}{2} &\left|1 + \tan\frac{\theta_1}{2}\tan\frac{\theta}{2}\,\mathrm{e}^{\mathrm{i}\phi}\right| \\ &\times \left|1 + \tan\frac{\theta_2}{2}\tan\frac{\theta}{2}\,\mathrm{e}^{\mathrm{i}(\phi-\phi_2)}\right| \left|1 + \tan\frac{\theta_3}{2}\tan\frac{\theta}{2}\,\mathrm{e}^{\mathrm{i}(\phi-\phi_3)}\right|,\end{aligned} \tag{5.21}$$

figure 4(I), of the gravitational field with respect to the canonical reference tetrad.

Of course, for any *conformally flat* spacetime the radiation vanishes entirely because $\Psi_j^{\mathrm{i}} = 0$ for all j. This is the case of, for example, the Friedman–Robertson–Walker solutions which admit $\mathcal{I}$.

There exist alternative choices of the reference tetrad, e.g., those which respect the symmetry of the radiation pattern. For spacetimes of *type D* the directional structure indicated in figure 4(D) admits two planes of symmetry. It is thus natural to choose the tetrad $\mathbf{q}'_{\mathrm{o}}, \mathbf{r}'_{\mathrm{o}}, \mathbf{s}'_{\mathrm{o}}$ adapted to them: we require that one (double degenerate) PND has inclination θ_{s} with respect to $\mathbf{q}'_{\mathrm{o}}$, the second PND has the *same* inclination with respect to $-\mathbf{q}'_{\mathrm{o}}$ (i.e. $\theta_{\mathrm{s}} = (\pi - \theta_1)/2$), and that the vector $\mathbf{s}'_{\mathrm{o}}$ is perpendicular to the plane spanned by these PNDs (see [118] for more details). With respect to this reference tetrad the PNDs are parametrized by the coefficients $R_1 = R_2 = \tan\frac{\theta_{\mathrm{s}}}{2}$ and $R_3 = R_4 = \cot\frac{\theta_{\mathrm{s}}}{2}$. Moreover, for type D there exists a

natural normalization of the field which is different from that discussed above. One can evaluate the components Ψ_j^{s} in the *algebraically special null tetrad* with $\mathbf{k}_{\mathrm{s}}$ and $\mathbf{l}_{\mathrm{s}}$ given by the degenerate PNDs—it follows from the definition of PNDs that only the component Ψ_2^{s} would be non-vanishing. This component is independent of a choice of the tetrad vectors orthogonal to PNDs, and of the scaling of PNDs (assuming $\mathbf{k}_{\mathrm{s}} \cdot \mathbf{l}_{\mathrm{s}} = -1$), cf (4.6) with $s = 2$. We may thus use Ψ_2^{s} to normalize the directional structure of radiation. Using the relation

$$\Psi_4^{\mathrm{o}'} = \tfrac{3}{2} \tan^2 \theta_{\mathrm{s}} \Psi_2^{\mathrm{s}}, \tag{5.22}$$

see [118], the radiation pattern (5.12) parametrized by angles θ', ϕ' with respect to the reference tetrad $\mathbf{t}'_{\mathrm{o}}$, $\mathbf{q}'_{\mathrm{o}}$, $\mathbf{r}'_{\mathrm{o}}$, $\mathbf{s}'_{\mathrm{o}}$ reads

$$\left|\Psi_4^{\mathrm{i}}\right| \approx \frac{1}{|\eta|} \frac{3}{2} \frac{\left|\Psi_{2*}^{\mathrm{s}}\right|}{\cos^2 \theta_{\mathrm{s}}} |\sin\theta' + \sin\theta_{\mathrm{s}} \cos\phi' - \mathrm{i} \sin\theta_{\mathrm{s}} \cos\theta' \sin\phi'|^2. \tag{5.23}$$

This coincides with the expression for the asymptotic directional structure of radiation in the C-metric spacetime with $\Lambda > 0$, as previously presented in [102].

For a completely general choice of the reference tetrad near a de Sitter-like conformal infinity, the dominant radiative term (5.12) of any gravitational field can asymptotically be written in terms of spherical angles θ, ϕ as

$$\left|\Psi_4^{\mathrm{i}}\right| \approx \frac{\left|\Psi_{4*}^{\mathrm{o}}\right|}{|\eta|} \cos^4 \frac{\theta}{2} \prod_{n=1,2,3,4} \left|1 + \tan \frac{\theta_n}{2} \tan \frac{\theta}{2} \mathrm{e}^{\mathrm{i}(\phi - \phi_n)}\right|, \tag{5.24}$$

where θ_n, ϕ_n identify the principal null directions $\mathbf{k}_n$ with respect to the reference tetrad. In a similar way, when $\Psi_{4*}^{\mathrm{o}} = 0$, $\Psi_{0*}^{\mathrm{o}} \neq 0$ we obtain from (4.20)

$$\begin{aligned} \left|\Psi_4^{\mathrm{i}}\right| &\approx \frac{\left|\Psi_{0*}^{\mathrm{o}}\right|}{|\eta|} |1 + |R_{\mathfrak{a}}|^2|^{-2} \left|1 - \frac{R_{1\mathfrak{a}}}{R}\right| \left|1 - \frac{R_{2\mathfrak{a}}}{R}\right| \left|1 - \frac{R_{3\mathfrak{a}}}{R}\right| \left|1 - \frac{R_{4\mathfrak{a}}}{R}\right| \\ &= \frac{\left|\Psi_{0*}^{\mathrm{o}}\right|}{|\eta|} \sin^4 \frac{\theta}{2} \prod_{n=1,2,3,4} \left|1 + \cot \frac{\theta_n}{2} \cot \frac{\theta}{2} \mathrm{e}^{\mathrm{i}(\phi - \phi_n)}\right|. \end{aligned} \tag{5.25}$$

An analogous discussion also applies to electromagnetic field (5.13). Moreover, it turns out that the square of Φ_2^{i} is the magnitude of the Poynting vector with respect to the interpretation tetrad, $|\mathbf{S}_{\mathrm{i}}| \approx \frac{1}{4\pi} \left|\Phi_2^{\mathrm{i}}\right|^2$. If the two PNDs of the electromagnetic field coincide ($R_1 = R_2 = 0$), the directional dependence of the Poynting vector at $\mathcal{I}$ with respect to the canonical reference tetrad is the same as in equation (5.16), figure 4(N). If they differ ($R_1 = \tan \frac{\theta_1}{2}$, $R_2 = 0$), the asymptotic directional structure of $|\mathbf{S}_{\mathrm{i}}|$ is given by equation (5.19), illustrated in figure 4(D). The latter result was first obtained for the test field of uniformly accelerated charges in de Sitter spacetime [101] and then recovered in the context of the charged C-metric spacetime [102].

The above discussion and explicit forms of the radiative directional patterns apply both to future conformal infinity $\mathcal{I}^+$ and past $\mathcal{I}^-$. In particular, it means that not only *outgoing* radiation does not vanish in a generic direction, but also that the *ingoing* field has a radiative ($\sim\eta^{-1}$) term along a generic null geodesic coming from the past infinity. This result can be related to Penrose's discussion of the nature of an incoming field near a spacelike infinity [28, 100] which has been studied in more detail in [104] and identified as the insufficiency of purely retarded fields.

5.5. Radiation on timelike $\mathcal{I}$

Now we shall explicitly analyse the dependence of radiation on the direction of a null geodesic near the 'anti-de Sitter-like', i.e. timelike, conformal infinity [117]. With respect to a suitable

reference tetrad $\mathbf{t}_\mathrm{o}, \mathbf{q}_\mathrm{o}, \mathbf{r}_\mathrm{o}, \mathbf{s}_\mathrm{o}$ these directions are parametrized by the complex parameter R, or its 'Lorentzian angles' ψ, ϕ and the orientation ϵ, related to R by pseudo-stereographic representation, see (5.11) and figure 3. The directional structure of radiation is given by expression (4.19) for $\sigma = +1$,

$$\Psi_4^\mathrm{i} \approx \frac{\Psi_{4*}^\mathrm{o}}{\eta}(1-|R|^2)^{-2}\left(1-\frac{R_1}{R_\mathrm{m}}\right)\left(1-\frac{R_2}{R_\mathrm{m}}\right)\left(1-\frac{R_3}{R_\mathrm{m}}\right)\left(1-\frac{R_4}{R_\mathrm{m}}\right), \tag{5.26}$$

$$\Phi_2^\mathrm{i} \approx \epsilon_0\frac{\Phi_{2*}^\mathrm{o}}{\eta}(1-|R|^2)^{-1}\left(1-\frac{R_1}{R_\mathrm{m}}\right)\left(1-\frac{R_2}{R_\mathrm{m}}\right). \tag{5.27}$$

Here, the complex number R_m is

$$R_\mathrm{m} = \bar{R}^{-1} = \coth^{\epsilon\epsilon_\mathrm{o}}\left(\frac{\psi}{2}\right)\exp(-\mathrm{i}\phi), \tag{5.28}$$

see (5.11). It characterizes a direction obtained from the direction R by a *reflection with respect to* $\mathcal{I}$, i.e., the *mirrored* direction with $\psi_\mathrm{m} = \psi, \phi_\mathrm{m} = \phi$ but opposite orientation $\epsilon_\mathrm{m} = -\epsilon$. Near an anti-de Sitter-like conformal infinity, a generic gravitational field thus takes the asymptotic form

$$\left|\Psi_4^\mathrm{i}\right| \approx \frac{\left|\Psi_{4*}^\mathrm{o}\right|}{|\eta|}\left(\frac{\cosh\psi+\epsilon\epsilon_\mathrm{o}}{2}\right)^2\prod_{n=1,2,3,4}\left|1-\tanh^{\epsilon_n\epsilon_\mathrm{o}}\left(\frac{\psi_n}{2}\right)\tanh^{\epsilon\epsilon_\mathrm{o}}\left(\frac{\psi}{2}\right)\mathrm{e}^{\mathrm{i}(\phi-\phi_n)}\right|, \tag{5.29}$$

where $\psi_n, \phi_n, \epsilon_n$ identify the principal null directions $\mathbf{k}_n$, including their orientation with respect to $\mathcal{I}$.

Expression (5.26) has been derived assuming $\Psi_4^\mathrm{o} \neq 0$, i.e., $R_n \neq \infty$. However, to describe the PND oriented along $\mathbf{l}_\mathrm{o}$ it is necessary to use a different component Ψ_j^o as a normalization factor. With $\Psi_0^\mathrm{o} = \Psi_4^\mathrm{o} R_1 R_2 R_3 R_4$ we obtain

$$\begin{aligned}\left|\Psi_4^\mathrm{i}\right| &\approx \frac{\left|\Psi_{0*}^\mathrm{o}\right|}{|\eta|}|1-|R_\mathrm{m}|^2\,|^{-2}\left|1-\frac{R_{1\mathrm{m}}}{R}\right|\left|1-\frac{R_{2\mathrm{m}}}{R}\right|\left|1-\frac{R_{3\mathrm{m}}}{R}\right|\left|1-\frac{R_{4\mathrm{m}}}{R}\right| \\ &= \frac{\left|\Psi_{0*}^\mathrm{o}\right|}{|\eta|}\left(\frac{\cosh\psi-\epsilon\epsilon_\mathrm{o}}{2}\right)^2\prod_{n=1,2,3,4}\left|1-\coth^{\epsilon_n\epsilon_\mathrm{o}}\left(\frac{\psi_n}{2}\right)\coth^{\epsilon\epsilon_\mathrm{o}}\left(\frac{\psi}{2}\right)\mathrm{e}^{\mathrm{i}(\phi-\phi_n)}\right|.\end{aligned} \tag{5.30}$$

Interestingly, the radiation pattern has thus the same form if all PNDs are reflected, $R_n \to (R_n)_\mathrm{m}$, and ingoing and outgoing directions switched, $R \to R_\mathrm{m}$.

Both expressions (5.26) and (5.30) characterize the asymptotic behaviour of the fields near anti-de Sitter-like infinity. First, we observe from (5.26) that the radiation 'blows up' for directions with $|R| = 1$ (i.e., $\psi \to \infty$). These are null directions *tangent* to $\mathcal{I}$, and thus they do not represent a direction of any geodesic approaching $\mathcal{I}$ from the 'interior' of spacetime. The reason for this divergent behaviour is 'kinematic': when we required the 'comparable' approach of geodesics to infinity (see discussion nearby (3.10)), we had fixed the component of $\mathbf{k}_\mathrm{i}$ normal to $\mathcal{I}$, equation (3.16). Clearly, such a condition implies an 'infinite' rescaling if $\mathbf{k}_\mathrm{i}$ is tangent to $\mathcal{I}$ which results in the divergence of $\left|\Psi_4^\mathrm{i}\right|$.

The divergence at $|R| = 1$ splits the radiation pattern into two components—the pattern for *outgoing* geodesics ($\epsilon = +1$) and that for *ingoing* geodesics ($\epsilon = -1$). These two different patterns are separately depicted in figures 5 and 6.

From equation (5.26) it is obvious that there are, in general, *four* directions along which the radiation *vanishes*, namely PNDs *reflected with respect to* $\mathcal{I}$, given by $R = (R_n)_\mathrm{m}$. Outgoing PNDs give rise to zeros in the radiation pattern for ingoing null geodesics, and vice versa. A qualitative shape of the radiation pattern thus depends on

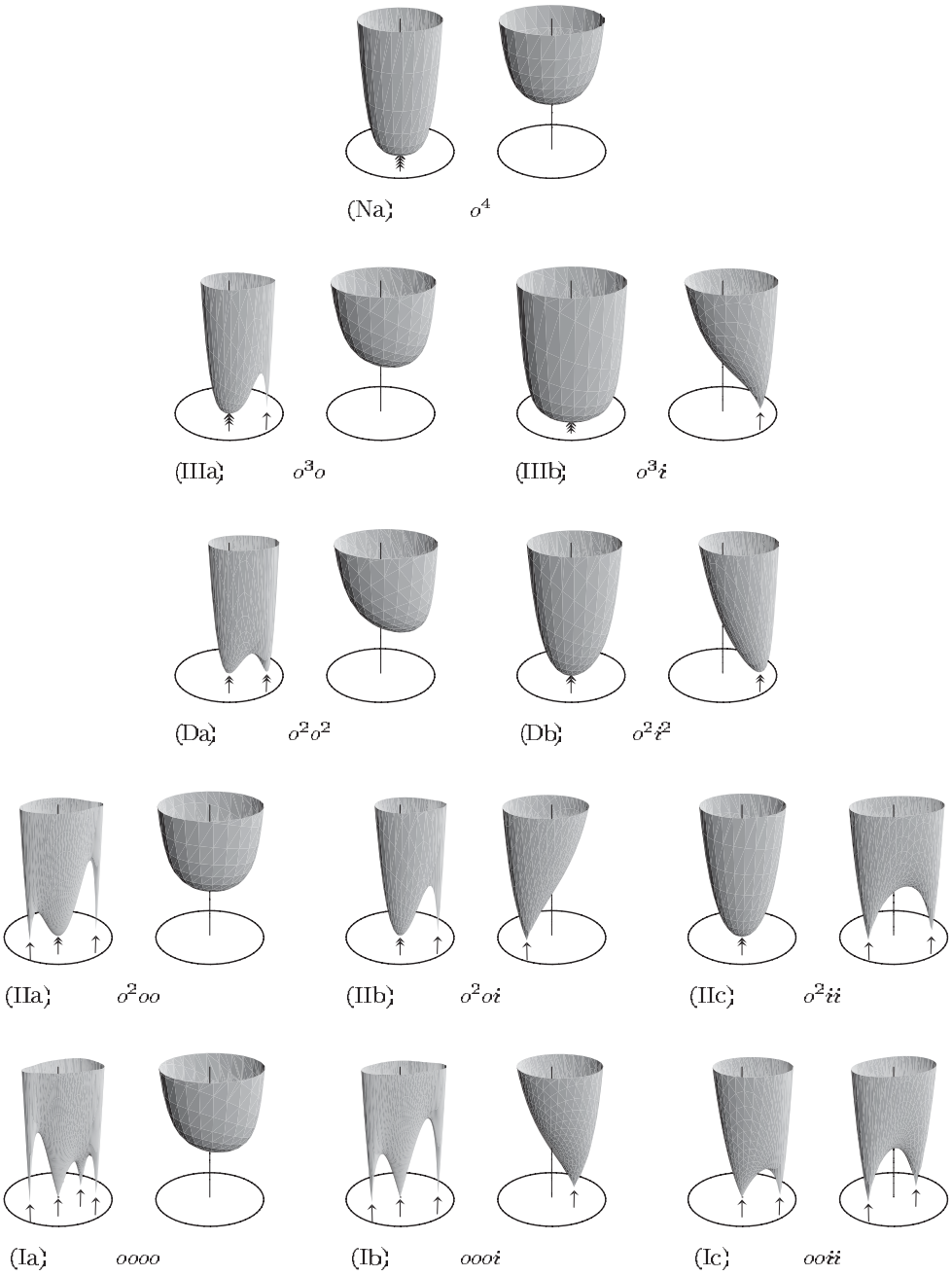

Figure 5. Directional structure of radiation near a timelike $\mathcal{I}$. All 11 qualitatively different shapes of the pattern when PNDs are not tangent to $\mathcal{I}$ are shown (the remaining nine are related by a simple reflection with respect to $\mathcal{I}$). Each diagram consists of patterns for ingoing (left) and outgoing geodesics (right). $\left|\Psi_4^{\mathrm{i}}\right|$ is drawn on the vertical axis, directions of geodesics are represented on the horizontal disc by coordinates ρ, ϕ introduced in figure 3. *Reflected* [degenerated] PNDs are indicated by [multiple] arrows under the discs. For PNDs that are not tangent to $\mathcal{I}$ these are directions of vanishing radiation. The Petrov types (N, III, D, II, I) corresponding to the degeneracy of PNDs are indicated by labels of diagrams, the number of ingoing and outgoing PNDs is also displayed using the notation of table 1.

Table 1. All 51 qualitatively different directional structures of gravitational radiation near a timelike conformal infinity. For various algebraic Petrov types, given by the degeneracy of principal null directions, the specific structure is determined by the orientation of these PNDs with respect to $\mathcal{I}$. We denote outgoing, tangent and ingoing PNDs by the symbols o, t and i, respectively, and their degeneracy by the corresponding power. The possibilities for each Petrov type which are presented in the third line are obtained from those in the first line by the duality between outgoing and ingoing directions, i.e. by interchanging o with i.

Type	PND degeneracy	Different possible orientations of PNDs
N	4	o^4 t^4 i^4
III	3 + 1	o^3o o^3t o^3i t^3o t^3t i^3i i^3t i^3o t^3i
D	2 + 2	o^2o^2 o^2t^2 o^2i^2 t^2t^2 i^2i^2 i^2t^2
II	2 + 1 + 1	o^2oo o^2ot o^2oi o^2ii o^2it o^2tt t^2oo t^2ot t^2oi t^2tt i^2ii i^2it i^2io i^2oo i^2ot i^2tt t^2ii t^2it
I	1 + 1 + 1 + 1	$oooo$ $ooot$ $oooi$ $ooit$ $oott$ $ottt$ $ooii$ $oitt$ $tttt$ $iiii$ $iiit$ $iiio$ $iiot$ $iitt$ $ittt$

(i) *degeneracy* of the PNDs (Petrov type of the spacetime),

(ii) *orientation* of these PNDs with respect to $\mathcal{I}$ (the number of outgoing/tangent/ingoing principal null directions).

Depending on these factors there are *51 qualitatively different shapes of the radiation patterns* (3 for Petrov type N spacetimes, 9 for type III, 6 for D, 18 for II and 15 for type I spacetimes); 21 pairs of them are related by the duality of equations (5.26) and (5.30). All the different possibilities are summarized in table 1. The corresponding directional patterns with PNDs not tangent to $\mathcal{I}$ are shown in figure 5, some examples of those with PNDs tangent to $\mathcal{I}$ can be found in figure 6.

As we have said before, the reference tetrad can be chosen to capture the geometry of the spacetime. To simplify the radiation pattern we can also adapt it to the algebraic structure, i.e., to correlate the tetrad with PNDs, as we did thoroughly for spacelike $\mathcal{I}$ in the previous section. In the case of timelike conformal infinity, however, the choice of canonical reference tetrads adjusted to PNDs is not very transparent—it splits to a lengthy discussion of separate cases depending on orientation of the PNDs with respect to $\mathcal{I}$. We do not include such a discussion here. We will only mention the simplest case of type N fields, and investigate in some more detail the cases of PNDs tangent to $\mathcal{I}$, the presence of which is specific for spacetimes with timelike infinity.

For type N fields with the quadruply degenerate PND, which is *not* tangent to $\mathcal{I}$, we can align the vector $\mathbf{k}_o$ along this algebraically special direction, i.e., $\mathbf{k}_o = \mathbf{k}_1 (= \mathbf{k}_2 = \mathbf{k}_3 = \mathbf{k}_4)$. The vector $\mathbf{l}_o$ is fixed by the adjustment condition (3.25). (The spatial vectors $\mathbf{m}_o, \bar{\mathbf{m}}_o$ cannot be fixed canonically by the algebraic structure—they have to be specified by other means.) The PNDs are then given by $R_n = 0$, i.e., $\psi_n = 0$ with orientations $\epsilon_n = \epsilon_o, n = 1, 2, 3, 4$. The directional dependence of radiation (5.29) thus reduces to

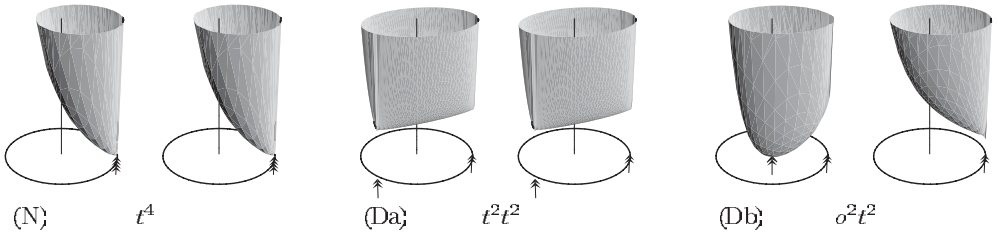

Figure 6. Examples of directional structure of radiation near a timelike $\mathcal{I}$ when PNDs are tangent to $\mathcal{I}$. Only the patterns for types N and D are shown. The notation and meaning of the diagrams are the same as in figure 5.

$$\left|\Psi_4^{\mathrm{i}}\right| \approx \frac{\left|\Psi_{4*}^{\mathrm{o}}\right|}{|\eta|}\left(\frac{\cosh\psi + \epsilon\epsilon_{\mathrm{o}}}{2}\right)^2, \tag{5.31}$$

illustrated in figure 5(N). Similarly, the radiative component of a general spin-s field of type N would be

$$\left|\Upsilon_{2s}^{\mathrm{i}}\right| \approx \frac{\left|\Upsilon_{2s*}^{\mathrm{o}}\right|}{|\eta|}\left(\frac{\cosh\psi + \epsilon\epsilon_{\mathrm{o}}}{2}\right)^s. \tag{5.32}$$

It is possible to introduce naturally the reference tetrads adjusted to the algebraic structure for Petrov type D gravitational fields or, in general, for fields with two equivalent special algebraic directions as, e.g., for a generic electromagnetic field. Such a tetrad is analogous to that introduced above (5.23) near a spacelike $\mathcal{I}$. A detailed discussion of these tetrads and of the normalization of the field can be found in [118] (cf also (5.36)).

We now turn to a special situation specific for the fields near a timelike infinity $\mathcal{I}$. Up to now we have discussed principal null directions which are either *incoming* or *outgoing* from the spacetime. However, PNDs can also be *tangent* to $\mathcal{I}$, and in the following we will discuss the consequences of such special orientation of PNDs for the radiation pattern. We do not expect PNDs to be tangent to $\mathcal{I}$ at generic points. However, they can be tangent on some lower-dimensional subspace such as the intersection of $\mathcal{I}$ with Killing horizons—cf the anti-de Sitter C-metric [103]. These subspaces can be important, e.g., as in the context of the Randall–Sundrum model: a brane constructed from the C-metric reaches infinity with PNDs tangent both to it and to $\mathcal{I}$ [119].

In the case when all PNDs *are tangent* to the conformal infinity, $R_n = \exp(-\mathrm{i}\phi_n)$, the directional pattern (4.19) for a general spin-s field reduces to

$$\left|\Upsilon_{2s}^{\mathrm{i}}\right| \approx \left|\Upsilon_{2s*}^{\mathrm{o}}\right| |\eta|^{-1} \prod_{n=1}^{2s} (\cosh\psi - \sinh\psi\cos(\phi - \phi_n))^{1/2}. \tag{5.33}$$

The field has, in general, no directions of vanishing radiation. It can only vanish along unphysical directions $R = R_n$ (unphysical because they are tangent to $\mathcal{I}$), provided the PND $\mathbf{k}_n$ is at least triple degenerate.

For type N fields, when all PNDs are the same, we can choose the reference tetrad in such a way that $R_n = 1$, i.e., $\phi_n = 0$, and we obtain

$$\left|\Upsilon_{2s}^{\mathrm{i}}\right| \approx \left|\Upsilon_{2s*}^{\mathrm{o}}\right| |\eta|^{-1} (\cosh\psi - \sinh\psi\cos\phi)^s. \tag{5.34}$$

In particular, for a gravitational field

$$\left|\Psi_4^{\mathrm{i}}\right| \approx \left|\Psi_{4*}^{\mathrm{o}}\right| |\eta|^{-1} (\cosh\psi - \sinh\psi\cos\phi)^2, \tag{5.35}$$

see figure 6(N).

For a gravitational field of Petrov type D with *both* double degenerate PNDs tangent to $\mathcal{I}$ (figure 6(Da)), we can choose the reference tetrad such that $R_1 = R_2 = 1$ and $R_3 = R_4 = -1$. The radiation pattern then becomes

$$\left|\Psi_4^{\mathrm{i}}\right| \approx \tfrac{3}{2}\left|\Psi_{2*}^{\mathrm{s}}\right| |\eta|^{-1} (1 + \sinh^2\psi \sin^2\phi), \tag{5.36}$$

where for normalization we have used the only non-vanishing field component Ψ_2^{s} in the algebraically special tetrad aligned along both PNDs: this is related to the reference tetrad field component by $\Psi_4^{\mathrm{o}} = \frac{3}{2}\Psi_2^{\mathrm{s}}$, see [118]. As we have said, there is no direction (even an unphysical one) of vanishing radiation in this case. However, directionally dependent limits $R \to R_1$ and $R \to R_4$, in general, do not diverge (cf figure 6(Da)). Finally, for a gravitational field of type D with *only one* PND tangent to $\mathcal{I}$, figure 6(Db), we can choose the reference tetrad so that $R_1 = R_2 = 1$, $R_3 = R_4 = 0$,

$$\left|\Psi_4^{\mathrm{i}}\right| \approx \left|\Psi_{4*}^{\mathrm{o}}\right| |\eta|^{-1} \frac{\cosh\psi + \epsilon\epsilon_{\mathrm{o}}}{2} (\cosh\psi - \sinh\psi\cos\phi). \tag{5.37}$$

To summarize, when $\mathcal{I}$ is not null the radiation fields depend on the direction along which the conformal infinity is approached. Analogously to the $\Lambda > 0$ case [116] the radiation pattern for $\Lambda < 0$ has a universal character determined by the *algebraic type* of the fields [117]. However, new features occur when $\Lambda < 0$: both *outgoing* and *ingoing* patterns have to be studied, their shapes depend also on the *orientation of the PNDs* with respect to $\mathcal{I}$, and an interesting possibility of PNDs *tangent to* $\mathcal{I}$ appears. Radiation vanishes only along directions which are reflections of PNDs with respect to $\mathcal{I}$. In a *generic* direction it is *non-vanishing*. The absence of η^{-1} terms thus cannot be used to distinguish nonradiative sources: near an anti-de Sitter-like infinity the radiative component reflects not only properties of sources but also their relation to the observer.

6. Conclusions

The investigation of the asymptotic structure of general fields in spacetimes with a non-vanishing cosmological constant Λ is motivated, among others, by the fact that these spacetimes have been commonly used in various branches of theoretical research, e.g. in inflationary models, brane cosmologies, supergravity or string theories. Perhaps most importantly, the possible presence of a positive Λ is also indicated by recent observations.

An understanding of the nature of radiation in spacetimes with a non-vanishing Λ is not so developed as that in spacetimes with $\Lambda = 0$. Standard techniques used for asymptotically flat spacetimes (such as the Bondi–Sachs approach) cannot be applied, and generalizations of other methods lead to results which are 'less unique'. In particular, we have documented that for $\Lambda \neq 0$ the field components with respect to a parallelly transported interpretation tetrad depend on a null direction along which infinity is approached—the feature which is absent in the $\Lambda = 0$ case. In Penrose's words (cf discussion after equation (9.7.38) in [33]): "on varying geodesic through P, the different components Ψ_j^{i} get mingled with each other". We derived this directional structure of radiation explicitly and we demonstrated that it is determined by the algebraic structure of the field. The asymptotic behaviour near $\mathcal{I}$ of the dominant component of any zero-rest-mass field of spin s is given by formula (4.19),

$$\Upsilon_{2s}^{\mathrm{i}} \propto \eta^{-1}(1 - \sigma R\bar{R})^{-s} \prod_{n=1}^{2s} (1 - \sigma R_n \bar{R}), \tag{6.1}$$

where η is the affine parameter. The coefficient $\sigma = -1, 0,$ or $+1$ denotes the spacelike, null or timelike character of the conformal infinity; in (electro)vacuum spacetimes $\sigma = -\operatorname{sign}\Lambda$.

The complex parameter R represents the direction of the outgoing/ingoing null geodesic along which a given point $P \in \mathcal{I}$ is approached as $\eta \to \pm\infty$. The complex constants R_n characterize the principal null directions, i.e. the algebraic structure of the field at P. Obviously, for $\mathcal{I}$ of a 'Minkowskian' type ($\sigma = 0$) the directional dependence completely vanishes. The specific dependence of $\Upsilon^{\mathrm{i}}_{2s}$ on the direction R of the geodesic occurs if $\sigma \neq 0$, i.e., near '(anti-)de Sitter-like' conformal infinity. Interestingly, in all spacetimes which are not conformally flat there are *at most* $2s$ directions along which the radiative part of the field (6.1) vanishes. These are directions antipodal to the principal null directions in the case of a spacelike $\mathcal{I}$, and mirror reflections of the PNDs with respect to $\mathcal{I}$ when its character is timelike. Along all other directions the radiation does *not* vanish, even if the field corresponds to a 'static' source.

Our results supplement and refine the peeling-off behaviour of zero-rest-mass fields. The 'peeling' is a well-known property of the fields near conformal infinity, and therefore we will emphasize again its relation to the above derived asymptotic directional structure of radiation. For example, in classical works [23, 30] one can find its very suggestive formulation: the curvature tensor expanded along null geodesics takes the form

$$\Psi = \mathrm{N}\eta^{-1} + \mathrm{III}\eta^{-2} + \mathrm{II}\eta^{-3} + \mathrm{I}\eta^{-4} + \cdots, \tag{6.2}$$

(see page 365 in [30] or equation (5.6) in [23]) where the terms N, III, II and I are algebraically special with quadruple, triple, double and non-degenerate PNDs, respectively. On this basis it is commonly stated that the radiative component ($\sim \eta^{-1}$) becomes asymptotically of Petrov type N with one quadruply degenerate PND. Our discussion above, however, demonstrates that such an interpretation is misleading or, at least, not precise. The separation of the terms having different algebraic structure into different orders of the asymptotic expansion in η is not due to the inherent properties of the Weyl tensor itself, but rather due to the asymptotic degeneracy of the tetrad with respect to which the Weyl tensor is evaluated. The coefficients in (6.2) are calculated in the *interpretation tetrad* which is parallelly transported along the null geodesic. We have seen that such a tetrad becomes infinitely boosted with respect to a regular tetrad defined in terms of the conformal geometry (see, e.g., relations (3.18), (2.19)). The Weyl tensor evaluated in the tetrad which is defined using the conformal techniques (i.e., the field calculated in the conformal geometry and then appropriately rescaled to obtain the physical quantity) has a typical behaviour $\Psi \sim \eta^{-3}$ (cf equation (4.18)) and it does *not* exhibit any peeling-off behaviour. It is the transformation to the interpretation tetrad (by the infinite boost, see equation (4.12)) which gives rise to peeling-off of the components with a different algebraic structure.

The field thus becomes asymptotically of type N only when viewed from the parallelly transported tetrad, with the algebraically special direction oriented along the tangent to the null geodesic approaching infinity. Already this dependence of the algebraically special direction, along which the field asymptotically aligns, on the direction of the geodesic, indicates that the asymptotic algebraic degeneracy suggested by (6.2) is not an invariant property of the field but an effect resulting from specific relation between the field and the observer.

As we said, near a *null* conformal infinity the magnitude of leading coefficient $\sim\eta^{-1}$ in the expansion (6.2) actually does *not* depend on the direction of the null geodesic (see (6.1) for $\sigma = 0$), and can thus be assigned a more invariant meaning—we may speak about non-radiative fields if this leading term is missing, and about radiative fields otherwise. However, for a *spacelike or timelike* conformal infinity we have found that the magnitude of the leading term *does* depend substantially on the direction R of the geodesic. Interestingly, such a dependence can be explicitly described in terms of the principal null directions of the field, see (6.1) and the discussion in sections 5.4 and 5.5.

To summarize: the peeling-off behaviour of a field near a spacelike or timelike infinity is not an invariant property of the field itself, but it is rather a statement about the behaviour of the field components evaluated in suitable tetrads propagated parallelly along null geodesics. For the full description of the components, the standard 'peeling' needs to be supplemented by their directional dependence which was presented above. We hope that our results may give some clues to the understanding of radiation in spacetimes which are not asymptotically flat.

It is very difficult to obtain an explicit general relation between the matter distribution and the corresponding distant gravitational field since the non-linearity of the Einstein equations effectively allows gravitation to act as its own source. Therefore, it remains an open problem to relate the structure of bounded sources to the principal null directions of the field at $\mathcal{I}$ which essentially determines the radiation structure at spacelike or timelike conformal infinities. Some insight in this direction could hopefully be obtained by investigating suitable exact model spacetimes.

Acknowledgments

We are grateful to Jiří Bičák, who brought our attention to the problem of radiation under the presence of a cosmological constant, for many valuable comments and suggestions. We also thank Jerry Griffiths and Marcello Ortaggio for careful reading of the manuscript. This work was supported by the grant GAČR 202/02/0735 of the Czech Republic.

Appendix A. Asymptotic polyhomogeneous expansions

In section 2.3 we integrated equation (2.13) for a physical affine parameter, and we obtained its expansion (2.17) in terms of the conformal affine parameter $\tilde\eta$. This can easily be inverted only in the leading order, $\tilde\eta = -1/\eta$. Here we derive the expansion of the conformal affine parameter $\tilde\eta$ in terms of η up to a higher order.

First, assuming smoothness of the conformal factor in the conformal affine parameter near $\mathcal{I}$, we have (cf equation (2.16))

$$\Omega = -\epsilon\tilde\eta + \Omega_2\tilde\eta^2 + \Omega_3\tilde\eta^3 + \cdots, \tag{A.1}$$

where Ω_i are constants. Expanding Ω^{-2}, the integration of (2.13) then leads to

$$\eta = -\frac{1}{\tilde\eta} + \big(2\epsilon\Omega_2 \ln|\tilde\eta| + \eta_0\big) + \big(3\Omega_2^2 + 2\epsilon\Omega_3\big)\tilde\eta + \cdots \tag{A.2}$$

(cf equation (2.17)), where η_0 is a constant of integration. This expression contains the logarithmic term $\ln|\tilde\eta|$ which means that the relation between η and $\tilde\eta$ is intrinsically non-analytic and cannot thus be inverted as a standard power expansion. We have to look for an inverse expansion in a broader class of functions, namely we admit functions which for small ξ can be written as

$$f(\xi) = \sum_{j=j_*}^{\infty} f_j(\ln^{-1}|\xi|)\xi^j, \tag{A.3}$$

where $j, j_* \in \mathbb{Z}$, and the 'coefficient' $f_j(\ln^{-1}|\xi|)$ in the power expansion is an (infinite) polynomial of the reciprocal logarithm $x = \ln^{-1}|\xi|$. More precisely, $f_j(x)$ is a function which is analytic (with a possible pole of a finite order $-k_*$ if $k_* < 0$) at $x = 0$,

$$f_j(x) = \sum_{k=k_*}^{\infty} f_{j,k}x^k. \tag{A.4}$$

Inspired by [90], we may call such an expansion polyhomogeneous. The expansion (A.3) with the leading coefficient $f_{j_*}(x)$ regular and non-vanishing at $x = 0$ can be substituted into another polyhomogeneous expansion and the result remains again in the class of polyhomogeneous expansions.

Expansion (A.2) is exactly of the form (A.3) for a small parameter $\tilde{\eta}$. We can seek the inverse relation as a polyhomogeneous expansion in the *small* parameter $\varepsilon = -\eta^{-1}$ (i.e., in the reciprocal physical affine parameter; notice the difference between ε and ϵ):

$$\tilde{\eta} = \varepsilon + \tilde{\eta}_2(\ln^{-1}|\varepsilon|)\varepsilon^2 + \tilde{\eta}_3(\ln^{-1}|\varepsilon|)\varepsilon^3 + \cdots. \tag{A.5}$$

Substituting into (A.2), expanding logarithmic terms, and requiring that the resulting expansion should lead to the single term $\eta = -\varepsilon^{-1}$, we find

$$\begin{aligned}\tilde{\eta} = \varepsilon - (2\epsilon\Omega_2 \ln|\varepsilon| + \eta_0)\varepsilon^2 + \big(&4\Omega_2^2 \ln^2|\varepsilon| + 4\Omega_2(\epsilon\eta_0 + \Omega_2)\ln|\varepsilon| + \eta_0^2 \\ &+ 2\epsilon\eta_0\Omega_2 - 3\Omega_2^2 - 2\epsilon\Omega_3\big)\varepsilon^3 + \cdots.\end{aligned} \tag{A.6}$$

Thus, the conformal factor (A.1) is

$$\begin{aligned}\Omega = -\epsilon\varepsilon + (2\Omega_2 \ln|\varepsilon| + \epsilon\eta_0 + \Omega_2)\varepsilon^2 - \epsilon\big(&4\Omega_2^2 \ln^2|\varepsilon| + 4\Omega_2^2(\epsilon\eta_0 + 2\Omega_2)\ln|\varepsilon| \\ &+ \eta_0^2 + 4\epsilon\eta_0\Omega_2 - 3\Omega_2^2 - 3\epsilon\Omega_3\big)\varepsilon^3 + \cdots.\end{aligned} \tag{A.7}$$

Integrating now equation (3.19) for parameter L, in which we expand Ω and the right-hand side in parameter $\tilde{\eta}$, see equations (A.1) and (3.20), we obtain

$$L = M_1 \ln|\tilde{\eta}| + L_0 + (M_2 + 2\epsilon M_1\Omega_2)\tilde{\eta} + \tfrac{1}{2}\big(M_3 + 2\epsilon M_2\Omega_2 + M_1\big(3\Omega_2^2 + 2\epsilon\Omega_3\big)\big)\tilde{\eta}^2 + \cdots, \tag{A.8}$$

and expressing this in terms of the reciprocal physical affine parameter using (A.6)

$$\begin{aligned}L = M_1 \ln|\varepsilon| + L_0 + (&-2\epsilon M_1\Omega_2 \ln|\varepsilon| + M_2 - M_1\eta_0 + 2\epsilon M_1\Omega_2)\varepsilon \\ &+ \big(2M_1\Omega_2^2 \ln^2|\varepsilon| - 2\epsilon(M_2 - M_1\eta_0)\Omega_2 \ln|\varepsilon| \\ &+ \tfrac{1}{2}\big(M_3 - 2M_2(\eta_0 - \epsilon\Omega_2) + M_1\big(\eta_0^2 - 3\Omega_2^2 - 2\epsilon\Omega_3\big)\big)\big)\varepsilon^2 + \cdots.\end{aligned} \tag{A.9}$$

Moreover, the coefficients Ω_i, M_i in expansions (2.16) and (3.20) can be expressed in terms of derivatives of Ω and $\bar{\mathbf{m}}^a_{\mathrm{a}}\mathbf{d}_a\Omega$ with respect of $\tilde{\eta}$. Namely, Ω_2 and M_1 are given by

$$\Omega_2 = \frac{1}{2}\frac{\mathrm{d}^2\Omega}{\mathrm{d}\tilde{\eta}^2}\bigg|_{\tilde{\eta}=0} = \ell^2\big(\tilde{\mathbf{k}}^b_{\mathrm{a}}\tilde{\mathbf{k}}^a_{\mathrm{a}}\tilde{\nabla}_b\mathbf{d}_a\Omega\big)\big|_{\mathcal{I}}, \tag{A.10}$$

$$M_1 = \sqrt{2}\ell\frac{\mathrm{d}}{\mathrm{d}\tilde{\eta}}\big(\tilde{\mathbf{m}}^a_{\mathrm{a}}\mathbf{d}_a\Omega\big)\bigg|_{\tilde{\eta}=0} = 2\ell^2\big(\tilde{\mathbf{k}}^b_{\mathrm{a}}\tilde{\mathbf{m}}^a_{\mathrm{a}}\tilde{\nabla}_b\mathbf{d}_a\Omega\big)\big|_{\mathcal{I}}, \tag{A.11}$$

where we used (3.11) and (3.12). Employing equations (2.3) and (2.8) we obtain

$$\tilde{\nabla}_b\mathbf{d}_a\Omega = \tfrac{1}{4}\tilde{\mathbf{g}}_{ab}\tilde{\Box}\Omega + \tfrac{1}{2}\Omega\big[\big(\mathbf{Ric}_{ab} - \tfrac{1}{4}R\mathbf{g}_{ab}\big) - \big(\tilde{\mathbf{Ric}}_{ab} - \tfrac{1}{4}\tilde{R}\tilde{\mathbf{g}}_{ab}\big)\big]. \tag{A.12}$$

Consequently,

$$\Omega_2 = \tfrac{1}{2}\ell^2\big(\Omega\tilde{\mathbf{k}}^b_{\mathrm{a}}\tilde{\mathbf{k}}^a_{\mathrm{a}}\big[\big(\mathbf{Ric}_{ab} - \tfrac{1}{4}R\mathbf{g}_{ab}\big) - \big(\tilde{\mathbf{Ric}}_{ab} - \tfrac{1}{4}\tilde{R}\tilde{\mathbf{g}}_{ab}\big)\big]\big)\big|_{\mathcal{I}}, \tag{A.13}$$

$$M_1 = \ell^2\big(\Omega\tilde{\mathbf{k}}^b_{\mathrm{a}}\tilde{\mathbf{m}}^a_{\mathrm{a}}\big[\big(\mathbf{Ric}_{ab} - \tfrac{1}{4}R\mathbf{g}_{ab}\big) - \big(\tilde{\mathbf{Ric}}_{ab} - \tfrac{1}{4}\tilde{R}\tilde{\mathbf{g}}_{ab}\big)\big]\big)\big|_{\mathcal{I}}, \tag{A.14}$$

We assume regularity of the conformal geometry near infinity so that the second terms in brackets, $\Omega\big(\tilde{\mathbf{Ric}}_{ab} - \frac{1}{4}\tilde{R}\tilde{\mathbf{g}}_{ab}\big)$, vanish on $\mathcal{I}$. The first terms can be expressed as the specific tetrad components of the traceless Ricci tensor [12], namely

$$\Phi^{\mathrm{a}}_{00} = \tfrac{1}{2}\big(\mathbf{Ric}_{ab} - \tfrac{1}{4}R\mathbf{g}_{ab}\big)\mathbf{k}^b\mathbf{k}^a, \qquad \Phi^{\mathrm{a}}_{01} = \tfrac{1}{2}\big(\mathbf{Ric}_{ab} - \tfrac{1}{4}R\mathbf{g}_{ab}\big)\mathbf{k}^b\mathbf{m}^a, \tag{A.15}$$

which in view of Einstein equations (2.9) are proportional to the corresponding components of the energy–momentum tensor. We thus obtain

$$\Omega_2 = \ell^2\big(\Omega^{-1}\Phi^{\mathrm{a}}_{00}\big)\big|_{\mathscr{I}} \sim \big(\tilde\eta^{-1}\Phi^{\mathrm{a}}_{00}\big)\big|_{\tilde\eta=0}, \tag{A.16}$$

$$M_1 = 2\ell^2\big(\Omega^{-1}\Phi^{\mathrm{a}}_{01}\big)\big|_{\mathscr{I}} \sim \big(\tilde\eta^{-1}\Phi^{\mathrm{a}}_{01}\big)\big|_{\tilde\eta=0}, \tag{A.17}$$

where Φ^{a}_{00} and Φ^{a}_{01} are evaluated with respect to the tetrad (3.14). These vanish identically for vacuum spacetimes. Moreover, Ω_2 and M_1 are zero also in non-vacuum cases such that near the conformal infinity the matter field decays faster than $\sim\tilde\eta$. It corresponds to the situation when Penrose's asymptotic Einstein condition (equation (2.20), cf (9.6.21) of [33]) is satisfied. With $\Omega_2 = 0$, $M_1 = 0$ the logarithmic terms in expansions (A.6)–(A.9) disappear.

Appendix B. Tetrads and fields in spinor formalism

Following, e.g., [33], the field of any spin $s = 0, \frac{1}{2}, 1, \frac{3}{2}, \cdots$ can be represented using the two-component symmetric spinor $\boldsymbol{\Upsilon}$ with $2s$ lower indices. To fix conventions for various signs and prefactors which alter in the literature we first summarize some general relations for spinors and their relation to tangent vectors.

Two-component spinors at a point x form two mutually conjugated complex vector spaces $\mathbf{S}_x\mathcal{M}$ and $\bar{\mathbf{S}}_x\mathcal{M}$ of dimension two. We use capital Latin letters for indices of spinors from $\mathbf{S}_x\mathcal{M}$ and letters with a bar for the conjugated spinors. Spinor spaces are equipped with *skew-symmetric metrics* $\boldsymbol{\epsilon}_{AB}$ and $\bar{\boldsymbol{\epsilon}}_{\bar A\bar B}$ respectively, and with their inverses $\boldsymbol{\epsilon}^{AB}$ and $\bar{\boldsymbol{\epsilon}}^{\bar A\bar B}$ (such that, e.g., $\boldsymbol{\epsilon}^{AM}\boldsymbol{\epsilon}_{BM} = \boldsymbol{\delta}^A_B$). These metrics are used for lowering and raising indices: $\boldsymbol{\psi}^A = \boldsymbol{\epsilon}^{AM}\boldsymbol{\psi}_M$, $\boldsymbol{\psi}_A = \boldsymbol{\psi}^M\boldsymbol{\epsilon}_{MA}$. The space of real bi-spinors (i.e., spinors $\boldsymbol{\alpha}^{A\bar A}$ such that $\boldsymbol{\alpha}^{A\bar A} = \bar{\boldsymbol{\alpha}}^{\bar A A}$) with metric $-\boldsymbol{\epsilon}_{AB}\bar{\boldsymbol{\epsilon}}_{\bar A\bar B}$ is isometric to the space of tangent vectors with metric spacetime $\mathbf{g}_{ab}$ through the *soldering form* $\boldsymbol{\sigma}^a{}_{A\bar A}$. The relation of both metrics is

$$\mathbf{g}^{ab} = -\boldsymbol{\sigma}^a{}_{A\bar A}\boldsymbol{\sigma}^b{}_{B\bar B}\boldsymbol{\epsilon}^{AB}\bar{\boldsymbol{\epsilon}}^{\bar A\bar B}, \qquad \boldsymbol{\epsilon}_{AB}\bar{\boldsymbol{\epsilon}}_{\bar A\bar B} = -\mathbf{g}_{ab}\boldsymbol{\sigma}^a{}_{A\bar A}\boldsymbol{\sigma}^b{}_{B\bar B}. \tag{B.1}$$

A spinor frame $\boldsymbol{o}, \boldsymbol{\iota}$ is called *normalized* if it satisfies

$$\boldsymbol{\epsilon}^{AB} = \boldsymbol{o}^A\boldsymbol{\iota}^B - \boldsymbol{\iota}^A\boldsymbol{o}^B, \qquad \text{i.e.,} \quad \boldsymbol{o}^A\boldsymbol{\iota}^B\boldsymbol{\epsilon}_{AB} = 1. \tag{B.2}$$

We can associate a normalized spinor frame $\boldsymbol{o}, \boldsymbol{\iota}$ with any null tetrad $\mathbf{k}, \mathbf{l}, \mathbf{m}, \bar{\mathbf{m}}$ in the following way:

$$\begin{aligned} \mathbf{k}^a &= \boldsymbol{\sigma}^a{}_{A\bar A}\boldsymbol{o}^A\bar{\boldsymbol{o}}^{\bar A}, & \mathbf{m}^a &= \boldsymbol{\sigma}^a{}_{A\bar A}\boldsymbol{o}^A\bar{\boldsymbol{\iota}}^{\bar A}, \\ \mathbf{l}^a &= \boldsymbol{\sigma}^a{}_{A\bar A}\boldsymbol{\iota}^A\bar{\boldsymbol{\iota}}^{\bar A}, & \bar{\mathbf{m}}^a &= \boldsymbol{\sigma}^a{}_{A\bar A}\boldsymbol{\iota}^A\bar{\boldsymbol{o}}^{\bar A}. \end{aligned} \tag{B.3}$$

Special Lorentz transformations (3.3), (3.4) and (3.5) correspond to transformations of the normalized spinor frame which leave (B.2) unchanged. Namely, for null rotation with $\mathbf{k}$ fixed we have

$$\begin{aligned} &\boldsymbol{o} = \boldsymbol{o}_{\mathrm{o}}, && \mathbf{k} = \mathbf{k}_{\mathrm{o}}, && \mathbf{m} = \mathbf{m}_{\mathrm{o}} + L\mathbf{k}_{\mathrm{o}}, \\ &\boldsymbol{\iota} = \boldsymbol{\iota}_{\mathrm{o}} + \bar L\boldsymbol{o}_{\mathrm{o}}, && \mathbf{l} = \mathbf{l}_{\mathrm{o}} + \bar L\mathbf{m}_{\mathrm{o}} + L\mathbf{m} + L\bar L\mathbf{k}, && \bar{\mathbf{m}} = \bar{\mathbf{m}}_{\mathrm{o}} + \bar L\mathbf{k}_{\mathrm{o}}, \end{aligned} \tag{B.4}$$

and for null rotation with $\mathbf{l}$ fixed,

$$\begin{aligned} &\boldsymbol{o} = \boldsymbol{o}_{\mathrm{o}} + K\boldsymbol{\iota}_{\mathrm{o}}, && \mathbf{k} = \mathbf{k}_{\mathrm{o}} + \bar K\mathbf{m}_{\mathrm{o}} + K\mathbf{m} + K\bar K\mathbf{k}, && \mathbf{m} = \mathbf{m}_{\mathrm{o}} + K\mathbf{k}_{\mathrm{o}}, \\ &\boldsymbol{\iota} = \boldsymbol{\iota}_{\mathrm{o}}, && \mathbf{l} = \mathbf{l}_{\mathrm{o}}, && \bar{\mathbf{m}} = \bar{\mathbf{m}}_{\mathrm{o}} + \bar K\mathbf{k}_{\mathrm{o}}. \end{aligned} \tag{B.5}$$

Boost and rotation are

$$\begin{aligned} &\boldsymbol{o} = B^{\frac12}\exp\big(\mathrm{i}\tfrac{\phi}{2}\big)\boldsymbol{o}_{\mathrm{o}}, && \mathbf{k} = B\mathbf{k}_{\mathrm{o}}, && \mathbf{m} = \exp(\mathrm{i}\phi)\mathbf{m}_{\mathrm{o}}, \\ &\boldsymbol{\iota} = B^{-\frac12}\exp\big(-\mathrm{i}\tfrac{\phi}{2}\big)\boldsymbol{\iota}_{\mathrm{o}}, && \mathbf{l} = B^{-1}\mathbf{l}_{\mathrm{o}}, && \bar{\mathbf{m}} = \exp(-\mathrm{i}\phi)\bar{\mathbf{m}}_{\mathrm{o}}. \end{aligned} \tag{B.6}$$

As we have said, the field of spin s can be represented by a spinor $\boldsymbol{\Upsilon}_{A_1\cdots A_{2s}}$ which is symmetric in all indices. The space of such symmetric spinors forms a representation space for the irreducible representation of type $(0, s)$ of the $\mathtt{SL}(2\mathbb{C})$ group, or of its $\mathtt{sl}(2\mathbb{C})$ Lie algebra which is isomorphic to Lie algebra $\mathtt{so}(1, 3)$ of the Lorenz group.

Field equations for the zero-rest-mass field of spin s are usually written in the form

$$\epsilon^{MN}\nabla_{M\bar{A}}\boldsymbol{\Upsilon}_{NA_2\cdots A_{2s}} = 0, \qquad \text{with} \quad \nabla_{A\bar{A}} = \boldsymbol{\sigma}^a{}_{A\bar{A}}\nabla_a. \tag{B.7}$$

It is well known [33] that such an equation is not consistent for $s > 2$ in a general curved background, and there are restrictions on curvature to achieve consistency for $s > 1$. However, the exact form of the field equations is not necessary for our discussion. We only assume that we may obtain the field $\boldsymbol{\Upsilon}$ from some unspecified theory which prescribes the behaviour of the field.

The examples are spinors $\boldsymbol{\Psi}_{ABCD}$ and $\boldsymbol{\Phi}_{AB}$ of spins 2 and 1 which represent the gravitational and electromagnetic fields, respectively. These spinors are related to the Weyl tensor $\mathbf{C}_{abcd}$ as

$$\begin{aligned}\mathbf{C}_{abcd} &= \boldsymbol{\sigma}_a{}^{A\bar{A}}\boldsymbol{\sigma}_b{}^{B\bar{B}}\boldsymbol{\sigma}_c{}^{C\bar{C}}\boldsymbol{\sigma}_d{}^{D\bar{D}}(\boldsymbol{\Psi}_{ABCD}\,\bar{\boldsymbol{\epsilon}}_{\bar{A}\bar{B}}\bar{\boldsymbol{\epsilon}}_{\bar{C}\bar{D}} + \bar{\boldsymbol{\Psi}}_{\bar{A}\bar{B}\bar{C}\bar{D}}\boldsymbol{\epsilon}_{AB}\boldsymbol{\epsilon}_{CD}),\\ \boldsymbol{\Psi}_{ABCD} &= \tfrac{1}{4}\boldsymbol{\sigma}^a{}_{A\bar{A}}\boldsymbol{\sigma}^b{}_{B\bar{B}}\boldsymbol{\sigma}^c{}_{C\bar{C}}\boldsymbol{\sigma}^d{}_{D\bar{D}}\mathbf{C}_{abcd}\bar{\boldsymbol{\epsilon}}^{\bar{A}\bar{B}}\bar{\boldsymbol{\epsilon}}^{\bar{C}\bar{D}},\end{aligned} \tag{B.8}$$

and to the electromagnetic tensor $\mathbf{F}_{ab}$ as

$$\begin{aligned}\mathbf{F}_{ab} &= \boldsymbol{\sigma}_a{}^{A\bar{A}}\boldsymbol{\sigma}_b{}^{B\bar{B}}(\boldsymbol{\Phi}_{AB}\bar{\boldsymbol{\epsilon}}_{\bar{A}\bar{B}} + \bar{\boldsymbol{\Phi}}_{\bar{A}\bar{B}}\boldsymbol{\epsilon}_{AB}),\\ \boldsymbol{\Phi}_{AB} &= \tfrac{1}{2}\boldsymbol{\sigma}^a{}_{A\bar{A}}\boldsymbol{\sigma}^b{}_{B\bar{B}}\mathbf{F}_{ab}\bar{\boldsymbol{\epsilon}}_{\bar{A}\bar{B}}.\end{aligned} \tag{B.9}$$

The field $\boldsymbol{\Upsilon}$ has $2s + 1$ independent components. In the normalized spinor frame $\boldsymbol{o}, \boldsymbol{\iota}$ these can be identified as

$$\Upsilon_j = \boldsymbol{\Upsilon}_{A_1\cdots A_jA_{j+1}\cdots A_{2s}}\boldsymbol{\iota}^{A_1}\cdots\boldsymbol{\iota}^{A_j}\boldsymbol{o}^{A_{j+1}}\cdots\boldsymbol{o}^{A_{2s}}, \qquad j = 0, 1, \ldots, 2s. \tag{B.10}$$

Substituting the transformations (B.4), (B.5) and (B.6) of the spinor frames into (B.10) we immediately obtain the transformation properties of the field components. Namely, we get

$$\Upsilon_j = \Upsilon_j^{\mathrm{o}} + \binom{j}{1}\bar{L}\Upsilon_{j-1}^{\mathrm{o}} + \binom{j}{2}\bar{L}^2\Upsilon_{j-2}^{\mathrm{o}} + \binom{j}{3}\bar{L}^3\Upsilon_{j-3}^{\mathrm{o}} + \cdots + \bar{L}^j\Upsilon_0^{\mathrm{o}} \tag{B.11}$$

for the null rotation with $\mathbf{k}$ fixed, and

$$\Upsilon_j = \Upsilon_j^{\mathrm{o}} + \binom{2s-j}{1}K\Upsilon_{j+1}^{\mathrm{o}} + \binom{2s-j}{2}K^2\Upsilon_{j+2}^{\mathrm{o}} + \cdots + K^{2s-j}\Upsilon_{2s}^{\mathrm{o}} \tag{B.12}$$

for the null rotation with $\mathbf{l}$ fixed. Finally, for the boost and the rotation we obtain

$$\Upsilon_j = B^{s-j}\exp(\mathrm{i}(s-j)\phi)\Upsilon_j^{\mathrm{o}}. \tag{B.13}$$

References

[1] Einstein A 1916 Näherungsweise Integration der Feldgleichungen der Gravitation *Preuss. Akad. Wiss. Sitz.* 688–96

[2] Einstein A 1918 Über Gravitationwellen *Preuss. Akad. Wiss. Sitz.* 154–67

[3] Weyl H 1919 *Raum-Zeit-Materie* (Berlin: Springer)

[4] Eddington A S 1923 The propagation of gravitational waves *Proc. R. Soc. Lond.* A **102** 268–82

[5] Bondi H, Pirani F A E and Robinson I 1959 Gravitational waves in general relativity: III. Exact plane waves *Proc. R. Soc. Lond.* A **251** 519–33

[6] Jordan P, Ehlers J and Kundt W 1960 Strenge Lösungen der Feldgleichungen der Allgemeinen Relativitätstheorie *Akad. Wiss. Lit. Mainz. Abhandl., Math.-Nat. Kl.* no 2

[7] Ehlers J and Kundt W 1962 Exact solutions of the gravitational field equations *Gravitation: an Introduction to Current Research* ed L Witten (New York: Wiley) pp 49–101

[8] Robinson I and Trautman A 1960 Spherical gravitational waves *Phys. Rev. Lett.* **4** 431–2
[9] Robinson I and Trautman A 1962 Some spherical gravitational waves in general relativity *Proc. R. Soc. Lond.* A **265** 463–73
[10] Bonnor W B and Swaminarayan N S 1964 An exact solutiou for uniformly accelerated particles in general relativity *Z. Phys.* **177** 240–56
[11] Bičák J 1968 Gravitational radiation from uniformly accelerated particles in general relativity *Proc. R. Soc. Lond.* A **302** 201–24
[12] Stephani H *et al* 2002 *Exact Solutions of Einstein's Field Equations* 2nd edn (Cambridge: Cambridge University Press)
[13] Bičák J 1985 On exact radiative solutions representing finite sources *Galaxies, Axisymmetric Systems and Relativity* ed M A H MacCaluum (Cambridge: Cambridge University Press) pp 91–124
[14] Bičák J 1987 Radiative properties of spacetimes with the axial and boost symmetries *Gravitation and Geometry (A volume in honour of Ivor Robinson)* ed W Rindler and A Trautman (Naples: Bibliopolis) pp 55–69
[15] Bičák J and Schmidt B G 1989 Asymptotically flat radiative space-times with boost-rotation symmetry: the general structure *Phys. Rev.* D **40** 1827–53
[16] Bonnor W B, Griffiths J B and MacCallum M A H 1994 Physical interpretation of vacuum solutions of Einstein's equations. Part II. Time-dependent solutions *Gen. Rel. Grav.* **26** 687–729
[17] Bičák J 1997 Radiative spacetimes: exact approaches *Relativistic Gravitation and Gravitational Radiation, Les Houches 1995* ed J A Marck and J P Lasota (Cambridge: Cambridge University Press) pp 67–87
[18] Bičák J 2000 Selected solutions of Einstein's field equations: Their role in general relativity and astrophysics *Einstein's Field Equations and Their Physical Implications* vol 540, ed B G Schmidt (Berlin: Springer) pp 1–126
[19] Bičák J and Krtouš P 2003 Radiative fields in spacetimes with Minkowski and de Sitter asymptotics *Recent Developments in Gravity (Proc. 10th Greek Relativity Meeting, Chalkidiki, May 2002)* ed K D Kokkotas and N Stergioulas (Singapore: World Scientific) pp 3–25
[20] Bondi H 1960 Gravitational waves in general relativity *Nature* **186** 535
[21] Bondi H, van der Burg M G J and Metzner A W K 1962 Gravitational waves in general relativity: VII. Waves from axi-symmetric isolated systems *Proc. R. Soc. Lond.* A **269** 21–52
[22] Sachs R 1961 Gravitational waves in general relativity: VI. The outgoing radiation condition *Proc. R. Soc. Lond.* A **264** 309–38
[23] Sachs R K 1962 Gravitational waves in general relativity: VII. Waves in asymptotically flat space-time *Proc. R. Soc. Lond.* A **270** 103–26
[24] van der Burg M G J 1969 Gravitational waves in general relativity X. Asymptotic expansions for the Einstein–Maxwell field *Proc. R. Soc. Lond.* A **310** 221–30
[25] Newman E T and Penrose R 1962 An approach to gravitational radiation by a method of spin coefficients *J. Math. Phys.* **3** 566–78
[26] Newman E T and Unti T W J 1962 Behavior of asymptotically flat empty spaces *J. Math. Phys.* **3** 891–901
[27] Penrose R 1963 Asymptotic properties of fields and space-times *Phys. Rev. Lett.* **10** 66–68
[28] Penrose R 1964 Conformal treatment of infinity *Relativity, Groups and Topology, Les Houches 1963* ed C DeWitt and B DeWitt (New York: Gordon and Breach) pp 563–84
[29] Penrose R 1965 Zero rest-mass fields including gravitation: asymptotic behaviour *Proc. R. Soc. Lond.* A **284** 159–203
[30] Pirani F A E 1965 Introduction to gravitational radiation theory *Brandeis Lectures on General Relativity* ed S Deser and K W Ford (Englewood Cliffs, NJ: Prentice-Hall) pp 249–372
[31] Geroch R P 1977 Asymptotic structure of space-time *Asymptotic Structure of Space-Time* ed F P Esposito and L Witten (New York: Plenum) pp 1–106
[32] Newman E T and Tod K P 1980 Asymptotically flat space-times *General Relativity and Gravitation* vol 2, ed A Held (New York: Plenum) pp 1–36
[33] Penrose R and Rindler W 1984, 1986 *Spinors and Space-Time* (Cambridge: Cambridge University Press)
[34] Friedrich H 1992 Asymptotic structure of space-time *Recent Advances in General Relativity* ed A I Janish and J R Porter (Basel: Birkhäuser)
[35] Stewart J 1993 *Advanced General Relativity* (Cambridge: Cambridge University Press)
[36] Friedrich H 1998 Einstein's equation and conformal structure *The Geometric Universe: Science, Geometry, and the Work of Roger Penrose* ed S A Huggett *et al* (Oxford: Oxford University Press) pp 81–98
[37] Sachs R K 1962 Aymptotic symmetries in gravitational theory *Phys. Rev.* **128** 2851–64
[38] van der Burg M G J 1966 Gravitational waves in general relativity IX. Conserved quantities *Proc. R. Soc. Lond.* A **294** 112–22
[39] Bičák J and Pravdová A 1998 Symmetries of asymptotically flat electro-vacuum spacetimes and radiation *J. Math. Phys.* **39** 6011–39

[40] Goldberg J N and Kerr R P 1964 Asymptotic properties of the electromagnetic field *J. Math. Phys.* **5** 172–6
[41] Petrov A Z 1954 Classification of spaces defined by gravitational fields *Sci. Not. Kazan. State Univ.* **114** 55
[42] Pirani F A E 1957 Invariant formulation of gravitational radiation theory *Phys. Rev.* **105** 1089–99
[43] Debever R 1959 Tenseur de super-énergie, tenseur de Riemann: cas singuliers *C. R. Acad. Sci., Paris* **249** 1744–6
[44] Penrose R 1960 A spinor approach to general relativity *Ann. Phys., NY* **10** 171–201
[45] Janish A I and Newman I T 1965 Structure of gravitational sources *J. Math. Phys.* **6** 902–14
[46] Szekeres P 1965 The gravitational compass *J. Math. Phys.* **6** 1387–91
[47] Bičák J and Podolský J 1999 Gravitational waves in vacuum spacetimes with cosmological constant. II: Deviation of geodesics and interpretation of non-twisting type N solutions *J. Math. Phys.* **40** 4506–17
[48] Penrose R 1968 Structure of space-time *Battelle Recontres* ed B DeWitt and J A Wheeler (New York: Benjamin) pp 121–235
[49] Winicour J H and Tamburino L A 1965 Lorentz-covariant gravitational energy–momentum linkages *Phys. Rev. Lett.* **15** 601–5
[50] Tamburino L A and Winicour J H 1966 Gravitational fields in finite and conformal Bondi frames *Phys. Rev.* **150** 1039–53
[51] Friedrich H 2002 Conformal Einstein evolution *The Conformal Structure of Space-Time: Geometry, Analysis, Numerics (Lecture Notes in Physics* vol 604*)* ed J Frauendiener and H Friedrich (Berlin: Springer) pp 1–50
[52] Ashtekar A and Magnon A 1984 Asymptotically anti-de Sitter space-times *Class. Quantum Grav.* **1** L39–44
[53] Ashtekar A and Das S 2000 Asymptotically anti-de Sitter spacetimes: conserved quantities *Class. Quantum Grav.* **17** L17–30
[54] Winicour J 1968 Some total invariance of asymptotically flat space-times *J. Math. Phys.* **9** 861–7
[55] Persides S 1979 A definition of asymptotically Minkowskian space-times *J. Math. Phys.* **20** 1731–40
[56] Schmidt B G 1987 Gravitational radiation near spatial and null infinity *Proc. R. Soc. Lond.* A **410** 201–8
[57] Chruściel P T, Jezierski J and MacCallum M A H 1998 Uniqueness of the Trautman–Bondi mass *Phys. Rev.* D **58** 084001
[58] Tafel J and Pukas S 2000 Comparison of the Bondi–Sachs and Penrose approaches to asymptotic flatness *Class. Quantum Grav.* **17** 1559–70
[59] Tafel J 2000 Bondi mass in terms of the Penrose conformal factor *Class. Quantum Grav.* **17** 4397–408
[60] Hawking S W and Ellis G F R 1973 *The Large Scale Structure of Space-Time* (Cambridge: Cambridge University Press)
[61] Wald R M 1984 *General Relativity* (Chicago, IL: The University of Chicago Press)
[62] Frauendiener J 2004 Conformal infinity *Liv. Rev. Rel.* **7** 2004-1 http://www.livingreviews.org/lrr-2004-1
[63] Friedrich H 1981 The asymptotic characteristic initial value problem for Einstein's vacuum field equations as an initial value problem for a first-order quasilinear symmetric hyperbolic system *Proc. R. Soc. Lond.* A **378** 401–21
[64] Friedrich H 1986 On the existence of n-geodesically complete or future complete solutions of Einstein's field equations with smooth asymptotic structure *Commun. Math. Phys.* **107** 587–609
[65] Friedrich H 1983 Cauchy problems for the conformal vacuum field equations in general relativity *Commun. Math. Phys.* **91** 445–72
[66] Friedrich H 1988 On static and radiative space-times *Commun. Math. Phys.* **119** 51–73
[67] Friedrich H 1991 On the global existence and the asymptotic behavior of solutions to the Einstein–Maxwell–Yang–Mills equations *J. Diffr. Geom.* **34** 275–345
[68] Friedrich H 1995 Einstein equations and conformal structure: existence of anti-de Sitter-type space-times *J. Geom. Phys.* **17** 125–84
[69] Friedrich H 1998 Gravitational fields near space-like and null infinity *J Geom. Phys.* **24** 83–163
[70] Cutler C and Wald R M 1989 Existence of radiating Einstein–Maxwell solutions which are $\mathcal{C}^\infty$ on all of $\mathcal{I}^+$ and $\mathcal{I}^-$ *Class. Quantum Grav.* **6** 453–66
[71] Christodoulou D and Klainerman S 1993 *The Global Nonlinear Stability of the Minkowski Space* (Princeton, NJ: Princeton University Press)
[72] Klainerman S and Nicolò F 1999 On local and global aspects of the Cauchy problem in general relativity *Class. Quantum Grav.* **16** R73–R157
[73] Klainerman S and Nicolò F 2003 Peeling properties of asymptotically flat solutions to the Einstein vacuum equations *Class. Quantum Grav.* **20** 3215–57
[74] Andersson L, Chruściel P T and Friedrich H 1992 On the regularity of solutions to the Yamabe equation and the existence of smooth hyperboloidal initial data for Einstein's field equations *Commun. Math. Phys.* **149** 587–612
[75] Andersson L and Chruściel P T 1996 On asymptotic behaviour of solutions of the constraint equations in general relativity with hyperboloidal boundary conditions *Diss. Math.* **355** 1–100

[76] Kánnár J 1996 Hyperboloidal initial data for the vacuum Einstein equations with cosmological constant *Class. Quantum Grav.* **13** 3075–84
[77] Corvino J 2000 Scalar curvature deformation and a gluing construction for the Einstein constraint equations *Commun. Math. Phys.* **214** 137–89
[78] Corvino J and Schoen R M 2003 On the asymptotics for the vacuum Einstein constraint equations *Preprint* gr-qc/0301071
[79] Chruściel P T and Delay E 2002 Existence of non-trivial, vacuum, asymptotically simple space-times *Class. Quantum Grav.* **19** L71–9
Chruściel P T and Delay E 2002 *Class. Quantum Grav.* **19** 3389 (erratum)
[80] Friedrich H 2003 Spin-2 fields on Minkowski space near space-like and null infinity *Class. Quantum Grav.* **20** 101–17
[81] Friedrich H 1998 Einstein's equation and geometric asymptotics *Gravitation and Relativity: At the Turn of the Millenium (Proc. GR-15 Conference)* ed N Dadhich and J Narlikar (Pune: Inter-University Centre for Astronomy and Astrophysics Press)
[82] Rendall A D 2002 Theorems on existence and global dynamics for the Einstein equations *Liv. Rev. Rel.* **5** 2002–6 http://www.livingreviews.org/lrr-2002-6
[83] Pravda V and Pravdová A 2000 Boost-rotation symmetric spacetimes—review *Czech. J. Phys.* **50** 333–75
[84] Ashtekar A and Dray T 1981 On the existence of solutions to Einstein's equation with non-zero Bondi news *Commun. Math. Phys.* **79** 581–9
[85] Andersson L and Chruściel P T 1993 On hyperboloidal Cauchy data for vacuum Einstein equations and obstructions to smoothness of 'null infinity' *Phys. Rev. Lett.* **70** 2829–32
[86] Andersson L and Chruściel P T 1994 On 'hyperboloidal' Cauchy data for vacuum Einstein equations and obstructions to smoothness of Scri *Commun. Math. Phys.* **161** 533–68
[87] Winicour J 1985 Logarithmic asymptotic flatness *Found. Phys.* **15** 605–16
[88] Damour T 1986 Analytical calculations of gravitational radiation *Proc. 4th Marcel Grossmann Meeting* vol A ed R Ruffini (Amsterdam: North-Holland) p 365
[89] Valiente Kroon J A 2004 A new class of obstructions to the smoothness of null infinity *Commun. Math. Phys.* **244** 133–56
[90] Chruściel P T, MacCallum M A H and Singleton P B 1995 Gravitational waves in general relativity XIV. Bondi expansions and the polyhomogeneity of $\mathcal{J}$ *Phil. Trans. R. Soc. Lond.* A **350** 113–41
[91] Valiente Kroon J A 2002 Polyhomogeneous expansions close to null and spatial infinity *The Conformal Structure of Space-Time: Geometry, Analysis, (Numerics Lecture Notes in Physics* vol 604*)* ed J Frauendiener and H Friedrich (Berlin: Springer) pp 135–59
[92] Trautman A 1958 Radiation and boundary conditions in the theory of gravitation *Bull. Acad. Pol. Sci., Sér. Sci. Math. Astron. Phys.* VI 407–12
[93] Newman E T and Penrose R 1965 10 exact gravitationally-conserved quantities *Phys. Rev. Lett.* **15** 231–3
[94] Newman E T and Penrose R 1968 New conservation laws for zero rest-mass fields in asymptotically flat space-time *Proc. R. Soc. Lond.* A **305** 175–204
[95] Exton A R, Newman E T and Penrose R 1969 Conserved quantities in the Einstein–Maxwell theory *J. Math. Phys.* **10** 1566–70
[96] Robinson D C 1969 Conserved quantities of Newman and Penrose *J. Math. Phys.* **10** 1745–53
[97] Glass E N and Goldberg J N 1970 Newman–Penrose constants and their invariant transformations *J. Math. Phys.* **11** 3400–13
[98] Valiente Kroon J A 1998 Conserved quantities for polyhomogeneous spacetimes *Class. Quantum Grav.* **15** 2479–91
[99] Valiente Kroon J A 2000 Polyhomogeneity and zero-rest-mass fields with applications to Newman–Penrose constants *Class. Quantum Grav.* **17** 605–21
[100] Penrose R 1967 Cosmological boundary conditions for zero rest-mass fields *The Nature of Time* ed T Gold (Ithaca, NY: Cornell University Press) pp 42–54
[101] Bičák J and Krtouš P 2002 The fields of uniformly accelerated charges in de Sitter spacetime *Phys. Rev. Lett.* **88** 211101
[102] Krtouš P and Podolský J 2003 Radiation from accelerated black holes in de Sitter universe *Phys. Rev.* D **68** 024005
[103] Podolský J, Ortaggio M and Krtouš P 2003 Radiation from accelerated black holes in an anti-de Sitter universe *Phys. Rev.* D **68** 124004
[104] Bičák J and Krtouš P 2001 Accelerated sources in de Sitter spacetime and the insufficiency of retarded fields *Phys. Rev.* D **64** 124020
[105] Avis S J, Isham C J and Storey D 1978 Quantum field theory in anti-de Sitter space-time *Phys. Rev.* D **18** 3565–76

[106] Hawking S W 1983 The boundary conditions for gauged supergravity *Phys. Lett.* B **126** 175–7
[107] Henneaux M and Teitelboim C 1985 Asymptotically anti-de Sitter spaces *Commun. Math. Phys.* **98** 391–424
[108] Bičák J and Krtouš P Fields of accelerated sources: Born in de Sitter (to be submitted)
[109] Kinnersley W and Walker M 1970 Uniformly accelerating charged mass in general relativity *Phys. Rev.* D **2** 1359–70
[110] Bičák J and Pravda V 1999 Spinning C-metric: radiative spacetime with accelerating, rotating black holes *Phys. Rev.* D **60** 044004
[111] Plebański J and Demiański M 1976 Rotating charged and uniformly accelerated mass in general relativity *Ann. Phys., NY* **98** 98–127
[112] Podolský J and Griffiths J B 2001 Uniformly accelerating black holes in a de Sitter universe *Phys. Rev.* D **63** 024006
[113] Podolský J 2002 Accelerating black holes in anti-de Sitter universe *Czech. J. Phys.* **52** 1–10
[114] Dias O J C and Lemos J P S 2003 Pair of accelerated black holes in an anti-de Sitter background: The AdS C metric *Phys. Rev.* D **67** 064001
[115] Dias O J C and Lemos J P S 2003 Pair of accelerated black holes in a de Sitter background: the dS C metric *Phys. Rev.* D **67** 084018
[116] Krtouš P, Podolský J and Bičák J 2003 Gravitational and electromagnetic fields near a de Sitter-like infinity *Phys. Rev. Lett.* **91** 061101
[117] Krtouš P and Podolský J 2004 Gravitational and electromagnetic fields near an anti-de Sitter-like infinity *Phys. Rev.* D **69** 084023
[118] Krtouš P and Podolský J Asymptotic directional structure of radiation for fields of algebraic type D *Czech. J. Phys.* (submitted)
[119] Emparan R, Horowitz G T and Myers R C 2000 Exact description of black holes on branes II: comparison with BTZ black holes and black strings *J. High Energy Phys.* JHEP01(2000)021

Asymptotic directional structure of radiation for fields of algebraic type D *)

Pavel Krtouš, Jiří Podolský

Institute of Theoretical Physics, Faculty of Mathematics and Physics, Charles University, V Holešovičkách 2, 180 00 Praha 8, Czech Republic

Received 7 September 2004

The directional behavior of dominant components of algebraically special spin-s fields near a spacelike, timelike or null conformal infinity is studied. By extending our previous general investigations, we concentrate on fields which admit a pair of equivalent algebraically special null directions, such as the Petrov type-D gravitational fields or algebraically general electromagnetic fields. We introduce and discuss a canonical choice of the reference tetrad near infinity in all possible situations, and we present the corresponding asymptotic directional structures using the most natural parametrizations.

PACS: 04.20.Ha, 98.80.Jk, 04.40.Nr
Key words: gravitational radiation, asymptotic structure, cosmological constant

1 Introduction

In the series of papers [1–4] we analyzed the asymptotic directional properties of electromagnetic and gravitational fields in spacetimes with a nonvanishing cosmological constant Λ. It had been known for a long time [5–7] that — contrary to the asymptotically flat spacetimes — the dominant (radiative) component of the fields is not unique since it substantially depends on the direction along which a null geodesic approaches a given point at conformal infinity $\mathcal{I}$. We demonstrated that, somewhat surprisingly, such directional structure of radiation can be described in closed explicit form. It has a universal character that is essentially determined by the algebraic type of the field, i.e., by the specific local degeneracy and orientation of the principal null directions.

Our results were summarized and thoroughly discussed in the recent topical review [8]. They apply not only to electromagnetic or gravitational fields but to any field of spin s. In addition, the expression representing the directional behavior of radiation can be written in a unified form which covers all three possibilities $\Lambda > 0$, $\Lambda < 0$ or $\Lambda = 0$, corresponding to a spacelike, timelike or null character of $\mathcal{I}$, respectively.

This paper further elaborates and supplements some aspects of our work reviewed in [8]. It extends possible definitions of the canonical reference tetrad for the algebraically simple fields — those which admit an equivalent pair of distinct (degenerate) principal null directions. We systematically describe the most natural choices of the reference tetrad for all possible algebraic structures of type D fields, and for any value of Λ.

*) Dedicated to Prof. Jiří Horáček on the occasion of his 60th birthday

The notation used in the present paper is the same as in [8]; in fact, we shall frequently employ the material already described and derived there. For brevity, we shall refer directly to the equations and sections of the review [8] by prefixing the letter 'R' in front of the reference: equation (R.1.1), section R.2.1, etc.

2 Summary of general results

We wish to study the behavior of radiative component of fields near conformal infinity $\mathcal{I}$. An overview of the concept of conformal infinity can be found in textbooks (e.g., [9]; our notation is described in section R.2 of the work [8]).

Let us only recall that it is possible to define a normalized vector $\mathbf{n}$ normal to the conformal infinity. The causal character of the infinity — spacelike, null, or timelike — is given by the sign of the square of this vector, $\sigma = \mathbf{n}\cdot\mathbf{n} = -1, 0, +1$ (see also Fig. 1). Here and in the following, the dot '$\cdot$' denotes the scalar product, defined using the spacetime metric $\mathbf{g}$. Typically, the causal character of $\mathcal{I}$ is correlated with the sign of the cosmological constant, $\sigma = -\operatorname{sign}\Lambda$ (see section R.2.2 for details).

2.1 Null tetrads

To study various components of the fields, we introduce suitable orthonormal, and associated with them null tetrads. We denote the vectors of an *orthonormal tetrad* as $\mathbf{t}$, $\mathbf{q}$, $\mathbf{r}$, $\mathbf{s}$, where $\mathbf{t}$ is a future-oriented unit timelike vector. With this tetrad we associate a *null tetrad* of null vectors $\mathbf{k}$, $\mathbf{l}$, $\mathbf{m}$, $\bar{\mathbf{m}}$ by

$$\mathbf{k} = \tfrac{1}{\sqrt{2}}(\mathbf{t}+\mathbf{q})\,, \quad \mathbf{l} = \tfrac{1}{\sqrt{2}}(\mathbf{t}-\mathbf{q})\,, \quad \mathbf{m} = \tfrac{1}{\sqrt{2}}(\mathbf{r}-\mathrm{i}\,\mathbf{s})\,, \quad \bar{\mathbf{m}} = \tfrac{1}{\sqrt{2}}(\mathbf{r}+\mathrm{i}\,\mathbf{s})\,. \tag{1}$$

The normalization conditions for these tetrads are

$$-\mathbf{t}\cdot\mathbf{t} = \mathbf{q}\cdot\mathbf{q} = \mathbf{r}\cdot\mathbf{r} = \mathbf{s}\cdot\mathbf{s} = 1\,, \quad -\mathbf{k}\cdot\mathbf{l} = \mathbf{m}\cdot\bar{\mathbf{m}} = 1\,, \tag{2}$$

respectively, with all other scalar products being zero.

The crucial tetrad in our study is the *interpretation tetrad* $\mathbf{k}_{\mathrm{i}}$, $\mathbf{l}_{\mathrm{i}}$, $\mathbf{m}_{\mathrm{i}}$, $\bar{\mathbf{m}}_{\mathrm{i}}$. It is a tetrad which is parallelly transported along a null geodesic $z(\eta)$, the vector $\mathbf{k}_{\mathrm{i}}$ being tangent to the geodesic. With respect to this tetrad we define the radiative component of the field. The precise definition and description of asymptotic behavior of the interpretation tetrad was thoroughly presented in sections R.3.3 and R.3.4, where more details can be found.

Here, we are going to concentrate on the *reference tetrad* $\mathbf{k}_{\mathrm{o}}$, $\mathbf{l}_{\mathrm{o}}$, $\mathbf{m}_{\mathrm{o}}$, $\bar{\mathbf{m}}_{\mathrm{o}}$. It is a tetrad conveniently defined near the conformal infinity. It serves as the reference frame for parametrization of directions near $\mathcal{I}$. It can be defined using special features of the spacetime geometry (e.g., the Killing vectors, direction toward sources, etc.). Alternatively, it can be adapted to the studied fields — namely, it can be 'aligned' with algebraically special directions of the fields under consideration. A general situation was discussed in sections R.5.4 and R.5.5. In the present work we will offer other possible privileged definitions of the reference tetrad for algebraically simple fields of type D.

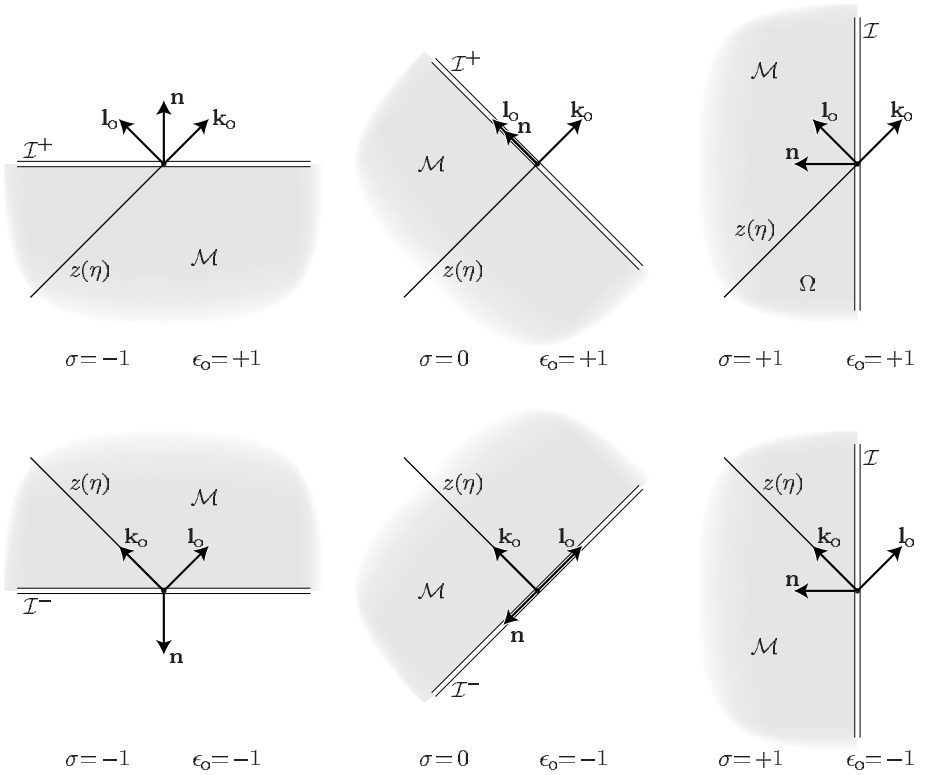

Fig. 1. The reference tetrad adjusted to conformal infinity $\mathcal{I}$ of various character, determined by σ which is a norm of the vector $\mathbf{n}$ normal to $\mathcal{I}$. If the vector $\mathbf{k}_o$ is oriented along an outgoing direction (outward from the physical spacetime $\mathcal{M}$) we have $\epsilon_o = +1$, if it is ingoing (oriented inward to $\mathcal{M}$) then $\epsilon_o = -1$.

Following [8], we require that the reference tetrad is *adjusted to conformal infinity*, i.e., that the vectors $\mathbf{k}_o$ and $\mathbf{l}_o$ satisfy the relation

$$\mathbf{n} = \epsilon_o \tfrac{1}{\sqrt{2}}(-\sigma \mathbf{k}_o + \mathbf{l}_o) \,, \tag{3}$$

where the sign $\epsilon_o = \pm 1$ indicates the outgoing/ingoing orientation of the vector $\mathbf{k}_o$ with respect to $\mathcal{I}$ (see also below). This adjustment condition guarantees that the vectors $\mathbf{k}_o$ and $\mathbf{l}_o$ are collinear with the normal $\mathbf{n}$ to $\mathcal{I}$, and normalized such that

$$\mathbf{n} = \begin{cases} \epsilon_o \, \mathbf{t}_o & \text{for a spacelike infinity } (\sigma = -1) \,, \\ -\epsilon_o \, \mathbf{q}_o & \text{for a timelike infinity } (\sigma = +1) \,, \\ \epsilon_o \, \mathbf{l}_o / \sqrt{2} & \text{for a null infinity } (\sigma = 0) \,. \end{cases} \tag{4}$$

All possible orientations of the reference tetrad with respect to $\mathcal{I}$ are shown in Fig. 1.

The normalization and adjustment conditions do not fix the reference tetrad uniquely. Additional necessary conditions — the alignment with the algebraically special directions — will be specified in Sect. 3.

2.2 Parametrization of null directions

In the following, it will be necessary to parametrize a general null direction $\mathbf{k}$ near $\mathcal{I}$. This can be done with respect to the reference tetrad by a complex *directional parameter* R:

$$\mathbf{k} \propto \mathbf{k}_{\mathrm{o}} + \bar{R}\,\mathbf{m}_{\mathrm{o}} + R\,\bar{\mathbf{m}}_{\mathrm{o}} + R\bar{R}\,\mathbf{l}_{\mathrm{o}} \,. \tag{5}$$

The value $R = \infty$ is also permitted — it corresponds to $\mathbf{k}$ oriented along $\mathbf{l}_{\mathrm{o}}$.

In addition, we introduce the *orientation parameter* ϵ which indicates whether the null direction $\mathbf{k}$ is an outgoing direction (pointing outside the spacetime), $\epsilon = +1$, or if it is an ingoing direction (pointing inside the spacetime), $\epsilon = -1$.

When the infinity $\mathcal{I}$ has a *spacelike* character, it is also possible to parametrize the null direction $\mathbf{k}$ using *spherical angles*, which specify its normalized spatial projection into $\mathcal{I}$. We define the angles θ, ϕ by

$$\mathbf{q} = \cos\theta\;\mathbf{q}_{\mathrm{o}} + \sin\theta\,(\cos\phi\;\mathbf{r}_{\mathrm{o}} + \sin\phi\;\mathbf{s}_{\mathrm{o}}) \,, \tag{6}$$

where $\mathbf{q}$ is the unit vector pointing into the spatial ($\mathbf{q}\cdot\mathbf{n} = 0$) direction given by $\mathbf{k}$, see (R.5.5). The complex parameter R of (5) is actually a stereographic representation of the spatial direction $\mathbf{q}$:

$$R = \tan\left(\tfrac{1}{2}\theta\right)\,\exp(-\mathrm{i}\phi) \,. \tag{7}$$

Near a *timelike* infinity $\mathcal{I}$ we can analogously describe null direction $\mathbf{k}$ by *pseudospherical parameters* ψ, ϕ of its projection into $\mathcal{I}$. If we label the normalized projection of $\mathbf{k}$ by $\mathbf{t}$, cf. (R.5.8), ψ and ϕ are given by

$$\mathbf{t} = \cosh\psi\;\mathbf{t}_{\mathrm{o}} + \sinh\psi\,(\cos\phi\;\mathbf{r}_{\mathrm{o}} + \sin\phi\;\mathbf{s}_{\mathrm{o}}) \,. \tag{8}$$

These parameters have to be supplemented by the orientation ϵ of $\mathbf{k}$ with respect to $\mathcal{I}$. The parameter R is the pseudostereographic representation of $\mathbf{t}$:

$$R = \tanh^{\epsilon\epsilon_{\mathrm{o}}}\left(\tfrac{1}{2}\psi\right)\,\exp(-\mathrm{i}\phi) \,. \tag{9}$$

In fact, we can introduce both these parametrizations simultaneously, independently of the causal character of the infinity, just with respect to the reference tetrad — the angles θ, ϕ using a projection onto the 3-space orthogonal to the time vector $\mathbf{t}_{\mathrm{o}}$ of the reference tetrad, and the parameters ψ, ϕ using a projection to the 2+1-space orthogonal to $\mathbf{q}_{\mathrm{o}}$. In such a case they are related by expressions

$$\tanh\psi = \sin\theta \,, \quad \sinh\psi = \tan\theta \,, \quad \cosh\psi = \cos^{-1}\theta \,, \quad \tanh\left(\tfrac{1}{2}\psi\right) = \tan\left(\tfrac{1}{2}\theta\right) \,. \tag{10}$$

If the infinity has a timelike character, all future-oriented null directions at one point at $\mathcal{I}$ naturally split into two families of outgoing and ingoing directions. The

directions of each of these families form a hemisphere which can be projected onto a unit circle, parametrized by ρ and ϕ, such that

$$\rho = \tanh\psi = \sin\theta \,, \tag{11}$$

see also figure R.3.

2.3 Asymptotic directional structure of radiation

The main result of paper [8] is derivation of the explicit dependence of the radiative component of the field on a direction along which the infinity is approached — we call this dependence the *asymptotic directional structure of radiation*.

In [8] we investigated a general spin-s field, and in more detail gravitational ($s = 2$) and electromagnetic ($s = 1$) fields. These fields can be characterized by $2s + 1$ complex components Υ_j, $j = 0, \ldots, 2s$, evaluated with respect to a null tetrad. Relation of these components to a spinor representation of the fields, and their transformation properties can be found in R.4.1 and appendix R.B. The components of gravitational and electromagnetic fields are traditionally called Ψ_j, $j = 0, \ldots, 4$, and Φ_j, $j = 0, 1, 2$, respectively — see [10] or equations (R.4.1) and (R.4.2).

To study the asymptotic behavior, we evaluated the field with respect to the interpretational tetrad — the tetrad which is parallelly transported along a null geodesic $z(\eta)$. It turned out that these field components satisfy the standard *peeling-off* property, namely that they exhibit a different fall-off in η when approaching $\mathcal{I}$, η being the affine parameter of the geodesic. The leading component of the field is the component $\Upsilon^{\mathrm{i}}_{2s}$ with the fall-off of order η^{-1}, and we call it the *radiative component*. In sections R.4.3 and R.4.4 we found that the radiative field component depends on the direction R of the null geodesic along which a fixed point at the infinity is approached. This directional structure is determined mainly by the algebraic structure of the field, and it reads

$$\Upsilon^{\mathrm{i}}_{2s} \approx \frac{1}{\eta}\, \epsilon_{\mathrm{o}}^{s} \Upsilon^{\mathrm{o}}_{2s*}\, \frac{\big(1-\sigma R_1\bar{R}\big)\big(1-\sigma R_2\bar{R}\big)\ldots\big(1-\sigma R_{2s}\bar{R}\big)}{\big(1-\sigma R\bar{R}\big)^{s}} \,. \tag{12}$$

The complex constants $R_1, \ldots, R_{2s}$ represent the *principal null directions* $\mathbf{k}_1, \ldots, \mathbf{k}_{2s}$ of the spin-s field, the sign $\sigma = \pm 1, 0$ specifies the causal character of the conformal infinity, ϵ_{o} denotes orientation of the reference tetrad, and $\Upsilon^{\mathrm{o}}_{2s*}$ is a constant normalization factor of the field evaluated with respect to the reference tetrad, $\Upsilon^{\mathrm{o}}_{2s} \approx \Upsilon^{\mathrm{o}}_{2s*}\eta^{-s-1}$ (cf. section R.4.4).

The principal null directions (PNDs) are special directions along which some of the field components vanish — see [9, 10] or section R.4.2 for a precise definition. The field of spin s has $2s$ PNDs. However, these can be degenerate and this degeneracy (or, more generally, mutual relations of all the PNDs) is called the *algebraic structure* of the field. Distinct PNDs are also called *algebraically special directions* of the field. The classification according to the degeneracy of PNDs for a gravitational field is the well-known Petrov classification.

3 Fields of type D

In this paper we wish to discuss the situation when the field has two distinct and equivalent algebraically special directions. This may occur only for fields of an *integer* spin, $s \in \mathbb{N}$, with PNDs having the degeneracy

$$\mathbf{k}_1 = \cdots = \mathbf{k}_s \quad \text{and} \quad \mathbf{k}_{s+1} = \cdots = \mathbf{k}_{2s} \,. \tag{13}$$

The directional structure (12) of such a field takes the form

$$\Upsilon^{\mathrm{i}}_{2s} \approx \frac{1}{\eta}\, \epsilon_{\mathrm{o}}^{s} \Upsilon^{\mathrm{o}}_{2s*}\, \frac{\left(1-\sigma R_1 \bar{R}\right)^s \left(1-\sigma R_{2s} \bar{R}\right)^s}{\left(1-\sigma R \bar{R}\right)^s} \,, \tag{14}$$

with the constants R_1 and R_{2s} parametrizing the two distinct PNDs. The directional dependence of the magnitude of a gravitational type-D field and of an algebraically general electromagnetic field are thus quite similar. This similarity is even closer if we recall that the square of the electromagnetic component Φ^{i}_2 is proportional to the magnitude of the Poynting vector with respect to the interpretation tetrad, $|\mathbf{S}_{\mathrm{i}}| \approx (1/4\pi) \left|\Phi^{\mathrm{i}}_2\right|^2$. Indeed, we have

$$\left|\Psi^{\mathrm{i}}_4\right| \approx \frac{1}{|\eta|}\, |\Psi^{\mathrm{o}}_{4*}|\, \frac{\left|1-\sigma R_1 \bar{R}\right|^2 \left|1-\sigma R_4 \bar{R}\right|^2}{\left|1-\sigma R \bar{R}\right|^2} \,, \tag{15}$$

$$4\pi\, |\mathbf{S}_{\mathrm{i}}| \approx \left|\Phi^{\mathrm{i}}_2\right|^2 \approx \frac{1}{\eta^2}\, |\Phi^{\mathrm{o}}_{2*}|^2\, \frac{\left|1-\sigma R_1 \bar{R}\right|^2 \left|1-\sigma R_2 \bar{R}\right|^2}{\left|1-\sigma R \bar{R}\right|^2} \,. \tag{16}$$

As discussed in section R.4.5, the form of the directional structure (12) depends on the choice of the normalization factor $\Upsilon^{\mathrm{o}}_{2s*}$. Other choices can sometimes be more convenient, in particular if the factor $\Upsilon^{\mathrm{o}}_{2s*}$ vanishes, which happens when one of the PNDs points along the direction $\mathbf{l}_{\mathrm{o}}$ of the reference tetrad. For the type-D fields there exists a more natural 'symmetric' choice of normalization of the directional structure of radiation which is guaranteed to be non-degenerate. For these fields we can define a *canonical field component*, namely, the only nonvanishing component with respect of the null tetrad associated with the PNDs (13).

Having two distinct algebraic directions $\mathbf{k}_1$ and $\mathbf{k}_{2s}$, we can define *algebraically special null tetrad* $\mathbf{k}_{\mathrm{s}}$, $\mathbf{l}_{\mathrm{s}}$, $\mathbf{m}_{\mathrm{s}}$, $\bar{\mathbf{m}}_{\mathrm{s}}$ (and associated orthonormal tetrad $\mathbf{t}_{\mathrm{s}}$, $\mathbf{q}_{\mathrm{s}}$, $\mathbf{r}_{\mathrm{s}}$, $\mathbf{s}_{\mathrm{s}}$) by requiring that $\mathbf{k}_{\mathrm{s}}$, $\mathbf{l}_{\mathrm{s}}$ are *proportional* to the PNDs and future-oriented, and that the spatial vector $\mathbf{s}_{\mathrm{s}}$ is *tangent* to $\mathcal{I}$,

$$\mathbf{k}_{\mathrm{s}} \propto \mathbf{k}_1 \,, \quad \mathbf{l}_{\mathrm{s}} \propto \mathbf{k}_{2s} \,, \quad \mathbf{s}_{\mathrm{s}} \cdot \mathbf{n} = 0 \,. \tag{17}$$

For PNDs, which are not tangent to the conformal infinity, the normalization of null vectors $\mathbf{k}_{\mathrm{s}}$, $\mathbf{l}_{\mathrm{s}}$ can be fixed by condition

$$\epsilon_1\, \mathbf{k}_{\mathrm{s}} \cdot \mathbf{n} = \epsilon_{2s}\, \mathbf{l}_{\mathrm{s}} \cdot \mathbf{n} \,, \tag{18}$$

where ϵ_1, $\epsilon_{2s} = \pm 1$ parametrize orientations of the PNDs with respect to $\mathcal{I}$. The special case of PNDs tangent to $\mathcal{I}$ will be discussed below.

Using the definition of PNDs (see section R.4.2), we find that the field components with respect to the algebraically special tetrad have very special form — only the component $\Upsilon^{\rm s}_s$ is nonvanishing ($\Psi^{\rm s}_2$ for gravitational and $\Phi^{\rm s}_1$ for electromagnetic fields). This component is, in fact, independent of the choice of the spatial vectors $\mathbf{r}_{\rm s}$, $\mathbf{s}_{\rm s}$, and thus it does not depend on the normal vector $\mathbf{n}$, which we used in the definition (17). It also does not depend on the normalization (18), provided that the normalization (2) is satisfied. We shall use the privileged component $\Upsilon^{\rm s}_s$ for the normalization of the directional structure of radiation. However, the algebraically special tetrad is *not* adjusted to the infinity (cf. condition (3)) since $\mathbf{k}_{\rm s}$ and $\mathbf{l}_{\rm s}$ are not in general collinear with $\mathbf{n}$ and thus it cannot be used as a reference tetrad.

Nevertheless, we can define privileged reference tetrad which is 'somehow aligned' with the algebraically special tetrad, and which shares some of the symmetries of the geometric situation. We shall always assume that the reference tetrad satisfies the normalization and adjustment conditions (2), (3), and we set $\mathbf{s}_{\rm o} = \mathbf{s}_{\rm s}$. This is, however, still not sufficient to completely fix the reference tetrad. The remaining necessary condition cannot be prescribed in general — we have to discuss separately several possible cases, depending on the character of the infinity $\mathcal{I}$, and on the orientation of the PNDs with respect to $\mathcal{I}$.

Below we shall define the reference tetrad for all possible cases. We shall present the relation between the component $\Upsilon^{\rm o}_{2s}$ and the canonical component $\Upsilon^{\rm s}_s$, which can be substituted into the directional structure (14). Finally, we shall rewrite the results in terms of the angular variables introduced with respect to the reference tetrad.

3.1 Spacelike $\mathcal{I}$

We begin with a spacelike conformal infinity, $\sigma = -1$. In this case the two distinct future-oriented algebraically special directions are either both ingoing or both outgoing, and we accordingly set the orientation $\epsilon_{\rm o}$ of the reference tetrad. We define the reference tetrad by conditions

$$\mathbf{q}_{\rm o} = \mathbf{q}_{\rm s} \,, \quad \mathbf{s}_{\rm o} = \mathbf{s}_{\rm s} \,, \quad \epsilon_{\rm o} = \epsilon_1 = \epsilon_{2s} \,, \tag{19}$$

and by adjustment condition (4). It follows that the algebraically special directions $\mathbf{k}_{\rm s}$ and $\mathbf{l}_{\rm s}$ are parametrized with respect to the reference tetrad by a single parameter $\theta_{\rm s}$ as

$$\begin{aligned} \mathbf{k}_{\rm s} &= \tfrac{1}{\sqrt{2}} \cos^{-1}\theta_{\rm s} \left(\mathbf{t}_{\rm o} + \cos\theta_{\rm s}\, \mathbf{q}_{\rm o} + \sin\theta_{\rm s}\, \mathbf{r}_{\rm o}\right) , \\ \mathbf{l}_{\rm s} &= \tfrac{1}{\sqrt{2}} \cos^{-1}\theta_{\rm s} \left(\mathbf{t}_{\rm o} - \cos\theta_{\rm s}\, \mathbf{q}_{\rm o} + \sin\theta_{\rm s}\, \mathbf{r}_{\rm o}\right) . \end{aligned} \tag{20}$$

The algebraically special and reference tetrads are thus related by

$$\mathbf{t}_{\rm s} = \cos^{-1}\theta_{\rm s}\, \mathbf{t}_{\rm o} + \tan\theta_{\rm s}\, \mathbf{r}_{\rm o} \,, \quad \mathbf{q}_{\rm s} = \mathbf{q}_{\rm o} \,, \quad \mathbf{r}_{\rm s} = \cos^{-1}\theta_{\rm s}\, \mathbf{r}_{\rm o} + \tan\theta_{\rm s}\, \mathbf{t}_{\rm o} \,, \quad \mathbf{s}_{\rm s} = \mathbf{s}_{\rm o} \,, \tag{21}$$

Pavel Krtouš and Jiří Podolský

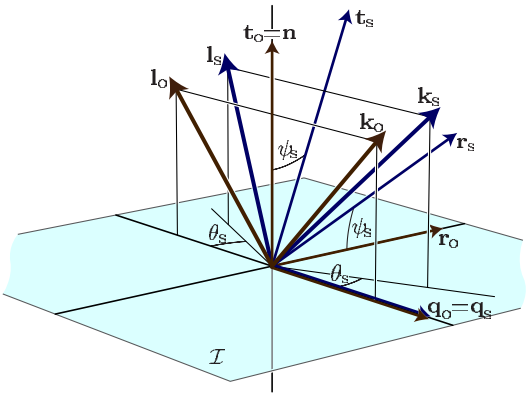

Fig. 2. Algebraically special and reference tetrads at a spacelike infinity. Vectors $\mathbf{k}_o$, $\mathbf{l}_o$ ($\mathbf{k}_s$, $\mathbf{l}_s$, respectively) of the null tetrad, and $\mathbf{t}_o$, $\mathbf{q}_o$, $\mathbf{r}_o$ ($\mathbf{t}_s$, $\mathbf{q}_s$, $\mathbf{r}_s$) of the orthonormal reference (algebraically special, respectively) tetrad are shown; the direction $\mathbf{s}_o = \mathbf{s}_s$ tangent to $\mathcal{I}$ and orthogonal to PNDs is hidden. The vectors $\mathbf{k}_s$, $\mathbf{l}_s$ are aligned with algebraically special directions (degenerate PNDs), $\mathbf{t}_o$ is normal to the infinity $\mathcal{I}$, and $\mathbf{q}_o$, $\mathbf{r}_o$ are tangent to $\mathcal{I}$. The relation of both the tetrads is parametrized by the angle θ_s between $\mathbf{q}_o$ and the projection of $\mathbf{k}_s$ onto $\mathcal{I}$. The special tetrad can be obtained from the reference tetrad by a boost in $\mathbf{t}_o$-$\mathbf{r}_o$ plane with rapidity parameter ψ_s given by $\sinh\psi_s = \tan\theta_s$, cf. (21).

which is actually a boost in $\mathbf{t}_o$-$\mathbf{r}_o$ plane with rapidity parameter ψ_s related to θ_s by (10), see Fig. 2.

Inspecting the spatial projections of $\mathbf{k}_s$ and $\mathbf{l}_s$ onto conformal infinity $\mathcal{I}$, we find that their angular coordinates with respect to the reference tetrad are $\theta_1 = \theta_s$, $\phi_1 = 0$, and $\theta_{2s} = \pi - \theta_s$, $\phi_{2s} = 0$, respectively. It means that the complex parameters R_1 and R_{2s} of both these algebraic special directions are

$$R_1 = \tan\left(\tfrac{1}{2}\theta_s\right) \ , \quad R_{2s} = \cot\left(\tfrac{1}{2}\theta_s\right) \ . \tag{22}$$

Straightforward calculation shows that the transformation (21) from the algebraically special to the reference tetrad can be decomposed into boost (R.3.5), subsequent null rotation with $\mathbf{k}$ fixed (R.3.4), and null rotation with $\mathbf{l}$ fixed (R.3.3), given by the parameters $B = 2(1+\cos^{-1}\theta_s)^{-1}$, $L = -\frac{1}{2}\tan\theta_s$, and $K = -\tan(\theta_s/2)$. Applying these transformations to the field components (relations (R.4.6), (R.4.5), and (R.4.4)) we easily find that

$$\Upsilon^o_{2s} = \binom{2s}{s} \bar{L}^s \, \Upsilon^s_s = (-1)^s \frac{(2s)!}{2^s (s!)^2} \tan^s\theta_s \, \Upsilon^s_s \ . \tag{23}$$

For gravitational and electromagnetic fields we can write explicit expressions for

all field components with respect to the reference tetrad as

$$\Psi_0^{\mathrm{o}} = \Psi_4^{\mathrm{o}} = \frac{3}{2}\tan^2\theta_{\mathrm{s}}\,\Psi_2^{\mathrm{s}}\,, \quad \Psi_1^{\mathrm{o}} = \Psi_3^{\mathrm{o}} = -\frac{3}{2}\frac{\tan\theta_{\mathrm{s}}}{\cos\theta_{\mathrm{s}}}\,\Psi_2^{\mathrm{s}}\,, \quad \Psi_2^{\mathrm{o}} = \Big(1+\frac{3}{2}\tan^2\theta_{\mathrm{s}}\Big)\Psi_2^{\mathrm{s}}\,, \tag{24}$$

$$\Phi_0^{\mathrm{o}} = \Phi_2^{\mathrm{o}} = -\tan\theta_{\mathrm{s}}\,\Phi_1^{\mathrm{s}}\,, \quad \Phi_1^{\mathrm{o}} = \cos^{-1}\theta_{\mathrm{s}}\,\Phi_1^{\mathrm{s}}\,. \tag{25}$$

Following the discussion in section R.4.4 we assume asymptotic behavior (R.4.18), i.e., $\Upsilon_j^{\mathrm{o}} \approx \Upsilon_{j*}^{\mathrm{o}}\,\eta^{-s-1}$ with constant coefficients $\Upsilon_{j*}^{\mathrm{o}}$. Similarly, we introduce the coefficient $\Upsilon_{s*}^{\mathrm{s}}$ by $\Upsilon_s^{\mathrm{s}} \approx \Upsilon_{s*}^{\mathrm{s}}\,\eta^{-s-1}$. Clearly, the relations (23)–(25) hold also in their 'stared' forms.

Substituting (22), the 'stared' version of (23), (7), and $\sigma = +1$ into (14) we finally obtain the asymptotic directional structure of radiation for type-D fields

$$\Upsilon_{2s}^{\mathrm{i}} \approx \frac{(-\epsilon_{\mathrm{o}})^s}{\eta}\,\frac{(2s)!}{2^s(s!)^2}\,\Upsilon_{s*}^{\mathrm{s}}\Big[\frac{\exp(\mathrm{i}\phi)}{\cos\theta_{\mathrm{s}}}\,\big(\sin\theta + \sin\theta_{\mathrm{s}}\cos\phi - \mathrm{i}\sin\theta_{\mathrm{s}}\cos\theta\sin\phi\big)\Big]^s\,. \tag{26}$$

The null direction along which the field is measured is parametrized by angles θ, ϕ, the field itself is characterized by the normalization component $\Upsilon_{s*}^{\mathrm{s}}$ and by the parameter θ_{s} which encodes the directions of the algebraically special directions with respect to a spacelike infinity $\mathcal{I}$. As discussed in section R.4.5, only the magnitude of this radiative component has a physical meaning. For the magnitude

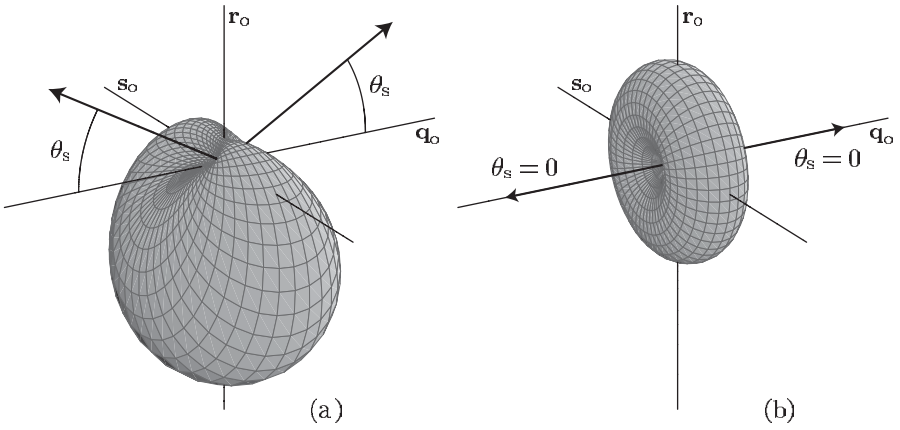

Fig. 3. Directional structure of radiation near a spacelike infinity. Directions in the diagrams correspond to spatial directions (projections onto $\mathcal{I}$) of null geodesics along which the infinity is approached. The diagrams show the directional dependence of the magnitude of the radiative-field component (27) (or (28)). The arrows depict the directions which are spatially opposite to algebraically special directions (PNDs); the radiative component evaluated along the geodesics in these directions is asymptotically vanishing. The diagram (a) shows a general orientation of algebraically special directions, the diagram (b) corresponds to the case, when both distinct PNDs are spatially opposite.

of the $\Psi_4^{\rm i}$ component of the gravitational field and for the Poynting vector of the electromagnetic field we thus obtain

$$\left|\Psi_4^{\rm i}\right| \approx \frac{1}{|\eta|}\,\frac{3}{2}\,\frac{|\Psi_{2*}^{\rm s}|}{\cos^2\theta_{\rm s}}\left|\sin\theta+\sin\theta_{\rm s}\cos\phi-{\rm i}\sin\theta_{\rm s}\cos\theta\sin\phi\right|^2 , \tag{27}$$

$$4\pi\,|\mathbf{S}_{\rm i}| \approx \left|\Phi_2^{\rm i}\right|^2 \approx \frac{1}{\eta^2}\,\frac{\left|\Phi_{1*}^{\rm s}\right|^2}{\cos^2\theta_{\rm s}}\left|\sin\theta+\sin\theta_{\rm s}\cos\phi-{\rm i}\sin\theta_{\rm s}\cos\theta\sin\phi\right|^2 . \tag{28}$$

These are exactly the expressions for the asymptotic directional structure of radiation as derived in [11] for test electromagnetic field of accelerated charges in de Sitter spacetime, and for gravitational field and electromagnetic fields of the C-metric spacetime with $\Lambda>0$, as presented in [1]. This directional structure is illustrated in Fig. 3.

3.2 Timelike $\mathcal{I}$ with non-tangent PNDs, $\epsilon_1 \neq \epsilon_{2s}$

Now we shall study the situation near a timelike conformal infinity ($\sigma=-1$), when both distinct algebraic directions are not tangent to $\mathcal{I}$, such that one of them is outgoing and the other ingoing, $\epsilon_1\neq\epsilon_{2s}$. In this case we require that the orientation $\epsilon_{\rm o}$ of the reference tetrad is adjusted to ϵ_1, and that $\mathbf{t}_{\rm s}$ is aligned along $\mathbf{t}_{\rm o}$,

$$\mathbf{t}_{\rm o}=\mathbf{t}_{\rm s}\ ,\quad \mathbf{s}_{\rm o}=\mathbf{s}_{\rm s}\ ,\quad \epsilon_{\rm o}=\epsilon_1=-\epsilon_{2s}\ , \tag{29}$$

together with the adjustment condition (4). Again, the algebraically special directions $\mathbf{k}_{\rm s}$ and $\mathbf{l}_{\rm s}$ are parametrized with respect to the reference tetrad by a single parameter $\theta_{\rm s}$:

$$\begin{aligned}\mathbf{k}_{\rm s}&=\tfrac{1}{\sqrt{2}}\left(\mathbf{t}_{\rm o}+\cos\theta_{\rm s}\,\mathbf{q}_{\rm o}+\sin\theta_{\rm s}\,\mathbf{r}_{\rm o}\right)\ ,\\ \mathbf{l}_{\rm s}&=\tfrac{1}{\sqrt{2}}\left(\mathbf{t}_{\rm o}-\cos\theta_{\rm s}\,\mathbf{q}_{\rm o}-\sin\theta_{\rm s}\,\mathbf{r}_{\rm o}\right)\ .\end{aligned} \tag{30}$$

The algebraically special and reference tetrads are thus related by

$$\mathbf{t}_{\rm s}=\mathbf{t}_{\rm o}\ ,\quad \mathbf{q}_{\rm s}=\cos\theta_{\rm s}\,\mathbf{q}_{\rm o}+\sin\theta_{\rm s}\,\mathbf{r}_{\rm o}\ ,\quad \mathbf{r}_{\rm s}=-\sin\theta_{\rm s}\,\mathbf{q}_{\rm o}+\cos\theta_{\rm s}\,\mathbf{r}_{\rm o}\ ,\quad \mathbf{s}_{\rm s}=\mathbf{s}_{\rm o}\ , \tag{31}$$

which is a spatial rotation in $\mathbf{q}_{\rm o}$-$\mathbf{r}_{\rm o}$ plane by angle $\theta_{\rm s}$, see Fig. 4a.

To read out the normalized projection into $\mathcal{I}$ of the null vectors $\mathbf{k}_{\rm s}$, $\mathbf{l}_{\rm s}$, it is useful to rewrite (30) in a different way

$$\begin{aligned}\mathbf{k}_{\rm s}&=\tfrac{1}{\sqrt{2}}\cosh^{-1}\psi_{\rm s}\left(\mathbf{q}_{\rm o}+\cosh\psi_{\rm s}\,\mathbf{t}_{\rm o}+\sinh\psi_{\rm s}\,\mathbf{r}_{\rm o}\right)\ ,\\ \mathbf{l}_{\rm s}&=\tfrac{1}{\sqrt{2}}\cosh^{-1}\psi_{\rm s}\left(-\mathbf{q}_{\rm o}+\cosh\psi_{\rm s}\,\mathbf{t}_{\rm o}-\sinh\psi_{\rm s}\,\mathbf{r}_{\rm o}\right)\ ,\end{aligned} \tag{32}$$

where we have used the parameter $\psi_{\rm s}$ instead of $\theta_{\rm s}$ related by (10). Comparing the normalized projections of $\mathbf{k}_1=\mathbf{k}_{\rm s}$ and $\mathbf{k}_{2s}=\mathbf{l}_{\rm s}$ with (8), we find that the pseudospherical parameters ψ, ϕ, ϵ of the algebraically special directions are $\psi_1=\psi_{\rm s}$, $\phi_1=0$, $\epsilon_1=\epsilon_{\rm o}$, and $\psi_{2s}=\psi_{\rm s}$, $\phi_{2s}=\pi$, $\epsilon_{2s}=-\epsilon_{\rm o}$ respectively. The corresponding complex parameters are

$$R_1=\tanh\left(\tfrac{1}{2}\psi_{\rm s}\right)\ ,\quad R_{2s}=-\coth\left(\tfrac{1}{2}\psi_{\rm s}\right)\ . \tag{33}$$

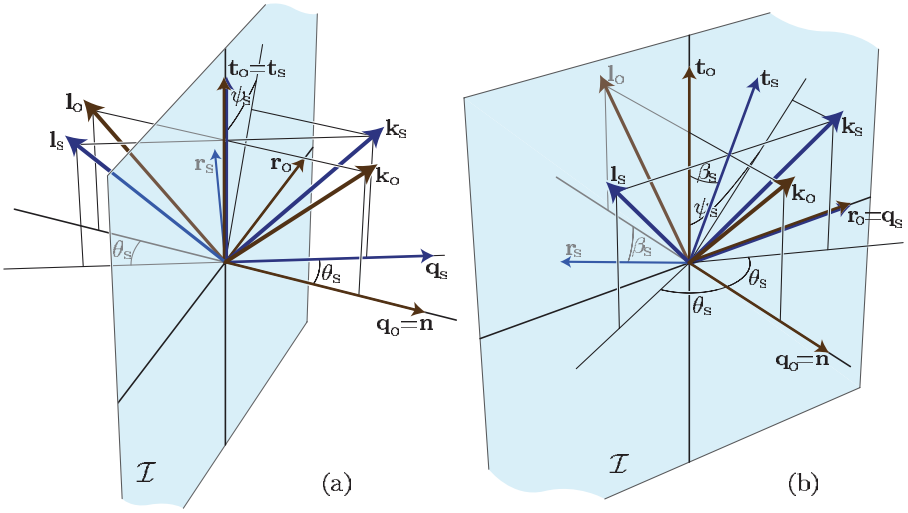

Fig. 4. Algebraically special and reference tetrads near a timelike infinity. Vectors $\mathbf{k}_o$, $\mathbf{l}_o$ ($\mathbf{k}_s$, $\mathbf{l}_s$) of the null reference (algebraically special, respectively) tetrad are shown. The axes correspond to the timelike direction $\mathbf{t}_o$ and the spatial directions $\mathbf{q}_o$, $\mathbf{r}_o$ of the reference tetrad. The direction $\mathbf{s}_o = \mathbf{s}_s$ tangent to $\mathcal{I}$ and orthogonal to PNDs is hidden. The vectors $\mathbf{k}_s$, $\mathbf{l}_s$ are aligned with the algebraically special directions (degenerate PNDs), $\mathbf{q}_o$ is normal to infinity $\mathcal{I}$ and $\mathbf{t}_o$, $\mathbf{r}_o$ are tangent to it. The vectors $\mathbf{t}_s$, $\mathbf{q}_s$, $\mathbf{r}_s$ of the algebraically special tetrad are drawn only in diagrams (a), (b) and (d); for simplicity they are omitted in the diagram (c), but see (53). Different diagrams correspond to different orientations of PNDs with respect to the infinity $\mathcal{I}$: in the diagram (a) one PND is ingoing and one is outgoing (cf. Subsect. 3.2), in (b) both PNDs are outgoing (or ingoing, respectively, cf. Subsect. 3.3), the diagram (c) shows the situation when one PND is tangent to $\mathcal{I}$ (Subsect. 3.4), and, finally, both PNDs are tangent in (d) (Subsect. 3.5). The relation of the reference and algebraically special tetrads in the generic cases (a) and (b) can be parametrized by the angle θ_s (the angle between $\mathbf{q}_o$ and the projection of $\mathbf{k}_s$ to the space normal to $\mathbf{t}_o$), or by pseudospherical parameter ψ_s (the lorenzian angle between $\mathbf{t}_o$ and the projection of $\mathbf{k}_s$ to $\mathcal{I}$). These parameters are related by (10). In the case (a) the special tetrad can be obtained from the reference tetrad by a spatial rotation in $\mathbf{q}_o$-$\mathbf{r}_o$ plane by θ_s, cf. (31); in the case (b) the special tetrad is the reference tetrad boosted by rapidity β_s given by $\sinh\beta_s = \cot\theta_s = \sinh^{-1}\psi_s$, cf. (42). (*continued*)

Again, the transformation (31) can be decomposed into boost, null rotation with $\mathbf{k}$ fixed, and null rotation with $\mathbf{l}$ fixed, given by $B = 2\cosh\psi_s(1+\cosh\psi_s)^{-1}$, $L = \frac{1}{2}\tanh\psi_s$, and $K = -\tanh(\psi_s/2)$. Applying these transformations to the field components we obtain

$$\Upsilon^{o}_{2s} = \frac{(2s)!}{2^s(s!)^2}\tanh^s\psi_s\,\Upsilon^{s}_{s}\,, \tag{34}$$

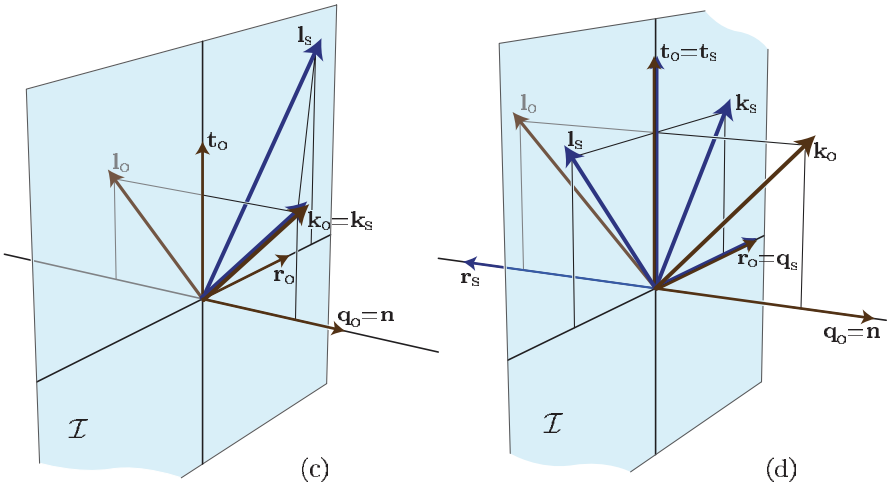

Fig. 4. (*continued*)

and, in more detail, for gravitational and electromagnetic fields

$$\Psi_0^\mathrm{o} = \Psi_4^\mathrm{o} = \tfrac{3}{2}\tanh^2\psi_\mathrm{s}\,\Psi_2^\mathrm{s}\,, \quad -\Psi_1^\mathrm{o} = \Psi_3^\mathrm{o} = \frac{3}{2}\frac{\tanh\psi_\mathrm{s}}{\cosh\psi_\mathrm{s}}\,\Psi_2^\mathrm{s}\,, \qquad \Psi_2^\mathrm{o} = \left(1-\tfrac{3}{2}\tanh^2\psi_\mathrm{s}\right)\Psi_2^\mathrm{s}\,, \tag{35}$$

$$-\Phi_0^\mathrm{o} = \Phi_2^\mathrm{o} = \tanh\psi_\mathrm{s}\,\Phi_1^\mathrm{s}\,, \quad \Phi_1^\mathrm{o} = \cosh^{-1}\psi_\mathrm{s}\,\Phi_1^\mathrm{s}\,. \tag{36}$$

Substituting (33), 'stared' version of (34), (9), and $\sigma = +1$ into expression (14), we obtain the asymptotic directional structure of radiation in the form

$$\Upsilon^\mathrm{i}_{2s} \approx \frac{\epsilon^s}{\eta}\,\frac{(2s)!}{2^s(s!)^2}\,\Upsilon^\mathrm{s}_{s*}\left[\frac{\exp(\mathrm{i}\phi)}{\cosh\psi_\mathrm{s}}\left(\sinh\psi + \epsilon\epsilon_\mathrm{o}\sinh\psi_\mathrm{s}\cos\phi - \mathrm{i}\sinh\psi_\mathrm{s}\cosh\psi\sin\phi\right)\right]^s . \tag{37}$$

The direction is given by pseudospherical parameters ψ, ϕ, ϵ, the field is characterized by the component Υ^s_{s*} and by the parameter ψ_s, which fixes the orientation of the algebraically special directions with respect to infinity $\mathcal{I}$. Again, only the magnitude of component Υ^i_{2s} has a physical meaning so that

$$\left|\Psi_4^\mathrm{i}\right| \approx \frac{1}{|\eta|}\,\frac{3}{2}\,\frac{|\Psi^\mathrm{s}_{2*}|}{\cosh^2\psi_\mathrm{s}}\left|\sinh\psi + \epsilon\epsilon_\mathrm{o}\sinh\psi_\mathrm{s}\cos\phi - \mathrm{i}\sinh\psi_\mathrm{s}\cosh\psi\sin\phi\right|^2 , \tag{38}$$

$$4\pi\,|\mathbf{S}_\mathrm{i}| \approx \left|\Phi_2^\mathrm{i}\right|^2 \approx \frac{1}{\eta^2}\,\frac{|\Phi^\mathrm{s}_{1*}|^2}{\cosh^2\psi_\mathrm{s}}\left|\sinh\psi + \epsilon\epsilon_\mathrm{o}\sinh\psi_\mathrm{s}\cos\phi - \mathrm{i}\sinh\psi_\mathrm{s}\cosh\psi\sin\phi\right|^2 . \tag{39}$$

This directional structure is illustrated in Fig. 5a.

3.3 Timelike $\mathcal{I}$ with non-tangent PNDs, $\epsilon_1 = \epsilon_{2s}$

In the previous case we have studied the directional structure of radiation near a timelike $\mathcal{I}$ with two PNDs oriented in opposite directions with respect to the infinity. Now, we shall discuss the situation when both PNDs are outgoing, or both ingoing, $\epsilon_1 = \epsilon_{2s}$. The derivation of the directional structure is similar to the previous case and we shall thus sketch it only briefly.

The reference tetrad is fixed by the conditions

$$\mathbf{r}_{\rm o} = \mathbf{q}_{\rm s} \ , \quad \mathbf{s}_{\rm o} = \mathbf{s}_{\rm s} \ , \quad \epsilon_{\rm o} = \epsilon_1 = \epsilon_{2s} \ , \tag{40}$$

together with the adjustment condition (4). Therefore

$$\begin{aligned} \mathbf{k}_{\rm s} &= \tfrac{1}{\sqrt{2}} \, \sin^{-1}\theta_{\rm s} \left(\mathbf{t}_{\rm o} + \cos\theta_{\rm s} \, \mathbf{q}_{\rm o} + \sin\theta_{\rm s} \, \mathbf{r}_{\rm o} \right) \\ &= \tfrac{1}{\sqrt{2}} \sinh^{-1} \psi_{\rm s} \left(\mathbf{q}_{\rm o} + \cosh\psi_{\rm s} \, \mathbf{t}_{\rm o} + \sinh\psi_{\rm s} \, \mathbf{r}_{\rm o} \right) , \\ \mathbf{l}_{\rm s} &= \tfrac{1}{\sqrt{2}} \, \sin^{-1}\theta_{\rm s} \left(\mathbf{t}_{\rm o} + \cos\theta_{\rm s} \, \mathbf{q}_{\rm o} - \sin\theta_{\rm s} \, \mathbf{r}_{\rm o} \right) \\ &= \tfrac{1}{\sqrt{2}} \sinh^{-1} \psi_{\rm s} \left(\mathbf{q}_{\rm o} + \cosh\psi_{\rm s} \, \mathbf{t}_{\rm o} - \sinh\psi_{\rm s} \, \mathbf{r}_{\rm o} \right) , \end{aligned} \tag{41}$$

where parameters $\theta_{\rm s}$ and $\psi_{\rm s}$ are again related by Eqs. (10). The algebraically special and reference tetrads are thus

$$\mathbf{t}_{\rm s} = \sin^{-1}\theta_{\rm s} \, \mathbf{t}_{\rm o} + \cot\theta_{\rm s} \, \mathbf{q}_{\rm o} \ , \quad \mathbf{q}_{\rm s} = \mathbf{r}_{\rm o} \ , \quad -\mathbf{r}_{\rm s} = \cot\theta_{\rm s} \, \mathbf{t}_{\rm o} + \sin^{-1}\theta_{\rm s} \, \mathbf{q}_{\rm o} \ , \quad \mathbf{s}_{\rm s} = \mathbf{s}_{\rm o} \ , \tag{42}$$

see Fig. 4(b). Pseudospherical parameters ψ, ϕ, ϵ of projections of the PNDs into $\mathcal{I}$ are $\psi_1 = \psi_{\rm s}$, $\phi_1 = 0$, $\epsilon_1 = \epsilon_{\rm o}$ and $\psi_{2s} = \psi_{\rm s}$, $\phi_{2s} = \pi$, $\epsilon_{2s} = \epsilon_{\rm o}$, respectively, i.e.,

$$R_1 = \tanh(\tfrac{1}{2}\psi_{\rm s}) \ , \quad R_{2s} = -\tanh(\tfrac{1}{2}\psi_{\rm s}) \ . \tag{43}$$

The transformation from the algebraically special to the reference tetrad can be decomposed into boost (R.3.5), null rotation with $\mathbf{k}$ fixed (R.3.4), and null rotation with $\mathbf{l}$ fixed (R.3.3) with parameters $B = 2\tanh(\psi_{\rm s}/2)$, $L = \frac{1}{2}\coth(\psi_{\rm s}/2)$, and $K = -\tanh(\psi_{\rm s}/2)$. For the field components we obtain

$$\Upsilon^{\rm o}_{2s} = \frac{(2s)!}{2^s (s!)^2} \coth^s \frac{\psi_{\rm s}}{2} \, \Upsilon^{\rm s}_s \ , \tag{44}$$

and, in more detail, for gravitational and electromagnetic fields

$$\Psi^{\rm o}_0 = \tfrac{3}{2} \tanh^2 \left(\tfrac{1}{2}\psi_{\rm s}\right) \, \Psi^{\rm s}_2 \ , \quad \Psi^{\rm o}_2 = -\tfrac{1}{2}\Psi^{\rm s}_2 \ , \quad \Psi^{\rm o}_4 = \tfrac{3}{2} \coth^2 \left(\tfrac{1}{2}\psi_{\rm s}\right) \, \Psi^{\rm s}_2 \ , \quad \Psi^{\rm o}_1 = \Psi^{\rm o}_3 = 0 \ , \tag{45}$$

$$\Phi^{\rm o}_0 = -\tanh\left(\tfrac{1}{2}\psi_{\rm s}\right) \, \Phi^{\rm s}_1 \ , \quad \Phi^{\rm o}_1 = 0 \ , \quad \Phi^{\rm o}_2 = \cot\left(\tfrac{1}{2}\psi_{\rm s}\right) \, \Phi^{\rm s}_1 \ . \tag{46}$$

Substituting into the expression (14) we finally obtain

$$\begin{aligned} \Upsilon^{\rm i}_{2s} \approx{}& \frac{\epsilon^s}{\eta} \, \frac{(2s)!}{2^s (s!)^2} \, \Upsilon^{\rm s}_{s*} \\ &\times \left[\frac{\exp(\mathrm{i}\phi)}{\sinh\psi_{\rm s}} \left((\cosh\psi + \epsilon\epsilon_{\rm o}\cosh\psi_{\rm s})\cos\phi - \mathrm{i}(\epsilon\epsilon_{\rm o} + \cosh\psi_{\rm s}\cosh\psi)\sin\phi \right) \right]^s . \end{aligned} \tag{47}$$

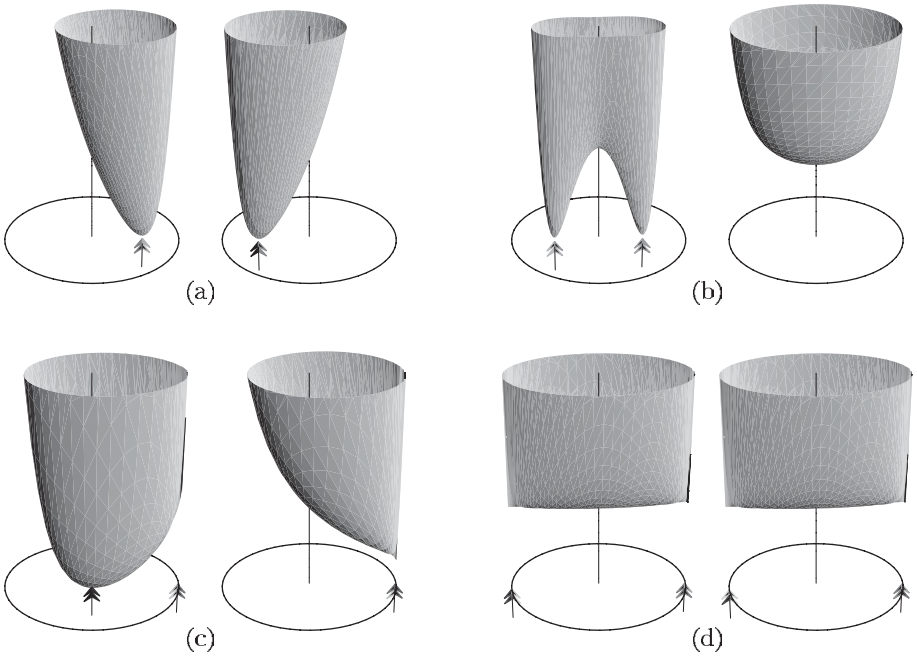

Fig. 5. Directional structure of gravitational radiation near a timelike infinity. The four diagrams, each consisting of a pair of radiation patterns, correspond to different orientation of algebraically special directions with respect to the infinity $\mathcal{I}$: (a) one PND outgoing and one ingoing (cf. Subsect. 3.2), (b) both PNDs outgoing (Subsect. 3.3; the case with both PNDs ingoing is analogous), (c) one PND tangent to $\mathcal{I}$ and one outgoing (Subsect. 3.4), (d) both PNDs tangent to $\mathcal{I}$ (Subsect. 3.5). In each diagram the circles in horizontal plane represent spatial projections of hemispheres of ingoing (left circle) and outgoing (right circle) directions. The circles are parametrized by coordinates ρ, ϕ defined in Subsect. 2.2, cf. Eq. (11). On the vertical axis the magnitude of the radiative field component is plotted (cf. (38), (49), (59) and (69)). The arrows indicate mirror reflections with respect to $\mathcal{I}$ of the algebraically special directions (PNDs). The radiative component evaluated along the geodesics in these directions is (for non-tangent PNDs) asymptotically vanishing. The radiative component diverges for unphysical geodesics tangent to $\mathcal{I}$ (the border of the circles) due to fixed normalization of the null directions — see section R.5.5.

The phase of this component is unphysical, its magnitude can be put into the form

$$|\Upsilon^{\mathrm{i}}_{2s}| \approx \frac{1}{|\eta|}\,\frac{(2s)!}{2^s(s!)^2}\;|\Upsilon^{\mathrm{s}}_{s*}|\;\Big(\sinh^{-2}\!\psi_{\mathrm{s}}\,\big(\cosh\psi_{\mathrm{s}}+\epsilon\epsilon_{\mathrm{o}}\cosh\psi\big)^2+\sinh^2\psi\sin^2\phi\Big)^{s/2}. \tag{48}$$

For gravitational and electromagnetic fields it gives

$$|\Psi^{\mathrm{i}}_{4}| \approx \frac{1}{|\eta|}\,\frac{3}{2}|\Psi^{\mathrm{s}}_{2*}|\,\Big(\sinh^{-2}\!\psi_{\mathrm{s}}\,\big(\cosh\psi_{\mathrm{s}}+\epsilon\epsilon_{\mathrm{o}}\cosh\psi\big)^2+\sinh^2\psi\sin^2\phi\Big)\,, \tag{49}$$

$$4\pi\,|\mathbf{S}_{\rm i}| \approx \left|\Phi_2^{\rm i}\right|^2 \approx \frac{1}{\eta^2}\,|\Phi_{1*}^{\rm s}|^2\left(\sinh^{-2}\psi_{\rm s}\left(\cosh\psi_{\rm s}+\epsilon\epsilon_{\rm o}\cosh\psi\right)^2+\sinh^2\psi\sin^2\phi\right), \tag{50}$$

which is illustrated in Fig. 5b.

3.4 Timelike $\mathcal{I}$, one PND tangent to $\mathcal{I}$

Until now we have concentrated on a generic orientation of algebraically special directions with respect to the conformal infinity. In this and the next sections we are going to study the special cases when the PNDs are *tangent* to $\mathcal{I}$. This can only occur for timelike or null conformal infinity, the latter case will be discussed in Subsect. 3.6.

First, we assume that only one of two distinct PNDs, say $\mathbf{k}_{2s}$, is tangent to $\mathcal{I}$. Let us note that in such a case we require normalization (18) only for the vector $\mathbf{k}_{\rm s}\propto\mathbf{k}_1$, the normalization of the other PND $\mathbf{l}_{\rm s}$ is fixed by the condition $\mathbf{k}_{\rm s}\cdot\mathbf{l}_{\rm s}=-1$. We use the PND $\mathbf{k}_{\rm s}$ as the vector $\mathbf{k}_{\rm o}$, i.e., we define the reference tetrad by conditions

$$\mathbf{k}_{\rm o}=\mathbf{k}_{\rm s}\,,\quad \mathbf{s}_{\rm o}=\mathbf{s}_{\rm s}\,,\quad \epsilon_{\rm o}=\epsilon_1\,, \tag{51}$$

together with the condition (4). The algebraically special directions $\mathbf{k}_{\rm s}$ and $\mathbf{l}_{\rm s}$ are then given in terms of the reference tetrad as

$$\mathbf{k}_{\rm s}=\frac{1}{\sqrt{2}}\left(\mathbf{t}_{\rm o}+\mathbf{q}_{\rm o}\right),\quad \mathbf{l}_{\rm s}=\sqrt{2}\left(\mathbf{t}_{\rm o}+\mathbf{r}_{\rm o}\right), \tag{52}$$

see Fig. 4c. The tetrads are related by

$$\mathbf{t}_{\rm s}=\tfrac{3}{2}\mathbf{t}_{\rm o}+\tfrac{1}{2}\mathbf{q}_{\rm o}+\mathbf{r}_{\rm o}\,,\quad \mathbf{q}_{\rm s}=-\tfrac{1}{2}\mathbf{t}_{\rm o}+\tfrac{1}{2}\mathbf{q}_{\rm o}-\mathbf{r}_{\rm o}\,,\quad \mathbf{r}_{\rm s}=\mathbf{t}_{\rm o}+\mathbf{q}_{\rm o}+\mathbf{r}_{\rm o}\,,\quad \mathbf{s}_{\rm s}=\mathbf{s}_{\rm o}\,. \tag{53}$$

Complex parametrizations of $\mathbf{k}_1$ and $\mathbf{k}_{2s}$ are then

$$R_1=0\,,\quad R_{2s}=+1\,. \tag{54}$$

The transformation from the algebraically special to the reference tetrad is just the null rotation with $\mathbf{k}$ fixed with $L=-1$. Applying this transformation, we obtain

$$\Upsilon_{2s}^{\rm o}=(-1)^s\frac{(2s)!}{(s!)^2}\,\Upsilon_s^{\rm s}\,, \tag{55}$$

specifically for $s=2$, 1,

$$\Psi_0^{\rm o}=\Psi_1^{\rm o}=0\,,\quad \Psi_2^{\rm o}=\Psi_2^{\rm s}\,,\quad \Psi_3^{\rm o}=-3\Psi_2^{\rm s}\,,\quad \Psi_4^{\rm o}=6\Psi_2^{\rm s}\,, \tag{56}$$

$$\Phi_0^{\rm o}=0\,,\quad \Phi_1^{\rm o}=\Phi_1^{\rm s}\,,\quad \Phi_2^{\rm o}=-2\Phi_1^{\rm s}\,. \tag{57}$$

Substituting into (14), we get the asymptotic directional structure of radiation

$$\Upsilon_{2s}^{\rm i}\approx\frac{\epsilon^s}{\eta}\,\frac{(2s)!}{2^s(s!)^2}\,\Upsilon_{s*}^{\rm s}\left(\epsilon\epsilon_{\rm o}+\cosh\psi-\sinh\psi\,\exp(\mathrm{i}\phi)\right)^s, \tag{58}$$

i.e.,

$$\left|\Psi_4^{\mathrm{i}}\right| \approx 3\frac{|\Psi_{2*}^{\mathrm{s}}|}{|\eta|}\left(\epsilon\epsilon_{\mathrm{o}}+\cosh\psi\right)\left(\cosh\psi-\sinh\psi\cos\phi\right), \tag{59}$$

$$4\pi\,|\mathbf{S}_{\mathrm{i}}| \approx \left|\Phi_2^{\mathrm{i}}\right|^2 \approx 2\frac{\left|\Phi_{1*}^{\mathrm{s}}\right|^2}{\eta^2}\left(\epsilon\epsilon_{\mathrm{o}}+\cosh\psi\right)\left(\cosh\psi-\sinh\psi\cos\phi\right), \tag{60}$$

for gravitational and electromagnetic field, see Fig. 5c and (R.5.37).

3.5 Timelike $\mathcal{I}$, two PNDs tangent to $\mathcal{I}$

Next, let both the PNDs be tangent to a timelike conformal infinity. In such a situation there exists no natural normalization of both PNDs analogous to the condition (18) used above. This is related to an ambiguity in the choice of the timelike unit vector $\mathbf{t}_{\mathrm{s}}$ — we can choose any of the (future-oriented) unit vectors in the plane $\mathbf{k}_1$–$\mathbf{k}_{2s}$. However, despite the fact that we cannot fix the algebraically special tetrad uniquely, the nonvanishing component Υ_s^{s} is independent of this ambiguity: different choices of the special tetrad only differ by a boost in $\mathbf{k}_1$–$\mathbf{k}_{2s}$ plane, and Υ_s^{s} does not change under such a boost. In the following, we arbitrarily choose one particular algebraically special tetrad with respect to which we define the reference tetrad. The reference tetrad thus shares the same ambiguity as the algebraically special tetrad.

The reference tetrad is simply fixed by conditions

$$\mathbf{t}_{\mathrm{o}}=\mathbf{t}_{\mathrm{s}}\,,\quad \mathbf{s}_{\mathrm{o}}=\mathbf{s}_{\mathrm{s}}\,,\quad \epsilon_{\mathrm{o}}=\epsilon_1\,, \tag{61}$$

and (4). PNDs $\mathbf{k}_{\mathrm{s}}$ and $\mathbf{l}_{\mathrm{s}}$ are given by

$$\mathbf{k}_{\mathrm{s}}=\tfrac{1}{\sqrt{2}}\left(\mathbf{t}_{\mathrm{o}}+\mathbf{r}_{\mathrm{o}}\right),\quad \mathbf{l}_{\mathrm{s}}=\tfrac{1}{\sqrt{2}}\left(\mathbf{t}_{\mathrm{o}}-\mathbf{r}_{\mathrm{o}}\right), \tag{62}$$

so that the algebraically special and reference tetrads are related by

$$\mathbf{t}_{\mathrm{s}}=\mathbf{t}_{\mathrm{o}}\,,\quad \mathbf{q}_{\mathrm{s}}=\mathbf{r}_{\mathrm{o}}\,,\quad \mathbf{r}_{\mathrm{s}}=-\mathbf{q}_{\mathrm{o}}\,,\quad \mathbf{s}_{\mathrm{s}}=\mathbf{s}_{\mathrm{o}}\,. \tag{63}$$

It is just a simple spatial rotation by $\pi/2$ in $\mathbf{q}_{\mathrm{o}}$-$\mathbf{r}_{\mathrm{o}}$ plane, as illustrated in Fig. 4d. The complex directional parameters of $\mathbf{k}_1$ and $\mathbf{k}_{2s}$ are

$$R_1=+1\,,\quad R_{2s}=-1\,. \tag{64}$$

The transformation can be decomposed into boost $B=2$, null rotation with $\mathbf{k}$ fixed $L=-1/2$, and null rotation with $\mathbf{l}$ fixed $K=1$. Applying them, we obtain

$$\Upsilon_{2s}^{\mathrm{o}}=(-1)^s\,\frac{(2s)!}{2^s(s!)^2}\,\Upsilon_s^{\mathrm{s}}\,, \tag{65}$$

and

$$\Psi_0^{\mathrm{o}}=\Psi_4^{\mathrm{o}}=\tfrac{3}{2}\,\Psi_2^{\mathrm{s}}\,,\quad \Psi_2^{\mathrm{o}}=-\tfrac{1}{2}\Psi_2^{\mathrm{s}}\,,\quad \Psi_1^{\mathrm{o}}=\Psi_3^{\mathrm{o}}=0\,, \tag{66}$$

$$\Phi_0^{\mathrm{o}}=-\Phi_2^{\mathrm{o}}=\Phi_1^{\mathrm{s}}\,,\quad \Phi_1^{\mathrm{o}}=0\,. \tag{67}$$

Substituting into (14), we get

$$\begin{aligned} \Upsilon^{\mathrm{i}}_{2s} &\approx \frac{(-\epsilon_{\mathrm{o}})^s}{\eta}\,\frac{(2s)!}{2^s(s!)^2}\,\Upsilon^{\mathrm{s}}_{s*}\left(\exp(\mathrm{i}\phi)\big(\cos\phi - \mathrm{i}\,\epsilon\epsilon_{\mathrm{o}}\cosh\psi\,\sin\phi\big)\right)^s , \\ \left|\Upsilon^{\mathrm{i}}_{2s}\right| &\approx \frac{1}{|\eta|}\,\frac{(2s)!}{2^s(s!)^2}\,\left|\Upsilon^{\mathrm{s}}_{s*}\right|\,\left(1+\sinh^2\psi\,\sin^2\phi\right)^{s/2} , \end{aligned} \tag{68}$$

which for gravitational and electromagnetic fields gives

$$\left|\Psi^{\mathrm{i}}_4\right| \approx \frac{3}{2}\frac{1}{|\eta|}\,\left|\Psi^{\mathrm{s}}_{2*}\right|\,\left(1+\sinh^2\psi\,\sin^2\phi\right) , \tag{69}$$

$$4\pi\,|\mathbf{S}_{\mathrm{i}}| \approx \left|\Phi^{\mathrm{i}}_2\right|^2 \approx \frac{1}{\eta^2}\,\left|\Phi^{\mathrm{s}}_{1*}\right|^2\left(1+\sinh^2\psi\,\sin^2\phi\right) , \tag{70}$$

see Fig. 5d and (R.5.36).

3.6 Null $\mathcal{I}$

Finally, we investigate the case of conformal infinity $\mathcal{I}$ of a null character, $\sigma = 0$. It can be easily observed from (12) (cf. section R.5.1 for more detail) that the directional structure of radiation near the null infinity is *independent* of the direction

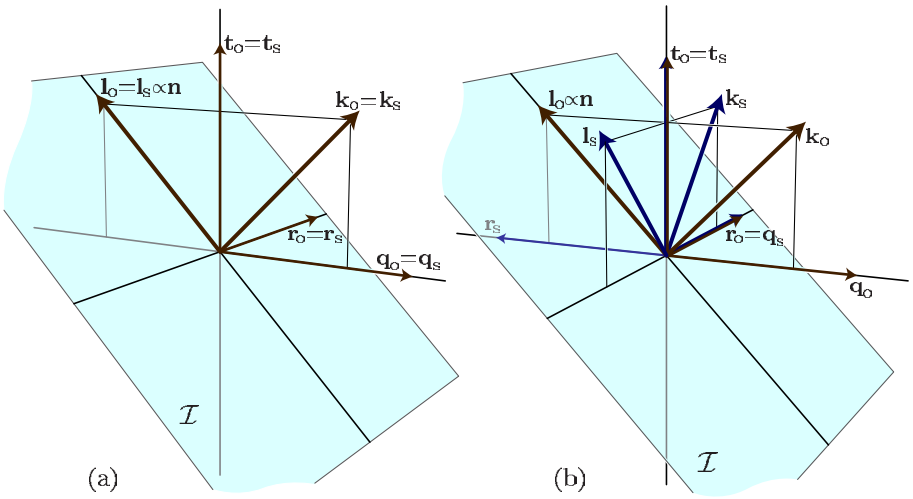

Fig. 6. Algebraically special and reference tetrads at a null infinity. Vectors $\mathbf{k}_{\mathrm{o}}$, $\mathbf{l}_{\mathrm{o}}$ ($\mathbf{k}_{\mathrm{s}}$, $\mathbf{l}_{\mathrm{s}}$) of the null tetrad, and $\mathbf{t}_{\mathrm{o}}$, $\mathbf{q}_{\mathrm{o}}$, $\mathbf{r}_{\mathrm{o}}$ ($\mathbf{t}_{\mathrm{s}}$, $\mathbf{q}_{\mathrm{s}}$, $\mathbf{r}_{\mathrm{s}}$) of the orthonormal reference (algebraically special, respectively) tetrad are shown; the direction $\mathbf{s}_{\mathrm{o}} = \mathbf{s}_{\mathrm{s}}$ tangent to $\mathcal{I}$ and orthogonal to PNDs is not plotted. The vectors $\mathbf{k}_{\mathrm{s}}$, $\mathbf{l}_{\mathrm{s}}$ are aligned with algebraically special directions. The diagram (a) depicts the situation with one PND tangent to $\mathcal{I}$. In this case the algebraically special tetrad can be used as the reference tetrad. In the diagram (b) neither of both distinct PNDs is tangent to $\mathcal{I}$. The algebraically special tetrad can be then obtained from the reference tetrad by a spatial rotation in $\mathbf{q}_{\mathrm{o}}$–$\mathbf{r}_{\mathrm{o}}$ plane by $\pi/2$.

along which the infinity is approached. The only interesting question is whether the dominant field component is vanishing or not — in other words: whether the field is radiative or nonradiative. It follows from the definition of PNDs that the normalization factor $\Upsilon^{\mathrm{o}}_{2s*}$ in (12) is vanishing if and only if one of the PNDs is tangent to $\mathcal{I}$. Thus, the tangency of PNDs to $\mathcal{I}$ serves as the geometrical characterization of radiative/nonradiative fields.

Let us first assume that one of the PNDs, say $\mathbf{l}_{\mathrm{s}}$, is tangent to $\mathcal{I}$. As in the previous section we cannot fix the normalization of algebraically special tetrad using the condition (18); the algebraically special tetrad cannot be selected uniquely. Nevertheless, the field component $\Upsilon^{\mathrm{s}}_{s}$ is still unique. If we choose one algebraically special tetrad, we can use it also as the reference tetrad — it satisfies the adjustment condition (4), cf. Fig. 6. As mentioned above, the component $\Upsilon^{\mathrm{o}}_{2s}$ is then vanishing:

$$\Upsilon^{\mathrm{i}}_{2s} \approx 0 \,. \tag{71}$$

If both distinct PNDs are not tangent to $\mathcal{I}$, we may normalize them by (18) and fix the reference tetrad by the condition $\mathbf{t}_{\mathrm{o}} = \mathbf{t}_{\mathrm{s}}$, namely,

$$\mathbf{t}_{\mathrm{o}} = \mathbf{t}_{\mathrm{s}} \,, \quad \mathbf{s}_{\mathrm{o}} = \mathbf{s}_{\mathrm{s}} \,, \quad \epsilon_{\mathrm{o}} = \epsilon_1 \,, \tag{72}$$

together with the adjustment condition (4), see Fig. 6. In terms of the reference tetrad the PNDs $\mathbf{k}_{\mathrm{s}}$ and $\mathbf{l}_{\mathrm{s}}$ are given by

$$\mathbf{k}_{\mathrm{s}} = \tfrac{1}{\sqrt{2}} \left(\mathbf{t}_{\mathrm{o}} + \mathbf{r}_{\mathrm{o}}\right) \,, \quad \mathbf{l}_{\mathrm{s}} = \tfrac{1}{\sqrt{2}} \left(\mathbf{t}_{\mathrm{o}} - \mathbf{r}_{\mathrm{o}}\right) \tag{73}$$

and their complex parameters are

$$R_1 = +1 \,, \quad R_{2s} = -1 \,. \tag{74}$$

The relation between the algebraically special and reference tetrads is thus the same as in Subsect. 3.5. Using (12), $\sigma = 0$, and relation (65), we find that the radiative component has no directional structure:

$$\Upsilon^{\mathrm{i}}_{2s} \approx \epsilon_{\mathrm{o}}^{s} \, \frac{(2s)!}{(s!)^2} \, \Upsilon^{\mathrm{s}}_{s*} \, \frac{1}{\eta} \,. \tag{75}$$

In particular, for gravitational and electromagnetic field we obtain

$$\left|\Psi^{\mathrm{i}}_4\right| \approx 3 \left|\Psi^{\mathrm{s}}_{2*}\right| \, \frac{1}{|\eta|} \,, \tag{76}$$

$$4\pi \left|\mathbf{S}_{\mathrm{i}}\right| \approx \left|\Phi^{\mathrm{i}}_2\right|^2 \approx 2 |\Phi^{\mathrm{s}}_{1*}|^2 \, \frac{1}{\eta^2} \,. \tag{77}$$

4 Conclusions

We have analyzed the asymptotic directional structure of fields, that are characterized by the existence of two distinct, but equivalent algebraicaly special null

directions. This involves a generic electromagnetic field ($s = 1$), the Petrov type D gravitational fields ($s = 2$) having double-degenerate principal null directions, and other possible fields of an integer spin s, which admit a pair of s-degenerate PNDs.

The structure of such fields near the conformal infinity depends on the specific orientation of these algebraically special directions with respect to $\mathcal{I}$, and on the causal character of $\mathcal{I}$. In the case of a spacelike conformal infinity ($\Lambda > 0$) there is essentially only one possibility which is described in Subsect. 3.1, whereas for a timelike conformal infinity ($\Lambda < 0$) four different situations may occur that have to be discussed separately, see Subsects. 3.2–3.5. For the conformal infinity having a null character ($\Lambda = 0$), the asymptotic directional structure disappears: when one of the (degenerate) PNDs is tangent to $\mathcal{I}$, the radiative component vanishes, otherwise the radiation is present and it is independent of the direction along which the infinity is approached, cf. Subsect. 3.6.

In all such cases we have introduced the privileged 'symmetric' reference tetrad which is naturally adapted to the algebraically special directions and to $\mathcal{I}$. These are illustrated in Figs. 2, 4, and 6. With respect to these reference tetrads it is possible to characterize any null direction by standard (pseudo)spherical parameters. The corresponding explicit directional structure of radiation for a spacelike $\mathcal{I}$ is presented in expression (26), and the four possibilities for a timelike $\mathcal{I}$ are given by (37), (47), (58), (68).

These results generalize our previous study of the asymptotic directional structure of gravitational and electromagnetic radiation in the C-metric spacetimes [1, 2] to other fields which are of the type D. On the other hand, the expressions presented here are more detailed and more explicit than those given in the review article [8]. It would now be an interesting task to apply them on particular exact model spacetimes of type D. This may provide a deeper insight into the geometric relation between the structure of the sources and the properties of radiation generated by them, as observed at spacelike or timelike conformal infinities.

This work was supported by the grant GAČR 202/02/0735.

References

[1] P. Krtouš and J. Podolský: Phys. Rev. D **68** (2003) 024005.

[2] J. Podolský, M. Ortaggio, and P. Krtouš: Phys. Rev. D **68** (2003) 124004.

[3] P. Krtouš, J. Podolský, and J. Bičák: Phys. Rev. Lett. **91** (2003) 061101.

[4] P. Krtouš and J. Podolský: Phys. Rev. D **69** (2004) 084023.

[5] R. Penrose: in *Relativity, Groups and Topology*, Les Houches 1963, (Eds. C. DeWitt and B. DeWitt), Gordon and Breach, New York, 1964, p. 563.

[6] R. Penrose: Proc. R. Soc. Lond., A **284** (1965) 159.

[7] R. Penrose: in *The Nature of Time*, (Ed. T. Gold), Cornell University Press, Ithaca, New York, 1967, p. 42.

[8] P. Krtouš and J. Podolský: Class. Quantum Grav. **21** (2004) R233–273.

[9] R. Penrose and W. Rindler: *Spinors and Space-Time*, Cambridge University Press, Cambridge (England), 1984; 1986.

[10] H. Stephani *et al.*: *Exact Solutions of Einstein's Field Equations*, Second Edition, Cambridge University Press, Cambridge (England), 2002.

[11] J. Bičák and P. Krtouš: Phys. Rev. Lett. **88** (2002) 211101.

PHYSICAL REVIEW D **71,** 124031 (2005)

Ultrarelativistic boost of the black ring

Marcello Ortaggio,* Pavel Krtouš,† and Jiří Podolský‡

Institute of Theoretical Physics, Faculty of Mathematics and Physics, Charles University in Prague, V Holešovičkách 2, 180 00 Prague 8, Czech Republic

(Received 15 April 2005; published 23 June 2005)

We investigate the ultrarelativistic boost of the five-dimensional Emparan-Reall nonrotating black ring. Following the classical method of Aichelburg and Sexl, we determine the gravitational field generated by a black ring moving ''with the speed of light'' in an arbitrary direction. In particular, we study in detail two different boosts along axes orthogonal and parallel to the plane of the ring circle, respectively. In both cases, after the limit one obtains a five-dimensional impulsive pp-wave propagating in Minkowski spacetime. The curvature singularity of the original static spacetime becomes a singular source within the wave front, in the shape of a ring or a rod according to the direction of the boost. In the case of an orthogonal boost, the wave front contains also a remnant of the original disk-shaped membrane as a component of the Ricci tensor (which is everywhere else vanishing). We also analyze the asymptotic properties of the boosted black ring at large spatial distances from the singularity, and its behavior near the sources. In the limit when the singularity shrinks to a point, one recovers the well-known five-dimensional analogue of the Aichelburg-Sexl monopole solution.

DOI: 10.1103/PhysRevD.71.124031 PACS numbers: 04.50.+h, 04.20.Jb

I. INTRODUCTION

The study of black holes in higher dimensions has been for a long time motivated by unified theories, in particular, string theory [1]. In the past few years, extra-dimension models of TeV gravity have raised further interest in view of possible black hole production at colliders [2–5]. According to [6,7], in semiclassical investigations of such high energy phenomena one can represent the incoming states with black hole metrics boosted ''to the speed of light.'' In the case of the four-dimensional Schwarzschild black hole, the corresponding ultrarelativistic gravitational field is described by the Aichelburg-Sexl impulsive pp-wave [8]. In the spirit of [2–5], however, one clearly needs to consider higher dimensional settings. Indeed, the boosting technique of [8] has been already applied to static (charged) black holes in higher dimensions [9] (and straightforwardly extended to the $D \geq 4$ Schwarzschild black hole in an external magnetic field [10]). Recent analyses of black hole production in high energy collisions [11–13] thus employed the Aichelburg-Sexl solution (or other impulsive waves) in $D \geq 4$ spacetime dimensions (see [14] for a subtler discussion). The very recent work [15] studied the more elaborate ultrarelativistic limit of the Myers-Perry solution [1] (a generalization of the rotating Kerr metric to arbitrary dimensions).

In fact, one of the most remarkable feature of general relativity in $D > 4$ is the nonuniqueness of the Myers-Perry spherical black holes. In five-dimensional vacuum gravity, there exist also asymptotically flat rotating black rings with an event horizon of topology $S^1 \times S^2$ [16]. It is our purpose to investigate the gravitational field generated by such rings when they move at the speed of light, in the sense of the Aichelburg-Sexl limit. In the present paper we will be focusing on the special subcase of zero angular momentum, i.e. on the static black rings found in [17]. We shall consider spinning rings in a separate subsequent work [18].

The structure of the paper is as follows. In Sec. II we briefly describe the static black ring of [17], which we intend to Lorentz-boost subsequently. In Sec. III we split the corresponding line element into flat space plus a term that becomes ''small'' at asymptotic infinity. We also introduce (asymptotically) Cartesian coordinates useful for performing the ultrarelativistic boost. Sections IV, V, and VI contain our main results. In Secs. IV and V we explicitly calculate the metric of the black ring boosted along a direction orthogonal and parallel to the plane of the ring circle, respectively. This leads to two different impulsive pp-waves that naturally ''recall'' the original curvature and conical singularities of the static ring (in a sense to be made clear later). We analyze several specific properties of such solutions, in particular the Ricci and Weyl tensors, and asymptotic expansions far from and close to the singularities, and near geometrically privileged axes and planes. In Sec. VI we briefly discuss a boost along an arbitrary direction. We again obtain an impulsive pp-wave, whose singular source is described by an ellipse. Our final remarks are presented in Sec. VII. Appendix A summarizes the definitions and properties of the complete elliptic integrals employed in Secs. IV and V, whereas Appendix B provides the explicit tetrad components of the Weyl tensor in the case of the orthogonal boost.

*Electronic address: marcello.ortaggio@comune.re.it
Also at INFN, Rome, Italy.
†Electronic address: Pavel.Krtous@mff.cuni.cz
‡Electronic address: Jiri.Podolsky@mff.cuni.cz

II. THE STATIC BLACK RING

In this section we briefly summarize the basic properties of the static black ring, referring to [17,19] for further details. In the coordinates of [19],[1] the line element reads

$$ds^2 = -\frac{F(y)}{F(x)}dt^2 + \frac{L^2}{(x-y)^2}F(x)\Big[(y^2-1)d\psi^2 + \frac{1}{F(y)}\frac{dy^2}{y^2-1} + \frac{1}{F(x)}\frac{dx^2}{1-x^2} + (1-x^2)d\phi^2\Big], \quad (1)$$

where

$$F(\zeta) = \frac{1+\lambda\zeta}{1-\lambda}, \qquad 0 \le \lambda < 1. \quad (2)$$

The parameter λ is dimensionless, and for $\lambda = 0$ (i.e., $F = 1$) the spacetime (1) is flat. The constant $L > 0$ represents a length related to the radius of the "central circle" of the ring. For a physical interpretation of the spacetime (1), we take

$$y \in (-\infty, -1], \qquad x \in [-1, +1], \quad (3)$$

and ψ and ϕ as periodic angular coordinates (see below). Now, y is an "area coordinate" that, loosely speaking, parametrizes "distances" from the ring circle. Surfaces of constant y have topology $S^1 \times S^2$, and area which is monotonically growing with y. The coordinate ψ runs along the S^1 factor, whereas (x, ϕ) parametrize S^2 (see [17,19] for illustrative pictures). At $y \to -\infty$ the spacetime has a curvature singularity, $y = -1/\lambda$ is a horizon of topology $S^1 \times S^2$, and spatial infinity corresponds to $x, y \to -1$. To avoid conical singularities at the axes $x = -1$ and $y = -1$, the angular coordinates must have the standard periodicity

$$\Delta\phi = 2\pi = \Delta\psi. \quad (4)$$

With this choice, however, there is a conical singularity at $x = +1$. This describes a disk-shaped membrane (with an excess angle) inside the ring which prevents the ring from collapsing under its self-gravity.[2] Nevertheless, the spacetime (1) is asymptotically flat [17], and the black ring has mass

$$M = \frac{3\pi L^2}{4}\frac{\lambda}{1-\lambda}. \quad (5)$$

[1]More precisely, one has to multiply $F(\zeta)$ by $(1-\lambda)$, and to divide ψ and ϕ by $\sqrt{1-\lambda}$ to obtain the corresponding quantities of [19]. The original notation of [17] is recovered with the transformations $y = (y' - \lambda)/(1 - \lambda y')$, $x = (x' - \lambda)/(1 - \lambda x')$, $\psi = \psi'/\sqrt{1+\lambda}$, $\phi = \phi'/\sqrt{1+\lambda}$, $L^2 = (1-\lambda^2)/A^2$.

[2]Alternatively, one can require regularity at $x = +1$ and place the conical singularity at $x = -1$, i.e., outside the ring [17]; we will not consider this case because the singularity would extend to infinity. There is no way to achieve regularity at both $x = -1$ and $x = +1$, unless the ring rotates [16].

Except on the disk membrane at $x = +1$, the metric (1) is a vacuum solution. It clearly admits three commuting orthogonal Killing vector fields ∂_t, ∂_ψ, ∂_ϕ and, in fact, it belongs to the generalized Weyl class of [17]. Interestingly, it has been proven recently [20] that vacuum black rings (with or without rotation) differ from the five-dimensional Myers-Perry black holes not only in the horizon topology, but also in the algebraic type of the Weyl tensor: black holes are of type D, whereas black rings are of the more general type I_i (type II on the horizon), according to the higher dimensional classification of [21].

III. SPLITTING OF THE METRIC AND CONVENIENT COORDINATES

For our purposes, it is convenient to decompose the line element (1) as

$$ds^2 = ds_0^2 + \lambda\Delta, \quad (6)$$

in which ds_0^2 is Minkowski spacetime [given by Eq. (1) with $\lambda = 0$, i.e., $F(x) = 1 = F(y)$], and

$$\Delta = \frac{x-y}{1+\lambda x}dt^2 + \frac{L^2}{(x-y)^2}\Big[\frac{x+1}{1-\lambda}(y^2-1)d\psi^2 + \frac{x-y}{1+\lambda y}\frac{dy^2}{y^2-1} + \frac{x+1}{1-\lambda}(1-x^2)d\phi^2\Big] \quad (7)$$

measures the deviation from flatness of the full black ring metric (1). Asymptotically ($x, y \to -1$), Δ becomes "negligible" (in the sense of the Minkowskian metric ds_0^2).

A boost is now naturally defined with respect to the flat background ds_0^2 (as well as with respect to asymptotic infinity), namely, by its isometries. We wish to visualize this in standard Cartesian coordinates. In order to introduce them, it is first convenient to replace the "C-metric" coordinates (y, x) with (ξ, η) via the substitution[3]

$$y = -\frac{\xi^2+\eta^2+L^2}{\sqrt{(\xi^2+\eta^2-L^2)^2+4L^2\eta^2}}, \qquad x = -\frac{\xi^2+\eta^2-L^2}{\sqrt{(\xi^2+\eta^2-L^2)^2+4L^2\eta^2}}. \quad (8)$$

The flat term ds_0^2 in Eq. (6) then takes the form of Minkowski space in double cylindrical coordinates

$$ds_0^2 = -dt^2 + d\eta^2 + \eta^2 d\phi^2 + d\xi^2 + \xi^2 d\psi^2, \quad (9)$$

and the additional quantity Δ reads

[3]We have simply inverted the relations $\xi = L\sqrt{y^2-1}/(x-y)$ and $\eta = L\sqrt{1-x^2}/(x-y)$ of [17].

$$\Delta = \frac{2L^2}{\Sigma(1+\lambda x)}dt^2 + 2L^2\frac{[(\xi^2-\eta^2-L^2)d\xi + 2\eta\xi d\eta]^2}{\Sigma^3(1+\lambda y)} + \frac{\Sigma-\eta^2-\xi^2+L^2}{\Sigma(1-\lambda)}(\xi^2 d\psi^2 + \eta^2 d\phi^2), \quad (10)$$

where we have denoted

$$\Sigma = \sqrt{(\xi^2+\eta^2-L^2)^2 + 4L^2\eta^2}. \quad (11)$$

In Eq. (10) we have kept an explicit simple dependence on the old coordinates (y, x) for brevity and for later convenience [but one can readily substitute Eq. (8) into Eq. (10) if necessary].

Cartesian coordinates are finally given by

$$x_1 = \eta\cos\phi, \qquad y_1 = \xi\cos\psi, \qquad x_2 = \eta\sin\phi, \qquad y_2 = \xi\sin\psi, \quad (12)$$

so that $\eta = \sqrt{x_1^2+x_2^2}$, $\xi = \sqrt{y_1^2+y_2^2}$, and the background is $ds_0^2 = -dt^2 + dx_1^2 + dx_2^2 + dy_1^2 + dy_2^2$.

In principle, one could now study a boost along a general direction. Since the original spacetime (1) is symmetric under (separate) rotations in the (x_1, x_2) and (y_1, y_2) planes, such a direction can be specified by a single parameter α, namely, introducing the rotated axes

$$z_1 = x_1\cos\alpha + y_1\sin\alpha, \qquad z_2 = -x_1\sin\alpha + y_1\cos\alpha. \quad (13)$$

Defining suitable double null coordinates (u', v') by

$$t = \frac{-u'+v'}{\sqrt{2}}, \qquad z_1 = \frac{u'+v'}{\sqrt{2}}, \quad (14)$$

a Lorentz boost along z_1 takes the simple form

$$u' = \epsilon^{-1}u, \qquad v' = \epsilon v. \quad (15)$$

The parameter $\epsilon > 0$ is related to the standard Lorentz factor via $\gamma = (\epsilon+\epsilon^{-1})/2$.

In the following, we will study in detail two different boosts of the black ring along the privileged axes x_1 ($\alpha = 0$) and y_1 ($\alpha = \pi/2$), which are, respectively, "orthogonal" and "parallel" to the ring. But we will also discuss a boost in a general direction. In particular, we will consider "ultrarelativistic" boosts to the speed of light, i.e. the transformation (15) in the limit $\epsilon \to 0$. Along with that, we will perform the standard mass rescaling [8]

$$M = \gamma^{-1}p = 2\epsilon(1+\epsilon^2)^{-1}p, \quad (16)$$

which keeps the total energy finite ($p > 0$ is a constant). From Eq. (5), in term of the dimensionless parameter λ the rescaling (16) becomes

$$\lambda = \lambda_\epsilon = \epsilon\frac{8p}{3\pi L^2 + \epsilon(8p+3\pi L^2\epsilon)}, \quad (17)$$

so that when $\epsilon \to 0$ then $\lambda_\epsilon \approx \epsilon(8p/3\pi L^2) \to 0$.

IV. ORTHOGONAL BOOST: $\alpha = 0$

A. Evaluation of the impulsive limit of the metric

For $\alpha = 0$ in Eq. (13), Eq. (14) reduces to

$$t = \frac{-u'+v'}{\sqrt{2}}, \qquad x_1 = \frac{u'+v'}{\sqrt{2}}, \quad (18)$$

so that the transformation (15) describes a Lorentz boost along the x_1 axis, which lies in the 2-plane spanned by (η, ϕ) [cf. Eq. (12)]. The latter is orthogonal to the 2-plane (ξ, ψ), which contains the ring circle. We wish now to evaluate how the black ring metric (1) [that is, Eq. (6) with Eqs. (9) and (10)] transforms under the boost (15) with $\alpha = 0$. Since the coordinates ξ and ψ remain unchanged in this case, it suffices to substitute only the first column of Eq. (12) into Eqs. (9) and (10). Then, we put Eq. (18) into the thus obtained expressions for ds_0^2 and for Δ (we omit the intermediate expressions, which are cumbersome and not of particular significance). Finally, we perform the boost (15). This leaves ds_0^2 invariant ($2du'dv' = 2dudv$), i.e.

$$ds_0^2 = 2dudv + dx_2^2 + d\xi^2 + \xi^2 d\psi^2, \quad (19)$$

and makes Δ dependent parametrically on ϵ. Using the shortcut

$$z_\epsilon = \frac{1}{\sqrt{2}}(\epsilon^{-1}u + \epsilon v), \quad (20)$$

one obtains[4]

$$\Delta_\epsilon = \frac{L^2(\epsilon^{-1}du - \epsilon dv)^2}{\Sigma_\epsilon(1+\lambda_\epsilon x)} + \frac{2L^2}{\Sigma_\epsilon^3(1+\lambda_\epsilon y)}\left([\xi^2 - z_\epsilon^2 - x_2^2 - L^2]d\xi + 2\xi\left[\frac{1}{\sqrt{2}}z_\epsilon(\epsilon^{-1}du + \epsilon dv) + x_2 dx_2\right]\right)^2 + \frac{\Sigma_\epsilon - z_\epsilon^2 - x_2^2 - \xi^2 + L^2}{\Sigma_\epsilon(1-\lambda_\epsilon)}\left(\xi^2 d\psi^2 + \frac{\frac{1}{2}[\sqrt{2}z_\epsilon dx_2 - x_2(\epsilon^{-1}du + \epsilon dv)]^2}{z_\epsilon^2 + x_2^2}\right). \quad (21)$$

[4]Again, for convenience in Eq. (21) we have left some expressions containing the old coordinates y and x [cf. Eq. (8)], which now depend on ϵ. However, these terms will not contribute to the final result in the limit $\epsilon \to 0$.

Here, the quantity Σ_ϵ comes from the expression (11) using the above described coordinate transformations and the boost (15), and it can be rewritten as

$$\Sigma_\epsilon = \sqrt{[z_\epsilon^2 + x_2^2 + (\xi + L)^2][z_\epsilon^2 + x_2^2 + (\xi - L)^2]}. \quad (22)$$

We are now interested in taking the ultrarelativistic limit $\epsilon \to 0$, i.e. in finding the resulting metric

$$ds^2 = ds_0^2 + \lim_{\epsilon\to 0} \lambda_\epsilon \Delta_\epsilon. \quad (23)$$

Recalling Eq. (17), one easily sees that $\lim_{\epsilon\to 0}(\lambda_\epsilon\Delta_\epsilon) = 0$ at any given spacetime point with $u \neq 0$ (and away from the ring singularity $y = -\infty$). At $u = 0$ this limit diverges, but in fact it represents a sound distribution supported on $u = 0$. By inspecting the various quantities in Eq. (21), it suffices to retain only the terms proportional to du^2, as the remaining ones become negligible for $\epsilon \to 0$. Similarly, we drop the factors $1 + \lambda_\epsilon x$, $1 + \lambda_\epsilon y$ and $1 - \lambda_\epsilon$, since $\lambda_\epsilon \to 0$ for $\epsilon \to 0$. Using Eqs. (17), (20), and (21), for $\epsilon \sim 0$ we can thus write

$$\lambda_\epsilon \Delta_\epsilon \approx \frac{8p}{3\pi L^2} \frac{1}{\epsilon} h_\perp(z_\epsilon) du^2, \quad (24)$$

where

$$h_\perp(z_\epsilon) = \frac{2L^2 - x_2^2}{2\Sigma_\epsilon} + \frac{4L^2\xi^2 z_\epsilon^2}{\Sigma_\epsilon^3} + \frac{x_2^2(L^2 - \xi^2)}{2(z_\epsilon^2 + x_2^2)\Sigma_\epsilon} + \frac{x_2^2}{2(z_\epsilon^2 + x_2^2)}. \quad (25)$$

We have emphasized the dependence of $h_\perp$ on z_ϵ (which gives the only dependence on ϵ) because this is essential in our limit (of course, $h_\perp$ depends on the coordinates x_2 and ξ as well). In taking the limit $\epsilon \to 0$ of Eq. (24), we can now apply the distributional identity [recall Eq. (20)]

$$\lim_{\epsilon\to 0} \frac{1}{\epsilon} f(z_\epsilon) = \sqrt{2}\delta(u) \int_{-\infty}^{+\infty} f(z) dz. \quad (26)$$

With this, the final metric is [cf. Eqs. (19) and (23)]

$$ds^2 = 2du dv + dx_2^2 + d\xi^2 + \xi^2 d\psi^2 + H_\perp(x_2, \xi)\delta(u) du^2, \quad (27)$$

with a profile function given by

$$H_\perp(x_2, \xi) = \frac{8\sqrt{2}p}{3\pi L^2}\left(\int_{-\infty}^{+\infty} h_\perp(z) dz\right). \quad (28)$$

It only remains to explicitly perform the integration in Eq. (28), with $h_\perp$ given by Eq. (25) with Eq. (22). The last term in Eq. (25) gives rise to the simple integral $\int_{-\infty}^{+\infty}(z^2 + x_2^2)^{-1} dz = \pi|x_2|^{-1}$. The first three terms lead to the elliptic integrals (A13)–(A15) of Appendix A. Combining the various quantities, we finally obtain

$$H_\perp(x_2, \xi) = \frac{8\sqrt{2}p}{3\pi L^2}\left[\left(3L^2 + \xi^2 + x_2^2 \frac{\xi + L}{\xi - L}\right)\frac{K(k)}{\sqrt{(\xi + L)^2 + x_2^2}} - \sqrt{(\xi + L)^2 + x_2^2} E(k) - \frac{\xi + L}{\xi - L}\frac{(\xi - L)^2 + x_2^2}{\sqrt{(\xi + L)^2 + x_2^2}}\Pi(\rho_0, k) + \frac{\pi}{2}|x_2|\right], \quad (29)$$

with

$$k = \sqrt{\frac{4\xi L}{(\xi + L)^2 + x_2^2}}, \qquad \rho_0 = -\frac{(\xi - L)^2}{x_2^2}. \quad (30)$$

One can reexpress the elliptic integral $\Pi(\rho_0, k)$ using identities (A4) and (A5) and obtain an alternative form of $H_\perp$, which will be useful for subsequent discussions,

$$H_\perp(x_2, \xi) = \frac{8\sqrt{2}p}{3\pi L^2}\left[\frac{3L^2 + \xi^2}{\sqrt{(\xi + L)^2 + x_2^2}} K(k) - \sqrt{(\xi + L)^2 + x_2^2} E(k) + \frac{\xi - L}{\xi + L}\frac{x_2^2}{\sqrt{(\xi + L)^2 + x_2^2}}\Pi(\rho, k) + \pi|x_2|\Theta(L - \xi)\right], \quad (31)$$

where

$$\rho = \frac{4\xi L}{(\xi + L)^2}, \quad (32)$$

and $\Theta(L - \xi)$ denotes the step function.

Let us observe that no singular coordinate transformation of the type of [8] had to be performed in the calculation above, since all the required integrals are convergent.

B. Properties of the solution

A static black ring boosted to the speed of light in a direction orthogonal to the ring circle is thus described by the metric (27), with $H_\perp$ given explicitly by Eq. (31). This is evidently a five-dimensional impulsive pp-wave propagating along the x_1 direction [see Eq. (18)]. Such a spacetime is flat everywhere except on the null hyperplane $u = 0$, which represents the impulsive wave front. In particular, the line element (27) is singular at the points satisfying $u = 0 = x_2$ and $\xi = L$ [$k = 1$ in Eq. (30)], i.e. on a *circle of radius L* contained within the wave front. This is a remnant of the curvature singularity ($y = -\infty$) of the original static black ring (1). Since the boost performed above was orthogonal to the ring circle, the latter has not Lorentz-contracted. We have plotted the profile function $H_\perp$ in Fig. 1.

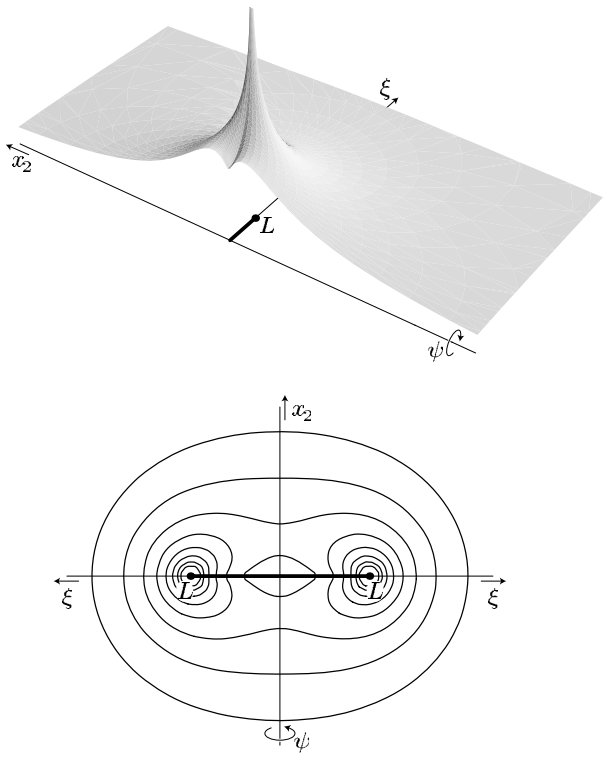

FIG. 1. The profile function $H_\perp(x_2, \xi)$ given by Eq. (31). The upper picture represents the values taken by $H_\perp$ over the plane (x_2, ξ), whereas the lower one displays curves along which $H_\perp$ is constant. This is the case of a static black ring boosted to the speed of light in a direction orthogonal to the plane (ξ, ψ), which contains the ring circle. The coordinates (x_2, ξ, ψ) span spatial sections of the impulsive wave front $u = 0$, cf. Eq. (27). Here the coordinate ψ is suppressed, since it just describes the orbits of a Killing vector field. The profile function $H_\perp$ diverges (only) at the *ring* singularity $x_2 = 0$, $\xi = L$, as indicated by the thick point(s) in the pictures. In addition, there is a disk membrane within the ring, i.e. at $x_2 = 0$, $\xi < L$ [cf. Eq. (34)], which manifests itself as a jump in $\partial H_\perp / \partial x_2$. This is drawn above as a thick line.

1. Killing vectors

The pp-wave line element (27) and (31) is obviously invariant under the transformations generated by the vector fields ∂_v and ∂_ψ. It has been demonstrated in four spacetime dimensions [22] that impulsive pp-waves admit more isometries than the same class of waves with a general profile. Similarly, it is easy to see that, thanks to the presence of $\delta(u)$, the line element (27) admits also the three commuting Killing vectors

$$u\partial_{x_2} - x_2\partial_v, \qquad u\partial_{y_1} - y_1\partial_v, \qquad u\partial_{y_2} - y_2\partial_v. \quad (33)$$

[Recall the simple relation (12) between (y_1, y_2) and (ξ, ψ).] These are generators of null rotations. Incidentally, we observe that impulsive waves in the four-dimensional (anti-)de Sitter universe can be described as a submanifold of five-dimensional impulsive pp-waves, and they admit symmetries very similar to the above [23].

2. The Ricci tensor

The static ring (1) is a vacuum spacetime ($R_{\mu\nu} = 0$) everywhere except on the disk membrane $x = +1$ (and of course on the ring singularity $y = -\infty$). Therefore, one would expect also the ultrarelativistic boosted ring to be a vacuum solution except at a possible remnant (after the boost) of the original disk membrane. To check the results, we have verified that the Ricci tensor associated to the spacetime (27) and (31) is indeed zero everywhere but at $u = 0 = x_2$, $\xi < L$, i.e. inside a two-dimensional disk lying on the wave front. Namely, using Eqs. (A6) one finds

$$R_{uu} = -\frac{1}{2}\Delta H_\perp \delta(u) = -\frac{8\sqrt{2}p}{3L^2}\Theta(L - \xi)\delta(x_2)\delta(u) \quad (34)$$

[the symbol Δ denotes the Laplace operator over the transverse flat space (x_2, ξ, ψ)]. This nonvanishing component arises only due to the last term in Eq. (31), a typical term associated to boosted conical singularities [24]. On the disk rim $u = 0 = x_2$, $\xi = L$ the metric (27), (31) is singular, and its exact structure may be not reflected correctly by Eq. (34).

3. The Weyl tensor

For any five-dimensional pp-wave written in the form $ds^2 = 2dudv + dx_2^2 + d\xi^2 + \xi^2 d\psi^2 + H_\perp du^2$, in the null/orthonormal frame

$$\boldsymbol{k} = du, \qquad \boldsymbol{l} = -dv - \frac{1}{2}H_\perp du, \\ \boldsymbol{m}_{(1)} = d\xi, \qquad \boldsymbol{m}_{(2)} = \xi d\psi, \qquad \boldsymbol{m}_{(3)} = dx_2, \tag{35}$$

the Weyl tensor is

$$\boldsymbol{C} = \Psi_{ij}[(\boldsymbol{k}\wedge\boldsymbol{m}_{(i)})\otimes(\boldsymbol{k}\wedge\boldsymbol{m}_{(j)}) + (\boldsymbol{k}\wedge\boldsymbol{m}_{(j)})\otimes(\boldsymbol{k}\wedge\boldsymbol{m}_{(i)})], \tag{36}$$

where summation over $i, j = 1, 2, 3$ is understood. This is the canonical form of type N spacetimes [21,25], and $\boldsymbol{k}$ is the unique principal null direction. The symbols [25]

$$\Psi_{ij} = \frac{1}{2}C_{\mu\nu\rho\sigma}l^\mu m^\nu_{(i)} l^\rho m^\sigma_{(j)}, \qquad i, j = 1, 2, 3 \tag{37}$$

define a 3×3 symmetric traceless matrix that expresses the independent frame components of the Weyl tensor, which are in general five in $D = 5$.[5] In particular, this demonstrates that in the ultrarelativistic boost studied above the original type I_i [20] of the static ring (1) has degenerated to the type N on the wave front of our specific pp-wave (27), (31). Moreover, for such a solution the symmetry under ∂_ψ implies $\Psi_{12} = 0 = \Psi_{23}$. One is thus left with

$$\Psi_{11} = -\frac{1}{2}\left(\frac{1}{2}\frac{\partial^2 H_\perp}{\partial\xi^2}\delta(u) + \frac{1}{3}R_{uu}\right), \\ \Psi_{13} = -\frac{1}{4}\frac{\partial^2 H_\perp}{\partial\xi\partial x_2}\delta(u), \\ \Psi_{22} = -\frac{1}{2}\left(\frac{1}{2\xi}\frac{\partial H_\perp}{\partial\xi}\delta(u) + \frac{1}{3}R_{uu}\right), \\ \Psi_{33} = -\frac{1}{2}\left(\frac{1}{2}\frac{\partial^2 H_\perp}{\partial x_2^2}\delta(u) + \frac{1}{3}R_{uu}\right). \tag{38}$$

The above components of the Weyl tensor confirm the presence of an impulsive gravitational wave at $u = 0$. For $H_\perp$ given by Eq. (31), the explicit form of the scalars Ψ_{ij} is presented in Appendix B. There one can observe that the elliptic integral $\Pi(\rho, k)$ disappears from such expressions.

4. Asymptotic behavior

The spacetime (27) is flat everywhere except on the wave front $u = 0$. If we restrict within the latter, it is interesting to analyze how the gravitational field generated by the boosted black ring behaves *at a large spatial distance from the center of the ring singularity* (given by $\xi = 0 = x_2$). Spatial sections of the wave front are three-dimensional spaces, in which we can introduce standard spherical coordinates (r, θ, ψ) by

$$x_2 = r\cos\theta, \qquad \xi = r\sin\theta. \tag{39}$$

Since r is a radial coordinate from the center of the ring ($r^2 = x_2^2 + \xi^2$) and L is the radius of the ring, we consider an expansion for small values of the dimensionless parameter L/r. This means considering Eq. (31) for k and ρ approaching zero. Using Eqs. (A7)–(A9), we obtain

$$H_\perp = \frac{1}{\sqrt{2}}\frac{8p}{3L}\left[3\frac{L}{r} - \frac{7}{8}(3\cos^2\theta - 1)\frac{L^3}{r^3} + O\left(\frac{L^5}{r^5}\right)\right]. \tag{40}$$

We recognize the standard multipole terms [indeed, for $\xi > L$, $H_\perp$ is a solution of a three-dimensional Laplace equation, cf. Eq. (34)]. Notice that the dipole term is missing, due to the geometry of the source. In the limit when the ring shrinks to a point, i.e. $L \to 0$, the expansion reduces just to the monopole term,

$$H_\perp^0 = \lim_{L\to 0} H_\perp = \frac{1}{\sqrt{2}}\frac{8p}{r}. \tag{41}$$

This exhibits the "Newtonian" $1/r$ falloff in three-dimensional space, with a "mass" proportional to p. The metric (27) with a profile function given by $H_\perp^0$ coincides with the five-dimensional analogue of the Aichelburg-Sexl solution, obtained by boosting the Schwarzschild line element to the speed of light [9] (cf. also, e.g., [10,11,13]).

In order to gain further physical insight, one can similarly consider other expansions near "special places." For example, *near the axis* $\xi = 0$ we obtain

$$H_\perp = \frac{8\sqrt{2}p}{3L^2}\left[\frac{L^2 - x_2^2}{\sqrt{L^2 + x_2^2}} + |x_2| + \frac{3L^2}{4}\frac{L^2 - x_2^2}{\sqrt{(L^2 + x_2^2)^5}}\xi^2 + O(\xi^4)\right]. \tag{42}$$

Near the plane of the ring $x_2 = 0$,

$$H_\perp = \frac{1}{\sqrt{2}}\frac{8p}{3\pi L^2}\left[2\frac{3L^2 + \xi^2}{L + \xi}K(\tilde{k}) - 2(L + \xi)E(\tilde{k}) + 2\pi|x_2|\Theta(L - \xi) - \left(\frac{1}{L + \xi}K(\tilde{k}) + \frac{5L^2 - \xi^2}{(L - \xi)^2(L + \xi)}E(\tilde{k})\right)x_2^2 + O(x_2^4)\right], \tag{43}$$

where $\tilde{k} = k(x_2 = 0) = \sqrt{4L\xi}/(L + \xi)$.

If we introduce suitable coordinates "centered on the ring"

$$x_2 = \tilde{r}\sin\tilde{\theta}, \qquad \xi = L + \tilde{r}\cos\tilde{\theta}, \tag{44}$$

using Eqs. (A10)–(A12), the expansion [of Eq. (29)] *near the singular ring* $\tilde{r} = 0$ is

[5]The quantities Ψ_{ij} can be understood as a generalization of the complex scalar Ψ_4, which fully characterizes type N spacetimes in the well-known $D = 4$ theory.

$$H_\perp = \frac{1}{\sqrt{2}}\frac{8p}{3\pi L}\left\{-4\left(1+\log\frac{\tilde r}{8L}\right)+2\tilde\theta\sin\tilde\theta\frac{\tilde r}{L} - \frac{1}{4}\left[1+\cos 2\tilde\theta\left(1+3\log\frac{\tilde r}{8L}\right)\right]\frac{\tilde r^2}{L^2}+O\left(\frac{\tilde r^3}{L^3}\right)\right\}. \tag{45}$$

The ring-shaped singularity is explicitly visible in the first logarithmic term.

V. PARALLEL BOOST: $\alpha = \pi/2$

A. Evaluation of the impulsive limit of the metric

For $\alpha = \pi/2$ in Eq. (13), Eq. (14) becomes

$$t = \frac{-u' + v'}{\sqrt{2}}, \qquad y_1 = \frac{u' + v'}{\sqrt{2}}, \tag{46}$$

so that the transformation (15) describes a boost in the y_1 direction, i.e. in the 2-plane (ξ, ψ) [cf. Eq. (12)] containing the ring circle. As for the previous orthogonal boost, we need to calculate how the black ring metric (1) transforms under the boost (15), and then take the limit $\epsilon \to 0$. In the present case ($\alpha = \pi/2$) the coordinates η and ϕ remain unchanged, hence we substitute the second column of Eq. (12) into Eqs. (9) and (10). Apart from this, we follow the same steps as in Sec. IV, and the derivation here will be therefore shortened in its straightforward parts. The flat, boost-invariant part of the decomposition (6) can now be written as

$$ds_0^2 = 2dudv + dy_2^2 + d\eta^2 + \eta^2 d\phi^2. \tag{47}$$

For the additional term $\lambda\Delta$, as $\epsilon \sim 0$ we get an expression analogous to Eq. (24), but with $h_\perp(z_\epsilon)$ replaced by

$$h_{||}(z_\epsilon) = \frac{4L^2 - y_2^2}{2\Sigma_\epsilon} - \frac{4L^2\eta^2 z_\epsilon^2}{\Sigma_\epsilon^3} - \frac{y_2^2(L^2+\eta^2)}{2(z_\epsilon^2+y_2^2)\Sigma_\epsilon} + \frac{y_2^2}{2(z_\epsilon^2+y_2^2)}, \tag{48}$$

and

$$\Sigma_\epsilon = \sqrt{z_\epsilon^4 + 2(y_2^2+\eta^2-L^2)z_\epsilon^2 + a^4}, \tag{49}$$

with

$$a = [(\eta^2 + y_2^2 - L^2)^2 + 4\eta^2 L^2]^{1/4}. \tag{50}$$

Again employing identity (26), the final boosted metric is now

$$ds^2 = 2dudv + dy_2^2 + d\eta^2 + \eta^2 d\phi^2 + H_{||}(y_2, \eta)\delta(u)du^2, \tag{51}$$

with a profile function

$$H_{||}(y_2, \eta) = \frac{8\sqrt{2}p}{3\pi L^2}\left(\int_{-\infty}^{+\infty} h_{||}(z)dz\right). \tag{52}$$

We employ the elliptic integrals (A17)–(A19) of Appendix A in order to perform the integration in Eq. (52) [with $h_{||}$ given by Eqs. (48) and (49)]. Combining all the terms, and using identity (A5) to reexpress the elliptic integral Π in a more convenient form, we obtain

$$H_{||}(y_2, \eta) = \frac{8\sqrt{2}p}{3\pi L^2}\left[\frac{5L^2+\eta^2+2a^2}{2a}K(k) - 2aE(k) + \frac{\eta^2+L^2}{2a}\frac{a^2+y_2^2}{a^2-y_2^2}\Pi(\rho, k) + \pi|y_2|\Theta(y_2^2-a^2)\right], \tag{53}$$

where

$$k = \frac{(a^2-\eta^2-y_2^2+L^2)^{1/2}}{\sqrt{2}a}, \qquad \rho = -2y_2^2\frac{a^2-\eta^2-y_2^2+L^2}{(a^2-y_2^2)^2}, \tag{54}$$

and a as in Eq. (50).

B. Properties of the solution

A static black ring boosted to the speed of light in a direction contained in the plane of the ring circle is thus represented by the metric (51) and (53). As in the case of the orthogonal boost of Sec. IV, this is a five-dimensional impulsive pp-wave. It propagates along the y_1 direction, and it is singular at the points satisfying $u = 0 = \eta$ and $|y_2| \le L$ [$k = 1$ in Eq. (54)], i.e. on a *rod of length* $2L$ contained within the wave front. This is a remnant of the curvature singularity of the original static black ring (1), which has Lorentz-contracted because of the ultrarelativistic boost in the plane of the ring. On the contrary, notice that the apparent divergence of $H_{||}$ at $y_2^2 = a^2$ is only a fictitious effect: the singular behavior of the coefficient of Π in Eq. (53) is compensated if one takes into account the form of ρ [Eq. (54)] and the step function in the last term. The profile function $H_{||}$ is plotted in Fig. 2.

The discussion of further properties of the solution (51) and (53) is now shortened, since it follows the similar one in Sec. IV. There exist isometries generated by the Killing vector fields ∂_v, ∂_ϕ, $u\partial_{y_2} - y_2\partial_v$, $u\partial_{x_1} - x_1\partial_v$ and $u\partial_{x_2} - x_2\partial_v$ [cf. Eq. (33)].

During the parallel boost, also the original disk membrane has Lorentz contracted, and it is now located on the singular region $u = 0 = \eta$, $|y_2| \le L$. We will not discuss the behavior of the solution there. Except on this singular rod, the Ricci tensor associated to the spacetime (51) and (53) is vanishing, as we verified using identities (A6).

Similarly as in Sec. IV, one can cast the Weyl tensor in the type N canonical form using the frame (35) with the replacements $\xi \to \eta$, $\psi \to \phi$, $x_2 \to y_2$ and, of course, $H_\perp \to H_{||}$. Analogously, one obtains the corresponding

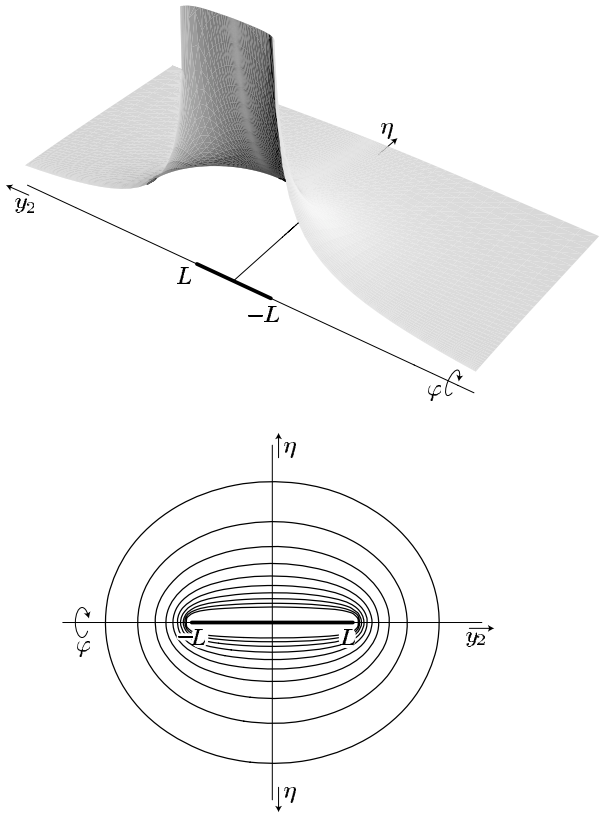

FIG. 2. Plot of the profile function $H_{||}(y_2, \eta)$ given by Eq. (53). This is the case of a static black ring boosted to the speed of light along a direction contained within the plane of the ring circle, i.e. (ξ, ψ). The coordinates (y_2, η, ϕ) span spatial sections of the impulsive wave front $u = 0$, cf. Eq. (51). The Killing coordinate ϕ is suppressed in the figures. The profile function $H_{||}$ diverges (only) at the *rod* singularity $\eta = 0$, $|y_2| \le L$, as indicated by the thick line in the pictures.

Weyl components from Eq. (38). In this case, we omit the explicit form of the scalars Ψ_{ij}, which is rather complicated and does not provide any immediate physical insight. We just notice that, again, the elliptic integral Π disappears.

Following the corresponding analysis of Sec. IV, we can analyze how the gravitational field generated by the boosted black ring (51) behaves *at a large spatial distance from the center of the rod singularity* (given by $\eta = 0 = y_2$). With spherical coordinates defined on the wave front by

$$y_2 = r\cos\theta, \qquad \eta = r\sin\theta, \tag{55}$$

we now obtain

$$H_{||} = \frac{1}{\sqrt{2}}\frac{8p}{3L}\left[3\frac{L}{r} + \frac{5}{8}(3\cos^2\theta - 1)\frac{L^3}{r^3} + O\left(\frac{L^5}{r^5}\right)\right]. \tag{56}$$

The monopole term coincides with that obtained in the case of $H_\perp$, cf. (40) and (41), and for $L \to 0$ (i.e., when the rod shrinks to a point) it gives rise to the five-dimensional Aichelburg-Sexl solution. Again, there is no dipole, but the quadrupole term is different from that of Eq. (40).

In addition, we can consider an expansion of $H_{||}$ *near the axis* $\eta = 0$. The rod singularity lies exactly at $\eta = 0$, for $|y_2| \le L$. Therefore, we have to study the two cases $|y_2| > L$ and $|y_2| < L$ separately. For $|y_2| > L$, one has

$$H_{||} = \frac{8\sqrt{2}p}{3L^2}\left[\frac{L^2}{\sqrt{y_2^2 - L^2}} + |y_2| - \sqrt{y_2^2 - L^2} - \frac{3}{4}\frac{L^2 y_2^2}{\sqrt{(y_2^2 - L^2)^5}}\eta^2 + O(\eta^4)\right]. \tag{57}$$

The case $|y_2| < L$ is more delicate and one has to employ expansions (A10)–(A12). At the end,

$$H_{||} = \frac{8\sqrt{2}p}{3\pi L^2}\left[\frac{y_2^2 - 2L^2}{\sqrt{L^2 - y_2^2}}\log\frac{L^2\eta^2}{16(L^2 - y_2^2)^2} - 2\sqrt{L^2 - y_2^2} + |y_2|\operatorname{arccot}\frac{L^2 - 2y_2^2}{2|y_2|\sqrt{L^2 - y_2^2}} + O(\eta^2)\right], \tag{58}$$

where "arccot" takes values in $[0, \pi]$. The first term carries the singular behavior at the rod $\eta = 0$.

VI. GENERAL BOOST: AN ARBITRARY α

We finally consider the boost in a general direction z_1, which is characterized by the angular parameter α, see Eqs. (13)–(15). We employ the method of the previous sections, and after straightforward calculations we again obtain an impulsive pp-wave

$$ds^2 = 2dudv + dx_2^2 + dy_2^2 + dz_2^2 + H(x_2, y_2, z_2)\delta(u)du^2. \tag{59}$$

Now the profile function

$$H(x_2, y_2, z_2) = \frac{8\sqrt{2}p}{3\pi L^2}\left(\int_{-\infty}^{+\infty} h(z)dz\right), \tag{60}$$

is an integral of the function

$$h(z) = \frac{L^2}{\Sigma} + \frac{L^2}{\Sigma^3}\left[\left(\xi^2 - \eta^2 - L^2\right)\frac{y_1}{\xi}\sin\alpha + 2\xi x_1\cos\alpha\right]^2 + \frac{1}{2}\left(1 - \frac{\xi^2 + \eta^2 - L^2}{\Sigma}\right)\left(\frac{y_2^2}{\xi^2}\sin^2\alpha + \frac{x_2^2}{\eta^2}\cos\alpha\right). \tag{61}$$

Here the dependence on z is contained in

$$y_1 = z\sin\alpha + z_2\cos\alpha, \qquad \xi^2 = y_1^2 + y_2^2,$$
$$x_1 = z\cos\alpha - z_2\sin\alpha, \qquad \eta^2 = x_1^2 + x_2^2, \tag{62}$$

and in Σ, given by Eq. (11). In order to perform the above

integration, it is convenient to factorize Σ as

$$\Sigma = \sqrt{[(z-r_1)^2 + s_1^2][(z+r_1)^2 + s_2^2]}, \tag{63}$$

where the parameters s_1 and s_2 are defined by

$$s_1^2 = r_1^2 + A - \frac{2B}{r_1}, \qquad s_2^2 = r_1^2 + A + \frac{2B}{r_1}, \tag{64}$$

and r_1 by the equation (of third order in r_1^2)

$$r_1^6 + A r_1^4 + \frac{1}{4}(A^2 - C) r_1^2 - B^2 = 0, \tag{65}$$

with

$$\begin{aligned} A &= x_2^2 + y_2^2 + z_2^2 - L^2 + 2L^2 \cos^2\alpha, \\ B &= L^2 z_2 \sin\alpha \cos\alpha, \\ C &= (x_2^2 + y_2^2 + z_2^2 - L^2)^2 + 4L^2(x_2^2 + z_2^2 \sin^2\alpha). \end{aligned} \tag{66}$$

Using Cardano's formula we may write the root r_1^2 as

$$r_1^2 = -\frac{A}{3} + \sqrt[3]{-\frac{q}{2} + \sqrt{Q}} + \sqrt[3]{-\frac{q}{2} - \sqrt{Q}}, \tag{67}$$

where

$$\begin{aligned} Q &= \left(\frac{p}{3}\right)^3 + \left(\frac{q}{2}\right)^2, \qquad p = -\frac{1}{3}A^2 + \frac{1}{4}(A^2 - C), \\ q &= \frac{2}{27}A^3 - \frac{1}{12}A(A^2 - C) - B^2. \end{aligned} \tag{68}$$

Notice that for the particular case of the orthogonal boost ($\alpha = 0$) we obtain $r_1 = 0$, $s_1^2 = x_2^2 + (\xi + L)^2$, $s_2^2 = x_2^2 + (\xi - L)^2$, which coincides with Eq. (22), while for the parallel boost ($\alpha = \frac{\pi}{2}$) one has $2r_1^2 = a^2 - y_2^2 - \eta^2 + L^2$ and $2s_1^2 = 2s_2^2 = a^2 + y_2^2 + \eta^2 - L^2$, which is equivalent to Eq. (49) [a is defined in Eq. (50)]. For any α, the integral (60) could now be expressed using elliptic integrals, in principle (because Σ is a square root of a fourth order polynomial in z) [26,27]. For example, the simplest first term in Eq. (61) leads to [27]

$$\int_{-\infty}^{+\infty} \frac{dz}{\Sigma(z)} = \frac{2}{\sqrt{s_1 s_2 k_1}} K(k), \tag{69}$$

where

$$\begin{aligned} k^2 &= \frac{k_1^2 - 1}{k_1^2}, \qquad k_1 = \sqrt{D^2 - 1} + D, \\ D &= \frac{4r_1^2 + s_1^2 + s_2^2}{2 s_1 s_2}. \end{aligned} \tag{70}$$

We can investigate the location of the singularity of the expression (69). This occurs when $k = 1$, i.e. for $s_1 s_2 = 0$. From (64) one gets $s_1^2 s_2^2 = -3r_1^4 - 2Ar_1^2 + C$, so that the singularity is at $r_1^2 = -\frac{1}{3}(A + \sqrt{A^2 + 3C})$. This exactly corresponds to the explicit expression (67) for $Q = 0$, i.e. $27q^2 = -4p^3$. Using the relations (66) and (68), it is straightforward (but somewhat lengthy) to demonstrate that this polynomial condition is satisfied for

$$x_2 = 0, \qquad z_2^2 = (L^2 - y_2^2)\cos^2\alpha. \tag{71}$$

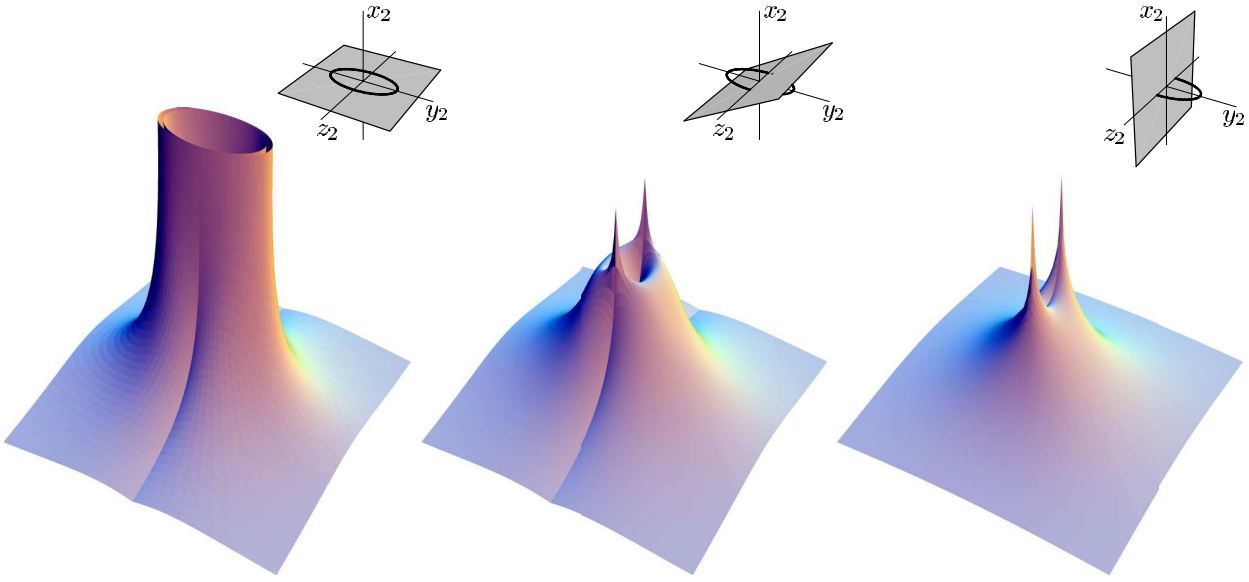

FIG. 3 (color online). Plot of the profile function $H(x_2, y_2, z_2)$ given by Eqs. (60) and (61). The integration in Eq. (60) has been performed numerically. The coordinates (x_2, y_2, z_2) span spatial sections of the impulsive wave front $u = 0$, cf. Eq. (59). Since this plot corresponds to a boost in a general direction z_1, the function H is not axially symmetry. We have thus depicted representative plots of the values taken by H over different sections of the three space (x_2, y_2, z_2). In the left figure, in particular, it is evident the ellipse-shaped singularity, cf. Eq. (72).

This singular behavior of the term (69) suggests that there is a singular source located on the wave front ($u = 0$) of the metric (59), precisely in the plane $x_2 = 0$ on the ellipse

$$\left(\frac{y_2}{L}\right)^2 + \left(\frac{z_2}{L\cos\alpha}\right)^2 = 1. \tag{72}$$

Of course the above argument is not conclusive. Rigorously, we should integrate also all the other terms in Eq. (61). This could in principle be done, but it would lead to an involved expression without much practical use. We rather prefer to integrate numerically the full function (61), and display the thus obtained profile H in Fig. 3, which indeed confirms the presence of a singular ellipse within the wave front. This also corresponds to intuitive expectations, since the original static circular source has been boosted in a general direction. [Moreover, it agrees with the following argument: the source of the black ring (1) was located at $y = -\infty$, i.e. $\eta = 0$ and $\xi = L$. In view of Eq. (62), these conditions become Eq. (71), which is unchanged under the boost (15).]

VII. CONCLUSIONS

We have derived the gravitational field generated by a five-dimensional static black ring moving "with the speed of light." More precisely, we have calculated how the Emparan-Reall line element transforms under appropriate boosts, and studied the ultrarelativistic limit when the boost velocity approaches the speed of light. In particular, we have studied in detail two complementary boosts along privileged directions, namely, those orthogonal and parallel to the plane containing the ring circle. The resulting line elements represent impulsive pp-waves. These are exact vacuum solutions everywhere except at singular points that are a remnant of the original curvature singularity of the static black ring. In addition, in the case of the orthogonal boost, there is a disk-shaped membrane inside the ring directly inherited from the conical singularity of the static Emparan-Reall spacetime. [Notice that the profile functions obtained via the boosting procedure ultimately provide solutions to equivalent problems of three-dimensional electrostatics (or Newtonian gravity) with a disk or a nonuniform rod source.] Further analysis of the solutions has been supplemented via graphical plots and via suitable expansions of the metric functions. We may also observe here that, if necessary, one could introduce a coordinate system in which the metric coefficients take a continuous form, using the general transformation presented in [6].

It is also worth remarking that, in contradistinction to the well-known situation in four dimensions [8], we did not need to perform any infinite subtractions during our calculations. This is essentially due to the faster falloff of the gravitational potential of a "monopole" in $D > 4$, which ensures that all the required integrals are finite. The same simplification occurred in previous investigations of ultrarelativistic boosts in higher dimensions [9,10,15], as well as in the case of the boost of particles with multipole moments in $D = 4$ (Weyl solutions) [28].

We have concentrated on a static ring containing a disk membrane at $x = +1$, for which there is no conical singularity at infinity. A generalization to the case of a ring with a deficit membrane at $x = -1$ (which extends to infinity) would be straightforward. It would be more interesting to extend our results to the case of rotating black rings. Such work is currently in progress [18].

ACKNOWLEDGMENTS

M. O. is supported by the Istituto Nazionale di Fisica Nucleare (bando n.10068/03).

APPENDIX A: ELLIPTIC INTEGRALS

In this appendix we summarize the definitions and the properties of the complete elliptic integrals employed in the main text, following references [26,27].

1. Definitions

The complete elliptic integrals in trigonometric form are defined by [26]

$$K(k) = \int_0^{\pi/2} \frac{d\alpha}{\sqrt{1 - k^2\sin^2\alpha}}, \tag{A1}$$

$$E(k) = \int_0^{\pi/2} \sqrt{1 - k^2\sin^2\alpha}\, d\alpha, \tag{A2}$$

$$\Pi(\rho, k) = \int_0^{\pi/2} \frac{d\alpha}{(1 - \rho\sin^2\alpha)\sqrt{1 - k^2\sin^2\alpha}}. \tag{A3}$$

2. Useful identities

They satisfy the identities [27]

$$(k^2 - \rho)\Pi(\rho, k) = k^2K(k) - \frac{\rho(1 - k^2)}{1 - \rho}\Pi\left(\frac{k^2 - \rho}{1 - \rho}, k\right), \tag{A4}$$

$$\Pi(\rho, k) = K(k) - \Pi\left(\frac{k^2}{\rho}, k\right) + \frac{\pi}{2}\sqrt{\frac{-\rho}{(1 - \rho)(k^2 - \rho)}}, \quad \text{with } \rho(1 - \rho)^{-1}(k^2 - \rho)^{-1} < 0. \tag{A5}$$

3. Differential relations

Derivatives of elliptic integrals lead to combinations of the same integrals:

$$\frac{dK(k)}{dk} = \frac{E(k)}{k(1-k^2)} - \frac{K(k)}{k},$$
$$\frac{dE(k)}{dk} = \frac{E(k)-K(k)}{k},$$
$$\frac{\partial\Pi(\rho,k)}{\partial k} = \frac{k}{k^2-\rho}\left[-\Pi(\rho,k) + \frac{E(k)}{1-k^2}\right], \tag{A6}$$
$$\frac{\partial\Pi(\rho,k)}{\partial\rho} = \frac{1}{2\rho(1-\rho)}\left[\frac{k^2-\rho^2}{k^2-\rho}\Pi(\rho,k) - K(k) - \frac{\rho}{k^2-\rho}E(k)\right].$$

4. Series representations

The behavior near $k = 0$ is given by

$$K(k) = \frac{\pi}{2}\left(1 + \frac{1}{4}k^2 + \frac{9}{64}k^4 + O(k^6)\right), \tag{A7}$$

$$E(k) = \frac{\pi}{2}\left(1 - \frac{1}{4}k^2 - \frac{3}{64}k^4 + O(k^6)\right), \tag{A8}$$

$$\Pi(\rho,k) = \frac{\pi}{2}\sum_{\mu=0}^{\infty}\sum_{\nu=0}^{\mu}\frac{(2\mu-1)!!(2\nu-1)!!}{(2\mu)!!(2\nu)!!}k^{2\nu}\rho^{\mu-\nu}, \quad \text{with } |\rho|<1. \tag{A9}$$

Near the singular point $k = 1$ one has

$$K(k) = -\frac{1}{2}\log\frac{1-k^2}{16} - \frac{1}{8}\left(2 + \log\frac{1-k^2}{16}\right)(1-k^2) - \frac{9}{128}\left(\frac{7}{3} + \log\frac{1-k^2}{16}\right)(1-k^2)^2 + O((1-k^2)^3), \tag{A10}$$

$$E(k) = 1 - \frac{1}{4}\left(1 + \log\frac{1-k^2}{16}\right)(1-k^2) - \frac{3}{32}\left(\frac{13}{6} + \log\frac{1-k^2}{16}\right)(1-k^2)^2 + O((1-k^2)^3), \tag{A11}$$

$$\Pi(\rho,k) = \frac{1}{1-\rho}\log\frac{4}{\sqrt{1-k^2}} + \frac{\sqrt{-\rho}}{1-\rho}\arctan\sqrt{-\rho} + O(1-k^2), \quad \text{with } \rho<0. \tag{A12}$$

5. Useful integrals: orthogonal boost

In Sec. IV we employed the following integrals:

$$\int_0^\infty \frac{dz}{\sqrt{(z^2+a^2)(z^2+b^2)}} = \frac{1}{a}K(k), \tag{A13}$$

$$\int_0^\infty \frac{z^2dz}{\sqrt{(z^2+a^2)^3(z^2+b^2)^3}} = \frac{a^2+b^2}{a(a^2-b^2)^2}K(k) - \frac{2a}{(a^2-b^2)^2}E(k), \tag{A14}$$

$$\int_0^\infty \frac{dz}{(z^2+c^2)\sqrt{(z^2+a^2)(z^2+b^2)}} = \frac{1}{a(b^2-c^2)}\left[\frac{b^2}{c^2}\Pi\left(-\frac{b^2-c^2}{c^2},k\right) - K(k)\right], \tag{A15}$$

where

$$k = \frac{\sqrt{a^2-b^2}}{a}, \qquad a>b>0, \qquad c\neq 0. \tag{A16}$$

6. Useful integrals: parallel boost

The integrals used in Sec. V are

$$\int_0^\infty \frac{dz}{\sqrt{z^4+2b^2z^2+a^4}} = \frac{1}{a}K(k), \tag{A17}$$

$$\int_0^\infty \frac{z^2dz}{\sqrt{(z^4+2b^2z^2+a^4)^3}} = \frac{a}{a^4-b^4}E(k) - \frac{1}{2a(a^2-b^2)}K(k), \tag{A18}$$

$$\int_0^\infty \frac{dz}{(z^2+c^2)\sqrt{z^4+2b^2z^2+a^4}} = \frac{1}{a(a^2-c^2)}\left[\frac{a^2+c^2}{2c^2}\Pi\left(-\frac{(a^2-c^2)^2}{4c^2a^2},k\right) - K(k)\right], \tag{A19}$$

with

$$k = \frac{\sqrt{a^2-b^2}}{\sqrt{2}a}, \qquad a^2>b^2>-\infty, \qquad a^2>0, \qquad c\neq 0. \tag{A20}$$

APPENDIX B: THE WEYL TENSOR FOR $H_\perp$

Here we present explicitly the frame components of the Weyl tensor in the case of the metric (27) and (31) describing a black ring boosted in an orthogonal direction. Using Eq. (A6), from Eq. (38) with Eq. (31) we obtain

$$\Psi_{11} = \frac{2\sqrt{2}p}{3\pi L^2}\frac{1}{\xi^2\sqrt{[(\xi+L)^2+x_2^2]^3}}\Big\{-[L^6+(x_2^2-2\xi^2)L^4+(\xi^4-x_2^4+8\xi^2x_2^2)L^2-x_2^2(x_2^2+\xi^2)^2]\frac{K(k)}{(\xi-L)^2+x_2^2}$$
$$+[L^8+(2x_2^2-7\xi^2)L^6+\xi^2(11\xi^2+7x_2^2)L^4-(x_2^2+\xi^2)(2x_2^4-13\xi^2x_2^2+5\xi^4)L^2-x_2^2(x_2^2+\xi^2)^3]$$
$$\times\frac{E(k)}{[(\xi-L)^2+x_2^2]^2}\Big\}\delta(u)-\frac{1}{6}R_{uu}, \tag{B1}$$

$$\Psi_{13} = \frac{2\sqrt{2}p}{3\pi L^2}\frac{x_2}{\xi\sqrt{[(\xi+L)^2+x_2^2]^3}}\Big\{-\frac{3L^4+4(x_2^2-\xi^2)L^2+(\xi^2+x_2^2)^2}{(\xi-L)^2+x_2^2}K(k)$$
$$+[3L^6+(11\xi^2+7x_2^2)L^4+5(x_2^2-3\xi^2)(x_2^2+\xi^2)L^2+(x_2^2+\xi^2)^3]\frac{E(k)}{[(\xi-L)^2+x_2^2]^2}\Big\}\delta(u), \tag{B2}$$

$$\Psi_{22} = \frac{4\sqrt{2}p}{3\pi L^2}\frac{1}{\xi\sqrt{(\xi+L)^2+x_2^2}}\Big\{(L^2-\xi^2-x_2^2)K(k)-\frac{L^4-(\xi^2+x_2^2)^2}{(\xi-L)^2+x_2^2}E(k)\Big\}\delta(u)-\frac{1}{6}R_{uu}, \tag{B3}$$

$$\Psi_{33} = -(\Psi_{11}+\Psi_{22}). \tag{B4}$$

The last equation follows from the tracelessness of the Weyl tensor.

[1] R. C. Myers and M. J. Perry, Ann. Phys. (N.Y.) **172**, 304 (1986).
[2] T. Banks and W. Fischler, hep-th/9906038.
[3] R. Emparan, G. T. Horowitz, and R. C. Myers, Phys. Rev. Lett. **85**, 499 (2000).
[4] S. B. Giddings and S. Thomas, Phys. Rev. D **65**, 056010 (2002).
[5] S. Dimopoulos and G. Landsberg, Phys. Rev. Lett. **87**, 161602 (2001).
[6] T. Dray and G. 't Hooft, Nucl. Phys. **B253**, 173 (1985).
[7] G. 't Hooft, Phys. Lett. B **198**, 61 (1987).
[8] P. C. Aichelburg and R. U. Sexl, Gen. Relativ. Gravit. **2**, 303 (1971).
[9] C. O. Loustó and N. Sánchez, Int. J. Mod. Phys. A **5**, 915 (1990).
[10] M. Ortaggio, J. High Energy Phys. 05 (2005) 048.
[11] D. M. Eardley and S. B. Giddings, Phys. Rev. D **66**, 044011 (2002).
[12] E. Kohlprath and G. Veneziano, J. High Energy Phys. 06 (2002) 057.
[13] H. Yoshino and Y. Nambu, Phys. Rev. D **66**, 065004 (2002).
[14] S. B. Giddings and V. S. Rychkov, Phys. Rev. D **70**, 104026 (2004).
[15] H. Yoshino, Phys. Rev. D **71**, 044032 (2005).
[16] R. Emparan and H. S. Reall, Phys. Rev. Lett. **88**, 101101 (2002).
[17] R. Emparan and H. S. Reall, Phys. Rev. D **65**, 084025 (2002).
[18] M. Ortaggio, P. Krtouš, and J. Podolský, gr-qc/0506064.
[19] R. Emparan, J. High Energy Phys. 03 (2004) 064.
[20] V. Pravda and A. Pravdová, gr-qc/0501003.
[21] A. Coley, R. Milson, V. Pravda, and A. Pravdová, Classical Quantum Gravity **21**, L35 (2004).
[22] P. C. Aichelburg and H. Balasin, Classical Quantum Gravity **13**, 723 (1996).
[23] J. Podolský and M. Ortaggio, Classical Quantum Gravity **18**, 2689 (2001).
[24] C. O. Loustó and N. Sánchez, Nucl. Phys. **B355**, 231 (1991).
[25] V. Pravda, A. Pravdová, A. Coley, and R. Milson, Classical Quantum Gravity **21**, 2873 (2004).
[26] I. S. Gradshteyn and I. M. Ryzhik, *Table of Integrals, Series, and Products* (Academic Press, San Diego, 2000), 6th ed.
[27] W. Gröbner and N. Hofreiter, *Integraltafel* (Springer-Verlag, Wien, 1966), Vol. 2.
[28] J. Podolský and J. B. Griffiths, Phys. Rev. D **58**, 124024 (1998).

Fields of accelerated sources: Born in de Sitter*

Jiří Bičák† and Pavel Krtouš‡
Institute of Theoretical Physics, Charles University, V Holešovičkách 2, 180 00 Prague 8, Czech Republic
and
Max-Planck Institute for Gravitational Physics (Albert Einstein Institute), 14476 Golm, Germany
(Received 8 June 2005; Accepted 6 July 2005; Published 27 October 2005)

This paper deals thoroughly with the scalar and electromagnetic fields of uniformly accelerated charges in de Sitter spacetime. It gives details and makes various extensions of our Physical Review Letter from 2002. The basic properties of the classical Born solutions representing two uniformly accelerated charges in flat spacetime are first summarized. The worldlines of uniformly accelerated particles in de Sitter universe are defined and described in a number of coordinate frames, some of them being of cosmological significance, the other are tied naturally to the particles. The scalar and electromagnetic fields due to the accelerated charges are constructed by using conformal relations between Minkowski and de Sitter space. The properties of the generalized "cosmological" Born solutions are analyzed and elucidated in various coordinate systems. In particular, a limiting procedure is demonstrated which brings the cosmological Born fields in de Sitter space back to the classical Born solutions in Minkowski space. In an extensive Appendix, which can be used independently of the main text, nine families of coordinate systems in de Sitter spacetime are described analytically and illustrated graphically in a number of conformal diagrams.

PACS numbers: 04.20.-q, 04.40.Nr, 98.80.Jk, 03.50.-z

I. INTRODUCTION

In 1969, on the sixtieth anniversary of Max Born's [1] first analysis of the field of a uniformly accelerated charge, Ginzburg, Nobelist in 2003, reanalyzed [2–4] this—what he called—"perpetual problem of classical physics," with the conclusion that the problem "is already clear enough not to be regarded as perpetual." Ginzburg confirmed the presence of radiation and emphasized that the vanishing of the radiation reaction force during the uniformly accelerated motion of the charge "is in no way paradoxical, in spite of the presence of radiation," since "a non-zero total energy flux through a surface surrounding a charge at a zero radiation force is exactly equal to the decrease of the field energy in the volume enclosed by this surface." Despite Ginzburg's view, however, the problem does not seem to lose its "perpetuity." A number of distinguished physicists who dealt with it before Ginzburg like Sommerfeld, Schott, von Laue, Pauli and others have, after Ginzburg, been followed by such authors as, for example, Bondi [5], Boulware [6], Peierls [7], Thirring [8] and others [9–12].

The fields and radiation patterns from uniformly accelerated general multipole particles were also studied [13]. The December 2000 issue of Annals of Physics contains three papers by Eriksen and Grøn [14–16] with numerous references on "electrodynamics of hyperbolically accelerated charges". (Yet, except for [1] and [6], the explicit citations above are not contained in [14–16].)

Spacetimes describing "uniformly accelerated particles or black holes" play fundamental role in general relativity. They are the only explicit solutions of Einstein's field equations known which are radiative and represent the fields of finite sources. Born fields in electrodynamics are produced by two charges moving along an "axis of symmetry" in opposite directions with uniform accelerations of the same magnitude. They have two symmetries: they are axially symmetric and symmetric with respect to the boosts along the axis of symmetry. Their general-relativistic counterparts, the boost rotation symmetric spacetimes, are unique because of a theorem which roughly states that in axially symmetric, locally asymptotically flat spacetimes the only additional symmetry that does not exclude radiation is the boost symmetry. The boost-rotation symmetric spacetimes have been used in gravitational radiation theory, quantum gravity, and as test beds in numerical relativity; their general structure is described in [17], their applications and new references are given in the reviews [18–20]. One of the best known examples, the so-called C-metric, describing uniformly accelerated black holes, is the only boost-rotation symmetric solution known also for a nonvanishing cosmological constant Λ. Asymptotically this "generalized" C-metric approaches de Sitter spacetime if $\Lambda > 0$. It is well-known from the classical work of Penrose [21] on the asymptotic properties of fields and spacetimes that, in contrast to asymptotically Minkowskian spacetimes with null (lightlike) conformal infinities $\mathcal{I}^{\pm}$, asymptotically de Sitter vacuum spacetimes have two disjoint conformal infinities, past and future, which are both *spacelike*. When $\Lambda < 0$, as in anti-de Sitter space, the conformal

*Published in J. Math. Phys. **46**, 102504 (2005).
This version differs only by a more compact formatting.
†bicak@mbox.troja.mff.cuni.cz
‡Pavel.Krtous@mff.cuni.cz

infinity is timelike, and it is not disjoint. (In the analytically extended C-metrics, there is an infinite number of such infinities which can be reached by going "through" black holes like with a Reissner-Nordtröm black hole, but this is not pertinent to the present work.)

The importance of de Sitter spacetime in the history of modern cosmology seems to grow steadily. The "flat" de Sitter universe became the standard cosmological model in steady state theory, more recently, as the "first approximation" of inflationary models, and today, with indications that $\Lambda > 0$ in our Universe, it is an asymptote of all indefinitely expanding Friedmann-Robertson-Walker models with $\Lambda > 0$. In fact much more general cosmological models with $\Lambda > 0$ approach de Sitter model asymptotically in time. This manifestation of the validity of the "cosmic no-hair conjecture" [22], [23] will also be noticed in the properties of the fields analyzed in this work.

Motivated by the role of the Born solution in classical electrodynamics, by the importance of the boost-rotation symmetric spacetimes in general relativity, and by the relevance of de Sitter space in contemporary cosmology, we have recently generalized the Born solution for scalar and electromagnetic fields to the case of two charges uniformly accelerated in de Sitter universe [24]. In the present paper we give calculations and detailed proofs of the results and statements briefly sketched in our paper [25]. In addition, we investigate the character of the field in a number of various coordinate systems which are relevant either in a general-relativistic context or from a cosmological perspective.

The appropriate coordinates and corresponding tetrad fields were important in finding our recent results on a general asymptotic behavior of fields in the neighborhood of future infinity $\mathcal{I}^+$ in asymptotically de Sitter spacetimes [26]. In obtaining these results we were inspired by the inspection of the electromagnetic fields from uniformly accelerated charges in de Sitter universe.

It was known from the work of Penrose since late 1960's that the radiation field is "less invariantly" defined when $\mathcal{I}^+$ is spacelike—that it depends on the direction in which $\mathcal{I}^+$ is approached. However, no explicit models were available. The investigation of the test fields of accelerated charges in de Sitter universe has served as a useful example; it was then generalized also to the study of asymptotic and radiative properties of the C-metric with $\Lambda > 0$ [27], as well as to the case of the C-metric with $\Lambda < 0$ when infinity is timelike [28]. (For other recent works on the "cosmological" C-metric, see, e.g., [29, 30].) These studies led to more general conclusions [26]: the directional pattern of gravitational and electromagnetic radiation near de Sitter-like conformal infinity has a universal character, determined by the algebraic (Petrov) type of a solution of the Maxwell/Einstein equations considered. In particular, the radiation field vanishes along directions opposite to principal null directions. Very recently analogous conclusions have been obtained for spacetimes with anti-de Sitter asymptotics [31].

Since past and future infinities are spacelike in de Sitter spacetime, there exist particle and event horizons. Under the presence of the horizons, purely retarded fields (appropriately defined) become singular or even cannot be constructed at the "creation light cones", i.e., at future light cones of the "points" at $\mathcal{I}^-$ at which the sources "enter" the universe. In [24] we analyzed this phenomenon in detail and constructed smooth (outside the sources) fields involving both retarded and advanced effects. As demonstrated in [24], to be "born in de Sitter" is quite a different matter than to be "born in Minkowski". This reveals the double meaning of the second—perhaps somewhat enigmatic—part of the title of this paper.

Its plan is as follows. In order to gain an understanding of the generalized Born solution in de Sitter space it is advantageous to be familiar with some details of the classical Born solution in Minkowski space. Hence, its properties most relevant for our purpose are summarized in Section II. Here we also discuss why in Minkowski space problems with purely retarded fields of uniformly accelerated particles do not arise.

There exists vast literature on de Sitter space in which various types of coordinates are employed. We shall construct fields in de Sitter space by using its conformal relations to Minkowski space. For our aim coordinate systems on conformally compactified spaces and their properties will be particularly useful. These, together with several "cosmological" and "static" coordinate systems, will be described and graphically illustrated in conformal diagrams in Section III. What is meant by "uniformly accelerated particles in de Sitter space" is defined and the properties of the corresponding worldlines are studied in Section IV. For technical reasons it is more advantageous to consider particles which asymptotically start and end at the poles of coordinates covering de Sitter space, i.e., particles "born at the poles" (Section IV A). In order to find a direct relation between the standard form of the Born solution produced by two charges at each time located symmetrically with respect to the origin of Minkowski space and the generalized Born solution in de Sitter space, it is necessary to construct also worldlines of uniformly accelerated particles which are "born at the equator" (Section IV B).

With the worldlines of accelerated particles available, it is advantageous to consider coordinates in de Sitter space which are centered on these worldlines. These "accelerated coordinates" and "Robinson-Trautman coordinates" are obtained, in a constructive manner, in Section V.

Section VI is devoted to the fields from particles "born at the poles". Here we also study in detail their properties in various coordinate systems introduced before. The fields of particles "born at the equator" are found in Section VII by a simple rotation. Starting from these fields we demonstrate by means of which limiting procedure the standard Born field in Minkowski space can be regained. Finally, we conclude by few remarks in Section VIII.

The paper contains a rather extensive Appendix in which nine families of coordinate systems employed in the main text are described in detail, illustrated graphically, their relations are given, and corresponding metric forms as well as orthonormal tetrads are presented. We believe the Appendix can be used as a general-purpose catalogue in other studies of physics in de Sitter spacetime.

II. BORN IN MINKOWSKI

It was Einstein in 1908, inspired by a letter from Planck, who first defined a *uniformly accelerated* motion in special relativity [32, 33]. A particle is in uniformly accelerated motion if its acceleration has a fixed constant value in instantaneous rest frames of the particle. This can be stated in a covariant form (see, e.g., [34]) as

$$\mathrm{P}^{\alpha}_{\mu}\,\dot{\mathrm{a}}^{\mu} = \dot{\mathrm{a}}^{\alpha} - (\mathrm{a}^{\mu}\,\mathrm{a}_{\mu})\,\mathrm{u}^{\alpha} = 0\,, \tag{2.1}$$

u^{α} being four-velocity, $\dot{} \equiv \mathrm{u}^{\mu}\nabla_{\mu}$ covariant derivative with respect to proper time, $\mathrm{a}^{\alpha} = \dot{\mathrm{u}}^{\alpha}$ four-acceleration, and $\mathrm{P}^{\alpha}_{\mu} = \delta^{\alpha}_{\mu} + \mathrm{u}^{\alpha}\,\mathrm{u}_{\mu}$ is the projection tensor into the hypersurface orthogonal to u^{α}. Eq. (2.1) implies $\dot{\mathrm{a}}^{\mu}\mathrm{a}_{\mu} = 0$ so that the condition of uniform acceleration guarantees that the magnitude of the four-acceleration is constant,

$$a_{\mathrm{M}} = \sqrt{\mathrm{a}^{\mu}\,\mathrm{a}_{\mu}} = \text{constant}, \tag{2.2}$$

although $\dot{\mathrm{a}}^{\mu} \neq 0$. Integrating Eq. (2.1) in Minkowski spacetime, one finds that the worldline of a uniformly accelerated particle is a hyperbola [35, 36]. One can then choose an inertial frame, in which the initial three-velocity and three-acceleration are parallel; in such frames the motion is spatially 1-dimensional. It can be produced by putting a test charged particle into a homogenous electric field with initial velocity aligned with the field. The motion along the z axis is illustrated in Fig. 1. There, in fact, *two* particles uniformly accelerated in opposite directions are shown, the one moving along the positive ($\varepsilon = +1$ for particle $w_{\oplus}$ in the figure) and the second one along the negative z axis ($\varepsilon = -1$ for particle $w_{\ominus}$); their worldlines parametrized by proper time λ_{M} are

$$z = \varepsilon\, b_{\mathrm{o}} \cosh\frac{\lambda_{\mathrm{M}}}{b_{\mathrm{o}}}\,, \quad t = b_{\mathrm{o}} \sinh\frac{\lambda_{\mathrm{M}}}{b_{\mathrm{o}}}\,, \quad x = y = 0\,, \tag{2.3}$$

or

$$z = \varepsilon\sqrt{t^2 + b_{\mathrm{o}}^2}\,. \tag{2.4}$$

Here we have chosen the particles to be at rest at $z = \varepsilon b_{\mathrm{o}}$ at $t = 0$. Then their three-acceleration at initial moment $t = 0$ is $a_{\mathrm{M}} = \left|d^2z/dt^2\right| = 1/b_{\mathrm{o}}$. As $t \to \infty$, the three-velocity $v_{\mathrm{M}} = |dz/dt| = t/\sqrt{t^2 + b_{\mathrm{o}}^2}$ approaches the velocity of light. This is the well-known *hyperbolic motion*.

The worldlines of the particles coincide with the orbits of the boost Killing vector in the t-z plane,

$$\xi_{\mathrm{boost}} = z\frac{\partial}{\partial t} + t\frac{\partial}{\partial z}\,. \tag{2.5}$$

These orbits, given by $-t^2 + z^2 = \text{constant}$, x, $y = \text{constant}$, are timelike at $-t^2 + z^2 > 0$, but they are spacelike at $-t^2 + z^2 < 0$. The fields (scalar, electromagnetic, higher-spin) produced by charged particles in the hyperbolic motion will have boost-rotational symmetry. They are thus static in the region $-t^2 + z^2 > 0$—"below the roof" as introduced in [17], however, we can expect them to be radiative in the region $-t^2 + z^2 < 0$—"above the roof".

Consider a massless scalar field Φ with the scalar charge source S satisfying, in a general 4-dimensional spacetime, the wave equation

$$\left[\Box - \tfrac{1}{6}R\right]\Phi = S\,, \tag{2.6}$$

in which $\Box \equiv g^{\mu\nu}\nabla_{\mu}\nabla_{\nu}$ is the curved-space d'Alambertian, and R is the scalar curvature (of course, in Minkowski space $R = 0$). We are interested in a field due to two monopole particles with the same constant scalar charge of magnitude s moving along hyperbolae (2.3). The source at a spacetime point x is thus given by

$$S = S_{\oplus} + S_{\ominus}\,, \quad S_{\varepsilon} = s\int \delta(x - w_{\varepsilon}(\lambda_{\mathrm{M}}))\,d\lambda_{\mathrm{M}}\,, \tag{2.7}$$

where $w_{\varepsilon}(\lambda_{\mathrm{M}})$ denotes the worldlines of the particles. The resulting fields may be written as

$$\Phi = \Phi_{\oplus} + \Phi_{\ominus}\,, \tag{2.8}$$

where Φ_{ε} is produced by S_{ε}. The retarded and advanced fields of these sources are constructed and analyzed in detail in Ref. [17]. It can be demonstrated that the retarded and advanced fields due to the particle $w_{\oplus}$ or $w_{\ominus}$ are all given by exactly *identical* expression

$$\Phi_{\mathrm{BM}} = \frac{s}{4\pi}\frac{1}{\mathcal{R}}\,, \tag{2.9}$$

which, however, is valid in different regions of spacetime. Namely,

$$\Phi_{\mathrm{ret/adv}\,\varepsilon} = \frac{s}{4\pi}\frac{1}{\mathcal{R}}\,\theta(\varepsilon z \pm t)\,, \tag{2.10}$$

θ being the step function and upper/lower sign is valid for retarded/advanced case. The quantity $\mathcal{R}$ in the denominator is given by

$$\mathcal{R} = \frac{1}{2b_{\mathrm{o}}}\left(\left(b_{\mathrm{o}}^2 + t^2 - r^2\right)^2 + 4b_{\mathrm{o}}^2 r^2\sin^2\vartheta\right)^{\frac{1}{2}}\,. \tag{2.11}$$

It has the meaning of a *retarded* or *advanced distance*—it is a spatial distance of the "observation" (field) point from the position of the source at retarded or advanced time. Here, as usual, $x = r\sin\vartheta\cos\varphi$, $y = r\sin\vartheta\sin\varphi$, $z = r\cos\vartheta$. The fields (2.9), as well as (2.10), are, at first glance, axially (rotationally) symmetric. They are also unchanged under the boost along the z axis.

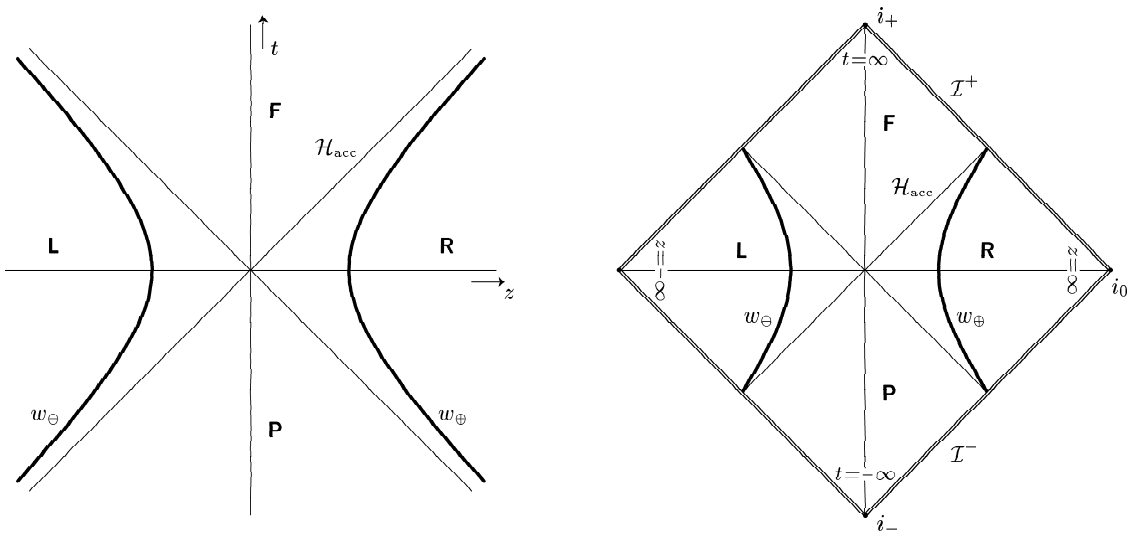

Figure 1: A pair of uniformly accelerated charges in Minkowski spacetime (with the conformal diagram on the right). The boost Killing vector is timelike in regions **L** and **R**; it is spacelike in **F** and **P**. The charges are causally disconnected by null hypersurfaces ("the roof") $-t^2+z^2=0$. These hypersurfaces represent the acceleration horizon for uniformly accelerated observers with respect to which the charges are at rest.

The field $\Phi_{\rm BM}$ can, in fact, be viewed as the field due to both accelerated particles, i.e., as the field corresponding to the source (2.7). Inspecting regions at which the retarded and advanced fields (2.10) are non-vanishing we discover that $\Phi_{\rm BM}$ admits the interpretation as arising from 1-parametric combination of retarded and advanced effects from both particles:

$$\Phi_{\rm BM}=\xi\Phi_{{\rm ret}\oplus}+(1-\xi)\Phi_{{\rm adv}\oplus}+(1-\xi)\Phi_{{\rm ret}\ominus}+\xi\Phi_{{\rm adv}\ominus}\,, \tag{2.12}$$

where $\xi\in\mathbb{R}$ is an arbitrary constant parameter. In particular, choosing $\xi=\frac{1}{2}$, the field $\Phi_{\rm BM}$ arises from $\frac{1}{2}(\Phi_{\rm ret}+\Phi_{\rm adv})$ from both particles. With $\xi=1$, the field can be interpreted as being caused by purely retarded effects from particle $w_\oplus$ in region $z+t>0$, and by purely advanced effects from particle $w_\ominus$ in region $z+t<0$.

The case of electrodynamics is very similar. The solution corresponding to the scalar field (2.9) was found by Born in 1909 [1]. It is customarily given in cylindrical coordinates (see, e.g., [14, 34, 37]), however, in order to compare it with its generalization to de Sitter universe, it is more convenient to write it down in spherical coordinates:

$$\begin{aligned}\mathrm{F}_{\rm BM}=&-\frac{e}{4\pi}\frac{1}{2b_0}\frac{1}{\mathcal{R}^3}\\ &\times\Big(-(b_0^2+t^2-r^2)\cos\vartheta\,\mathrm{d}t\wedge\mathrm{d}r\\ &\quad+(b_0^2+t^2+r^2)\,r\sin\vartheta\,\mathrm{d}t\wedge\mathrm{d}\vartheta\\ &\quad-2\,t\,r^2\sin\vartheta\,\mathrm{d}r\wedge\mathrm{d}\vartheta\Big)\,.\end{aligned} \tag{2.13}$$

The field can be obtained from the Liénard-Wiechert retarded and advanced potentials of two charged particles moving along hyperbolae (2.3), however, in contrast to the scalar case when charges are exactly the same, the electric charges have *opposite* signs. Similarly to the scalar case, the field is smooth everywhere, except for the places where the particles occur. $\mathrm{F}_{\rm BM}$ can be interpreted in the precisely same way as the scalar field (2.9), i.e., as the 1-parametric combination of retarded and advanced effects from both charges, analogously to Eq. (2.12). However, in the electromagnetic case an exact form of retarded and advanced fields from a single particle is a more subtle issue. Considering that the field in the region $z+t>0$ may be interpreted as the retarded effect emitted from the charge which moves along $z>0$, it is natural to try to exclude advanced effects of the other particle by requiring the field to vanish in the region $z+t<0$ (cf. Fig. 1). The field is then not smooth at the null hypersurface $z=-t$. In the scalar case such a field *does* represent the pure retarded field of the single particle, cf. Eq. (2.10). However, in the electromagnetic case the field $\mathrm{F}_{\rm BM}\,\theta(z+t)$ corresponds to sources consisting not only of the particle but also of a "charged wall" moving along hypersurface $z+t=0$ with velocity of light [5, 38]. Nevertheless, it is possible to obtain a pure retarded field of the only single particle by modifying the field with a delta function valued term localized on $z+t=0$ [6, 39, 40].

In de Sitter space such a modification is not feasible because the advanced fields cannot be excluded. The underlying cause is the *null* character of the past conformal infinity in Minkowski spacetime, whereas in de Sitter spacetime both future and past conformal infinities are *spacelike*. As a consequence, the Gauss constraint restricts the data at the spacelike past infinity, and it

can be shown that a purely retarded field of a point-like charge cannot satisfy this constraint [24]. The absence of purely retarded fields is also related to a different character of the past horizon of a particle. Since the worldline of a particle "enters" the universe through the past spacelike infinity, there exists the past particle horizon, called also the *creation light cone*. In de Sitter space a purely retarded electromagnetic field of a point-like charge cannot be constructed on the whole cone. In Minkowski spacetime the creation light cone of a particle moving asymptotically in the past freely, coincides with the whole past null infinity, and thus it does not belong to the physical spacetime. Eternally accelerated particles can "enter" the Minkowski spacetime at a point of the past null infinity—as, for example, uniformly accelerated particles do. Like in de Sitter case, in conformal spacetime the past horizon of such particles forms the null cone but, in contrast to de Sitter space, it has *one generator in common* with the null infinity. In physical spacetime this horizon thus corresponds to a null hyperplane—for the particle $w_\oplus$ it is just the hyperplane $z + t = 0$ (cf. Fig. 1)—and so its spatial sections are not compact. Thanks to this non-compactness the "bad" behavior of the retarded field on the horizon can be "pushed *out of sight*" to the infinity. We analyzed this issue in detail in Ref. [24].

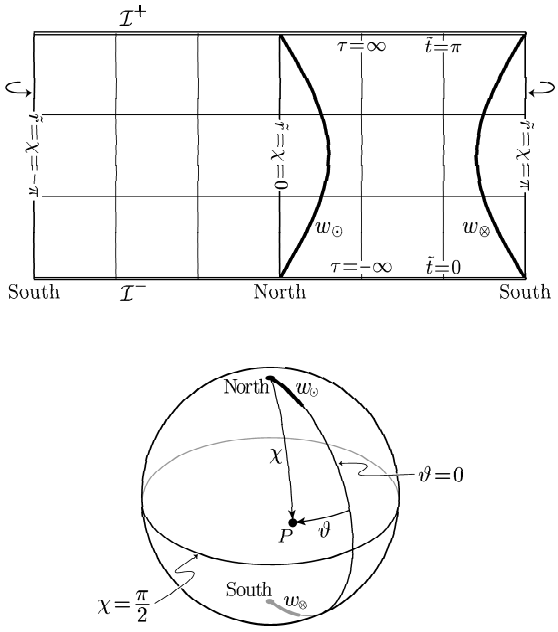

Figure 2: The spherical cosmological coordinates and a pair of uniformly accelerated particles $w_\odot$ and $w_\otimes$ in de Sitter universe: the conformal diagram (above) and projection on *the spacelike cut* $\tau = constant$ *in the standard cosmological* spherical coordinates (angle φ suppressed). The whole de Sitter spacetime could be represented by just the "right half" of the conformal diagram. For convenience, we admit negative values of radial coordinates and identify $\tilde{r} = \chi = -\pi$ and $\tilde{r} = \chi = \pi$ (see the text below Eq. (3.12) and the Appendix).

III. MANY FACES OF DE SITTER

The fields due to various types of uniformly accelerated sources in de Sitter spacetime found in [24], as well as those described briefly in Ref. [25], were constructed by employing the conformal relation between Minkowski and de Sitter spacetimes. When analyzing the worldlines of the sources in de Sitter spacetime and their relation to the corresponding worldlines in Minkowski spacetime we need to introduce appropriate coordinate systems. Suitable coordinates will later be used to exhibit various properties of the fields. An extensive literature exists on various types of coordinates in de Sitter space (e.g. [41, 42]), but we want to survey some of them in this section. In particular, we relate them to the corresponding coordinates on conformally related Minkowski spaces since this does not appear to be given elsewhere. In the next section, after identifying the worldlines of uniformly accelerated particles in de Sitter space, we shall construct new coordinate systems tied to such particles, such as Rindler-type "accelerated" coordinates, or Robinson-Trautman-type coordinates in which the null cones emanating from the particles have especially simple forms. These coordinate systems will turn out to be very useful in analyzing the fields. Here, in the main text, however, only a brief description of relevant coordinates will be given. More details, including both formulas and illustrations, are relegated to the Appendix.

As it is well-known from textbooks on general relativity (for a recent pedagogical exposition, see [43]), de Sitter spacetime, which is the solution of Einstein vacuum equations with a cosmological term $\Lambda > 0$, is best visualized as the 4-dimensional hyperboloid imbedded in flat 5-dimensional Minkowski space. It is the homogeneous space of constant curvature equal to 4Λ. Hereafter, we use the quantity

$$\ell_\Lambda = \sqrt{\frac{3}{\Lambda}} \tag{3.1}$$

(with the dimension of length) to parametrize the radius of the curvature.

The entire de Sitter spacetime can be covered by a single coordinate system—which we call *standard coordinates*—$\tau \in \mathbb{R}$, $\chi \in (0, \pi)$, $\vartheta \in (0, \pi)$, $\varphi \in (-\pi, \pi)$ in which the metric reads

$$g_{\rm ds} = -\mathrm{d}\tau^2 + \ell_\Lambda^2 \cosh^2 \frac{\tau}{\ell_\Lambda} \left(\mathrm{d}\chi^2 + \sin^2\chi \, \mathrm{d}\omega^2 \right), \tag{3.2}$$

$$\mathrm{d}\omega^2 = \mathrm{d}\vartheta^2 + \sin^2\vartheta \, \mathrm{d}\varphi^2 \, . \tag{3.3}$$

Clearly, we can imagine the spacetime as the time evolution of a 3-sphere which shrinks from infinite extension at $\tau \to -\infty$ to a radius ℓ_Λ, and then expands again in a

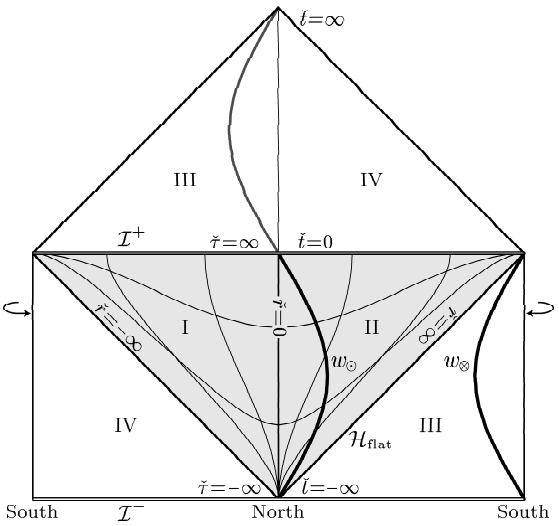

Figure 3: The flat cosmological coordinates and particles $w_\odot$, $w_\otimes$ in de Sitter space and in conformally related Minkowski space. The flat cosmological coordinates cover shaded region. Its boundary, $\check{r}=\pm\infty$, represents the horizon for observers at rest in these coordinates.

time-symmetric way. Hence, we also call τ, χ the *spherical cosmological coordinates*. The coordinate lines are shown in the conformal diagram, Fig. 2.

In cosmology the most popular "flat" de Sitter universe is obtained by considering only a half of de Sitter hyperboloid foliated by flat 3-dimensional spacelike hypersurfaces labeled by timelike coordinate $\check{\tau}\in\mathbb{R}$, cf. Fig. 3. Together with appropriate radial coordinate $\check{r}\in\mathbb{R}^+$, the new coordinates, which we call *flat cosmological coordinates*, are given in terms of τ, χ by

$$\begin{aligned}\check{\tau} &= \ell_\Lambda \log\Big(\sinh\frac{\tau}{\ell_\Lambda}+\cosh\frac{\tau}{\ell_\Lambda}\cos\chi\Big)\,,\\ \check{r} &= \ell_\Lambda\frac{\sin\chi}{\cos\chi+\tanh(\tau/\ell_\Lambda)}\,,\end{aligned}\tag{3.4}$$

implying the well-known "inflationary" metric

$$g_{\rm dS}=-\mathrm{d}\check{\tau}^2+\exp\frac{2\check{\tau}}{\ell_\Lambda}\Big(\mathrm{d}\check{r}^2+\check{r}^2\,\mathrm{d}\omega^2\Big)\,.\tag{3.5}$$

These coordinates cover only "one-half" of de Sitter space as indicated by shading in Fig. 3.

de Sitter introduced his model in what we call *hyperbolic cosmological coordinates* $\eta\in\mathbb{R}$, $\rho\in\mathbb{R}^+$ (see Fig. 4) related to τ, χ by

$$\begin{aligned}\cosh\frac{\eta}{\ell_\Lambda} &= \cosh\frac{\tau}{\ell_\Lambda}\cos\chi\,,\\ \tanh\frac{\rho}{\ell_\Lambda} &= \coth\frac{\tau}{\ell_\Lambda}\sin\chi\,.\end{aligned}\tag{3.6}$$

The metric

$$g_{\rm dS}=-\mathrm{d}\eta^2+\sinh^2\frac{\eta}{\ell_\Lambda}\Big(\mathrm{d}\rho^2+\ell_\Lambda^2\sinh^2\frac{\rho}{\ell_\Lambda}\,\mathrm{d}\omega^2\Big)\tag{3.7}$$

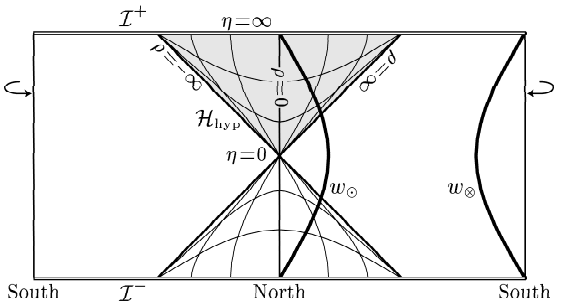

Figure 4: The hyperbolic cosmological coordinates. They cover only the shaded region and, therefore, only a part of the worldline $w_\odot$. The horizon $\mathcal{H}_{\rm hyp}$ arises for the observers who are at rest in the hyperbolic cosmological coordinates.

shows that the time slices $\eta=$ constant have the geometry of constant negative curvature, i.e., as the standard time slices in an open FRW universe.

The last commonly used coordinates in de Sitter spacetime are *static coordinates* $T\in\mathbb{R}$, $R\in(0,\ell_\Lambda)$:

$$\begin{aligned}T &= \frac{\ell_\Lambda}{2}\log\left|\frac{\cos\chi+\tanh(\tau/\ell_\Lambda)}{\cos\chi-\tanh(\tau/\ell_\Lambda)}\right|\,,\\ R &= \ell_\Lambda\cosh\frac{\tau}{\ell_\Lambda}\,\sin\chi\,,\end{aligned}\tag{3.8}$$

covering also only a part of the universe. The metric in these coordinates reads

$$g_{\rm dS}=-\Big(1-\frac{R^2}{\ell_\Lambda^2}\Big)\,\mathrm{d}T^2+\Big(1-\frac{R^2}{\ell_\Lambda^2}\Big)^{-1}\mathrm{d}R^2+R^2\,\mathrm{d}\omega^2\,,\tag{3.9}$$

revealing that $\partial/\partial T$ is a timelike Killing vector in the region $0<R<\ell_\Lambda$.

Among the coordinates introduced until now only the standard coordinates τ, χ, ϑ, φ cover the whole de Sitter spacetime globally. One can easily extend flat cosmological coordinates to cover (though not smoothly) the whole de Sitter hyperboloid, which will be useful in discussion of the conformally related Minkowski spacetime, cf. Eq. (3.13). We shall also use extensions of the static coordinates into the whole spacetime, using definitions (3.8), but allowing $R\in\mathbb{R}^+$. In regions where $R>\ell_\Lambda$ coordinates T and R interchange their character, $\partial/\partial T$ becomes a spacelike Killing vector (analogously to $\partial/\partial t$ inside a Schwarzschild black hole). However, the static coordinates T, R are not globally smooth and uniquely valued. Namely, $T\to\infty$ at the cosmological horizons $R=\ell_\Lambda$. The static coordinates, extended to the whole de Sitter space, are illustrated in Fig. 5. Here we also indicate the regions in which $\partial/\partial T$ is spacelike by bold **F** ("future") and **P** ("past"), whereas the regions in which it is timelike are denoted by **N** (containing the "north pole" $\chi=0$) and **S** (containing the "south pole" $\chi=\pi$). Hereafter, this notation will be used repeatedly.

The conformal structure of Minkowski and de Sitter spacetimes, their conformal relation, and their confor-

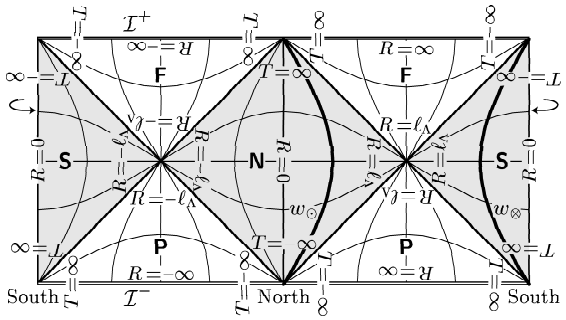

Figure 5: The static coordinates and the wordlines of particles $w_\odot$ and $w_\otimes$. These coordinates can be defined in the whole spacetime, however several coordinate patches, in diagram indicated by shaded and nonshaded regions, have to be used (cf. Appendix A 5 and A 6). These regions are separated by the cosmological horizons at $R = \ell_\Lambda$, where $T = \pm\infty$. The vector $\partial/\partial T$ is a Killing vector of de Sitter spacetime. It is timelike in the domains **N** and **S** (shaded regions) and spacelike in the domains **F** and **P**. The histories of both particles $w_\odot$ and $w_\otimes$ belong to the domains **N** and **S**.

mal relation to various regions of the Einstein static universe have been discussed extensively in literature (see, e.g., [44–47]). The complete compactified picture of these spacetimes, in particular the 3-dimensional diagram of the compactified Minkowski and de Sitter spaces $M^\#$ as parts of the Einstein universe represented by a *solid* cylinder can be found in [24]. We refer the reader especially to Section III of [24] where we explain and illustrate the compactification in detail. In the present paper we shall confine ourselves to the 2-dimensional Penrose diagrams.

The basic *standard rescaled coordinates* covering globally de Sitter spacetime including the conformal infinity are simply related to the standard coordinates as follows:

$$\tan\frac{\tilde t}{2} = \exp\frac{\tau}{\ell_\Lambda}\,, \quad \tilde r = \chi\,, \tag{3.10}$$

$\tilde t \in (0,\pi)$, $\tilde r \in (0,\pi)$. The metric (3.2) becomes

$$g_{\rm dS} = \ell_\Lambda^2\,\sin^{-2}\tilde t\,\left(-{\rm d}\tilde t^2 + {\rm d}\tilde r^2 + \sin^2\tilde r\,{\rm d}\omega^2\right)\,, \tag{3.11}$$

demonstrating explicitly the conformal relations of de Sitter spacetime to the Einstein universe:

$$g_{\rm E} = \Omega_{\rm dS}^2\, g_{\rm dS}\,, \quad \Omega_{\rm dS} = \sin\tilde t\,. \tag{3.12}$$

Therefore, we also call coordinates $\tilde t$, $\tilde r$ the *conformally Einstein coordinates*. The conformal diagram of de Sitter spacetime is illustrated in Fig. 2. The past and future infinities, $\tilde t = 0$ and $\tilde t = \pi$ are spacelike, the worldlines of the north and south poles (given by the choice of the origin of the coordinates) are described by $\tilde r = \chi = 0$ and $\tilde r = \chi = \pi$.

The whole de Sitter spacetime could be represented by just the "right half" of Fig. 2. Indeed, it is customary to draw this half only and to consider any point in the figure as a 2-sphere, except for the poles $\tilde r = 0, \pi$. As we shall see, the formulas relating coordinates on the conformally related de Sitter and Minkowski spacetimes have simpler forms if we admit negative values of the radial coordinate $\tilde r \in (-\pi, 0)$ covering the left half of the diagram. We shall thus consider the 2-dimensional diagrams as in Fig. 2 to represent the cuts of de Sitter spacetime along the axis going through the origins (through north and south poles—analogously to the cuts along the z axis in E^3). The axis, i.e., the main circle of the spatial spherical section of de Sitter spacetime, is typically chosen as $\vartheta = 0, \pi$. Thus, in the diagram the point with $\tilde r = -\tilde r_{\rm o} < 0$, $\vartheta = \vartheta_{\rm o}$, $\varphi = \varphi_{\rm o}$ is identical to that with $\tilde r = \tilde r_{\rm o}$, $\vartheta = \pi - \vartheta_{\rm o}$, and $\varphi = \varphi_{\rm o} + \pi$. We use the same convention also for other radial coordinates appearing later, as explicitly stated in the Appendix (cf. also Appendix in [24]). We admit negative radial coordinates only when describing various relations between the coordinate systems. In the expressions for the fields in the following sections only positive radial coordinates are considered.

As mentioned above, in [24] we constructed fields on de Sitter spacetime by conformally transforming the fields from Minkowski spacetime. Now "different Minkowski spaces" can be used in the conformal relation to de Sitter space, depending on which region of a Minkowski space is mapped onto which region of de Sitter space. Consider, for example, Minkowski space with metric $g_{\rm M}$ given in spherical coordinates $\check t$, $\check r$, ϑ, φ. Identify it with de Sitter space by relations

$$\check t = \frac{\ell_\Lambda \sin\tilde t}{\cos\tilde t - \cos\tilde r}\,, \quad \check r = \frac{\ell_\Lambda \sin\tilde r}{\cos\tilde r - \cos\tilde t}\,, \tag{3.13}$$

the inverse relation (A11) is given in the Appendix. In the coordinates $\check t$, $\check r$, ϑ, φ the de Sitter metric (3.11) becomes

$$g_{\rm dS} = \frac{\ell_\Lambda^2}{\check t^2}\left(-{\rm d}\check t^2 + {\rm d}\check r^2 + \check r^2\,{\rm d}\omega^2\right)\,, \tag{3.14}$$

so that

$$g_{\rm dS} = \Omega_{\rm M}^2 g_{\rm M}\,, \quad \Omega_{\rm M} = \frac{\ell_\Lambda}{\check t}\,. \tag{3.15}$$

The coordinates $\check t$, $\check r$, ϑ, φ can, of course, be used in both de Sitter and Minkowski spaces. Fig. 3 illustrates the coordinate lines. It also shows how four regions I, II, III, and IV of Minkowski space are mapped onto four regions of de Sitter space by relations (3.13). We call $\check t$, $\check r$ *rescaled flat cosmological coordinates* since their radial coordinate $\check r$ coincides with that of the flat cosmological coordinates (3.4) and the time coordinate is simply related to $\check r$ as

$$\check t = -\ell_\Lambda\,\exp(-\check r/\ell_\Lambda)\,. \tag{3.16}$$

The caron or the check (still better "háček") "∨" formed by cosmological horizon at $\check t = \pm\infty$ in de Sitter space (cf. Fig. 3) inspired our notation of these coordinates. It

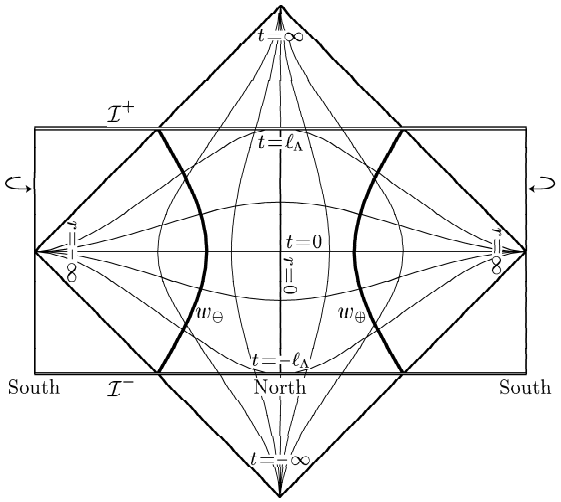

Figure 6: The conformally Minkowski coordinates. They cover the whole conformally related Minkowski space but only a part of corresponding de Sitter space. This Minkowski space is related to that in Fig. 3 by a shift "downwards" by $\pi/2$ in the direction of the conformally Einstein coordinate $\tilde{t}$.

is possible to introduce analogously the coordinates $\hat{t}$, $\hat{r}$ given in the Appendix, Eqs. (A39), (A40), that cover nicely the past conformal infinity but are not smooth at the cosmological horizon $\hat{t} = \pm\infty$; in this case they form the hat "$\wedge$" in the conformal diagram (see Fig. 16 in the Appendix).

From relations (3.13) it is explicitly seen why, when writing down mappings between de Sitter and Minkowski spaces and drawing the corresponding 2-dimensional conformal diagrams, it is advantageous to admit negative radial coordinates. If we would restrict all radial coordinates to be non-negative, we would have to consider the second relation in Eq. (3.13) with different signs for regions III and II in de Sitter space: in III $\check{r} = \ell_\Lambda \sin\tilde{r}/(\cos\tilde{r} - \cos\tilde{t})$, but in III we would have $\check{r} = -\ell_\Lambda \sin\tilde{r}/(\cos\tilde{r} - \cos\tilde{t})$.

Another mapping of Minkowski on de Sitter space will be used to advantage in the explicit manifestation that the generalized Born solution in de Sitter space goes over to the classical solution (2.13). Instead of the mapping (3.13), consider the relations

$$t = -\frac{\ell_\Lambda \cos\tilde{t}}{\cos\tilde{r} + \sin\tilde{t}}\,, \quad r = \frac{\ell_\Lambda \sin\tilde{r}}{\cos\tilde{r} + \sin\tilde{t}} \tag{3.17}$$

(see Eq. (A17) for the inverse mapping), which turn the metric (3.11) into

$$g_{\text{dS}} = \Big(\frac{2\,\ell_\Lambda^2}{\ell_\Lambda^2 - t^2 + r^2}\Big)^2 \Big(-\mathrm{d}t^2 + \mathrm{d}r^2 + r^2\,\mathrm{d}\omega^2\Big)\,. \tag{3.18}$$

We again obtain the de Sitter metric in the form explicitly conformal to the Minkowski metric with, however, a different conformal factor from that in Eq. (3.15):

$$g_{\text{dS}} = \Omega_{\text{M}}^2\, g_{\text{M}}\,, \quad \Omega_{\text{M}} = \frac{2\,\ell_\Lambda^2}{\ell_\Lambda^2 - t^2 + r^2}\,. \tag{3.19}$$

(For the use of the de Sitter metric in "atypical" form (3.18) in the work on the domain wall spacetimes, see [48].) The relation of Minkowski space to de Sitter space based on the mapping (3.17) is illustrated in Fig. 6. Clearly, the Minkowski space in this figure is shifted "downwards" by $\pi/2$ in $\tilde{t}$ coordinate, as compared with Minkowski space in Fig. 3 (Eq. (3.13)). Indeed, replacing $\tilde{t}$ by $\tilde{t} + \frac{\pi}{2}$ in Eq. (3.13), we get $\check{t} = t$, $\check{r} = r$ with t, r given by Eq. (3.17). Since coordinates t, r, ϑ, φ are not connected directly with any cosmological model and correspond to Minkowski space "centered" on de Sitter space (Fig. 6), we just call them *conformally Minkowski coordinates*.

In Ref. [24] still another Minkowski space is related to de Sitter space—one which is shifted "downward" in $\tilde{t}$ coordinate by another $\pi/2$. As mentioned below Eq. (3.16), the cosmological horizon forms hat "$\wedge$" in this case and the corresponding coordinates are accordingly denoted as $\hat{t}$, $\hat{r}$. They are given explicitly in Appendix A 3 and Fig. 16.

The three sets of coordinates $\check{t}$, $\check{r}$, t, r, and $\hat{t}$, $\hat{r}$ (with the same ϑ, φ) relating naturally "three" Minkowski spaces to de Sitter space are suitable for different purposes. The third set describes conveniently the past infinity of de Sitter space—that is why it was used extensively in [24] where we were interested in how the sources enter (are "born in") de Sitter universe. The second set will be needed in Section VII for exhibiting the flat-space limit of the generalized Born solution. The first set describes nicely the future infinity and will be employed when analyzing radiative properties of the fields.

With all the coordinates discussed above, corresponding double null coordinates can be associated; some of them will also be used in the following. Their more detailed description and illustration is presented in section A 10 of the Appendix.

Before concluding this section let us notice that the observers which are at rest in cosmological coordinate systems τ, χ, $\check{\tau}$, $\check{r}$, and η, ρ move along the geodesics with proper time τ, $\check{\tau}$, and η respectively. These geodesics are also the orbits of the conformal Killing vectors. Indeed, the symmetries of Minkowski spacetime and of the Einstein universe become conformal symmetries in conformally related de Sitter spacetime. In particular, we shall employ the fact that since $\partial/\partial\check{t}$ and $\partial/\partial t$ are timelike Killing vectors in Minkowski spacetime and $\partial/\partial\tilde{t}$ is a timelike Killing vector in the Einstein universe, the vectors

$$\frac{\partial}{\partial\tilde{t}}\,, \quad \frac{\partial}{\partial\check{t}}\,, \quad \text{and} \quad \frac{\partial}{\partial t} \tag{3.20}$$

are timelike conformal Killing vectors in de Sitter spacetime. As mentioned below Eq. (3.9), $\partial/\partial T$ is a Killing vector which is timelike for $|R| < \ell_\Lambda$.

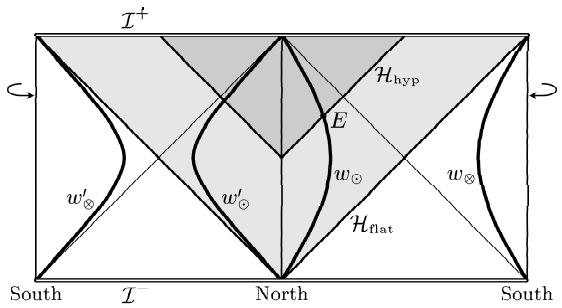

Figure 7: The worldlines of uniformly accelerated charges. The particles $w_\odot$ and $w'_\odot$ start and end at the "north pole," $w_\otimes$, $w'_\otimes$ start and end at the south pole. Particles $w'_\odot$, $w'_\otimes$ have a higher magnitude of acceleration $a_{\rm dS}$ than particles $w_\odot$, $w_\otimes$. They are characterized by a negative parameter $\alpha_{\rm o}$, whereas particles $w_\odot$, $w_\otimes$ have a positive $\alpha_{\rm o}$.

IV. UNIFORMLY ACCELERATED PARTICLES IN DE SITTER

A. Particles born at the poles

In Section II we defined uniformly accelerated motion in Minkowski spacetime. However, the formulas given there, being in covariant forms, remain valid in de Sitter spacetime. As explained in [24] in detail, a simple way of obtaining a worldline of a uniformly accelerated particle in de Sitter spacetime is to consider a suitable particle moving with a *uniform velocity* in Minkowski spacetime and use the conformal relation between the spaces.

Consider a particle moving with a constant velocity of magnitude

$$v_{\check{\rm M}} = \tanh\alpha_{\rm o} = \text{constant}\,, \tag{4.1}$$

such that for $\alpha_{\rm o} > 0$ it moves in a negative direction along the $\check{z}$ axis of the inertial frame in Minkowski space $\check{M}$ with coordinates $\check{t}$, $\check{r}$, ϑ, φ and passes through $\check{r} = 0$ at $\check{t} = 0$:

$$\begin{aligned} \check{t} &= \lambda_{\check{\rm M}}\,\cosh\alpha_o\,, \\ \check{r} &= -\lambda_{\check{\rm M}}\sinh\alpha_{\rm o}\,, \quad \vartheta = 0\,. \end{aligned} \tag{4.2}$$

Substituting into transformation (A11), we find

$$\begin{aligned} \tilde{t} &= \arctan\Big(-2\ell_\Lambda\frac{\lambda_{\check{\rm M}}\cosh\alpha_{\rm o}}{\lambda_{\check{\rm M}}^2 - \ell_\Lambda^2}\Big)\,, \\ \tilde{r} &= \arctan\Big(-2\ell_\Lambda\frac{\lambda_{\check{\rm M}}\sinh\alpha_{\rm o}}{\lambda_{\check{\rm M}}^2 + \ell_\Lambda^2}\Big)\,, \end{aligned} \tag{4.3}$$

or expressing Minkowski proper time $\lambda_{\check{\rm M}}$ in terms of the proper time of de Sitter spacetime,

$$\lambda_{\check{\rm M}} = \mp\ell_\Lambda\exp\big(\mp(\cosh\alpha_{\rm o})\,\lambda_{\rm dS}/\ell_\Lambda\big)\,, \tag{4.4}$$

we obtain

$$\begin{aligned} \tilde{t} &= \operatorname{arccot}\Big(-\frac{\sinh\big((\cosh\alpha_{\rm o})\,\lambda_{\rm dS}/\ell_\Lambda\big)}{\cosh\alpha_{\rm o}}\Big)\,, \\ \tilde{r} &= \operatorname{arccot}\Big(\pm\frac{\cosh\big((\cosh\alpha_{\rm o})\,\lambda_{\rm dS}/\ell_\Lambda\big)}{\sinh\alpha_{\rm o}}\Big)\,, \quad \vartheta = 0\,. \end{aligned} \tag{4.5}$$

Here $\lambda_{\rm dS}\in\mathbb{R}$, arccot takes values such that $\tilde{t}\in(0,\pi)$ and $\tilde{r}\in(0,\pi)$ for $\alpha_{\rm o} > 0$, or $\tilde{r}\in(-\pi,0)$ for $\alpha_{\rm o} < 0$. Upper sign is valid for the particle starting and ending with $\tilde{r} = 0$ (particle $w_\odot$ in Fig. 7), lower sign for the particle starting and ending at $\tilde{r} = \pi$ (particle $w_\otimes$ in Fig. 7).

One can make sure by direct calculations of the four-acceleration (for its simplest form in the static coordinates, see below) that these worldlines describe the uniformly accelerated motion as defined in Section II, the magnitude of the acceleration being

$$a_{\rm dS} = \sqrt{\mathrm{a}^\mu\mathrm{a}_\mu} = \big|\ell_\Lambda^{-1}\,\sinh\alpha_{\rm o}\big|\,. \tag{4.6}$$

Since de Sitter universe represents the asymptotic state of all three types of indefinitely expanding FRW models with $\Lambda > 0$, it is of interest to find out the form of these worldlines in the three types of cosmological frames—spherical, flat, and hyperbolic—introduced in Section II.

In terms of cosmological spherical coordinates the worldlines are given by

$$\begin{aligned} \tau &= \ell_\Lambda\,\operatorname{arcsinh}\left(\frac{\sinh\big((\cosh\alpha_{\rm o})\,\lambda_{\rm dS}/\ell_\Lambda\big)}{\cosh\alpha_{\rm o}}\right)\,, \\ \chi &= \operatorname{arccot}\left(\pm\frac{\cosh\big((\cosh\alpha_{\rm o})\,\lambda_{\rm dS}/\ell_\Lambda\big)}{\sinh\alpha_{\rm o}}\right)\,, \quad \vartheta = 0\,. \end{aligned} \tag{4.7}$$

In flat cosmological coordinates, which cover only half of de Sitter space, we obtain just particle $w_\odot$ described by the worldline

$$\begin{aligned} \check{\tau} &= \lambda_{\rm dS}\,\cosh\alpha_{\rm o} - \ell_\Lambda\log\cosh\alpha_{\rm o}\,, \\ \check{r} &= \ell_\Lambda\sinh\alpha_{\rm o}\;\exp\big\{-(\cosh\alpha_{\rm o})\,\lambda_{\rm dS}/\ell_\Lambda\big\}\,. \end{aligned} \tag{4.8}$$

Finally, in hyperbolic cosmological coordinates, which are also not global, we obtain again one particle's worldline only given in terms of its proper time as

$$\begin{aligned} \eta &= \ell_\Lambda\,\operatorname{arccosh}\frac{\cosh\big((\cosh\alpha_{\rm o})\,\lambda_{\rm dS}/\ell_\Lambda\big)}{\cosh\alpha_{\rm o}}\,, \\ \rho &= \ell_\Lambda\,\operatorname{arccoth}\frac{\sinh\big((\cosh\alpha_{\rm o})\,\lambda_{\rm dS}/\ell_\Lambda\big)}{\sinh\alpha_{\rm o}}\,. \end{aligned} \tag{4.9}$$

These formulas have no meaning for $|\lambda_{\rm dS}/\ell_\Lambda\,\cosh\alpha_{\rm o}| < |\alpha_{\rm o}|$ where the inverse hyperbolic functions are not defined. This corresponds to the fact that for such $\lambda_{\rm dS}$ the particle occurs in the region where the hyperbolic cosmological coordinates are not defined (cf. Fig. 4). Excluding the proper time we find the worldlines to be given by remarkably simple formulas in the three systems of the cosmological coordinates:

(a) spherical,

$$\sin\chi = \pm\tanh\alpha_{\rm o}\Big/\cosh\frac{\tau}{\ell_\Lambda}\ ; \tag{4.10}$$

(b) flat,

$$\frac{\check r}{\ell_\Lambda} = \tanh\alpha_{\rm o}\Big/\exp\frac{\check\tau}{\ell_\Lambda}\ ; \tag{4.11}$$

c) hyperbolic,

$$\sinh\frac{\rho}{\ell_\Lambda} = \tanh\alpha_{\rm o}\Big/\sinh\frac{\eta}{\ell_\Lambda}\ . \tag{4.12}$$

It is of interest to see what are the physical radial velocities which will be observed by three types of the fundamental cosmological observers, i.e., those with fixed χ, $\check r$, and ρ, respectively, whose proper times are τ, $\check\tau$, and η, respectively. Such velocities can be defined by the covariant expression

$$v_{\rm obs} = {\rm u}_\alpha\, {\rm e}^\alpha_{\rm I}\,\frac{d\lambda_{\rm dS}}{d\lambda_{\rm obs}}\ , \tag{4.13}$$

where u^α is the particle's four-velocity, $\lambda_{\rm dS}$ its proper time, $\mathrm{e}^\alpha_{\rm I}$ is the unit spacelike vector in the direction of the radial coordinate $x^1 = \chi$, $\check r$,, and ρ, respectively, i.e., in directions $\partial/\partial\chi$, $\partial/\partial\check r$ and $\partial/\partial\rho$, and $\lambda_{\rm obs}$ is the proper time of an observer, i.e., τ, $\check\tau$, or η, respectively. Since all three cosmological metrics are diagonal the expression (4.13) takes on the form

$$v_{obs} = \sqrt{g_{dS11}}\,\frac{dx^1}{d\lambda_{\rm obs}}\ . \tag{4.14}$$

The results are of interest:

$$v_{\rm obs(\chi)} = \mp\frac{\operatorname{sign}\tau\,\sinh\alpha_{\rm o}}{\sqrt{\sinh^2\alpha_{\rm o} + \coth^2(\tau/\ell_\Lambda)}}\ , \tag{4.15}$$

$$v_{\rm obs(\check r)} = -\tanh\alpha_o\ , \tag{4.16}$$

$$v_{\rm obs(\rho)} = -\frac{\sinh\alpha_{\rm o}}{\sqrt{\sinh^2\alpha_{\rm o} + \tanh^2(\eta/\ell_\Lambda)}}\ . \tag{4.17}$$

Consider first the picture in spherical cosmological coordinates, Eqs. (4.7) and (4.10). Only in this frame both particles are present. They start asymptotically at antipodes of the spatial section of de Sitter space at $\mathcal{I}^-$ ($\tau\to-\infty$) and move one towards the other until $\tau = 0$, the moment of maximal contraction of de Sitter space ("the neck" of de Sitter hyperboloid), when they stop, $v_{\rm obs(\chi)} = 0$. Then they move, in a time-symmetric manner, apart from each other until they reach future infinity asymptotically at the antipodes from which they started. In contrast to the flat space case, the particles do not approach the velocity of light in this global spherical cosmological coordinate system, the asymptotical magnitude of their velocity being equal to $|\tanh\alpha_{\rm o}|$ (cf. Eq. (4.15)). Hence, curiously enough, the particles approach the antipodes asymptotically with a finite nonvanishing velocity (for an intuitive insight into this effect, see below).

Although the particles $w_\odot$ and $w_\otimes$ do not approach infinities with velocity of light, they *are* causally disconnected as the analogous pair of particles in Minkowski space (cf. Fig. 1 and Fig. 7). No retarded or advanced effects from the particle $w_\odot$ can reach the particle $w_\otimes$ and vice versa.

Next, consider flat and hyperbolic observers. As seen from Eq. (4.16), with respect to the flat cosmological coordinates the particle $w_\odot$ moves with the same velocity $|\tanh\alpha_{\rm o}|$ all the time. And the same velocity is asymptotically, at $\eta\to\infty$, reached by this particle in the hyperbolic cosmological coordinates. The magnitude of the asymptotic values of the velocity at $\mathcal{I}^+$ is, in fact, equal to the velocity (4.1) of the particle in Minkowski space from which we constructed uniformly accelerated worldlines by a conformal transformation. The identity of all these velocities is understandable: the magnitude of the velocity with respect to an observer can be determined by projecting the particle's four-velocity on the observer's four-velocity, i.e., by the angle between these directions. In de Sitter space all three types of cosmological observers reach $\mathcal{I}^+$ with the same four-velocity; moreover, this four-velocity is at $\mathcal{I}^+$ identical to the four-velocity of observers at rest in conformally related Minkowski space. But a conformal transformation preserves the angles and thus, the velocities with respect to the three types of cosmological observers in de Sitter space and the velocity in the conformally related Minkowski space must all be equal—given by the "Lorentzian" angle α_o.

It is worth noticing yet what is the *initial* velocity of the particle $w_\odot$ in hyperbolic cosmological coordinates. Regarding Fig. 4 we have $\eta\to-\infty$, $\rho\to 0$ at the "starting point" of the particle at $\mathcal{I}^-$. From Eq. (4.17) we get $v_{\rm obs(\rho)}\to-\tanh\alpha_{\rm o}$ which in the magnitude is the same as in spherical cosmological coordinates but has opposite sign since the particle moves in the direction of increasing negative ρ. More interesting is how the particle enters the upper region of the hyperbolic coordinates. Fig. 4 suggests that its velocity must approach the velocity of light since at this boundary the fundamental observers of the hyperbolic cosmological frame themselves approach the velocity of light. Indeed, at this boundary $\eta = 0$, $\rho = \infty$, and the expression (4.17) implies $v_{\rm obs(\rho)}\to-1$.

By far the simplest description of the particles is obtained in the static coordinates T, R. Using, for example, the relation $R = \ell_\Lambda\sin\tilde r/\sin\tilde t$ (cf. Eqs. (A64), (A77)), and substituting from Eq. (4.5), we find that the worldlines of both particles $w_\odot$ and $w_\otimes$ are given by remarkably lucid forms

$$\begin{aligned} T &= \lambda_{\rm dS}\,\cosh\alpha_{\rm o} = \frac{\lambda_{\rm dS}}{\sqrt{1-R_{\rm o}^2/\ell_\Lambda^2}}\ , \\ R &= \ell_\Lambda\tanh\alpha_{\rm o} \equiv R_{\rm o}\ . \end{aligned} \tag{4.18}$$

These expressions imply that the four-acceleration

$\mathrm{a}^\alpha = \mathrm{u}^\mu \nabla_\mu \mathrm{u}^\alpha$ is simply

$$\mathrm{a} = -\frac{R_\mathrm{o}}{\ell_\Lambda^2}\frac{\partial}{\partial R} = -\frac{1}{\ell_\Lambda}\tanh\alpha_\mathrm{o}\frac{\partial}{\partial R} = a_\mathrm{o}\mathrm{e}_R\,, \qquad (4.19)$$

where e_R is a unit spatial vector in the direction $\partial/\partial R$ of the static radial coordinate R, and we introduced constant

$$a_\mathrm{o} = -\ell_\Lambda^{-1}\sinh\alpha_\mathrm{o} = -\frac{R_\mathrm{o}/\ell_\Lambda^2}{\sqrt{1-R_\mathrm{o}^2/\ell_\Lambda^2}} \qquad (4.20)$$

which represents the "oriented" value of the acceleration of the particles.

We thus find the uniformly accelerated particles in de Sitter spacetime to be at rest in the static coordinates at fixed values $R = R_\mathrm{o}$ of the radial coordinate. Two charges moving along the orbits of the boost Killing vector (2.5) in Minkowski space are at rest in the Rindler coordinate system and have a constant distance from the spacetime origin, as measured along the slices orthogonal to the Killing vector. Similarly, we see that the worldlines $w_\odot$ and $w_\otimes$ are the orbits of the static Killing vector $\partial/\partial T$ of de Sitter space. The particle $w_\odot$ (respectively, $w_\otimes$) has, as measured at fixed T, a constant proper distance from the origin $\tilde{t} = \pi/2$ ($\tau = 0$), $\tilde{r} = \chi = 0$ (respectively, $\tilde{r} = \chi = \pi$). As with Rindler coordinates in Minkowski space, the static coordinates cover only a "half" of de Sitter space. In the other half the Killing vector becomes spacelike. Owing to "cosmic repulsion" caused by the presence of Λ, fundamental cosmological observers moving along geodesics χ, ϑ, φ constant are "repelled" one from the others. Their initial implosion starting at $\tau \to -\infty$ is stopped at $\tau = 0$ and changes into expansion. Clearly, a particle with constant $R = R_\mathrm{o}$—hence a constant proper distance from the particle at $R = 0 = \chi$—must be accelerated towards that "central" particle.

In Eq. (4.20) we have denoted the radial tetrad component of the acceleration in the static coordinates by a_o; notice that, in contrast to the magnitude of the acceleration $a_\mathrm{dS} = |a_\mathrm{o}|$ (cf. Eq. (4.6)), a_o can be negative as, in fact, it is the case with *both* particles $w_\odot$ and $w_\otimes$, assuming that the static radial coordinate of the particles is positive, $R = R_\mathrm{o} > 0$. Geometrically, the four-vectors of the acceleration of the particles point in opposite directions—towards $\chi = 0$, the other towards $\chi = \pi$. Since, however, one needs two sets of the static coordinates to cover both particles, and the radial coordinate R increases from both $\chi = 0$ and $\chi = \pi$ worldlines (cf. Fig. 5), the accelerations of both particles point in the direction of decreasing R's and is thus negative. All the particles we are considering perform 1-dimensional motion only, hence we use for the description of their worldlines the same convention as for the 2-dimensional diagrams with time and radial coordinates—we allow the radial coordinate to take negative values. Thus, for example, consider a particle with worldline $w'_\odot$ which is a "reflection" of the worldline $w_\odot$ with respect to $\tilde{r} = \chi = 0$ (see Fig. 7). The particle $w'_\odot$ moves in the region of negative $\tilde{r}$, respectively R, it has an acceleration positive, $a_\mathrm{o} = -\ell_\Lambda^{-1}\sinh\alpha_\mathrm{o} > 0$ (i.e., $\alpha_\mathrm{o} < 0$), and its four-acceleration vector is pointing in the direction of increasing R. With our convention, the particle $w'_\odot$ is just that which moves from $\chi = 0$ along the $\vartheta = \pi$ direction. This convention will be particularly useful when we shall construct worldlines of uniformly accelerated particles which start and end at the equator. Those which move in the region $\chi > \pi/2$ will have negative a_o, those moving with $\chi < \pi/2$ will have positive a_o—see Section IV B.

An intuitive geometrical understanding of the worldlines of uniformly accelerated particles in de Sitter spacetime can be gained by considering de Sitter space as a 4-dimensional hyperboloid $-{Z_0}^2 + {Z_1}^2 + {Z_2}^2 + {Z_3}^2 + {Z_4}^2 = \ell_\Lambda^2$ in 5-dimensional Minkowski space. The spherical cosmological coordinates τ, χ, ϑ, φ are then identical to the hyperspherical coordinates on this hyperboloid. The worldlines of the north and south poles, $\chi = 0, \pi$, can be obtained by cutting the hyperboloid by a timelike 2-plane $\mathcal{T}_2$, given by $Z_2 = Z_3 = Z_4 = 0$. The worldlines of our uniformly accelerated particles $w_\odot$ and $w_\otimes$ then arise when the hyperboloid is cut by a timelike 2-plane $\mathcal{T}_2^*$ parallel to $\mathcal{T}_2$ at a distance $R_\mathrm{o} = \ell_\Lambda\tanh(\alpha_\mathrm{o}/\ell_\Lambda)$ from the origin [43]. $\mathcal{T}_2^*$ is thus given by $Z_2 = R_\mathrm{o}$, $Z_3 = Z_4 = 0$. From the definition of the hyperspherical coordinates it follows $\vartheta = 0, \pi$ and $Z_2 = \ell_\Lambda\cosh(\tau/\ell_\Lambda)\sin\chi\cos\vartheta = R_\mathrm{o}$, i.e., $\sin\chi = \pm\tanh\alpha_\mathrm{o}/\cosh(\tau/\ell_\Lambda)$, which is just Eq. (4.10) describing $w_\odot$ and $w_\otimes$.

From this construction, the curious result mentioned above—that $w_\odot$ and $w_\otimes$ approach antipodes $\chi = 0$ and $\chi = \pi$ asymptotically with a fixed speed $|\tanh\alpha_\mathrm{o}|$ in spherical cosmological coordinates is not so surprising: thanks to the expansion of de Sitter spacetime all fundamental cosmological observers with arbitrarily small $\chi = \text{constant} > 0$ will, in the limit $\tau \to \infty$, eventually cross the plane $\mathcal{T}_2^*$, and thus the particle $w_\odot$; however at any finite but arbitrarily large τ there will be observers with $\chi = \text{constant}$ which are still moving towards the particle $w_\odot$. The same, of course, is true with the symmetrically located particle $w_\otimes$ and corresponding observers close to $\chi = \pi$.

B. Particles born at the equator

In the classical Born solutions both charges are, at all times, located symmetrically with respect to the origin of the Minkowski coordinates (see Fig. 1). In order to demonstrate explicitly that a limiting procedure exists in which our generalized Born's solution goes over to its classical counterpart, we shall now construct the pair of uniformly accelerated particles which are, at all times, symmetrically located with respect to the origin of the standard spherical coordinates in de Sitter space, i.e., with respect to the "north pole" at $\chi = 0$. Asymptotically at $\tau \to -\infty$ these two particles both start ("are

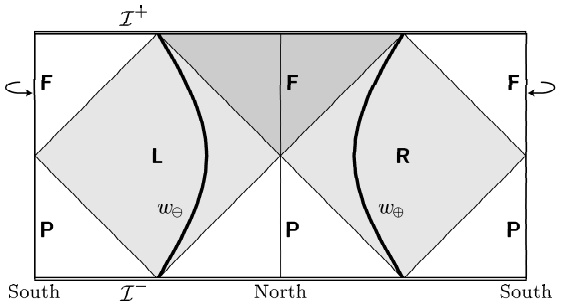

Figure 8: The worldlines of uniformly accelerated charges located symmetrically with respect to the origin (north pole) of the standard spherical coordinates in de Sitter space. The particles "start" and "end" at the equator. They are causally disconnected as a corresponding pair in Minkowski space (cf. Fig. 1). The "oriented" value a_o of the acceleration of these particles is positive (cf. the "rotated" version of Eq. (4.20)).

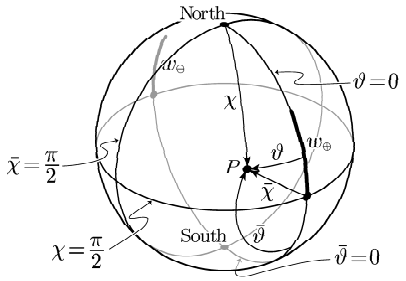

Figure 9: The rotated spherical coordinates $\bar\chi$, $\bar\vartheta$ on 3-sphere (the cut $\varphi=$ constant). The relation between the coordinates is given in Eq. (4.21).

born") with the same speed at the equator, $\chi=\pi/2$, at the antipodal points $\vartheta=0$ and $\vartheta=\pi$. As the universe contracts, they both move symmetrically along the axis $\vartheta=0,\pi$, reach some limiting value χ_o at the moment of time symmetry, and accelerate back towards the equator, reaching the initial positions asymptotically at $\tau\to+\infty$. These two particles are illustrated in Fig. 8, with their worldlines denoted by $w_\oplus$ and $w_\ominus$. In Fig. 9, a snapshot at $\tau=$ constant is depicted. Comparing Fig. 8 with Fig. 7, it is evident that the particles $w_\oplus$ and $w_\ominus$ are located with respect to the point $\chi=\pi/2$, $\vartheta=0$ in exactly the same manner as the particles $w_\odot$ and $w_\otimes$ are located with respect to the pole $\chi=0$ (or, rather, as the particles $w'_\odot$, $w'_\otimes$, since we chose $w_\oplus$, $w_\ominus$ to have positive a_o in Fig. 8).

Owing to the global homogeneity of de Sitter space and the spherical geometry of its slices $\tau=$ constant, the worldlines of the particles $w_\oplus$ and $w_\ominus$ can be constructed by a suitable rotation of the worldlines of the particles $w_\odot$ and $w_\otimes$. In Section VII the same rotation will be applied to obtain the fields of these particles "born at the equator." We rotate the coordinates χ, ϑ, φ into new coordinates $\bar\chi$, $\bar\vartheta$, $\bar\varphi$ which, as a pole, have the point $\chi=\pi/2$, $\vartheta=0$ (see Fig. 9). The relations between these coordinates follow from the spherical geometry:

$$\cos\bar\chi=\sin\chi\cos\vartheta\ ,\quad \tan\bar\vartheta=-\tan\chi\sin\vartheta\ ,\quad \bar\varphi=\varphi\ . \tag{4.21}$$

The new worldlines, $w_\oplus$ and $w_\ominus$, will then be given by Eqs. (4.7) in which χ, ϑ, φ are replaced by rotated coordinates $\bar\chi$, $\bar\vartheta$, $\bar\varphi$. Substituting for these by using relations (4.21), we find the worldlines $w_\oplus$, $w_\ominus$ in the original coordinates to be described by the expressions:

$$\begin{aligned}
\tau&=\ell_\Lambda\,\mathrm{arcsinh}\left(\frac{\sinh\big((\cosh\alpha_o)\,\lambda_{ds}/\ell_\Lambda\big)}{\cosh\alpha_o}\right)\ ,\\
\chi&=\pm\arctan\left(-\frac{\cosh\big((\cosh\alpha_o)\,\lambda_{ds}/\ell_\Lambda\big)}{\sinh\alpha_o}\right)\ ,\\
\vartheta&=0\ ,
\end{aligned}\tag{4.22}$$

with the values of arctan from $(0,\pi)$ and upper (lower) sign corresponding to the particle starting at the positive (negative) value of χ, i.e., to the particle $w_\oplus$ (or $w_\ominus$, respectively).

Excluding the proper time λ_{ds}, we arrive at simple result (cf. Eq. (4.10))

$$\cos\chi=-\frac{\tanh\alpha_o}{\cosh(\tau/\ell_\Lambda)}\ . \tag{4.23}$$

As $\tau\to\pm\infty$, then indeed $|\chi|\to\pi/2$; at $\tau=0$, $|\chi|=\arccos(-\tanh\alpha_o)=\arccos(-R_o/\ell_\Lambda)$, in agreement with the "deviation" of the "original" particles $w_\odot$, $w_\otimes$ from $\chi=0$ at $\tau=0$. In the spherical rescaled coordinates, Eqs. (4.22) read

$$\begin{aligned}
\tilde t&=\mathrm{arccot}\left(-\frac{\sinh\big((\cosh\alpha_o)\,\lambda_{ds}/\ell_\Lambda\big)}{\cosh\alpha_o}\right)\ ,\\
\tilde r&=\pm\arctan\left(-\frac{\cosh\big((\cosh\alpha_o)\,\lambda_{ds}/\ell_\Lambda\big)}{\sinh\alpha_o}\right)\ ,\\
\vartheta&=0\ ,
\end{aligned}\tag{4.24}$$

again with the values of arctan and arccot from $(0,\pi)$. Eq. (4.23) becomes

$$\cos\tilde r=-\tanh\alpha_o\sin\tilde t\ . \tag{4.25}$$

Although the flat (rescaled) cosmological coordinates cover only parts of the worldlines $w_\oplus$, $w_\ominus$ (see Figs. 8 and 3), we transcribe the equations above also into these frames in which the particles "emerge" at $\check r$, $\check t\to-\infty$ at the cosmological horizon at $\check r=\pm\infty$. We find

$$\begin{aligned}
\frac{\check\tau}{\ell_\Lambda}&=-\log\left(\frac{-\cosh\alpha_o}{-\sinh\big((\cosh\alpha_o)\,\lambda_{ds}/\ell_\Lambda\big)+\sinh\alpha_o}\right)\ ,\\
\frac{\check t}{\ell_\Lambda}&=\frac{\cosh\alpha_o}{-\sinh\big((\cosh\alpha_o)\,\lambda_{ds}/\ell_\Lambda\big)+\sinh\alpha_o}\ ,\\
\frac{\check r}{\ell_\Lambda}&=\mp\frac{\cosh\big((\cosh\alpha_o)\,\lambda_{ds}/\ell_\Lambda\big)}{-\sinh\big((\cosh\alpha_o)\,\lambda_{ds}/\ell_\Lambda\big)+\sinh\alpha_o}\ ,
\end{aligned}\tag{4.26}$$

so that Eq. (4.25) translates into the relations

$$\check{r} = \pm\sqrt{\ell_\Lambda^2 + \check{t}^2 - 2\,\ell_\Lambda \check{t}\tanh\alpha_0}\ ,$$
$$\check{r} = \pm\ell_\Lambda\sqrt{1 + 2\tanh\alpha_0\,\exp(-\check{\tau}/\ell_\Lambda) + \exp(-2\check{\tau}/\ell_\Lambda)}\ . \tag{4.27}$$

As $\check{\tau}\to+\infty$, we have $\check{r}\to\pm\ell_\Lambda$, as it corresponds to $\chi\to\pm\pi/2$; at $\check{\tau}\to-\infty$, we get $\check{r}\to\pm\infty$—here the particles enter flat cosmological frame at the horizon (cf. Fig. 8).

The worldlines $w_\oplus$, $w_\ominus$ are situated outside the regions covered by our choice of the hyperbolic cosmological coordinates. Similarly, we get only finite parts of $w_\oplus$, $w_\ominus$ in our static coordinates. Of course, we could rotate the static coordinates to cover both particles but then we arrive at exactly the same picture as with the particles $w_\odot$, $w_\otimes$ considered above.

Our primary reason to discuss the pair $w_\oplus$, $w_\ominus$ is to demonstrate explicitly how our fields go over into the classical Born solution in the limit of vanishing Λ. For this purpose, it will be important to have available also the description of the worldlines $w_\oplus$, $w_\ominus$ in the Minkowski coordinates introduced in Eqs. (3.17). As it is obvious from Fig. 6, these coordinates cover both worldlines $w_\oplus$ and $w_\ominus$ completely. Using the relations inverse to Eqs. (3.17) given in the Appendix, Eq. (A17), we find Eqs. (4.24) to imply

$$t = b_0\sinh\frac{\lambda_{\rm M}}{b_0}\ ,\quad r = \pm b_0\cosh\frac{\lambda_{\rm M}}{b_0}\ ,\quad \vartheta = 0\ , \tag{4.28}$$

where

$$\frac{b_0}{\ell_\Lambda} = \exp\alpha_0 = \sqrt{1 + a_0^2\ell_\Lambda^{-2}} - a_0\ell_\Lambda = \sqrt{\frac{\ell_\Lambda + R_0}{\ell_\Lambda - R_0}}\ , \tag{4.29}$$

and $\lambda_{\rm M}$ is the proper time measured in Minkowski space M related to de Sitter space by conformal mapping (3.18), (3.19):

$$\lambda_{\rm M} = \exp\alpha_0\,\cosh\alpha_0\,\lambda_{\rm dS}\ . \tag{4.30}$$

Consequently,

$$r = \pm\sqrt{t^2 + b_0^2}\ ,\quad \vartheta = 0\ , \tag{4.31}$$

which is the simplest form of the hyperbolic motion with the uniform acceleration $1/b_0$ as measured in Minkowski space (cf. Eqs. (2.3)).

V. FRAMES CENTERED ON ACCELERATED PARTICLES

For the investigation of the radiative properties and other physical aspects of the fields, the use of (physically equivalent) particles $w_\odot$, $w_\otimes$, i.e., those "born at the poles" of spherical coordinates is technically more advantageous. We shall now return back and construct frames with the origins located directly on these particles. In such frames, various properties of the fields will become more transparent than in the coordinates introduced so far.

As we have seen in the preceding section, the uniformly accelerated particles $w_\odot$ and $w_\otimes$ are at rest in static coordinates T, R at given $R = R_0 = -a_0\ell_\Lambda^2/\sqrt{1 + a_0^2\ell_\Lambda^2}$, where $|a_0|$ is the magnitude of the acceleration. In order to investigate the properties of the fields, in particular, in order to see what is the structure of the field along the null cones with vertices at the particle's position, i.e., what is the field "emitted" by the particle at a given time, it is useful to construct coordinate frames centered on the accelerated particles. Such systems of coordinates are used to describe accelerating black holes in general relativity (like C-metrics, known also for $\Lambda\neq 0$, cf. [27, 28]), so that their properties on de Sitter background may indicate what is their meaning in more general cases—in situations when they are centered on gravitating objects *rather than on test particles*.

We shall now describe three coordinate systems of this type: the *accelerated coordinates*, the *C-metric-like coordinates*, and the *Robinson-Trautman coordinates*, all centered on the worldlines $w_\odot$ and $w_\otimes$. Instead of writing down just the transformation formulas, we wish to indicate some steps how these coordinates can be obtained naturally. We list only the main transformation relations here, many other formulas and forms of the metrics can be found in the Appendix. Let us also note that in this section we assume R_0, $\alpha_0 > 0$, i.e., $a_0 < 0$, and we use only static radial coordinate with positive values, i.e., $R > 0$.

A. Accelerated coordinates

We begin with the construction of *accelerated coordinates* T', R', ϑ', φ. This type of coordinates was recently introduced [49] by another method in the context of the C-metric with $\Lambda > 0$. In the preceding section we obtained the worldlines $w_\odot$, $w_\otimes$ of uniformly accelerated particles in de Sitter space by starting from a particle moving with a uniform velocity $v_{\check{\rm M}} = \tanh\alpha_0$ in a negative direction of the $\check{z}$ axis in the inertial frame $\check{t}$, $\check{r}$, ϑ, φ in Minkowski space $\check{M}$ which passes through $\check{r} = 0$ at $\check{t} = 0$ (see Eqs. (4.1), (4.2)); and we used then the conformal relation between Minkowski and de Sitter spaces to find $w_\odot$, $w_\otimes$. Therefore, let us first construct a frame centered on the uniformly moving particle in $\check{M}$. Using spherical coordinates again, this boosted frame denoted by primes is related to the original one simply by

$$\begin{aligned}\check{t}' &= \check{t}\cosh\alpha_0 + \check{r}\cos\vartheta\sinh\alpha_0\ ,\\ \check{r}'\cos\vartheta' &= \check{t}\sinh\alpha_0 + \check{r}\cos\vartheta\cosh\alpha_0\ ,\\ \check{r}'\sin\vartheta' &= \check{r}\sin\vartheta\ ,\end{aligned} \tag{5.1}$$

the φ-coordinate does not change and will be suppressed

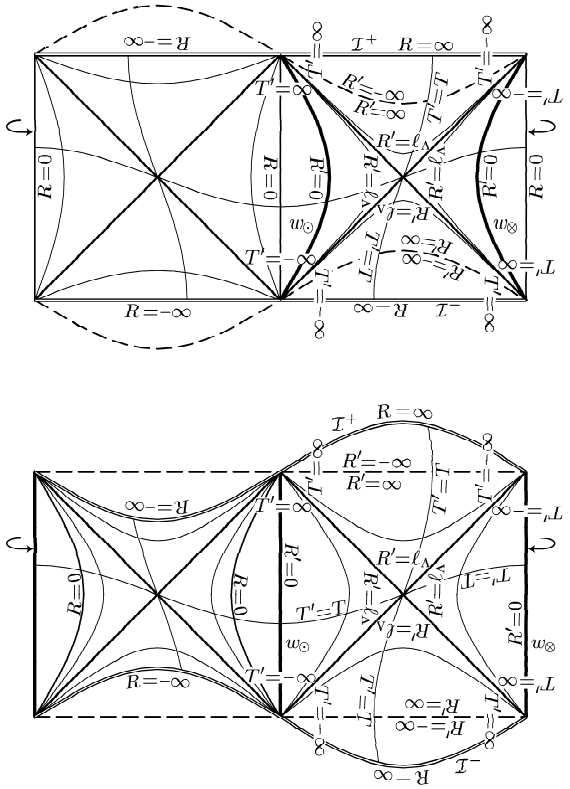

Figure 10: The 2-dimensional conformal diagrams of de Sitter space based on the static, non-accelerated coordinates (upper diagram), and on the accelerated coordinates (lower diagram). Starting from static coordinates T, R, ϑ, φ, one can draw the conformal diagram of the axis $\vartheta = 0, \pi$ in which the conformal past and future infinities, $\mathcal{I}^{\pm}$ ($R = \pm\infty$), are horizontal (double) lines. In addition to static coordinates T, R, also accelerated coordinates T', R' are indicated in both diagrams. These have a coordinate singularity for $R' = \infty$ (drawn as a dashed line). The origins of the accelerated coordinates, $R' = 0$ (thick lines), are worldlines of uniformly accelerated particles. In the conformal diagram of the axis $\vartheta' = 0, \pi$ based on accelerated coordinates, the origins $R' = 0$ and the coordinate singularity $R' = \infty$ of the accelerated frame are straight lines; the true infinities $\mathcal{I}^{\pm}$ have a "bulge" upwards or "downwards", depending on the angle ϑ'. The hypersurface $R' = \infty$ corresponds to the boosted hyperplane $\check{t}' = 0$, whereas the conformal infinity corresponds to $\check{t} = 0$ (the relation of both hyperplanes can be well understood in the diagram of the conformally related Minkowski space $\check{M}$). The diagrams in which the conformal infinities $\mathcal{I}^{\pm}$ are *not* straight naturally arise in the studies of the C-metric with $\Lambda > 0$ (de Sitter space being a special case of this class of the metrics)—see [27]. In general, outside the axis $\vartheta = \vartheta' = 0, \pi$, the transformations between the static and accelerated coordinates mix radial and angular coordinates R, ϑ and R', ϑ', as is seen also in the following Fig. 11. The sections $\vartheta' =$ constant (for some general ϑ') are also shown in Fig. 21 in the Appendix.

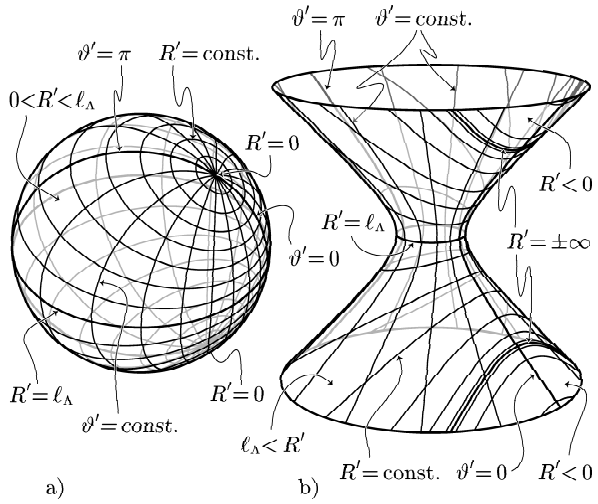

Figure 11: The accelerated coordinates R', ϑ' on the sections $T' =$ constant of de Sitter space (coordinate φ suppressed). In the region where $\partial/\partial T'$ is timelike ($0 < R' < \ell_\Lambda$), the cut $T' =$ constant is a spacelike sphere (diagram a). In the region where $\partial/\partial T'$ is spacelike ($\ell_\Lambda < R'$ and $R' < 0$), it is a timelike hyperboloid (diagram b). The diagrams are not in the same scale—the radius of the sphere and of the neck of the hyperboloid should be the same. The axis $\vartheta' = 0, \pi$ corresponds to the lines $T' =$ constant of Fig. 10. The coordinate singularity $R' = \pm\infty$ is also indicated. For more details see the text.

in the following. From here

$$-\check{t}'^2 + \check{r}'^2 = -\check{t}^2 + \check{r}^2 \,,$$
$$\tan\vartheta' = \frac{\sin\vartheta}{(\check{t}/\check{r})\sinh\alpha_{\rm o} + \cos\vartheta\cosh\alpha_{\rm o}} \,. \tag{5.2}$$

The original frame $\check{t}$, $\check{r}$, ϑ in Minkowski space $\check{M}$ is related to the static coordinates T, R, ϑ in de Sitter space by (cf. Eqs. (A67), (A80))

$$T = -\frac{\ell_\Lambda}{2}\log\left|\frac{\check{t}^2 - \check{r}^2}{\ell_\Lambda^2}\right| \,, \quad R = -\ell_\Lambda\frac{\check{r}}{\check{t}} \,, \quad \vartheta = \vartheta \,. \tag{5.3}$$

The metrics of the two spaces are related by $g_{\rm ds} = (\ell_\Lambda^2/\check{t}^2)g_{\check{\rm M}}$, $g_{\rm ds}$ being given by Eq. (3.9)—cf. Eq. (3.14). Now, let us introduce coordinates T', R', ϑ' given in terms of $\check{t}'$, $\check{r}'$, ϑ' by exactly the same formulas as coordinates T, R, ϑ are given in terms of $\check{t}$, $\check{r}$, ϑ in Eq. (5.3). In this way we obtain $g_{{\rm ds}'} = (\ell_\Lambda^2/\check{t}'^2)g_{\check{\rm M}}$. Combining the last relation with $g_{\rm ds} = (\ell_\Lambda^2/\check{t}^2)g_{\check{\rm M}}$, we find the metric of the original de Sitter space in the new coordinates T', R', ϑ' in the form

$$g_{\rm ds} = \frac{\check{t}'^2}{\check{t}^2}\, g_{{\rm ds}'} \,, \tag{5.4}$$

$g_{{\rm ds}'}$ is given by the "primed" version of Eq. (3.9). Expressing then the factor $(\check{t}'/\check{t})^2$ by using Eqs. (5.1), (5.2), and "primed" relations (5.3), we arrive at the de Sitter

metric in the accelerated coordinates in the form

$$g_{\rm as} = \frac{1 - R_{\rm o}^2/\ell_\Lambda^2}{\left[1 + (R' R_{\rm o}/\ell_\Lambda^2)\,\cos\vartheta'\right]^2}\left(-\left(1 - \frac{R'^2}{\ell_\Lambda^2}\right)\mathrm{d}T'^2 + \left(1 - \frac{R'^2}{\ell_\Lambda^2}\right)^{-1}\mathrm{d}R'^2 + R'^2\left(\mathrm{d}\vartheta'^2 + \sin^2\vartheta'\,\mathrm{d}\varphi^2\right)\right) . \tag{5.5}$$

Here the accelerated coordinates T', R', ϑ', φ are given in terms of static coordinates by the relation obtained by the procedure described above as follows:

$$R' = \ell_\Lambda \sqrt{1 - \frac{\left(1 - R^2/\ell_\Lambda^2\right)\left(1 - R_{\rm o}^2/\ell_\Lambda^2\right)}{\left[1 - (R R_{\rm o}/\ell_\Lambda^2)\,\cos\vartheta\right]^2}} ,$$
$$T' = T , \quad \tan\vartheta' = \frac{\sqrt{1 - R_{\rm o}^2/\ell_\Lambda^2}\, R\sin\vartheta}{R\cos\vartheta - R_{\rm o}} . \tag{5.6}$$

Notice that the time coordinate of static and accelerated frames coincide. Technically, this is easy to see from the first relation in Eqs. (5.2) and Eq. (5.3). Intuitively, this is evident since the uniformly accelerated particles are at rest in the static coordinates, as well as in the accelerated coordinates, the only difference being that they are located *at the origin* of the accelerated frame. Setting $R_{\rm o} = 0$ in Eq. (5.6), we get $R' = R$, $\vartheta' = \vartheta$, as expected. The static coordinates are centered on the poles $\chi = 0, \pi$, hence, on the *un*accelerated worldlines. The name *accelerated* coordinates is thus inspired by the fact that their origin *is* accelerated, and the value of this acceleration enters the form of the metric (5.5) explicitly through the quantity $R_{\rm o}$.

The 2-dimensional conformal diagram of de Sitter space with coordinate lines $T' = $ constant, $R' = $ constant of the accelerated frame is given in Fig. 10. For details, see the figure caption. Here let us just notice that the cosmological horizons are still described by $R'^2 = \ell_\Lambda^2$. Infinite values of R' can, however, be encountered "before" the conformal infinities $\mathcal{I}^\pm$ are reached. This depends on the angle ϑ'. Indeed, $R' = \infty$ corresponds to $\check{t}' = 0$, whereas $\mathcal{I}^\pm$ is given by $\check{t} = 0$, i.e.,

$$R' = -\frac{\ell_\Lambda^2}{R_{\rm o}}\frac{1}{\cos\vartheta'} , \tag{5.7}$$

(cf. metric (5.5)). Relation of these two surfaces is best viewed in Minkowski space $\check{M}$. We see that for $\vartheta, \vartheta' < \pi/2$, the conformal infinity $\mathcal{I}^+$ ($\mathcal{I}^-$) lies "above" ("below") the surface $R' = \pm\infty$. Thus the infinity $R' = \pm\infty$ is just a coordinate singularity, which can be removed using, for example, the C-metric-like coordinate υ introduced below.

Fig. 11a shows the cut $T = T' = $ constant located in the region of de Sitter space where the Killing vector $\partial/\partial T = \partial/\partial T'$ is timelike ($R, R' < \ell_\Lambda$); φ-direction is suppressed. The cut is a *spacelike* sphere S^3 with homogeneous spherical metric. The coordinate lines $R' = $ constant and $\vartheta' = $ constant are plotted, with two origins $R' = 0$ indicated: here the accelerated particles occur. The coordinate R' grows from $R' = 0$ at the origins to the equator where $R' = \ell_\Lambda$. In Fig. 11b the cut $T = T' = $ constant located in the regions where $\partial/\partial T = \partial/\partial T'$ is spacelike ($R, R' > \ell_\Lambda$) is illustrated, again with φ-direction suppressed. Here the cut is *timelike* with the geometry of three-dimensional de Sitter space. The coordinate lines $R' = $ constant and $\vartheta' = $ constant are also shown.

As we have just seen, the points with $R' = \infty$ can be "nice" points in de Sitter manifold. It may thus be convenient to introduce the inverse of R' as a new coordinate. Also, we consider $-\cos\vartheta'$ as a new coordinate, and make the time coordinate dimensionless. We thus arrive at the *C-metric-like coordinates* τ, υ, ξ, φ:

$$\tau = \frac{T'}{\ell_\Lambda} , \quad \upsilon = \frac{\ell_\Lambda}{R'} , \quad \xi = -\cos\vartheta' . \tag{5.8}$$

The metric (5.5) becomes

$$g_{\rm as} = \mathfrak{r}^2\left(-(\upsilon^2 - 1)\,\mathrm{d}\tau^2 + \frac{1}{\upsilon^2 - 1}\,\mathrm{d}\upsilon^2 + \frac{1}{1 - \xi^2}\,\mathrm{d}\xi^2 + (1 - \xi^2)\,\mathrm{d}\varphi^2\right) , \tag{5.9}$$

with the conformal factor $\mathfrak{r}$ given by

$$\mathfrak{r} = \frac{\ell_\Lambda}{\upsilon\cosh\alpha_{\rm o} - \xi\sinh\alpha_{\rm o}} . \tag{5.10}$$

This is de Sitter spacetime in the "C-metric form": setting the mass and charge parameters, m and e, equal to zero in the the C-metric with a positive cosmological constant (written in the form (2.8) of Ref. [27]), and choosing the acceleration parameter equal to $A = \ell_\Lambda^{-1}\,|\sinh\alpha_{\rm o}| = |a_{\rm o}|$, we obtain the metric (5.9).

B. Robinson-Trautman coordinates

In order to arrive naturally to the Robinson-Trautman form of the metric, notice that the coefficients in the metric (5.9) become singular at $\upsilon \to \pm 1$, similarly as they do on the horizon of the Schwarzschild spacetime in the standard Schwarzschild coordinates. Analogously to that case, we choose a "tortoise-type" coordinate $\upsilon_\star$ by

$$\upsilon_\star = \frac{1}{2}\log\left|\frac{1 - \upsilon}{1 + \upsilon}\right| . \tag{5.11}$$

Similarly to the Schwarzschild case again, we introduce a suitable *null* coordinate $\mathfrak{u}$ in terms of the radial and time coordinates τ and $\upsilon_\star$ as follows:

$$\mathfrak{u} = (\ell_\Lambda \tanh\alpha_{\rm o})\,(\tau + \upsilon_\star) . \tag{5.12}$$

Together with the conformal factor $\mathfrak{r}$ defined in Eq. (5.10), we arrive at the de Sitter metric in coordinates $\mathfrak{u}$, $\mathfrak{r}$, ξ, φ (cf. Eq. (A109)) which is very near to being in the Robinson-Trautman form. However, there is a

non-vanishing mixed metric coefficient at $\mathrm{d}\mathfrak{u} \vee \mathrm{d}\xi$ which is absent in the Robinson-Trautman metric. Such a term can be made to vanish by introducing a new angular coordinate ψ by

$$\psi = \operatorname{arctanh}\xi + \frac{\mathfrak{u}}{\ell_\Lambda}\sinh\alpha_0 \,. \tag{5.13}$$

The de Sitter metric then becomes

$$g_{\mathrm{ds}} = -H\,\mathrm{d}\mathfrak{u}^2 - \mathrm{d}\mathfrak{u}\vee\mathrm{d}\mathfrak{r} + \frac{\mathfrak{r}^2}{P^2}\left(\mathrm{d}\psi^2+\mathrm{d}\varphi^2\right), \tag{5.14}$$

where

$$H = -\frac{\mathfrak{r}^2}{\ell_\Lambda^2} + 2\frac{\mathfrak{r}}{\ell_\Lambda}\sinh\alpha_0\,\tanh\Big(\psi - \frac{\mathfrak{u}}{\ell_\Lambda}\sinh\alpha_0\Big) + 1\,,$$
$$P = \cosh\Big(\psi - \frac{\mathfrak{u}}{\ell_\Lambda}\sinh\alpha_0\Big)\,. \tag{5.15}$$

This is precisely the form of the Robinson-Trautman metric—see, e.g., [50]. Tracking back the transformations leading to the metric (5.14), the connection between the Robinson-Trautman coordinates and the static coordinates T, R, ϑ, φ turns out to be not as complicated as our procedure might have indicated, in particular, for the radial coordinate. We find a nice formula for $\mathfrak{r}$,

$$\mathfrak{r} = \frac{\ell_\Lambda}{\sqrt{1-\frac{R_0^2}{\ell_\Lambda^2}}}\left(\left(1-\frac{RR_0}{\ell_\Lambda^2}\cos\vartheta\right)^2 - \left(1-\frac{R^2}{\ell_\Lambda^2}\right)\left(1-\frac{R_0^2}{\ell_\Lambda^2}\right)\right)^{\frac{1}{2}}, \tag{5.16}$$

whereas the other two coordinates are simply expressed only in terms of accelerated coordinates $T'=T$, R', ϑ', φ:

$$\mathfrak{u} = \sqrt{1-\frac{R_0^2}{\ell_\Lambda^2}}\left(T' + \frac{\ell_\Lambda}{2}\log\left|\frac{R'-\ell_\Lambda}{R'+\ell_\Lambda}\right|\right), \tag{5.17}$$
$$\psi = \frac{R_0}{\ell_\Lambda}\left(\frac{T'}{\ell_\Lambda} + \frac{1}{2}\log\left|\frac{R'-\ell_\Lambda}{R'+\ell_\Lambda}\right|\right) + \log\left|\tan\frac{\vartheta'}{2}\right|\,.$$

Coordinates R', ϑ' can then be obtained in terms of the original static coordinates by using Eqs. (5.6).

The Robinson-Trautman coordinates with metric (5.14) are centered on the accelerated particles. As with static or accelerated frames, we need two sets of such coordinates to cover both $w_\odot$ and $w_\otimes$. The relations to the static coordinates become, of course, much simpler if the particles are not accelerated, $R_0 = 0$, and when both the Robinson-Trautman and static coordinates are centered on the pole $\chi = 0$:

$$\mathfrak{r} = R\,,\quad \psi = \log\tan\frac{\vartheta}{2}\,,$$
$$\mathfrak{u} = T + \frac{\ell_\Lambda}{2}\log\left|\frac{R-\ell_\Lambda}{R+\ell_\Lambda}\right|\,. \tag{5.18}$$

However, even "accelerated" Robinson-Trautman coordinates possess some very convenient features. The radial coordinate $\mathfrak{r}$ is an affine parameter along null rays

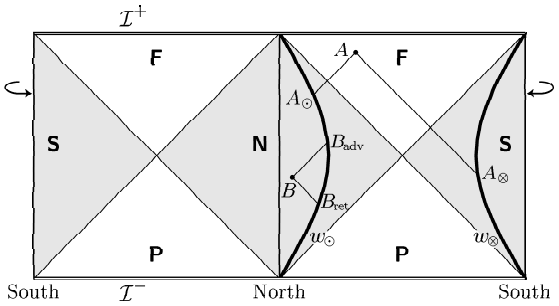

Figure 12: The field at an event A can be interpreted as 1/2 of the sum of the retarded fields produced by particle $w_\odot$ at $A_\odot$ and particle $w_\otimes$ at $A_\otimes$. The field at B can be interpreted as 1/2 of the sum of the retarded and advanced effects from particle $w_\odot$. The affine parameter distances BB_{ret} and BB_{adv} are equal, the same being true for the distances $AA_\odot$ and $AA_\otimes$.

$\mathfrak{u}$, ψ, φ = constants, normalized at the particle's worldline by the condition

$$\frac{\partial^\mu}{\partial\mathfrak{r}}\,g_{\mathrm{ds}\mu\nu}\,\mathfrak{u}^\nu = -1\,, \tag{5.19}$$

where $\mathfrak{u}$ is the particle's four-velocity. These null rays form a diverging but nonshearing and nonrotating congruence of geodesics. The null vector $\partial/\partial\mathfrak{r}$, tangent to the rays, is parallelly propagated along them. Its divergence is given by $\nabla_\mu\frac{\partial^\mu}{\partial\mathfrak{r}} = 2/\mathfrak{r}$ so that $\mathfrak{r}$ is both the affine parameter and the luminosity distance (see, e.g., [51]). With Robinson-Trautman coordinates, one can also associate a null tetrad (explicitly written down in the Appendix, Eq. (A114)) which is parallelly transported along the null rays from the particle ($\mathfrak{r}=0$) up to infinity ($\mathfrak{r}=\infty$).

Owing to the boost symmetry of both the worldlines and de Sitter space, an interesting feature arises, which is analogous to the situation in Minkowski space. Consider a point B in region **N** (Fig. 12). There are two generators of the null cone with the origin at B which cross the worldline $w_\odot$ at two points, B_{ret} and B_{adv}. Then the affine parameter distance BB_{ret} is the same as BB_{adv}. (In order to go towards the past from B_{adv} to B, the "advanced" Robinson-Trautman coordinates built on the past null cones with origins on $w_\odot$ can easily be introduced.) This is evident because B lies on one orbit of the boost Killing vector $\partial/\partial T$ and a boost can be applied which leaves the worldline $w_\odot$ invariant but moves B into event B' on the slice of time symmetry, $\tau = 0$ (also $T = T' = 0$), where the particle is at rest. Then B_{adv} and B_{ret} move to the new points B'_{adv}, B'_{ret}, which are located symmetrically with respect to $\tau = 0$. The equality of the affine parameter distances then follows from the symmetry immediately. Similarly, for an event A in region **F** one can show that the affine parameter distance $AA_\odot$ is equal to the distance $AA_\otimes$ (see Fig. 12). The point A lies on a boost orbit (which now has a spatial character) along which it

can be brought, by an appropriate boost, to the point located symmetrically between the worldlines $w_\odot$ and $w_\otimes$ (lying so on the equator, $\chi = \pi/2$). The same consideration can, of course, be applied to an event in the "past" region **P**—showing that the affine distances along future-oriented null rays from an event to the particles are equal.

Although the symmetries just described are common to the worldlines of uniformly accelerated particles in Minkowski and de Sitter spacetimes, an important difference exists. In Minkowski space, the affine parameter distance along the null ray from an event on particle's worldline, such as $A_\odot$, to an "observation" point A is equal to the proper distance between $A_\perp$ and $A_\odot$ where $A_\perp$ is the *orthogonal* projection of A onto the spacelike slice $T = T(A_\odot)$. This is not the case in de Sitter space if, as it appears natural, under an 'orthogonal projection' we understand the projection of the observation point A onto the spacelike slice $T =$ constant containing $A_\odot$ performed along a timelike geodesic orthogonal to such a slice. Nevertheless, the proper distance s between $A_\odot$ and $A_\perp$ is still related to the affine parameter distance $\mathfrak{r}$ by a simple expression:

$$\frac{\mathfrak{r}}{\ell_\Lambda} = \tan\frac{s}{\ell_\Lambda} \,. \tag{5.20}$$

This relation can be derived as follows. Consider, without loss of generality, $A_\odot$ located at the turning point of the particle $w_\odot$ at $T = 0$. The condition that the events A and $A_\odot$ are connected by a null ray implies that the distance s between $A_\odot$ and $A_\perp$ is the same as the time interval between $A_\perp$ and A as measured by the metric (3.12) of the conformally related static Einstein universe. Since A occurs at some time $\tilde{t}$ whereas $A_\odot$ and $A_\perp$ at $\tilde{t} = \pi/2$ (i.e., at static time $T = 0$), this time interval is equal to $\ell_\Lambda(\tilde{t} - \pi/2)$, cf. Eq. (3.11). The static radial coordinate R of A thus reads (cf. Eqs. (A64), (A77))

$$R = \frac{\sin\tilde{r}}{\sin\tilde{t}} = \frac{\sin\tilde{r}}{\cos(s/\ell_\Lambda)} \,. \tag{5.21}$$

The slice $T = 0$ has a geometry of the 3-sphere of radius ℓ_Λ. Using the standard law of cosines in spherical trigonometry for the sides of the triangle spanned by $A_\odot$, $A_\perp$, and the north pole, we can eliminate $\tilde{r}$. Finally, employing Eq. (5.16), we obtain the result (5.20). Clearly, near the particle $w_\odot$ we have $s \ll \ell_\Lambda$, and Eq. (5.20) then gives $\mathfrak{r} \approx s$, as in Minkowski space.

In the following section we shall explore the character of the fields of the particles $w_\odot$ and $w_\otimes$. We shall see that the affine parameter distance $\mathfrak{r}$ will play most important role, simplifying their description enormously. Namely, as we will see in Section VIB, Eq. (6.28), the affine parameter $\mathfrak{r}$ is identical to the factor $\mathcal{Q}$ which will be introduced in the following and will appear in all expressions for the fields.

VI. FIELDS OF UNIFORMLY ACCELERATED SOURCES AND THEIR MANY FACES

In this section we wish to construct the scalar and electromagnetic fields of uniformly accelerated (scalar and electric) charges in de Sitter universe. A general procedure, suitable in case of any—not necessarily uniform—acceleration would be to seek for appropriate Green's functions. Alternatively, in particular for sources moving along uniformly accelerated worldlines, we can make use of the conformal relations between Minkowski and de Sitter spaces, and of the properties of scalar and electromagnetic fields under conformal mappings. This method is advantageous not only for finding the fields in de Sitter spacetime, but also for understanding their relationships to the known fields of corresponding sources in special relativity. The only delicate issue is the fact that there are *no conformal mappings between Minkowski and de Sitter* space which are globally smooth. We discussed, in Section III, how various regions of one space can be mapped onto the regions of the other space. In Ref. [24] we carefully treated the fields at the hypersurfaces where the conformal transformation fails to be regular. In order to obtain well-behaved fields, one must continue analytically across such a hypersuface the field obtained in one region into the whole de Sitter space. In Section II in Ref. [24], we also analyzed in detail the behavior of the scalar field wave equation with sources and of Maxwell's equations with sources under (general) conformal transformations.

In Ref. [24] we primarily concentrated on the absence of purely retarded fields at the past infinity $\mathcal{I}^-$ of de Sitter spacetime—in fact, in any spacetime in which $\mathcal{I}^-$ is spacelike. In order to analyze this problem we also considered, in addition to monopole charges, more complicated sources like rigid and geodesic dipoles; and we constructed some retarded solutions to show their patological features. However, we confined ourselves to the sources the worldlines of which start and end at the poles; we did not employ coordinates best suited for exhibiting the properties of the fields at future infinity $\mathcal{I}^+$, and the frames corresponding to cosmological models like flat ($k = 0$) or hyperbolic ($k = -1$) cosmological coordinates; and we did not give the physical components of the fields. In the following we shall find the fields and discuss their properties in various physically important coordinate systems, in particular those significant at $\mathcal{I}^+$ or in a cosmological context. In the next section, we also obtain the fields due to the uniformly accelerated scalar and electric charges starting at $\mathcal{I}^-$ at $\chi = \pi/2$ ("born at the equator"). This, among others, will be important when we wish to regain the classical Born fields in the limit $\Lambda \to 0$.

We start by using the analysis of the conformal behavior of the fields and sources given in Section II in [24], and we also take over from [24] the resulting forms of the fields due to the sources starting and ending at the poles of de Sitter space, as described in standard coordinates.

A. Fields in coordinates centered on the poles

Consider two uniformly accelerated point sources starting at $\mathcal{I}^-$ (i.e., at $\tau \to -\infty$, $\tilde{t} \to 0$) at the poles $\chi = \tilde{r} = 0$ and $\chi = \tilde{r} = \pi$ (Fig. 7). Their worldlines $w_\odot$, $w_\otimes$ are given by Eqs. (4.7) (or (4.24)) in these standard (rescaled) coordinates, by Eqs. (4.8) and (4.9) in the flat and hyperbolic cosmological coordinates, and by Eqs. (4.18) in the static coordinates. Their simplest description is, of course, given by $R' = 0$ and $\mathfrak{r} = 0$ in the accelerated and Robinson-Trautman coordinates since these frames are centered exactly on their worldlines. In Section IV we discussed physical velocities and other properties of these particles.

Now, as noticed at the beginning of Section IV, these *two* worldlines can be obtained by conformally mapping the worldline of *one* uniformly moving particle in Minkowski space into de Sitter space. The fields of *uniformly moving* sources in Minkowski space are just boosted Coulomb fields. Under a conformal rescaling of the metric, $g_{\alpha\beta} \to \hat{g}_{\alpha\beta} = \Omega^2 g_{\alpha\beta}$, the fields behave as follows: $\Phi \to \hat{\Phi} = \Omega^{-1}\Phi$, $\mathrm{F}_{\alpha\beta} \to \hat{\mathrm{F}}_{\alpha\beta} = \mathrm{F}_{\alpha\beta}$ (see [24], Section II, where the behavior of the source terms is also analyzed). Hence, the fields due to two *uniformly accelerated* sources in de Sitter spacetime can be obtained by conformally transforming the boosted Coulomb fields in Minkowski spacetime. Employing the conformal mapping (3.13) (3.15), we arrive at the following results (note [52]). The scalar field is given by the expression

$$\Phi = \frac{s}{4\pi}\frac{1}{\mathcal{Q}}\,, \tag{6.1}$$

where

$$\mathcal{Q} = \ell_\Lambda \Big[\Big(\sqrt{1+a_o^2\ell_\Lambda^2} + a_o\ell_\Lambda \cosh\frac{\tau}{\ell_\Lambda} \sin\chi\cos\vartheta \Big)^2 - \Big(1 - \cosh^2\frac{\tau}{\ell_\Lambda}\sin^2\chi \Big) \Big]^{\frac{1}{2}}\,, \tag{6.2}$$

or, written in the standard rescaled coordinates,

$$\mathcal{Q} = \ell_\Lambda \Big[\Big(\sqrt{1+a_o^2\ell_\Lambda^2} + a_o\ell_\Lambda \frac{\sin\tilde{r}}{\sin\tilde{t}}\cos\vartheta \Big)^2 - 1 + \frac{\sin^2\tilde{r}}{\sin^2\tilde{t}} \Big]^{\frac{1}{2}}\,. \tag{6.3}$$

This field is produced by *two* identical charges of magnitude s moving along worldlines $w_\odot$ and $w_\otimes$. It is smooth everywhere outside the charges and it can be written as a symmetric combination of retarded and advanced effects from both charges (cf. Eq. (6.6) in [24]).

Similarly to the scalar-field case, by using conformal technique the electromagnetic field produced by two uniformly accelerated charges moving along $w_\odot$ and $w_\otimes$ can be obtained in the form

$$\begin{aligned}\mathrm{F} = \frac{e}{4\pi}\frac{\ell_\Lambda^2}{\mathcal{Q}^3}\cosh\frac{\tau}{\ell_\Lambda} \Big[& a_o\ell_\Lambda \sin\chi\cos\chi\sin\vartheta\, \mathrm{d}\tau\wedge\mathrm{d}\vartheta \\ & - \Big(\sqrt{1+a_o^2\ell_\Lambda^2}\cosh\frac{\tau}{\ell_\Lambda}\sin\chi + a_o\ell_\Lambda\cos\vartheta \Big)\mathrm{d}\tau\wedge\mathrm{d}\chi \\ & + a_o\ell_\Lambda^2 \sinh\frac{\tau}{\ell_\Lambda}\cosh\frac{\tau}{\ell_\Lambda}\sin^2\chi\sin\vartheta\,\mathrm{d}\chi\wedge\mathrm{d}\vartheta \Big]\,,\end{aligned} \tag{6.4}$$

where $\mathcal{Q}$ is again given by Eq. (6.2). As in the scalar-field case, the field is smooth, non-vanishing in the whole de Sitter spacetime and involving thus both retarded and advanced effects (cf. Section VIIA in [24]). However, an important difference between the scalar and electromagnetic case exists: the magnitude of the scalar charges is the same, whereas the electromagnetic charges producing the fields (6.4) have *opposite* signs. This is analogous to the situation in Minkowski spacetime described in Section II (see the discussion below Eq. (2.13)). At the root of this fact appears to be CPT theorem—cf. [53] for the analogous gravitational case where the masses of the particles uniformly accelerated in the opposite direction are the same. In de Sitter spacetime, as in any spacetime with compact spacelike sections, a simpler argument exists: the total charge in a compact space must vanish as a consequence of the Gauss theorem [24].

To gain a better physical insight into the electromagnetic fields, we shall introduce the orthonormal tetrad $\{\mathrm{e}_\mu\}$ and the dual tetrad $\{\mathrm{e}^\mu\}$ tied to each coordinate frame used, and we shall decompose the electromagnetic field F into the electric and magnetic parts. Such a decomposition, of course, depends on the choice of the tetrad. For example, in the standard spherical coordinates τ, χ, ϑ, φ the electromagnetic field (2-form) F can be written as

$$\begin{aligned}\mathrm{F} = {} & \mathrm{E}^\chi\,\mathrm{e}^\chi\wedge\mathrm{e}^\tau + \mathrm{E}^\vartheta\,\mathrm{e}^\vartheta\wedge\mathrm{e}^\tau + \mathrm{E}^\varphi\,\mathrm{e}^\varphi\wedge\mathrm{e}^\tau \\ & + \mathrm{B}^\chi\,\mathrm{e}^\vartheta\wedge\mathrm{e}^\varphi + \mathrm{B}^\vartheta\,\mathrm{e}^\varphi\wedge\mathrm{e}^\chi + \mathrm{B}^\varphi\,\mathrm{e}^\chi\wedge\mathrm{e}^\vartheta\,,\end{aligned} \tag{6.5}$$

and the electric and magnetic field spatial vectors are given in terms of their *frame* components as follows:

$$\begin{aligned}\mathrm{E} &= \mathrm{E}^\chi\,\mathrm{e}_\chi + \mathrm{E}^\vartheta\,\mathrm{e}_\vartheta + \mathrm{E}^\varphi\,\mathrm{e}_\varphi\,, \\ \mathrm{B} &= \mathrm{B}^\chi\,\mathrm{e}_\chi + \mathrm{B}^\vartheta\,\mathrm{e}_\vartheta + \mathrm{B}^\varphi\,\mathrm{e}_\varphi\,.\end{aligned} \tag{6.6}$$

In the present case of the standard spherical coordinates, using the explicit forms of the tetrad given in the Appendix (Eqs. (A10)), we find

$$\begin{aligned}\mathrm{E}_{\mathrm{sph}} &= \frac{e}{4\pi}\frac{\ell_\Lambda}{\mathcal{Q}^3}\Big[-a_o\ell_\Lambda\cos\chi\sin\vartheta\,\mathrm{e}_\vartheta \\ &\qquad + \Big(\sqrt{1+a_o^2\ell_\Lambda^2}\cosh\frac{\tau}{\ell_\Lambda}\sin\chi + a_o\ell_\Lambda\cos\vartheta \Big)\mathrm{e}_\chi \Big]\,, \\ \mathrm{B}_{\mathrm{sph}} &= \frac{e}{4\pi}\frac{a_o\ell_\Lambda^2}{\mathcal{Q}^3}\sinh\frac{\tau}{\ell_\Lambda}\sin\chi\sin\vartheta\,\mathrm{e}_\varphi\,.\end{aligned} \tag{6.7}$$

In the Appendix the orthonormal tetrads tied to the coordinate systems considered in this paper are all listed explicitly. The only exception is the Robinson-Trautman coordinate system with one coordinate null and thus with a nondiagonal metric; in this case the null tetrad is given in which the Newman-Penrose-type components are more telling.

The tetrad components of the electric intensity and the magnetic induction vectors are physically meaningful objects: they can be measured by observers who move with the four-velocities given by the timelike vector of the

tetrad (as, e.g., e_τ for spherical cosmological observers), and are equipped with an orthonormal triad of the space-like vectors (e.g., e_χ, e_ϑ, e_φ).

We first list the resulting electromagnetic field tensor and its electric and magnetic parts in the coordinate systems centered on the poles $\chi = 0, \pi$. The scalar field is always given by expression (6.1), the explicit form of the scalar factor $\mathcal{Q}$ changes according to the coordinates used. Since this factor enters all the electromagnetic quantities as well, we always give $\mathcal{Q}$ first and then write the electromagnetic field quantities.

In the flat cosmological coordinates (see Eqs. (3.4), (3.5)) we find:

$$\mathcal{Q} = \ell_\Lambda \Big[\Big(\cosh\alpha_\mathrm{o} - \sinh\alpha_\mathrm{o} \frac{\check r}{\ell_\Lambda} \exp\frac{\check\tau}{\ell_\Lambda} \cos\vartheta \Big)^2 - \Big(1 - \frac{\check r^2}{\ell_\Lambda^2} \exp\Big(2\frac{\check\tau}{\ell_\Lambda}\Big)\Big)\Big]^{\frac12} , \tag{6.8}$$

$$\begin{aligned} \mathrm{F} = -\frac{e}{4\pi}\frac{1}{\mathcal{Q}^3} \exp\frac{\check\tau}{\ell_\Lambda} \Big[& \ell_\Lambda \check r \sinh\alpha_\mathrm{o} \sin\vartheta \, \mathrm{d}\check\tau\wedge\mathrm{d}\vartheta \\ & + \Big(\check r \cosh\alpha_\mathrm{o} \exp\frac{\check\tau}{\ell_\Lambda} - \ell_\Lambda \sinh\alpha_\mathrm{o} \cos\vartheta \Big) \mathrm{d}\check\tau\wedge\mathrm{d}\check r \\ & + \check r^2 \sinh\alpha_\mathrm{o} \exp\Big(2\frac{\check\tau}{\ell_\Lambda}\Big) \sin\vartheta \, \mathrm{d}\check r\wedge\mathrm{d}\vartheta \Big] , \end{aligned} \tag{6.9}$$

$$\begin{aligned} \mathrm{E}_{\mathrm{flat}} &= \frac{e}{4\pi}\frac{\ell_\Lambda}{\mathcal{Q}^3} \Big[\sinh\alpha_o \sin\vartheta \, \mathrm{e}_\vartheta \\ &\quad - \Big(\cosh\alpha_\mathrm{o} \frac{\check r}{\ell_\Lambda} \exp\frac{\check\tau}{\ell_\Lambda} - \sinh\alpha_\mathrm{o}\cos\vartheta \Big) \mathrm{e}_{\check r} \Big] , \\ \mathrm{B}_{\mathrm{flat}} &= -\frac{e}{4\pi}\frac{\ell_\Lambda \sinh\alpha_\mathrm{o}}{\mathcal{Q}^3} \frac{\check r}{\ell_\Lambda} \exp\frac{\check\tau}{\ell_\Lambda} \sin\vartheta \, \mathrm{e}_\varphi . \end{aligned} \tag{6.10}$$

In the hyperbolic cosmological coordinates (see Eqs. (3.6), (3.7)), the results are slightly lengthier:

$$\mathcal{Q} = \ell_\Lambda \Big[\Big(\cosh\alpha_\mathrm{o} - \sinh\alpha_\mathrm{o} \sinh\frac{\eta}{\ell_\Lambda} \sinh\frac{\rho}{\ell_\Lambda} \cos\vartheta \Big)^2 - \Big(1 - \sinh^2\frac{\eta}{\ell_\Lambda} \sinh^2\frac{\rho}{\ell_\Lambda} \Big)\Big]^{\frac12} , \tag{6.11}$$

$$\begin{aligned} \mathrm{F} = -\frac{e}{4\pi}\frac{\ell_\Lambda}{\mathcal{Q}^3} \Big[& \sinh\frac{\eta}{\ell_\Lambda} \\ & \times \Big(\cosh\alpha_o \sinh\frac{\eta}{\ell_\Lambda} \sinh\frac{\rho}{\ell_\Lambda} - \sinh\alpha_o \cos\vartheta \Big) \mathrm{d}\eta\wedge\mathrm{d}\rho \\ & + \sinh\alpha_\mathrm{o} \sinh\frac{\eta}{\ell_\Lambda} \sinh\frac{\rho}{\ell_\Lambda} \cosh\frac{\rho}{\ell_\Lambda} \sin\vartheta \, \ell_\Lambda \mathrm{d}\eta\wedge\mathrm{d}\vartheta \\ & + \sinh\alpha_\mathrm{o} \sinh^2\frac{\eta}{\ell_\Lambda} \cosh\frac{\eta}{\ell_\Lambda} \sinh^2\frac{\rho}{\ell_\Lambda} \sin\vartheta \, \ell_\Lambda \mathrm{d}\rho\wedge\mathrm{d}\vartheta \Big] , \end{aligned} \tag{6.12}$$

$$\begin{aligned} \mathrm{E}_{\mathrm{hyp}} &= \frac{e}{4\pi}\frac{\ell_\Lambda}{\mathcal{Q}^3} \Big[\sinh\alpha_\mathrm{o} \cosh\frac{\rho}{\ell_\Lambda} \sin\vartheta \, \mathrm{e}_\vartheta \\ &\quad + \Big(\cosh\alpha_\mathrm{o} \sinh\frac{\eta}{\ell_\Lambda} \sinh\frac{\rho}{\ell_\Lambda} - \sinh\alpha_\mathrm{o}\cos\vartheta \Big) \mathrm{e}_\rho \Big] , \\ \mathrm{B}_{\mathrm{hyp}} &= -\frac{e}{4\pi}\frac{\ell_\Lambda}{\mathcal{Q}^3} \sinh\alpha_\mathrm{o} \cosh\frac{\eta}{\ell_\Lambda} \sinh\frac{\rho}{\ell_\Lambda} \sin\vartheta \, \mathrm{c}_\varphi . \end{aligned} \tag{6.13}$$

Much simpler expressions for the fields arise in the static coordinates (see Eqs. (3.8), (3.9)). We obtain

$$\mathcal{Q}^2 = \frac{(\ell_\Lambda^2 - R R_\mathrm{o}\cos\vartheta)^2}{(\ell_\Lambda^2 - R_\mathrm{o}^2)} - (\ell_\Lambda^2 - R^2) , \tag{6.14}$$

$$\begin{aligned} \mathrm{F} = -\frac{e}{4\pi} \frac{\ell_\Lambda}{\sqrt{\ell_\Lambda^2 - R_\mathrm{o}^2}} \frac{1}{\mathcal{Q}^3} \Big[& (R - R_\mathrm{o}\cos\vartheta) \, \mathrm{d}T\wedge\mathrm{d}R \\ & + \Big(1 - \frac{R^2}{\ell_\Lambda^2} \Big) R R_\mathrm{o} \sin\vartheta \, \mathrm{d}T\wedge\mathrm{d}\vartheta \Big] , \end{aligned} \tag{6.15}$$

$$\begin{aligned} \mathrm{E}_{\mathit{stat}} &= \frac{e}{4\pi}\frac{1}{\mathcal{Q}^3} \Big[\frac{\ell_\Lambda (R - R_\mathrm{o}\cos\vartheta)}{\sqrt{\ell_\Lambda^2 - R_\mathrm{o}^2}} \mathrm{e}_R + R_\mathrm{o}\sin\vartheta \, \mathrm{e}_\vartheta \Big] , \\ \mathrm{B}_{\mathit{stat}} &= 0 . \end{aligned} \tag{6.16}$$

Since for practical calculations and for an understanding of the conformal relations between Minkowski and de Sitter spaces the rescaled coordinates are very useful, we also give the fields in these coordinates. The rescaled coordinates are tied with the same orthonormal tetrad as non-rescaled ones, and they define the same splitting into electric and magnetic parts (E and B are the same spatial vectors); the functional dependence on the coordinates, however, is different. In the standard rescaled (conformally Einstein) coordinates (see Eqs. (3.10)–(3.12)), which cover the whole de Sitter spacetime including its conformal infinities globally, we get Eq. (6.3) for $\mathcal{Q}$ and

$$\begin{aligned} \mathrm{F} = -\frac{e}{4\pi}\frac{1}{\mathcal{Q}^3}\frac{\ell_\Lambda^3}{\sin^3\tilde t} \Big[& a_\mathrm{o}\ell_\Lambda \cos\tilde t \sin^2\tilde r \sin\vartheta \, \mathrm{d}\tilde r\wedge\mathrm{d}\vartheta \\ & + \Big(\sqrt{1 + a_\mathrm{o}^2\ell_\Lambda^2} \sin\tilde r + a_\mathrm{o}\ell_\Lambda \sin\tilde t\cos\vartheta \Big) \mathrm{d}\tilde t\wedge\mathrm{d}\tilde r \\ & - a_o\ell_\Lambda \sin\tilde t\cos\tilde r \sin\tilde r \sin\vartheta \, \mathrm{d}\tilde t\wedge\mathrm{d}\vartheta \Big] , \end{aligned} \tag{6.17}$$

$$\begin{aligned} \mathrm{E}_{\mathrm{sph}} &= \frac{e}{4\pi}\frac{\ell_\Lambda}{\mathcal{Q}^3} \Big[-a_\mathrm{o}\ell_\Lambda \cos\tilde r \sin\vartheta \, \mathrm{e}_\vartheta \\ &\quad + \Big(\sqrt{1 + a_\mathrm{o}^2\ell_\Lambda^2} \frac{\sin\tilde r}{\sin\tilde t} + a_\mathrm{o}\ell_\Lambda\cos\vartheta \Big) \mathrm{e}_\chi \Big] , \\ \mathrm{B}_{\mathrm{sph}} &= -\frac{e}{4\pi}\frac{a_\mathrm{o}\ell_\Lambda^2}{\mathcal{Q}^3} \cot\tilde t \sin\tilde r \sin\vartheta \, \mathrm{e}_\varphi , \end{aligned} \tag{6.18}$$

whereas in the flat rescaled cosmological coordinates (3.13) (3.15), which cover globally the conformally related Minkowski space (see also Fig. 3), we arrive at

$$\mathcal{Q} = \ell_\Lambda \Big[\Big(\cosh\alpha_\mathrm{o} + \sinh\alpha_\mathrm{o} \frac{\check r}{\check t}\cos\vartheta \Big)^2 - \Big(1 - \frac{\check r^2}{\check t^2} \Big)\Big]^{\frac12} , \tag{6.19}$$

$$\begin{aligned} \mathrm{F} = \frac{e}{4\pi}\frac{1}{\mathcal{Q}^3}\frac{\ell_\Lambda^3}{\check t^3} \Big[& \sinh\alpha_\mathrm{o} \, \check r^2 \sin\vartheta \, \mathrm{d}\check r\wedge\mathrm{d}\vartheta \\ & + \big(\cosh\alpha_\mathrm{o} \, \check r + \sinh\alpha_\mathrm{o} \, \check t\cos\vartheta \big) \mathrm{d}\check t\wedge\mathrm{d}\check r \\ & - \sinh\alpha_\mathrm{o} \, \check t \, \check r \sin\vartheta \, \mathrm{d}\check t\wedge\mathrm{d}\vartheta \Big] , \end{aligned} \tag{6.20}$$

$$\mathrm{E}_{\mathrm{flat}} = \frac{e}{4\pi}\frac{\ell_\Lambda}{\mathcal{Q}^3}\Big[\sinh\alpha_{\mathrm{o}}\,\sin\vartheta\,\mathrm{e}_\vartheta - \Big(\cosh\alpha_{\mathrm{o}}\,\frac{\check r}{\check t} + \sinh\alpha_{\mathrm{o}}\cos\vartheta\Big)\,\mathrm{e}_{\check r}\Big]\,, \qquad (6.21)$$

$$\mathrm{B}_{\mathrm{flat}} = \frac{e}{4\pi}\,\frac{\ell_\Lambda\sinh\alpha_{\mathrm{o}}}{\mathcal{Q}^3}\,\frac{\check r}{\check t}\,\sin\vartheta\,\mathrm{e}_\varphi\,.$$

In various contexts the electromagnetic field four-potential form A, implying the field $\mathrm{F} = \mathrm{dA}$, may be needed. In the standard rescaled (conformally Einstein) coordinates the potential reads

$$\mathrm{A} = -\frac{e}{4\pi}\frac{1}{\mathcal{Q}}\frac{\ell_\Lambda}{\sin\tilde t}\,\frac{\sqrt{1+a_{\mathrm{o}}^2\ell_\Lambda^2}\,\sin\tilde l + a_{\mathrm{o}}\ell_\Lambda\sin\tilde r\cos\vartheta}{\sin^2\tilde l - \sin^2\tilde r} \times\Big(\sin\tilde t\cos\tilde r\,\mathrm{d}\tilde t - \cos\tilde t\sin\tilde r\,\mathrm{d}\tilde r\Big)\,. \qquad (6.22)$$

From this expression the frame components can easily be obtained and the four-potential form can be transformed directly to any coordinate system of interest. The four-potential acquires a particularly simple form in static coordinates:

$$\mathrm{A} = -\frac{e}{4\pi}\,\frac{1}{\mathcal{Q}}\,\frac{\ell_\Lambda^2 - RR_{\mathrm{o}}\cos\vartheta}{\ell_\Lambda\sqrt{\ell_\Lambda^2 - R_{\mathrm{o}}^2}}\,\mathrm{d}T\,. \qquad (6.23)$$

Inspecting now the expressions (6.4)–(6.21), we first notice few basic features of the fields. As a consequence of the axisymmetry, the azimuthal φ component of the electric field vanishes. On the other hand, only the azimuthal φ component of the magnetic field is non-zero. At the axis of symmetry, $\vartheta = 0, \pi$, the latitudinal ϑ component of the electric field and magnetic field vanish as $\sim \sin\vartheta$. The electric field points along the axis.

In the classical Born solution in Minkowski space, both charges are, at any time, located symmetrically with respect to the equatorial plane $\vartheta = \pi/2$. Consequently, the radial part of the electric field vanishes for $\vartheta = \pi/2$ (cf. Eq. (2.13)). In de Sitter spacetime the charges outgoing from the poles are, at all times, symmetrically located with respect to the sphere $\chi = \pi/2$ (illustrated as the circle in Fig. 2). We thus expect the ϑ component of the electric field to vanish for $\chi = \pi/2$. This, indeed, follows from Eq. (6.7). This symmetry can be seen only in the standard spherical coordinates since the sphere $\chi = \pi/2$ is not covered by the hyperbolic cosmological coordinates and in the flat cosmological coordinates only one particle occurs.

Another typical feature of the Born solution in Minkowski space is its time symmetry. As a consequence, the magnetic field vanishes at $t = 0$ (cf. Eq. (2.13)). In the past, it was this fact which led some investigators, W. Pauli [54] among them, to the conclusion that there is "no formation of a wave zone nor any corresponding radiation" since $\mathrm{B} = 0$ at $t = 0$. However, it is not at a spacelike hypersurface $t =$ constant but at $\mathcal{I}^+$, which is reached by taking $u = t - r$ constant, $t, r \to \infty$, where the Born field has typical radiative features, i.e., $|\mathrm{E}| = |\mathrm{B}| \sim r^{-1}$ (see [37], [53], [25]). In our generalized Born solution, the time symmetry of the fields is clearly demonstrated in the global standard coordinates: under inversion $\tau \to -\tau$ the electric field in Eq. (6.7) is invariant, whereas the magnetic field changes the sign; $\mathrm{B}_\varphi = 0$ at $\tau = 0$. The field also exhibits radiative character when we approach $\mathcal{I}^+$ in an appropriate way, as it is briefly indicated in [25]. As mentioned in the Introduction, a detailed analysis of the radiative properties of the generalized Born field will be given elsewhere.

The fields take the simplest form in the static coordinates, Eq. (6.15). In these coordinates the particles are at rest, and they both have a constant distance from the poles; their world lines are the orbits of the "static" Killing vector $\partial/\partial T$ of de Sitter space. The electric field is time independent, the magnetic field vanishes. This is fully analogous to the Born field in Minkowski spacetime: it is static, and purely electric in the Rindler coordinates, the time coordinate of which is aligned along the orbit of the boost Killing vectors (see, e.g., [6]). However, as we discussed in Section III, the static coordinates cover only a "half" of de Sitter space. In the other half, the Killing vector $\partial/\partial T$ becomes spacelike. It is in this non-static domain (regions **F** and **P** in Fig. 12) where we expect, in analogy with the results in Minkowski spacetime, to find fields which have radiative properties. $\partial/\partial T$ is the Killing vector also in the non-static regions, however, it is spacelike here, as it is typical for a boost Killing vector in Minkowski space. The fields of uniformly accelerated charges in de Sitter spacetime are invariant under the boosts along $\partial/\partial T$ everywhere. They are thus boost-rotation symmetric as the Born fields in Minkowski spacetime.

In the cosmological coordinates, respectively, in their rescaled versions, the fields are, of course, time dependent. Here we expect the effects of the expansion/contraction of de Sitter universe to be manifested. Indeed, considering in any of the cosmological frames the spatial coordinates fixed, and examining the fields along the timelike geodesics, we discover that the fields exponentially decay at large times, i.e., as $\mathcal{I}^+$ is approached. More specifically, with the spherical coordinates χ, ϑ, φ fixed, the factor $\mathcal{Q}$ behaves as $\exp(\tau/\ell_\Lambda)$ at large times τ, and hence, we obtain $\mathrm{E}_{\mathrm{sph}} \approx c_1\exp(-2\tau/\ell_\Lambda)\mathrm{e}_\chi + c_2\exp(-3\tau/\ell_\Lambda)\mathrm{e}_\vartheta$, $\mathrm{B}_{\mathrm{sph}} \approx b_1\exp(-2\tau/\ell_\Lambda)\mathrm{e}_\varphi$, c_1, c_2, b_1 being constants. The electric field thus becomes radial at large τ. Similarly, in flat cosmological coordinates we find $\mathrm{E}_{\mathrm{flat}} \approx c_1\exp(-2\check\tau/\ell_\Lambda)\mathrm{e}_{\check r}$, $\mathrm{B}_{\mathrm{flat}} \approx b_1\exp(-2\check\tau/\ell_\Lambda)\mathrm{e}_\varphi$. In the hyperbolic cosmological coordinates the proper time η appears instead of $\check\tau$. The rapid decay of the fields along timelike worldlines at large times is caused by the exponential expansion (at large times) of the spatial slices $\tau =$ constant (respectively $\check\tau$, $\eta =$ constant). Although our fields are just test fields, their exponential decay is another manifestation of the "cosmic no-hair phenomenon": geodesic observers in spacetimes with $\Lambda > 0$ see at large times these spacetimes to approach the de Sitter universe exponentially fast—the universe becomes

"bald" (see, e.g., [22, 23]). Clearly, as one approaches *past* infinity $\mathcal{I}^-$ ($\tau \to -\infty$), the fields also decay exponentially.

It is interesting to notice the character of the field as it would be seen by the observers at rest with respect to the hyperbolic cosmological coordinates in the limit at which the particles "enter" the region covered by these observers across the horizon $\tilde{t} = \tilde{r}$ (cf. Fig. 4), given in the hyperbolic coordinates by $\eta \to 0$, $\rho \to \infty$. As discussed in Section IV, the observed velocity (4.17) of the charges at this boundary is (in the limit) equal to the velocity of light. Employing the transformation formulas (A86), it is easy to see that at this boundary $|\sinh(\eta/\ell_\Lambda)\, \sinh(\rho/\ell_\Lambda)| \to 1$. Hence, the factor $\mathcal{Q}$ is finite here (as it is evident from its scalar character and its finiteness in the global standard coordinates). Also, the radial part of the electric field remains finite. However, E^{ϑ} diverges as $\exp(\rho/\ell_\Lambda)$ here, indicating that the field has a character of an impulse, in fact, rather of an impulsive wave: indeed, Eq. (6.10) implies $\left|\mathrm{E}^{\vartheta}\right| = |\mathrm{B}^{\varphi}|$. The situation appears to be analogous to the field of a static charge viewed from an inertial frame boosted to the velocity of light in Minkowski spacetime (see, e.g., [55]).

B. Fields in coordinates centered on the particles

As expected, a remarkable simplification occurs when the fields are evaluated in the coordinates at the origin of which the charges are situated at all times. Since the accelerated coordinates T', R', ϑ' and the C-metric-like coordinates are simply related by Eqs. (5.8), the discussion of the field properties is the same in both these frames. Namely, notice that both coordinate systems are tied with the same orthonormal tetrad, and they thus define the same splitting of the field into the electric and magnetic parts. In these coordinates, we find the factor $\mathcal{Q}$ to read

$$\begin{aligned}\mathcal{Q} &= \cosh\alpha_o\, \frac{1}{R'} + \sinh\alpha_o\, \frac{1}{\ell_\Lambda}\cos\vartheta' \\ &= \frac{1}{\ell_\Lambda}\big(\upsilon\cosh\alpha_o - \xi\sinh\alpha_o\big)\,.\end{aligned} \tag{6.24}$$

The scalar field is again given by $\Phi = (s/4\pi)\,\mathcal{Q}^{-1}$, and the electromagnetic field also acquires now an extremely simple form:

$$\mathrm{F} = \frac{e}{4\pi}\,\frac{1}{R'^2}\,\mathrm{d}R'\wedge\mathrm{d}T' = \frac{e}{4\pi}\,\mathrm{d}\tau\wedge\mathrm{d}\upsilon\,, \tag{6.25}$$

$$\mathrm{E}_{\mathrm{acc}} = \frac{e}{4\pi}\,\frac{1}{\mathcal{Q}^2}\,\mathrm{e}_{R'}\,,\quad \mathrm{B}_{\mathrm{acc}} = 0\,. \tag{6.26}$$

The magnetic field vanishes in the frame tied to the accelerated and C-metric coordinates, the electric field has precisely the Coulomb form, with the factor $\mathcal{Q}$ playing the role of a distance.

As signalized above already, the factor $\mathcal{Q}$ turns out to be the Robinson-Trautman radial coordinate (see Eq. (6.28) below), i.e., the affine parameter distance along null geodesics. The geometrical role of $\mathcal{Q}$ was elucidated in Section V B. Considering a fixed point in de Sitter universe and a light cone emanating from this point, three typical situations can arise as illustrated in Fig. 12. For a point B from the regions **N** or **S**, there are two null geodesics, one past-pointing, the other future-pointing, each of which crosses the worldline of *the same* particle, say $w_{\odot}$ (in case of B from **N**), at points B_{ret} and B_{adv} (see Fig. 12). Since $\mathcal{Q}$ is equal to the (specific) affine parameter distance which is the same from B_{ret} as from B_{adv} (see Section V B), we can interpret the field (6.26) as arising from purely retarded, respectively, advanced effects from B_{ret}, respectively B_{adv}; or, equivalently, as a combination of retarded and advanced effects from these points. In the second situation, when the fixed point, say A, is located "above the roof" (in the region **F**), there are two past-oriented null geodesics emanating from it which cross now *both* particles $w_{\odot}$ and $w_{\otimes}$ at points $A_{\odot}$ and $A_{\otimes}$ (see Fig. 12). The field can be interpreted as arising from retarded effects only, either as a combination from both particles $w_{\odot}$ and $w_{\otimes}$, or as the retarded field from just one of them. Finally, for a point from the region **P** the field can analogously be interpreted in terms of advanced effects.

As we discussed in Section V A and illustrated in detail in the Appendix, the accelerated coordinates (similarly as the static coordinates to which they go over for a vanishing acceleration) are *static*, i.e., the vector $\partial/\partial T'$ tangent to the orbits of the Killing vector is timelike, only in the regions **N** and **S** (cf. Figs. 10, 12). Observers following the orbits of the Killing vector are thus confined to the regions **N** and **S**, and they cannot detect the fields in the region **F** (respectively **P**). Nevertheless, notice that although the time coordinate T' diverges at the horizon $R = \ell_\Lambda$, the radial coordinate R' is perfectly finite there, $R' = \ell_\Lambda$ (cf. Eq. (5.6) with $R = \ell_\Lambda$), and the field (6.25) is meaningful in the region **F** (or **P**) as well. Since here the roles of the coordinates R' and T' are interchanged, R' becoming a *time coordinate*, the field becomes *time-dependent*. As mentioned above, we do not expect to find radiative properties in the regions **N** and **S**. Indeed, in accelerated coordinates the field (6.26) is static Coulomb field, with $\mathcal{Q}$ playing the role of a distance. However, the radiative properties of the whole field in the wave zone in the region **F** are not evident from the time-dependent, purely electric field in the accelerated coordinates with R' as a time coordinate.

It is worthwhile to recall that with finite sources in Minkowski spacetime the field at *any* event is of a *general* algebraic type; only asymptotically, at large distances, its features approach those of a *null field* ($\mathrm{E}^2 - \mathrm{B}^2 = 0$, $\mathrm{E}\cdot\mathrm{B} = 0$), if there is a radiation (see, e.g., [45, 56]). In case of a non-null field, one can always introduce a frame in which the electric and magnetic fields are collinear, or, in the language of the Newman-Penrose formalism,

to choose such a null tetrad k, l, m, $\bar{\mathrm{m}}$, corresponding to the orthonormal tetrad, that the only non-vanishing null-tetrad component is $\Phi_1 = \frac{1}{2\sqrt{2}}(\mathrm{E} - i\mathrm{B}) \cdot (\mathrm{k} - \mathrm{l})$ (see Eqs. (A114) for the explicit expressions of the null tetrad and Eqs. (A4) for the null-tetrad components of the electromagnetic field). Such a situation arises precisely for the null tetrad associated with the accelerated coordinates: the null-tetrad components are simply

$$\Phi_1^{\mathrm{acc}} = -\frac{1}{2}\frac{e}{4\pi}\frac{1}{\mathcal{Q}^2}\,, \quad \Phi_0^{\mathrm{acc}} = \Phi_2^{\mathrm{acc}} = 0\,. \tag{6.27}$$

The vanishing of the other two null-tetrad components, Φ_0^{acc} and Φ_2^{acc}, has a deeper algebraic explanation: the null tetrad tied to the accelerated coordinates is special in the sense that it contains *both* principal null directions of the electromagnetic field. Inspecting the form of the null tetrad constructed from the orthonormal tetrad (A95), we observe that both these principal null directions are tangent to the "radial" surfaces ϑ', φ = constant in the accelerated coordinates.

The radiative properties are well exhibited in the *Robinson-Trautman coordinates*. As we discussed in Section V B, these coordinates are tied to the future null cones centered on the worldline of a particle. We consider the null cones with vertices on the particle $w_{\ominus}$. Let us recall that the radial coordinate $\mathfrak{r}$ is the affine parameter along the generators of the null cones, each of which is given by $\mathfrak{u}$, ψ, φ fixed. Now, as mentioned above, it turns out that the *factor $\mathcal{Q}$ is precisely equal to this affine parameter $\mathfrak{r}$*:

$$\mathcal{Q} = \mathfrak{r}\,. \tag{6.28}$$

The scalar field is then simply given by

$$\Phi = \frac{s}{4\pi}\frac{1}{\mathfrak{r}}\,. \tag{6.29}$$

A remarkably nice form also acquires the electromagnetic field:

$$\begin{aligned}\mathrm{F} &= \frac{e}{4\pi}\left(\frac{1}{\mathfrak{r}^2}\,\mathrm{d}\mathfrak{u}\wedge\mathrm{d}\mathfrak{r} + a_{\mathrm{o}}\sin^2\vartheta'\,\mathrm{d}\mathfrak{u}\wedge\mathrm{d}\vartheta'\right)\\ &= \frac{e}{4\pi}\left(\frac{1}{\mathfrak{r}^2}\,\mathrm{d}\mathfrak{u}\wedge\mathrm{d}\mathfrak{r} + a_{\mathrm{o}}\sin^2\vartheta'\,\mathrm{d}\mathfrak{u}\wedge\mathrm{d}\psi\right)\,.\end{aligned} \tag{6.30}$$

The Newman-Penrose scalars are defined in terms of the null tetrad (A114), which is parallelly propagated from the source to the "observation point" along the rays $\mathfrak{u}$, ψ, φ = constant. They look as follows:

$$\begin{aligned}\Phi_0^{\mathrm{RT}} &= 0\,,\\ \Phi_1^{\mathrm{RT}} &= -\frac{1}{2}\frac{e}{4\pi}\frac{1}{\mathfrak{r}^2}\,,\\ \Phi_2^{\mathrm{RT}} &= \frac{1}{\sqrt{2}}\frac{e}{4\pi}\frac{1}{\mathfrak{r}}a_{\mathrm{o}}\sin\vartheta'\,.\end{aligned} \tag{6.31}$$

Now the radiative character of the field is transparent: the first term entering the peeling behavior, the scalar Φ_2, decays indeed as $\mathfrak{r}^{-1}$, and it is non-vanishing for a non-zero acceleration a_{o}. In the expressions (6.30) and (6.31), the de Sitter background is completely "hidden". The same form of the fields are obtained in case of uniformly accelerated charges in Minkowski space if the coordinates built on the null cones emanating from the particles are employed. A difference between both cases reveals itself only in the explicit dependence of the affine parameter $\mathfrak{r}$ on the coordinates of spacetime points.

VII. BORN IN DE SITTER

Finally, we turn to the fields from the particles symmetrically located with respect to the origin $\chi = 0$ (the "north pole") of the standard spherical coordinates. The particles are thus "born" asymptotically at the equator, $\chi = \pi/2$, at $\tau \to -\infty$, and return back at $\tau \to \infty$ with the opposite speeds (Fig. 8). Their fields, of course, are intrinsically the same as those considered in the preceding section but only now they represent the *direct* generalization of the classical Born solutions due to uniformly accelerated charges symmetrically located with respect to the origin of Minkowski space.

We shall find the generalized Born fields easily by using the transformation (4.21) which we applied to obtain the worldlines of the particles born at the equator from those born at the poles. The scalar field due to two equal scalar charges s moving along the worldlines $w_{\oplus}$ and $w_{\ominus}$ reads

$$\Phi = \frac{s}{4\pi}\,\Omega_{\mathrm{M}}^{-1}\,\frac{1}{\mathcal{R}}\,, \tag{7.1}$$

where the factor $\mathcal{R}$ is determined by

$$\begin{aligned}\mathcal{R} = \frac{\ell_\Lambda}{1+\cosh\frac{\tau}{\ell_\Lambda}\cos\chi}\Big[&\cosh^2\frac{\tau}{\ell_\Lambda}\,\sin^2\chi\,\sin^2\vartheta\\ &+\left(\sqrt{1+a_{\mathrm{o}}^2\ell_\Lambda^2}\,\cosh\frac{\tau}{\ell_\Lambda}\,\cos\chi - a_{\mathrm{o}}\ell_\Lambda\right)^2\Big]^{\frac{1}{2}}\,,\end{aligned} \tag{7.2}$$

and the conformal factor Ω_{M} is given by (cf. Eq. (3.19))

$$\Omega_{\mathrm{M}} = 1 + \cosh\frac{\tau}{\ell_\Lambda}\cos\chi\,. \tag{7.3}$$

This factor is left in the explicit form here, in contrast to the preceding section, since it explicitly exhibits conformal relation of the scalar field under conformal mappings (3.19) between de Sitter space and Minkowski space M. This relation will be used in the following to perform the limit from the Born field in de Sitter to the Born field in Minkowski spacetime.

The electromagnetic field produced by charge e moving along the worldline $w_{\oplus}$ and by symmetrically located

charge $-e$ moving along $w_\ominus$ has the following form:

$$\begin{aligned}\mathrm{F}_{\mathrm{BdS}} = {} & \frac{e}{4\pi}\frac{\ell_\Lambda^2}{\mathcal{R}^3}\frac{\cosh\frac{\tau}{\ell_\Lambda}\,\sin\vartheta}{(1+\cosh\frac{\tau}{\ell_\Lambda}\cos\chi)^3} \\ & \times\Big[a_{\mathrm{o}}\ell_\Lambda^2\sinh\frac{\tau}{\ell_\Lambda}\,\cosh\frac{\tau}{\ell_\Lambda}\,\sin^2\chi\,\mathrm{d}\chi\wedge\mathrm{d}\vartheta \\ & +\Big(\sqrt{1+a_{\mathrm{o}}^2\ell_\Lambda^2}\cosh\frac{\tau}{\ell_\Lambda}\,\cos\chi - a_{\mathrm{o}}\ell_\Lambda\Big)\,\cot\vartheta\,\mathrm{d}\tau\wedge\mathrm{d}\chi \\ & -\Big(\sqrt{1+a_{\mathrm{o}}^2\ell_\Lambda^2}\cosh\frac{\tau}{\ell_\Lambda} - a_{\mathrm{o}}\ell_\Lambda\cos\chi\Big)\,\sin\chi\,\mathrm{d}\tau\wedge\mathrm{d}\vartheta\Big]\,,\end{aligned} \tag{7.4}$$

with factor $\mathcal{R}$ given by (7.2). In the tetrad tied to the standard spherical coordinates the electric and magnetic fields become

$$\begin{aligned}\mathrm{E}^{\mathrm{BdS}}_{\mathrm{sph}} = {} & -\frac{e}{4\pi}\frac{\ell_\Lambda}{\mathcal{R}^3}\frac{1}{(1+\cosh\frac{\tau}{\ell_\Lambda}\cos\chi)^3} \\ & \times\Big[\Big(\sqrt{1+a_{\mathrm{o}}^2\ell_\Lambda^2}\cosh\frac{\tau}{\ell_\Lambda}\,\cos\chi - a_{\mathrm{o}}\ell_\Lambda\Big)\cot\vartheta\,\mathrm{e}_\chi \\ & -\Big(\sqrt{1+a_{\mathrm{o}}^2\ell_\Lambda^2}\cosh\frac{\tau}{\ell_\Lambda} - a_{\mathrm{o}}\ell_\Lambda\cos\chi\Big)\sin\chi\,\mathrm{e}_\vartheta\Big]\,, \\ \mathrm{B}^{\mathrm{BdS}}_{\mathrm{sph}} = {} & \frac{e}{4\pi}\frac{a_{\mathrm{o}}\ell_\Lambda^2}{\mathcal{R}^3}\frac{\sinh\frac{\tau}{\ell_\Lambda}\,\sin\chi\,\sin\vartheta}{(1+\cosh\frac{\tau}{\ell_\Lambda}\cos\chi)^3}\,\mathrm{e}_\varphi\,.\end{aligned} \tag{7.5}$$

In the standard rescaled (conformally Einstein) coordinates the expressions (7.4)–(7.5) slightly simplify:

$$\frac{\mathcal{R}}{\ell_\Lambda} = \frac{\big[(a_{\mathrm{o}}\ell_\Lambda\sin\tilde t - \sqrt{1+a_{\mathrm{o}}^2\ell_\Lambda^2}\cos\tilde r)^2 + \sin^2\tilde r\sin^2\vartheta\big]^{\frac12}}{\sin\tilde t+\cos\tilde r}\,, \tag{7.6}$$

$$\Omega_{\mathrm{M}} = \frac{\cos\tilde r+\sin\tilde t}{\sin\tilde t}\,, \tag{7.7}$$

$$\begin{aligned}\mathrm{F}_{\mathrm{BdS}} = {} & -\frac{e}{4\pi}\frac{\ell_\Lambda^3}{\mathcal{R}^3}\frac{\sin\vartheta}{(\sin\tilde t+\cos\tilde r)^3}\Big[a_{\mathrm{o}}\ell_\Lambda\sin^2\tilde r\cos\tilde t\,\mathrm{d}\tilde r\wedge\mathrm{d}\vartheta \\ & -\big(\sqrt{1+a_{\mathrm{o}}^2\ell_\Lambda^2}\cos\tilde r - a_{\mathrm{o}}\ell_\Lambda\sin\tilde t\big)\,\cot\vartheta\,\mathrm{d}\tilde t\wedge\mathrm{d}\tilde r \\ & +\big(\sqrt{1+a_{\mathrm{o}}^2\ell_\Lambda^2} - a_{\mathrm{o}}\ell_\Lambda\cos\tilde r\sin\tilde t\big)\,\sin\tilde r\,\mathrm{d}\tilde t\wedge\mathrm{d}\vartheta\Big]\,,\end{aligned} \tag{7.8}$$

$$\begin{aligned}\mathrm{E}^{\mathrm{BdS}}_{\mathrm{CE}} = {} & \frac{e}{4\pi}\frac{\ell_\Lambda\sin^2\tilde t}{\mathcal{R}^3(\sin\tilde t+\cos\tilde r)^3} \\ & \times\Big[-\big(\sqrt{1+a_{\mathrm{o}}^2\ell_\Lambda^2}\cos\tilde r - a_{\mathrm{o}}\ell_\Lambda\sin\tilde t\big)\cos\vartheta\,\mathrm{e}_{\tilde r} \\ & +\big(\sqrt{1+a_{\mathrm{o}}^2\ell_\Lambda^2} - a_{\mathrm{o}}\ell_\Lambda\sin\tilde t\cos\tilde r\big)\sin\vartheta\,\mathrm{e}_\vartheta\Big]\,, \\ \mathrm{B}^{\mathrm{BdS}}_{\mathrm{CE}} = {} & -\frac{e}{4\pi}\frac{a_{\mathrm{o}}\ell_\Lambda^2\sin^2\tilde t}{\mathcal{R}^3(\sin\tilde t+\cos\tilde r)^3}\cos\tilde t\sin\tilde r\sin\vartheta\,\mathrm{e}_\varphi\,.\end{aligned} \tag{7.9}$$

The character of these fields was discussed in the preceding section for the particles $w_\ominus$ and $w_\otimes$. One must only rotate all the structures by $\pi/2$ in the χ direction; hence, for example, the sphere of symmetry changes from $\chi=\pi/2$ to $\vartheta=\pi/2$.

There is some interest in having the fields available also in the hyperbolic cosmological coordinates. They cover only those regions of the fields in which we assume the radiative properties will be manifested. The sources producing the fields are not covered by these coordinates (cf. Fig. 8). The fields in the hyperbolic cosmological coordinates look as follows:

$$\begin{aligned}\mathcal{R} = {} & \frac{1}{2b_{\mathrm{o}}}\Big[\Big(b_{\mathrm{o}}^2+\ell_\Lambda^2\tanh^2\frac{\eta}{2\ell_\Lambda}\Big)^2 \\ & +4\,b_{\mathrm{o}}^2\,\tanh^2\frac{\eta}{2\ell_\Lambda}\sinh^2\frac{\rho}{\ell_\Lambda}\sin^2\vartheta\Big]^{\frac12}\,,\end{aligned} \tag{7.10}$$

$$\Omega_{\mathrm{M}} = 1+\cosh\frac{\eta}{\ell_\Lambda} = 2\cosh^2\frac{\eta}{2\ell_\Lambda}\,, \tag{7.11}$$

$$\begin{aligned}\mathrm{F}_{\mathrm{BdS}} = {} & \frac{e}{4\pi}\frac{\ell_\Lambda^3}{\mathcal{R}^3}\frac{1}{2b_{\mathrm{o}}\Omega_{\mathrm{M}}^2}\Big[\Big(\frac{b_{\mathrm{o}}^2}{\ell_\Lambda^2}+\tanh^2\frac{\eta}{2\ell_\Lambda}\Big)\sinh\frac{\eta}{\ell_\Lambda} \\ & \times\Big(\frac{1}{\ell_\Lambda}\cos\vartheta\,\mathrm{d}\eta\wedge\mathrm{d}\rho - \sinh\frac{\rho}{\ell_\Lambda}\cosh\frac{\rho}{\ell_\Lambda}\sin\vartheta\,\mathrm{d}\eta\wedge\mathrm{d}\vartheta\Big) \\ & -\Big(\frac{b_{\mathrm{o}}^2}{\ell_\Lambda^2}-\tanh^2\frac{\eta}{2\ell_\Lambda}\Big)\sinh^2\frac{\eta}{\ell_\Lambda}\,\sinh^2\frac{\rho}{\ell_\Lambda}\sin\vartheta\,\mathrm{d}\rho\wedge\mathrm{d}\vartheta\Big]\,,\end{aligned} \tag{7.12}$$

$$\begin{aligned}\mathrm{E}^{\mathrm{BdS}}_{\mathrm{hyp}} = {} & \frac{e}{4\pi}\frac{\ell_\Lambda^2}{\mathcal{R}^3}\frac{1}{2b_{\mathrm{o}}\Omega_M^2}\Big(\frac{b_{\mathrm{o}}^2}{\ell_\Lambda^2}+\tanh^2\frac{\eta}{2\ell_\Lambda}\Big) \\ & \times\Big(-\cos\vartheta\,\mathrm{e}_\rho+\cosh\frac{\rho}{\ell_\Lambda}\sin\vartheta\,\mathrm{e}_\vartheta\Big)\,,\end{aligned} \tag{7.13}$$

$$\mathrm{B}^{\mathrm{BdS}}_{\mathrm{hyp}} = -\frac{e}{4\pi}\frac{\ell_\Lambda^2}{\mathcal{R}^3}\frac{\sinh\frac{\rho}{\ell_\Lambda}}{2b_{\mathrm{o}}\Omega_{\mathrm{M}}^2}\Big(\frac{b_{\mathrm{o}}^2}{\ell_\Lambda^2}-\tanh^2\frac{\eta}{2\ell_\Lambda}\Big)\sin\vartheta\,\mathrm{e}_\varphi\,.$$

We shall use these results in the forthcoming paper on the radiative properties of the generalized Born solution.

Here, finally, we wish to describe the limiting procedure which leads from the generalized Born solutions directly to their counterparts in Minkowski spacetime. For this purpose it is natural to employ the conformally Minkowski coordinates t, r, ϑ, φ introduced in Eq. (3.17), with the inverse transformation given in the Appendix, Eq. (A17). Transforming the fields of the particles $w_\oplus$, $w_\ominus$ from the conformally Einstein coordinates to the conformally Minkowski coordinates, we arrive at the following intriguing forms. The scalar field is given by Eq. (7.1) where now the factors $\mathcal{R}$ and Ω_{M} are determined by

$$\mathcal{R} = \frac{1}{2b_{\mathrm{o}}}\sqrt{(b_{\mathrm{o}}^2+t^2-r^2)^2+4\,b_{\mathrm{o}}^2\,r^2\sin^2\vartheta}\,, \tag{7.14}$$

$$\Omega_{\mathrm{M}} = \frac{2\,\ell_\Lambda^2}{\ell_\Lambda^2-t^2+r^2}\,. \tag{7.15}$$

Notice that factor $\mathcal{R}$ coincides with the expression (2.11) in Minkowski space. The electromagnetic field reads

$$\begin{aligned}\mathrm{F}_{\mathrm{BdS}} = {} & -\frac{e}{4\pi}\frac{1}{2b_{\mathrm{o}}}\frac{1}{\mathcal{R}^3}\Big[-2\,t\,r^2\sin\vartheta\,\mathrm{d}r\wedge\mathrm{d}\vartheta \\ & -(b_{\mathrm{o}}^2+t^2-r^2)\cos\vartheta\,\mathrm{d}t\wedge\mathrm{d}r \\ & +r\,(b_{\mathrm{o}}^2+t^2+r^2)\sin\vartheta\,\mathrm{d}t\wedge\mathrm{d}\vartheta\Big]\,,\end{aligned} \tag{7.16}$$

and the electric and magnetic parts of the field turn out to be

$$\mathrm{E}^{\mathrm{BdS}}_{\mathrm{CM}} = \frac{e}{4\pi}\,\frac{1}{\mathcal{R}^3}\,\frac{1}{2b_0\Omega_{\mathrm{M}}^2}\Big[(b_o^2+t^2-r^2)\cos\vartheta\,\mathrm{e}_r - (b_o^2+t^2+r^2)\sin\vartheta\,\mathrm{e}_\vartheta\Big]\,, \quad (7.17)$$

$$\mathrm{B}^{\mathrm{BdS}}_{\mathrm{CM}} = \frac{e}{4\pi}\,\frac{1}{\mathcal{R}^3}\,\frac{1}{b_0\Omega_{\mathrm{M}}^2}\,t\,r\sin\vartheta\,\mathrm{e}_\varphi\,.$$

To connect these fields with their counterparts in flat space, note that they are conformally related by the conformal transformation (3.19). Under the conformal mapping, the field Φ_{BdS} must be multiplied by factor Ω_{M}, which gives $\Phi_{\mathrm{M}} = (s/4\pi)\,\mathcal{R}^{-1}$, and $\mathrm{F}_{\mathrm{BdS}}$ in (7.16) remains unchanged. The transformed fields then coincide with the classical Born fields (2.9), (2.11), and (2.13).

In order to see the limit for $\Lambda \to 0$, we parametrize the sequence of de Sitter spaces by Λ, and identify them in terms of coordinates t, r, ϑ, φ. As $\Lambda = 3/\ell_\Lambda^2 \to 0$, Eq. (3.19) implies $(\Omega_{\mathrm{M}})_\Lambda \to 2$, $(g_{\mathrm{dS}})_\Lambda \to 4g_{\mathrm{M}}$. After the trivial rescaling of t, r by factor 2, the standard Minkowski metric is obtained. The limit of the scalar and electromagnetic fields (7.1) and (7.16), in which b_0 is kept constant (with $a_0 = (1 - b_0^2\ell_\Lambda^{-2})/(2b_0)$ cf. Eq. (4.29)), leads precisely to the scalar and electromagnetic Born fields (2.9) and (2.13) in flat space. Because of the rescaling of the coordinates by factor 2, we get the physical acceleration equal to $1/b_0 = 2a_0$, and the scalar field rescaled by 1/2. The explicit limiting procedure carrying the generalized Born fields in de Sitter universe back into the classical Born solution in Minkowski space has thus been demonstrated.

VIII. CONCLUDING REMARKS

Since 1998 the observations of high-redshift supernovae indicate, with an increasing evidence, that we live in an accelerating universe with a positive cosmological constant (for most recent observations see, e.g., [57]). Vacuum energy seems to dominate in the universe and it is thus of interest to understand fundamental physics in the vacuum dominated de Sitter spacetime.

In the present work, we constructed the fields of uniformly accelerated charges in this universe. They go over to the classical Born fields in Minkowski space in the limit of a vanishing cosmological constant. Aside from some similarities found, the generalized fields provide the models showing how a positive cosmological constant implies essential differences from physics in flat spacetime. For example, advanced effects occur inevitably due to the spacelike character of the past infinity $\mathcal{I}^-$ and its consequence—the existence of the past particles' horizons, respectively, of the "creation light cones" of the particles' worldlines.

Since de Sitter spacetime, according to our present understanding, appears to be not only an appropriate basic model for studying future cosmological epochs, but it is commonly used also for exploring the inflationary era, various physical processes have been investigated in de Sitter space from the perspective of the early universe, among them, the effects of quantum field theory. Also in quantum contexts, however, problems arise from combining the causal structure of the full de Sitter spacetime with the constraint equations (see [58] for a recent review). These problems are associated with the "insufficiency of purely retarded fields" in spacetimes with a spacelike $\mathcal{I}^-$. We analyzed this issue in detail for the classical electromagnetic and scalar fields with sources in Ref. [24].

Another intriguing implication of the rapid expansion of de Sitter universe due to a positive cosmological constant is manifested in the exponential decay of the fields at large times. We noticed this "cosmic no-hair phenomenon" explicitly on the late-time behaviour of the fields due to accelerated charges.

In the present paper we wished to give all details on the construction of the fields and on coordinate frames useful in understanding their various aspects, including their relation to their counterparts in flat spacetime. We did not here analyze the radiative characteristics of the fields. In the Introduction we indicated that radiative properties depend on the way in which a given point of infinity is approached. This is briefly described at the end of our paper [25].

In de Sitter spacetime it is not a priori clear, as it is in special relativity, how to define global physical quantities like energy or energy flux. Such issues connected with the question of radiation from "Born in de Sitter" will be considered in a future presentation.

Acknowledgments

The authors are grateful to the Division of geometric analysis and gravitation, Albert Einstein Institute, Golm, for the kind hospitality. Here most of the work was done. J.B. also thanks the Institute of Astronomy, University of Cambridge, for hospitality. We also acknowledge support by Grants GAČR 202/02/0735 of the Czech Republic and Research Project No. MSM113200004.

Appendix A: THE PALETTE OF COORDINATE SYSTEMS IN DE SITTER SPACETIME

Nine families of coordinate systems are here introduced, described analytically and illustrated graphically. The corresponding forms of de Sitter metric, orthonormal tetrads and interrelations between the systems are given. All these systems are suitable for exhibiting various features of de Sitter space; two families are directly associated with uniformly accelerated particles. Although the majority (though not all) of these coordinate systems undoubtedly appeared in literature in some form already, they are scattered and, as far as we know, not summarized as comprehensively as in the following. In the main text we refer frequently to this Appendix, but

the Appendix can be read independently. We hope it can serve as a catalogue useful for analyzing various aspects of physics in de Sitter universe.

By a *family of coordinate systems* we mean the systems with the *same* coordinate lines; e.g., $\{x^\mu\}$ and $\{y^\mu\}$ where $x^1 = x^1(y^1)$, $x^2 = x^2(y^2)$, etc. Seven of our families have the same spherical angular coordinates ϑ, φ, accelerated and Robinson-Trautman coordinates mix three coordinates, only azimuthal coordinate φ remains unchanged.

The homogeneous normalized metric on two-spheres (the metric "in angular direction") is denoted by

$$\mathrm{d}\omega^2 = \mathrm{d}\vartheta^2 + \sin^2\vartheta\,\mathrm{d}\varphi^2 \,. \tag{A1}$$

The radial coordinates label directions pointing out from the pole and acquire only positive values. However, transformations among coordinates take simpler forms if we allow radial coordinates to take on negative values as well. This causes no problems if, denoting by t and r the prototypes of time and radial coordinates, we adopt the convention that the following two values of coordinates describe the same point:

$$\{t,\, r,\, \vartheta,\, \varphi\} \;\leftrightarrow\; \{t,\, -r,\, \pi - \vartheta,\, \varphi + \pi\} \,. \tag{A2}$$

Hence, intuitively we may consider a point with $-r < 0$ and ϑ, φ fixed to lie on diametrically opposite side of the pole $r = 0$ with respect to the point $r > 0$, ϑ, φ.

The orthonormal tetrad e_t, e_r, e_ϑ, e_φ associated with a coordinate system is tangent to the coordinate lines and oriented (with few exceptions) in the directions of growing coordinates. It is chosen in such a way that the external product $e^t \wedge e^r \wedge e^\vartheta \wedge e^\varphi$ of 1-forms of the dual tetrad has always the same orientation. Since all forms of the metric contain the term (A1) the only component $(\mathrm{e}_\varphi)^\varphi$ of the tetrad vector e_φ in coordinate frame $\{\frac{\partial}{\partial x^\mu}\}$ is related to the ϑ-component of e_ϑ as

$$(\mathrm{e}_\varphi)^\varphi = \frac{1}{\sin\vartheta}\,(\mathrm{e}_\vartheta)^\vartheta \,, \tag{A3}$$

and we thus omit e_φ henceforth.

In the standard Newman-Penrose null complex tetrad k, l, m, $\bar{\mathrm{m}}$ with only nonvanishing inner products $\mathrm{k}\cdot\mathrm{l} = -1$, $\mathrm{m}\cdot\bar{\mathrm{m}} = 1$, the electromagnetic field F is represented by three complex components:

$$\begin{gathered}\Phi_0 = \mathrm{F}_{\alpha\beta}\,\mathrm{k}^\alpha\,\mathrm{m}^\beta \,, \quad \Phi_2 = \mathrm{F}_{\alpha\beta}\,\bar{\mathrm{m}}^\alpha\,\mathrm{l}^\beta \,, \\ \Phi_1 = \tfrac{1}{2}\,\mathrm{F}_{\alpha\beta}\left(\mathrm{k}^\alpha\,\mathrm{l}^\beta - \mathrm{m}^\alpha\,\bar{\mathrm{m}}^\beta\right) .\end{gathered} \tag{A4}$$

The null tetrad can be specified directly (as it will be done in the case of Robinson-Trautman coordinates in Eq. (A114)), or it can be associated with any orthonormal tetrad, say t, q, r, s, by relations

$$\begin{aligned}\mathrm{k} &= \tfrac{1}{\sqrt{2}}(\mathrm{t} + \mathrm{q}) \,, & \mathrm{l} &= \tfrac{1}{\sqrt{2}}(\mathrm{t} - \mathrm{q}) \,, \\ \mathrm{m} &= \tfrac{1}{\sqrt{2}}(\mathrm{r} - i\,\mathrm{s}) \,, & \bar{\mathrm{m}} &= \tfrac{1}{\sqrt{2}}(\mathrm{r} + i\,\mathrm{s}) \,.\end{aligned} \tag{A5}$$

Here, t and q are timelike and spacelike unit vectors respectively, typically in a direction of "time" and "radial" coordinate, and r, s are spacelike unit vectors in angular directions, $\mathrm{r} = \mathrm{e}_\vartheta$, $\mathrm{s} = \mathrm{e}_\varphi$.

For each coordinate family we give the diagram illustrating section ϑ, φ = constant with the radial coordinate taking on *both* positive and negative values. The diagrams thus represent the history of the *entire* main circle of the spatial spherical section of de Sitter universe. The left and right edges of the diagrams represent the south pole and should be considered as identified; the central vertical line describes the history of the north pole. Recalling the meaning of the negative radial coordinate we could eliminate the left half of each of the diagrams by transforming it into the right one by replacements $\{\vartheta,\, \varphi\} \to \{\pi - \vartheta,\, \varphi + \pi\}$. However, it is instructive to keep both halves for better understanding of the spatial topology of the sections. All diagrams are compactified—they are adapted to the standard rescaled coordinates $\tilde{t}$, $\tilde{r}$ (see below). The past and future conformal infinities are drawn as double lines. The ranges of time and radial coordinates are shown, the orientation of coordinate labels indicates the directions of the growth of corresponding coordinates.

We will also introduce several sign factors. The values of these factors in different domains of spacetime are indicated in Fig. 13.

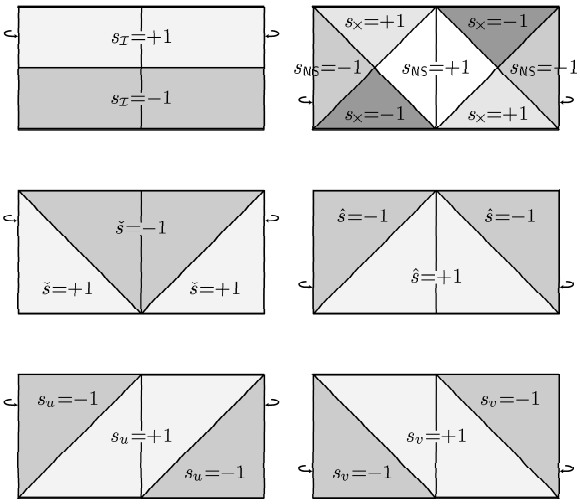

Figure 13: The values of the factors $s_{\mathcal{I}}$, s_{NS}, $s_\times$, $\check{s}$, $\hat{s}$, s_u and s_v in various regions of de Sitter space. The factors are defined in Eqs. (A73), (A61), (A74), (A21), (A36) and (A128), respectively. The factor $s_\times$ is used only in the expressions for static coordinates in the region where the Killing vector is spacelike. Therefore, we indicated the values of $s_\times$ only in those regions, although Eq. (A74) defines $s_\times$ everywhere. The factors $s_\times$, s_u, and s_v are defined only for any given section ϑ = constant, but not as unique functions on the whole spacetime (they are not symmetric with respect to the pole). This is related to our convention using negative radial coordinates, cf. the text below Eq. (A1).

1. The spherical cosmological family

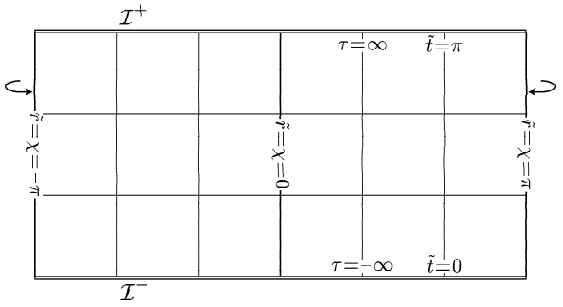

Figure 14: The spherical cosmological family of coordinates.

The first family consists of the *standard* or *spherical cosmological coordinates* τ, χ, ϑ, φ, and of the *standard rescaled* or *conformally Einstein coordinates* $\tilde t$, $\tilde r$, ϑ, φ (where $\tilde r \equiv \chi$). These coordinates cover de Sitter spacetime globally. They are associated with cosmological observers with homogeneous spatial sections of positive spatial curvature. The coordinates are adjusted to the spherical symmetry of the spatial sections: χ, ϑ, and φ are standard angular coordinates. The coordinate τ is a proper time along the worldlines of the cosmological observers given by χ, ϑ, $\varphi =$ constant. The vector $\partial/\partial\tau$ is a conformal Killing vector which is everywhere timelike. The rescaled coordinates $\tilde t$, $\tilde r$, ϑ, φ can also be viewed as the standard coordinates of the conformally related Einstein universe; they cover smoothly both conformal infinities $\mathcal{I}^\pm$ of de Sitter spacetime.

Metric and relation between coordinates

$$g = -\mathrm{d}\tau^2 + \ell_\Lambda^2 \cosh^2(\tau/\ell_\Lambda)\left(\mathrm{d}\chi^2 + \sin^2\chi\,\mathrm{d}\omega^2\right), \tag{A6}$$

$$g = \ell_\Lambda^2 \sin^{-2}\tilde t\left(-\mathrm{d}\tilde t^{\,2} + \mathrm{d}\tilde r^2 + \sin^2\tilde r\,\mathrm{d}\omega^2\right), \tag{A7}$$

$$\tan\frac{\tilde t}{2} = \exp\frac{\tau}{\ell_\Lambda}, \quad \cot\tilde t = -\sinh\frac{\tau}{\ell_\Lambda}, \qquad \sin\tilde l = \cosh^{-1}\frac{\tau}{\ell_\Lambda}, \quad \cos\tilde l = -\tanh\frac{\tau}{\ell_\Lambda}, \tag{A8a}$$

$$\tilde r = \chi\,. \tag{A8b}$$

The ranges of coordinates are

$$\tau\in\mathbb{R}, \quad \chi\in(-\pi,\pi), \qquad \tilde t\in(0,\pi), \quad \tilde r\in(-\pi,\pi), \tag{A9}$$

with negative values of radial coordinates χ, $\tilde r$ interpreted in accordance with Eq. (A2).

Orthonormal tetrad

$$\mathrm{e}_\tau = \frac{\partial}{\partial\tau} = \frac{1}{\ell_\Lambda}\sin\tilde l\,\frac{\partial}{\partial\tilde t}\,,$$

$$\mathrm{e}_\chi = \frac{1}{\ell_\Lambda}\cosh^{-1}\frac{\tau}{\ell_\Lambda}\,\frac{\partial}{\partial\chi} = \frac{1}{\ell_\Lambda}\sin\tilde t\,\frac{\partial}{\partial\tilde r}\,, \tag{A10}$$

$$\mathrm{e}_\vartheta = \frac{1}{\ell_\Lambda}\frac{1}{\cosh(\tau/\ell_\Lambda)\sin\chi}\frac{\partial}{\partial\vartheta} = \frac{1}{\ell_\Lambda}\frac{\sin\tilde t}{\sin\tilde r}\frac{\partial}{\partial\vartheta}\,.$$

Relation to flat cosmological family

$$\tan\tilde t = \frac{2\,\ell_\Lambda\hat t}{\ell_\Lambda^2 - \hat t^2 + \hat r^2} = \frac{2\,\ell_\Lambda\check t}{\ell_\Lambda^2 - \check t^2 + \check r^2}\,, \qquad \tan\tilde r = \frac{2\,\ell_\Lambda\hat r}{\ell_\Lambda^2 + \hat t^2 - \hat r^2} = \frac{2\,\ell_\Lambda\check r}{\ell_\Lambda^2 + \check t^2 - \check r^2}\,. \tag{A11}$$

Relation to hyperbolic cosmological coordinates

$$\cot\tilde t = -\sinh\frac{\eta}{\ell_\Lambda}\cosh\frac{\rho}{\ell_\Lambda}\,, \qquad \tan\tilde r = \tanh\frac{\eta}{\ell_\Lambda}\sinh\frac{\rho}{\ell_\Lambda}\,. \tag{A12}$$

Relation to static family in timelike domains **N**, **S**

$$\tan\tilde t = -s_{\mathsf{NS}}\frac{\ell_\Lambda}{\sqrt{\ell_\Lambda^2 - R^2}}\sinh^{-1}\frac{T}{\ell_\Lambda}\,, \qquad \tan\tilde r = s_{\mathsf{NS}}\frac{R}{\sqrt{\ell_\Lambda^2 - R^2}}\cosh^{-1}\frac{T}{\ell_\Lambda}\,, \tag{A13}$$

$$\tan\tilde l = -s_{\mathsf{NS}}\frac{\cosh\frac{\bar r}{\ell_\Lambda}}{\sinh\frac{\bar t}{\ell_\Lambda}}\,, \quad \tan\tilde r = s_{\mathsf{NS}}\frac{\sinh\frac{\bar r}{\ell_\Lambda}}{\cosh\frac{\bar t}{\ell_\Lambda}}\,, \tag{A14}$$

where $s_{\mathsf{NS}} = +1$ (-1) in domain **N** (**S**), cf. Eq. (A61).

Relation to static family in spacelike domains **F**, **P**

$$\tan\tilde t = \frac{-s_{\mathcal{I}}\,\ell_\Lambda}{\sqrt{R^2 - \ell_\Lambda^2}}\cosh^{-1}\frac{T}{\ell_\Lambda}\,, \qquad \tan\tilde r = \frac{s_{\mathcal{I}}\,R}{\sqrt{R^2 - \ell_\Lambda^2}}\sinh^{-1}\frac{T}{\ell_\Lambda}\,, \tag{A15}$$

$$\tan\tilde t = s_{\mathsf{X}}\frac{\sinh\frac{\bar r}{\ell_\Lambda}}{\cosh\frac{\bar t}{\ell_\Lambda}}\,, \quad \tan\tilde r = -s_{\mathsf{X}}\frac{\cosh\frac{\bar r}{\ell_\Lambda}}{\sinh\frac{\bar t}{\ell_\Lambda}}\,, \tag{A16}$$

where $s_{\mathcal{I}} = -\operatorname{sign}\cos\tilde t$ and $s_{\mathsf{X}} = -s_{\mathcal{I}}\operatorname{sign}\tilde r$, cf. Eqs. (A73) and (A74).

Relation to conformally Minkowski coordinates

$$\cot\tilde t = \frac{2\ell_\Lambda t}{t^2 - r^2 - \ell_\Lambda^2}\,, \quad \tan\tilde r = \frac{2\ell_\Lambda r}{t^2 - r^2 + \ell_\Lambda^2}\,. \tag{A17}$$

2. The flat cosmological family, type "∨"

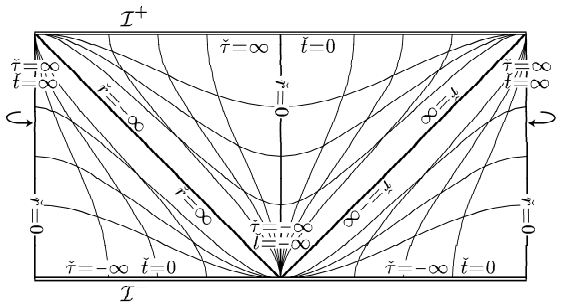

Figure 15: The flat cosmological family, type "∨".

The first flat cosmological coordinate family consists of the *flat cosmological coordinates* $\check\tau$, $\check r$, ϑ, φ and of the *rescaled flat cosmological coordinates* $\check t$, $\check r$, ϑ, φ. Hypersurfaces $\check\tau=$ constant are homogeneous flat spaces and coordinate lines $\check r$, ϑ, $\varphi=$ constant are worldlines of cosmological observers orthogonal to these hypersurfaces. They are geodesic with proper time $\check\tau$, the vector $\partial/\partial\check\tau$ is a conformal Killing vector. The coordinates cover de Sitter spacetime smoothly, except for the past cosmological horizon, $\check r=\check t$, of the north pole where $\check r$, $\check t\to\pm\infty$. The coordinates thus split into two coordinate patches—"above" and "below" the horizon. The domain above the horizon has a cosmological interpretation of an exponentially expanding flat three-space. The rescaled coordinates can be viewed as inertial coordinates in the conformally related Minkowski space $\check M$, cf. Fig. 3; the domain above the horizon corresponds to the "lower half", $\check t<0$, of $\check M$, the domain below corresponds to the "upper half", $\check t>0$.

Metric and relation between coordinates

$$g=\frac{\ell_\Lambda^2}{\check t^2}\left(-\mathrm{d}\check t^{\,2}+\mathrm{d}\check r^2+\check r^2\,\mathrm{d}\omega^2\right), \tag{A18}$$

$$g=-\mathrm{d}\check\tau^2+\exp\!\left(-\check s\,2\,\check\tau/\ell_\Lambda\right)\left(\mathrm{d}\check r^2+\check r^2\,\mathrm{d}\omega^2\right). \tag{A19}$$

$$\check t=\check s\,\ell_\Lambda\exp\!\left(\check s\frac{\check\tau}{\ell_\Lambda}\right), \tag{A20}$$

$$\check s=\operatorname{sign}\check t\,. \tag{A21}$$

The ranges of coordinates are

$$\begin{aligned}&\check\tau\in\mathbb{R}\,,\quad \check t\in\mathbb{R}^-\,,\quad \check r\in\mathbb{R}\quad\text{above the horizon}\,,\\ &\check\tau\in\mathbb{R}\,,\quad \check t\in\mathbb{R}^+\,,\quad \check r\in\mathbb{R}\quad\text{below the horizon}\,,\end{aligned} \tag{A22}$$

with negative values of radial coordinate $\check r$ interpreted as described in Eq. (A2).

Orthonormal tetrad

$$\begin{aligned}\mathrm{e}_{\check t}&=\frac{\partial}{\partial\check\tau}=\frac{\check s\,\check t}{\ell_\Lambda}\frac{\partial}{\partial\check t}\,,\quad \mathrm{e}_{\check r}=\exp\frac{\check s\check\tau}{\ell_\Lambda}\frac{\partial}{\partial\check r}=\frac{\check s\,\check t}{\ell_\Lambda}\frac{\partial}{\partial\check r}\,,\\ \mathrm{e}_\vartheta&=-\frac{\check s}{\check r}\exp\frac{\check s\check\tau}{\ell_\Lambda}\frac{\partial}{\partial\vartheta}=-\frac{1}{\ell_\Lambda}\frac{\check t}{\check r}\frac{\partial}{\partial\vartheta}\,.\end{aligned} \tag{A23}$$

Relation to spherical cosmological family

$$\check t=\frac{-\ell_\Lambda\cosh^{-1}(\tau/\ell_\Lambda)}{\cos\chi+\tanh(\tau/\ell_\Lambda)}\,,\quad \check r=\frac{\ell_\Lambda\cosh^{-1}(\tau/\ell_\Lambda)}{\cos\chi+\tanh(\tau/\ell_\Lambda)}\,. \tag{A24}$$

$$\check t=\frac{\ell_\Lambda\sin\tilde t}{\cos\tilde t-\cos\tilde r}\,,\quad \check r=\frac{\ell_\Lambda\sin\tilde r}{\cos\tilde r-\cos\tilde t}\,. \tag{A25}$$

Relation to flat cosmological family, type "∧"

$$\check t=-\frac{\hat t\,\ell_\Lambda^2}{\hat t^2-\hat r^2}\,,\quad \check r=\frac{\hat r\,\ell_\Lambda^2}{\hat t^2-\hat r^2}\,, \tag{A26}$$

$$\begin{aligned}&\check t\hat r+\hat t\check r=0\,,\quad \hat t\check t+\hat r\check r=-\ell_\Lambda^2\,,\\ &\left(-\hat t^2+\hat r^2\right)\left(-\check t^2+\check r^2\right)=\ell_\Lambda^4\,,\\ &(\hat t+\hat r)(\check t+\check r)=(\hat t-\hat r)(\check t-\check r)=-\ell_\Lambda^2\,.\end{aligned} \tag{A27}$$

Relation to static family in timelike domains **N**, **S**

$$\begin{aligned}\frac{\check t}{\ell_\Lambda}&=-s_{\mathsf{NS}}\frac{\ell_\Lambda}{\sqrt{\ell_\Lambda^2-R^2}}\exp\!\left(-\frac{T}{\ell_\Lambda}\right),\\ \frac{\check r}{\ell_\Lambda}&=\;\;s_{\mathsf{NS}}\frac{R}{\sqrt{\ell_\Lambda^2-R^2}}\exp\!\left(-\frac{T}{\ell_\Lambda}\right),\end{aligned} \tag{A28}$$

$$\begin{aligned}\check t&=-s_{\mathsf{NS}}\,\ell_\Lambda\exp\!\left(-\frac{\bar t}{\ell_\Lambda}\right)\cosh\frac{\bar r}{\ell_\Lambda}\,,\\ \check r&=\;\;s_{\mathsf{NS}}\ell_\Lambda\exp\!\left(-\frac{\bar t}{\ell_\Lambda}\right)\sinh\frac{\bar r}{\ell_\Lambda}\,,\end{aligned} \tag{A29}$$

where $s_{\mathsf{NS}}=+1$ (-1) in domain **N** (**S**), cf. Eq. (A61).

Relation to static family in spacelike domains **F**, **P**

$$\begin{aligned}\frac{\check t}{\ell_\Lambda}&=s_\times\frac{\ell_\Lambda}{\sqrt{R^2-\ell_\Lambda^2}}\exp\!\left(-\frac{T}{\ell_\Lambda}\right),\\ \frac{\check r}{\ell_\Lambda}&=-s_\times\frac{R}{\sqrt{R^2-\ell_\Lambda^2}}\exp\!\left(-\frac{T}{\ell_\Lambda}\right),\end{aligned} \tag{A30}$$

$$\begin{aligned}\check t&=s_\times\ell_\Lambda\exp\!\left(-\frac{\bar t}{\ell_\Lambda}\right)\sinh\frac{\bar r}{\ell_\Lambda}\,,\\ \check r&=-s_\times\ell_\Lambda\exp\!\left(-\frac{\bar t}{\ell_\Lambda}\right)\cosh\frac{\bar r}{\ell_\Lambda}\,,\end{aligned} \tag{A31}$$

where $s_\times=\operatorname{sign}\tilde r\,\operatorname{sign}\cos\tilde t$, cf. Eqs. (A73) and (A74).

Relation to conformally Minkowski coordinates

$$\frac{\check t}{\ell_\Lambda}=-\frac{\ell_\Lambda^2-t^2+r^2}{(\ell_\Lambda+t)^2-r^2}\,,\quad \frac{\check r}{\ell_\Lambda}=\frac{2\,\ell_\Lambda r}{(\ell_\Lambda+t)^2-r^2}\,. \tag{A32}$$

3. The flat cosmological family, type "Λ"

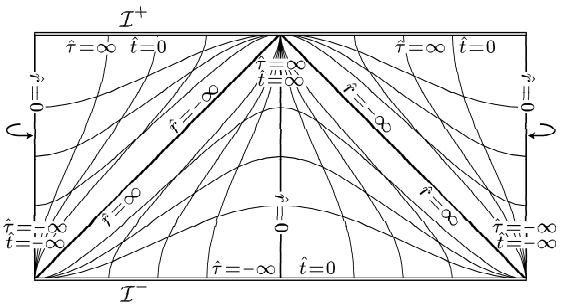

Figure 16: The flat cosmological family, type "Λ".

The second flat cosmological coordinate family consists of the *flat cosmological coordinates* $\hat\tau$, $\hat r$, ϑ, φ and of the *rescaled flat cosmological coordinates* $\hat t$, $\hat r$, ϑ, φ. They can be built analogously to the flat coordinates introduced above, with north and south poles interchanged only. They thus have similar properties: Hypersurfaces $\hat t=$ constant are homogeneous flat three-spaces, coordinate lines $\hat r$, ϑ, $\varphi=$ constant are geodesics with proper time $\hat\tau$, and $\partial/\partial\hat\tau$ is a conformal Killing vector. The coordinates cover de Sitter spacetime everywhere except the future cosmological horizon, $\tilde r=\pi-\tilde t$, of the north pole (i.e., the past horizon of the south pole), and the rescaled coordinates can be viewed as inertial coordinates in the conformally related Minkowski space $\hat M$.

Metric and relation between coordinates

$$g=\frac{\ell_\Lambda^2}{\hat t^2}\left(-\mathrm{d}\hat t^{\,2}+\mathrm{d}\hat r^2+\hat r^2\,\mathrm{d}\omega^2\right), \tag{A33}$$

$$g=-\mathrm{d}\hat\tau^2+\exp\bigl(-\hat s\,2\,\hat\tau/\ell_\Lambda\bigr)\left(\mathrm{d}\hat r^2+\hat r^2\,\mathrm{d}\omega^2\right), \tag{A34}$$

$$\hat t=\hat s\,\ell_\Lambda\exp\Bigl(\hat s\frac{\hat\tau}{\ell_\Lambda}\Bigr), \tag{A35}$$

where

$$\hat s=\operatorname{sign}\hat t\,. \tag{A36}$$

The ranges of coordinates are

$$\begin{aligned}&\hat\tau\in\mathbb{R}\,,\quad \hat t\in\mathbb{R}^-\,,\quad \hat r\in\mathbb{R}\quad\text{above the horizon}\,,\\ &\hat\tau\in\mathbb{R}\,,\quad \hat t\in\mathbb{R}^+\,,\quad \hat r\in\mathbb{R}\quad\text{below the horizon}\,,\end{aligned} \tag{A37}$$

with negative values of radial coordinate $\hat r$ interpreted as described in Eq. (A2).

Orthonormal tetrad

$$\begin{aligned}\mathrm{e}_{\hat t}&=\frac{\partial}{\partial\hat\tau}=\frac{\hat s\,\hat t}{\ell_\Lambda}\frac{\partial}{\partial\hat t}\,,\quad \mathrm{e}_{\hat r}=\exp\frac{\hat s\hat\tau}{\ell_\Lambda}\frac{\partial}{\partial\hat r}=\frac{\hat s\,\hat t}{\ell_\Lambda}\frac{\partial}{\partial\hat r}\,,\\ \mathrm{e}_{\vartheta}&=\frac{\hat s}{\hat r}\exp\frac{\hat s\hat\tau}{\ell_\Lambda}\frac{\partial}{\partial\vartheta}=\frac{1}{\ell_\Lambda}\frac{\hat t}{\hat r}\frac{\partial}{\partial\vartheta}\,.\end{aligned} \tag{A38}$$

Relation to spherical cosmological family

$$\hat t=\frac{\ell_\Lambda\cosh^{-1}(\tau/\ell_\Lambda)}{\cos\chi-\tanh(\tau/\ell_\Lambda)}\,,\quad \hat r=\frac{\ell_\Lambda\cosh^{-1}(\tau/\ell_\Lambda)}{\cos\chi-\tanh(\tau/\ell_\Lambda)}\,. \tag{A39}$$

$$\hat t=\frac{\ell_\Lambda\sin\tilde t}{\cos\tilde t+\cos\tilde r}\,,\quad \hat r=\frac{\ell_\Lambda\sin\tilde r}{\cos\tilde r+\cos\tilde t}\,. \tag{A40}$$

Relation to flat cosmological family, type "Λ"

$$\hat t=-\frac{\check t\,\ell_\Lambda^2}{\check t^2-\check r^2}\,,\quad \hat r=\frac{\check r\,\ell_\Lambda^2}{\check t^2-\check r^2}\,, \tag{A41}$$

$$\begin{gathered}\check t\,\hat r+\hat t\,\check r=0\,,\quad \hat t\,\check t+\hat r\,\check r=-\ell_\Lambda^2\,,\\ \bigl(-\hat t^2+\hat r^2\bigr)\bigl(-\check t^2+\check r^2\bigr)=\ell_\Lambda^4\,,\\ (\hat t+\hat r)(\check t+\check r)=(\hat t-\hat r)(\check t-\check r)=-\ell_\Lambda^2\,.\end{gathered} \tag{A42}$$

Relation to static family in timelike domains **N**, **S**

$$\begin{aligned}\frac{\hat t}{\ell_\Lambda}&=s_{\mathsf{NS}}\frac{\ell_\Lambda}{\sqrt{\ell_\Lambda^2-R^2}}\exp\frac{T}{\ell_\Lambda}\,,\\ \frac{\hat r}{\ell_\Lambda}&=s_{\mathsf{NS}}\frac{R}{\sqrt{\ell_\Lambda^2-R^2}}\exp\frac{T}{\ell_\Lambda}\,,\end{aligned} \tag{A43}$$

$$\begin{aligned}\hat t&=s_{\mathsf{NS}}\,\ell_\Lambda\exp\frac{\bar t}{\ell_\Lambda}\cosh\frac{\bar r}{\ell_\Lambda}\,,\\ \hat r&=s_{\mathsf{NS}}\,\ell_\Lambda\exp\frac{\bar t}{\ell_\Lambda}\sinh\frac{\bar r}{\ell_\Lambda}\,,\end{aligned} \tag{A44}$$

where $s_{\mathsf{NS}}=+1$ (-1) in domain **N** (**S**), cf. Eq. (A61).

Relation to static family in spacelike domains **F**, **P**

$$\begin{aligned}\frac{\hat t}{\ell_\Lambda}&=s_\times\frac{\ell_\Lambda}{\sqrt{R^2-\ell_\Lambda^2}}\exp\frac{T}{\ell_\Lambda}\,,\\ \frac{\hat r}{\ell_\Lambda}&=s_\times\frac{R}{\sqrt{R^2-\ell_\Lambda^2}}\exp\frac{T}{\ell_\Lambda}\,,\end{aligned} \tag{A45}$$

$$\begin{aligned}\hat t&=s_\times\,\ell_\Lambda\exp\frac{\bar t}{\ell_\Lambda}\sinh\frac{\bar r}{\ell_\Lambda}\,,\\ \hat r&=s_\times\,\ell_\Lambda\exp\frac{\bar t}{\ell_\Lambda}\cosh\frac{\bar r}{\ell_\Lambda}\,,\end{aligned} \tag{A46}$$

where $s_\times=\operatorname{sign}\tilde r\,\operatorname{sign}\cos\tilde t$, cf. Eqs. (A73) and (A74).

Relation to conformally Minkowski coordinates

$$\frac{\hat t}{\ell_\Lambda}=\frac{\ell_\Lambda^2-t^2+r^2}{(\ell_\Lambda-t)^2-r^2}\,,\quad \frac{\hat r}{\ell_\Lambda}=\frac{2\,\ell_\Lambda r}{(\ell_\Lambda-t)^2-r^2}\,. \tag{A47}$$

4. The conformally Minkowski family

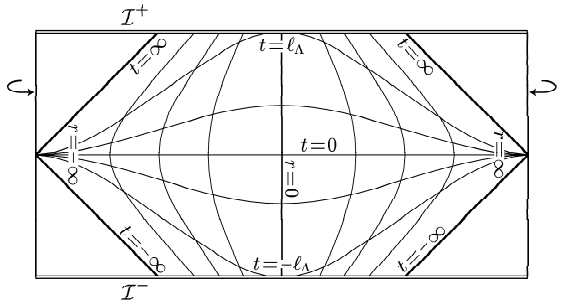

Figure 17: The conformally Minkowski family of coordinates.

The *conformally Minkowski coordinates* t, r, ϑ, φ can be understood as spherical coordinates in the conformally related Minkowski space M. The coordinates do not cover de Sitter spacetime globally—they cover only a region around north pole, see Fig. 17. The boundary of this region is given by the conformal infinity of the Minkowski spacetime. These coordinates are useful for studying the limit $\Lambda \to 0$.

The metric

$$g = \left(\frac{2\,\ell_\Lambda^2}{\ell_\Lambda^2 - t^2 + r^2}\right)^2 \left(-\mathrm{d}t^2 + \mathrm{d}r^2 + r^2\,\mathrm{d}\omega^2\right), \quad \text{(A48)}$$

the ranges of coordinates

$$t \in \mathbb{R}\,, \quad r \in \mathbb{R}\,, \quad \text{such that} \quad t^2 - r^2 < \ell_\Lambda^2\,, \quad \text{(A49)}$$

with negative values of radial coordinate r interpreted as described in Eq. (A2).

Orthonormal tetrad

$$\begin{aligned} \mathrm{e}_t &= \frac{\ell_\Lambda^2 - t^2 + r^2}{2\ell_\Lambda^2}\,\frac{\partial}{\partial t}\,, \\ \mathrm{e}_r &= \frac{\ell_\Lambda^2 - t^2 + r^2}{2\ell_\Lambda^2}\,\frac{\partial}{\partial r}\,, \\ \mathrm{e}_\vartheta &= \frac{\ell_\Lambda^2 - t^2 + r^2}{2\ell_\Lambda^2}\,\frac{1}{r}\,\frac{\partial}{\partial t}\,. \end{aligned} \quad \text{(A50)}$$

Relation to spherical cosmological family

$$\begin{aligned} t &= -\frac{\ell_\Lambda \cos\tilde{t}}{\cos\tilde{r} + \sin\tilde{t}}\,, \\ r &= \frac{\ell_\Lambda \sin\tilde{r}}{\cos\tilde{r} + \sin\tilde{t}}\,. \end{aligned} \quad \text{(A51)}$$

Relation to flat cosmological family

$$\begin{aligned} \frac{t}{\ell_\Lambda} &= -\frac{\ell_\Lambda^2 - \hat{t}^2 + \hat{r}^2}{(\ell_\Lambda + \hat{t})^2 - \hat{r}^2} = \frac{\ell_\Lambda^2 - \check{t}^2 + \check{r}^2}{(\ell_\Lambda - \check{t})^2 - \check{r}^2}\,, \\ \frac{r}{\ell_\Lambda} &= \frac{2\,\ell_\Lambda \hat{r}}{(\ell_\Lambda + \hat{t})^2 - \hat{r}^2} = \frac{2\,\ell_\Lambda \check{r}}{(\ell_\Lambda - \check{t})^2 - \check{r}^2}\,. \end{aligned} \quad \text{(A52)}$$

Relation to hyperbolic cosmological coordinates

$$\begin{aligned} \frac{t}{\ell_\Lambda} &= \tanh\frac{\eta}{2\ell_\Lambda}\,\cosh\frac{\beta}{\ell_\Lambda}\,, \\ \frac{r}{\ell_\Lambda} &= \tanh\frac{\eta}{2\ell_\Lambda}\,\sinh\frac{\beta}{\ell_\Lambda}\,. \end{aligned} \quad \text{(A53)}$$

Relation to static family in timelike domains **N**, **S**

$$\begin{aligned} \frac{t}{\ell_\Lambda} &= \frac{\sinh\frac{\bar{t}}{\ell_\Lambda}}{\cosh\frac{\bar{t}}{\ell_\Lambda} + s_{\mathsf{NS}}\cosh\frac{\bar{r}}{\ell_\Lambda}}\,, \\ \frac{r}{\ell_\Lambda} &= \frac{\sinh\frac{\bar{r}}{\ell_\Lambda}}{\cosh\frac{r}{\ell_\Lambda} + s_{\mathsf{NS}}\cosh\frac{\bar{t}}{\ell_\Lambda}}\,, \end{aligned} \quad \text{(A54)}$$

$$\begin{aligned} \frac{t}{\ell_\Lambda} &= \frac{\sqrt{\ell_\Lambda^2 - R^2}\,\sinh\frac{T}{\ell_\Lambda}}{s_{\mathsf{NS}}\ell_\Lambda + \sqrt{\ell_\Lambda^2 - R^2}\,\cosh\frac{T}{\ell_\Lambda}}\,, \\ \frac{r}{\ell_\Lambda} &= \frac{R}{\ell_\Lambda + s_{\mathsf{NS}}\sqrt{\ell_\Lambda^2 - R^2}\,\cosh\frac{T}{\ell_\Lambda}}\,, \end{aligned} \quad \text{(A55)}$$

where $s_{\mathsf{NS}} = +1$ (-1) in domain **N** (**S**), cf. Eq. (A61).

Relation to static family in spacelike domains **F**, **P**

$$\begin{aligned} \frac{t}{\ell_\Lambda} &= \frac{\cosh\frac{\bar{t}}{\ell_\Lambda}}{\sinh\frac{\bar{t}}{\ell_\Lambda} - s_\times\sinh\frac{\bar{r}}{\ell_\Lambda}}\,, \\ \frac{r}{\ell_\Lambda} &= \frac{\cosh\frac{\bar{r}}{\ell_\Lambda}}{\sinh\frac{\bar{r}}{\ell_\Lambda} - s_\times\cosh\frac{\bar{t}}{\ell_\Lambda}}\,, \end{aligned} \quad \text{(A56)}$$

$$\begin{aligned} \frac{t}{\ell_\Lambda} &= \frac{\sqrt{R^2 - \ell_\Lambda^2}\,\cosh\frac{T}{\ell_\Lambda}}{-s_\times\ell_\Lambda + \sqrt{R^2 - \ell_\Lambda^2}\,\sinh\frac{T}{\ell_\Lambda}}\,, \\ \frac{r}{\ell_\Lambda} &= \frac{R}{\ell_\Lambda - s_\times\sqrt{R^2 - \ell_\Lambda^2}\,\sinh\frac{T}{\ell_\Lambda}}\,, \end{aligned} \quad \text{(A57)}$$

with $s_\times = \operatorname{sign}\tilde{r}\,\operatorname{sign}\cos\tilde{t}$, cf. Eqs. (A73) and (A74).

5. The static family in timelike domains N and S

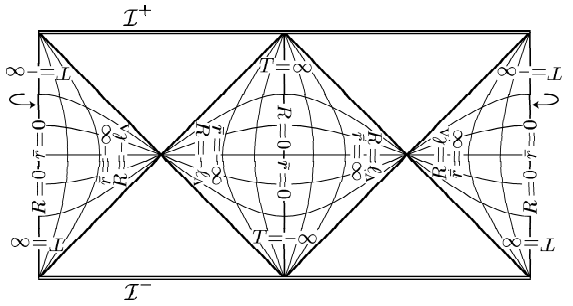

Figure 18: The static family of coordinates, timelike domains.

This family consists of the *static coordinates* T, R, ϑ, φ and the *"tortoidal" static coordinates* $\bar t$, $\bar r$, ϑ, φ. The metric does not depend on time coordinate $T=\bar t$—the coordinates are associated with a Killing vector. Since the Killing vector changes its character, the coordinates do not cover the spacetime smoothly. We first describe the static coordinates in domains **N** and **S**, where the Killing vector is timelike. In domain **N** the orbits of the Killing vector (corresponding to the worldlines of static observers) start and end at the north pole, in domain **S**—at the south pole. They are orthogonal to slices $T=$ constant, each of which consists of two hemispheres (one in domain **N**, the other in **S**) with homogeneous spherical 3-metric. The distances between static observers (measured within these slices) do not change. Since the static observers must overcome first the cosmological contraction and then the expansion, they move with a (uniform) acceleration.

Metric and relation between coordinates

$$g=\cosh^{-2}\frac{\bar r}{\ell_\Lambda}\left(-\mathrm{d}\bar t^2+\mathrm{d}\bar r^2+\ell_\Lambda^2\sinh^2\frac{\bar r}{\ell_\Lambda}\,\mathrm{d}\omega^2\right), \tag{A58}$$

$$g=-\left(1-\frac{R^2}{\ell_\Lambda^2}\right)\mathrm{d}T^2+\left(1-\frac{R^2}{\ell_\Lambda^2}\right)^{-1}\mathrm{d}R^2+R^2\,\mathrm{d}\omega^2, \tag{A59}$$

$$T=\bar t\,, \tag{A60a}$$

$$\exp\frac{\bar r}{\ell_\Lambda}=\sqrt{\frac{\ell_\Lambda+R}{\ell_\Lambda-R}}\,,\quad \sinh\frac{\bar r}{\ell_\Lambda}=\frac{R}{\sqrt{\ell_\Lambda^2-R^2}}\,,$$
$$\tanh\frac{\bar r}{\ell_\Lambda}=\frac{R}{\ell_\Lambda}\,,\qquad \cosh\frac{\bar r}{\ell_\Lambda}=\frac{\ell_\Lambda}{\sqrt{\ell_\Lambda^2-R^2}}\,, \tag{A60b}$$

$$s_{\mathsf{NS}}=\begin{cases}+1 & \text{in domain } \mathbf{N}\,,\\ -1 & \text{in domain } \mathbf{S}\,.\end{cases} \tag{A61}$$

The ranges of coordinates are

$$T\in\mathbb{R}\,,\quad R\in(-\ell_\Lambda,\ell_\Lambda)\,,$$
$$\bar t\in\mathbb{R}\,,\quad \bar r\in\mathbb{R}\,, \tag{A62}$$

with negative values of radial coordinate R and $\bar r$ interpreted as described in Eq. (A2).

Orthonormal tetrad

$$\mathrm{e}_T=\left(1-\frac{R^2}{\ell_\Lambda^2}\right)^{-1/2}\frac{\partial}{\partial T}=\cosh\frac{\bar r}{\ell_\Lambda}\frac{\partial}{\partial\bar t}\,,$$
$$\mathrm{e}_R=\left(1-\frac{R^2}{\ell_\Lambda^2}\right)^{1/2}\frac{\partial}{\partial R}=\cosh^{-1}\frac{\bar r}{\ell_\Lambda}\frac{\partial}{\partial\bar r}\,, \tag{A63}$$
$$\mathrm{e}_\vartheta=\frac{1}{R}\frac{\partial}{\partial\vartheta}=\frac{1}{\ell_\Lambda}\coth\frac{\bar r}{\ell_\Lambda}\frac{\partial}{\partial\vartheta}\,.$$

Relation to spherical cosmological family

$$T=\frac{\ell_\Lambda}{2}\log\frac{\cos\tilde r-\cos\tilde t}{\cos\tilde r+\cos\tilde t}\,,\quad R=\ell_\Lambda\frac{\sin\tilde r}{\sin\tilde t}\,, \tag{A64}$$

$$t=\frac{\ell_\Lambda}{2}\log\Big(\tan\frac{\tilde t+\tilde r}{2}\,\tan\frac{\tilde t-\tilde r}{2}\Big)\,, \tag{A65a}$$

$$\exp\frac{\bar t}{\ell_\Lambda}=\sqrt{\frac{\cos\tilde r-\cos\tilde t}{\cos\tilde r+\cos\tilde t}}\,,\quad \sinh\frac{\bar t}{\ell_\Lambda}=\frac{-s_{\mathsf{NS}}\cos\tilde t}{\sqrt{\cos^2\tilde r-\cos^2\tilde t}}\,,$$
$$\tanh\frac{\bar t}{\ell_\Lambda}=-\frac{\cos\tilde t}{\cos\tilde r}\,,\qquad \cosh\frac{\bar t}{\ell_\Lambda}=\frac{s_{\mathsf{NS}}\cos\tilde r}{\sqrt{\cos^2\tilde r-\cos^2\tilde t}}\,,$$

$$\bar r=\frac{\ell_\Lambda}{2}\log\Big(\tan\frac{\tilde t+\tilde r}{2}\,\cot\frac{\tilde t-\tilde r}{2}\Big)\,, \tag{A65b}$$

$$\exp\frac{\bar r}{\ell_\Lambda}=\sqrt{\frac{\sin\tilde t+\sin\tilde r}{\sin\tilde t-\sin\tilde r}}\,,\quad \sinh\frac{\bar r}{\ell_\Lambda}=\frac{\sin\tilde r}{\sqrt{\sin^2\tilde t-\sin^2\tilde r}}\,,$$
$$\tanh\frac{\bar r}{\ell_\Lambda}=\frac{\sin\tilde r}{\sin\tilde t}\,,\qquad \cosh\frac{\bar r}{\ell_\Lambda}=\frac{\sin\tilde t}{\sqrt{\sin^2\tilde t-\sin^2\tilde r}}\,.$$

Relation to flat cosmological family

$$\bar t=\frac{\ell_\Lambda}{2}\log\frac{\hat t^2-\hat r^2}{\ell_\Lambda^2}=-\frac{\ell_\Lambda}{2}\log\frac{\check t^2-\check r^2}{\ell_\Lambda^2}\,,$$
$$\bar r=\frac{\ell_\Lambda}{2}\log\frac{\hat t+\hat r}{\hat t-\hat r}=\frac{\ell_\Lambda}{2}\log\frac{\check t-\check r}{\check t+\check r}\,, \tag{A66}$$

$$\frac{T}{\ell_\Lambda}=\frac{1}{2}\log\frac{\hat t^2-\hat r^2}{\ell_\Lambda^2}=-\frac{1}{2}\log\frac{\check t^2-\check r^2}{\ell_\Lambda^2}\,,$$
$$\frac{R}{\ell_\Lambda}=\frac{\hat r}{\hat t}=-\frac{\check r}{\check t}\,. \tag{A67}$$

Relation to conformally Minkowski coordinates

$$\tanh\frac{T}{\ell_\Lambda}=\frac{2\,\ell_\Lambda t}{\ell_\Lambda^2+t^2-r^2}\,,\quad \frac{R}{\ell_\Lambda}=\frac{2\,\ell_\Lambda r}{\ell_\Lambda^2+r^2-t^2}\,, \tag{A68}$$

$$\bar t=\frac{\ell_\Lambda}{2}\log\frac{(\ell_\Lambda+t)^2-r^2}{(\ell_\Lambda-t)^2-r^2}\,,\quad \bar r=\frac{\ell_\Lambda}{2}\log\frac{(\ell_\Lambda+r)^2-t^2}{(\ell_\Lambda-r)^2-t^2}\,. \tag{A69}$$

6. The static family in spacelike domains F and P

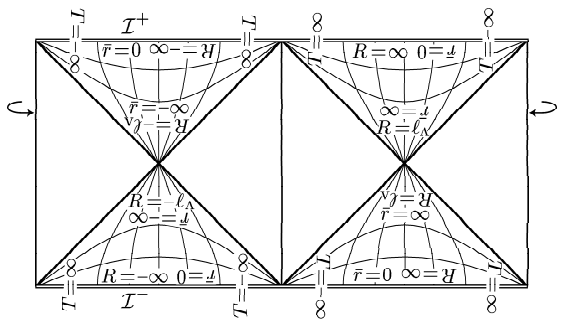

Figure 19: The static family of coordinates, spacelike domains.

Here we describe the *static coordinates* T, R, ϑ, φ and the *"tortoidal" static coordinates* $\bar t$, $\bar r$, ϑ, φ from the preceding section in domains **F** and **S** where the Killing vector is spacelike. These "non-static" domains extend up to infinity, namely, domain **F** up to $\mathcal{I}^+$, domain **P** up to $\mathcal{I}^-$. The orbits of the Killing vector start at the south pole and end at the north pole in **F**, and they point in opposite direction in **P**. The motion along them could thus be characterized as a "translation" from one pole to the other. The Lorentzian hypersurfaces $T=$ constant are homogeneous spaces with positive curvature, i.e., 3-dimensional de Sitter spacetimes.

Metric and relation between coordinates

$$g=\sinh^{-2}\frac{\bar r}{\ell_\Lambda}\left(-\mathrm{d}\bar r^2+\mathrm{d}\bar l^2+\ell_\Lambda^2\cosh^2\frac{\bar r}{\ell_\Lambda}\,\mathrm{d}\omega^2\right), \tag{A70}$$

$$g=-\Big(1-\frac{R^2}{\ell_\Lambda^2}\Big)\,\mathrm{d}T^2+\Big(1-\frac{R^2}{\ell_\Lambda^2}\Big)^{-1}\mathrm{d}R^2+R^2\,\mathrm{d}\omega^2, \tag{A71}$$

$$T=\bar t\,, \tag{A72a}$$

$$\exp\frac{\bar r}{\ell_\Lambda}=\sqrt{\frac{R+\ell_\Lambda}{R-\ell_\Lambda}}\,,\quad \left|\sinh\frac{\bar r}{\ell_\Lambda}\right|=\frac{\ell_\Lambda}{\sqrt{R^2-\ell_\Lambda^2}}\,,$$
$$\tanh\frac{\bar r}{\ell_\Lambda}=\frac{\ell_\Lambda}{R}\,,\qquad \cosh\frac{\bar r}{\ell_\Lambda}=\frac{|R|}{\sqrt{R^2-\ell_\Lambda^2}}\,. \tag{A72b}$$

The signature factors $s_{\mathcal{I}}$ and $s_\times$ are defined as

$$s_{\mathcal{I}}=\begin{cases}+1 & \text{in domain } \mathbf{F}\,,\\ -1 & \text{in domain } \mathbf{P}\,,\end{cases} \tag{A73}$$

and

$$s_\times=-s_\tau\,\operatorname{sign}\tilde r\,. \tag{A74}$$

The coordinates ranges are

$$T\in\mathbb{R}\,,\quad |R|\in(\ell_\Lambda,\infty)\,,$$
$$\bar t\in\mathbb{R}\,,\quad \bar r\in\mathbb{R}\,, \tag{A75}$$

with negative values of radial coordinate R and $\bar r$ interpreted as described in Eq. (A2).

Orthonormal tetrad

$$\mathrm{e}_T=\Big(\frac{R^2}{\ell_\Lambda^2}-1\Big)^{-1/2}\frac{\partial}{\partial T}=\left|\sinh\frac{\bar r}{\ell_\Lambda}\right|\frac{\partial}{\partial\bar t}\,,$$
$$\mathrm{e}_R=\Big(\frac{R^2}{\ell_\Lambda^2}-1\Big)^{1/2}\frac{\partial}{\partial R}=-\left|\sinh^{-1}\frac{\bar r}{\ell_\Lambda}\right|\frac{\partial}{\partial\bar r}\,, \tag{A76}$$
$$\mathrm{e}_\vartheta=\frac{1}{R}\frac{\partial}{\partial\vartheta}=\frac{1}{\ell_\Lambda}\left|\tanh\frac{\bar r}{\ell_\Lambda}\right|\frac{\partial}{\partial\vartheta}\,.$$

Relation to spherical cosmological family

$$T=\frac{\ell_\Lambda}{2}\log\frac{\cos\tilde t-\cos\tilde r}{\cos\tilde t+\cos\tilde r}\,,\quad R=\ell_\Lambda\frac{\sin\tilde r}{\sin\tilde t}\,, \tag{A77}$$

$$\bar t=\frac{\ell_\Lambda}{2}\log\Big(-\tan\frac{\tilde t+\tilde r}{2}\,\tan\frac{\tilde t-\tilde r}{2}\Big)\,, \tag{A78a}$$

$$\exp\frac{\bar t}{\ell_\Lambda}=\sqrt{\frac{\cos\tilde t-\cos\tilde r}{\cos\tilde t+\cos\tilde r}}\,,\quad \sinh\frac{\bar t}{\ell_\Lambda}=\frac{s_{\mathcal{I}}\cos\tilde r}{\sqrt{\cos^2\tilde t-\cos^2\tilde r}}\,,$$
$$\tanh\frac{\bar t}{\ell_\Lambda}=-\frac{\cos\tilde r}{\cos\tilde t}\,,\qquad \cosh\frac{\bar t}{\ell_\Lambda}=\frac{-s_{\mathcal{I}}\cos\tilde t}{\sqrt{\cos^2\tilde t-\cos^2\tilde r}}\,,$$

$$\bar r=\frac{\ell_\Lambda}{2}\log\Big(-\tan\frac{\tilde t+\tilde r}{2}\,\cot\frac{\tilde t-\tilde r}{2}\Big)\,, \tag{A78b}$$

$$\exp\frac{\bar r}{\ell_\Lambda}=\sqrt{\frac{\sin\tilde r+\sin\tilde t}{\sin\tilde r-\sin\tilde t}}\,,\quad \left|\sinh\frac{\bar r}{\ell_\Lambda}\right|=\frac{\sin\tilde t}{\sqrt{\sin^2\tilde r-\sin^2\tilde t}}\,,$$
$$\tanh\frac{\bar r}{\ell_\Lambda}=\frac{\sin\tilde t}{\sin\tilde r}\,,\qquad \cosh\frac{\bar r}{\ell_\Lambda}=\frac{|\sin\tilde r|}{\sqrt{\sin^2\tilde r-\sin^2\tilde t}}\,.$$

Relation to flat cosmological family

$$\bar t=\frac{\ell_\Lambda}{2}\log\frac{-\hat t^2+\hat r^2}{\ell_\Lambda^2}=-\frac{\ell_\Lambda}{2}\log\frac{-\check t^2+\check r^2}{\ell_\Lambda^2}\,,$$
$$\bar r=\frac{\ell_\Lambda}{2}\log\frac{\hat r+\hat t}{\hat r-\hat t}=\frac{\ell_\Lambda}{2}\log\frac{\check r-\check t}{\check r+\check t}\,, \tag{A79}$$

$$\frac{T}{\ell_\Lambda}=\frac{1}{2}\log\frac{-\hat t^2+\hat r^2}{\ell_\Lambda^2}=-\frac{1}{2}\log\frac{-\check t^2+\check r^2}{\ell_\Lambda^2}\,,$$
$$\frac{R}{\ell_\Lambda}=\frac{\hat r}{\hat t}=-\frac{\check r}{\check t}\,. \tag{A80}$$

Relation to conformally Minkowski coordinates

$$\coth\frac{T}{\ell_\Lambda}=\frac{2\,\ell_\Lambda t}{\ell_\Lambda^2+t^2-r^2}\,,\quad \frac{R}{\ell_\Lambda}=\frac{2\,\ell_\Lambda r}{\ell_\Lambda^2+r^2-t^2}\,, \tag{A81}$$

$$\bar t=\frac{\ell_\Lambda}{2}\log\Big(-\frac{(\ell_\Lambda+t)^2-r^2}{(\ell_\Lambda-t)^2-r^2}\Big)\,,$$
$$\bar r=\frac{\ell_\Lambda}{2}\log\Big(-\frac{(\ell_\Lambda+r)^2-t^2}{(\ell_\Lambda-r)^2-t^2}\Big)\,, \tag{A82}$$

7. The hyperbolic cosmological family

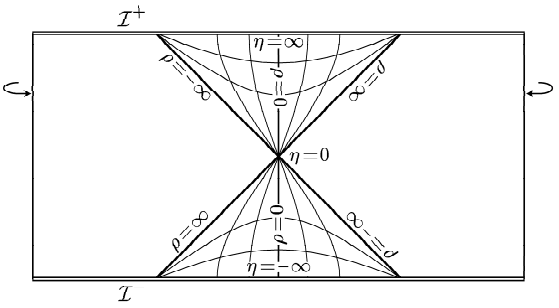

Figure 20: The hyperbolic cosmological family of coordinates.

The third type of cosmological coordinates are the hyperbolic cosmological coordinates η, ρ, ϑ, φ. The hypersurfaces $\eta =$ constant are homogeneous spaces with negative curvature, coordinate lines $\rho, \vartheta, \varphi =$ constant correspond to the worldlines of cosmological observers orthogonal to these slices, and the vector $\partial/\partial\eta$ is a timelike conformal Killing vector. The coordinates cover spacetime only partially—they can be introduced in two disconnected domains near the north pole, namely, in the past of the event $\tilde{t} = \pi/2$, $\tilde{r} = 0$ (where $\eta < 0$), and in the future of this event (where $\eta > 0$).

The metric

$$g = -\mathrm{d}\eta^2 + \sinh^2\tfrac{\eta}{\ell_\Lambda}\left(\mathrm{d}\rho^2 + \ell_\Lambda^2 \sinh^2\tfrac{\rho}{\ell_\Lambda}\,\mathrm{d}\omega^2\right), \qquad \text{(A83)}$$

The ranges of coordinates and the signature factor $s_\mathcal{I}$ are

$$\begin{aligned} &\eta \in \mathbb{R}^+\,, \quad \rho \in \mathbb{R}\,, \quad s_\mathcal{I} = +1 \quad \text{in the future patch}\,,\\ &\eta \in \mathbb{R}^-\,, \quad \rho \in \mathbb{R}\,, \quad s_\mathcal{I} = -1 \quad \text{in the past patch}\,, \end{aligned} \qquad \text{(A84)}$$

with negative values of radial coordinate ρ interpreted as described in Eq. (A2).

Orthonormal tetrad

$$\begin{aligned} \mathrm{e}_\eta &= \frac{\partial}{\partial\eta}\,, \quad \mathrm{e}_\rho = \sinh^{-1}\frac{\eta}{\ell_\Lambda}\,\frac{\partial}{\partial\rho}\,,\\ \mathrm{e}_\vartheta &= \sinh^{-1}\frac{\eta}{\ell_\Lambda}\,\sinh^{-1}\frac{\rho}{\ell_\Lambda}\,\frac{\partial}{\partial\rho}\,. \end{aligned} \qquad \text{(A85)}$$

Relation to spherical cosmological family

$$\tanh\frac{\eta}{2\ell_\Lambda} = s_\mathcal{I}\sqrt{\frac{\cos\tilde{r}-\sin\tilde{t}}{\cos\tilde{r}+\sin\tilde{t}}}\,, \quad \tanh\frac{\rho}{\ell_\Lambda} = -\frac{\sin\tilde{r}}{\cos\tilde{t}}\,. \qquad \text{(A86)}$$

Relation to conformally Minkowski coordinates

$$\tanh\frac{\eta}{2\ell_\Lambda} = s_\mathcal{I}\frac{\sqrt{t^2-r^2}}{\ell_\Lambda}\,, \quad \tanh\frac{\rho}{\ell_\Lambda} = \frac{r}{t}\,. \qquad \text{(A87)}$$

8. The accelerated coordinate family

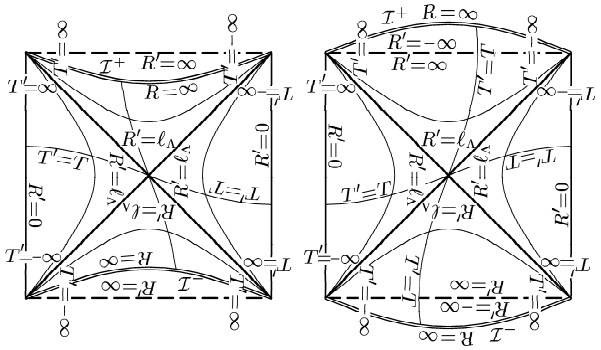

Figure 21: The accelerated family of coordinates.

This family consists of the *accelerated coordinates* T', R', ϑ', φ, and the *C-metric-like* coordinates τ, υ, ξ, φ (τ being different from τ of the standard coordinates). Contrary to the previous cases the accelerated coordinates are centered on uniformly accelerate origins: $R' = 0$ corresponds to two worldlines with acceleration $|a_\mathrm{o}|$. The transformation relations to the systems introduced above mix these three coordinates in general.

The accelerated coordinates are closely related to the static system. Their time coordinates coincide, $T'=T$, and coordinate lines $R', \vartheta', \varphi =$ constant are the same as those with $R, \vartheta, \varphi =$ constant. Both coordinate systems are identical for $a_\mathrm{o} = 0$. Sections $T, T', \varphi =$ constant with $R, R' < \ell_\Lambda$ have geometry of 2-sphere with parallels and meridians given by the coordinate lines of the static coordinates R, ϑ. The lines of coordinates R', ϑ' are the deformed version of static ones, their poles are shifted along meridian $\vartheta = 0$ towards each other, cf. Fig. 11.

Two conformal diagrams of sections $\vartheta', \varphi =$ constant ($\vartheta' < \pi/2$ on the right, $\vartheta' > \pi/2$ on the left), adapted to the accelerated coordinates, are depicted in Fig. 21. The shape of the diagram varies with different values of ϑ'; indeed, the position of infinity is given by $R' = -\ell_\Lambda^2/R_\mathrm{o}\,\cos^{-1}\vartheta'$. See also Fig. 10 for sections $\vartheta' = 0, \pi$.

The C-metric-like coordinates rescale only the values of the accelerated coordinates and regularize the coordinate singularity $R' = \pm\infty$. de Sitter metric in these coordinates is a zero-mass limit of the C-metric (the metric describing accelerated black holes; see, e.g., [28, 29]).

Finally, we use four parameters a_o, α_o, R_o, b_o to parametrize the acceleration.They are related as follows:

$$\begin{aligned} \sinh\alpha_\mathrm{o} &= \frac{R_o}{\sqrt{\ell_\Lambda^2 - R_\mathrm{o}^2}} = \frac{b_\mathrm{o}^2-\ell_\Lambda^2}{2\,\ell_\Lambda b_\mathrm{o}} = \quad -a_\mathrm{o}\ell_\Lambda\,,\\ \cosh\alpha_\mathrm{o} &= \frac{\ell_\Lambda}{\sqrt{\ell_\Lambda^2 - R_\mathrm{o}^2}} = \frac{b_\mathrm{o}^2+\ell_\Lambda^2}{2\,\ell_\Lambda b_\mathrm{o}} = \sqrt{1+a_\mathrm{o}^2\ell_\Lambda^2}\,,\\ \tanh\alpha_o &= \frac{R_\mathrm{o}}{\ell_\Lambda} = \frac{b_\mathrm{o}^2-\ell_\Lambda^2}{b_\mathrm{o}^2+\ell_\Lambda^2} = -\frac{a_\mathrm{o}\ell_\Lambda}{\sqrt{1+a_\mathrm{o}^2\ell_\Lambda^2}}\,,\\ \exp\alpha_\mathrm{o} &= \sqrt{\frac{\ell_\Lambda+R_\mathrm{o}}{\ell_\Lambda-R_\mathrm{o}}} = \frac{b_\mathrm{o}}{\ell_\Lambda} = \sqrt{1+a_\mathrm{o}^2\ell_\Lambda^2} - a_\mathrm{o}\ell_\Lambda\,. \end{aligned} \qquad \text{(A88)}$$

33 Fields of accelerated sources: Born in de Sitter

J. Math. Phys. **46**, 102504 (2005) [reformatted]

Metric and relation between coordinates

$$g=\Omega^2\left[-\left(1-\frac{R'^2}{\ell_\Lambda^2}\right)\mathrm{d}T'^2+\left(1-\frac{R'^2}{\ell_\Lambda^2}\right)^{-1}\mathrm{d}R'^2+R'^2\,\mathrm{d}\omega^{2\prime}\right], \tag{A89}$$

$$g=\mathfrak{r}^2\left[-(\upsilon^2-1)\,\mathrm{d}\tau^2+\frac{1}{\upsilon^2-1}\,\mathrm{d}\upsilon^2+\frac{1}{1-\xi^2}\,\mathrm{d}\xi^2+(1-\xi^2)\,\mathrm{d}\varphi^2\right], \tag{A90}$$

where

$$\mathrm{d}\omega^{2\prime}=\left(\mathrm{d}\vartheta'^2+\sin^2\vartheta'\,\mathrm{d}\varphi^2\right), \tag{A91}$$

$$\Omega=\frac{\sqrt{1-R_\mathrm{o}^2/\ell_\Lambda^2}}{1+(R'R_\mathrm{o}/\ell_\Lambda^2)\cos\vartheta'}=\frac{\mathfrak{r}}{R'}=\frac{\mathfrak{r}\,\upsilon}{\ell_\Lambda}, \tag{A92}$$

$$\mathfrak{r}=\frac{\ell_\Lambda}{\upsilon\cosh\alpha_\mathrm{o}-\xi\sinh\alpha_\mathrm{o}}=\Omega\,R'=\Omega\,\frac{\ell_\Lambda}{\upsilon}. \tag{A93}$$

$$\tau=\frac{T'}{\ell_\Lambda}\qquad \upsilon=\frac{\ell_\Lambda}{R'}\qquad \xi=-\cos\vartheta', \tag{A94}$$

Orthonormal tetrad

$$\begin{aligned}
\mathrm{e}_{T'}&=|\Omega|^{-1}\left(1-\frac{R'^2}{\ell_\Lambda^2}\right)^{-1/2}\frac{\partial}{\partial T'}=\frac{1}{\mathfrak{r}\sqrt{\upsilon^2-1}}\,\frac{\partial}{\partial T'},\\
\mathrm{e}_{R'}&=|\Omega|^{-1}\left(1-\frac{R'^2}{\ell_\Lambda^2}\right)^{1/2}\frac{\partial}{\partial R'}=\frac{1}{\mathfrak{r}}\sqrt{\upsilon^2-1}\,\frac{\partial}{\partial R'},\\
\mathrm{e}_{\vartheta'}&=\frac{1}{\Omega R'}\,\frac{\partial}{\partial\vartheta'}=\frac{1}{\mathfrak{r}}\,\frac{\partial}{\partial\vartheta'}.
\end{aligned} \tag{A95}$$

Relation to static coordinates

$$T=T'$$

$$\begin{aligned}
R\cos\vartheta&=\frac{R'\cos\vartheta'+R_\mathrm{o}}{1+(R'R_\mathrm{o}/\ell_\Lambda^2)\cos\vartheta'},\\
R\sin\vartheta&=\frac{R'\sin\vartheta'\sqrt{1-\frac{R_\mathrm{o}^2}{\ell_\Lambda^2}}}{1+(R'R_\mathrm{o}/\ell_\Lambda^2)\cos\vartheta'},\\
\frac{R^2}{\ell_\Lambda^2}&=1-\frac{\left(1-R'^2/\ell_\Lambda^2\right)\left(1-R_\mathrm{o}^2/\ell_\Lambda^2\right)}{\left(1+(R'R_\mathrm{o}/\ell_\Lambda^2)\cos\vartheta'\right)^2},\\
\tan\vartheta&=\frac{R'\sin\vartheta'\sqrt{1-\frac{R_\mathrm{o}^2}{\ell_\Lambda^2}}}{R'\cos\vartheta'+R_\mathrm{o}}.
\end{aligned} \tag{A96}$$

The inverse relations have the same form with T, R, ϑ and T', R', ϑ' interchanged only and α_o replaced by $-\alpha_\mathrm{o}$.

$$\Omega=\frac{\sqrt{1-R_\mathrm{o}^2/\ell_\Lambda^2}}{1+(R'R_\mathrm{o}/\ell_\Lambda^2)\cos\vartheta'}=\frac{1-(RR_\mathrm{o}/\ell_\Lambda^2)\cos\vartheta}{\sqrt{1-R_\mathrm{o}^2/\ell_\Lambda^2}}, \tag{A97}$$

$$\left(1+\frac{R'R_\mathrm{o}}{\ell_\Lambda^2}\cos\vartheta'\right)\left(1-\frac{RR_\mathrm{o}}{\ell_\Lambda^2}\cos\vartheta\right)=1-\frac{R_\mathrm{o}^2}{\ell_\Lambda^2}, \tag{A98}$$

$$\frac{1-R'^2/\ell_\Lambda^2}{1+(R'R_\mathrm{o}/\ell_\Lambda^2)\cos\vartheta'}=\frac{1-R^2/\ell_\Lambda^2}{1-(RR_\mathrm{o}/\ell_\Lambda^2)\cos\vartheta}. \tag{A99}$$

Relation to Robinson-Trautman coordinates

$$\begin{aligned}
T'&=\mathfrak{u}\cosh\alpha_\mathrm{o}-\frac{\ell_\Lambda}{2}\log\left|\frac{\ell_\Lambda-\mathfrak{r}\,(\sinh\alpha_\mathrm{o}\cos\vartheta'+\cosh\alpha_\mathrm{o})}{\ell_\Lambda-\mathfrak{r}\,(\sinh\alpha_\mathrm{o}\cos\vartheta'-\cosh\alpha_\mathrm{o})}\right|,\\
R'&=\frac{\mathfrak{r}\cosh\alpha_\mathrm{o}}{1-(\mathfrak{r}/\ell_\Lambda)\sinh\alpha_\mathrm{o}\cos\vartheta'},\\
\left|\tan\frac{\vartheta'}{2}\right|&=\exp\left(\psi-\frac{\mathfrak{u}}{\ell_\Lambda}\sinh\alpha_\mathrm{o}\right),
\end{aligned} \tag{A100}$$

$$\begin{aligned}
\tau&=\frac{\mathfrak{u}}{\ell_\Lambda}\cosh\alpha_\mathrm{o}-\frac{1}{2}\log\left|\frac{\ell_\Lambda-\mathfrak{r}\,(\sinh\alpha_\mathrm{o}\cos\vartheta'+\cosh\alpha_\mathrm{o})}{\ell_\Lambda-\mathfrak{r}\,(\sinh\alpha_\mathrm{o}\cos\vartheta'-\cosh\alpha_\mathrm{o})}\right|,\\
\upsilon&=\frac{\ell_\Lambda}{\mathfrak{r}\cosh\alpha_\mathrm{o}}-\tanh\alpha_\mathrm{o}\cos\vartheta',\\
\xi&=\tanh\left(\psi-\frac{\mathfrak{u}}{\ell_\Lambda}\sinh\alpha_\mathrm{o}\right),
\end{aligned} \tag{A101}$$

where $\cos\vartheta'=-\xi$ is given in terms of the Robinson-Trautman coordinates by the last equation.

Relation to flat cosmological family

If we introduce the spherical coordinates $\check{t}'$, $\check{r}'$, ϑ', φ boosted with respect to the flat cosmological coordinates $\check{t}$, $\check{r}$, ϑ, φ by a boost α_o (in the sense of Minkowski space $\check{M}$), we find that the accelerated coordinates T', R' are related to $\check{t}'$, $\check{r}'$ in exactly the same way as the static coordinates T, R are related to the coordinates $\check{t}$, $\check{r}$. The boost $\check{t}'=\check{t}\cosh\alpha_\mathrm{o}+\check{z}\sinh\alpha_\mathrm{o}$, $\check{x}'=\check{x}$, $\check{y}'=\check{y}$, $\check{z}'=\check{t}\sinh\alpha_\mathrm{o}+\check{z}\cosh\alpha_\mathrm{o}$, rewritten in the spherical coordinates $\check{r}'\cos\vartheta'=\check{z}'$, $\check{r}'\sin\vartheta'=\sqrt{\check{x}'^2+\check{y}'^2}$, reads

$$\begin{aligned}
\check{t}'&=\check{t}\cosh\alpha_\mathrm{o}+\check{r}\cos\vartheta\sinh\alpha_\mathrm{o},\\
\check{r}'\cos\vartheta'&=\check{t}\sinh\alpha_\mathrm{o}+\check{r}\cos\vartheta\cosh\alpha_\mathrm{o},\\
\check{r}'\sin\vartheta'&=\check{r}\sin\vartheta,
\end{aligned} \tag{A102}$$

and relations analogous to Eqs. (A67) and (A80) are:

$$T'=-\frac{\ell_\Lambda}{2}\log\left|\frac{\check{t}'^2-\check{r}'^2}{\ell_\Lambda^2}\right|,\quad R'=-\ell_\Lambda\frac{\check{r}'}{\check{t}'}. \tag{A103}$$

Similarly, the formulas relating the accelerated coordinates to the coordinates $\hat{t}$, $\hat{r}$, ϑ are:

$$\begin{aligned}
\hat{t}'&=\hat{t}\cosh\alpha_\mathrm{o}-\hat{r}\cos\vartheta\sinh\alpha_\mathrm{o},\\
\hat{r}'\cos\vartheta'&=-\hat{t}\sinh\alpha_\mathrm{o}+\hat{r}\cos\vartheta\cosh\alpha_\mathrm{o},\\
\hat{r}'\sin\vartheta'&=\hat{r}\sin\vartheta,
\end{aligned} \tag{A104}$$

$$T'=\frac{\ell_\Lambda}{2}\log\left|\frac{\hat{t}'^2-\hat{r}'^2}{\ell_\Lambda^2}\right|,\quad R'=\ell_\Lambda\frac{\hat{r}'}{\hat{t}'}. \tag{A105}$$

The conformal factor takes the form

$$\Omega=\frac{\check{t}'}{\check{t}}=\frac{\hat{t}'}{\hat{t}}=\cosh\alpha_\mathrm{o}-\frac{R}{\ell_\Lambda}\sinh\alpha_\mathrm{o}\cos\vartheta. \tag{A106}$$

9. The Robinson-Trautman coordinates

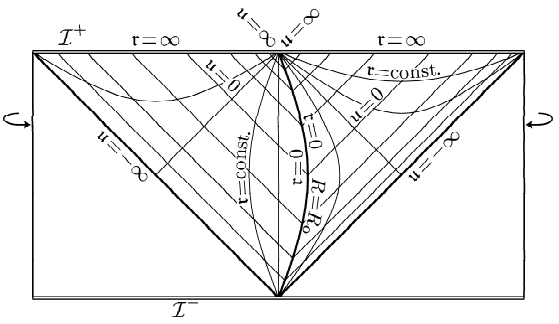

Figure 22: The Robinson-Trautman coordinates.

In the *Robinson-Trautman coordinates* $\mathfrak{u}$, $\mathfrak{r}$, ψ, φ (or in their complex version $\mathfrak{u}$, $\mathfrak{r}$, ζ, $\bar\zeta$), de Sitter metric takes the standard Robinson-Trautman form [50]. The coordinate $\mathfrak{u}$ is null, the "radial" coordinate $\mathfrak{r}$ is an affine parameter along coordinate lines $\mathfrak{u}, \psi, \varphi$ = constant. These lines are null geodesics generating light cones with vertices at the origin $\mathfrak{r}=0$. The coordinates ψ, φ (or ζ, $\bar\zeta$) are angular coordinates, however, they are not functions of the accelerated angular coordinates ϑ', φ only (cf. Eq. (A112)). Because ϑ', φ have a clearer geometrical meaning, we list some formulas also in the mixed coordinate system $\mathfrak{u}$, $\mathfrak{r}$, ϑ', φ.

The origin $\mathfrak{r}=0$ of the Robinson-Trautman coordinates is centered on the worldline of the uniformly accelerated observer moving with the acceleration $|a_o| = |\ell_\Lambda^{-1} \sinh\alpha_o|$. The coordinates are thus closely related to the accelerated coordinates.

The coordinates $\mathfrak{u}$, $\mathfrak{r}$, ψ, φ do not cover the whole spacetime smoothly. They can be introduced smoothly in the future of the north pole, or in the past of the south pole. At the boundary of these two domains, $\mathfrak{u} \to \pm\infty$.

Metric and relation between coordinates

$$g = -H\,\mathrm{d}\mathfrak{u}^2 - \mathrm{d}\mathfrak{u}\vee\mathrm{d}\mathfrak{r} + \frac{\mathfrak{r}^2}{P^2}\left(\mathrm{d}\psi^2+\mathrm{d}\varphi^2\right), \tag{A107}$$

$$g = -H\,\mathrm{d}\mathfrak{u}^2 - \mathrm{d}\mathfrak{u}\vee\mathrm{d}\mathfrak{r} + \frac{\mathfrak{r}^2}{P^2}\,\mathrm{d}\zeta\vee\mathrm{d}\bar\zeta, \tag{A108}$$

$$\begin{aligned} g = &-\cosh^2\alpha_o\,\frac{\mathfrak{r}^2}{\ell_\Lambda^2}\,(v^2-1)\,\mathrm{d}\mathfrak{u}^2 - \mathrm{d}\mathfrak{u}\vee\mathrm{d}\mathfrak{r} \\ &+ \cosh\alpha_o\,\frac{\mathfrak{r}^2}{\ell_\Lambda}\,\sin\vartheta'\,\mathrm{d}\mathfrak{u}\vee\mathrm{d}\vartheta' + \mathfrak{r}^2\left(\mathrm{d}\vartheta'^2+\sin^2\vartheta'\,\mathrm{d}\varphi^2\right), \end{aligned} \tag{A109}$$

$$\begin{aligned} H &= -\frac{\mathfrak{r}^2}{\ell_\Lambda^2} + 2\,\frac{\mathfrak{r}}{\ell_\Lambda}\,\sinh\alpha_o\,\tanh\Big(\psi - \frac{\mathfrak{u}}{\ell_\Lambda}\,\sinh\alpha_o\Big) + 1 \\ &= -\frac{\mathfrak{r}^2}{\ell_\Lambda^2} - 2\,\frac{\mathfrak{r}}{\ell_\Lambda}\,\sinh\alpha_o\,\cos\vartheta' + 1\,, \end{aligned} \tag{A110}$$

$$P = \cosh\Big(\psi - \frac{\mathfrak{u}}{\ell_\Lambda}\,\sinh\alpha_o\Big) = \frac{1}{\sin\vartheta'}\,. \tag{A111}$$

$$\begin{aligned} \psi &= \frac{\mathfrak{u}}{\ell_\Lambda}\,\sinh\alpha_o + \log\left|\tan\frac{\vartheta'}{2}\right|\,, \\ \left|\tan\frac{\vartheta'}{2}\right| &= \exp\Big(\psi - \frac{\mathfrak{u}}{\ell_\Lambda}\,\sinh\alpha_o\Big)\,, \end{aligned} \tag{A112}$$

$$\begin{aligned} \zeta &= \frac{1}{\sqrt2}(\psi - i\varphi)\,, \quad \psi = \frac{1}{\sqrt2}(\zeta+\bar\zeta)\,, \\ \bar\zeta &= \frac{1}{\sqrt2}(\psi + i\varphi)\,, \quad \varphi = \frac{i}{\sqrt2}(\zeta-\bar\zeta)\,. \end{aligned} \tag{A113}$$

Null tetrad

Since the Robinson-Trautman coordinates are closely related to the congruence of null geodesics, it is convenient to introduce the null tetrad which is parallelly transported along these geodesics $\mathfrak{u}, \psi, \varphi$ = constant:

$$\begin{aligned} \mathrm{k}_{\mathrm{RT}} &= \frac{1}{\sqrt2}\frac{\partial}{\partial\mathfrak{r}}\,, \quad \mathrm{l}_{\mathrm{RT}} = -\frac{1}{\sqrt2}H\,\frac{\partial}{\partial\mathfrak{r}} + \sqrt2\,\frac{\partial}{\partial\mathfrak{u}}\,, \\ \mathrm{m}_{\mathrm{RT}} &= \frac{1}{\sqrt2}\,\frac{P}{\mathfrak{r}}\left(\frac{\partial}{\partial\psi} - i\frac{\partial}{\partial\varphi}\right), \\ \bar{\mathrm{m}}_{\mathrm{RT}} &= \frac{1}{\sqrt2}\,\frac{P}{\mathfrak{r}}\left(\frac{\partial}{\partial\psi} + i\frac{\partial}{\partial\varphi}\right). \end{aligned} \tag{A114}$$

Relation to accelerated coordinate family

$$\begin{aligned} \mathfrak{r} &= \frac{R'\sqrt{1-R_o^2/\ell_\Lambda^2}}{1+(R'R_o/\ell_\Lambda^2)\cos\vartheta'}\,, \\ \mathfrak{u} &= \sqrt{1-\frac{R_o^2}{\ell_\Lambda^2}}\left(T' + \frac{\ell_\Lambda}{2}\log\left|\frac{R'-\ell_\Lambda}{R'+\ell_\Lambda}\right|\right), \\ \psi &= \frac{R_o}{\ell_\Lambda}\left(\frac{T'}{\ell_\Lambda} + \frac{1}{2}\log\left|\frac{R'-\ell_\Lambda}{R'+\ell_\Lambda}\right|\right) + \log\left|\tan\frac{\vartheta'}{2}\right|, \end{aligned} \tag{A115}$$

$$\begin{aligned} \mathfrak{r} &= \frac{\ell_\Lambda}{v\cosh\alpha_o - \xi\sinh\alpha_o}\,, \\ \mathfrak{u} &= \frac{\ell_\Lambda}{\cosh\alpha_o}\left(\tau + \frac{1}{2}\log\left|\frac{1-v}{1+v}\right|\right), \\ \psi &= \tanh\alpha_o\left(\tau + \frac{1}{2}\log\left|\frac{1-v}{1+v}\right|\right) + \frac{1}{2}\log\left|\frac{1+\xi}{1-\xi}\right|\,. \end{aligned} \tag{A116}$$

Relation to static family

$$\mathfrak{r} = \frac{\ell_\Lambda}{\sqrt{1-R_o^2/\ell_\Lambda^2}}\left[\left(1-\frac{RR_o}{\ell_\Lambda^2}\cos\vartheta\right)^2 - \left(1-\frac{R^2}{\ell_\Lambda^2}\right)\left(1-\frac{R_o^2}{\ell_\Lambda^2}\right)\right]^{\frac12}, \tag{A117}$$

$$\mathfrak{r}\sin\vartheta' = R\sin\vartheta\,, \quad \mathfrak{r}\cos\vartheta' = \frac{R\cos\vartheta - R_o}{\sqrt{1-R_o^2/\ell_\Lambda^2}}\,. \tag{A118}$$

$$\begin{aligned} R\sin\vartheta &= \mathfrak{r}\sin\vartheta'\,, \\ R\cos\vartheta &= \mathfrak{r}\cos\vartheta'\sqrt{1-R_o^2/\ell_\Lambda^2} + R_o\,. \end{aligned} \tag{A119}$$

10. The null family

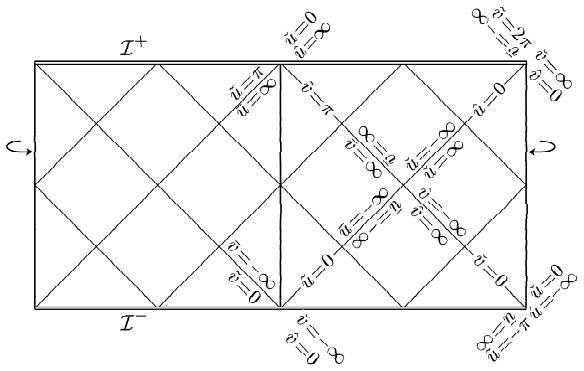

Figure 23: The null family of coordinates

Finally, we return back to the coordinate systems which employ standard coordinates ϑ, φ. Time and radial coordinates can be transformed into two null coordinates. Such null coordinates can be associated with most coordinate families introduced above. Coordinates $\tilde{u}$, $\tilde{v}$ are related to the standard coordinates; $\check{u}$, $\check{v}$ and $\hat{u}$, $\hat{v}$ to the flat cosmological coordinates; u, v to the conformally Minkowski; and $\bar{u}$, $\bar{v}$ to the static coordinates. Coordinate vectors $\{\partial/\partial\tilde{u}, \partial/\partial\tilde{v}\}$, $\{\partial/\partial\check{u}, \partial/\partial\check{v}\}$, etc., are the pairs of independent null vectors in the radial 2-slices $\vartheta, \varphi =$ constant. We do not allow the radial coordinate to be negative in the definitions of null coordinates because this would interchange the meaning of u and v. The null coordinates are thus drawn in the right half of Fig. 23 only.

Metric and relation to other coordinates

$$g = \frac{\ell_\Lambda^2}{1-\cos(\tilde{u}+\tilde{v})}\Big(-\mathrm{d}\tilde{u}\vee\mathrm{d}\tilde{v} + \big(1-\cos(\tilde{u}-\tilde{v})\big)\,\mathrm{d}\omega^2\Big)\,, \tag{A120}$$

$$g = \frac{\ell_\Lambda^2}{(\hat{u}+\hat{v})^2}\left(-2\,\mathrm{d}\hat{u}\vee\mathrm{d}\hat{v} + (\hat{u}-\hat{v})^2\,\mathrm{d}\omega^2\right), \tag{A121}$$

$$g = \frac{\ell_\Lambda^2}{(\check{u}+\check{v})^2}\left(-2\,\mathrm{d}\check{u}\vee\mathrm{d}\check{v} + (\check{u}-\check{v})^2\,\mathrm{d}\omega^2\right), \tag{A122}$$

$$g = \left(\frac{\ell_\Lambda^2}{\ell_\Lambda^2-uv}\right)^2\left(-2\,\mathrm{d}u\vee\mathrm{d}v + (u-v)^2\,\mathrm{d}\omega^2\right), \tag{A123}$$

$$g = \left(\exp\frac{\bar{u}}{\ell_\Lambda} + \exp\frac{\bar{v}}{\ell_\Lambda}\right)^{-2} \tag{A124}$$
$$\times\left(-2\exp\frac{\bar{u}+\bar{v}}{\ell_\Lambda}\,\mathrm{d}\bar{u}\vee\mathrm{d}\bar{v} + \ell_\Lambda^2\left(\exp\frac{\bar{u}}{\ell_\Lambda} - \exp\frac{\bar{v}}{\ell_\Lambda}\right)^2\mathrm{d}\omega^2\right).$$

The relation of time and radial coordinates $\overset{*}{t}$, $\overset{*}{r}$ to the corresponding null coordinates $\overset{*}{u}$, $\overset{*}{v}$ is given by usual formulas:

$$\begin{aligned} \overset{*}{t} &= \tfrac{1}{2}(\overset{*}{v}+\overset{*}{u})\,, \quad \overset{*}{u} = \overset{*}{t}-\overset{*}{r}\,, \\ \overset{*}{r} &= \tfrac{1}{2}(\overset{*}{v}-\overset{*}{u})\,, \quad \overset{*}{v} = \overset{*}{t}+\overset{*}{r}\,. \end{aligned} \tag{A125}$$

Here $\{\overset{*}{t}, \overset{*}{r}\}$ stands for $\{\tilde{t}, \tilde{r}\}$, $\{\check{t}, \check{r}\}$, $\{\hat{t}, \hat{r}\}$, $\{t, r\}$, and $\{\bar{t}, r\}$ respectively; similarly with $\{\overset{*}{u}, \overset{*}{v}\}$.

Relation between null coordinates

The coordinates $\hat{u}$, $\hat{v}$, u, v, and $\check{u}$, $\check{v}$ can be viewed as null coordinates in the conformally related Minkowski spaces $\hat{M}$, M, and $\check{M}$; these are shifted with respect to each other by $\frac{\pi}{2}$ in the direction of the conformally Einstein time coordinate $\tilde{t}$, or associated null coordinates:

$$\begin{aligned} \frac{\hat{u}}{\ell_\Lambda} &= \tan\frac{\tilde{u}}{2}\,, & \frac{\hat{v}}{\ell_\Lambda} &= \tan\frac{\tilde{v}}{2}\,, \\ \frac{u}{\ell_\Lambda} &= \tan\Big(\frac{\tilde{u}}{2}-\frac{\pi}{4}\Big)\,, & \frac{v}{\ell_\Lambda} &= \tan\Big(\frac{\tilde{v}}{2}-\frac{\pi}{4}\Big)\,, \\ \frac{\check{u}}{\ell_\Lambda} &= \tan\Big(\frac{\tilde{u}}{2}-\frac{\pi}{2}\Big)\,, & \frac{\check{v}}{\ell_\Lambda} &= \tan\Big(\frac{\tilde{v}}{2}-\frac{\pi}{2}\Big)\,. \end{aligned} \tag{A126}$$

The remaining coordinates $\bar{u}$, $\bar{v}$ are related to the conformally Einstein null coordinates $\tilde{u}$, $\tilde{v}$ by the "compactification transformation":

$$\tan\frac{\tilde{u}}{2} = s_u\exp\frac{\bar{u}}{\ell_\Lambda}\,, \quad \tan\frac{\tilde{v}}{2} = s_v\exp\frac{\bar{v}}{\ell_\Lambda}\,. \tag{A127}$$

Here the sign factors s_u and s_v are given by

$$s_u = \operatorname{sign}\tan\frac{\tilde{u}}{2}\,, \quad s_v = \operatorname{sign}\tan\frac{\tilde{v}}{2}\,. \tag{A128}$$

Relations (A126), (A127) between null coordinates can also be rewritten as follows:

$$\tan\frac{\tilde{u}}{2} = s_u\exp\frac{\bar{u}}{\ell_\Lambda} = \frac{\hat{u}}{\ell_\Lambda} = -\frac{\ell_\Lambda}{\check{u}} = \frac{\ell_\Lambda+u}{\ell_\Lambda-u}\,, \tag{A129}$$

$$\tan\bar{u} = -s_u\sinh^{-1}\frac{\bar{u}}{\ell_\Lambda} = \frac{2\hat{u}\ell_\Lambda}{\ell_\Lambda^2-\hat{u}^2} = \frac{2\check{u}\ell_\Lambda}{\ell_\Lambda^2-\check{u}^2} = \frac{u^2-\ell_\Lambda^2}{2u\ell_\Lambda}\,,$$

$$\sin\tilde{u} = s_u\cosh^{-1}\frac{\bar{u}}{\ell_\Lambda} = \frac{2\hat{u}\ell_\Lambda}{\ell_\Lambda^2+\hat{u}^2} = \frac{-2\check{u}\ell_\Lambda}{\ell_\Lambda^2+\check{u}^2} = \frac{\ell_\Lambda^2-u^2}{\ell_\Lambda^2+u^2}\,,$$

$$\cos\tilde{u} = -\tanh\frac{\bar{u}}{\ell_\Lambda} = \frac{\ell_\Lambda^2-\hat{u}^2}{\ell_\Lambda^2+\hat{u}^2} = \frac{\hat{u}^2-\ell_\Lambda^2}{\hat{u}^2+\ell_\Lambda^2} = \frac{-2u\ell_\Lambda}{\ell_\Lambda^2+u^2}\,,$$

$$\frac{\hat{u}}{\ell_\Lambda} = \tan\frac{\tilde{u}}{2} = s_u\exp\frac{\bar{u}}{\ell_\Lambda} = -\frac{\ell_\Lambda}{\check{u}} = \frac{\ell_\Lambda+u}{\ell_\Lambda-u}\,, \tag{A130}$$

$$-\frac{\check{u}}{\ell_\Lambda} = \cot\frac{\tilde{u}}{2} = s_u\exp\Big(-\frac{\bar{u}}{\ell_\Lambda}\Big) = \frac{\ell_\Lambda}{\hat{u}} = \frac{\ell_\Lambda-u}{\ell_\Lambda+u}\,, \tag{A131}$$

$$\begin{aligned} \frac{u}{\ell_\Lambda} &= -\frac{1-\sin\tilde{u}}{\cos\tilde{u}} = -\frac{\cos\tilde{u}}{1+\sin\tilde{u}} \\ &= \Big(\tanh\frac{\bar{u}}{2\ell_\Lambda}\Big)^{s_u} = \frac{\hat{u}-\ell_\Lambda}{\hat{u}+\ell_\Lambda} = \frac{\ell_\Lambda+\check{u}}{\ell_\Lambda-\check{u}}\,, \end{aligned} \tag{A132}$$

$$\begin{aligned} \frac{u}{\ell_\Lambda} &= \log\left|\tan\frac{\tilde{u}}{2}\right| = \log\left|\frac{\hat{u}}{\ell_\Lambda}\right| = \log\left|\frac{\ell_\Lambda}{\check{u}}\right| \\ &= \log\left|\frac{\ell_\Lambda+u}{\ell_\Lambda-u}\right| = 2\operatorname{arctanh}\Big(\frac{u}{\ell_\Lambda}\Big)^{s_u}\,. \end{aligned} \tag{A133}$$

$$\hat{u}\check{u} = -\ell_\Lambda^2\,, \quad \frac{\hat{u}}{\ell_\Lambda} + \frac{\ell_\Lambda}{\check{u}} = 0\,. \tag{A134}$$

The same relations hold for coordinates v.

[1] M. Born, Ann. Phys. (Leipzig) **30**, 1 (1909).
[2] V. L. Ginzburg, Soviet Physics Uspekhi **12**, 565 (1970).
[3] V. L. Ginzburg, *Theoretical Physics and Astrophysics* (Pergamon Press, Oxford, 1979).
[4] V. L. Ginzburg, *Applications of Electrodynamics in Theoretical Physics and Astrophysics* (Gordon and Breach, New York, 1989).
[5] H. Bondi, Proc. R. Soc. Lond., Ser A **376**, 493 (1981).
[6] D. G. Boulware, Ann. Phys. (N.Y.) **124**, 169 (1980).
[7] R. Peierls, in *Surprises in Theoretical Physics* (Princeton University Press, Princeton, 1979).
[8] W. Thirring, *A Course in Mathematical Physics II: Classical Field Theory* (Springer, New York, Wien, 1986).
[9] L. Herrera, Il Nuov. Cim. **78B**, 156 (1983).
[10] A. Harpaz and N. Soker, Gen. Rel. Grav. **30**, 1217 (1998).
[11] A. Gupta and T. Padmanabhan, Phys. Rev. D **57**, 7241 (1998).
[12] A. Shariati and M. Khorrami, Found. Phys. Lett. **12**, 427 (1999).
[13] J. Bičák and R. Muschall, Wiss. Zeits. der Friedrich-Schiller-Universität Jena **39**, 1827 (1990).
[14] E. Eriksen and Ø. Grøn, Ann. Phys. (N.Y.) **286**, 320 (2000).
[15] E. Eriksen and Ø. Grøn, Ann. Phys. (N.Y.) **286**, 343 (2000).
[16] E. Eriksen and Ø. Grøn, Ann. Phys. (N.Y.) **286**, 373 (2000).
[17] J. Bičák and B. G. Schmidt, Phys. Rev. D **40**, 1827 (1989). See in particular Section IVB and Appendix A there, but beware that the conventions we are using here are different to comply with the conventions used in [24, 25].
[18] J. Bičák, *Selected Solutions of Einstein's Field Equations: Their Role in General Relativity and Astrophysics*, in *Einstein's Field Equations and Their Physical Implications (Selected Essays in Honour of Jürgen Ehlers)*, edited by B. G. Schmidt, Lecture Notes in Physics **540** (Springer, Berlin, 2000), pp. 1–126, gr-qc/0004016.
[19] J. Bičák and P. Krtouš, in *Recent Developments in Gravity (Proceedings of 10th Greek Relativity Meeting, Chalkidiki, May 2002)*, edited by K. D. Kokkotas and N. Stergioulas (World Scientific, Singapore, 2003), pp. 3–25, gr-qc/0303091.
[20] V. Pravda and A. Pravdová, Czech. J. Phys. **50**, 333 (2000), gr-qc/0003067.
[21] R. Penrose, Proc. R. Soc. Lond., Ser A **284**, 159 (1965).
[22] K. Maeda, in *Proceedings of the Fifth M. Grossman Meeting on General Relativity, Perth, Australia, 1988*, edited by D. G. Blair, M. J. Buckingham, and R. Ruffini (World Scientific, Singapore, 1989).
[23] A. D. Rendall, Ann. H. Poincaré **5**, 1041 (2004), gr-qc/0312020.
[24] J. Bičák and P. Krtouš, Phys. Rev. D **64**, 124020 (2001), gr-qc/0107078.
[25] J. Bičák and P. Krtouš, Phys. Rev. Lett. **88**, 211101 (2002), gr-qc/0207010.
[26] P. Krtouš, J. Podolský, and J. Bičák, Phys. Rev. Lett. **91**, 061101 (2003), gr-qc/0308004.
[27] P. Krtouš and J. Podolský, Phys. Rev. D **68**, 024005 (2003), gr-qc/0301110.
[28] J. Podolský, M. Ortaggio, and P. Krtouš, Phys. Rev. D **68**, 124004 (2003), gr-qc/0307108. The coordinates τ, v, ξ, φ differ from the "standard" coordinates t, x, y, φ of [59] (where only case $\Lambda = 0$ is considered) by a simple rescaling $t = \tau \tanh \alpha_o$, $y = v \coth \alpha_o$, and $x = -\xi$. The conformal factor is then given by $\mathfrak{r} = \big(A(x+y)\big)^{-1}$.
[29] O. J. C. Dias and J. P. S. Lemos, Phys. Rev. D **67**, 084018 (2003), hep-th/0301046.
[30] O. J. C. Dias and J. P. S. Lemos, Phys. Rev. D **67**, 064001 (2003), hep-th/0210065.
[31] P. Krtouš and J. Podolský, Phys. Rev. D **69**, 084023 (2004), gr-qc/0310089.
[32] A. Einstein, Jahrb. d. Radioaktivität u. Elektronik **4**, 411 (1907).
[33] A. Einstein, Jahrb. d. Radioaktivität u. Elektronik **5**, 98 (1908).
[34] F. Rohrlich, *Classical Charged Particles* (Addison-Wesley, Reading, 1965).
[35] E. L. Hill, Phys. Rev. **67**, 358 (1945).
[36] E. L. Hill, Phys. Rev. **72**, 143 (1947).
[37] T. Fulton and F. Rohrlich, Ann. Phys. (N.Y.) **9**, 499 (1960).
[38] C. Leibovitz and A. Peres, Ann. Phys. (N.Y.) **25**, 400 (1963).
[39] H. Bondi and T. Gold, Proc. R. Soc. Lond., Ser A **229**, 416 (1955).
[40] P. Krtouš, *Physical fields of uniformly accelerated sources*, Master thesis (Charles University, Prague, Czechoslovakia, 1991), in Czech.
[41] H. J. Schmidt, Fortschr. d. Physik **41**, 179 (1993).
[42] E. Eriksen and Ø. Grøn, Int. J. Mod. Phys. **D4**, 115 (1995).
[43] W. Rindler, *Relativity: special, general, and cosmological* (Oxford University Press, Oxford, 2001).
[44] R. Penrose, in *Battelle Recontres*, edited by B. DeWitt and J. A. Wheeler (Benjamin, New York, 1968), pp. 121–235.
[45] R. Penrose and W. Rindler, *Spinors and Space-Time* (Cambridge University Press, Cambridge, England, 1984, 1986).
[46] S. W. Hawking and G. F. R. Ellis, *The Large Scale Structure of Space-Time* (Cambridge University Press, Cambridge, England, 1973).
[47] R. M. Wald, *General Relativity* (The University of Chicago Press, Chicago and London, 1984).
[48] M. Cvetič, S. Griffies, and H. H. Soleng, Phys. Rev. D **48**, 2613 (1993).
[49] J. Podolský and J. B. Griffiths, Phys. Rev. D **63**, 024006 (2001), gr-qc/0010109.
[50] H. Stephani, D. Kramer, M. Maccallum, C. Hoenselaers, and E. Herlt, *Exact Solutions of Einstein's Field Equations, Second Edition* (Cambridge University Press, Cambridge, England, 2003).
[51] H. Bondi, M. G. J. van der Burg, and A. W. K. Metzner, Proc. R. Soc. Lond., Ser A **269**, 21 (1962).
[52] For the detailed derivation, see [24], Section V. The field (6.1), with $\mathcal{Q}$ given by (6.3), is the field (5.2) in [24]. Notice, however, the following changes in notation: the quantities α, β_o and $\mathcal{X}$ in [24] are, in the present paper, denoted by ℓ_Λ, α_o and $\sqrt{\ell_\Lambda^2 - R_o^2}\,\mathcal{Q}$ with R_o again given

by Eq. (4.20). Since the field (6.1) (as well as the electromagnetic field (6.4)) can be written as a symmetric combination of retarded and advanced effects from both charges, we called it "symmetric" in [24] and used a subscript "sym". Such a notation was necessary in Ref. [24], but is not used here.

[53] J. Bičák, Proc. R. Soc. Lond., Ser A **302**, 201 (1968).
[54] W. Pauli, *Theory of Relativity* (Pergamon Press, London, 1958).
[55] J. D. Jackson, *Classical Electrodynamics* (J. Wiley, New York, London, 1975).
[56] J. N. Goldberg and R. P. Kerr, J. Math. Phys. **5**, 172 (1964).
[57] A. G. Riess et al (20 authors), Ap. J. **607**, 665 (2004).
[58] R. P. Woodard, in *Deserfest: A celebration of the life and works of Stanley Deser* edited by J. T. Liu and K. Stelle (World Scientific, New Jersey, London, Singapore, 2005), gr-qc/0408002.
[59] W. Kinnersley and M. Walker, Phys. Rev. D **2**, 1359 (1970).

Published by Institute of Physics Publishing for SISSA
Received: *August 3, 2005*
Revised: *November 4, 2005*
Accepted: *November 7, 2005*
Published: *December 1, 2005*

Ultrarelativistic boost of spinning black rings

Marcello Ortaggio,* Jiří Podolský and Pavel Krtouš

Institute of Theoretical Physics, Faculty of Mathematics and Physics
Charles University in Prague
V Holešovičkách 2, 180 00 Prague 8, Czech Republic
E-mail: marcello.ortaggio@comune.re.it, Jiri.Podolsky@mff.cuni.cz, Pavel.Krtous@mff.cuni.cz

Abstract: We study the $D = 5$ Emparan-Reall spinning black ring under an ultrarelativistic boost along an arbitrary direction. We analytically determine the resulting shock *pp*-wave, in particular for boosts along axes orthogonal and parallel to the plane of rotation. The solution becomes physically more interesting and simpler if one enforces equilibrium between the forces on the ring. We also comment on the ultrarelativistic limit of recently found supersymmetric black rings with two independent angular momenta. Essential distinct features with respect to the boosted Myers-Perry black holes are pointed out.

Keywords: Black Holes, Classical Theories of Gravity.

*Also at INFN, Rome, Italy.

Contents

1. Introduction

Shock *pp*-wave geometries describe the spacetime surrounding very fast moving objects, and are thus relevant to the study of planckian scattering [1]. They are also of interest in string theory, since strings may be exactly solved in such backgrounds [2, 3]. The prototype of shock wave solutions is the Aichelburg-Sexl spacetime, which represents the gravitational field of a massless point particle. It was originally obtained by boosting the Schwarzschild black hole to the speed of light, while rescaling the mass to zero in an appropriate way [4]. According to recent extra-dimension scenarios, the fundamental Planck scale of (higher dimensional) gravity could be as low as a few TeV. This has stimulated renewed interest in the study of gravitational effects in high energy collisions, especially in view of the possible observation of microscopic black holes at near future colliders [5 – 8] (see, e.g., [9] for a recent review and for further references). It has been shown that closed trapped surfaces do indeed form in the ultrarelativistic collision of Aichelburg-Sexl point particles [10, 11] and of finite-size beams [12], which can more accurately model string-size effects. Nevertheless, it is desirable to understand how other effects could influence high energy scattering. A first step in this direction is to investigate more general shock wave solutions of higher dimensional gravity, which can naturally be obtained by applying the boosting technique of [4] to black hole spacetimes. This has been done in any $D \geq 4$ for static black holes with

electric charge [13] or immersed in an external magnetic field [14, 15]. The ultrarelativistic limit of the Myers-Perry rotating black holes [16] has been studied in [17] (for the case of one non-vanishing spin). However, a striking feature of General Relativity in $D > 4$ is the non-uniqueness of the spherical black holes of [16]. In five-dimensional vacuum gravity, there exist also asymptotically flat rotating black rings with an event horizon of topology $S^1 \times S^2$ [18]. In the present contribution, we aim at studying the gravitational field generated by such rings in the Aichelburg-Sexl limit. As we will see in detail, this results in shock waves generated by extended lightlike sources (with a characteristic length-scale) which are remnants of the ring singularity of the original spacetime [18]. Our recent results on boosted non-rotating black rings [19] will be recovered as a special subcase. In general, the presence of spin is important because it allows black rings to be in equilibrium [18] without introducing "unphysical" membranes via conical singularities [20]. This will be reflected also in the shock geometry resulting from the boost. From a supergravity and string theory point of view, it is remarkable that supersymmetric black rings have been also constructed [21 – 24]. We will conclude this article with a brief comment on the boost of such solutions. In the Appendix, we compare our results with those obtained for the ultrarelativistic limit of Myers-Perry black holes [17] in $D = 5$.

2. The black ring solution

In this section we briefly summarize the basic properties of the black ring, referring to [18, 25] for details. In the coordinates of [25],[1] the line element reads

$$\begin{aligned} \mathrm{d}s^2 = & -\frac{F(y)}{F(x)}\left(\mathrm{d}t + C(\nu,\lambda)L\frac{1+y}{F(y)}\mathrm{d}\psi\right)^2 + \\ & + \frac{L^2}{(x-y)^2}F(x)\left[-\frac{G(y)}{F(y)}\mathrm{d}\psi^2 - \frac{\mathrm{d}y^2}{G(y)} + \frac{\mathrm{d}x^2}{G(x)} + \frac{G(x)}{F(x)}\mathrm{d}\phi^2\right], \end{aligned} \tag{2.1}$$

where

$$F(\zeta) = \frac{1+\lambda\zeta}{1-\lambda}, \qquad G(\zeta) = (1-\zeta^2)\frac{1+\nu\zeta}{1-\nu}, \qquad C(\nu,\lambda) = \sqrt{\frac{\lambda(\lambda-\nu)(1+\lambda)}{(1-\nu)(1-\lambda)^3}}. \tag{2.2}$$

The dimensionless parameters λ and ν satisfy $0 \leq \nu \leq \lambda < 1$, and for $\lambda = 0 = \nu$ the spacetime (2.1) is flat. The constant $L > 0$ represents a length related to the radius of the "central circle" of the ring. For a physical interpretation of the spacetime (2.1) we take $y \in (-\infty, -1]$, $x \in [-1, +1]$ (see a discussion in [26] for other possible choices) and ψ and ϕ as periodic angular coordinates (see below). Surfaces of constant y have topology $S^1 \times S^2$. The coordinate ψ runs along the S^1 factor, whereas (x, ϕ) parametrize S^2 (see [20, 25, 22] for illustrative pictures). Within the above range, y parametrizes "distances" from the ring circle. At $y \to -\infty$ the spacetime has a inner spacelike curvature singularity, $y = -1/\nu$

[1] Up to simple constant rescalings of $F(\zeta)$, $G(\zeta)$, $C(\lambda,\nu)$, ψ and ϕ, cf. eqs. (2.2) and (2.4) with the corresponding ones in [25]. In addition, multiply our L^2 by $(1-\nu)/(1-\lambda)$ to obtain the parameter used in [25].

is a horizon and $y=-1/\lambda$ an ergosurface, both with topology $S^1\times S^2$. The black ring solution (2.1) is asymptotically flat near spatial infinity $x,y\to-1$, where it tends to Minkowski spacetime in the form

$$\mathrm{d}s_0^2=-\mathrm{d}t^2+\frac{L^2}{(x-y)^2}\left[(y^2-1)\mathrm{d}\psi^2+\frac{\mathrm{d}y^2}{y^2-1}+\frac{\mathrm{d}x^2}{1-x^2}+(1-x^2)\mathrm{d}\phi^2\right]. \tag{2.3}$$

To avoid conical singularities at the axes $x=-1$ and $y=-1$, the angular coordinates must have the standard periodicity

$$\Delta\phi=2\pi=\Delta\psi\,. \tag{2.4}$$

Centrifugal repulsion and gravitational self-attraction of the ring are in balance if conical singularities are absent also at $x=+1$, which requires

$$\lambda=\frac{2\nu}{1+\nu^2}\,. \tag{2.5}$$

When this equilibrium condition holds, the metric (2.1) is a vacuum solution (of $D=5$ General Relativity) everywhere. With different choices (e.g., in the static limit $\nu=\lambda$ [20]), the conical singularity at $x=+1$ describes a disk-shaped membrane inside the ring.

The mass, angular momentum and angular velocity (at the horizon) of the black ring are

$$M=\frac{3\pi L^2}{4}\frac{\lambda}{1-\lambda}\,,\qquad J=\frac{\pi L^3}{2}\sqrt{\frac{\lambda(\lambda-\nu)(1+\lambda)}{(1-\nu)(1-\lambda)^3}}\,,\qquad \Omega=\frac{1}{L}\sqrt{\frac{(\lambda-\nu)(1-\lambda)}{\lambda(1+\lambda)(1-\nu)}}\,. \tag{2.6}$$

The algebraic type of the Weyl tensor of the ring spacetime is I_i [26].

3. General boost

For our purposes, it is convenient to decompose the line element (2.1) as

$$\mathrm{d}s^2=\mathrm{d}s_0^2+\Delta\,, \tag{3.1}$$

in which $\mathrm{d}s_0^2$ is Minkowski spacetime (2.3) and

$$\begin{aligned}\Delta=\;&\lambda\frac{x-y}{1+\lambda x}\mathrm{d}t^2-2(1-\lambda)C(\lambda,\nu)L\frac{1+y}{1+\lambda x}\mathrm{d}t\,\mathrm{d}\psi\\
&+\frac{\lambda-\nu}{1-\nu}\frac{L^2}{1+\lambda y}\left[-\lambda\frac{1+\lambda}{1-\lambda}\frac{(1+y)^2}{1+\lambda x}+\frac{y^2-1}{x-y}\right]\mathrm{d}\psi^2+\\
&+\frac{L^2}{(x-y)^2}\left[\nu\frac{x+1}{1-\nu}(y^2-1)\mathrm{d}\psi^2+\frac{\lambda(1-\nu)(x-y)+(\lambda-\nu)(1+y)}{(1-\lambda)(1+\nu y)}\frac{\mathrm{d}y^2}{y^2-1}+\right.\\
&\left.+\frac{\lambda-\nu}{1-\lambda}\frac{\mathrm{d}x^2}{(1-x)(1+\nu x)}+\nu\frac{x+1}{1-\nu}(1-x^2)\mathrm{d}\phi^2\right].\end{aligned} \tag{3.2}$$

The above splitting is such that near infinity ($x,y\to-1$) one has $\mathrm{d}s^2\to\mathrm{d}s_0^2$, while Δ becomes "negligible" (in the sense of the "background" metric $\mathrm{d}s_0^2$). This enables us to define a notion of Lorentz boost using the symmetries of the asymptotic minkowskian

background $\mathrm{d}s_0^2$. Cartesian coordinates will visualize it most naturally. These can be introduced in two steps. First, we replace the coordinates (y, x) with new coordinates (ξ, η) via the substitution

$$y = -\frac{\xi^2 + \eta^2 + L^2}{\Sigma}\,, \qquad x = -\frac{\xi^2 + \eta^2 - L^2}{\Sigma}\,, \tag{3.3}$$

where

$$\Sigma = \sqrt{(\eta^2 + \xi^2 - L^2)^2 + 4L^2\eta^2}\,. \tag{3.4}$$

The flat term $\mathrm{d}s_0^2$ in eq. (3.1) now takes the form $\mathrm{d}s_0^2 = -\mathrm{d}t^2 + \mathrm{d}\eta^2 + \eta^2\mathrm{d}\phi^2 + \mathrm{d}\xi^2 + \xi^2\mathrm{d}\psi^2$. Then, cartesian coordinates adapted to the Killing vectors ∂_ϕ and ∂_ψ are given by

$$x_1 = \eta\cos\phi\,, \qquad x_2 = \eta\sin\phi\,, \qquad y_1 = \xi\cos\psi\,, \qquad y_2 = \xi\sin\psi\,, \tag{3.5}$$

so that $\eta = \sqrt{x_1^2 + x_2^2}$, $\xi = \sqrt{y_1^2 + y_2^2}$, and $\mathrm{d}s_0^2 = -\mathrm{d}t^2 + \mathrm{d}x_1^2 + \mathrm{d}x_2^2 + \mathrm{d}y_1^2 + \mathrm{d}y_2^2$. This enables us to study a boost along a general direction. Since the original spacetime (2.1) is symmetric under (separate) rotations in the (x_1, x_2) and (y_1, y_2) planes, such a direction can be specified by a single parameter α, namely introducing rotated axes z_1 and z_2

$$x_1 = z_1\cos\alpha - z_2\sin\alpha\,, \qquad y_1 = z_1\sin\alpha + z_2\cos\alpha\,. \tag{3.6}$$

Defining now suitable double null coordinates (u', v') by

$$t = \frac{-u' + v'}{\sqrt{2}}\,, \qquad z_1 = \frac{u' + v'}{\sqrt{2}}\,, \tag{3.7}$$

a Lorentz boost along z_1 takes the simple form

$$u' = \epsilon^{-1}u\,, \qquad v' = \epsilon v\,. \tag{3.8}$$

The parameter $\epsilon > 0$ is related to the standard Lorentz factor via $\gamma = (\epsilon + \epsilon^{-1})/2$. We are interested in "ultrarelativistic" boosts to the speed of light, i.e. in taking the limit $\epsilon \to 0$ in the transformation (3.8). While $\epsilon \to 0$, we will rescale the mass as $M = \gamma^{-1}p_M \approx 2\epsilon p_M$ [4], which physically means that the total energy remains finite in the limit ($p_M > 0$ is a constant). Moreover, during the ultrarelativistic limit we wish to keep the angular velocity Ω finite (a similar condition was imposed in [17]), and to allow for the possibility of black rings in equilibrium (when the condition (2.5) holds). From eq. (2.6), these requirements imply the rescalings[2]

$$\lambda = \epsilon p_\lambda\,, \qquad \nu = \epsilon p_\nu\,, \tag{3.9}$$

where $p_\lambda = 8p_M/(3\pi L^2)$ and p_ν is another positive constant such that $p_\lambda \geq p_\nu$. In terms of these parameters, for $\epsilon \to 0$ the equilibrium condition (2.5) becomes

$$p_\lambda = 2p_\nu\,. \tag{3.10}$$

[2]This appears to be physically the most interesting and simple choice. See Footnote 3 for a subtler, slightly more general comment.

Values $p_\nu \le p_\lambda < 2p_\nu$ correspond to black rings (2.1) which are "underspinning" before the boost (and therefore balanced by a membrane of negative energy density), values $p_\lambda > 2p_\nu$ to "overspinning" black rings (with a membrane of positive energy density). Notice, however, that under the limit $\epsilon \to 0$ the angular momentum J will tend to zero (as $\sim \epsilon$).

We can now evaluate how the black ring metric (2.1) (that is, eq. (3.1) with eqs. (2.3) and (3.2)) transforms under the boost (3.8). We have first to substitute eq. (3.3) into eqs. (2.3) and (3.2). Then, we apply the sequence of substitutions (3.5)–(3.7) into the thus obtained expressions for $\mathrm{d}s_0^2$ and for Δ. Finally, we perform the boost (3.8) with the rescalings (3.9), which make $\Delta = \Delta_\epsilon$ dependent on ϵ. The $\mathrm{d}s_0^2$ is invariant under the boost and at the end it reads

$$\mathrm{d}s_0^2 = 2\mathrm{d}u\mathrm{d}v + \mathrm{d}x_2^2 + \mathrm{d}y_2^2 + \mathrm{d}z_2^2 \,. \tag{3.11}$$

The next step is to take the ultrarelativistic limit $\mathrm{d}s^2 = \mathrm{d}s_0^2 + \lim_{\epsilon\to 0} \Delta_\epsilon$. This is delicate because the expansion of Δ_ϵ in ϵ has a different structure in different regions of the spacetime (even away from the singularity $y = -\infty$). In particular, a peculiar behaviour is obtained for $u = 0$, because Δ_ϵ depends on u through the combination

$$z_\epsilon = \frac{1}{\sqrt{2}}(\epsilon^{-1}u + \epsilon v) \,. \tag{3.12}$$

In order to have control over the exact distributional structure of the limit, it is convenient to isolate such dependence on $\epsilon^{-1}u$ by performing first an expansion of Δ_ϵ with z_ϵ unexpanded. This leads to an expression

$$\Delta_\epsilon = \frac{1}{\epsilon} h(z_\epsilon)\mathrm{d}u^2 + [k_1(z_\epsilon)\mathrm{d}x_2 + k_2(z_\epsilon)\mathrm{d}y_2 + k_3(z_\epsilon)\mathrm{d}z_2 + k_4(z_\epsilon)\mathrm{d}u]\,\mathrm{d}u + \cdots \,, \tag{3.13}$$

where the dots denote terms proportional to higher powers of ϵ, which are negligible in the limit. We have emphasized here the dependence of the functions h and k_i ($i = 1, \ldots, 4$) on z_ϵ (and thus on ϵ), because this is essential in our limit, but they depend also on x_2, y_2 and z_2. The quantities k_i are rather involved, but it suffices to observe here that $\lim_{\epsilon\to 0} k_i(z_\epsilon) = 0$. We can thus also drop all the terms of order ϵ^0 in (3.13).[3] For h, after all the steps described above, we obtain explicitly

$$\begin{aligned} h(z_\epsilon) = \; & p_\lambda \frac{L^2}{\Sigma} + p_\nu \frac{L^2}{\Sigma^3}\left[(\xi^2 - \eta^2 - L^2)\frac{y_1}{\xi}\sin\alpha + 2\xi x_1 \cos\alpha\right]^2 + \\ & + \frac{1}{2}(2p_\nu - p_\lambda)\left(1 - \frac{\xi^2 + \eta^2 - L^2}{\Sigma}\right)\left(\frac{y_2^2}{\xi^2}\sin^2\alpha + \frac{x_2^2}{\eta^2}\cos\alpha\right) + \\ & + \sqrt{p_\lambda(p_\lambda - p_\nu)}\frac{L y_2 \sin\alpha}{\xi^2}\left(-1 + \frac{\xi^2 + \eta^2 + L^2}{\Sigma}\right) + (p_\lambda - p_\nu)\frac{L^2 y_2^2}{\xi^2 \Sigma}\sin^2\alpha + \\ & + \frac{1}{2}(p_\lambda - p_\nu)\left(1 - \frac{\xi^2 + \eta^2 - L^2}{\Sigma}\right). \end{aligned} \tag{3.14}$$

[3] A remark on the "triviality" of the ϵ^0 terms is in order, since they could be non-vanishing for certain more general scalings of the original metric parameters. While with higher order (in ϵ) corrections in eq. (3.9) $\lim_{\epsilon\to 0} k_i(z_\epsilon) = 0$ would still hold, we could introduce a non-vanishing contribution by allowing an ϵ-dependence in the ring "radius" via $L_\epsilon = L + c_1\epsilon + c_2\epsilon^2 + \ldots$. The convergence of the integral (3.17) would then require $c_1 = 0$, but the quantity $c_2\epsilon^2$ would affect the limit of (3.13) via $\lim_{\epsilon\to 0} k_4(z_\epsilon) = c_2$. The resulting term $c_2\mathrm{d}u^2$ is, however, obviously removable with a coordinate transformation.

Recall that the dependence of h on ϵ is contained in x_1 and y_1 via eqs. (3.6)–(3.8), in η and ξ via eq. (3.5) and in Σ via eq. (3.4). In taking the limit $\epsilon \to 0$ of eq. (3.13), we apply the distributional identity

$$\lim_{\epsilon\to 0} \frac{1}{\epsilon} f\left(z_\epsilon\right) = \sqrt{2}\,\delta(u) \int_{-\infty}^{+\infty} f(z)\mathrm{d}z\,. \tag{3.15}$$

The final metric is thus (cf. eqs. (3.11) and (3.13))

$$\mathrm{d}s^2 = 2\mathrm{d}u\mathrm{d}v + \mathrm{d}x_2^2 + \mathrm{d}y_2^2 + \mathrm{d}z_2^2 + H(x_2, y_2, z_2)\delta(u)\mathrm{d}u^2\,, \tag{3.16}$$

with a profile function given by

$$H(x_2, y_2, z_2) = \sqrt{2} \int_{-\infty}^{+\infty} h(z)\mathrm{d}z\,. \tag{3.17}$$

A black ring boosted to the speed of light in a general direction z_1 is thus described by the metric (3.16) with eq. (3.17). This is evidently a $D = 5$ impulsive pp-wave with wave vector ∂_v. Such a spacetime is flat everywhere except on the null hyperplane $u = 0$, which represents the impulsive wave front. Note that the equilibrium condition (3.10) has not yet been enforced in the above expression for h (in particular, in the static limit $p_\nu = p_\lambda$ we recover the result of [19]). In order to write the solutions in a completely explicit form, it only remains to perform the integration in eq. (3.17), with h given by eq. (3.14) with eqs. (3.4)–(3.8) and (3.12). For any α, this integral is always convergent and can in principle be expressed using elliptic integrals (because Σ is a square root of a fourth order polynomial in z, see [19] for related comments). Therefore, no singular coordinate transformation of the type of [4] has to be performed. In the following, we will explicitly calculate the integral, and study the corresponding solution in the case of two different boosts of the black ring along the privileged axes x_1 ($\alpha = 0$) and y_1 ($\alpha = \pi/2$), which are respectively "orthogonal" and "parallel" to the 2-plane (y_1, y_2) (i.e., (ξ, ψ)) in which the ring rotates.

4. Orthogonal boost: $\alpha = 0$

For the orthogonal boost $\alpha = 0$, from eq. (3.6) one has $z_1 = x_1$ and $z_2 = y_1$, so that the general pp-wave (3.16) reduces to

$$\mathrm{d}s^2 = 2\mathrm{d}u\mathrm{d}v + \mathrm{d}x_2^2 + \mathrm{d}y_1^2 + \mathrm{d}y_2^2 + H_\perp(x_2, y_1, y_2)\delta(u)\mathrm{d}u^2\,. \tag{4.1}$$

Also, it is now convenient to rewrite h in eq. (3.14) as

$$\begin{aligned} h_\perp(z_\epsilon) = {} & \left[3p_\lambda L^2 - (p_\lambda - p_\nu)\xi^2 - p_\nu(x_2^2 + L^2)\right] \frac{1}{2\Sigma} + p_\nu \frac{4L^2\xi^2 z_\epsilon^2}{\Sigma^3} + \\ & + \frac{1}{2}(2p_\nu - p_\lambda)\left[\frac{x_2^2(L^2 - \xi^2)}{(z_\epsilon^2 + x_2^2)\Sigma} + \frac{x_2^2}{z_\epsilon^2 + x_2^2}\right] + \frac{1}{2}(p_\lambda - p_\nu)\left(1 - \frac{z_\epsilon^2}{\Sigma}\right), \end{aligned} \tag{4.2}$$

and Σ (from eq. (3.4)) as

$$\Sigma = \sqrt{\left[z_\epsilon^2 + x_2^2 + (\xi + L)^2\right]\left[z_\epsilon^2 + x_2^2 + (\xi - L)^2\right]}. \tag{4.3}$$

Hereafter, it is understood that $\xi = \sqrt{y_1^2 + y_2^2}$. In the orthogonal boost there is no contribution to $h_\perp$ from the off-diagonal term $g_{t\psi}$ in the metric (2.1). Performing the integration (3.17) with h given by eqs. (4.2) and (4.3), we find

$$\begin{aligned} H_\perp(x_2, y_1, y_2) = \sqrt{2}\,\frac{3p_\lambda L^2 + (2p_\nu - p_\lambda)\xi^2}{\sqrt{(\xi+L)^2 + x_2^2}}\,K(k) + \sqrt{2}(2p_\nu - p_\lambda) \times \\ \times \left[-\sqrt{(\xi+L)^2 + x_2^2}\,E(k) + \frac{\xi - L}{\xi + L}\,\frac{x_2^2}{\sqrt{(\xi+L)^2 + x_2^2}}\,\Pi(\rho, k) + \right. \\ \left. + \pi |x_2| \Theta(L - \xi) \right], \end{aligned} \tag{4.4}$$

where

$$k = \sqrt{\frac{4\xi L}{(\xi+L)^2 + x_2^2}}\,, \qquad \rho = \frac{4\xi L}{(\xi+L)^2}\,, \tag{4.5}$$

and $\Theta(L - \xi)$ denotes the step function. In the above calculation, we have used the standard elliptic integrals and their properties summarized in the Appendix of [19], and the additional integral (Σ given by eq. (4.3) with z_ϵ replaced by z)

$$\int_0^\infty \left(1 - \frac{z^2}{\Sigma}\right) \mathrm{d}z = \sqrt{(\xi+L)^2 + x_2^2}\,E(k)\,. \tag{4.6}$$

In order to gain physical insight, it is useful to visualize the behaviour of the gravitational field at a large spatial distance within the wave front $u = 0$. Defining the coordinates (r, θ)

$$x_2 = r\cos\theta\,, \qquad \xi = r\sin\theta\,, \tag{4.7}$$

an expansion for small values of the dimensionless parameter L/r (using the identities summarized in [19]) leads to

$$\begin{aligned} H_\perp = \frac{\pi}{\sqrt{2}} p_\lambda L \left[3\frac{L}{r} - \left(\frac{5}{8} + \frac{p_\nu}{4p_\lambda}\right)(3\cos^2\theta - 1)\frac{L^3}{r^3} + \right. \\ \left. + \left(\frac{7}{64} + \frac{p_\nu}{16p_\lambda}\right)(35\cos^4\theta - 30\cos^2\theta + 3)\frac{L^5}{r^5} + O\left(\frac{L^7}{r^7}\right) \right]. \end{aligned} \tag{4.8}$$

We recognize the standard form of multipole terms. The monopole is essentially an Aichelburg-Sexl term. The dipole and the octupole are missing, due to the geometry of the source. The quadrupole and 16-pole reflect the shape of the singularity and depend on the spin of the original black ring, but they persist even in the static limit $p_\nu = p_\lambda$ [19] (when, in fact, they reach their maximal strength).

It is remarkable that for the physically more interesting case of *black rings in equilibrium*, i.e. those satisfying $p_\lambda = 2p_\nu$ (see eq. (3.10)), the profile function simplifies significantly to

$$H_\perp^e(x_2, y_1, y_2) = \frac{3\sqrt{2}\,p_\lambda L^2}{\sqrt{(\xi+L)^2 + x_2^2}}\,K(k)\,. \tag{4.9}$$

Interestingly, this is just the newtonian potential generated by a *uniform ring of radius* L and linear density $\mu = 3\sqrt{2}p_\lambda L/4$ located at $x_2 = 0$ in the flat three-dimensional space (x_2, y_1, y_2). Since for a general pp-wave (4.1) the only component of the Ricci tensor is

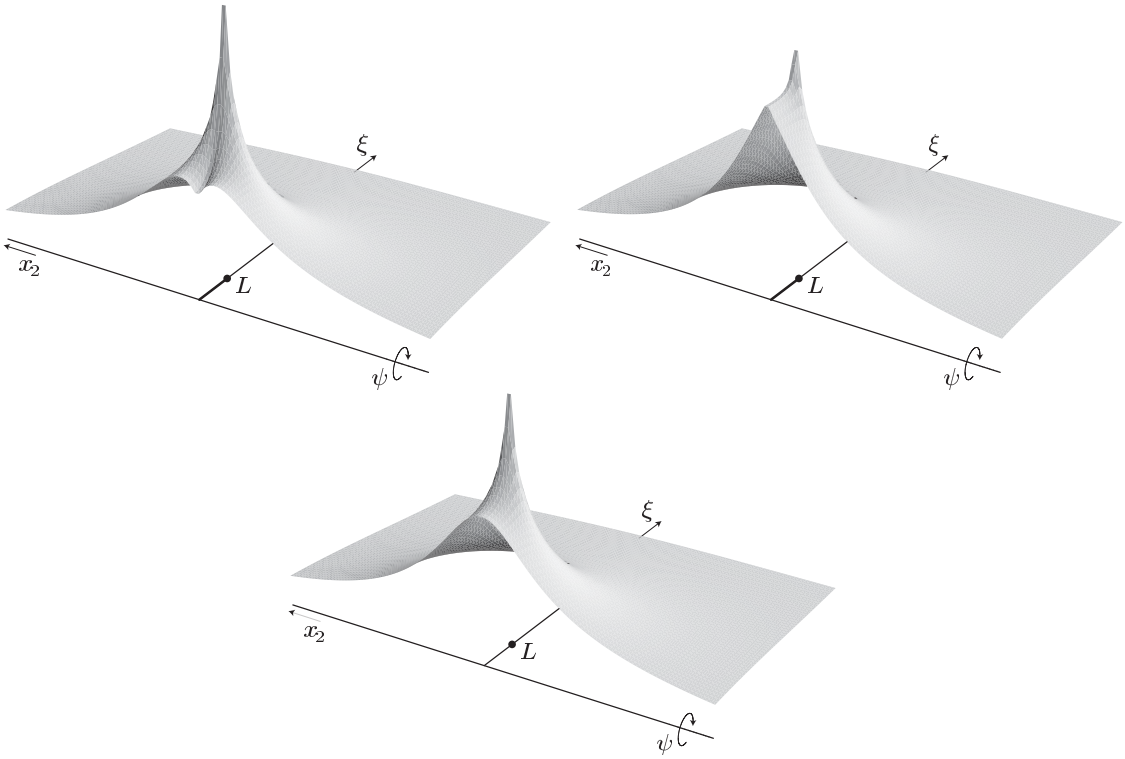

Figure 1: The profile function $H_\perp$, given by eq. (4.4), in the case of underspinning ($p_\lambda < 2p_\nu$, left), overspinning ($p_\lambda > 2p_\nu$, right) and balanced ($p_\lambda = 2p_\nu$, bottom) black rings (cf. eq. (3.10)) boosted along an orthogonal direction x_1. It is represented over the plane (x_2, ξ) (cf. eq. (3.5)), and the Killing coordinate ψ is suppressed. In the equilibrium case, $H_\perp$ reduces to $H^e_\perp$ of eq. (4.9) and the disk membrane at $x_2 = 0$, $\xi < L$ disappears (no jump of $\partial H^e_\perp/\partial x_2$ occurs at $x_2 = 0$). In all cases, there is a ring singularity at $x_2 = 0$, $\xi = L$, as indicated by the thick points in the pictures.

$R_{uu} = -\frac{1}{2}\delta(u)\mathbf{\Delta} H_\perp$, $\mathbf{\Delta}$ denoting the Laplace operator over the transverse space (x_2, y_1, y_2), it follows that the profile function (4.9) represents a spacetime which is vacuum everywhere except on the circle $u = 0 = x_2$, $\xi = L$ (so that $k = 1$ in eq. (4.5)). This lies on the wave front and corresponds to a singular ring-shaped source moving with the speed of light. It is obviously a remnant of the curvature singularity ($y = -\infty$) of the original stationary black ring (2.1). For the non-equilibrium solution (4.4), the discontinuous term proportional to $\Theta(L - \xi)$ is responsible for a disk memebrane supporting the ring [19]. We have plotted typical profile functions $H_\perp$ and $H^e_\perp$ in figure 1.

5. Parallel boost: $\alpha = \pi/2$

For the parallel boost $\alpha = \pi/2$, from eq. (3.6) one has $z_1 = y_1$ and $z_2 = -x_1$, and the general pp-wave (3.16) reduces to

$$\mathrm{d}s^2 = 2\mathrm{d}u\mathrm{d}v + \mathrm{d}x_1^2 + \mathrm{d}x_2^2 + \mathrm{d}y_2^2 + H_{||}(x_1, x_2, y_2)\delta(u)\mathrm{d}u^2 \,. \tag{5.1}$$

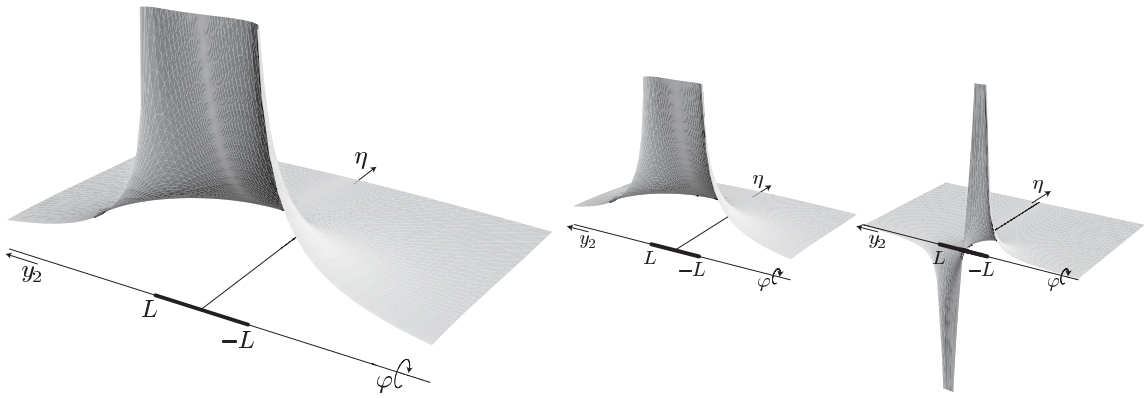

Figure 2: Plot of the profile function $H^e_{||}$, given by eq. (5.10), for balanced black rings ($p_\lambda = 2p_\nu$) boosted along the direction y_1 in the plane of rotation. It is depicted over the plane (y_2, η) (cf. eq. (3.5)), and the Killing coordinate ϕ is suppressed. The profile function $H^e_{||}$ diverges at the rod singularity $\eta = 0$, $|y_2| \le L$, as indicated by the thick line. The two smaller pictures represent the symmetric and antisymmetric part (with respect to the origin of the y_2-axis) of $H^e_{||}$, respectively. The case of unbalanced black rings, eq. (5.5), does not produce qualitative changes, since the disk membrane Lorentz-contracts to the singular rod region.

The function h can be reexpressed as

$$\begin{aligned} h_{||}(z_\epsilon) = {} & \left[(3p_\lambda + p_\nu)L^2 - p_\nu y_2^2 + 2\sqrt{p_\lambda(p_\lambda - p_\nu)}Ly_2 - (p_\lambda - p_\nu)\eta^2\right]\frac{1}{2\Sigma} - p_\nu\frac{4L^2\eta^2 z_\epsilon^2}{\Sigma^3} + \\ & + \frac{1}{2}\left[(2p_\nu - p_\lambda)y_2^2 - 2\sqrt{p_\lambda(p_\lambda - p_\nu)}Ly_2\right]\left[-\frac{L^2+\eta^2}{(z_\epsilon^2 + y_2^2)\Sigma} + \frac{1}{z_\epsilon^2 + y_2^2}\right] + \\ & + \frac{1}{2}(p_\lambda - p_\nu)\left(1 - \frac{z_\epsilon^2}{\Sigma}\right), \end{aligned} \tag{5.2}$$

and

$$\Sigma = \sqrt{z_\epsilon^4 + 2(y_2^2 + \eta^2 - L^2)z_\epsilon^2 + a^4}\,, \tag{5.3}$$

with

$$a = \left[(\eta^2 + y_2^2 - L^2)^2 + 4\eta^2 L^2\right]^{1/4}. \tag{5.4}$$

It is understood that $\eta = \sqrt{x_1^2 + x_2^2}$. Performing the integration (3.17) with h given by eqs. (5.2)–(5.4), one obtains

$$\begin{aligned} H_{||}(x_1, x_2, y_2) = {} & \left[2(2p_\lambda - p_\nu)L^2 + (2p_\nu - p_\lambda)a^2\left(1 + \frac{L^2+\eta^2}{a^2 - y_2^2}\right) + \right. \\ & \left. + 2\sqrt{p_\lambda(p_\lambda - p_\nu)}Ly_2\left(1 - \frac{L^2+\eta^2}{a^2 - y_2^2}\right)\right]\frac{\sqrt{2}}{a}K(k) - 2\sqrt{2}(2p_\nu - p_\lambda)aE(k) + \\ & + \frac{\sqrt{2}}{2}\left[(2p_\nu - p_\lambda)y_2 - 2\sqrt{p_\lambda(p_\lambda - p_\nu)}L\right] \times \\ & \times \left[-\frac{\eta^2 + L^2}{ay_2}\frac{a^2 + y_2^2}{a^2 - y_2^2}\,\Pi(\rho, k) + \pi\,\mathrm{sgn}(y_2)\right], \end{aligned} \tag{5.5}$$

where

$$k = \frac{\left(a^2 - \eta^2 - y_2^2 + L^2\right)^{1/2}}{\sqrt{2}a}\,, \qquad \rho = -\frac{(a^2 - y_2^2)^2}{4a^2 y_2^2}\,. \tag{5.6}$$

Again, we refer to the [19, appendix], the only additional integral used here being (Σ given by eq. (5.3) with z_ϵ replaced by z)

$$\int_0^\infty \left(1 - \frac{z^2}{\Sigma}\right) \mathrm{d}z = 2aE(k) - aK(k)\,. \tag{5.7}$$

With the coordinates

$$y_2 = r\cos\theta\,, \qquad \eta = r\sin\theta\,, \tag{5.8}$$

the behaviour at large spatial distances is given by

$$\begin{aligned} H_{||} = \frac{\pi}{\sqrt{2}} p_\lambda L \Bigg[& 3\frac{L}{r} + 2\sqrt{\frac{p_\lambda - p_\nu}{p_\lambda}}\cos\theta\,\frac{L^2}{r^2} + \left(\frac{7}{8} - \frac{p_\nu}{4p_\lambda}\right)(3\cos^2\theta - 1)\frac{L^3}{r^3} + \\ & + \frac{3}{4}\sqrt{\frac{p_\lambda - p_\nu}{p_\lambda}}(5\cos^3\theta - 3\cos\theta)\frac{L^4}{r^4} + \\ & + \left(\frac{11}{64} - \frac{p_\nu}{16p_\lambda}\right)(35\cos^4\theta - 30\cos^2\theta + 3)\frac{L^5}{r^5} + O\left(\frac{L^6}{r^6}\right)\Bigg]\,. \end{aligned} \tag{5.9}$$

Notice that now there appear also a dipole and an octupole term, as a remnant of the angular momentum of the black ring.

We are especially interested in *black rings in equilibrium* (3.10), for which one is left with

$$\begin{aligned} H^e_{||}(x_1, x_2, y_2) = {} & p_\lambda L \left[\frac{3\sqrt{2}L}{a} + \frac{2y_2}{a}\left(1 - \frac{L^2 + \eta^2}{a^2 - y_2^2}\right)\right] K(k) + \\ & + p_\lambda L \left[\frac{\eta^2 + L^2}{a y_2}\frac{a^2 + y_2^2}{a^2 - y_2^2}\,\Pi(\rho, k) - \pi\,\mathrm{sgn}(y_2)\right]\,. \end{aligned} \tag{5.10}$$

This function is singular at the points satisfying $u = 0 = \eta$ and $|y_2| \le L$ ($k = 1$ in eq. (5.6)), i.e. on a *rod of length* $2L$ contained within the wave front. This is a remnant of the curvature singularity of the original stationary black ring (2.1), which has (infinitely) Lorentz-contracted because of the ultrarelativistic boost in the plane of the ring. For the same reason, and because the original ring was rotating, the rod-source corresponding to eq. (5.10) is not uniform. The profile (5.10) corresponds to a vacuum spacetime everywhere except on the rod. Notice also that the apparent divergences of $H^e_{||}$ at $y_2^2 = a^2$ and $y_2 = 0$ is only a fictitious effect: the singular behaviour of the coefficient of Π in eq. (5.10) is exactly compensated from that of K in the first case and from the $\mathrm{sgn}(y_2)$ function in the second case (recall also the form of ρ in eq. (5.6)). Finally, it is interesting to observe that the antisymmetric part (in the coordinate y_2) of $H_{||}$ and $H^e_{||}$ comes entirely from the off-diagonal term $g_{t\psi}$ in the metric (2.1), which was responsible for rotation before the boost (and produces the terms even in $\cos\theta$ in the expansion (5.9)). The profile function $H^e_{||}$ is plotted in figure 2.

6. Boost of the supersymmetric black ring

To conclude, we demonstrate that the above method can also be employed to calculate the gravitational field generated by other black rings in the ultrarelativistic limit. The first supersymmetric black ring (solution of $D = 5$ minimal supergravity) was presented in [21] (and subsequently generalized in [22–24]). The line element reads

$$\mathrm{d}s^2 = -f^2(\mathrm{d}t + \omega_\psi \mathrm{d}\psi + \omega_\phi \mathrm{d}\phi)^2 + f^{-1}(\mathrm{d}s_0^2 + \mathrm{d}t^2)\,, \tag{6.1}$$

with $\mathrm{d}s_0^2$ as in eq. (2.3) and

$$f^{-1} = 1 + \frac{Q-q^2}{2L^2}(x-y) - \frac{q^2}{4L^2}(x^2-y^2)\,, \tag{6.2}$$

$$\omega_\psi = \frac{3}{2}q(1+y) + \frac{q}{8L^2}(1-y^2)\left[3Q - q^2(3+x+y)\right], \tag{6.3}$$

$$\omega_\phi = -\frac{q}{8L^2}(1-x^2)\left[3Q - q^2(3+x+y)\right]. \tag{6.4}$$

The $S^1 \times S^2$ horizon is localized at $y \to -\infty$, and asymptotic infinity at $x, y \to -1$. The Maxwell field $F = \mathrm{d}A$ is determined by

$$A = \frac{\sqrt{3}}{2} f(\mathrm{d}t + \omega_\psi \mathrm{d}\psi + \omega_\phi \mathrm{d}\phi) - \frac{\sqrt{3}}{4} q[(1+x)\mathrm{d}\phi + (1+y)\mathrm{d}\psi]. \tag{6.5}$$

The net electric charge and the local dipole magnetic charge are proportional to the positive parameters Q and q, respectively, which (for a physical interpretation) are assumed to satisfy $Q \geq q^2$ and $L < (Q-q^2)/(2q)$ [21]. The mass and angular momenta of the ring are

$$M = \frac{3\pi}{4}Q\,, \qquad J_\psi = \frac{\pi}{8}q(6L^2 + 3Q - q^2)\,, \qquad J_\phi = \frac{\pi}{8}q(3Q - q^2)\,. \tag{6.6}$$

In the limit $q = 0$ the black ring becomes a static charged naked singularity, solution of the pure Einstein-Maxwell theory. In order to boost the line element (6.1), we can follow a procedure almost identical to the one used for the vacuum ring. The standard mass rescaling of [4] together with the inequality $L < (Q-q^2)/(2q)$ suggests that during the boost we rescale the charges as

$$Q = \epsilon p_Q\,, \qquad q = \epsilon p_q \qquad (p_Q > 2L p_q)\,. \tag{6.7}$$

Omitting straightforward intermediate steps, in the case of a boost orthogonal to the plane (ξ, ψ) we obtain a shock pp-wave (4.1) with

$$H^s_\perp(x_2, y_1, y_2) = \frac{3\sqrt{2}\,p_Q}{\sqrt{(\xi+L)^2 + x_2^2}}\,K(k), \tag{6.8}$$

and k given by eq. (4.5). For a parallel boost, we obtain the metric (5.1) with

$$H^s_{||}(x_1, x_2, y_2) = 3\sqrt{2}\left[p_Q\frac{1}{a} + p_q\frac{y_2}{a}\left(1 - \frac{L^2+\eta^2}{a^2-y_2^2}\right)\right]K(k) + \\ + \frac{3\sqrt{2}p_q}{2}\left[\frac{\eta^2+L^2}{a y_2}\frac{a^2+y_2^2}{a^2-y_2^2}\,\Pi(\rho,k) - \pi\,\mathrm{sgn}(y_2)\right], \tag{6.9}$$

where k and ρ as in eq. (5.6). To obtain the field of a boosted naked singularity ($q = 0$) just set $p_q = 0$ in eq. (6.9). Notice that the dipole charge q has an effect only in the case of a parallel boost, since p_q does not appear in $H^s_\perp$ [which is in fact equivalent to the expression (4.9) for balanced vacuum rings]. This is related to the "asymmetry" between the angular momenta J_ψ and J_ϕ in eq. (6.6). In both boosts, one also finds that $F = \mathrm{d}A$ tends to zero together with its associated energy-momentum tensor (so that the "peculiar configuration" of [13] does not arise here). In fact, both $H^s_\perp$ and $H^s_{||}$ correspond to vacuum pp-waves. In principle, rescalings different from eq. (6.7) can be considered if one drops the requirement $L < (Q - q^2)/(2q)$. The detailed investigation of this and other possibilities is left for possible future work.

Acknowledgments

M.O. is supported by a post-doctoral fellowship from Istituto Nazionale di Fisica Nucleare (bando n.10068/03).

A. Results for the boosted $D = 5$ Myers-Perry black hole

Ref. [17] analyzed the ultrarelativistic boost of D-dimensional Myers-Perry black holes [16] with a single non-vanishing angular momentum. As in the present work, the calculation was performed in the case of two particular boosts orthogonal and parallel to the plane of rotation, and for $D = 5$ it resulted in impulsive pp-waves of the type (4.1) and (5.1), respectively. It is thus interesting to compare the results of [17] to ours. First of all, the angular momentum of black holes in $D = 5$ must obey a Kerr-like bound $a^2 < \mu$ [16]. Since, in the Aichelburg-Sexl limit, ref. [17] sent the mass parameter μ to zero while keeping the spin parameter a fixed, for $D = 5$ the final metrics refer to boosted naked singularities rather than black holes [17]. On the other hand, there is no upper limit on the spin of black rings [18], so that in our limit the rings do remain "black" until the final pp-wave is obtained (the same applies to the solutions of [17] in $D \geq 6$, when also black holes can be ultra-spinning). In the rest of this appendix we shall present the profile functions of [17] (for the case $D = 5$) using an explicit form adapted to our notation,[4] and we shall compare them with our functions (4.4) and (5.5).

A.1 Orthogonal boost

For an orthogonal boost, the result of [17] can be rearranged as

$$\tilde{H}_\perp(x_2, y_1, y_2) = \frac{8\sqrt{2}\,p_M}{3\pi}\left[\frac{2\sqrt{2}}{(\xi^2 + x_2^2 + L^2 + b^2)^{1/2}}\,K(k_1) + \frac{\sqrt{2}}{L^2}(\xi^2 + x_2^2 + L^2 + b^2)^{1/2} \times \right.$$
$$\left. \times\, E(k_1) - \frac{2\sqrt{2}}{L^2}\frac{b^2}{(\xi^2 + x_2^2 + L^2 + b^2)^{1/2}}\,\Pi(\rho_1, k_1)\right], \qquad \text{(A.1)}$$

[4] In particular, the quantity L will replace the original spin parameter a.

where

$$k_1 = \left(\frac{\xi^2+x_2^2+L^2-b^2}{\xi^2+x_2^2+L^2+b^2}\right)^{1/2}, \qquad \rho_1 = -\frac{(\xi^2+x_2^2-L^2-b^2)^2}{4L^2x_2^2},$$
$$b = [(\xi^2+x_2^2-L^2)^2+4x_2^2L^2]^{1/4}. \tag{A.2}$$

The above elliptic functions are singular for $k_1 = 1$, that is on a circle of radius L given by $x_2 = 0$, $\xi = L$. This was already remarked in [17] and it resembles our results of section 4. Other physical properties are more "hidden" in the expression (A.1). First of all, for $x_2 \to 0$ one has $\rho_1 \to 0$ if $\xi > L$, whereas ρ_1 diverges if $\xi < L$. This implies (with [19, identity (A5)]) that, when $\xi < L$ and x_2 is small, $H_{\perp}$ contains a non-smooth term proportional to $|x_2|$, namely there is an additional membrane at $x_2 = 0$ and $\xi < L$ (i.e. within the ring singularity discussed above). The presence of such a disk-shaped source is related to the structure of the singularities of the Myers-Perry solutions [16], and it should be contrasted with the simpler profile function (4.9) for balanced black rings, which has only a "uniform" circle as a source. From a complementary viewpoint, we can compare an expansion of the profile function (A.1) at large spatial distances with the analogous result (4.8) for the black ring. From eq. (A.1) we obtain

$$\tilde{H}_{\perp} = \frac{1}{\sqrt{2}}\frac{8\,p_M}{3L}\left[3\frac{L}{r} - \frac{5}{8}(3\cos^2\theta-1)\frac{L^3}{r^3} + \frac{7}{64}(35\cos^4\theta-30\cos^2\theta+3)\frac{L^5}{r^5} + O\left(\frac{L^7}{r^7}\right)\right]. \tag{A.3}$$

The monopole term coincides with the one in the corresponding expression (4.8) for the black ring, which we should expect since we are boosting objects with the same mass (which scales as $M = \gamma^{-1}p_M$). However, eqs. (A.3) and (4.8) in general differ already in the quadrupole term, in particular for the physically most interesting case of balanced rings $p_\lambda = 2p_\nu$. They coincide only in the limiting case $p_\nu = 0$, corresponding to $\nu = 0$, when the black ring in fact reduces to a naked singularity isometric to that of Myers and Perry (see the discussion above about the Kerr bound). In addition, in the limit of vanishing rotation $L = 0$ of eq. (A.3) only the Aichelburg-Sexl monopole survives, which corresponds to the ultrarelativistic boost of the $D = 5$ Schwarzschild-Tangherlini black hole.[5]

A.2 Parallel boost

For a parallel boost, the profile function of [17] is

$$\tilde{H}_{||}(x_1,x_2,y_2) = \frac{8\sqrt{2}\,p_M}{3\pi}\left[\frac{4}{a}\left(1+\frac{\eta^2+y_2^2+L^2+a^2}{2Ly_2}\right)K(k) + \frac{2a}{L^2}E(k) - \right.$$
$$\left. - \frac{2L+y_2}{a}\frac{\eta^2+y_2^2+L^2+a^2}{L^2y_2}\Pi(\rho_1,k)\right], \tag{A.4}$$

with a as in eq. (5.4), k as in eq. (5.6) and

$$\rho_1 = -\frac{\eta^2+y_2^2+L^2-a^2}{2a^2}. \tag{A.5}$$

[5]Recall that, instead, balanced black rings can not be static, while unbalanced static rings correspond to setting $p_\nu = p_\lambda$ in eq. (4.8) [19] (and *not* $L = 0$).

Similarly as in section 5, the elliptic integrals are singular at $k = 1$, i.e. on a rod of length $2L$ located at $\eta = 0$, $|y_2| \leq L$ [17]. At large spatial distances, the expression (A.4) behaves as

$$\tilde{H}_{||} = \frac{1}{\sqrt{2}} \frac{8\, p_M}{3L} \left[3\frac{L}{r} + 2\cos\theta\, \frac{L^2}{r^2} + \frac{7}{8}(3\cos^2\theta - 1)\frac{L^3}{r^3} + \frac{3}{4}(5\cos^3\theta - 3\cos\theta)\frac{L^4}{r^4} + \right.$$
$$\left. + \frac{11}{64}(35\cos^4\theta - 30\cos^2\theta + 3)\frac{L^5}{r^5} + O\left(\frac{L^6}{r^6}\right) \right]. \qquad \text{(A.6)}$$

The discussion is similar as the one above for $\tilde{H}_{\perp}$. Again, the monopole term coincides with the one in the corresponding expression (5.9) for the black ring. Higher multipoles in general differ, in particular for balanced rings. Boosted black holes reduce to the Aichelburg-Sexl monopole in the static limit $L = 0$.

References

[1] G. 't Hooft, *Graviton dominance in ultrahigh-energy scattering*, *Phys. Lett.* **B 198** (1987) 61.

[2] D. Amati and C. Klimčík, *Strings in a shock wave background and generation of curved geometry from flat space string theory*, *Phys. Lett.* **B 210** (1988) 92.

[3] H.J. de Vega and N. Sánchez, *Quantum string scattering in the Aichelburg-Sexl geometry*, *Nucl. Phys.* **B 317** (1989) 706.

[4] P.C. Aichelburg and R.U. Sexl, *On the gravitational field of a massless particle*, *Gen. Rel. Grav.* **2** (1971) 303.

[5] T. Banks and W. Fischler, *A model for high energy scattering in quantum gravity*, `hep-th/9906038`.

[6] R. Emparan, G.T. Horowitz and R.C. Myers, *Black holes radiate mainly on the brane*, *Phys. Rev. Lett.* **85** (2000) 499 [`hep-th/0003118`].

[7] S.B. Giddings and S.D. Thomas, *High energy colliders as black hole factories: the end of short distance physics*, *Phys. Rev.* **D 65** (2002) 056010 [`hep-ph/0106219`].

[8] S. Dimopoulos and G. Landsberg, *Black holes at the LHC*, *Phys. Rev. Lett.* **87** (2001) 161602 [`hep-ph/0106295`].

[9] V. Cardoso, E. Berti and M. Cavagliá, *What we (don't) know about black hole formation in high-energy collisions*, *Class. and Quant. Grav.* **22** (2005) L61 [`hep-ph/0505125`].

[10] D.M. Eardley and S.B. Giddings, *Classical black hole production in high-energy collisions*, *Phys. Rev.* **D 66** (2002) 044011 [`gr-qc/0201034`].

[11] H. Yoshino and Y. Nambu, *High-energy head-on collisions of particles and hoop conjecture*, *Phys. Rev.* **D 66** (2002) 065004 [`gr-qc/0204060`].

[12] E. Kohlprath and G. Veneziano, *Black holes from high-energy beam-beam collisions*, *JHEP* **06** (2002) 057 [`gr-qc/0203093`].

[13] C.O. Loustó and N. Sánchez, *The curved shock wave space-time of ultrarelativistic charged particles and their scattering*, *Int. J. Mod. Phys.* **A 5** (1990) 915.

[14] M. Ortaggio, *Ultrarelativistic black hole in an external electromagnetic field and gravitational waves in the Melvin universe*, *Phys. Rev.* **D 69** (2004) 064034 [`gr-qc/0311088`].

[15] M. Ortaggio, *Higher dimensional black holes in external magnetic fields*, *JHEP* **05** (2005) 048 [gr-qc/0410048].

[16] R.C. Myers and M.J. Perry, *Black holes in higher dimensional space-times*, *Ann. Phys. (NY)* **172** (1986) 304.

[17] H. Yoshino, *Lightlike limit of the boosted Kerr black holes in higher-dimensional spacetimes*, *Phys. Rev.* **D 71** (2005) 044032 [gr-qc/0412071].

[18] R. Emparan and H.S. Reall, *A rotating black ring in five dimensions*, *Phys. Rev. Lett.* **88** (2002) 101101 [hep-th/0110260].

[19] M. Ortaggio, P. Krtouš and J. Podolský, *Ultrarelativistic boost of the black ring*, *Phys. Rev.* **D 71** (2005) 124031 [gr-qc/0503026].

[20] R. Emparan and H.S. Reall, *Generalized Weyl solutions*, *Phys. Rev.* **D 65** (2002) 084025 [hep-th/0110258].

[21] H. Elvang, R. Emparan, D. Mateos and H.S. Reall, *A supersymmetric black ring*, *Phys. Rev. Lett.* **93** (2004) 211302 [hep-th/0407065].

[22] H. Elvang, R. Emparan, D. Mateos and H.S. Reall, *Supersymmetric black rings and three-charge supertubes*, *Phys. Rev.* **D 71** (2005) 024033 [hep-th/0408120].

[23] I. Bena and N.P. Warner, *One ring to rule them all ... and in the darkness bind them?*, hep-th/0408106.

[24] J.P. Gauntlett and J.B. Gutowski, *General concentric black rings*, *Phys. Rev.* **D 71** (2005) 045002 [hep-th/0408122].

[25] R. Emparan, *Rotating circular strings and infinite non-uniqueness of black rings*, *JHEP* **03** (2004) 064 [hep-th/0402149].

[26] V. Pravda and A. Pravdová, *WANDs of the black ring*, *Gen. Rel. Grav.* **37** (2005) 1277.

PHYSICAL REVIEW D **72,** 124019 (2005)

Accelerated black holes in an anti-de Sitter universe

Pavel Krtouš*

Institute of Theoretical Physics, Faculty of Mathematics and Physics, Charles University in Prague, V Holešovičkách 2, 180 00 Prague 8, Czech Republic

(Received 23 October 2005; published 19 December 2005)

The *C*-metric is one of few known exact solutions of Einstein's field equations which describes the gravitational field of moving sources. For a vanishing or positive cosmological constant, the *C*-metric represents two accelerated black holes in asymptotically flat or de Sitter spacetime. For a negative cosmological constant the structure of the spacetime is more complicated. Depending on the value of the acceleration, it can represent one black hole or a sequence of pairs of accelerated black holes in the spacetime with an anti-de Sitter-like infinity. The global structure of this spacetime is analyzed and compared with an empty anti-de Sitter universe. It is illustrated by 3D conformal-like diagrams.

DOI: 10.1103/PhysRevD.72.124019 PACS numbers: 04.20.Ha, 04.20.Jb

I. INTRODUCTION

The *C*-metric without cosmological constant Λ is a well-known solution of the Einstein(-Maxwell) equations. It belongs to a class of spacetimes with boost-rotational symmetry [1] which represent the gravitational field of uniformly accelerated sources. The *C*-metric was discovered back in 1917 by Levi-Civita [2] and Weyl [3], and named by Ehlers and Kundt [4]. An understanding of the global structure of the *C*-metric spacetime as a universe with a pair of accelerated black holes came with the fundamental papers by Kinnersley and Walker [5], Ashtekar and Dray [6], and Bonnor [7]. Various aspects and properties of this solution were consequently studied, including the generalization to spinning black holes. References and overviews can be found, e.g., in Refs. [1,8–10]; for recent results see, e.g., Refs. [11–13].

A generalization of the standard *C*-metric for nonvanishing cosmological constant Λ has also been known for a long time [14–16]. However, until recently a complete understanding of global structure of this solution was missing. It was elucidated in a series of papers [17–19] in the case $\Lambda > 0$, and in Refs. [20–22] for $\Lambda < 0$ (cf. also Refs. [23–26] for related work and discussion of special and degenerated cases).

The *C*-metric is one of few explicitly known spacetimes representing the gravitational field of nontrivially moving sources. Therefore, it is interesting, for example, as a test bed for numerical simulations. It plays also an important role in a study of radiative properties of gravitational fields. Namely, in the case of a nonvanishing cosmological constant it may provide us with an insight into the character of radiation, which in the asymptotically nontrivial spacetimes is not yet well understood. In Refs. [19,22] the *C*-metric spacetimes with $\Lambda \neq 0$ were used to investigate the directional structure of radiation. These results were later generalized [27,28] for general spacetimes with spacelike and timelike conformal infinity. The *C*-metric spacetimes have found also a successful application to the problem of cosmological pair creation of black holes [29–34]. In addition to spacetime with accelerated black holes, the *C*-metric can also describe accelerated naked singularities or, for special choice of parameters, empty spacetime described in a coordinate system adapted to accelerated observers [17,35,36].

In the present work we wish to give a complete description of the case when the *C*-metric describes black holes moving with an acceleration in anti-de Sitter universe. As was already observed in [21,22,26], there are three qualitatively different cases according to value of the black hole acceleration A. For small values of acceleration, $A < 1/\ell$, (ℓ being a length scale given by the cosmological constant, cf. Eq. (2.3)) the *C*-metric describes one accelerated black hole in asymptotically anti-de Sitter spacetime. For large acceleration, $A > 1/\ell$, it describes a sequence of pairs of black holes. In the critical case $A = 1/\ell$ it describes a sequence of single accelerated black holes entering and leaving asymptotically anti-de Sitter spacetime. Here we concentrate on the generic situation $A \neq 1/\ell$; the critical case will be discussed separately [37] (cf. also Refs. [24,25]).

The main goal of the work is to give a clear visual representation of the global structure of the spacetimes. It is achieved with help of a number of two-dimensional and three-dimensional diagrams. Also, the relation to an empty anti-de Sitter universe is explored. Understanding of the anti-de Sitter spacetime in accelerated coordinates plays a key role in the construction of three-dimensional diagrams for the full *C*-metric spacetime.

The paper is organized as follows. In Sec. II we overview the *C*-metric solution with a negative cosmological constant in various coordinate systems. Namely, we introduce coordinates τ, ν, ξ, φ, closely related to those of [5,14], accelerated static coordinates T, R, Θ, Φ, very useful for physical interpretation, and global null coordinates u, v essential for a study of the global structure. In Secs. III and IV we discuss the two qualitatively different cases of small and large acceleration, respectively. Finally,

*Electronic address: Pavel.Krtous@mff.cuni.cz

Sec. V studies the weak field limit, i.e., the limit of vanishing mass and charge. In this case the *C*-metric describes empty anti-de Sitter universe in accelerated coordinates. The relation of these coordinates to the standard cosmological coordinates is presented, again separately for $A \lessgtr 1/\ell$.

An even more elaborated visual presentation of the studied spacetimes, including animations and interactive three-dimensional diagrams, can be found in [38]. Let us also note that the online version of this work includes figures in color.

II. THE *C*-METRIC WITH A NEGATIVE COSMOLOGICAL CONSTANT

The *C*-metric with a cosmological constant $\Lambda < 0$ can be written as

$$\mathbf{g} = \frac{1}{A^2(x+y)^2}\left(-F\mathbf{d}t^2 + \frac{1}{F}\mathbf{d}y^2 + \frac{1}{G}\mathbf{d}x^2 + G\mathbf{d}\varphi^2\right), \tag{2.1}$$

where F and G are polynomially dependent on y and z, respectively,

$$\begin{aligned} F &= \frac{1}{A^2\ell^2} - 1 + y^2 - 2mAy^3 + e^2A^2y^4, \\ G &= 1 - x^2 - 2mAx^3 - e^2A^2x^4. \end{aligned} \tag{2.2}$$

Here ℓ is a length scale given by the cosmological constant Λ,

$$\ell = \sqrt{-\frac{3}{\Lambda}}. \tag{2.3}$$

The metric is a solution of the Einstein-Maxwell equations with the electromagnetic field given by

$$\mathbf{F} = e\mathbf{d}y \wedge \mathbf{d}t. \tag{2.4}$$

Depending on the choice of parameters and of ranges of coordinates, the metric (2.1) can describe different spacetimes. In the physically most interesting cases, it describes black holes uniformly accelerated in anti-de Sitter universe. In these cases the constants A, m, e, and C (such that $\varphi \in (-\pi C, \pi C)$) characterize the acceleration, mass, and charge of the black holes, and the conicity of the φ symmetry axis, respectively. These parameters have to satisfy $m \geq 0$, $e^2 < m^2$, $A, C > 0$, and the function G must be vanishing for four different values of x in the charged case ($e, m \neq 0$), or for three different values in the uncharged case ($e = 0, m \neq 0$). The coordinate x must belong to an interval around zero on which G is positive, and $y \in (-x, \infty)$, cf. Figures 1 and 5. It follows that $0 \leq G \leq 1$. The boundary values of the allowed range of the coordinate x correspond to different parts of the axis of φ symmetry separated from each other by black holes.

The spacetime described by the *C*-metric is static and axially symmetric with Killing vectors $\boldsymbol{\partial}_t$ and $\boldsymbol{\partial}_\varphi$, respectively. Killing horizons of the vector $\boldsymbol{\partial}_t$ are given by condition $F = 0$. They coincide with horizons of various kinds as will be described below. Beside the Killing vectors, the geometry of spacetime possesses one conformal Killing tensor $\mathbf{Q}$,

$$\mathbf{Q} = \frac{1}{A^4(x+y)^4}\left(F\mathbf{d}t^2 - \frac{1}{F}\mathbf{d}y^2 + \frac{1}{G}\mathbf{d}x^2 + G\mathbf{d}\varphi^2\right). \tag{2.5}$$

There exist two doubly degenerate principal null directions

$$\mathbf{k}_1 \propto \boldsymbol{\partial}_t - F\boldsymbol{\partial}_y, \qquad \mathbf{k}_2 \propto \boldsymbol{\partial}_t + F\boldsymbol{\partial}_y, \tag{2.6}$$

so that the spacetime is of the Petrov type *D*. The metric has a curvature singularity for $y \to \pm\infty$.

The constants m and e parametrize the mass and charge of black holes. Let us emphasize that they are not directly the mass or charge defined through some invariant integral procedure. For example, the total charge defined by integration of the electric field over a surface around one black hole is $Q = \frac{1}{2}\Delta x C e$. It is proportional to e, but besides the trivial dependence on the conicity C, it depends also on the mass and the acceleration parameters through the length Δx of the allowed range of the coordinate x.

The parameter C defines a range of the angular coordinate φ, and thus it governs a regularity of the φ symmetry axis. Typically, the axis has a conical singularity which corresponds to a string or strut. By an appropriate choice of C, a part of the axis can be made regular. However, for nonvanishing acceleration it is not possible to achieve regularity of the whole axis—objects on the axis are physically responsible for the 'accelerated motion' of black holes.

The constant A parametrizes the acceleration of the black holes. But it is not a simple task to define what is the *acceleration* of a black hole. The acceleration of a test particle is defined with respect of a local inertial frame given by a background spacetime. However, black holes are objects which deform the spacetime in which they are moving; they define the notion of inertial observers, and they are actually dragging inertial frames with themselves. Therefore, it is not possible to measure the acceleration of black holes with respect to their surroundings. The motion of black holes can be partially deduced from a structure of the whole spacetime, e.g., from a relation of black holes and asymptotically free observers, and partially by investigating a weak field limit in which the black holes become test particles and cease to deform the spacetime around them. Namely, in the limit of vanishing mass and charge, the spacetime (2.1) reduces to the anti-de Sitter universe with black holes changed into world lines of uniformly accelerated particles. Such a limit will be discussed in Sec. V.

Depending on the value of the parameter A, the metric (2.1) describes qualitatively different spacetimes. For A smaller then a critical value $1/\ell$ given by the cosmological constant, cf. Eq. (2.3), the metric represents asymptotically anti-de Sitter universe with one uniformly accelerated black hole inside.[1] For $A > 1/\ell$ the metric (2.1) describes asymptotically anti-de Sitter spacetime which contains a sequence of pairs of uniformly accelerated black holes which enter and leave the universe through its conformal infinity.[2] The extremal case $A = 1/\ell$ corresponds to accelerated black holes entering and leaving the anti-de Sitter universe, one at a time. This extreme case will not be discussed here; however, see Refs. [24,25,37].

Coordinates t, y, x, φ can be rescaled in a various way. We will introduce coordinates τ, v, ξ, φ and closely related accelerated static coordinates T, R, Θ, Φ which are appropriate for a discussion of the limits of weak field and of vanishing acceleration. They will be used thoroughly in the following sections. We will also mention coordinates $\mathfrak{t}$, $\mathfrak{y}$, $\mathfrak{x}$, ϕ (used in Ref. [14]) in which the global prefactor A^{-2} in the metric (2.1) is transformed into metric functions, coordinates τ, ω, σ, φ adapted to the infinity, and global null coordinates u, v, ξ, φ. However, detailed transformations among these coordinates differs for the qualitatively different cases $A \lessgtr 1/\ell$. Therefore, we list first only metric forms in these coordinate systems and coordinate transformation which are general, and we postpone specific definitions to the next sections.

The metric (2.1) in the coordinate systems t, y, x, φ, τ, v, ξ, φ, and $\mathfrak{t}$, $\mathfrak{y}$, $\mathfrak{x}$, ϕ has actually the same form, only with different metric functions (cf. Eqs. (3.5), (3.7), and (4.5), (4.7))

$$\mathbf{g} = \frac{\ell^2}{\omega^2}\left(-\mathcal{F}\mathbf{d}\tau^2 + \frac{1}{\mathcal{F}}\mathbf{d}v^2 + \frac{1}{\mathcal{G}}\mathbf{d}\xi^2 + \mathcal{G}\mathbf{d}\varphi^2\right). \quad (2.7)$$

$$\mathbf{g} = \frac{\ell^2}{(\mathfrak{x}+\mathfrak{y})^2}\left(-\mathfrak{F}\mathbf{d}\mathfrak{t}^2 + \frac{1}{\mathfrak{F}}\mathbf{d}\mathfrak{y}^2 + \frac{1}{\mathfrak{G}}\mathbf{d}\mathfrak{x}^2 + \mathfrak{G}\mathbf{d}\phi^2\right). \quad (2.8)$$

Accelerated static coordinates T, R, Θ, Φ are given by

$$T = \ell\tau, \qquad R = \frac{\ell}{v}, \qquad \Phi = \varphi,$$
$$\mathbf{d}\Theta^2 = \frac{1}{\sqrt{\mathcal{G}}}\mathbf{d}\xi, \qquad \Theta = \frac{\pi}{2} \quad \text{for} \quad \xi = 0. \quad (2.9)$$

The metric takes a form

$$\mathbf{g} = \frac{\ell^2}{\omega^2 R^2}\left(-\mathcal{H}\mathbf{d}T^2 + \frac{1}{\mathcal{H}}\mathbf{d}R^2 + R^2(\mathbf{d}\Theta^2 + \mathcal{G}\mathbf{d}\Phi^2)\right), \quad (2.10)$$

$$\mathcal{H} = \frac{1}{v}\mathcal{F}; \quad (2.11)$$

see (3.9) and (4.8).

The coordinate R is not well defined at $v = 0$. It is a coordinate singularity which can be avoided by using the coordinate v. However, near the black hole, the coordinate R has a more direct physical meaning—it is the radial coordinate measured by area, at least in the conformally related geometry. Because v can be negative, R can take also negative values. However, it happens only far away from the black holes or in spacetime domains in which R changes into a time coordinate.

The coordinate ξ is given by $\xi = -x$ (cf. Eqs. (3.2) and (4.2)), so we can use what was said about range of definition of x. Let $[\xi_\mathrm{b}, \xi_\mathrm{f}]$ be the interval of allowed values of ξ, i.e., the interval where $\mathcal{G}$ is positive and $\xi_\mathrm{b} < 0 < \xi_\mathrm{f}$. The value ξ_f corresponds to the axis of φ symmetry (since $\mathcal{G} = 0$ at $\xi = \xi_\mathrm{f}$) pointing out of the black hole in the forward direction of the motion.[3] The value ξ_b corresponds to the axis (again, $\mathcal{G}|_{\xi=\xi_\mathrm{b}} = 0$) going in the opposite (backward) direction. Integrating $1/\sqrt{\mathcal{G}}$ in (2.9), we find that the longitudinal angular coordinate Θ belongs into an interval $[\Theta_\mathrm{b}, \Theta_\mathrm{f}]$ which, in general, differs from $[0, \pi]$.

If we use the conformal prefactor in the metric (2.7) as a coordinate, and if we find a complementary coordinate σ such that the metric is diagonal (see (3.10) and (4.9)), we get

$$\mathbf{g} = \frac{\ell^2}{\omega^2}\left(-\mathcal{F}\mathbf{d}\tau^2 + \frac{1}{\mathcal{E}}(\mathbf{d}\omega^2 + \mathcal{F}\mathcal{G}\mathbf{d}\sigma^2) + \mathcal{G}\mathbf{d}\varphi^2\right). \quad (2.12)$$

This coordinate system is well adapted to the infinity $\mathcal{I}$, since $\mathcal{I}$ is given by $\omega = 0$.

Finally, for discussion of global structure of the spacetime it is useful to introduce global null coordinates[4] u, v, ξ, φ. We start with the 'tortoise' coordinate v_*

$$\mathbf{d}\,v_* = \frac{1}{\mathcal{F}}\mathbf{d}v. \quad (2.13)$$

It expands each of the intervals between successive zeros of $\mathcal{F}$ to the whole real line. Next we define null coordinates $\bar{u}$, $\bar{v}$

[1] As for nonaccelerated black holes, it is possible to extend the spacetime through the interior of the black hole to other asymptotically anti-de Sitter domain(s). However, for $A < 1/\ell$, there is only one black hole in each of these domains.

[2] Again, there can be more asymptotically anti-de Sitter domains, each of them with the described structure.

[3] By the direction of motion we mean the direction from which the black hole is pulled by the cosmic string or toward which it is pushed by the strut. In the weak field limit it is the direction of the acceleration.

[4] Notice the difference between v (v) and v (upsilon). It should be always clear from the context if we speak about null v or radial v.

$$\bar{u} = v_* + \tau, \qquad \bar{v} = v_* - \tau. \tag{2.14}$$

These coordinates cover distinct domains of the spacetime which are separated from each other by horizons, i.e., by null surfaces $\mathcal{F} = 0$. The coordinates can be extended across a chosen horizon with help of global coordinates u, v:

$$\tan\frac{u}{2} = (-1)^m \exp\frac{\bar{u}}{2|\delta|}, \qquad \tan\frac{v}{2} = (-1)^n \exp\frac{\bar{v}}{2|\delta|}. \tag{2.15}$$

Integers m, n label the domains; see Figs. 2, 6, and 16 below. δ is a real constant. The metric reads[5]

$$\mathbf{g} = \frac{\ell^2}{\omega^2}\left(\frac{2\delta^2\mathcal{F}}{\sin u \sin v}\mathbf{d}u \vee \mathbf{d}v + \frac{1}{\mathcal{G}}\mathbf{d}\xi^2 + \mathcal{G}\mathbf{d}\varphi^2\right). \tag{2.16}$$

For a suitable choice of the constant δ the metric coefficients turn to be smooth and nondegenerate as functions of coordinates u, v across a chosen horizon. For such a choice we require that the coordinate map u, v, ξ, φ on a neighborhood of that horizon belongs to the differential atlas of the manifold. The metric is thus smoothly extended across the chosen horizon.

III. A SINGLE ACCELERATED BLACK HOLE

A. Coordinate systems

We start a specific discussion with the simpler case

$$A < \frac{1}{\ell}. \tag{3.1}$$

The coordinates τ, v, ξ, φ and $\mathfrak{t}$, $\mathfrak{y}$, $\mathfrak{x}$, ϕ are in this case defined by

$$\begin{aligned} \tau &= \cos\chi_o \mathfrak{t} = \cot\chi_o t, & v &= \tfrac{1}{\cos\chi_o}\mathfrak{y} = \tan\chi_o y, \\ \varphi &= \sin\chi_o \phi = \varphi, & \xi &= -\frac{1}{\sin\chi_o}\mathfrak{x} = -x, \end{aligned} \tag{3.2}$$

where $\chi_o \in [0, \frac{\pi}{2})$ is a parameter characterizing the acceleration,

$$A = \frac{1}{\ell}\sin\chi_o. \tag{3.3}$$

Its geometrical meaning in the weak field limit will be discussed in Sec. V. The metric functions in (2.7) and (2.8) are given by

$$\mathcal{F} = 1 + v^2 - 2\frac{m}{\ell}\cos\chi_o\, v^3 + \frac{e^2}{\ell^2}\cos^2\chi_o\, v^4, \tag{3.4}$$

$$\begin{aligned} \mathcal{G} &= 1 - \xi^2 + 2\frac{m}{\ell}\sin\chi_o\,\xi^3 - \frac{e^2}{\ell^2}\sin^2\chi_o\,\xi^4, \\ \omega &= v\cos\chi_o - \xi\sin\chi_o, \end{aligned} \tag{3.5}$$

and

$$\begin{aligned} \mathfrak{F} &= \cos^2\chi_o + \mathfrak{y}^2 - 2\frac{m}{\ell}\mathfrak{y}^3 + \frac{e^2}{\ell^2}\mathfrak{y}^4, \\ \mathfrak{G} &= \sin^2\chi_o - \mathfrak{x}^2 - 2\frac{m}{\ell}\mathfrak{x}^3 - \frac{e^2}{\ell^2}\mathfrak{x}^4. \end{aligned} \tag{3.6}$$

They are related by

$$\begin{aligned} \mathcal{F} &= \cos^{-2}\chi_o\,\mathfrak{F} = \tan^2\chi_o\, F = 1 - \frac{\ell^2}{\cos^2\chi_o} S\left(\frac{\cos\chi_o}{\ell} v\right), \\ \mathcal{G} &= \sin^{-2}\chi_o\mathfrak{G} = G = 1 + \frac{\ell^2}{\sin^2\chi_o} S\left(\frac{\sin\chi_o}{\ell}\xi\right), \end{aligned} \tag{3.7}$$

where $S(w)$ is a simple polynomial

$$S(w) = -w^2(1 - 2mw + e^2w^2). \tag{3.8}$$

The functions $\mathcal{H}$ is (cf. Eq. (2.11))

$$\mathcal{H} = 1 + \frac{R^2}{\ell^2} - \cos\chi_o\frac{2m}{R} + \cos^2\chi_o\frac{e^2}{R^2}. \tag{3.9}$$

The coordinate ω was already defined in Eq. (3.5). The complementary orthogonal coordinate σ can be, in general, given simply only in differential form[6]

$$\begin{aligned} \mathbf{d}\,\sigma &= \frac{\sin\chi_o}{\mathcal{F}}\mathbf{d}v + \frac{\cos\chi_o}{\mathcal{G}}\mathbf{d}\xi, \\ \mathbf{d}\omega &= -\cos\chi_o\mathbf{d}v + \sin\chi_o\mathbf{d}\xi. \end{aligned} \tag{3.10}$$

(Here we included also the gradient of ω for completeness.) The metric function ξ is given by

$$\mathcal{E} = \mathcal{F}\cos^2\chi_o + \mathcal{G}\sin^2\chi_o. \tag{3.11}$$

At infinity, $\omega = 0$ and $\xi = 1$.

B. Global structure

Now we are prepared to discuss the global structure of the spacetime in more details. We start inspecting the metric in the accelerated static coordinates (2.10) with $\mathcal{H}$ given by (3.9). It has a familiar form—if we ignore prefactor $\ell^2/(\omega R)^2$ we get the metric of a nonaccelerated black hole in anti-de Sitter universe in standard static coordinates—except for a different range of Θ and except for $\mathcal{G}$ instead of $\sin^2\Theta$ in front of the $\mathbf{d}\Phi^2$ term. Fortunately, $\sqrt{\mathcal{G}}$ on the allowed range of Θ resembles $\sin\Theta$, and the difference does not affect qualitative properties of the geometry.[7] The conformal prefactor $\ell^2/(\omega R)^2$

[5] $\mathbf{d}u \vee \mathbf{d}v = \mathbf{d}u\mathbf{d}v + \mathbf{d}v\mathbf{d}u$ is a symmetric tensor product, which is usually loosely written as $2\mathbf{d}u\mathbf{d}v$.

[6] The relations are integrable since $\mathcal{F}$ depends only on v and $\mathcal{G}$ on ξ.

[7] Let us mention that for $A = 0$, i.e., for $\chi_o = 0$, the metric (2.10) becomes exactly the Reissner-Nordström–anti-de Sitter solution with $\xi = -\cos\Theta$, $\mathcal{G} = \sin^2\Theta$, and $\mathcal{H} = 1 + \frac{R^2}{\ell^2} - \frac{2m}{R} + \frac{e^2}{R^2}$.

does not change the causal structure of the black hole. It justifies our claim that the spacetime contains a black hole. It also gives the interpretation for the coordinates—the accelerated static coordinates are centered around the hole, with R being a radial coordinate, and Θ and Φ longitudinal and latitudinal angular coordinates. T is a time coordinate of external observers staying at a constant distance above the horizon of the black hole. The coordinates $\tau, \upsilon, \xi, \varphi$ are only a different parametrization of the time, radial, and angular directions.

However, the prefactor $\ell^2/(\omega R)^2$ in (2.10) changes the 'position' of the infinity—the conformal infinity $\mathcal{I}$ is localized at $\omega = 0$, i.e., at

$$\upsilon = \tan\chi_o\, \xi. \tag{3.12}$$

It means that the radial position of the infinity depends on the direction ξ. This corresponds to the fact that the black hole is not in a symmetrical position with respect to the asymptotically anti-de Sitter universe. Nevertheless, it is in equilibrium—the cosmological compression of anti-de Sitter spacetime (which would push a test body toward any chosen center of the universe) is compensated by a string (or strut) on the axis which keeps the black hole in a static nonsymmetric position with respect to the infinity. We can thus say that the black hole is moving with uniform acceleration equal to the cosmological compression, despite the fact that it cannot be measured locally. Remember that in anti-de Sitter universe a static observer which stays at a fixed spatial position in the spacetime eternally feels the cosmological deceleration of a constant magnitude from the range $[0, 1/\ell)$, depending on his position. This corresponds to the assumption (3.1). As we will see in a moment, we are dealing with *one* black hole which stays *eternally* in equilibrium in asymptotically anti-de Sitter spacetime.

We already said that zeros of $\mathcal{F}$ correspond to Killing horizons of the Killing vector $\boldsymbol{\partial}_\tau$. Inspecting properties of the polynomial $S(w)$, we find that $\mathcal{F} = 0$ for two values $\upsilon = \upsilon_o$, υ_i ($\upsilon_o < \upsilon_i$) in the charged case ($e, m \neq 0$), and for just one value $\upsilon = \upsilon_o$ if $e = 0, m \neq 0$. The null surface $\upsilon = \upsilon_o$ corresponds to the outer black hole horizon, and $\upsilon = \upsilon_i$ corresponds to the inner black hole horizon.

Allowed ranges of coordinates υ, ξ are shown in Fig. 1. Boundary 'zigzag' lines correspond to the curvature singularity at $\upsilon, \xi \to \pm\infty$. The horizons separate the allowed range into qualitatively different regions II, III, and IV. Region II describes the asymptotically anti-de Sitter domain outside of the black hole, and regions III and IV correspond to the interior of the black hole.

The coordinate systems $\tau, \upsilon, \xi, \varphi$ or T, R, Θ, Φ are defined in each of the regions II, III, IV; however, they are singular at the horizons. To extend the spacetime through the horizons, global null coordinates u, v, ξ, φ can be used. It turns out that the global manifold contains more domains of the type II, III, IV, labeled by integers m, n; see

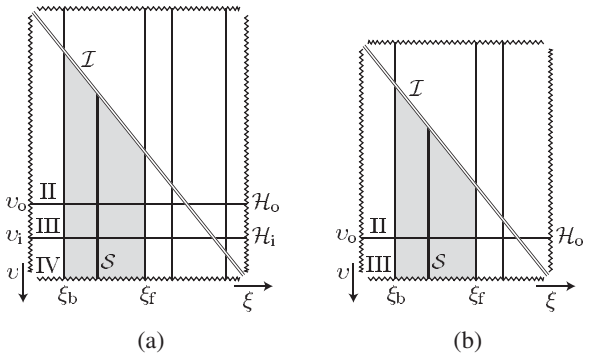

FIG. 1. The diagrams of the allowed range of coordinates υ and ξ (the shaded region) in the case of small acceleration $A < 1/\ell$. Diagram (a) is applicable in the charged case, (b) is valid for $m \neq 0$, $e = 0$. ξ_b and ξ_f are zeros of the metric function $\mathcal{G}$ closest to $\xi = 0$. These values correspond to the axis of φ symmetry. The diagonal double line represents the infinity, cf. Eq. (3.12). The bottom zigzag line is the singularity at $\upsilon = \infty$. υ_o and υ_i are zeros of the metric function $\mathcal{F}$. They define the outer and inner black hole horizons. They separate the allowed range of coordinates into regions II, III, and IV. These regions correspond to different domains in spacetime, each of them covered by its own coordinates $\tau, \upsilon, \xi, \varphi$. These coordinate systems cannot be smoothly extended over the horizon. Coordinates smooth across the horizon are used in Fig. 2, where sections $\xi =$ constant are depicted. Such a section is represented in the diagrams above by the vertical thick line.

Eq. (2.15). From the domain II outside the outer black hole horizon, the spacetime continues into two domains III inside the black hole. These are connected to other asymptotically anti-de Sitter domains II (behind the Einstein-Rosen bridge through the black hole), and, in the charged case, to domains IV behind inner black hole horizons. Each of these domains is covered by its own coordinate system $\tau, \upsilon, \xi, \varphi$. This global structure is well illustrated in two-dimensional conformal diagrams of $\xi, \varphi =$ constant sections; see Fig. 2.

As already mentioned, the inner structure of the black hole is qualitatively the same as the structure of the interior of the standard Schwarzschild or Reissner-Nordström black holes. Therefore we focus mainly on the exterior of the black hole. A more detailed conformal diagram of the domain outside of the outer horizon can be found in Fig. 3(b). The position of the infinity in the diagrams for various values of ξ changes according to (3.12). We can glue sheets of different ξ together into a three-dimensional diagram in Fig. 3(a), where only the coordinate φ is suppressed. The 'gluing' is done using an intuition that ξ is a 'deformed cosine' of longitudinal angle and that υ parametrizes the radial direction. The three-dimensional diagram in Fig. 3(a) is thus obtained by a rotation of the conformal diagram in Fig. 3(b).

The outer black hole horizon has a form of two conelike surfaces joined in the neck of the black hole. The conical

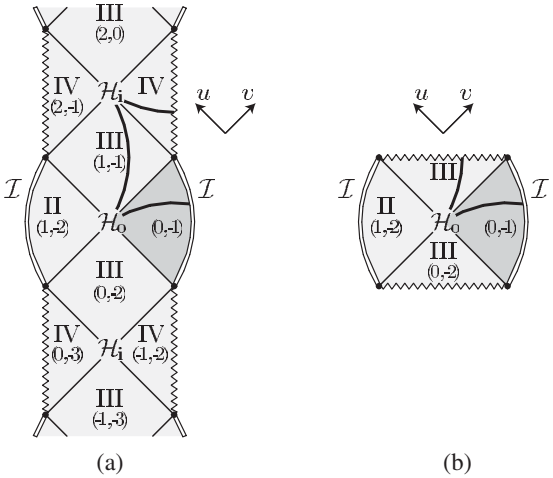

FIG. 2. The conformal diagrams of the sections $\xi, \varphi =$ constant for (a) charged and (b) uncharged C-metric with the acceleration $A < 1/\ell$. These diagrams are based on null coordinates u, v which grow in diagonal directions. Integers (m, n) in the diagrams, identifying different spacetime domains, are those from definition (2.15). Double lines represent conformal infinity $\mathcal{I}$ (cf. Eq. (3.12)), zigzag lines the singularity at $v = +\infty$, and thin diagonal lines the outer and inner black hole horizons $v = v_o$ and $v = v_i$, respectively. We can recognize familiar structure of the interior of Reissner-Nordström or Schwarzschild black holes, respectively, (domains III and IV). The exterior of the black holes is, however, asymptotically different—it has the asymptotics of anti-de Sitter universe. The whole spacetime consists of more exterior domains II which are connected (not necessary causally) with each other through the black holes. A more detailed diagram of a typical domain outside of the black hole (a darker area indicated above) can be found in Fig. 3(b). The thick line corresponds to a section $\tau =$ constant which is discussed in Fig. 1.

shape suggests that horizon is a null surface with null generators originating from the neck. Of course, the three-dimensional diagram does not have the nice feature of the two-dimensional conformal diagrams that each line with angle $\pi/4$ from the vertical is null; however, for Fig. 3(a) this feature still holds for lines in radial planes, i.e., it holds for generators of the black hole horizon.

In the weak field limit the black hole changes into a test particle. For such a transformation the diagram in Fig. 3(a) is not very intuitive—the black hole is represented there as an 'extended' object, and the qualitative shape of the horizon does not change with varying mass and charge. For this reason it is useful to draw another diagram in which the black hole horizon is deformed into a shape composed of two droplike surfaces, see Fig. 4. The conical form of the horizon from Fig. 3(a) is squeezed into more localized form, which in the limit of vanishing mass and charge shrinks into a world line of the particle—cf. Figure 13(b) in Sec. V.

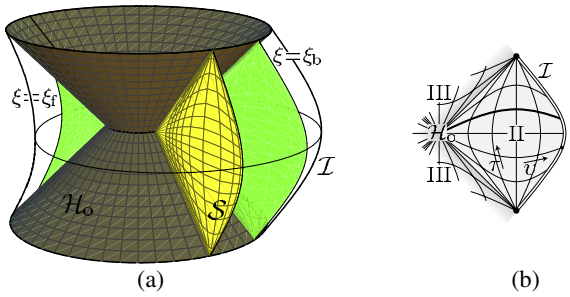

FIG. 3 (color online). (a) Three-dimensional representation of the *exterior* of the black hole accelerated in anti-de Sitter universe with acceleration smaller than $1/\ell$. The dark surface represents the outer black hole horizon $\mathcal{H}_o$, and the boundary of the diagram corresponds to the conformal infinity $\mathcal{I}$. Embeddings of a typical section $\xi =$ constant (section S) and of the axis $\xi = \xi_f$, ξ_b are shown. The nonsymmetric shape of the infinity reflects the fact that the coordinate system used is centered around the black hole which is moving with acceleration with respect to the infinity. (b) Two-dimensional conformal diagram of $\xi =$ constant section. Only the exterior of the black hole is shown (compare with Fig. 2). This part of the conformal diagram corresponds exactly to the section $\xi =$ constant indicated in the diagram on the left.

Because of the assumption $A < 1/\ell$, we cannot take a limit of a vanishing cosmological constant keeping $A \neq 0$. It is possible to set $A = 0$ first which leads to Reissner-Nordström–anti-de Sitter spacetime, cf. footnote 7. After that an appropriate limit of vanishing Λ gives a Reissner-Nordström metric representing a single unaccelerated black hole.

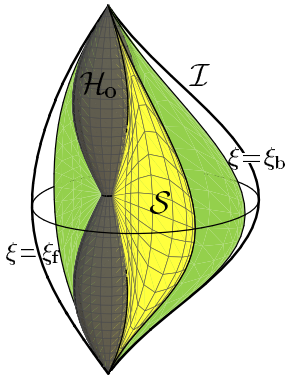

FIG. 4 (color online). Another three-dimensional representation of the exterior of the accelerated black hole with $A < 1/\ell$. The outer black hole horizon of a conical shape from Fig. 3(a) is here deformed to the surface of a shape of two joined drops. The black hole is thus represented as a localized object. Such a representation is useful for a study of the weak field limit when the black hole changes into the world line of a point particle.

IV. PAIRS OF ACCELERATED BLACK HOLES

A. Coordinate systems

Next we turn to the discussion of the more intricate case of the acceleration bigger than the critical one,

$$A > 1/\ell. \tag{4.1}$$

First, the coordinates $\mathfrak{t}$, $\mathfrak{y}$, $\mathfrak{x}$, ϕ and τ, ξ, υ, φ can be defined in an analogous way as in the previous section:

$$\begin{aligned} \tau &= \mathrm{sh}\alpha_\mathrm{o}\,\mathfrak{t} = \tanh\alpha_\mathrm{o}\, t, \qquad \upsilon = \frac{1}{\mathrm{sh}\alpha_\mathrm{o}}\mathfrak{y} = \coth\alpha_\mathrm{o}\, y, \\ \varphi &= \mathrm{ch}\alpha_\mathrm{o}\,\phi = \varphi, \qquad \xi = -\frac{1}{\mathrm{ch}\alpha_\mathrm{o}}\mathfrak{x} = -x. \end{aligned} \tag{4.2}$$

Ranges of the coordinates υ, ξ are indicated in Fig. 5. The acceleration is parametrized by the parameter $\alpha_\mathrm{o} \in \mathbb{R}^+$,

$$A = \frac{1}{\ell}\cosh\alpha_\mathrm{o}. \tag{4.3}$$

The metric functions in (2.7) and (2.8) are

$$\begin{aligned} -\mathcal{F} &= 1 - \upsilon^2 + 2\frac{m}{\ell}\mathrm{sh}\alpha_\mathrm{o}\,\upsilon^3 - \frac{e^2}{\ell^2}\mathrm{sh}^2\alpha_\mathrm{o}\,\upsilon^4, \\ \mathcal{G} &= 1 - \xi^2 + 2\frac{m}{\ell}\mathrm{ch}\alpha_\mathrm{o}\,\xi^3 - \frac{e^2}{\ell^2}\mathrm{ch}^2\alpha_\mathrm{o}\,\xi^4, \end{aligned} \tag{4.4}$$

$$\omega = \upsilon\mathrm{sh}\alpha_\mathrm{o} - \xi\mathrm{ch}\alpha_\mathrm{o}, \tag{4.5}$$

and

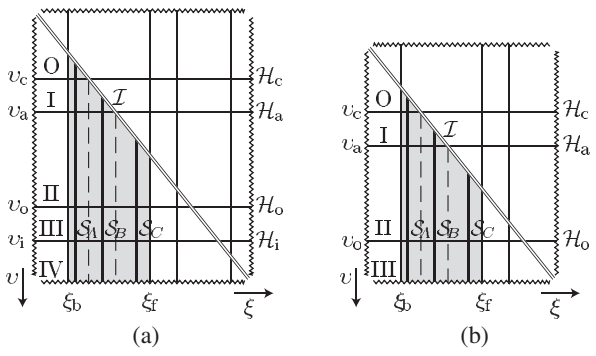

FIG. 5. Diagrams analogous to Fig. 1 in the case $A > 1/\ell$. The allowed range of coordinates υ, ξ (shaded area) is again restricted by the infinity (diagonal double line), by the axis (vertical border lines), and by the singularity (zigzag line). Additionally to outer and inner black hole horizons, acceleration and cosmological horizons (at $\upsilon = \upsilon_\mathrm{a}$ and $\upsilon = \upsilon_\mathrm{c}$) are also present. Horizons divide the allowed range into regions O–IV which corresponds to qualitatively different domains of spacetime; cf. Figure 6. Different sections ξ = constant cross different number of horizons. Typical representatives S_A, S_B, and S_C of these sections are indicated by thick vertical lines. They correspond to different shapes of the conformal diagrams in Fig. 6.

$$\begin{aligned} -\mathfrak{F} &= \mathrm{sh}^2\alpha_\mathrm{o} - \mathfrak{y}^2 + 2\frac{m}{\ell}\mathfrak{y}^3 - \frac{e^2}{\ell^2}\mathfrak{y}^4, \\ \mathfrak{G} &= \mathrm{ch}^2\alpha_\mathrm{o} - \mathfrak{x}^2 + 2\frac{m}{\ell}\mathfrak{x}^3 - \frac{e^2}{\ell^2}\mathfrak{x}^4. \end{aligned} \tag{4.6}$$

They are again related to the polynomial (3.8)

$$\begin{aligned} -\mathcal{F} &= -\mathrm{sh}^{-2}\chi_\mathrm{o}\,\mathfrak{F} = -\coth^2\chi_\mathrm{o}\,F \\ &= 1 + \frac{\ell^2}{\mathrm{sh}^2\alpha_\mathrm{o}} S\Big(\frac{\mathrm{sh}\alpha_\mathrm{o}}{\ell}\upsilon\Big), \\ \mathcal{G} &= \mathrm{ch}^{-2}\alpha_\mathrm{o}\mathfrak{G} = G = 1 + \frac{\ell^2}{\mathrm{ch}^2\alpha_\mathrm{o}} S\Big(\frac{\mathrm{ch}\alpha_\mathrm{o}}{\ell}\xi\Big). \end{aligned} \tag{4.7}$$

For the metric function $\mathcal{H}$, given by Eq. (2.11), we obtain

$$\mathcal{H} = 1 - \frac{R^2}{\ell^2} - \mathrm{sh}\alpha_\mathrm{o}\frac{2m}{R} + \mathrm{sh}^2\alpha_\mathrm{o}\frac{e^2}{R^2}. \tag{4.8}$$

Differential relations for the coordinates σ and ω are

$$\begin{aligned} \mathbf{d}\,\sigma &= \frac{\mathrm{ch}\alpha_\mathrm{o}}{\mathcal{F}}\mathbf{d}\upsilon + \frac{\mathrm{sh}\alpha_\mathrm{o}}{\mathcal{G}}\mathbf{d}\xi, \\ \mathbf{d}\omega &= -\mathrm{sh}\alpha_\mathrm{o}\mathbf{d}\upsilon + \mathrm{ch}\alpha_\mathrm{o}\mathbf{d}\xi, \end{aligned} \tag{4.9}$$

and the metric function ξ takes the form

$$\mathcal{E} = \mathcal{F}\mathrm{sh}^2\alpha_\mathrm{o} + \mathcal{G}\mathrm{ch}^2\alpha_\mathrm{o}. \tag{4.10}$$

B. Global structure

As in the previous case, we start with a discussion of the metric in accelerated static coordinates, Eq. (2.10). Near the outer and inner horizon (the smallest two zeros of $\mathcal{H}$), the metric function (4.8) has a similar behavior as the function (3.9). It means that we deal again with a black hole, and near (or inside of) the black hole we can apply the previous discussion. Namely, T is again a time coordinate for observers staying outside the black hole, R is a radial coordinate, and Θ, Φ are spherical-like angular coordinates. A similar interpretation holds for the coordinates τ, υ, ξ, φ. However, for $A > 1/\ell$ the metric function $\mathcal{H}$ (or, equivalently, $\mathcal{F}$, cf. Eq. (2.11)) has two additional zeros for $R = R_\mathrm{a}, R_\mathrm{c}$ ($\upsilon = \upsilon_\mathrm{a}, \upsilon_\mathrm{c}$, respectively), which correspond to acceleration and cosmological horizons. It means that we have to expect a more complicated structure of spacetime outside the black hole.

Indeed, from the ξ-υ diagram in Fig. 5 we see that new zeros divide the allowed range of coordinates into more regions O, I, II, III, and IV. An exact way how these domains can be reached through the horizons can be seen from the conformal diagrams of the sections ξ, φ = constant. However, in Fig. 5 we see that sections ξ, φ = constant can cross a different number of horizons, depending on the value of ξ, since they can reach the infinity, given in this case by

$$\upsilon = \coth\alpha_\mathrm{o}\,\xi, \tag{4.11}$$

before they cross the acceleration or cosmological horizons. There are three different generic classes of sections $\xi, \varphi =$ constant labeled S_A (sections crossing all horizons), S_B (sections which do not cross cosmological horizons), and S_C (which cross only black hole horizons). Special limiting cases are $\xi = \xi_c = v_c \tanh\alpha_o$ and $\xi = \xi_a = v_a \tanh\alpha_o$. For each of these sections a different shape of conformal diagram is obtained as can be found in Fig. 6. For section S_A the domain II outside a black hole is connected through the acceleration horizon to domains of type I which are connected through other acceleration horizons to another domain II with another black hole. The domain I is also connected through the cosmological horizon with two domains of type O. From these domains it is possible to reach another domain I, and so on.

The spacetime thus seems to describe a universe which at one moment contains a pair of black holes (domains III and IV) separated by the acceleration horizon (domains II and I), and at another moment does not contain any black hole (domains I and O)—see Fig. 6(a). However, the sections S_B do not contain domains O, and sections S_C do not even contain the domains I. How is it possible that one spacetime is described by three qualitatively different diagrams? And how is it possible that the spacetime with

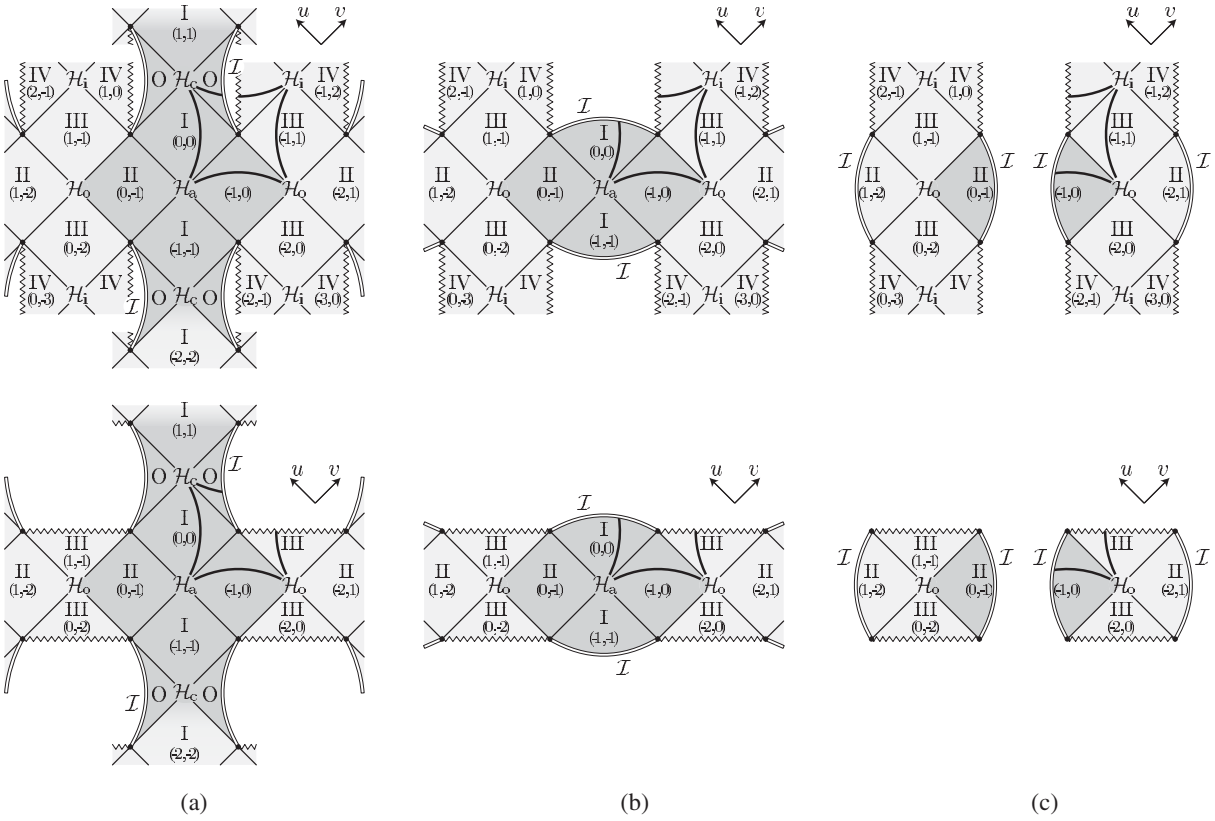

FIG. 6. The conformal diagrams of the sections $\xi, \varphi =$ constant for $A > 1/\ell$. The top diagrams are valid for $m, e \neq 0$, the bottom ones are for the uncharged case. The diagrams are based on coordinates u, v. Integers (m, n) from definition (2.15) identify different domains of the spacetime. Analogously to Fig. 2, double lines represent the infinity, zigzag lines the singularity, and diagonal lines the horizons. Domains O–II correspond to the exterior of black holes and domains III and IV to interiors of black holes. The interior has a similar causal structure to that of unaccelerated black holes. The spacetime contains more asymptotic domains, one of which is indicated by dark shading. The description below is from a point of view of this domain. Three different shapes of the diagrams correspond to the sections with a different value of the coordinate ξ. On the left, section S_A is spanned between two black holes which are moving with respect to each other along a common axis. It is also spanned between different pairs of such black holes through the domains O and I. In the middle, section S_B is spanned only between two black holes. It does not continue to the other pair of black hole because it intersects the conformal infinity in spacelike lines located inside domains I. The section S_C, depicted on the right, goes from each black hole directly into infinity—it does not connect different black holes through the exterior domains. These three sections correspond to thick vertical lines in Fig. 5. Thick lines in the diagrams above represent the section $\tau =$ constant, i.e., exactly the section discussed in Fig. 5. The embedding of these two-dimensional diagrams into spacetime is shown in Figs. 8–10. More detailed two-dimensional diagrams of the exterior of black holes (the dark area above) are also presented there.

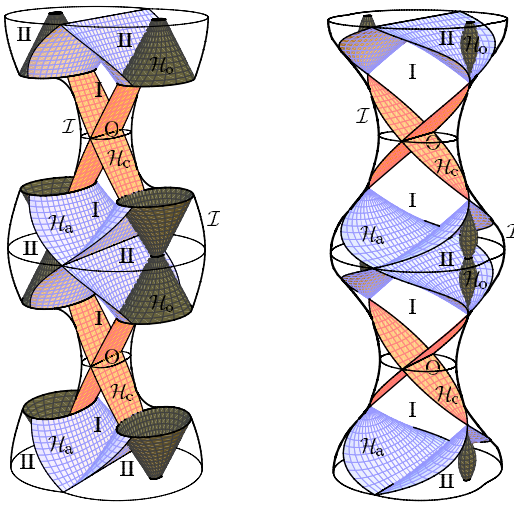

FIG. 7 (color online). Three-dimensional visualizations of the *exterior* of black holes which are moving with acceleration parameter $A > 1/\ell$ in asymptotically anti-de Sitter universe. The diagrams show a compactified picture of the whole universe—borders of the diagrams correspond to the conformal infinity. Diagram (a) is obtained by gluing together two-dimensional diagrams from Fig. 6. Black hole outer horizons $\mathcal{H}_o$ are represented by dark surfaces of a conical shape which indicates the null character of these surfaces. In the alternative representation (b), the black hole outer horizons are squeezed into droplike shapes. Such a representation shows the black hole as a localized object and it is useful in the weak field limit when the black hole changes to a pointlike particle—compare with Fig. 17(b). The universe represents a sequence of pairs of black holes which repeatedly enter and leave the universe through their timelike infinity—the diagrams should continue periodically in the vertical direction. Black holes of each pair are causally separated by the acceleration horizon $\mathcal{H}_a$; consequent pairs of black holes are separated by cosmological horizons $\mathcal{H}_c$. These are null surfaces—light cones of the entry points of black holes into the spacetime. Embedding of different types of two-dimensional conformal diagrams into the three-dimensional one is depicted in Figs. 8–10.

anti-de Sitter asymptotic has a conformal diagram with conformal infinity which looks spacelike as it occurs for sections S_B [see Fig. 6(b)]?

The answer can be given by drawing a three-dimensional diagram obtained by 'gluing' different sections of $\xi =$ constant together. The inspiration how to do it can be obtained by a study of accelerated static coordinates in empty anti-de Sitter universe as will be done in Sec. V. There we will learn that coordinates τ, υ, ξ, φ (or T, R, Θ, Φ) are sorts of bipolar coordinates—coordinates with two poles centered on two black holes. The coordinate R (respectively υ) is running through domain II from both black holes toward the acceleration horizon. It plays the role of a radial coordinate in domain II, but it changes its meaning into a time coordinate above and below the acceleration horizon, in domains of type I. It becomes again a space coordinate in domains O. The angular coordinates Θ, Φ (or ξ, φ) label different directions connecting the two holes. With this insight we can draw the three-dimensional diagrams reflecting the global structure of the universe, see Fig. 7. Embeddings of three typical surfaces $\xi, \varphi =$ constant into such a diagram are shown in Figs. 8–10. Here we can see an origin of different shapes of conformal diagrams.

The global picture of the universe is thus the following: into an empty anti-de Sitter-like universe (domains O and I) enters through the infinity $\mathcal{I}$ a pair of black holes (domains III and IV). The holes are flying toward each other (domains II) with deceleration until they stop and fly back to the infinity where they leave the universe. They are causally disconnected by the acceleration horizon. There follows a new phase without black holes (again, the domain I and O) followed by a new phase with a pair of black holes. Different pairs of black holes are separated by cosmological horizons.

Again, for the purpose of the weak field limit it is convenient to use a visualization with squeezed black hole horizons in Fig. 7(b). In this representation, the infinity has a shape which one would expect for asymptotically anti-de Sitter universe. The deformation of the infinity is related to the fact that we use coordinates centered around the black holes. Indeed, the black holes are drawn along straight lines in the vertical direction. As we will see in the next section, such a deformation of the

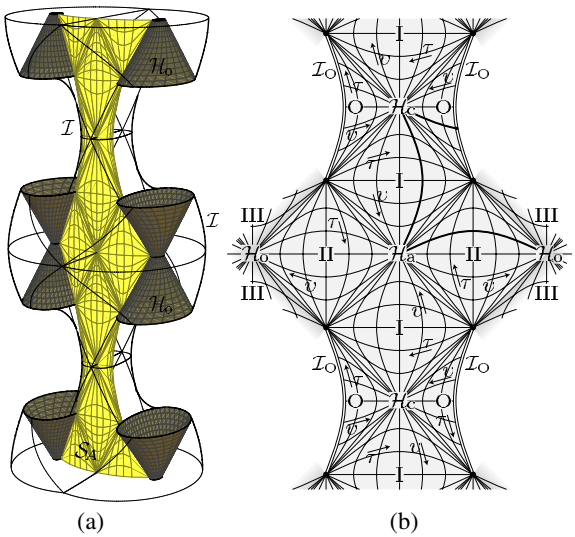

FIG. 8 (color online). (a) Embedding of section S_A [cf. Figs. 5 and 6(a)] into a three-dimensional representation of the C-metric spacetime. (b) The part of the two-dimensional conformal diagram of S_A representing the exterior of the black holes [corresponds to the dark area in Fig. 6(a)].

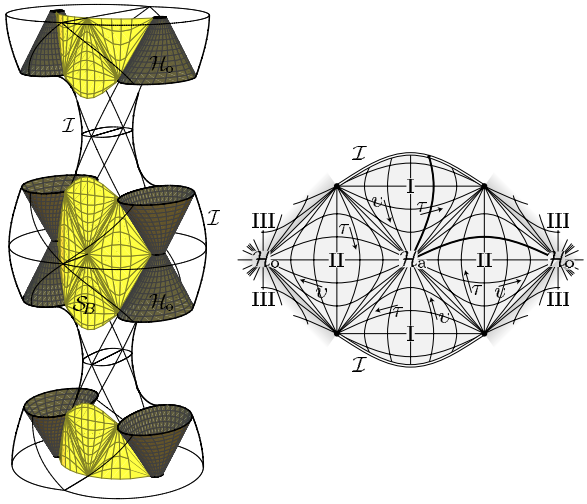

(a) (b)

FIG. 9 (color online). (a) Embedding of section S_B [cf. Figs. 5 and 6(b)] into a three-dimensional picture of spacetime. (b) The corresponding part of the two-dimensional conformal diagram of S_B [cf. the dark area in Fig. 6(b)].

infinity is obtained even for an empty anti-de Sitter universe if it is represented using accelerated coordinates.

In the case $A > 1/\ell$ there is no lower bound on the cosmological constant. An appropriate limit of vanishing Λ leads to C-metric spacetime with $\Lambda = 0$ representing a pair of accelerated black holes in the asymptotically flat universe.

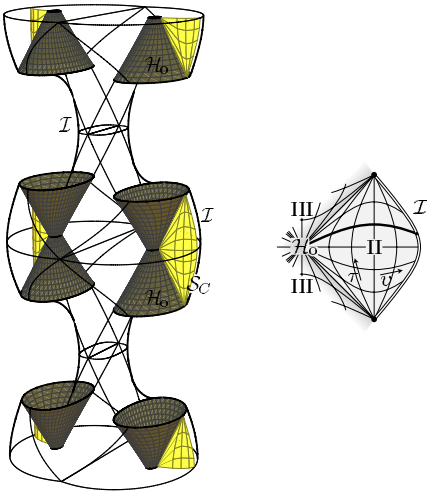

(a) (b)

FIG. 10 (color online). (a) Embedding of section S_C [cf. Fig. 5 and 6(c)] into a three-dimensional diagram. (b) The corresponding part of the two-dimensional conformal diagram of S_C [cf. the dark areas in Fig. 6(c)].

V. ANTI-DE SITTER UNIVERSE IN ACCELERATED COORDINATES

The spacetime (2.1) reduces to the anti-de Sitter universe for $m = 0$, $e = 0$. However, the limiting metric is not the anti-de Sitter metric in standard cosmological coordinates. Instead, it is the anti-de Sitter metric in so-called accelerated coordinates which prefer certain accelerated observers. These observers are remnants of the black holes. Investigating this form of the anti-de Sitter metric is useful for understanding of asymptotical structure of the C-metric universe, and of the nature of the coordinate systems used.

The anti-de Sitter metric can be written in cosmological spherical coordinates $\tilde{t}$, χ, ϑ, φ as

$$\mathbf{g}_{\text{AdS}} = \frac{\ell^2}{\cos^2\chi}(-\mathbf{d}\tilde{t} + \mathbf{d}\chi^2 + \sin^2\chi(\mathbf{d}\vartheta^2 + \sin^2\vartheta\mathbf{d}\varphi^2)). \tag{5.1}$$

They can be also called conformally Einstein because they are the standard coordinates on the conformally related Einstein universe. Another useful set of coordinates are cosmological cylindrical coordinates $\tilde{t}$, ζ, ρ, φ which redefine coordinates χ and ϑ. Surfaces $\tilde{t}, \rho =$ constant represent cylinders of constant distance from the axis, and surfaces $\tilde{t}, \zeta =$ constant are planes orthogonal to the axis. They are related to spherical coordinates by a rotation on the conformally related sphere of the Einstein universe by an angle $\pi/2$:

$$\begin{aligned} \cos\chi &= \cos\zeta\cos\rho, \qquad \sin\zeta = \sin\chi\cos\vartheta, \\ \tan\vartheta &= \cot\zeta\sin\rho, \qquad \tan\rho = \tan\chi\sin\vartheta. \end{aligned} \tag{5.2}$$

The metric in the cylindrical coordinates reads

$$\mathbf{g}_{\text{AdS}} = \frac{\ell^2}{\cos^2\zeta\cos^2\rho} \times (-\mathbf{d}\tilde{t}^2 + \mathbf{d}\zeta^2 + \cos^2\zeta(\mathbf{d}\rho^2 + \sin^2\rho\mathbf{d}\varphi^2)). \tag{5.3}$$

The anti-de Sitter universe admits four qualitatively different types of Killing vectors representing time translations, boosts, null boosts, and spatial rotations. Orbits of time translations and boosts correspond to world lines of observers with uniform acceleration. The limit of the C-metric is related exactly to these observers. The cases $A < 1/\ell$ and $A > 1/\ell$ correspond to time translation and boost Killing vectors respectively; the case $A = 1/\ell$ corresponds to a null boost Killing vector.

It is possible to introduce static coordinates associated with the Killing vector that is at least partially timelike. In the case of the time translation Killing vector, both cosmological spherical and cylindrical coordinates play the roles of such coordinates. It is also possible to rescale the

radial coordinate χ to obtain metric in 'standard static' form. Namely, defining static coordinates of type I

$$T_{\rm I} = \ell\tilde{t}, \quad R_{\rm I} = \ell\tan\chi, \quad \Theta_{\rm I} = \vartheta, \quad \Phi_{\rm I} = \varphi \tag{5.4}$$

we obtain

$$\mathbf{g}_{\rm AdS} = -\left(1+\frac{R_{\rm I}^2}{\ell^2}\right)\mathbf{d}T_{\rm I}^2 + \left(1+\frac{R_{\rm I}^2}{\ell^2}\right)^{-1}\mathbf{d}R_{\rm I}^2 + R_{\rm I}^2(\mathbf{d}\Theta_{\rm I}^2 + \sin^2\Theta_{\rm I}\mathbf{d}\Phi_{\rm I}^2). \tag{5.5}$$

Static coordinates of type II are associated with the boost Killing vector and can be related to the cosmological cylindrical coordinates

$$T_{\rm II} = \frac{\ell}{2}\log\left|\frac{\sin\tilde{t}-\sin\zeta}{\sin\tilde{t}+\sin\zeta}\right|, \qquad R_{\rm II} = \ell\frac{\cos\zeta}{\cos\tilde{t}}, \qquad \Theta_{\rm II} = \rho, \qquad \Phi_{\rm II} = \varphi, \tag{5.6}$$

leading to the metric

$$\mathbf{g}_{\rm AdS} = \frac{\ell^2}{R_{\rm II}^2\cos^2\Theta_{\rm II}}\left[-\left(1-\frac{R_{\rm II}^2}{\ell^2}\right)\mathbf{d}T_{\rm II}^2 + \left(1-\frac{R_{\rm II}^2}{\ell^2}\right)^{-1}\mathbf{d}R_{\rm II}^2 + R_{\rm II}^2(\mathbf{d}\Theta_{\rm II}^2 + \sin^2\Theta_{\rm II}\mathbf{d}\Phi_{\rm II}^2)\right]. \tag{5.7}$$

In the case of the full C-metric we do not have to use a different notation for coordinates defined in the case $A < 1/\ell$ and $A > 1/\ell$, because these two cases describe completely different spacetimes, and the coordinates cannot be mixed. However, in the weak field limit both cases describe one spacetime—anti-de Sitter universe—and we have a whole set of coordinate systems, parametrized by acceleration, living on this spacetime. To avoid a confusion, in the next two subsections we add a prime and subscript I (for $A < 1/\ell$) or II (for $A > 1/\ell$) to all coordinates introduced in the previous sections.[8] For example, accelerated static coordinates T, R, Θ, Φ will be renamed as $T'_{\rm I}$, $R'_{\rm I}$, $\Theta'_{\rm I}$, $\Phi'_{\rm I}$ or $T'_{\rm II}$, $R'_{\rm II}$, $\Theta'_{\rm II}$, $\Phi'_{\rm II}$ for small or large acceleration, respectively.

Let us note that for both cases $A \lessgtr 1/\ell$ in the weak field limit, the metric function $\mathcal{G}$ reduces to $\mathcal{G} = 1-\xi^2$ (see (3.4) and (4.4)). By integrating (2.9) we then get $\xi = -\cos\Theta$ and $\mathcal{G} = \sin^2\Theta$.

A. $A < 1/\ell$

In the limit of vanishing mass and charge, the metric (2.10) with $\mathcal{H}$ given by Eq. (3.9) takes the form

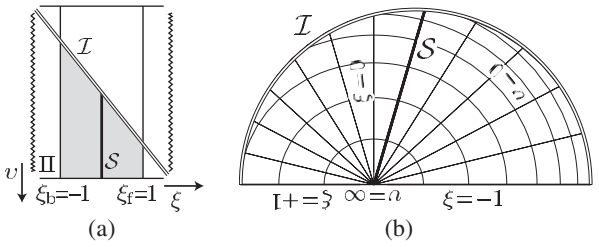

FIG. 11. A shaded region in diagram (a) indicates allowed ranges of coordinates $v \equiv v'_{\rm I} = \ell/R'_{\rm I} = \cot\chi'_{\rm I}$ and $\xi \equiv \xi'_{\rm I} = -\cos\Theta'_{\rm I} = -\cos\vartheta'_{\rm I}$. The diagonal double line corresponds to the infinity, vertical borders to the axis of symmetry, and the bottom line to the origin $\chi'_{\rm I} = 0$. The diagram (a) is an analogue of Fig. 1. However, this diagram does not respect the angular meaning of the ξ coordinate. A more natural representation (b) of the shaded region is obtained by shrinking the bottom line to a point, forming thus a deformed semicircle.

$$\mathbf{g} = \frac{\ell^2}{(\ell\cos\chi_{\rm o} + R'^2_{\rm I}\sin\chi_{\rm o}\cos\Theta'_{\rm I})^2}\left[-\left(1+\frac{R'^2_{\rm I}}{\ell^2}\right)\mathbf{d}T'^2_{\rm I} + \left(1+\frac{R'^2_{\rm I}}{\ell^2}\right)^{-1}\mathbf{d}R'^2_{\rm I} + R'^2_{\rm I}(\mathbf{d}\Theta'^2_{\rm I} + \sin^2\Theta'_{\rm I}\mathbf{d}\Phi'^2_{\rm I})\right]. \tag{5.8}$$

The allowed ranges of coordinates can be read from Fig. 11. For vanishing acceleration, $\chi_{\rm o} = 0$, the metric becomes exactly of the form (5.5); i.e., C-metric accelerated static coordinates become anti-de Sitter static coordinates of type I. For nonvanishing acceleration the form of the metric (5.8) differs from (5.5) by a scalar prefactor. However, we still claim that $\mathbf{g} = \mathbf{g}_{\rm AdS}$. The relation between coordinates $T_{\rm I}$, $R_{\rm I}$, $\Theta_{\rm I}$, $\Phi_{\rm I}$ and $T'_{\rm I}$, $R'_{\rm I}$, $\Theta'_{\rm I}$, $\Phi'_{\rm I}$ is thus a coordinate conformal transformation of anti-de Sitter space. It has a nice geometrical interpretation: if we define accelerated spherical coordinates of type I, $\tilde{t}'_{\rm I}$, $\chi'_{\rm I}$, $\vartheta'_{\rm I}$, $\varphi'_{\rm I}$, related to $T'_{\rm I}$, $R'_{\rm I}$, $\Theta'_{\rm I}$, $\Phi'_{\rm I}$ analogously to definition (5.4), these coordinates differ from $\tilde{t}$, χ, ϑ, φ only by a rotation of the Einstein sphere in the direction of the axis $\vartheta = \pi$ by the angle $\chi_{\rm o}$,

$$\tilde{t}'_{\rm I} = \tilde{t}, \qquad \cos\chi'_{\rm I} = \cos\chi_{\rm o}\cos\chi - \sin\chi_{\rm o}\sin\chi\cos\vartheta,$$
$$\varphi'_{\rm I} = \varphi, \qquad \cot\vartheta'_{\rm I} = \cos\chi_{\rm o}\cot\vartheta + \sin\chi_{\rm o}\cot\chi\sin^{-1}\vartheta. \tag{5.9}$$

Coordinates $\tilde{t}'_{\rm I}$, $\chi'_{\rm I}$, $\vartheta'_{\rm I}$, $\varphi'_{\rm I}$ are thus sort of spherical coordinates[9] centered on the observer given by $\chi = \chi_{\rm o}$, $\vartheta = \pi$. This observer remains eternally at a constant distance from the origin $\chi = 0$, and has a unique acceleration of magnitude $A = \sin\chi_{\rm o}$ which compensates for the cos-

[8] We use the subscript to distinguish two qualitatively different cases (although, we still have a hidden parametrization of the coordinate systems by the acceleration), and the prime to indicate a nontrivial acceleration. Corresponding unprimed coordinates refer to special values of the acceleration: $A = 0$ in the case I, and $A = 1/\ell$ in the case II. This notation is consistent with Ref. [36].

[9] They are spherical in the sense of conformally related Einstein universe.

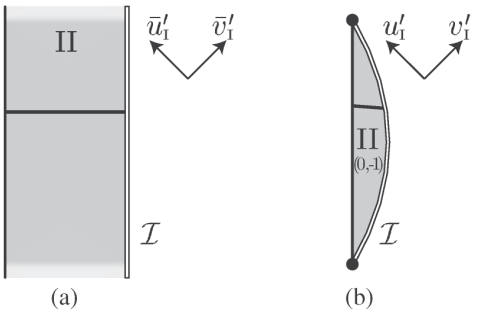

FIG. 12. Conformal diagrams of the section $\Theta'_{\rm I}$, $\Phi'_{\rm I}$ = constant (or, equivalently, $\vartheta'_{\rm I}$, $\varphi'_{\rm I}$ = constant). Diagram (a) is based on coordinates $\bar{u}'_{\rm I}$, $\bar{v}'_{\rm I}$. Horizontal and vertical lines are given by coordinate lines $\tilde{t}'_{\rm I}$ = constant and $\chi'_{\rm I}$ = constant, since for $m, e = 0$, definitions (2.13) and (2.14) give $\bar{u}'_{\rm I} = \chi'_{\rm I} + \tilde{t}'_{\rm I}$ and $\bar{v}'_{\rm I} = \chi'_{\rm I} - \tilde{t}'_{\rm I}$. The coordinate $\chi'_{\rm I}$ is a radial coordinate; the left border of the diagram thus corresponds to the world line of an accelerated observer at the origin. The right double line represents conformal infinity $\mathcal{I}$ (formed by limiting end points of spacelike and null geodetics). The diagram should continue infinitely in the vertical direction. (b) Compactified version of the same conformal diagram based on the coordinates $u'_{\rm I}$, $v'_{\rm I}$, related to $\bar{u}'_{\rm I}$, $\bar{v}'_{\rm I}$ by Eq. (2.15). The whole spacetime is here squeezed into a compact region which beside the conformal infinity includes also pointlike future and past infinities (limiting end points of timelike geodesics). This diagram is analogous to those in Fig. 2. An exact position of $\mathcal{I}$ depends on an angular direction of the plane of the diagram (i.e., on a value of coordinate $\vartheta'_{\rm I}$) through the relation $\tan\chi'_{\rm I} = -\ell\cot\chi_{\rm o}/\cos\vartheta'_{\rm I}$ [cf. Eq. (3.12)]. For $A = 0$ these diagrams reduce to the standard conformal diagrams based on the cosmological spherical coordinates.

mological compression of anti-de Sitter universe. For more details see [36].

Two-dimensional conformal diagrams of $T'_{\rm I}$-$R'_{\rm I}$ sections (i.e., of $\tilde{t}'_{\rm I}$-$\chi'_{\rm I}$ sections) can be found in Fig. 12. Three-dimensional diagrams obtained by gluing together two-dimensional sections with changing $\Theta'_{\rm I}$ are in Fig. 13. The diagram in Fig. 13(b) is clearly the limiting case of Fig. 4.

B. $A > 1/\ell$

In this case, the metric (2.10) with $\mathcal{H}$ given by Eq. (4.8) for vanishing mass and charge becomes

$$\mathbf{g} = \frac{\ell^2}{(\ell\,\mathrm{sh}\alpha_{\rm o} + R'_{\rm II}\mathrm{ch}\alpha_{\rm o}\cos\Theta'_{\rm II})^2} \times \left[-\left(1 - \frac{R'^2_{\rm II}}{\ell^2}\right)\mathbf{d}T'^2_{\rm II} + \left(1 - \frac{R'^2_{\rm II}}{\ell^2}\right)^{-1}\mathbf{d}R'^2_{\rm II} + R^2(\mathbf{d}\Theta'^2_{\rm II} + \sin^2\Theta'_{\rm II}\mathbf{d}\Phi'^2_{\rm II}) \right]. \quad (5.10)$$

The allowed range of coordinates $R'_{\rm II}$, $\Theta'_{\rm II}$ can be read from

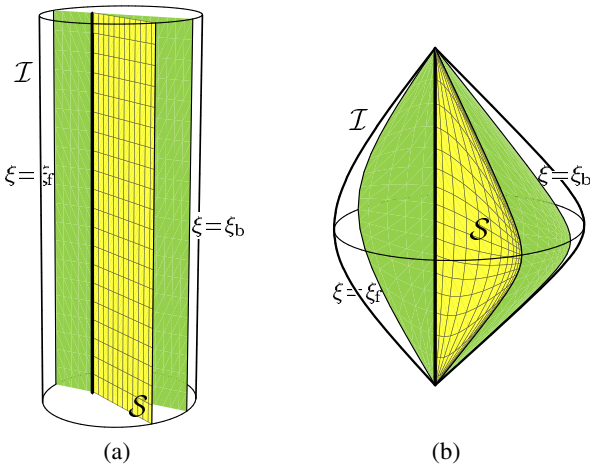

FIG. 13 (color online). Three-dimensional schematical diagrams of anti-de Sitter universe obtained by rotation (varying angular coordinate $\vartheta'_{\rm I}$) of two-dimensional diagrams from Fig. 12. The diagrams are centered on the world line of a static observer (thick line) which is accelerated with acceleration $A < 1/\ell$. The horizontal section $\tilde{t}$ = constant corresponds to two copies of Fig. 11(b) (one copy for $\varphi = 0$, another for $\varphi = \pi$).

Fig. 14. For $\alpha_{\rm o} = 0$ (i.e., in the limit $A \to 1/\ell$) we get exactly the metric (5.7). For nonzero $\alpha_{\rm o}$ both metrics (5.10) and (5.7) have the same form up to a scalar prefactor. However, as in the previous case, it is possible to find a transformation between $T'_{\rm II}$, $R'_{\rm II}$, $\Theta'_{\rm II}$, $\Phi'_{\rm II}$ and $T_{\rm II}$, $R_{\rm II}$, $\Theta_{\rm II}$, $\Phi_{\rm II}$ such that $\mathbf{g} = \mathbf{g}_{\rm AdS}$. First, we introduce accelerated spheri-

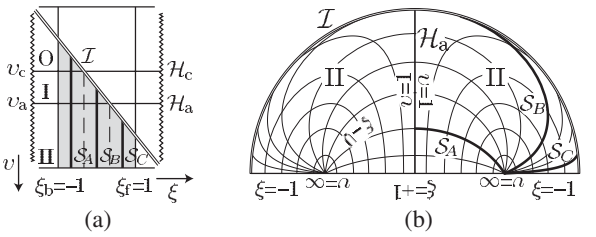

FIG. 14. A shaded region in diagram (a) represents the allowed range of coordinates $\upsilon \equiv \upsilon'_{\rm II} = \ell/R'_{\rm II}$ and $\xi \equiv \xi'_{\rm II} = -\cos\Theta'_{\rm II}$. The notation is the same as in Fig. 5, except there are no black hole horizons, and the bottom line does not represent a singularity but poles of the coordinates. Diagram (a) does not respect the bipolar nature of coordinates υ and ξ. A more accurate picture of region II is drawn in diagram (b). It depicts section $\tilde{t}, \varphi = 0$ through two spacetime domains of type II. Each of them contains one pole of the coordinate system. Both domains are separated by an acceleration horizon. The coordinate υ decreases from $\upsilon = +\infty$ at poles to $\upsilon = \upsilon_{\rm a}$ at the acceleration horizon, and the coordinate ξ labels different coordinate lines starting from the poles.

cal and cylindrical coordinates of type II, $\tilde{t}'_{\rm II}$, $\chi'_{\rm II}$, $\vartheta'_{\rm II}$, $\varphi'_{\rm II}$ and $\tilde{t}'_{\rm II}$, $\zeta'_{\rm II}$, $\rho'_{\rm II}$, $\varphi'_{\rm II}$, which are related to $T'_{\rm II}$, $R'_{\rm II}$, $\Theta'_{\rm II}$, $\Phi'_{\rm II}$ as $\tilde{t}$, χ, ϑ, φ and $\tilde{t}$, ζ, ρ, φ are related to $T_{\rm II}$, $R_{\rm II}$, $\Theta_{\rm II}$, $\Phi_{\rm II}$, i.e., by the relations (5.2) and (5.6). Transformations between cosmological and accelerated coordinates then are

$$\begin{aligned}\cot\tilde{t}'_{\rm II} &= \frac{{\rm ch}\alpha_{\rm o}\cos\tilde{t} - {\rm sh}\alpha_{\rm o}\cos\chi}{\sin\tilde{t}},\\ \cot\chi'_{\rm II} &= \frac{-{\rm sh}\alpha_{\rm o}\cos\tilde{t} + {\rm ch}\alpha_{\rm o}\cos\chi}{\sin\chi},\\ \vartheta'_{\rm II} &= \vartheta, \qquad \varphi'_{\rm II} = \varphi.\end{aligned} \tag{5.11}$$

It is interesting, that these transformations leave angular coordinates untouched. It means that they are a time dependent *radial* 'sqeezing' of anti-de Sitter universe; see Fig. 15.

Surprisingly, if we compose all partial transformations between $T'_{\rm II}$, $R'_{\rm II}$, $\Theta'_{\rm II}$, $\Phi'_{\rm II}$ and $T_{\rm II}$, $R_{\rm II}$, $\Theta_{\rm II}$, $\Phi_{\rm II}$ together, the resulting transformation is such that $T'_{\rm II} = T_{\rm II}$ and $\Phi'_{\rm II} = \Phi_{\rm II}$, see Ref. [36]—time surfaces of both the static coordinates of type II and of the accelerated static coordinates are the same.

Now, let us study global null coordinates $u_{\rm II}$, $v_{\rm II}$ related to the static coordinates of type II $T_{\rm II}$, $R_{\rm II}$ by the relations (2.14) and (2.15). With vanishing mass and charge (and setting $\delta = 1/2$ in (2.15)) these definitions give

$$\begin{aligned}&u_{\rm II} = \tilde{t} - \zeta, \qquad \Theta_{\rm II} = \rho, \qquad v_{\rm II} = \tilde{t} + \zeta,\\ &\Phi_{\rm II} = \varphi.\end{aligned} \tag{5.12}$$

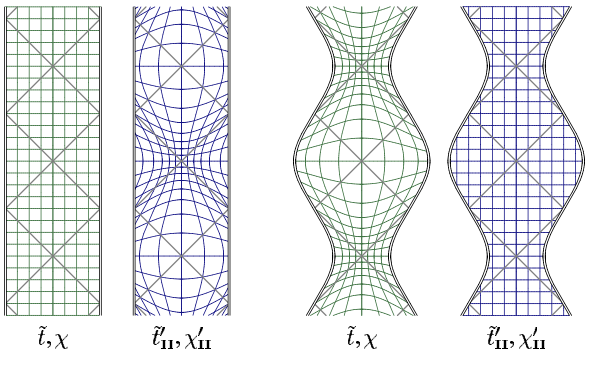

FIG. 15 (color online). Cosmological spherical coordinates $\tilde{t}$, χ and accelerated spherical coordinates $\tilde{t}'_{\rm II}$, $\chi'_{\rm II}$ drawn on a two-dimensional section of anti-de Sitter universe. The coordinate systems are related by the 'squeezing transformation' (5.11). Left: Coordinate lines of both systems drawn in such a way that lines $\tilde{t}$ = constant and χ = constant are horizontal and vertical, respectively. Right: A complementary representation with vertical and horizontal lines given by coordinate system $\tilde{t}'_{\rm II}$, $\chi'_{\rm II}$. The conformal infinity is given by $\chi = \pi/2$ and is thus deformed in the squeezed diagram on the right.

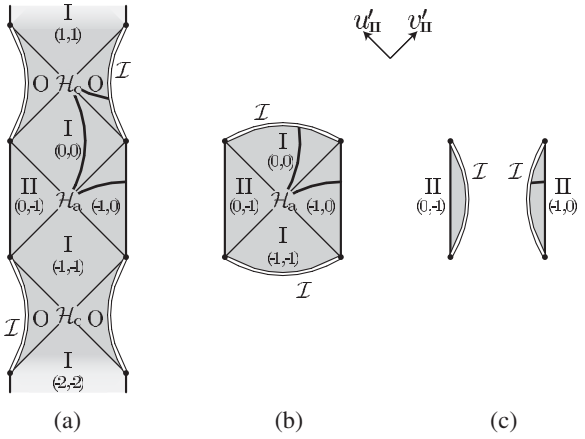

FIG. 16. The conformal diagrams of sections $\xi'_{\rm II}$, $\varphi'_{\rm II}$ = constant (or, equivalently, $\rho'_{\rm II}$, $\varphi'_{\rm II}$ = constant) for different values of $\xi \equiv \xi'_{\rm II}$. The diagrams are based on null coordinates $u'_{\rm II}$, $v'_{\rm II}$. They are spanned between two poles which correspond to observers with uniform acceleration $A > 1/\ell$ (straight vertical lines on the border of the diagrams, cf. also Fig. 17 for the three-dimensional localization of the poles). Three different shapes of the diagrams correspond to qualitatively different possibilities of how sections $\xi'_{\rm II}$, $\varphi'_{\rm II}$ = constant are embedded into the anti-de Sitter universe. They correspond to the three sections ξ = constant indicated in Fig. 14. Diagonal lines represent acceleration and cosmological horizons. The acceleration horizon causally separates both poles. It is formed by future light cones of points where the poles enter the anti-de Sitter universe. The cosmological horizon is formed by future light cones of points where the poles leave the universe. The thick line is an example of $\upsilon \equiv \upsilon'_{\rm II}$ = constant section—it corresponds to the diagram in Fig. 11. Gluing together diagram (a) for $\xi'_{\rm II} = -1$ (the axis $\rho'_{\rm II} = \Theta'_{\rm II} = 0$ between poles) with diagram (c) for $\xi'_{\rm II} = +1$ (the axis $\rho'_{\rm II} = \Theta'_{\rm II} = \pi$) gives the history of the whole axis of symmetry. It is the same section as that depicted in Fig. 15.

Horizontal and vertical lines of the conformal diagram based on $u_{\rm II}$, $v_{\rm II}$ are thus coordinate lines $\tilde{t}$ = constant and ζ = constant. The surface of this conformal diagram, i.e., the surface ρ, φ = constant, is a history of a line with a constant distance from the axis of symmetry. All such lines have common limiting end points $\zeta = \pm\pi/2$ located at the infinity of the anti-de Sitter universe. We will call them poles of the cylindrical coordinates.[10]

The conformal diagrams constructed in Sec. IV are based on coordinates $u'_{\rm II}$, $v'_{\rm II}$, i.e., on an 'accelerated'

[10]Lines of constant distance from the axis are not geodesics (except the axis itself) in the sense of the Lobachevsky geometry of the spatial section $\tilde{t}$ = constant. However, in the conformally related spherical geometry of the spatial section of Einstein universe, these lines are meridians with common poles. These two poles lie on the boundary of the hemisphere which corresponds to the Lobachevsky plane, i.e., at its infinity.

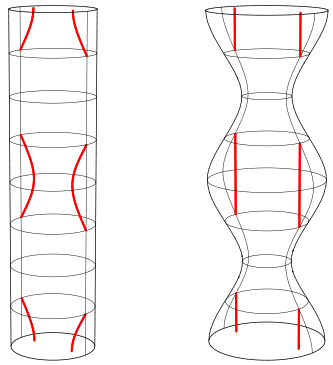

(a) (b)

FIG. 17 (color online). Three-dimensional representations of anti-de Sitter universe based (a) on cosmological coordinates $\tilde{t}$, χ, ϑ, φ and (b) on 'squeezed' accelerated coordinates $\tilde{t}'_{\rm II}$, $\chi'_{\rm II}$, $\vartheta'_{\rm II}$, $\varphi'_{\rm II}$. They can be obtained by a rotation of the corresponding diagrams from Fig. 15. Alternatively, they can be constructed by gluing together two-dimensional diagrams from Fig. 16. These are spanned between world lines of poles moving with the uniform acceleration $A = 1/\ell$ along the axis. World lines of the poles are indicated in the diagrams by thick lines. A pair of the poles enter anti-de Sitter universe through the conformal infinity, they approach each other, and then return back to the infinity—all this in a finite cosmological time $\Delta\tilde{t} = \pi$. After a stage without poles, a new pair of poles enters the universe, and so on. The diagram (b) is clearly the limit of Fig. 7(b) in which the black holes are shrunk to the accelerated particles located at the poles.

version of u, v discussed in the previous paragraph. For $m, e = 0$, these diagrams are depicted in Fig. 16. Different sections $\rho'_{\rm II}$, $\varphi'_{\rm II} =$ constant again correspond to histories of curves which end at common poles $\zeta'_{\rm II} = \pm\pi/2$. However, the infinity of the anti-de Sitter universe in accelerated cylindrical coordinates is given by (cf. (4.11))

$$\cos\zeta'_{\rm II}\cos\rho'_{\rm II} = -\tanh\alpha_{\rm o}\cos\tilde{t}'_{\rm II}\,. \qquad (5.13)$$

The poles thus, in general, do not lie at the infinity. Coordinates $\tilde{t}'_{\rm II}$, $\zeta'_{\rm II}$, $\rho'_{\rm II}$, $\varphi'_{\rm II}$ are sort of 'bipolar coordinates' with poles which correspond to the observers with acceleration $A > 1/\ell$; see Fig. 11(b). These observers, however, do not remain in anti-de Sitter universe eternally. Their histories periodically enter and leave the spacetime as shown in Fig. 17. The section $\rho'_{\rm II}$, $\varphi'_{\rm II} =$ constant, spanned between the poles, intersect anti-de Sitter universe in various ways, depending on a value of $\rho'_{\rm II}$. Different intersections lead to qualitatively different conformal diagrams in Fig. 16. This is in the agreement with analogous discussion in Sec. IV.

ACKNOWLEDGMENTS

The work was supported in part by program 360/2005 of Ministry of Education, Youth and Sports of Czech Republic. The author is grateful for kind hospitality at the Division of Geometric Analysis and Gravitation, Albert Einstein Institute, Golm, Germany, and the Department of Physics, University of Alberta, Edmonton, Canada where this work was partially done. He also thanks Don N. Page for reading the manuscript.

[1] J. Bičák and B. G. Schmidt, Phys. Rev. D **40**, 1827 (1989).
[2] T. Levi-Civita, Atti Accad. Naz. Lincei, Cl. Sci. Fis., Mat. Nat. Rend. **26**, 307 (1917).
[3] H. Weyl, Ann. Phys. (Berlin) **59**, 185 (1918).
[4] J. Ehlers and W. Kundt, in *Gravitation: an Introduction to Current Research*, edited by L. Witten (John Wiley, New York, 1962), p. 49.
[5] W. Kinnersley and M. Walker, Phys. Rev. D **2**, 1359 (1970).
[6] A. Ashtekar and T. Dray, Commun. Math. Phys. **79**, 581 (1981).
[7] W. B. Bonnor, Gen. Relativ. Gravit. **15**, 535 (1983).
[8] J. Bičák and V. Pravda, Phys. Rev. D **60**, 044004 (1999).
[9] P. S. Letelier and S. R. Oliveira, Phys. Rev. D **64**, 064005 (2001).
[10] V. Pravda and A. Pravdová, Czech. J. Phys. **50**, 333 (2000).
[11] K. Hong and E. Teo, Classical Quantum Gravity **20**, 3269 (2003).
[12] K. Hong and E. Teo, Classical Quantum Gravity **22**, 109 (2005).
[13] J. B. Griffiths and J. Podolsky, Classical Quantum Gravity **22**, 3467 (2005).
[14] J. Plebański and M. Demiański, Ann. Phys. (N.Y.) **98**, 98 (1976).
[15] B. Carter, Commun. Math. Phys. **10**, 280 (1968).
[16] R. Debever, Bull. Soc. Math. Belg. **23**, 360 (1971).
[17] J. Podolský and J. B. Griffiths, Phys. Rev. D **63**, 024006 (2001).
[18] O. J. C. Dias and J. P. S. Lemos, Phys. Rev. D **67**, 084018 (2003).
[19] P. Krtouš and J. Podolský, Phys. Rev. D **68**, 024005 (2003).
[20] J. Podolský, Czech. J. Phys. **52**, 1 (2002).
[21] O. J. C. Dias and J. P. S. Lemos, Phys. Rev. D **67**, 064001 (2003).
[22] J. Podolský, M. Ortaggio, and P. Krtouš, Phys. Rev. D **68**, 124004 (2003).
[23] O. J. C. Dias and J. P. S. Lemos, Phys. Rev. D **68**, 104010 (2003).

[24] R. Emparan, G. T. Horowitz, and R. C. Myers, J. High Energy Phys. 01 (2000) 007.
[25] A. Chamblin, Classical Quantum Gravity **18**, L17 (2001).
[26] R. Emparan, G. T. Horowitz, and R. C. Myers, J. High Energy Phys. 01 (2000) 021.
[27] P. Krtouš and J. Podolský, Classical Quantum Gravity **21**, R233 (2004).
[28] P. Krtouš and J. Podolský, Czech. J. Phys. **55**, 119 (2005).
[29] R. Emparan, Phys. Rev. Lett. **75**, 3386 (1995).
[30] R. Emparan, Phys. Rev. D **52**, 6976 (1995).
[31] R. B. Mann, Classical Quantum Gravity **14**, L109 (1997).
[32] I. S. Booth and R. B. Mann, Nucl. Phys. **B539**, 267 (1999).
[33] O. J. C. Dias and J. P. S. Lemos, Phys. Rev. D **69**, 084006 (2004).
[34] O. J. C. Dias, Phys. Rev. D **70**, 024007 (2004).
[35] J. Bičák and P. Krtouš, J. Math. Phys. (N.Y.) **46**, 102504 (2005).
[36] P. Krtouš, in preparation.
[37] P. Sládek and P. Krtouš, in preparation.
[38] P. Krtouš, Accelerated black holes, web presentation at http://utf.mff.cuni.cz/~krtous/physics.

Asymptotic structure of radiation in higher dimensions

Pavel Krtouš and Jiří Podolský

Institute of Theoretical Physics, Faculty of Mathematics and Physics,
Charles University in Prague,
V Holešovičkách 2, 180 00 Prague 8, Czech Republic

E-mail: Pavel.Krtous@mff.cuni.cz, Jiri.Podolsky@mff.cuni.cz

Abstract. We characterize a general gravitational field near conformal infinity (null, spacelike, or timelike) in spacetimes of any dimension. This is based on an explicit evaluation of the dependence of the radiative component of the Weyl tensor on the null direction from which infinity is approached. The behaviour similar to peeling property is recovered, and it is shown that the directional structure of radiation has a universal character that is determined by the algebraic type of the spacetime. This is a natural generalization of analogous results obtained previously in the four-dimensional case.

Submitted to: *Class. Quantum Grav.*

PACS numbers: 04.20.Ha, 04.50.+h, 98.80.Jk

1. Introduction

There has been a growing interest in studies of higher dimensional spacetimes, mainly motivated by finding particular models in the contexts of string theory and brane cosmology. However, some fundamental questions such as the mathematical classification of manifolds based on the algebraic structure of the Riemann and Weyl tensor, or investigation of the asymptotic behaviour of fields in higher dimensions have only recently been initiated [1–6].

As a contribution to this topic, in the present work we study asymptotic properties of a gravitational field as represented by the Weyl tensor in an arbitrary dimension. In particular, we analyze the directional structure at conformal infinity of the leading component of the field which corresponds to radiation. In fact, this is a natural extension of our previous work [7–10] in which we completely described the asymptotic directional structure of radiation in four-dimensional spacetimes with conformal infinity of any character (null, spacelike, or timelike). We demonstrated that this directional structure has universal properties that are basically given by the algebraic type of given spacetime, namely the degeneracy and orientation of principal null directions of the Weyl tensor. In the present article we show that these results—which are valid in standard $n = 4$ general relativity—can be directly generalized to higher dimensional spacetimes. Below we prove that the asymptotic directional structure of gravitational radiation in any dimension is given by the specific properties of Weyl aligned null directions at conformal infinity, i.e., by algebraic type of spacetime at infinity.

The paper is organized as follows. In section 2 we introduce necessary geometrical concepts and objects, and we set up the notation. In section 3 we first summarize the algebraic classification of the Weyl tensor in higher dimensions, and then we derive the expression which explicitly describes the behaviour of the field at conformal infinity. Subsequently, we discuss the directional structure of radiation in case of null, spacelike, and timelike infinity, in particular for the simplest algebraically special spacetimes. In the appendix, the relation between the higher-dimensional formalism used and the standard NP formalism in $n = 4$ is presented.

For brevity, we refer to equations of the review paper [9] directly as, e.g., (R2.13).

2. Geometrical preliminaries

2.1. Conformal infinity and null geodesics

First, we briefly review the context in which we study the asymptotic behaviour of the gravitational field. For details see the introductory section 2 of [9], where the discussion was not restricted to a particular number of dimensions.

We wish to study spacetimes with a conformal infinity. We therefore assume existence of an extension of the spacetime to an auxiliary manifold with metric $\tilde{\mathbf{g}}$ to which the physical metric $\mathbf{g}$ is (at least locally) conformaly related by $\tilde{\mathbf{g}} = \Omega^2\mathbf{g}$. In the physical spacetime, the conformal factor Ω is positive; the hypersurface $\Omega = 0$ corresponds to the spacetime infinity—called *conformal infinity* $\mathcal{I}$. We assume regularity of the conformal geometry across $\mathcal{I}$, even though it is known that in higher dimensions this is a more subtle issue than in the case $n = 4$, cf. [4,5]. We will return to this question shortly in section 3.3.

We introduce a vector $\mathbf{n}$ normal to $\mathcal{I}$, $\mathbf{n} \propto \mathbf{d}\Omega$, normalized using the physical

metric,[2] $\mathbf{n}\cdot\mathbf{n}=\sigma$, where the constant factor σ indicates the character of infinity: $\sigma=-1$ for spacelike $\mathcal{I}$, $\sigma=0$ for mull $\mathcal{I}$, and $\sigma=+1$ for timelike $\mathcal{I}$. From Einstein's field equations, assuming a vanishing trace of the energy-momentum tensor, it follows [9,11] that the character of infinity is correlated with the sign of cosmological constant, $\sigma=-\operatorname{sign}\Lambda$.

By radiative component we understand the leading component of the field measured with respect of a specific frame along a future oriented *null* geodesic $z(\eta)$ approaching $\mathcal{I}$. We are interested in the dependence of such a component on a *direction* along which infinity is approached. To compare the field along different geodesics, we have to fix the normalization of the affine parameter of these geodesics. We require that the projection of the tangent vector of the geodesic to $\mathbf{n}$ is independent of the direction of the geodesic. Using the relation to conformal geometry it can be shown (see (R2.13), (R2.14)) that near the infinity we have

$$\frac{d\,\Omega}{d\,\eta}\approx-\epsilon\,\Omega^2\,. \tag{2.1}$$

Here, the sign ϵ characterizes the orientation of the geodesic with respect to conformal infinity:

$$\epsilon=\begin{cases}+1: & \text{for } \textit{outgoing geodesics}, \quad \eta\to+\infty \text{ on } \mathcal{I},\\ -1: & \text{for } \textit{ingoing geodesics}, \quad \eta\to-\infty \text{ on } \mathcal{I}.\end{cases} \tag{2.2}$$

From (2.1) it follows that

$$\Omega=\epsilon\,\eta^{-1}+\dots\,. \tag{2.3}$$

2.2. Null frames and their transformations

In four dimensions, it is convenient to introduce complex null tetrads (R3.1). In the case of higher dimensions, we have to choose a slightly different normalization of the vectors of a real frame. Following [3], we call the frame $\mathbf{k}$, $\mathbf{l}$, $\mathbf{m}_i$ the *null frame* if $\mathbf{k}$, $\mathbf{l}$ are future oriented null vectors, and $\mathbf{m}_i$, $i=1,2,\dots,n-2$, are spatial real vectors satisfying

$$\mathbf{k}\cdot\mathbf{l}=-1\,,\quad \mathbf{k}\cdot\mathbf{m}_i=0\,,\quad \mathbf{l}\cdot\mathbf{m}_i=0\,,\quad \mathbf{m}_i\cdot\mathbf{m}_j=\delta_{ij}\,. \tag{2.4}$$

We use indices $a,b,c,\dots$ to refer to all spacetime dimensions, and indices $i,j,k,\dots=1,2,\dots,n-2$ to label spatial directions orthogonal to $\mathbf{k},\mathbf{l}$. Thanks to the orthonormality relation (2.4), components of any spatial vector $\mathbf{V}$ spanned on the vectors $\mathbf{m}_i$, i.e. $\mathbf{V}=V^i\mathbf{m}_i$, satisfy $V^i=V_i$. We also use a standard shorthand for square of the magnitude $|V|^2=\mathbf{V}\cdot\mathbf{V}=V^iV_i$.

We denote the vectors of an associated *orthonormal frame* as $\mathbf{t}$, $\mathbf{q}$, $\mathbf{m}_i$, where

$$\mathbf{t}=\tfrac{1}{\sqrt{2}}(\mathbf{k}+\mathbf{l})\,,\quad \mathbf{q}=\tfrac{1}{\sqrt{2}}(\mathbf{k}-\mathbf{l})\,. \tag{2.5}$$

We will distinguish different null frames by an additional lower roman index. For example, below in section 2.3 we will introduce *reference frame* denoted as $\mathbf{k}_{\mathrm{o}}$, $\mathbf{l}_{\mathrm{o}}$, $\mathbf{m}_{\mathrm{o}i}$.

[2] The dot '$\cdot$' denotes a scalar product defined by the physical metric $\mathbf{g}$. Strictly speaking, at infinity we should define a normal $\tilde{\mathbf{n}}$ normalized using conformal geometry to which the vector $\mathbf{n}$ is related by rescaling by Ω (which degenerates on $\mathcal{I}$). However, it is common to use formally the normal $\mathbf{n}$—see discussion in [9].

General transformations between different null frames can be composed from the following simple Lorentz transformations:

- *null rotation with* $\mathbf{k}$ *fixed* (parametrized by a spatial vector $\mathbf{L} = L^i\mathbf{m}_i$):[3]

$$\mathbf{k} = \mathbf{k}_\mathrm{o} , \qquad \mathbf{l} = \mathbf{l}_\mathrm{o} + \sqrt{2}L^i\mathbf{m}_{\mathrm{o}i} + |L|^2\,\mathbf{k}_\mathrm{o} , \qquad \mathbf{m}_i = \mathbf{m}_{\mathrm{o}i} + \sqrt{2}\,L_i\,\mathbf{k}_\mathrm{o} , \tag{2.6}$$

- *null rotation with* $\mathbf{l}$ *fixed* (parametrized by a vector $\mathbf{K} = K^i\mathbf{m}_i$):

$$\mathbf{k} = \mathbf{k}_\mathrm{o} + \sqrt{2}K^i\mathbf{m}_{\mathrm{o}i} + |K|^2\,\mathbf{l}_\mathrm{o} , \qquad \mathbf{l} = \mathbf{l}_\mathrm{o} , \qquad \mathbf{m}_i = \mathbf{m}_{\mathrm{o}i} + \sqrt{2}\,K_i\,\mathbf{l}_\mathrm{o} , \tag{2.7}$$

- *boost in the* $\mathbf{k}$-$\mathbf{l}$ *plane* (parametrized by a real number B):

$$\mathbf{k} = B\,\mathbf{k}_\mathrm{o} , \qquad \mathbf{l} = B^{-1}\,\mathbf{l}_\mathrm{o} , \qquad \mathbf{m}_i = \mathbf{m}_{\mathrm{o}i} , \tag{2.8}$$

- *spatial rotation in the space spaned on* $\mathbf{m}_i$ (parametrized by an orthogonal matrix ${\Phi_i}^j$):

$$\mathbf{k} = \mathbf{k}_\mathrm{o} , \qquad \mathbf{l} = \mathbf{l}_\mathrm{o} , \qquad \mathbf{m}_i = {\Phi_i}^j\,\mathbf{m}_{\mathrm{o}j} , \qquad \text{with} \quad {\Phi_i}^j\,{\Phi_k}^l\,\delta_{jl} = \delta_{ik} . \tag{2.9}$$

We say that a null frame is *adjusted to conformal infinity* $\mathcal{I}$ if the null vectors $\mathbf{k}$ and $\mathbf{l}$ on $\mathcal{I}$ are coplanar with normal $\mathbf{n}$ to the conformal infinity, and they satisfy the relation

$$\mathbf{n} = \epsilon\tfrac{1}{\sqrt{2}}(-\sigma\mathbf{k} + \mathbf{l}) , \qquad \text{where} \quad \epsilon = \pm 1 . \tag{2.10}$$

It follows that for a spacelike infinity ($\sigma = -1$) $\mathbf{n} = \epsilon\,\mathbf{t}$, for a timelike $\mathcal{I}$ ($\sigma = +1$) $\mathbf{n} = -\epsilon\,\mathbf{q}$, and $\mathbf{n} = \epsilon\,\mathbf{l}/\sqrt{2}$ for null $\mathcal{I}$ ($\sigma = 0$). Clearly, the vectors $\mathbf{m}_i$ of the adjusted frame are tangent to $\mathcal{I}$. If the null vector $\mathbf{k}$ is oriented along the null geodesic $z(\eta)$, the parameter ϵ indicates whether the geodesic is outgoing ($\epsilon = +1$) or ingoing ($\epsilon = -1$) (cf. fig. 2 of [9]).

2.3. The reference frame and parametrization of null directions

To parametrize a null direction along which $\mathcal{I}$ is approached, we fix at conformal infinity a reference frame $\mathbf{k}_\mathrm{o}$, $\mathbf{l}_\mathrm{o}$, $\mathbf{m}_{\mathrm{o}i}$. We require that this is adjusted to infinity in the sense of (2.10) and that it is smooth[4] along $\mathcal{I}$.

In view of (2.7), with respect to the reference frame, a null direction along a future oriented vector $\mathbf{k}$ can be parametrized by a spatial vector $\mathbf{R} = R^i\,\mathbf{m}_{\mathrm{o}i}$ which is orthogonal to $\mathbf{k}_\mathrm{o}$, $\mathbf{l}_\mathrm{o}$:

$$\mathbf{k} \propto \mathbf{k}_\mathrm{o} + \sqrt{2}\,\mathbf{R} + |R|^2\,\mathbf{l}_\mathrm{o} . \tag{2.11}$$

Consequently, the null direction $\mathbf{k}$ projected onto a space orthogonal to $\mathbf{t}_\mathrm{o}$ (cf. (R5.5)) can be represented by a unit spatial vector $\mathbf{q}$

$$\mathbf{q} = \frac{1}{1 + |R|^2}\big((1 - |R|^2)\,\mathbf{q}_\mathrm{o} + 2\,\mathbf{R}\big) . \tag{2.12}$$

[3] Note that our parametrization of null rotations differs from that used in [3] by factor $\sqrt{2}$.
[4] Again, at infinity we should define the frame normalized in conformal geometry to which the frame $\mathbf{k}_\mathrm{o}$, $\mathbf{l}_\mathrm{o}$, $\mathbf{m}_{\mathrm{o}i}$ is related by isotropic rescaling by Ω—see the related discussion in [9].

The vector $\mathbf{R}$ is a thus a *stereographic representation* of the vector $\mathbf{q}$, and hence of $\mathbf{k}$. Indeed, if we introduce an angle θ between $\mathbf{q}_\mathrm{o}$ and $\mathbf{q}$, and a unit direction $\mathbf{e}$ of the vector $\mathbf{R}$, we obtain

$$\mathbf{q} = \cos\theta\, \mathbf{q}_\mathrm{o} + \sin\theta\, \mathbf{e}\,, \qquad \mathbf{e} = \mathbf{R}/\left|R\right|\,, \qquad \left|R\right| = \tan\frac{\theta}{2}\,. \tag{2.13}$$

Complementarily, a normalized projection $\mathbf{t}$ of the null direction $\mathbf{k}$ onto a timelike hypersurface $\mathcal{H}_\mathrm{o}$ orthogonal to $\mathbf{q}_\mathrm{o}$ (cf. (R5.8)) is given by

$$\mathbf{t} = \frac{1}{\left|1-\left|R\right|^2\right|}\left((1+\left|R\right|^2)\,\mathbf{t}_\mathrm{o} + 2\,\mathbf{R}\right)\,. \tag{2.14}$$

In this case, the vector $\mathbf{R}$ is a *pseudostereographic representation* of the vector $\mathbf{t}$. In contrast to $\mathbf{q}$, the vector $\mathbf{t}$ does not represent a null direction $\mathbf{k}$ uniquely—the null direction obtained by reflection of $\mathbf{k}$ with respect to the hypersurface $\mathcal{H}_\mathrm{o}$ leads to the same vector $\mathbf{t}$. Therefore, we introduce the sign $\varsigma = \mathrm{sign}(1-\left|R\right|^2)$ which indicates if the vectors $\mathbf{k}$ and $\mathbf{k}_\mathrm{o}$ have the same orientation with respect to $\mathcal{H}_\mathrm{o}$. Introducing a rapidity parameter ψ between $\mathbf{t}_\mathrm{o}$ and $\mathbf{t}$ we can write

$$\mathbf{t} = \cosh\psi\, \mathbf{t}_\mathrm{o} + \sinh\psi\, \mathbf{e}\,, \qquad \mathbf{e} = \mathbf{R}/\left|R\right|\,, \qquad \left|R\right| = \left(\tanh\frac{\psi}{2}\right)^{\varsigma}\,. \tag{2.15}$$

Clearly, parametrization of the null direction $\mathbf{k}$ using the vector $\mathbf{q}$ and angle θ is useful for spacelike infinity $\mathcal{I}$ where $\mathbf{n} \propto \mathbf{t}_\mathrm{o}$ while the parametrization using $\mathbf{t}$, ψ, and ς is more appropriate for timelike $\mathcal{I}$ where $\mathbf{n} \propto \mathbf{q}_\mathrm{o}$.

Finally, let us note that the null direction $\mathbf{k}_\mathfrak{a}$ *antipodal* to $\mathbf{k}$, which is defined by $\mathbf{q}_\mathfrak{a} = -\mathbf{q}$, is given by $\mathbf{R}_\mathfrak{a} = -\mathbf{R}/\left|R\right|^2$, and that the *mirrored* direction $\mathbf{k}_\mathfrak{m}$ obtained from $\mathbf{k}$ by reflection with respect to the hypersurface $\mathcal{H}_\mathrm{o}$ is given by $\mathbf{t}_\mathfrak{m} = \mathbf{t}$, $\varsigma_\mathfrak{m} = -\varsigma$, so that $\mathbf{R} = \mathbf{R}/\left|R\right|^2$.

2.4. The interpretation frame

By *interpretation frame* $\mathbf{k}_\mathrm{i}$, $\mathbf{l}_\mathrm{i}$, $\mathbf{m}_{\mathrm{i}i}$ we understand a null frame that is parallelly transported along a null geodesic $z(\eta)$ to infinity $\mathcal{I}$ with the vector $\mathbf{k}_\mathrm{i}$ tangent to the geodesic. As in [9], we fix $\mathbf{k}_\mathrm{i} = \frac{1}{\sqrt{2}}\frac{Dz}{d\eta}$. Because we have already normalized the affine parameter η by (2.1), this choice guarantees that both the geodesics and the interpretation frames approach infinity from different directions in a comparable way.

The interpretation frame, however, is not uniquely fixed. One may perform transformations which leave $\mathbf{k}$ unchanged, namely the null rotation (2.6) and the spatial rotation (2.9). This non-uniqueness corresponds to the freedom in a choice of initial conditions for the frame.

A crucial observation which was first realized by Penrose is that the interpretation frame (boosted by the conformal factor Ω) *becomes adjusted* to infinity $\mathcal{I}$, independently of its initial conditions.

This fact can be derived by comparing the boosted frame $\mathbf{k}_\mathrm{b} = \Omega\mathbf{k}_\mathrm{i}$, $\mathbf{l}_\mathrm{b} = \Omega^{-1}\mathbf{l}_\mathrm{i}$, $\mathbf{m}_{\mathrm{b}i} = \mathbf{m}_{\mathrm{i}i}$ with a frame parallelly transported in the conformal geometry. Namely, we may define the auxiliary frame $\mathbf{k}_\mathrm{a}$, $\mathbf{l}_\mathrm{a}$, $\mathbf{m}_{\mathrm{a}i}$ as a frame parallelly transported along the geodesic in the conformal geometry, isotropically rescaled by Ω to become normalized in the physical geometry (see [9] for a detailed discussion). In addition, we require

that the auxiliary frame is adjusted to infinity. Following the steps leading to (R3.22), we analogously obtain that these two frames are related by

$$\mathbf{k}_{\rm b} = \mathbf{k}_{\rm a} \ , \quad \mathbf{l}_{\rm b} = \mathbf{l}_{\rm a} + \sqrt{2} L^i \mathbf{m}_{{\rm a}i} + |L|^2 \ \mathbf{k}_{\rm a} \ , \quad \mathbf{m}_{{\rm b}i} = \Phi_i{}^j \left(\mathbf{m}_{{\rm a}j} + \sqrt{2}\, L_j \, \mathbf{k}_{\rm a} \right) , \tag{2.16}$$

with parameters $L^i(\eta)$ and $\Phi_i{}^j(\eta)$ for large affine parameter η given by

$$\Phi_i{}^j = \Phi_{(0)i}{}^j \ , \qquad L^i = -\epsilon M^i_{(1)} \, \eta^{-1} \ln|\eta| + \epsilon L^i_{(0)} \, \eta^{-1} + \dots \ . \tag{2.17}$$

Here, $L^i_{(0)}$ and $\Phi_{(0)i}{}^j$ are constants of integration exactly corresponding to the freedom in the choice of initial conditions for the interpretation frame. The coefficients $M^i_{(1)}$ follow from the expansion of derivatives of Ω in the affine parameter η along the geodesic, see equation (R3.20). Typically—in the vacuum case or for matter satisfying the asymptotic Einstein condition (R2.20)—$M^i_{(1)}$ vanish, cf. eqation (R3.23) and discussion therein.

In any case, we observe that the boosted interpretation frame $\mathbf{k}_{\rm b}$, $\mathbf{l}_{\rm b}$, $\mathbf{m}_{{\rm b}i}$ at infinity becomes equal to the auxiliary frame, i.e., it becomes adjusted to $\mathcal{I}$, independently of the parameter $L^i_{(0)}$. However, the dependence on the spatial rotation $\Phi_{(0)i}{}^j$ persists. Because (on the general level) we are not able to fix the initial conditions for the interpretation frame uniquely, we do not know a particular value of $\Phi_{(0)i}{}^j$ and its dependence on the direction of the geodesic. Therefore, we will extract only information about radiation which is independent of the choice of spatial rotation. For this reason, in the following we may ignore any additional dependence on the spatial rotation.

We wish to characterize the interpretation frame with respect to the reference frame. Both the auxiliary and the reference frame are adjusted to infinity, i.e. they are related by a transformation which leaves the normal (2.10) unchanged. If the direction $\mathbf{k}_{\rm a} \propto \mathbf{k}_{\rm i}$ is specified by the parameters R^i via (2.11), the transformation from the reference to the auxiliary frame can be obtained by consecutive application of the null rotation (2.6) with $\mathbf{k}$ fixed, the null rotation (2.7) with $\mathbf{l}$ fixed, the boost (2.8), and the spatial rotation (2.9), given by parameters

$$L^i = \sigma R^i \ , \quad K^i = \frac{R^i}{1 - \sigma \, |R|^2} \ , \quad B = \epsilon\epsilon_{\rm o}(1 - \sigma \, |R|^2) \ , \tag{2.18}$$

and some orthonormal matrix $\Phi_i{}^j$, which can be ignored. The signs $\epsilon_{\rm o}$ and ϵ indicate orientations of the vectors $\mathbf{k}_{\rm o}$ and $\mathbf{k}_{\rm a} \propto \mathbf{k}_{\rm i}$ with respect to infinity $\mathcal{I}$, cf. eq. (2.1). Finally, the interpretation frame is simply obtained from the auxiliary one by the boost (2.8) with $B = \Omega$.

3. The graviational field and its asymptotic structure

We want to analyze the asymptotic behaviour of the gravitational field. For this we need to understand its algebraic structure. However, in a dimension higher than 4, it is quite complicated. It was investigated only recently in [1, 3]. Fortunately, these studies analyzed the structure of the Weyl tensor in the way which can immediately be used to generalize our previous results [9]. We thus start with a short overview of the algebraic structure of the Weyl tensor in higher dimensions. We will introduce a notation for its components which is convenient for our purposes.

3.1. Weyl tensor components and their transformation properties

We denote the frame components of the Weyl tensor as C^{o}_{abcd}, with index 'o' indicating that the reference frame is considered. Inspired by the notation of [3] we define the function $C^{\mathrm{o}}_{abcd}\left[K^i\right]_{\text{l-fixed}}$ of the argument K^i as a Weyl tensor component C_{abcd} evaluated with respect of the frame which is obtained from the reference frame by the null rotation (2.7) with the parameters K^i. Thanks to (2.7) it is a polynomial in K^i of the fourth order. Similarly, we define the polynomials $C^{\mathrm{o}}_{abcd}\left[L^i\right]_{\text{k-fixed}}$, $C^{\mathrm{o}}_{abcd}\left[B\right]_{\text{boost}}$, and $C^{\mathrm{o}}_{abcd}\left[\Phi_i{}^j\right]_{\text{rotation}}$. The explicit form of these functions can be easily obtained using equations (2.6)–(2.9), but some of the expressions are rather cumbersome and we will not list them here. Some particular transformations can be found in (3.1) and (3.5).

The Weyl tensor frame components can be separated into various groups according to their transformation properties under the boost (2.8). Any component C_{abcd} changes under the boost in a very simple way, namely,

$$C^{\mathrm{o}}_{abcd}\left[B\right]_{\text{boost}} = B^{w(abcd)}\, C^{\mathrm{o}}_{abcd}\,, \tag{3.1}$$

where the power $w(abcd)$ is called *boost weight* [3]. For each set of frame indices a, b, c, d it is simply the number of indices corresponding to the vector $\mathbf{k}_{\mathrm{o}}$ minus the number of indices corresponding to the vector $\mathbf{l}_{\mathrm{o}}$. For the Weyl tensor, the boost weights take the values $-2, -1, 0, 1, 2$. Components with various boost weights w are the analogues of the NP components Ψ_m of the Weyl tensor in four dimensions with $m = w + 2$. However, in a higher dimension, for each weight there are more than two independent real components, so they cannot be combined into suitable complex coefficients as when $n = 4$. Nevertheless, we may still introduce an analogous convenient notation, and we distinguish different components by additional indices.[5] We thus define real Weyl tensor components $\Psi_{m\ldots}$ grouped by their boost weight $w = m - 2$ as:

$$\Psi_{0\,ij} = C_{abcd}\, k^a\, m^b_i\, k^c\, m^d_j\,, \tag{3.2a}$$

$$\Psi_{1\,ijk} = C_{abcd}\, k^a\, m^b_i\, m^c_j\, m^d_k\,, \qquad \Psi_{1\mathrm{T}\,i} = C_{abcd}\, k^a\, l^b\, k^c\, m^d_i\,, \tag{3.2b}$$

$$\begin{aligned} \Psi_{2\,ijkl} &= C_{abcd}\, m^a_i\, m^b_j\, m^c_k\, m^d_l\,, & \Psi_{2\mathrm{S}} &= 2C_{abcd}\, k^a\, l^b\, l^c\, k^d\,, \\ \Psi_{2\,ij} &= C_{abcd}\, k^a\, l^b\, m^c_i\, m^d_j\,, & \Psi_{2\mathrm{T}\,ij} &= 2C_{abcd}\, k^a\, m^b_i\, l^c\, m^d_j\,, \end{aligned} \tag{3.2c}$$

$$\Psi_{3\,ijk} = C_{abcd}\, l^a\, m^b_i\, m^c_j\, m^d_k\,, \qquad \Psi_{3\mathrm{T}\,i} = C_{abcd}\, l^a\, k^b\, l^c\, m^d_i\,, \tag{3.2d}$$

$$\Psi_{4\,ij} = C_{abcd}\, l^a\, m^b_i\, l^c\, m^d_j\,. \tag{3.2e}$$

All other components can be obtained with the help of the symmetries of the Weyl tensor. Moreover, the listed components are mutually related. The components $\Psi_{0\,ij}$, $\Psi_{1\,ijk}$, $\Psi_{2\,ijkl}$, $\Psi_{2\,ij}$, $\Psi_{3\,ijk}$, and $\Psi_{4\,ij}$ are independent up to constraints following from the properties of the Weyl tensor:

$$\Psi_{0\,[ij]} = 0\,, \quad \Psi_{0\,k}{}^{k} = 0\,, \tag{3.3a}$$

$$\Psi_{1\,i(kl)} = 0\,, \quad \Psi_{1\,[ikl]} = 0\,, \tag{3.3b}$$

$$\Psi_{2\,ijkl} = \Psi_{2\,klij}\,, \quad \Psi_{2\,(ij)kl} = \Psi_{2\,ij(kl)} = \Psi_{2\,i[jkl]} = 0\,, \quad \Psi_{2\,(ij)} = 0\,, \tag{3.3c}$$

$$\Psi_{3\,i(kl)} = 0\,, \quad \Psi_{3\,[ikl]} = 0\,, \tag{3.3d}$$

$$\Psi_{4\,[ij]} = 0\,, \quad \Psi_{4\,k}{}^{k} = 0\,. \tag{3.3e}$$

[5] See the appendix for the relation to standard NP notation in the case $n = 4$.

The remaining components are not independent—they are given by

$$\begin{aligned}
&\Psi_{1\mathrm{T}\,i} = \Psi_{1\,k}{}^{k}{}_{i}\,,\\
&\Psi_{2\mathrm{T}\,ij} = \Psi_{2\,ikj}{}^{k} + \Psi_{2\,ij}\\
&\Psi_{2\mathrm{S}} = \Psi_{2\mathrm{T}\,k}{}^{k} = \Psi_{2\,kl}{}^{kl}\,,\\
&\Psi_{3\mathrm{T}\,i} = \Psi_{3\,k}{}^{k}{}_{i}\,.
\end{aligned} \tag{3.4}$$

Below we will mainly need the following transformation property of the $\Psi_{4\,ij}$ component under the null rotation (2.6):

$$\begin{aligned}
&\Psi_{4\,ij} = \Psi^{\circ}_{4\,ij}\left[L^{k}\right]_{\text{k-fixed}} =\\
&= \Psi^{\circ}_{4\,ij}\\
&\quad + 2\sqrt{2}\big(-\Psi^{\circ}_{3\,(ij)k}L^{k} + \Psi^{\circ}_{3\mathrm{T}\,(i}L_{j)}\big)\\
&\quad + \big(2\Psi^{\circ}_{2\,ikjl}L^{k}L^{l} - 2\Psi^{\circ}_{2\mathrm{T}\,k(i}L_{j)}L^{k} + \Psi^{\circ}_{2\mathrm{T}\,(ij)}\,|L|^{2} - \Psi^{\circ}_{2\mathrm{S}}\,L_{i}L_{j} - 4\Psi^{\circ}_{2\,k(i}L_{j)}L^{k}\big)\\
&\quad - 2\sqrt{2}\big(2\Psi^{\circ}_{1\,kl(i}L_{j)}L^{k}L^{l} + \Psi^{\circ}_{1\,(ij)k}L^{k}\,|L|^{2} + \Psi^{\circ}_{1\mathrm{T}\,(i}L_{j)}\,|L|^{2} - 2\Psi^{\circ}_{1\mathrm{T}\,k}L^{k}L_{i}L_{j}\big)\\
&\quad + \big(4\Psi^{\circ}_{0\,kl}L^{k}L^{l}L_{i}L_{j} - 4\Psi^{\circ}_{0\,k(i}L_{j)}L^{k}\,|L|^{2} + \Psi^{\circ}_{0\,ij}\,|L|^{4}\big)\,.
\end{aligned} \tag{3.5}$$

3.2. Weyl aligned null directions and algebraic classification in higher dimensions

Following [1, 3], we call the null direction $\mathbf{k}$ for which all the components $\Psi_{0\,ij}$ with respect to the null frame $\mathbf{k}$, $\mathbf{l}$, $\mathbf{m}_i$ vanish *Weyl aligned null direction* (WAND). This definition is independent of the choice of the normalization of $\mathbf{k}$ and of the choice of other vectors $\mathbf{l}$, $\mathbf{m}_i$ of the frame because under transformations which leave the direction $\mathbf{k}$ unchanged, $\Psi_{0\,ij}$ behave as

$$\Psi_{0\,ij}\left[L^{k}\right]_{\text{k-fixed}} = \Psi_{0\,ij}\,,\quad \Psi_{0\,ij}[B]_{\text{boost}} = B^{2}\Psi_{0\,ij}\,,\quad \Psi_{0\,ij}\left[\Phi_{k}{}^{l}\right]_{\text{rotation}} = \Phi_{i}{}^{k}\,\Phi_{j}{}^{l}\,\Psi_{0\,kl}\,. \tag{3.6}$$

If, in addition, all the components $\Psi_{m\,\ldots}$, $m = 0, \ldots, o-1$, with respect the null frame $\mathbf{k}$, $\mathbf{l}$, $\mathbf{m}_i$ also vanish, WAND $\mathbf{k}$ is said to be of *alignment order o*. Again, such an order of the alignment depends only on the direction of $\mathbf{k}$.

If we parametrize the null vector $\mathbf{k}$ with respect to the reference frame using the parameters R^{k} according to (2.11), the conditions that $\mathbf{k}$ is a WAND of alignment order o become

$$\Psi^{\circ}_{m\,ij}\left[R^{k}\right]_{\text{l-fixed}} = 0 \qquad \text{for} \quad m = 0, \ldots, o-1\,, \tag{3.7}$$

which are called *aligment equations* [3].

In four-dimensional spacetimes WANDs always exist and are exactly the principal null directions of the standard algebraic classification. In higher dimensions, the alignment equation (3.7) even of the first alignment order can be too restrictive and in a generic situation no WAND exists. If the alignment equations admit solutions, the spacetime is called algebraically special. Such spacetimes can be naturally classified according to the maximum alignment order of WANDs. The highest alignment order o of the WAND $\mathbf{k}$ is called the *principal alignment type*. For $o = 0, 1, 2, 3, 4$, and 5 we say that the spacetime is of principal type G (general), I, II, III, N (null), and O (trivial), respectively.

Additionally, if we set the vector $\mathbf{k}$ of the null frame $\mathbf{k}$, $\mathbf{l}$, $\mathbf{m}_i$ to be a WAND of the maximal alignment order, the highest possible aligment order of the vector $\mathbf{l}$ is said to be of *secondary aligment type*. We call the null frame with such chosen vectors $\mathbf{k}$, $\mathbf{l}$ the *frame aligned with the algebraic structure of the Weyl tensor*. From the duality between the vectors $\mathbf{k}$ and $\mathbf{l}$ and the components Ψ_m and Ψ_{4-m}, we conclude that for a spacetime of principal and secondary alignment type p and s the Weyl tensor components Ψ_m in the aligned null frame vanish for $m = 0, \dots, p-1$ and $m = 4-s+1, \dots, 4$, and the components Ψ_p and Ψ_{4-s} are nonvanishing.

Obviously, such a classification is a generalization of the standard algebraic classification in four dimensions. The main difference is that WANDs may not exist (i.e., the principal and secondary types can be zero). In other words, in four dimensions there are allowed only types that are labeled by principal and secondary type (p, s) as $(1, 1)$—Petrov type I, $(2, 1)$—Petrov type II, $(2, 2)$—Petrov type D, $(3, 1)$—Petrov type III, $(4, 0)$—Petrov type N, and the trivial $(5, 5)$—Petrov type O. In higher dimensions there are additional types $(0, 0)$—type G, $(1, 0)$, $(2, 0)$, and $(3, 0)$; see [1,3] for more detailed discussion.

3.3. Asymptotic behaviour of the field components

Now we should specify behaviour of the gravitational field at conformal infinity. However, it is not our goal here to study a specific 'fall-off' of the field in a general number of dimensions—such a task goes far beyond the scope of this work. We are interested in the *directional structure* of the 'far' field and it turns out that qualitatively this structure is *not* affected by a specific fall-off property of the field. We will thus make a general assumption that the Weyl tensor C_{abcd} behaves near infinity as Ω^{q-2}, q being some constant depending on the dimension (and maybe even on a particular solution),[6] cf. [6]. In $n = 4$ the well-known behaviour of the Weyl tensor is characterized by $q = 1$. For higher number of dimensions it is not clear if a similar property holds in a general situation (see, e.g., [4, 5]). However, our assumption is rather 'weak' and we expect it to be valid for a wide class of solutions.

Assuming the above fall-off of the Weyl tensor we can write down asymptotic behaviour of its components. Combining (3.2), (2.3) and considering the normalization of the reference frame[7] as $\mathbf{k}_{\mathrm{o}}, \mathbf{l}_{\mathrm{o}}, \mathbf{m}_{\mathrm{o}i} \sim \Omega$ we get

$$\Psi^{\mathrm{o}}_{m\dots} \approx \hat{\Psi}^{\mathrm{o}}_{m\dots}\, \eta^{-q-2}\,, \tag{3.8}$$

where $\hat{\Psi}^{\mathrm{o}}_{m\dots}$ are constant finite coefficients. We may also define $\hat{\Psi}^{\mathrm{o}}_{m\dots}\big[L^k\big]_{\text{k-fixed}}$ in a similar way as $\Psi^{\mathrm{o}}_{m\dots}\big[L^k\big]_{\text{k-fixed}}$. It is a polynomial in L^k with $\hat{\Psi}^{\mathrm{o}}_{m\dots}$ being coefficients.

The relation between the interpreation and reference frames was described in section 2.4. In particular, the interpretation tetrad can be obtained by the sequence of null rotations, boost, and spatial rotation with parameters (2.18) followed by the (asymptotically singular) boost $B = \Omega$. The field components with respect to the interpreation frame are thus

$$\Psi^{\mathrm{i}}_{m\dots} \overset{*}{\approx} \Omega^{2-m}\, \Psi^{\mathrm{a}}_{m\dots}\,, \tag{3.9}$$

since the interpretation frame is related to the adjusted auxiliary one by the boost. Here and in the following, we ignore spatial rotations acting on indices i, j which

[6] Alternatively, we could say that the fall-off of the conformally related Weyl tensor is $\tilde{\mathbf{C}}_{abc}{}^{d} \sim \Omega^q$.
[7] At $\mathcal{I}$, the conformally rescaled frame $\Omega^{-1}\mathbf{k}_{\mathrm{o}}, \Omega^{-1}\mathbf{l}_{\mathrm{o}}, \Omega^{-1}\mathbf{m}_{\mathrm{o}i}$, normalized in the unphysical metric $\tilde{\mathbf{g}}$, is regular.

can arise from the non-uniqueness of the interpretation frame or from the relation to the reference frame. This will be indicated by a star '$*$' above the equality symbol. Because asymptotically $\Omega \sim \eta^{-1}$, cf. (2.3), and the transformation from the auxiliary frame to the reference frame is regular, we see that different components of the Weyl tensor peel-off with different powers of the affine parameter η according to their boost weights labeled by m. This is the analogue of the well-known peeling-off theorem in four dimensions [11] — see also the recent analysis of this topic [6] in higher dimensions.

We will now study only the leading component of the gravitational field which is $\Psi^{\mathrm{i}}_{4\,ij}$. Performing the transformation (2.18) from the auxiliary frame to the reference frame we obtain

$$\Psi^{\mathrm{a}}_{4\,ij} \overset{*}{\approx} \frac{1}{(1-\sigma\,|R|^2)^2}\,\Psi^{\mathrm{o}}_{4\,ij}\left[\sigma R^k\right]_{\text{k-fixed}}\,, \tag{3.10}$$

where we parametrized the direction $\mathbf{k}_{\mathrm{i}}$ of the geodesic by R^k via (2.11). Using (3.9), (2.3), and (3.8) we finally get

$$\Psi^{\mathrm{i}}_{4\,ij} \overset{*}{\approx} \frac{\eta^{-q}}{(1-\sigma\,|R|^2)^2}\,\hat\Psi^{\mathrm{o}}_{4\,ij}\left[\sigma R^k\right]_{\text{k-fixed}}\,. \tag{3.11}$$

The explicit form of the expression $\hat\Psi^{\mathrm{o}}_{4\,ij}\left[L^k\right]_{\text{k-fixed}}$ is given in (3.5).

3.4. Directional structure of radiation

We have thus derived the asymptotic directional structure of gravitational radiation in higher dimensions which is a generalization of the main result of [9]. It describes the dependence of the leading field component on a direction along which the infinity is approached. Let us now briefly discuss some properties of this dependence.

First, as we mentioned earlier, we have ignored an arbitrary rotation of the field (3.11) 'in indices ij'. On the general level, we cannot control the spatial rotation (2.9) in these indices and therefore the only physically relevant quantities are invariants which we can construct from the matrix (3.11). Thanks to the properties of the Weyl tensor, the matrix of the radiative field component $\Psi^{\mathrm{i}}_{4\,ij}$ is symmetric, cf. (3.3e). Therefore, the invariants under spatial rotation are real eigenvalues of the matrix. Alternative invariants are the traces of powers of the matrix. Because $\Psi^{\mathrm{i}}_{4\,ij}$ is traceless, the independent invariants are

$$\underbrace{\Psi^{\mathrm{i}}_{4\,i}{}^{j}\;\Psi^{\mathrm{i}}_{4\,j}{}^{k}\;\ldots\;\Psi^{\mathrm{i}}_{4\,l}{}^{i}}_{m\text{-times}} \qquad \text{for} \quad m=2,\ldots,n-2\,. \tag{3.12}$$

Substituting the relation (3.11) into (3.12), one obtains expressions which are polynomial in the directional parameter R^k. Clearly, if all the invariants are zero, the complete leading term also vanishes.

The location of the zeros of the directional pattern (3.11) follows from a simple argument. The pattern is proportional to $\Psi^{\mathrm{a}}_{4\,ij}$. Analogous to the alignment equations (3.7), the vanishing of these Weyl tensor components means that the null vector $\mathbf{l}_{\mathrm{a}}$ is asymptotically[8] WAND. However, the auxiliary frame is adjusted to infinity, i.e.,

[8] The word 'asymptotically' refers to the fact that we define WANDs at conformal infinity using the components $\hat\Psi^{\mathrm{o}}_{m\ldots}$ instead of $\Psi^{\mathrm{o}}_{m\ldots}$, i.e., using the Weyl tensor isotropically rescaled by a factor $\sim\Omega^{-3}$. Such a definition of asymptotic WANDs is justified by the observation that a finite isotropic rescaling of the Weyl tensor does not change the notion of WANDs.

the vectors $\mathbf{k}_{\rm a}$ and $\mathbf{l}_{\rm a}$ are related by (2.10). Hence, the direction of the geodesic $\mathbf{k}_{\rm i} \propto \mathbf{k}_{\rm a}$ along which the leading term of the field vanishes has to be 'opposite' to a WAND $\mathbf{l}_{\rm a}$ in the sense of the relation (2.10). If the direction $\mathbf{k}_{\rm i} \propto \mathbf{k}_{\rm a}$ is given by the directional parameter R^k through (2.11), such a direction $\mathbf{l}_{\rm a}$ is given by the parameter $\sigma^{-1} R^k / |R|^2$.

For $\sigma \neq 0$, it is also possible to reach the same conclusions using the identity

$$\hat{\Psi}^{\rm o}_{4\,ij}\,[L^p]_{\text{k-fixed}} = |L|^4\ \big(\delta^k_i - 2L_iL^k/|L|^2\big)\big(\delta^l_j - 2L_jL^l/|L|^2\big)\ \hat{\Psi}^{\rm o}_{0\,kl}\left[L^p/|L|^2\right]_{\text{l-fixed}} \quad (3.13)$$

which relates transformations of the components $\Psi^{\rm o}_{4\,ij}$ and $\Psi^{\rm o}_{0\,ij}$. Applying this identity to the directional structure (3.11), and using the fact that matrix $(\delta^k_i - 2L_iL^k/|L|^2)$ is orthogonal we obtain

$$\Psi^{\rm i}_{4\,ij} \overset{*}{\approx} \frac{\eta^{-q}\,|R|^4}{(1-\sigma\,|R|^2)^2}\ \hat{\Psi}^{\rm o}_{0\,ij}\left[\sigma^{-1}R^k/|R|^2\right]_{\text{l-fixed}}, \qquad \text{for} \quad \sigma \neq 0\,. \quad (3.14)$$

Clearly, this vanishes iff the direction given by the parameter $\sigma^{-1}R^k/|R|^2$ is a WAND.

For $\sigma = 0$, equation (3.11) reduces to

$$\Psi^{\rm i}_{4\,ij} \overset{*}{\approx} \eta^{-q}\,\hat{\Psi}^{\rm o}_{4\,ij}\,. \quad (3.15)$$

Thus $\hat{\Psi}^{\rm o}_{4\,ij}$ vanishes if the vector $\mathbf{l}_{\rm o}$ is asymptotically WAND. However, $\mathbf{l}_{\rm o}$ is described by an infinite value of directional parameter (2.11), so that the leading term $\Psi^{\rm i}_{4\,ij}$ again vanishes again iff the direction $\sigma^{-1}R^k/|R|^2 = \infty$ is a WAND.

Let us now discuss the directional structure of radiation separately for a different character of the conformal infinity $\mathcal{I}$. For *null character* of the infinity, $\sigma = 0$, we find that the leading term (3.15) is independent of the direction of the null geodesic along which the infinity is approached. It vanishes if the null direction $\mathbf{l}_{\rm o}$ tangent to the infinity (cf. adjustment condition (2.10) for $\sigma = 0$) is asymptotically a WAND. This fact may be used for an invariant characterization of the presence of gravitational radiation in higher-dimensional spacetimes.

For a *spacelike* conformal infinity, $\sigma = -1$, it is natural to parametrize the null direction $\mathbf{k}$ of the geodesic using its normalized projection $\mathbf{q}$ to $\mathcal{I}$, cf. equation (2.12). It can be expressed in terms of the angle θ and of the complementary directional vector $\mathbf{e} = e^k\mathbf{m}_{{\rm o}k}$, see (2.13). The directional structure (3.11) then reads

$$\Psi^{\rm i}_{4\,ij} \overset{*}{\approx} \eta^{-q}\,\cos^4\tfrac{\theta}{2}\ \hat{\Psi}^{\rm o}_{4\,ij}\left[-\tan\tfrac{\theta}{2}\ e^k\right]_{\text{k-fixed}}. \quad (3.16)$$

The leading term of the field vanishes if the direction $\mathbf{k}_{\mathfrak{a}}$ antipodal to $\mathbf{k}$ is a WAND. Let us recall that the antipodal direction has the opposite projection to $\mathcal{I}$, $\mathbf{q}_{\mathfrak{a}} = -\mathbf{q}$ (see the end of section 2.3).

For a *timelike* infinity $\mathcal{I}$, $\sigma = +1$, we parametrize the null direction $\mathbf{k}$ of the geodesic by its normalized projection $\mathbf{t}$ to $\mathcal{I}$ (unit timelike future oriented vector, cf. (2.14)) and by the parameter $\epsilon = \pm 1$ which describes to which side of infinity the vector $\mathbf{k}$ points (cf. equation (2.2)). If we express the vector $\mathbf{t}$ through the rapidity ψ and the directional vector $\mathbf{e}$, see equation (2.15), we obtain

$$\Psi^{\rm i}_{4\,ij} \overset{*}{\approx} \eta^{-q}\,\tfrac{1}{4}(\cosh\psi + \epsilon\epsilon_{\rm o})^2\ \hat{\Psi}^{\rm o}_{4\,ij}\left[\tanh^{\epsilon\epsilon_{\rm o}\frac{\psi}{2}}\ e^k\right]_{\text{k-fixed}}. \quad (3.17)$$

This vanishes if the mirror reflection $\mathbf{k}_{\mathtt{m}}$ of the direction $\mathbf{k}$ with respect to the infinity is a WAND (see again the end of section 2.3).

We conclude that all these results are direct generalizations of the analogous results of [9]. As in four dimensions, the directional structure of radiation is given by the algebraic structure of the Weyl tensor. Also, the directions of vanishing radiation are determined by WANDs which are generalizations of the principal null directions which are known from $n = 4$ general relativity.

3.5. Algebraically special spacetimes

The general explicit form of the directional dependence of the radiative component is rather cumbersome, cf. equation (3.11) combined with (3.5). It simplifies for algebraically special spacetimes, i.e., in spacetimes which posses some WANDs, see section 3.2. Let us emphasize, however, that in higher dimensions the condition that the spacetime is algebraically special can be rather restrictive—as we mentioned above, a generic spacetime has no WANDs. It is also not clear if an algebraically special spacetime can admit a regular global infinity $\mathcal{I}$. Fortunately, our discussion requires only the *local* existence and regularity of the conformal infinity, and we restrict only to the cases when such an infinity exists.

Although the directional structure of radiation simplifies for algebraically special spacetimes, it is still parameterized by more independent components of the Weyl tensor than in the case of four dimensions. The resulting expressions thus typically remain lengthy. We will present them only in two most special cases—for spacetimes of type N and of type III.

A substantial simplification of the directional structure (3.11) occurs only for maximally special (nontrivial) spacetimes of type N. In this case there exists a WAND of the alignment order 4. If we choose the reference tetrad in such a way that $\mathbf{k}_{\mathrm{o}}$ is asymptotically this WAND, the alignment equations tell us that only the components $\hat\Psi^{\mathrm{o}}_{4\,ij}$ are nonvanishing. In view of (3.5), the directional structure of the radiative field components thus takes a simple form

$$\begin{aligned}\Psi^{\mathrm{i}}_{4\,ij} &\overset{*}{\approx} \frac{\eta^{-q}}{(1-\sigma\,|R|^2)^2}\,\hat\Psi^{\mathrm{o}}_{4\,ij} \\ &\overset{*}{\approx} \eta^{-q}\,\cos^4\tfrac{\theta}{2}\,\hat\Psi^{\mathrm{o}}_{4\,ij} \overset{*}{\approx} \eta^{-q}\,\tfrac14(\cosh\psi+\epsilon\epsilon_{\mathrm{o}})^2\,\hat\Psi^{\mathrm{o}}_{4\,ij}\,.\end{aligned} \tag{3.18}$$

Here $\hat\Psi^{\mathrm{o}}_{4\,ij}$ are constants characterizing the 'strength' and 'polarization' of the field. In this case, it is more convenient to choose as invariants (which ignore unknown polarization) the eigenvalues of $\Psi^{\mathrm{i}}_{4\,ij}$ instead of the traces (3.12)—these are proportional to the eigenvalues of $\hat\Psi^{\mathrm{o}}_{4\,ij}$ with a common factor which can be read from equation (3.18).

The next simplest case is that of spacetimes of type III (we do not need to distinguish the type according the secondary alignment type in our discussion). In this case, we may choose the reference tetrad with $\mathbf{k}_{\mathrm{o}}$ pointing asymptotically along a WAND of alignment order 3. It follows that the components $\hat\Psi^{\mathrm{o}}_{m\ldots}$, $m=0,1,2$, are vanishing and the leading field component thus reads

$$\Psi^{\mathrm{i}}_{4\,ij} \overset{*}{\approx} \frac{\eta^{-q}}{(1-\sigma\,|R|^2)^2}\left(\hat\Psi^{\mathrm{o}}_{4\,ij}+\sigma\,2\sqrt2\left(-\hat\Psi^{\mathrm{o}}_{3\,(ij)k}R^k+\hat\Psi^{\mathrm{o}}_{3\mathrm{T}\,(i}R_{j)}\right)\right). \tag{3.19}$$

It would be possible to use a more detailed structure of the field components $\hat{\Psi}^{\mathrm{o}}_{4\,ij}$ and $\hat{\Psi}^{\mathrm{o}}_{3\,ijk}$ to select a 'canonical' reference frame (e.g., $\hat{\Psi}^{\mathrm{o}}_{3\mathrm{T}\,i}$ identifies an additional spatial direction, etc.) with respect to which (3.19) would have a slightly more specific form. However, such a discussion would not bring any significant additional understanding of the directional structure of the field and we will not enter it here.

4. Conclusion

In recent years a great effort has been devoted to the investigation of gravitational theories in higher dimensional spacetimes. Several exact solutions of (generalized) Einstein's equations with properties either analogous to the four-dimensional case or with completely new features (such as, e.g., the existence of black rings) were found. However, many useful concepts and methods known from the four-dimensional gravity still have not been generalized to higher dimensions.

Our work is a contribution to such possible generalizations, namely to a discussion of an asymptotic behaviour of the gravitational field in higher dimensions. It does not address in detail such questions as what exactly radiation is or which part of the gravitational field is relevant for physical observers (e.g., in brane-world scenarios we should restrict only to the part of the conformal infinity near the brane). However, it demonstrates that the structure of the leading field components—in the sense of the peeling theorem—can be described in an analogous way as in four dimensions. It shows, that the directional ambiguity of the leading components in the case of a non-vanishing cosmological constant can again be characterized in terms of the asymptotic algebraic structure of the Weyl tensor. Due to the more complicated algebraic properties of the Weyl tensor in higher dimensions, the directional structure of the radiative components is, not surprisingly, more intricate.

A. Relation to complex notation in $n = 4$

In standard $n = 4$ general relativity it is convenient to introduce a *complex null tetrad* and to parametrize the Weyl tensor by the corresponding five *complex* components. These NP quantities are closely related to the *real* quantities introduced in our text. Here we present a 'dictionary' relating these two notations.

In four dimensions the transverse indices i, j, k, l run only over two values $1, 2$ and we can combine the real vectors $\mathbf{m}_i$ into the complex vectors

$$\mathbf{m} = \tfrac{1}{\sqrt{2}}\,(\mathbf{m}_1 - i\mathbf{m}_2)\,, \quad \bar{\mathbf{m}} = \tfrac{1}{\sqrt{2}}\,(\mathbf{m}_1 + i\mathbf{m}_2)\,. \tag{A.1}$$

Any real vector $\mathbf{V}$ spanned on $\mathbf{m}_1, \mathbf{m}_2$ can be parametrized by a complex number V by the relation

$$\mathbf{V} = V^1\mathbf{m}_1 + V^2\mathbf{m}_2 = \tfrac{1}{\sqrt{2}}\,(\bar{V}\mathbf{m} + V\bar{\mathbf{m}})\,. \tag{A.2}$$

It follows that

$$V = V^1 - iV^2\,, \quad |V|^2 = (V^1)^2 + (V^2)^2 = V\bar{V}\,. \tag{A.3}$$

The transformation properties of the null tetrad under, for example, a null rotation with $\mathbf{k}$ fixed (2.6) then reads

$$\mathbf{k} = \mathbf{k}_{\mathrm{o}}\,, \qquad \mathbf{l} = \mathbf{l}_{\mathrm{o}} + \bar{L}\,\mathbf{m}_{\mathrm{o}} + L\,\bar{\mathbf{m}}_{\mathrm{o}} + |L|^2\,\mathbf{k}_{\mathrm{o}}\,, \qquad \mathbf{m} = \mathbf{m}_{\mathrm{o}} + L\,\mathbf{k}_{\mathrm{o}}\,. \tag{A.4}$$

This is the standard four-dimensional expression for a null rotation, see, e.g., [9].

Moreover, in four dimensions there are only two real independent components of the Weyl tensor for each boost weight, namely

$$\Psi_{0\,11} = -\Psi_{0\,22} \,, \quad \Psi_{0\,12} = \Psi_{0\,21} \,, \tag{A.5a}$$

$$\Psi_{1\mathrm{T}\,1} = \Psi_{1\,221} = -\Psi_{1\,212} \,, \quad \Psi_{1\mathrm{T}\,2} = \Psi_{1\,112} = -\Psi_{1\,121} \,, \tag{A.5b}$$

$$\begin{aligned} &\Psi_{2\,1212} = \Psi_{2\,2121} = -\Psi_{2\,2112} = -\Psi_{2\,1221} = \Psi_{2\mathrm{T}\,11} = \Psi_{2\mathrm{T}\,22} = \tfrac{1}{2}\Psi_{2\mathrm{S}} \,, \\ &\Psi_{2\,12} = -\Psi_{2\,21} = \Psi_{2\mathrm{T}\,12} = -\Psi_{2\mathrm{T}\,21} \,, \end{aligned} \tag{A.5c}$$

$$\Psi_{3\mathrm{T}\,1} = \Psi_{3\,221} = -\Psi_{3\,212} \,, \quad \Psi_{3\mathrm{T}\,2} = \Psi_{3\,112} = -\Psi_{3\,121} \,, \tag{A.5d}$$

$$\Psi_{4\,11} = -\Psi_{4\,22} \,, \quad \Psi_{4\,12} = \Psi_{4\,21} \,. \tag{A.5e}$$

These can be combined into complex NP components defined by

$$\Psi_0 = C_{abcd}\, k^a\, m^b\, k^c\, m^d \,, \tag{A.6a}$$

$$\Psi_1 = C_{abcd}\, k^a\, l^b\, k^c\, m^d \,, \tag{A.6b}$$

$$\Psi_2 = C_{abcd}\, k^a\, m^b\, \bar{m}^c\, l^d \,, \tag{A.6c}$$

$$\Psi_3 = C_{abcd}\, l^a\, k^b\, l^c\, \bar{m}^d \,, \tag{A.6d}$$

$$\Psi_4 = C_{abcd}\, l^a\, \bar{m}^b\, l^c\, \bar{m}^d \,, \tag{A.6e}$$

via

$$\Psi_0 = \Psi_{0\,11} - i\Psi_{0\,12} \,, \tag{A.7a}$$

$$\Psi_1 = \tfrac{1}{\sqrt{2}}(\Psi_{1\mathrm{T}\,1} - i\Psi_{1\mathrm{T}\,2}) \,, \tag{A.7b}$$

$$\Psi_2 = -(\Psi_{2\,1212} + i\Psi_{2\,12}) \,, \tag{A.7c}$$

$$\Psi_3 = \tfrac{1}{\sqrt{2}}(\Psi_{3\mathrm{T}\,1} + i\Psi_{3\mathrm{T}\,2}) \,, \tag{A.7d}$$

$$\Psi_4 = \Psi_{4\,11} + i\Psi_{4\,12} \,. \tag{A.7e}$$

References

[1] Coley A, Milson R, Pravda V, and Pravdová A 2004 Classification of the Weyl Tensor in Higher Dimensions *Class. Quantum Grav.* **21** L35–L42

[2] Pravda V, Pravdová A, Coley A, and Milson R 2004 Bianchi identities in higher dimensions *Class. Quantum Grav.* **21** 2873-2898

[3] Milson R, Coley A, Pravda V, and Pravdová A 2005 Alignment and algebraically special tensors in Lorentzian geometry *Int. J. Geom. Meth. Mod. Phys.* **2** 41–61

[4] Hollands S and Wald R. M 2004 Conformal Null Infinity Does Not Exist for Radiating Solutions in Odd Spacetime Dimensions *Class. Quantum Grav.* **21** 5139-5146

[5] Hollands S and Ishibashi A 2005 Asymptotic Flatness and Bondi Energy in Higher Dimensional Gravity *J. Math. Phys.* **46** 022503

[6] Pravdová A, Pravda V, and Coley A 2005 A note on the peeling theorem in higher dimensions *Class. Quantum Grav.* **22** 2535-2538

[7] Krtouš P, Podolský J, and Bičák J 2003 Gravitational and electromagnetic fields near a de Sitter-like infinity *Phys. Rev. Lett.* **91** 061101

[8] Krtouš P and Podolský J 2004 Gravitational and electromagnetic fields near an anti-de Sitter-like infinity *Phys. Rev. D* **69** 084023

[9] Krtouš P and Podolský J 2004 Asymptotic directional structure of radiative fields in spacetimes with a cosmological constant *Class. Quantum Grav.* **21** R233–R273

[10] Krtouš P and Podolský J 2005 Asymptotic directional structure of radiation for fields of algebraic type D *Czech. J. Phys.* **55** 119-138

[11] Penrose R and Rindler W 1984, 1986 *Spinors and Space-Time* (Cambridge, England: Cambridge University Press)